Alternative therapeutic approaches in blocking the oncogenic role of the Siglec-15/Sialyl-Tn axis in Colorectal Cancer

Author: Mohammed Saqif Ahmad

Supervisory team: Dr Shoib Siddiqui, Dr Maria Braoudaki and Dr Lisa Lione

Submitted to the University of Hertfordshire in partial fulfilment of the requirement of the degree of Doctor of Philosophy

SEPTEMBER, 2024

UNIVERSITY OF HERTFORDSHIRE

College Lane, Hatfield AL10 9AB

Abstract

Colorectal cancer (CRC) malignancies are among the highest mortality and morbidity rates worldwide. Despite the emergence of numerous screening programs to reduce CRC incidence, the number of CRC and early-onset CRC diagnoses has risen exponentially, resulting in difficulties in curative surgical control and subsequent tumour related deaths. Thus, there is an unmet clinical need for developing targeted strategies in CRC treatment. As an emerging immune checkpoint protein, Siglec-15 is overexpressed in several malignancies and is correlated to the development of the tumour microenvironment through establishing immunosuppression upon binding with its putative ligand, Sialyl-Tn (STn). However, the role of Siglec-15 particularly relating to CRC remains elusive. The identification of regulatory mechanisms surrounding the Siglec-15/STn axis is poorly understood, and current therapeutic approaches have only shown a positive response in a small subset of cancer patients. Thus, underlining the clinical role of oncogenic targets such as Siglec-15 and the significant tumour heterogeneity that CRC tumours pose. As more recent approaches are focused on the development of monoclonal antibodies for Siglec-15 targeting, the development of small molecule therapeutic agents for Siglec-15 inhibition has not yet been elucidated. Hence, this study aimed to investigate the potential of key sialyltransferases as therapeutic targets in CRC by investigating the regulatory mechanisms that are associated with their expression profiles, the role they play in glycan biosynthesis, tumour progression, and the production of the STn antigen, respectively. Moreover, we aimed to experimentally demonstrate the characterisation of the cytotoxic profile of a β-amino carbonyl compound (SHG-8) and aleplasinin for Siglec-15 targeting within *in vitro* cell models as feasible treatment alternatives.

Initial datamining of the sialyltransferases *ST6GALNAC1*, *ST6GALNAC2*, *ST3GAL4* and *ST6GAL1* were performed using readily available transcriptomics tools including UALCAN and miRNA target prediction (TargetScan, MiRSystem, MiRDB and MirWalk) databases and binding site software for sialyltransferase expression profiles in colon adenocarcinoma tumours, pathologically the most frequently occurring CRC tumour type. Following this, tumour hallmarks associated with CRC progression were determined in relation to sialyltransferase expression through gene set enrichment analysis (GSEA). Similarly, their expression in association with the abundance of myeloid cell populations and prevalent immune checkpoint proteins were also demonstrated with integrated repositories readily available with the TIMER and TISIDB databases. Lastly, the expression of ST6GalNAc1 and ST6GalNAc2 at the protein level was determined via immunohistochemical analysis to underline their importance in the production of the STn antigen. Furthermore, molecular docking simulations were utilised to illustrate the potential of SHG-8 and aleplasinin as competitive small molecule inhibitors to the V-set binding domain of the Siglec-15 protein structure, rendering the STn antigen unable to directly bind to the R143 residue. Moreover, the characterisation of small molecule inhibitors on tumour viability, migration and colonisation via functional assays was determined *in vitro* on mammalian cell models SW480 and HCT116, both of which are representative of the large proportion of CRC diagnoses. In addition, apoptosis staining methods were performed to assess cellular arrest and apoptosis induction. Conversely, RNA sequencing methods were utilised to underline the expression profiles of miRNAs and gene targets following treatment exposure. Further exploration of these targets were also determined to elucidate potential CRC mechanisms of action.

The sialyltransferases revealed downregulated expression profiles excluding *ST6GAL1* in CRC adenocarcinoma tumours. Similarly, the identified interactive partners all exhibited varied expression profiles. Furthermore, common miRNAs involved in regulating sialyltransferases that play major roles in glycan biosynthesis were identified and exhibited high binding

affinities. Enrichment analysis revealed several dysregulated tumorigenic hallmarks associated with CRC progression. Furthermore, the association of myeloid cells and prevalent immune checkpoint proteins underlined the multifaceted roles of the sialyltransferases in CRC. The immunohistochemistry analysis revealed that STn production is independent of ST6GalNAc1/2 activity in CRC. Moreover, aleplasinin and SHG-8 exhibited a high binding affinity to the V-set binding domain of the Siglec-15 protein structure. Both compounds exerted dose-dependent cytotoxicity on cellular viability, migration and colonisation. Apoptosis staining methods demonstrated late apoptosis induction and nuclear fragmentation at higher treatment concentrations. Sequencing analysis methods demonstrated that the miR-6715b-3p/*PTTG1IP* and let-7a-5p/*ACSL6* axes could be involved in CRC progression following treatment exposure.

The evidence presented in this study suggested possible approaches for disrupting the Siglec-15/Sia axis and underlined the roles of sialyltransferases as potential therapeutic targets in CRC tumours. Furthermore, we have expanded the therapeutic landscape of Siglec-15 and highlighted treatment alternatives in Siglec-15^{+} tumours in contrast to current conventional therapeutic agents. Therefore, this will greatly help in the transition of novel therapeutic agents towards a clinical setting to address the challenges that is facing Siglec-15 mediated CRC progression. Ultimately, a multifaceted treatment approach based on our findings would offer the novel development of further inhibitors in targeting Siglec-15 and significantly advance the field of oncology.

Keywords: Colorectal cancer, Siglec-15, Sialyl-Tn, microRNAs, small molecule inhibitor, sialyltransferase

Dedication

আমি আমার পরিবারের অটল সমর্থন এবং স্নেহের জন্য কৃতজ্ঞ, যারা আমার একাডেমিক সাধনার জন্য একটি দৃঢ় ভিত্তি প্রদানে মৌলিক ভূমিকা পালন করেছেন। বিশেষ করে, আমার প্রয়াত দাদা আমাদের হৃদয়ে একটি গুরুত্বপূর্ণ এবং লালিত স্থান ধারণ করেন। আমি শ্রদ্ধার সাথে এই থিসিসটি তাদের কাছে উৎসর্গ করতেছি যারা আমার কাছে অপরিমেয় মূল্যবান।

Acknowledgments

The journey of finally reaching the conclusion of my PhD cannot be understated and I am incredibly indebted to a great many people who have supported, encouraged, and inspired me along the way.

First and foremost, I would like to express my deepest gratitude towards my supervisor Dr Shoib Siddiqui. Over the past few years since my master's degree, your unwavering patience, guidance, constant encouragement and kindness has been nothing short of invaluable. You have been more than just my supervisor, you have also been my mentor, my teacher and my friend. You have been a constant source of motivation and have helped me navigate through the highs and lows over the past few years. Your insight and wisdom has challenged me to critically think and push myself beyond the limits of my work, and your patience in navigating through my successes and struggles has helped in large part for me to grow both academically and personally. I will forever be grateful for the countless hours you have dedicated to my work and for always believing in my potential.

I would also like to extend my deepest heartfelt appreciation to Dr Maria Braoudaki, who has been my second mother throughout my time at the University of Hertfordshire since I was a small undergrad. Your belief in me helped my confidence, even when I didn't believe in myself and for having provided an ear to listen when I was struggling. Your wisdom has helped strengthen all aspects of my work in more ways than I can count. I appreciate the time you spent in helping in every way no matter how small and for broadening my perspectives.

Additionally, I would also like to give a heartfelt thanks to Dr Lisa Lione. Your wisdom, thoughtful critique, and willingness to engage with my work has strengthened this thesis and my research. The feedback I received from you has been a crucial pillar in shaping the final version of this research work.

To my colleagues and fellow PhD candidates in CPBS, thank you for being a source of camaraderie, inspiration, and collaboration. Whether it was through engaging in academic discussions (more likely big conversations about food), moral support during challenging times, or to relax and hang out, you made this journey far less isolating. Special thanks to Denis Mustafov and Altin Kocinaj, their understanding during the busiest periods and your

encouragement when I needed it most have meant the world to me. To Alex Selby, thank you for standing by me throughout this journey, for celebrating the small wins, and for picking me up during the inevitable lows. Your friendship has been a source of joy, sanity, and strength. The shared experiences of triumphs and tribulations were made all the more meaningful by having you all by my side.

I am deeply grateful to the University of Hertfordshire for providing an environment that is now a second home, which encouraged curiosity and growth since my first day all the way back in 2017. In addition, a special acknowledgment goes to the QR funding provided by the University of Hertfordshire for providing the financial support that enabled me to carry out this research, without which this experience wouldn't have been made possible. I would like to extend my heartfelt gratitude to my collaborators, Dr Irshad Ahmad and Dr Shagufta, for their invaluable contributions to my research. Their expertise and willingness to share their knowledge significantly enhanced the quality and depth of my work. A special thank you to the entire CPBS technical team for all their help and a special appreciation to Di Francis and Lee Rixon for their guidance and willingness to help even if I did break a lot of things!

To my family, I am forever indebted to you for your endless patience, love, and understanding. To my parents, Mohammed Abdus Salam and Syeda Nasima Begum, thank you for your endless sacrifices, for teaching me the value of education, and for always believing in me. Your unwavering support has been the foundation upon which this accomplishment rests and is as much your accomplishment as it is mine. To my brother, Mohammed Tauqir Ahmad, thank you for your constant encouragement, humour, and perspective, which kept me grounded through the most challenging phases.

Finally, to Cyntia Christurajah, you have always been the rock and steadfast support that carried me through this journey. Thank you for always being there, for encouraging me to push forward even when the path felt uncertain and celebrating every step of the way, no matter how small. I am deeply grateful for your presence in the many late nights, long weekends and the emotional ups and downs. I couldn't have imagined doing this by myself. Thank you for making me feel I am enough.

Table of Contents

List of Figures

List of tables

Abbreviations List

3-(4-bromophenyl)-1-phenyl-3-(phenylamino)propan-1-one - SHG-8
3-(4,5-dimethylthiazol-2-yl)-2,5-diphenyltetrazolium bromide – MTT
5-FU - 5-fluorouracil
ACSF2 - acyl-CoA synthetase family member 2
ACSL6 - acyl-CoA synthetase long chain family member 6
ACSS2 - acyl-CoA synthetase short chain family member 2
AGR2 - gene anterior gradient 2
AHSG - α-2-HS-glycoprotein
ALCC - average local clustering coefficient
AML - acute myeloid leukaemia
AMPK - AMP-activated protein kinase
AO/EB - Acridine orange/ Ethidium bromide
APC - adenomatous polyposis coli
Arid1a - Chromatin remodelling factor AT-rich interaction domain 1A
ASR - age standardised rate
AT - cancer adjacent colon tissue
B3GAL2, B3GAL5 - β-1,3-galactosyltransferase-2/-5
B3GNT6 - UDP-GlcNAc:βGal β-1,3-N-acetylglucosaminyltransferase 6
B4GALT1, B4GALT2, B4GALT3 - β-1,4-galactosyltransferase
BACH1-IT2 - BTB domain and CNC homolog 1 intrinsic transport 2
BAD - Bcl-2 associated agonist of cell death
BAK - Bcl-2 antagonist/killer 1
BAX - Bcl-2 associated X, apoptosis regulator
BIM - Bcl-2 interacting mediator of cell death
BSA – bovine serum albumin
C1GALT1 - Core 1 synthase glycoprotein-N-acetylgalactosamine 3-β -galactosyltransferase
C1GALT1C1; COSMC - C1GALT1 specific chaperone 1
ccRCC - clear-cell renal cell carcinoma
CD – Crohn's disease
CD22 – Siglec-2
CHK1 - checkpoint kinase 1
CHK2 - checkpoint kinase 2
CHST - carbohydrate sulphotransferase
CHST2 - carbohydrate sulphotransferase 2
CHST5 - carbohydrate sulphotransferase 5
CHST6 - carbohydrate sulphotransferase 6
CI - confidence interval
CIMP pathway - CpG island methylation phenotype
CIN – chromosomal instability
CKI - casein kinase I
CMAH - cytidine monophospho-N-acetylneuraminic acid hydroxylase
CMAS - N-acetylneuraminic acid synthetase
CMP - cytidine monophosphate
CoA - acetyl-coenzyme A
COAD – colon adenocarcinoma
CPT1 - carnitine palmitoyl transferase 1
CPT1A - carnitine palmitoyl transferase 1A
CRC – Colorectal cancer

CTLA-4 - cytotoxic T-lymphocyte associated protein 4
DAP12 - 12 kDa DNAX-activating protein-12
DDB2 - damage specific DNA binding protein 2
DE - differentially expressed
DMMR – DNA mismatch repair genes
DMSO - dimethyl sulfoxide
DUSP1 - dual specificity phosphatase 1
Dvl2 - dishevelled segment polarity protein 2
EDTA - disodium ethylenediaminetetraacetic acid
EEF1A2 - eukaryotic translation elongation factor 1α-2
EGFR - epidermal growth factor receptor
ELISA - enzyme-linked immunosorbent assay
EMT - epithelial to mesenchymal transition
EO-CRC - early-onset CRC
ER - endoplasmic reticulum
ER^+ - oestrogen receptor positive
ESI - electrospray ionisation
ESI-MS - electrospray ionisation mass spectrometry
EZH2 - enhancer of zeste homolog 2
FADD - FAS-associated death domain protein
FasL - Fas ligand
FASN - fatty acid synthase
FDA - food and drug administration
FIT - faecal immunohistochemistry testing
FUT – fucosyltransferase
FUT1 - fucosyltransferase-1
FUT2 – fucosyltransferase-2
FUT3 - fucosyltransferase-3
FUT4 - fucosyltransferase-4
FZD - frizzled
FZD3 - frizzled receptor 3
Gal - galactose
GalNAc - N-acetylgalactosamine
GALNT - N-acetylgalactosaminyltransferase
GALNT6 - N-acetylgalactosaminyltransferase 6
GB – glioblastoma
GC - gastric cancer
GCNT1 - glucosaminyl (N-acetyl) transferase 1
GlcNAc - N-acetylglucosamine
GO – Gene ontology
GSEA - Gene Set Enrichment Analysis
GSK3β - glycogen synthase kinase 3β
GSVA - gene set variation analysis
HDI - human development index
HNPCC - hereditary nonpolyposis colorectal cancer
HNSCC - head and neck squamous cell carcinoma
HR - hazard ratio
HRMS - High-resolution mass spectrum
IBD – inflammatory bowel disease
ICAM-1 - intercellular adhesion molecule-1

ICIs - immune checkpoint inhibitors
ICPs - immune checkpoint proteins
IF – Immunofluorescence
IgC_2 - constant set (C-set) domain
IgV - variable set (V-set) domain
IMRT - intensity-modulated radiation therapy
ITAM - immune receptor tyrosine-based activating motif
ITBCC - international tumour budding consensus conference
ITIM - immune receptor tyrosine-based inhibitory motif
KEGG - Kyoto Encyclopedia of Genes and Genomes
KM-plot - Kaplan-Meier plot
Kpnβ1 - karyopherin β1
KRAS - ki-ras2 Kirsten rat sarcoma viral oncogene homolog
LAG-3 - lymphocyte activating gene-3
LATS1 - large tumour suppressor kinase 1
LATS2 - large tumour suppressor kinase 2
lncRNA - long non-coding RNA
LPS – lipopolysaccharide
LRP5/6 - LDL receptor related protein 5 and protein 6
LSCC - lung squamous cell carcinoma
LUAD - lung adenocarcinoma
LUSC - lung squamous cell carcinoma
M-CSF - macrophage colony stimulating factor
MAG – Siglec-4
mCRC - metastatic CRC
MDM2 - MDM2 proto-oncogene
MDSC – myeloid derived suppressor cells
MFI – mean fluorescence intensity
MHC - major histocompatibility complexes
MiRNAs - MicroRNAs
MSI - microsatellite instability
MSI-H - high-microsatellite instability
MSS – microsatellite stable
MST1 - hippo kinase 1
MST2 - hippo kinase 2
MUC1 - mucin-1
NAT - adjacent normal colon tissue
NCAM - neuronal cell adhesion molecule
Necl-2 - nectin-like molecule 2
Neu5Ac - N-acetylneuraminic acid
Neu5Ac-P - N-acetylneuraminic acid phosphate
Neu5Gc - N-glycolylneuraminic acid
NF-κB - nuclear factor-kappa B
NICE - national institute for health and care excellence
NK cells – natural killer cells
NSCLC - non-small-cell lung cancer
OS - overall survival
OV - ovarian cancer
p21 - cyclin dependent kinase inhibitor 1A
PAI-1/SERPINE1 - plasminogen activator inhibitor-1

PBS – phosphate buffered saline
PD-1 - programmed cell death protein-1
PD-L1 - programmed death ligand-1
PDAC - pancreatic ductal adenocarcinoma
PDB - protein databank
PDX - patient derived xenografted
PFA – paraformaldehyde
PHYH - phytanoyl-CoA 2-hydroxylase
PI - propidium iodide
PI3K/AKT - phosphoinositide 3-kinase/protein kinase B
PLK1 - Ser/Thr mitotic kinase
PMA - phorbol-12-myristate-13-acetate
POU2F1 - POU class 2 homeobox transcription factor 1
PPI - protein-protein interactions
PPS - post-progression survival
Pri-miRNA – primary miRNA
PSA - polysialic acids
PSGL-1 - P-selectin glycoprotein ligand-1
PTTG1IP - pituitary tumour-transforming 1 protein interacting protein
RFS - relapse-free survival
RISC - RNA-induced silencing complex
RNF43 - ring finger protein 43
ROS - Reactive Oxygen Species
RT - room temperature
RT-qPCR - reverse transcription quantitative polymerase chain reaction
RXRB - retinoid X receptor β
SAFSNS - sulfonic acid functionalised silica nanospheres nano-catalyst
SAMPs - self-associated molecular patterns
SDGs - United Nations Sustainable Goals
SESN1 - sestrin 1
SFN – stratifin
Sfold - statistical folding of nucleic acids and studies of regulatory RNAs
SHIP - SH2 domain-containing inositol phosphatase
SHP-1 - Src homology region 2 domain-containing phosphatase-1
SHP-2 - Src homology region 2 domain-containing phosphatase-2
Sia – sialoglycan
Sialoadhesin – Siglec-1
Siglecs - sialic-acid binding immunoglobulin-like lectins
siRNA - silencing RNA
SNAIL - Zinc finger protein SNAI1
snoRNA - small nucleolar RNA
SOX2 - SRY-related HMG box 2
SPRR2D - small proline-rich protein 2D
SRCC - Spearman's rank correlation coefficient
sRNA-seq - small RNA-sequencing
ST3GalIV - ST3 β-galactoside α-2,3-sialyltransferase 4
ST6Gal1 – ST6 β-galactoside α-2,6-sialyltransferase 1
ST6GalNAc1 – ST6 α-N-acetylgalactosaminide α-2,6-sialyltransferase 1
ST6GalNAc2 – ST6 α-N-acetylgalactosaminide α-2,6-sialyltransferase 2
ST6GALNAC4 - ST6 α-N-acetylgalactosaminide α-2,6-sialyltransferase 4

ST8SIA5 - ST8 α-N-Acetyl-Neuraminide α-2,8-Sialyltransferase 5
STn – Sialyl-Tn antigen
STRING - Search Tool for the Retrieval of Interacting Genes/Proteins
Syk - spleen tyrosine kinase
TAMs - tumour associated macrophages
TAZ - PDZ-binding motif tafazzin
TCF/LEF1 - T cell factor/lymph enhancer factor 1
TCR - T-cell receptor
TGFβR1 and TGFβR2
TIGIT - T-cell immunoreceptor with Ig and ITIM domains
TLC - thin layer chromatography
TLR7/8 - toll-like receptor 7/8
TME - tumour microenvironment
TNBC – triple negative breast cancer
TNFR1 – tumour necrosis factor receptor 1
TNM - tumour node metastasis
TP53 - tumour protein p53
TPM - transcript per million
TRAIL - tumour necrosis factor-related apoptosis-inducing ligand
T_{regs} - regulatory T-cells
UC – ulcerative colitis
ULK1 - UNC-51-like kinase 1
UTR - untranslated region
V-set - variable set
WHO - World Health Organisation
XPC - XPC complex subunit, DNA damage recognition and repair factor
Xxylt1 - Xyloside Xylosyltransferase 1
YAP - yes-associated protein
ZEB2 - Zinc finger E-box-binding homeobox
ZNF16 - zinc finger protein 16
ZNF660 - zinc-finger protein 660

Chapter 1 - Siglec-15 mediated CRC progression

1.1 Introduction

1.1.1 Background overview of colorectal cancer malignancies

Colorectal cancer (CRC) is a malignancy that occurs through the differentiation and metastasis of normal epithelial mucosa to precursor lesions termed polyps (Øines et al., 2017). Within the epithelial lining of the colon/rectum, these lesions are categorised as adenomatous in nature or serrated and are concurrently classified based on growth patterns that are confirmed through histological examination (Li et al., 2021; Øines et al., 2017). Furthermore, the frequency of CRC development from these polyps is sporadic and can vary between patients among several criteria, including tumour localisation and metastasis, with colon adenocarcinomas constituting the majority of CRC cases, accounting for approximately 70% - 85% of all CRC diagnoses (Hong, 2018).

The most common pathway for CRC development is the canonical transition of benign adenomatous colon polyps to the pathophysiological characteristics of colorectal adenocarcinomas, which are associated with various somatic and germline mutations (Bien et al., 2019). Tumour development associated with this pathway utilises specific gene expression patterns relating to adenomatous polyposis coli (*APC*), ki-ras2 Kirsten rat sarcoma viral oncogene homolog (*KRAS*) and tumour protein p53 (*TP53*) in what is referred to as the Vogelstein model (Fearon & Vogelstein, 1990). As illustrated in figure 1, morphological advancement of the adenoma is induced by the deregulation of the *APC* gene, likely occurring through inactivation mutations/deletions. From this, cellular proliferation is sustained to generate adenocarcinomas which are driven by increased activity of oncogenes, including *KRAS* and the loss of function of *TP53* (Sameer, 2013). Consequently, over an extended period of time, tumour progression will result in metastasis to secondary organ sites, including the lungs and liver (Sameer, 2013).

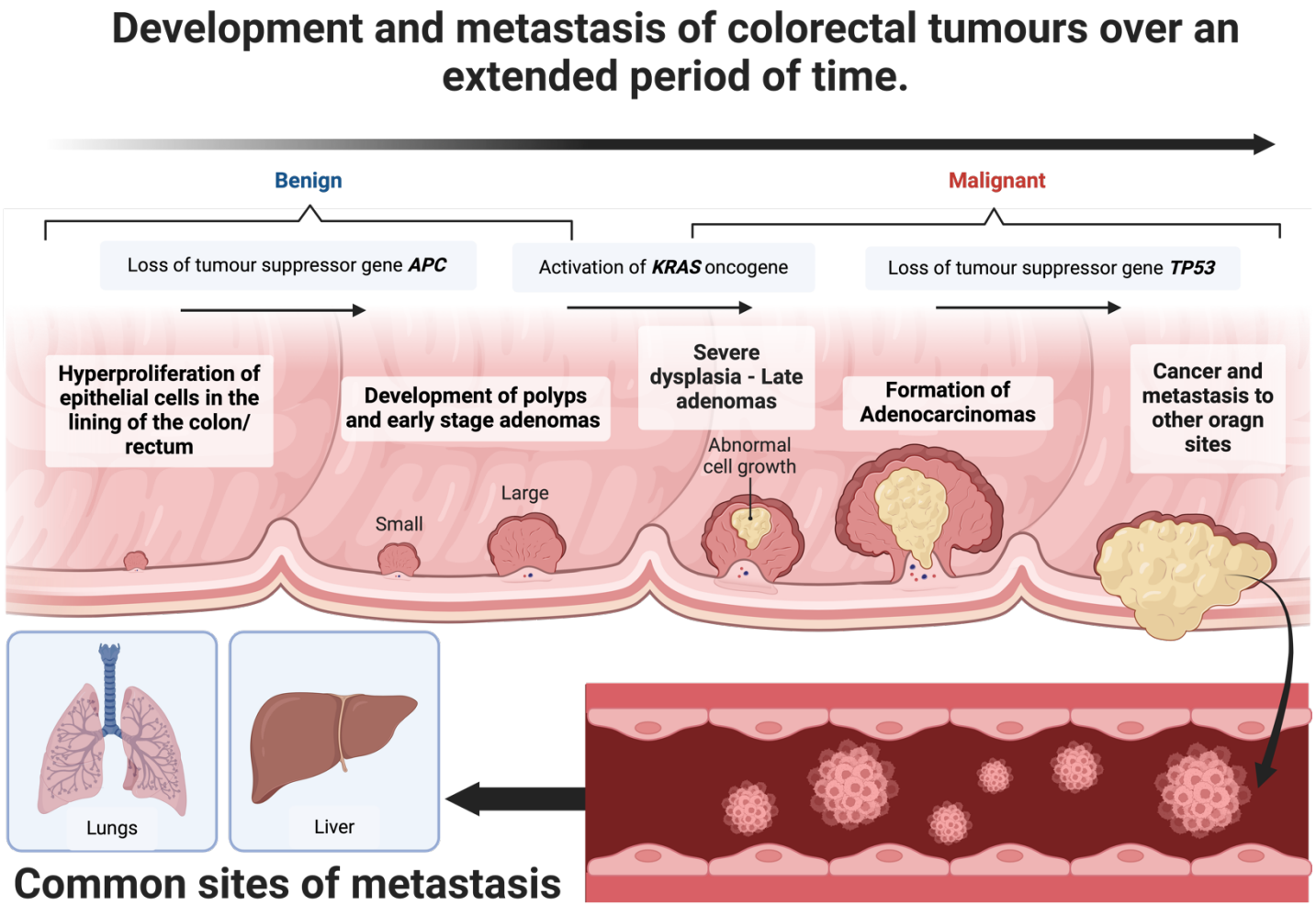

Figure 1: Vogelstein model of the multi-step canonical pathway of CRC tumorigenesis exhibiting the deregulated molecular alterations of adenomatous colon polyps. Within the normal epithelium, loss of function mutations in several tumour suppressor genes highlight the initial stages of tumour development, characterised by the generation of adenomatous colon polyps in the epithelial lining. Uncontrolled cellular proliferation and subsequent oncogenic mutations drive metastatic tumour growth resulting in metastasis and invasion to secondary organ sites [created with Biorender].

Alternatively, the non-canonical pathway for the development of CRC tumours occurs in approximately 10% - 25% of diagnoses via the traditional serrated pathway or serrated neoplasia pathway, which has only been recognised within the past couple of decades (Holme et al., 2015). As illustrated in figure 2, the serrated neoplasia pathway presents as a micro-vesicular hyperplastic polyp, which can progress to a sessile serrated adenoma and metastasise to microsatellite instability (MSI), or microsatellite stable (MSS) carcinomas based on genetic instability. Similarly, the traditional serrated pathway is depicted in which a goblet cell rich hyperplastic polyp can present as a traditional serrated adenoma transition to MSS carcinomas. A previous study highlighted that patients with serrated polyps develop CRC comparable to those with advanced adenomas (polyps >1cm in size) (Holme et al., 2015). However, tumours developed through this pathway possess distinct genetic characteristics not associated with adenomatous polyps (Leggett & Whitehall, 2010).

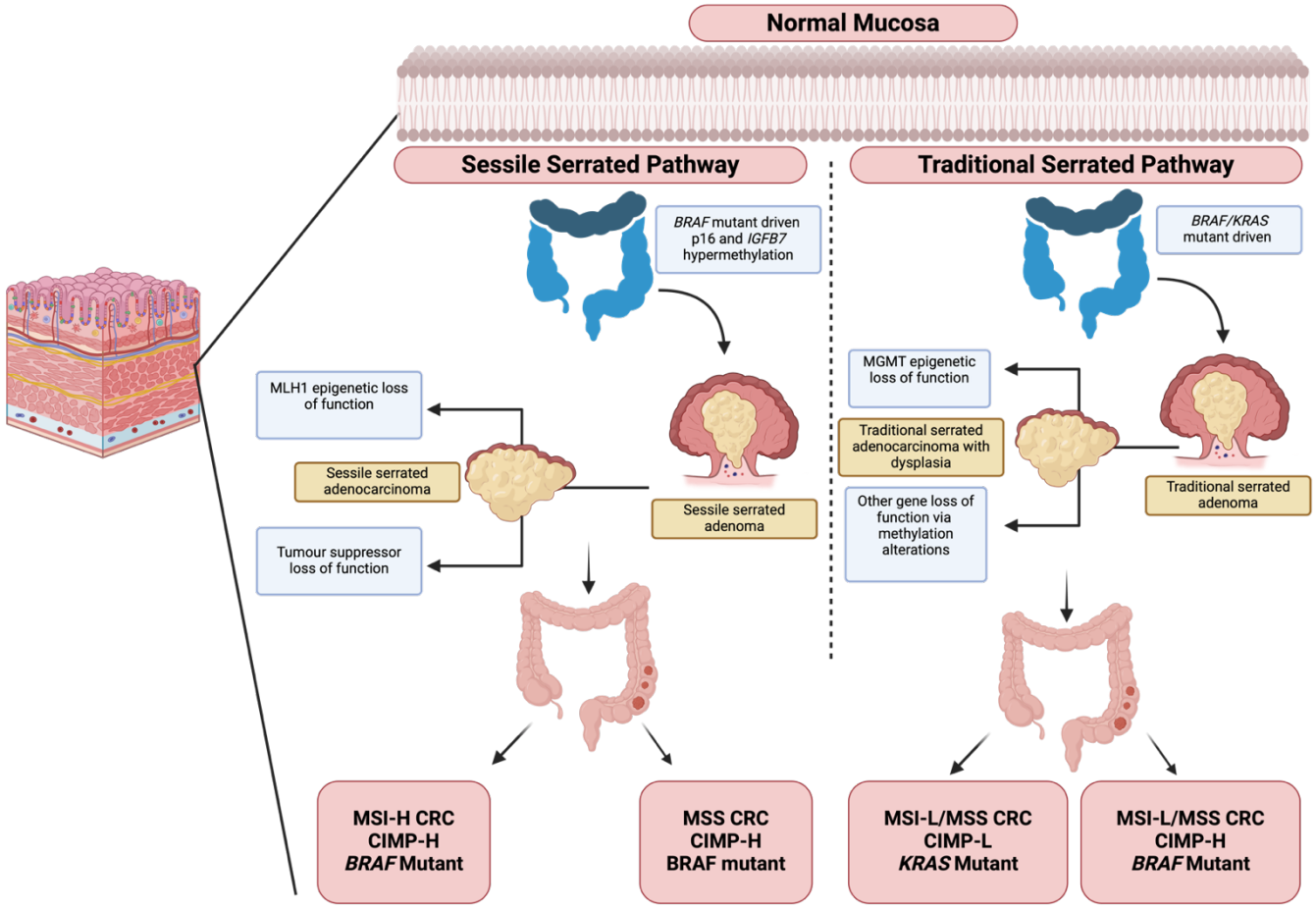

Figure 2: Non-canonical pathways of sessile serrated and traditional non-serrated neoplasia CRC development pathways. The sessile serrated neoplasia pathway is largely characterised by a high frequency of *BRAF* mutations and greater CpG island methylation. Hyperplastic polyps are outlined as initial lesions with extensive *KRAS* mutations; alongside the previously mentioned mutations, these polyps develop into sessile serrated adenomas or serrated lesions. Further genetic alterations of tumour suppressor genes and loss of function of *MLH1* transform these hyperplastic polyps into serrated adenocarcinomas. Conversely, the traditional non-serrated neoplasia pathway occurs more frequently and exhibits

greater *APC* mutations. Conventional adenomas are developed through a loss of function of *APC* and an increase in *KRAS* and *TP53* mutations. Significant accumulation of these mutations results in traditional adenocarcinoma development [created with BioRender].

The onset of CRC tumours can also be associated with other diseases, primarily presented in patients with colitis-related inflammation (Yashiro, 2014). Colitis-associated CRC can develop in patients with chronic inflammation and diagnosed with inflammatory bowel disease (IBD), including ulcerative colitis (UC) and Crohn's disease (CD) (Li et al., 2023). A meta-analysis study outlined CRC susceptibility significantly increased over a prolonged period of time by approximately 18% in UC patients (Eaden, 2004). Colitis-associated CRC shares a similar pathogenesis to sporadic CRC diagnoses, characterised by similar deregulation of oncogenes and tumour suppressor genes. However, differences in the molecular and clinicopathological features can outline distinct changes in tumour presentation (Huang et al., 2018).

Although the heterogeneity of CRC tumours exhibits irregular gene expression patterns that may not conform to a singular pathway, it is important to note that primary diagnosis for the onset of CRC stems from early identification and screening methods. Current screening methods employed in the UK comprise of the detection of blood in stool samples, and diagnosis is confirmed by faecal immunohistochemistry testing (FIT) and colonoscopy examination (Ladabaum et al., 2020). To determine a positive diagnosis, cases primarily adopt a quantification approach of faecal haemoglobin with a cut-off value of 150μg/g of blood, producing 70.8% sensitivity and 95.6% specificity (Jain et al., 2022). Furthermore, the predominant subtypes for the CRC phenotype are characterised by a handful of molecular alterations of diagnostic biomarkers at the gene level, which can determine diagnosis by biopsy extraction and analysis.

1.1.2 CRC molecular subtypes and TNM stage

Only a small percentage of cases have shown a genetic predisposition relating to familial history, with most cases stemming from sporadic mutations emphasising its tumour heterogeneity. Four distinct mechanistic pathways have been identified in CRC development and tumour progression (Figure 3), with each molecular subtype exhibiting unique clinicopathological characteristics (Bogaert & Prenen, 2014).

1.1.2.1 CRC molecular subtypes

The most common molecular subtype, also known as the chromosomal instability (CIN) pathway, is categorised by an abnormal chromosome number, the loss of heterozygosity of tumour suppressor genes and abnormal chromosomal rearrangement (Al-Sohaily et al., 2012; Valle et al., 2019). In addition, there are structural mutations in DNA mismatch repair (DMMR) genes, stimulating Wnt signalling, a main characteristic of CIN CRC tumours (Sullivan et al., 2022). The deregulation of Wnt signalling in CIN tumours poses as one of the earliest events in the development of adenomatous colon polyps (Guinney et al., 2015). A previous study demonstrated colonic/intestinal stem cell differentiation to adenoma morphology stemmed from the loss of function of *APC* and enhanced activity of Wnt signalling (Roper et al., 2017). Furthermore, common mutations that also resulted in the CIN molecular subtype included *PIK3CA, SMAD2 and SMAD4*, all of which are involved in the latter stages of adenoma-carcinoma development (Sullivan et al., 2022). The various genetic and epigenetic alterations at the gene level outline CRC heterogeneity. The CpG island methylation phenotype (CIMP pathway), associated with most of the CRC molecular subtypes, has shown an association with gene mutation and gene silencing of several genes, controlling the cell cycle and DNA mismatch repair (Deen et al., 2016). DNA hypermethylation of CpG islands, particularly in the promoter regions of genes, poses a critical hallmark of CRC tumorigenesis (Deng et al., 2020). Furthermore, the binding of a methyl group to cytosine residues of CpG dinucleotides prevents the binding of transcription factors to induce gene expression, leading to gene silencing at the transcriptional level (Joo, 2015). CpG island methylation is accentuated by the activity of BRAF proteins and the promoter silencing of DNA repair genes. One prominent gene involved in DNA mismatch repair includes *MLH1*; its deregulated expression profile typically displays a tumorigenic phenotype similar to CRC MSI tumours and is particularly observed in elderly CRC patients (Freitas et al., 2018). Further deregulation of the

CIMP pathway is also attributed to the enhanced activity of DNA methyltransferases driving hypermethylation of these promoter regions and reduced activity of DNA methylases, with loss of function preventing methyl group removal (Chen et al., 2021). Lastly, another recognised pathway involves high-microsatellite instability (MSI-H) tumours, characterised by a deficiency in DMMR genes *MLH1, MSH2, MSH6* and *PMS2* responsible for correcting base errors during DNA replication (Vilar & Gruber, 2010). These mutations typically occur via accumulated insertion/deletion mutations on several short DMMR sequences (microsatellites) with approximately >12 mutations per 10^6 bases, resulting in the CRC phenotype (Ozcan et al., 2018; The Cancer Genome Atlas Network, 2012). Characterisation of these mutations shows a genetic predisposition to hereditary nonpolyposis Colorectal cancer (HNPCC), referred to as Lynch syndrome (Umar et al., 2004). Furthermore, MSI-H tumours share contrasting clinicopathological characteristics compared to MSS tumours (tumours with minimal DMMR mutations). Development of MSI-H tumours also enhances the production of neoantigens (tumour-specific antigens) and may modify the characteristics of the tumour microenvironment, resulting in decreased efficacy of immune checkpoint inhibitors (Lin et al., 2020). Only a small subset of patients has shown positive response to immunotherapy treatment which may highlight difficulties in CRC treatment. Each of the CRC molecular subtypes serves as independent predictors for CRC tumour onset. Particularly, each of the molecular subtypes have exhibited pathophysiological hallmarks stimulated by greater instances of CIN, MSI and CIMP pathways, underlining greater treatment resistance in CRC patients (Harada & Morlote, 2020). However, elucidating the deregulation of potential therapeutic targets related to CRC progression may highlight possible treatment approaches (De Rosa et al., 2015).

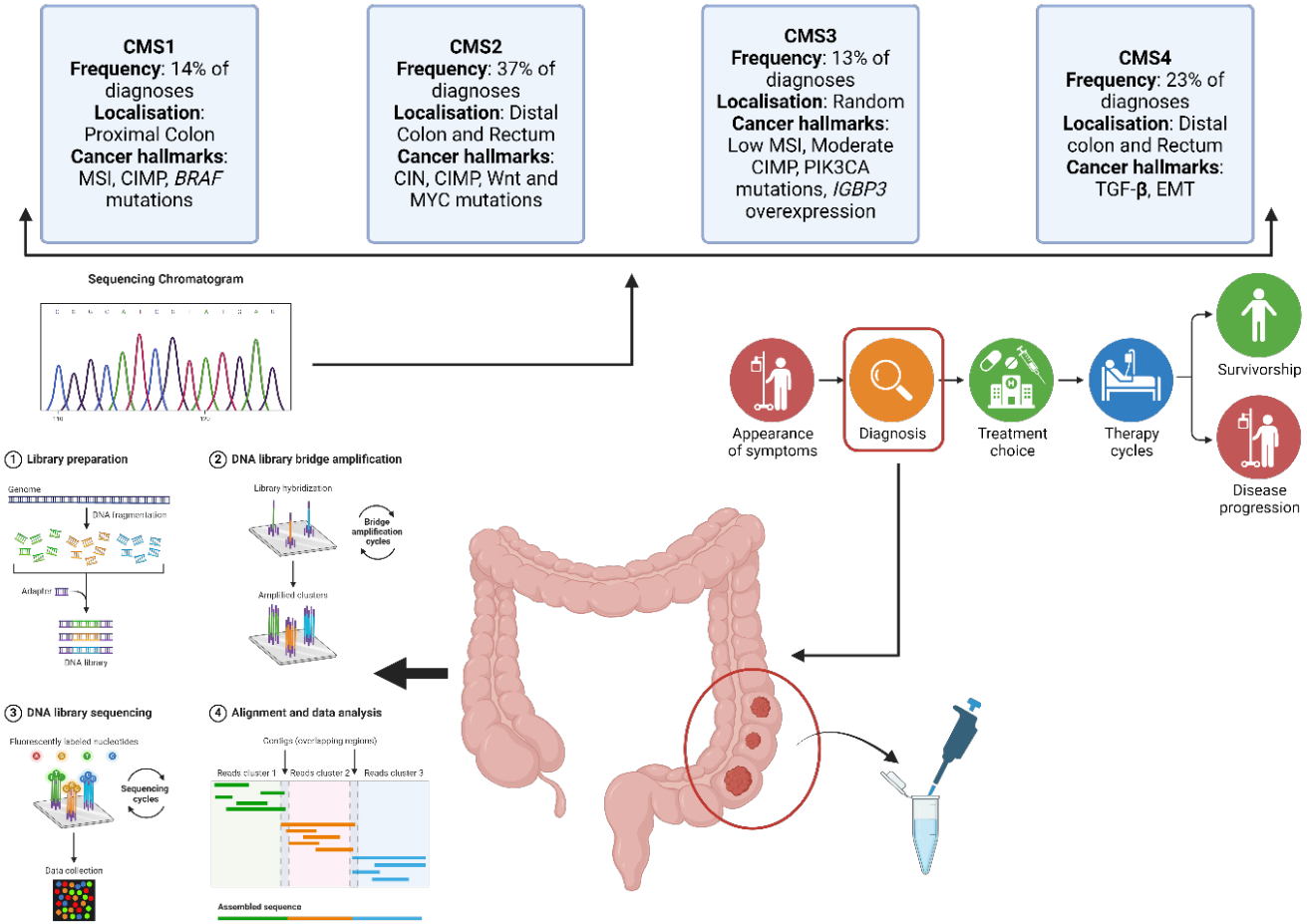

Figure 3: Genetic and epigenetic changes can promote molecular pathways, including chromosomal instability (CIN), CpG island methylation (CIMP) and microsatellite instability (MSI). To establish the diagnosis of a particular CRC subtype, sequencing analysis following a biopsy extraction categorises the tumour based on the following criteria, including cancer hallmarks and tumour localisation. Specific gene mutations also help in the identification of the tumour. CMS1 is classified as the immune subtype, and tumours are predominantly located in the proximal colon. The main hallmarks associated with CMS1 type tumours are typically high MSI and CIMP mutations and is driven by mutant BRAF. CMS2 classified tumours are the most frequent canonical tumours that occur in the distal colon and rectum. Alongside high CIMP

mutations, there is greater Wnt and MYC signalling that drive tumour progression. CMS3 classified tumours are metabolic type tumours that occur randomly. Although they appear less frequently, these tumours have greater KRAS mutations that drive tumorigenesis. CMS4 type tumours are more frequently observed within the distal colon and rectum and are associated with increased metastatic clinicopathological features including greater occurrence of EMT. This gives rise to the development of CRC and metastasis of colon tumours to secondary organ sites, including the lungs and liver [created with BioRender].

1.1.2.2 TNM staging and grading of CRC tumours

Conversely, tumour node metastasis (TNM) staging is used as a classification system for solid tumours and is utilised in determining the prognosis of CRC patients, following surgical resection of the tumour (Li, 2014). The T categorisation of the system involves the sizing of the primary tumour and is ranged from T1-T4, with increasing numbers indicating the greater invasion of tumour cells to nearby tissues. In addition, an X is denoted as a primary tumour that cannot be measured and a 0 is denoted as the inability to find/identify the primary tumour. Following this, the regional lymph nodes are subsequently classified (N). The lymph nodes are categorised from N1-N3 and refer to the number of lymph nodes which contain tumour cells and their localisation, respectively. Similar to the T categorisation, an X or 0 is also included in the N staging differential, which demonstrates the measuring of the lymph nodes containing cancer cells or if any lymph nodes possess tumour cells. In addition, the increase in N staging indicates a larger spread of the tumour to the lymph nodes. Lastly, the metastasis of solid tumours (M) is also categorised and classified as M0 or M1, which denotes whether the solid tumour is localised or metastasised to secondary tumour locations (Mahmoud, 2022). In addition, pathological features associated with CRC tumours, including molecular biomarkers associated with the molecular subtypes (Figure 3) and histological staining all determine tumour prognosis (Chen et al., 2021). At present, the histological grading scale for CRC tumours is provided by World Health Organisation (WHO) criteria (Ueno et al., 2012). From this, the histological grading of CRC tumours is dictated by the differentiation of normal epithelial cells to tumorigenic adenocarcinoma cells and is graded through stages I-IV. For CRC staging, stage I tumours are designated as early-stage tumours that are primarily localised to the epithelial wall of the colon/rectum and are without metastases in the lymph nodes. In comparison, stage II tumours are more defined but also lack lymph node metastases, similar to stage I tumours. Inversely, stage III tumours are more advanced and possess metastases within the lymph nodes. However, tumour invasion is limited, and tumours at secondary organ sites are rarely identified. Lastly, advanced stage IV tumours possess all the characteristics of the previous stage III but also exhibit metastases at secondary organ sites upon diagnosis, which are difficult to treat (Nagtegaal et al., 2020). As grade I tumours are more commonly associated with localised tumours within the colon/rectum, they also display a noticeable cellular pathology that closely resembles normal colonic mucosa (Iwama et al., 1993). In contrast, the higher-grade tumours are more prone to have aggressive characteristics associated with metastasis and tumour invasion (West et al., 2008). Thus, CRC patients exhibiting higher-grade

tumours (III-IV) have a poorer prognosis than lower grade CRC tumours. Furthermore, the increase in tumour grading is also characterised by poor differentiation and the lack of recognisability for standard epithelial morphology. However, standard tumour grading does not apply to rarer CRC histological subtypes, including signet ring cell, medullary, micropapillary and mucinous adenocarcinomas (Barresi et al., 2015). Conversely, tumour budding has been demonstrated as an independent prognostic marker for CRC tumours (Lugli et al., 2017). Tumour budding is primarily defined as a poorly differentiated cluster of tumour cells that are dissociated from the primary tumour that is involved in the initiation of invasion and metastasis of the tumour. In addition, tumour budding is also characterised by the international tumour budding consensus conference (ITBCC) criteria (Fujiyoshi et al., 2020). Although tumour budding may be found in several different malignancies, approximately 40% of CRC tumours have a greater proportion of tumour budding in advanced stage (III-IV) tumours (Zlobec et al., 2020). Histological staining of epithelial and mesenchymal markers such as cytokeratin and vimentin were co-expressed in a number of tumour buds, hinting tumour buds are able to adopt epithelial to mesenchymal transition (EMT) properties (Grigore et al., 2016). Ultimately, histological staining and other diagnostic tools pool together the staging/grade of the tumour to outline accurate patient diagnoses for determining treatment strategies with the best chance of success.

1.1.3 CRC epidemiology and mortality

With the most recent statistical data obtained from the WHO, CRC has been ranked as the fourth most prevalent tumour malignancy and ranks as the second most common cause of patient mortalities globally (Figure 4) (*Cancer Today*, n.d.). Furthermore, patient survival at both 5- and 10-years following diagnosis are estimated to be at 65% and 58%, respectively (Siegel et al., 2017, 2020). In 2020 alone, approximately 1,931,590 new cases were reported, leading to 935,137 patient deaths (Bray et al., 2018; *Cancer Today*, n.d.; Siegel et al., 2020). This rising trend in CRC incidence is projected to continue, with estimations suggesting that cancer-related deaths could reach a concerning 71.5% by 2035 and 3,200,000 new cases by 2040 (Siegel et al., 2020).

Moreover, CRC tumour burden has demonstrated significant variation based on geographical location. The developed countries such as Australia, the USA and regions in Europe, account for a large proportion of positive cases in comparison to low-income countries particularly

situated in Africa and Asia (Arnold et al., 2017). Furthermore, countries with the highest prevalence of CRC include Hungary, with 70.6 diagnoses per 100,000 of the population in men and Norway, with 29.3 diagnoses per 100,000 of the population in women, indicating variation amongst genders as well (Bray et al., 2018). However, external factors may affect the global incidence rate, as CRC diagnoses are concurrent with countries with a high human development index (HDI) typically associated with further developed countries (Rawla et al., 2019). This is greatly emphasised by disparities in the socioeconomic status of individuals and ethnic groups with poor clinical survival associated with low socioeconomic status (Coughlin, 2020).

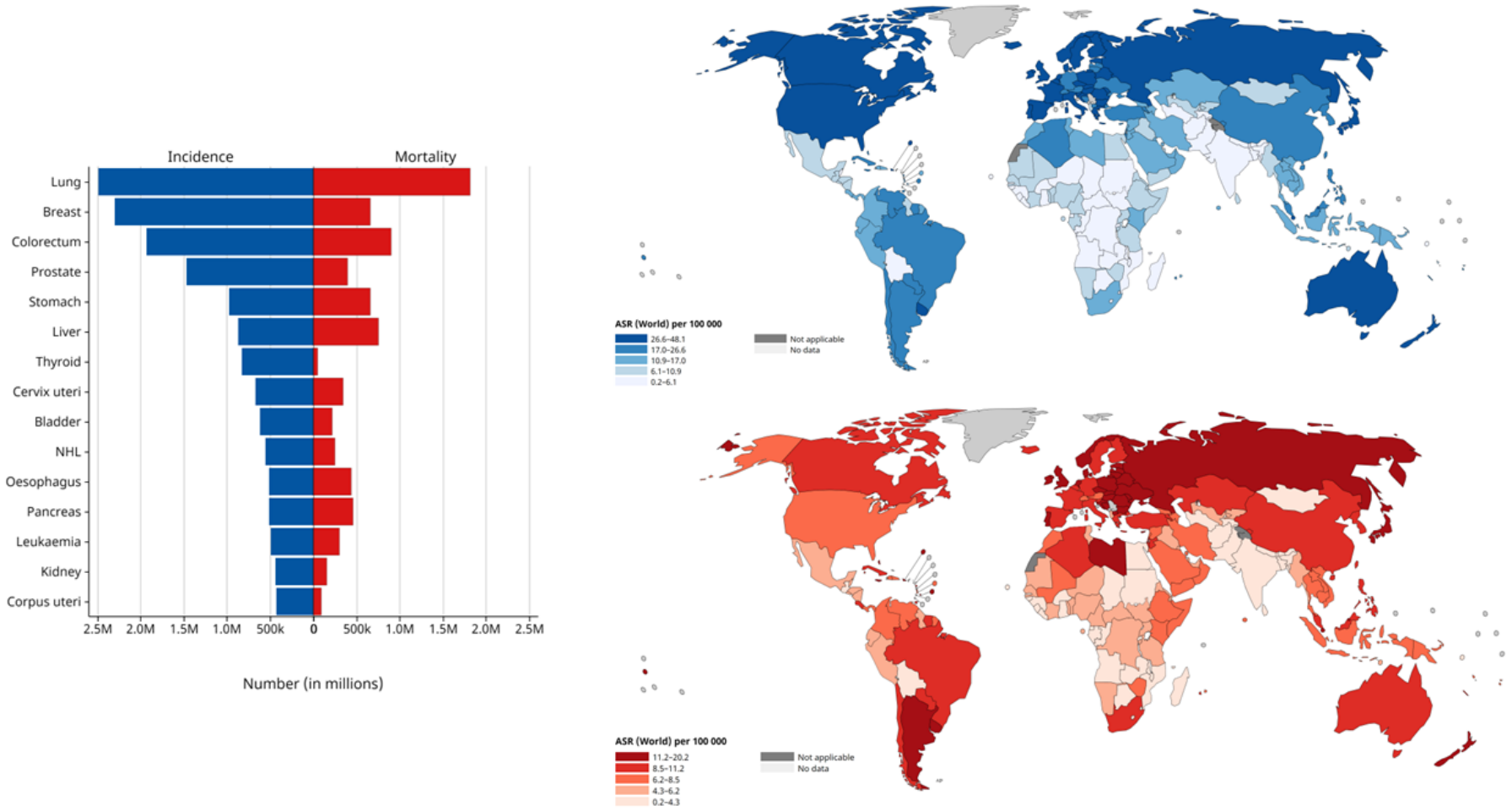

Figure 4: Absolute number of global incidence and mortality rates of the top 15 malignancies and age standardised rate (ASR) per 100,000 individuals of global incidence (blue) and mortality (red) of colorectal tumours in men and women obtained in 2022 [statistical data taken from the world health organisation (WHO)].

In addition, the economic development of undeveloped and developing countries as well as other external factors, are expected to correlate to the rising trend of CRC incidence. This may include changes in diet and lifestyle particularly relating to red and processed meats, excessive alcohol consumption and smoking as contributing factors for increased CRC susceptibility and tumour onset (Sawicki et al., 2021; Song et al., 2020; Vieira et al., 2017).

CRC prevalence has risen concurrently within older populations and presents more frequent diagnoses (Patel et al., 2013). However, the development of early-onset CRC (EO-CRC) (CRC diagnoses of patients <50yrs of age) represents a growing global concern. The prevalence of early-onset tumour diagnosis has exhibited a steadily rising trend, with an annual increase of 2% - 3% (Siegel et al., 2023). This has seen statistical numbers rise from 8.6 per 100,000 diagnoses in 1992 to 13.1 per 100,000 diagnoses in 2016 (Stoffel & Murphy, 2020). However, it is possible that this may be a result of reduced early screening in younger individuals (Venugopal & Carethers, 2022), and may not adequately reflect the identification of solid tumours. Moreover, CRC tumours themselves display significant heterogeneity within the tumour microenvironment (TME) and there is a greater importance to advance early screening and detection approaches to improve survival outcomes (Lam et al., 2021).

CRC mortality and morbidity highlight the interplay between the geographical variation disparities across individuals, gender and ethnic minorities. CRC presents a global challenge that necessitates greater importance to focus on the development of strategies related to prevention, screening, early detection, and therapeutic approaches to significantly improve patient clinical response and survival.

1.1.4 Current therapies in CRC treatment

Therapeutic interventions in CRC are pivotal in reducing tumour progression but also enhancing patient survival without the occurrence of remission. The integration of multiple treatment modalities, both adjuvant and neoadjuvant, has various effects on treatment outcomes. To date, a number of therapeutic approaches are available for the treatment of CRC tumours, and this is due to enhanced tumour heterogeneity and sporadic mutations that induce treatment resistance (Brandi, 2016). Moreover, CRC metastasis complicates the usage of adjuvant therapy and may not provide optimal response in patients, and this stems from both genetic and morphological changes between the primary tumour and secondary metastatic sites (Bedard et al., 2013). However, in low grade tumours (grade I-II), adjuvant chemotherapy approaches are more commonly used, demonstrating improvement in patient survival and response (Brandi, 2016). At initial stages of diagnosis, a large proportion of CRC patients have tumours that are localised to the colon/rectum, and according to the national institute for health and care excellence (NICE) guidelines, the first line of treatment is the surgical resection of the tumour (Van Cutsem et al., 2014).

1.1.4.1 Surgical methods in CRC treatment

Initially, surgical resection of CRC tumours is the first-line treatment for cancer patients with localised tumours (Van De Velde et al., 2014). Prior to a surgical procedure, a pre-operative assessment is also undertaken to consider a patient's suitability for surgery, including factors such as: patient's age, their fitness, post-surgical management plan, TNM stage of the tumour and the type of surgical procedure itself (Quirke et al., 2014). However, in more advanced CRC tumours, pre-operative neoadjuvant treatment such as chemotherapy or radiotherapy may be utilised to reduce the tumour size. Thus optimising the likelihood of a successful resection of the tumour (Breugom et al., 2014). The primary goal of surgical intervention in CRC treatment is the complete removal of the tumour with good margins to significantly improve the prognosis of the patient and reduce the occurrence of later remission. There are currently several methods that can be implemented in the treatment of CRC. Depending on tumour localisation within the colon/rectum, colectomy surgical procedures will be required to excise the tumour with the partial or complete removal of the colon (Chakedis & Schmidt, 2018). Additionally, laparoscopic surgery resections currently form the basis of primary CRC treatment. Due to the minimally invasive nature of the procedure, laparoscopic surgery

primarily involves the removal of tumours which are not overtly metastatic (Matsuda et al., 2018). Laparoscopic surgical methods reduce patient blood loss and complications in comparison to open surgery. Indications from several studies identified a higher efficiency using laparoscopic methods in CRC surgical treatment. However, laparoscopic surgical methods may prove difficult in executing due to factors including patient obesity, prior abdominal surgery and if the tumour is at an advanced stage and is overtly metastatic (Bonjer et al., 2015). Nevertheless, there are no apparent differences in short- and long-term outcomes of patients utilising either method (ElSherbiney et al., 2023; Fujii et al., 2016; Song et al., 2019). Furthermore, laparoscopic surgical methods provide better short-term survival outcomes in elderly patients diagnosed with common CRC tumours, which form the most at-risk groups (Zhou et al., 2019). Minimally invasive surgical procedures are being developed with novel techniques implemented to improve patient response to treatment. Possibilities to utilise trans-anal minimally invasive surgery for certain CRC tumours is one such approach that is currently under development to improve patient experience and survival (Zhou et al., 2022).

1.1.4.2 Chemotherapy approaches for solid CRC tumours

Following surgical interventions, common treatment methods include the use of adjuvant chemotherapies to prevent tumour recurrence (Figure 5), which has significantly higher beneficial outcomes in stage II and III CRC patients (Brown et al., 2019). Although there are several chemotherapeutic agents and inhibitors that are used, one of the first-line treatments used for CRC tumours is platinum-based chemotherapeutic agents such as Oxaliplatin. Similar to several platinum-based agents, Oxaliplatin is primarily used in the treatment of metastatic tumours. Its mechanism of action relies on dichloro-cyclohexane complexes exerting DNA damage, thus inhibiting DNA synthesis through cellular arrest (Alcindor & Beauger, 2011). However, due to CRC tumour heterogeneity, a number of other chemotherapeutic agents are also utilised alongside Oxaliplatin to prevent developmental resistance to treatment. Other chemotherapies that are typically used can involve the incorporation of 5-fluorouracil (5-FU) as part of adjuvant chemotherapy in stage II and III CRC tumours with expected 5-year survival rates of patients between 60% - 80% (Chan & Chee, 2019). 5-FU is structured as a heterocyclic aromatic uracil analogue with a fluorine atom that is located at the C5 position. The structure is highly similar to pyrimidines and can induce DNA damage once inserted into the DNA/RNA sequence (Blondy et al., 2020). 5-FU loaded gold nanoparticles were shown to enhance

apoptosis and reduce the proliferation of CRC cell lines when targeting EGFR proteins (Liszbinski et al., 2020). Similarly, 5-FU combination approaches with other chemotherapeutic agents demonstrated significant effectiveness in the treatment of CRC solid tumours (Xie et al., 2020). Other approaches can also utilise tipiracil as a viable chemotherapeutic agent. Mechanistically, tipiracil is an inhibitor of thymidine phosphorylase that is used in conjunction with trifluridine, a nucleoside analogue that inhibits DNA synthesis. The combination of both approaches was shown to have a positive clinical response in metastatic CRC patients who are resistant to 5-FU treatment (Kish & Uppal, 2016). Furthermore, adjuvant chemotherapies administered post-operatively are considered to improve 5-year survival and disease-free survival (Wu et al., 2012). However, the effectiveness of CRC chemotherapy treatments typically falls short. Patient response to treatment can become insignificant, and many patients develop chemoresistance towards 5-FU and other chemotherapeutic stratagems such as Oxaliplatin (Vodenkova et al., 2020). Other limitations include short half-life, high cellular toxicity and low bioavailability, all of which can reduce treatment efficacy for 5-FU based treatment regimens (Entezar-Almahdi et al., 2020).

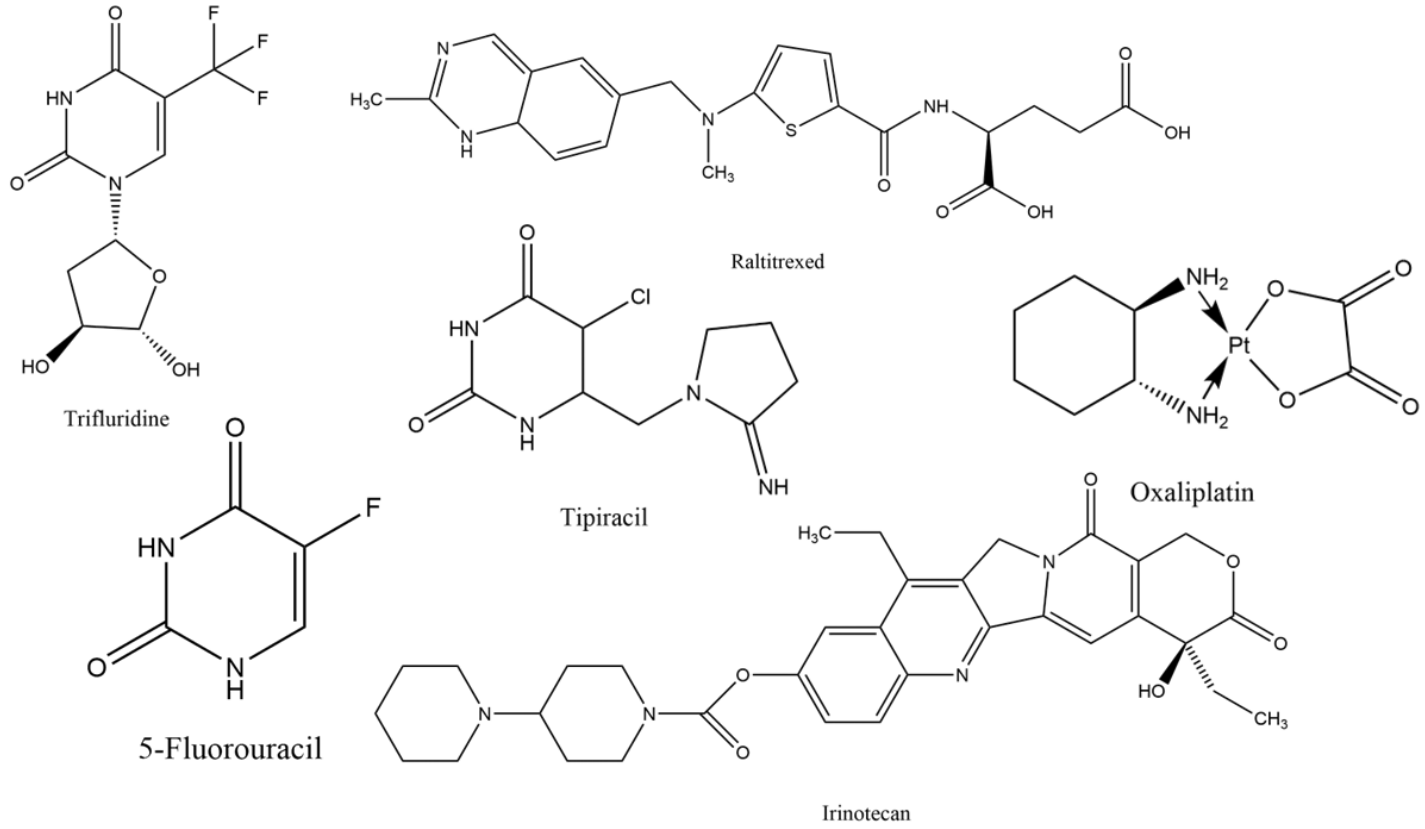

Figure 5: Chemical structures of several key chemotherapeutic agents utilised in the treatment of CRC tumours. Trifluoridine and Tipiracil are both used as a combination strategy for aggressive CRC tumours that have metastasised to secondary organ sites following poor response to primary chemotherapy treatment. Oxaliplatin is used as the first line treatment for CRC tumours following patients who have had surgical removal of the primary tumour. It is characterised by the ability to inhibit DNA synthesis; however, it presents a lot of off-target effects. Similarly, 5-FU administration is also commonly used in CRC treatment; however, is primarily used in a combination approach with other therapeutic agents due to a high level of recurrence and poor response rate to monotherapy. Irinotecan is primarily used for metastatic CRC tumours and is frequently used in conjunction with 5-FU and Oxaliplatin, which has demonstrated successful patient response and improved overall survival. Although not commonly used as compared to other chemotherapeutic agents mentioned, Raltitrexed is used as an alternative treatment approach to 5-FU in CRC

tumours with advanced tumour grade. Mechanistically, Raltitrexed inhibits the formation of precursor pyrimidine nucleotides by blocking thymidine synthase activity. Thus inhibiting the production of DNA/RNA molecules [created with Chemdraw].

1.1.4.3 Radiotherapy approaches for solid CRC tumours

Although used less frequently in early grade tumours, radiotherapy can also be employed as a treatment strategy for CRC patients. Selectively managing localised advanced stage tumours with stereotactic radiotherapy is predominantly used as a common treatment strategy (Häfner & Debus, 2016). The mechanism of action entails the exertion of ionising radiation disrupting DNA replication and transcription (Liu et al., 2021). On a molecular level, the interaction of radiation with H_2O molecules in cells causes the generation of free radicals affecting cellular components related to metabolism in a redox-mediated reaction (Liu et al., 2021). This method has been utilised with some success for various CRC tumours. Utilisation of stereotactic radiotherapy has been used in the treatment of lung metastases that originated from the primary localised CRC tumour (Jingu et al., 2018). However, treatment management of metastatic tumours originating from the colon is much more difficult to treat with radiation therapy and these tumours are more likely to become desensitised to treatment (Jingu et al., 2018). Application of stereotactic radiotherapy is more successful in managing tumours that are solely localised to the colon/rectum with significant patient response and low cytotoxic effects. However, this method typically highlights radio-resistance and reduced patient response following remission (Kobiela et al., 2018). Moreover, technological advances in the radiotherapeutic field have established techniques leading to more precise and targeted delivery of radiation, minimising cellular toxicity to surrounding healthy tissue. Another approach, intensity-modulated radiation therapy (IMRT), allows for the direct control of radiation beam intensity (Pointreau et al., 2022). Thus, this allows manageable distribution towards the whole tumour with good margins against healthy tissues, particularly against tumours surrounding internal organs including the small intestine and bladder (Pointreau et al., 2022).

1.1.4.4 Cancer immunotherapeutic treatments for solid CRC tumours

More recently, the use of novel immunotherapeutic agents has been suggested for translation to CRC immunotherapy treatment (Ganesh et al., 2019). Initially, the utilisation of immunotherapy approaches would boost/normalise the immune response in an immunosuppressive tumour environment (Esfahani et al., 2020). This approach requires the stimulated activation of T-cells, a group of lymphocytes that play a crucial role in active immunity against foreign pathogens and disease (Sun et al., 2023). In addition, T-cells are also broadly classified into $CD4^+$ helper and $CD8^+$ cytotoxic T-cells, and their function are dependent on their grouped classification (Hosokawa & Rothenberg, 2018). Mechanistically, T-cells are capable of recognising antigens expressed by major histocompatibility complexes (MHC) on neighbouring antigen presenting cells. Upon recognition of these antigens, binding commences between the antigen presenting cell and the T-cell via the T-cell receptor (TCR). Moreover, co-stimulatory molecules help facilitate the binding interactions. Furthermore, the release of cytokines stimulates the activation of naïve $CD4^+$ and $CD8^+$ lymphocytes, thus inducing a signalling cascade through clonal expansion and differentiation to their subsequent effector functions that regulate the immune response (Taniuchi, 2018; Teh et al., 1988). Following the activation of the immune response, a proportion of T-cells differentiate into memory T-cells, which provide the host with rapid effector function and lasting immunity against specifically recognised antigens. Conversely, a small group of $CD4^+$ lymphocytes differentiate into regulatory T-cells (T_{regs}) and maintain immune tolerance (Brugnera et al., 2000).

Current marketed immunotherapies such as Ipilimumab and Pembrolizumab target specific proteins that inhibit T-cell activation and are collectively known as immune checkpoint inhibitors. These inhibitors have targeted cytotoxic T-lymphocyte associated protein 4 (CTLA-4) and programmed cell death protein-1 (PD-1), demonstrating improved survival rates in melanoma and non-small-cell lung (NSCL) cancer patients, respectively, and in some cases in metastatic CRC (Ciardiello et al., 2019). Pembrolizumab promoted longer periods of progression-free survival in comparison to chemotherapy treatments for metastatic CRC patients (André et al., 2020). Adverse side effects of Pembrolizumab treatment were also shown to be reduced compared to chemotherapy treatments (André et al., 2020). Additional studies have begun to identify further novel immunotherapy treatments for metastatic DMMR-MSI CRC tumours (Lichtenstern et al., 2020). DMMR CRC solid tumours have currently

shown positive clinical responses to Nivolumab treatment, a PD-1 blocking antagonist, in phase II trials (Smith & Desai, 2018). Additionally, combination treatment strategies have proven beneficial in CRC treatment in comparison to mono-immunotherapy treatments. Atezolizumab, a programmed death ligand-1 (PD-L1) antagonist, was shown to have an effective patient response when combined with the MEK inhibitor Cobimetinib in DMMR CRC tumours (Tapia Rico & Price, 2018). Furthermore, the combination of Oxaliplatin and folinic acid achieved synergistic effects with 5-FU via nanoparticle co-delivery systems in CRC tumours with liver metastases. The mechanism of action induced immunogenic cell death and enhanced the activity of PD-L1 antagonists against liver metastases, therefore posing a substantial chemo-immunotherapy stratagem in metastatic CRC (Guo et al., 2020). Alternatively, bi-adjuvant neoantigen nano-vaccines utilising toll-like receptor-7/-8 (TLR7/8) agonists, proteins which participate in immune surveillance, were also developed for CRC treatment. They were observed to have a positive patient response and a complete regression of 70% of CRC tumours whilst demonstrating minimal systemic toxicity (Sun et al., 2022). With the premise of enhancing systemic immunity via modifications to $CD4^+$ and $CD8^+$ function, activation and proliferation, several pathways related to the immune function could potentiate an immune response and prevent cancer cell evasion (Bärenwaldt & Läubli, 2019). One such pathway that could benefit from this has been related to the Siglec/Sia axis, which has been associated with the inhibition of immune cell effectors (Bärenwaldt & Läubli, 2019).

Despite significant advancements in current treatment modalities, a notable number of patients continue to progress to high grade solid tumours and metastases (Costi, 2014). Thus, there is a shift in treatment interventions towards palliative care to improve the current quality of life. With more of a focus on pain management, there is reduced hospitalisation and enhanced decision-making, improving patient satisfaction and prognostic awareness (Bischoff et al., 2020).

1.1.5 Siglecs and immune checkpoint proteins

Unfortunately, conventional treatment modalities for CRC have limitations in achieving therapeutic success. Poor patient response, severe dose-limiting side effects and a lack of specificity of conventional treatments contribute to patient mortality and tumour recurrence (Weng et al., 2022). For instance, the effectiveness of immunotherapy is restricted to a limited number of patients, with the emergence of acquired treatment resistance being a concerning possibility (Weng et al., 2022). Consequently, exploring novel approaches and developing innovative treatment strategies are essential for effectively addressing this unmet medical need.

The identification of novel targets in immunotherapy treatment has shown positive responses in patients via the targeting of immune checkpoint proteins (ICPs). ICPs are a broad umbrella term for a classification of cell surface immunoreceptors that modulate the immune system against disease (Gaikwad et al., 2022). Within a tumour landscape, ICPs are expressed on the surface of cancer cells, functioning as protein receptor-ligands, preventing sufficient T-cell activation and immune response generation. As a result, this provides cancer cells to effectively evade the immune system and promote tumour progression. There have been several ICPs involved in tumour progression, including CTLA-4, PD-1, PD-L1, T-cell immunoreceptor with Ig and ITIM domains (TIGIT) and lymphocyte activating gene-3 (LAG-3). However, targeting immune checkpoint proteins with immune checkpoint inhibitors (ICIs) can only demonstrate a positive response in a small subset of cancer patients, highlighting the lack of targetable biomarkers (Tang et al., 2022).

One recently emerging immune checkpoint protein family are sialic-acid binding immunoglobulin-like lectins (Siglecs). Currently, a total of 15 human and 9 murine Siglecs have been identified and categorised into distinct groups based on homology between structure and function (Figure 6). Of those categorised, Siglec-1 (Sialoadhesin), Siglec-2 (CD22), Siglec-4 (myelin-associated glycoprotein; MAG) and Siglec-15 share 50-99% structural and functional homology (Duan & Paulson, 2020; Appendix 1). In contrast, the remaining Siglecs possess structural heterogeneity due to evolutionary duplication events of the CD33 gene and are collectively known as CD33-related Siglecs (Von Gunten & Bochner, 2008). Siglecs are type-I transmembrane proteins that comprise several distinct extracellular structural domains, a single intracellular domain and a transmembrane region (Jiang et al., 2022, Figure 6). In addition to this, each Siglec protein can possess a V-set binding domain located on the N-

terminus and serves as the primary region for sialoglycan ligand binding (Macauley et al., 2014). Direct contact and binding with the sialoglycan ligand rely on a conserved arginine residue on the V-set domain, forming a salt bridge with the respective sialoglycan carboxylate group (Von Gunten & Bochner, 2008). The tertiary structure of each Siglec member contains a cytoplasmic tyrosine residue intracellular motif that dictates Siglec function. They are commonly referred to as immune receptor tyrosine-based inhibitory motif (ITIM) or tyrosine-based activating motif (ITAM) that determine whether the Siglec protein is inhibitory or activating in nature (Jiang et al., 2022). Inhibitory Siglecs possessing an ITIM motif excluding Siglec-15 recruit tyrosine Src homology region 2 domain-containing phosphatase-1 (SHP-1) and Src homology region 2 domain-containing phosphatase-2 (SHP-2) for canonical downstream signalling related to inhibiting immune function (Crocker et al., 2007; Flores et al., 2019). Moreover, SH2 domain-containing inositol phosphatase (SHIP) enzymes also possess a similar function in Siglec binding via induced phosphatase recruitment upon partial ITAM binding (Dempke et al., 2018). However, there is an exception with one Siglec family member, primarily known as Siglec-XII. Siglec-XII is one of the most understudied Siglec family members that are unconventional due to an observed frameshift mutation (R122C) that removes the conserved arginine residues required for sialoglycan binding (Mitra et al., 2011). Nevertheless, Siglec-XII still possesses an intracellular ITIM motif capable of SHP-1/SHP-2 phosphorylation and downstream signalling (Lim et al., 2021; Mitra et al., 2011). Siglec-XII was capable of inhibitory signalling and tumour progression, which also correlated to poor clinical survival and advanced TNM stage (Siddiqui et al., 2021).

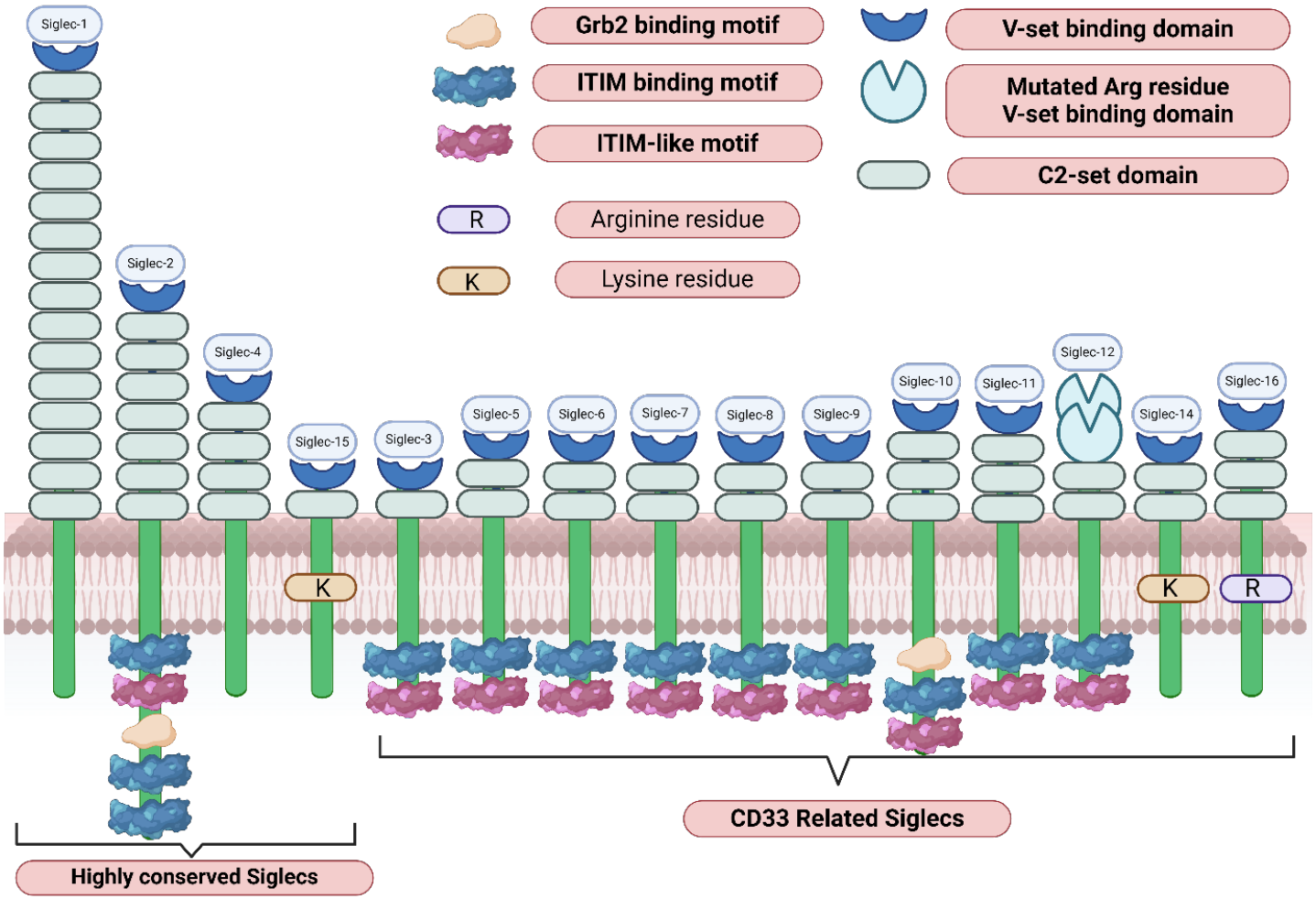

Figure 6: Siglec human family containing conserved and CD33-related non-conserved protein structures. The Siglec family comprises of a total of 15 human Siglecs that have been discovered. Only Siglec-1, Siglec-2, Siglec-3 and Siglec-15 share high conservation among their sequences. In contrast, the other Siglecs possess little similarities in their structural sequence [created with BioRender].

Siglec expression profiles in a subset of myeloid populations are heterogenous and were first characterised by the identification of Sialoadhesin (Crocker & Gordon, 1986). Furthermore, later experimental work also highlighted preferential interactions with sialoglycans, emphasising receptor ligand interactions and outlining possible heterogeneity in sialoglycan ligands (Crocker et al., 1991). With certain exceptions, the expression of Siglecs in the tumour landscape is immune cell specific and outlines the multifaceted roles in the regulation of the immune system (Siddiqui, 2023). For example, the expression of Sialoadhesin is characterised on the surface of macrophages, with a critical role in antigen recognition and is utilised as a monocytic differentiation marker (Duan & Paulson, 2020; Liu et al., 2020). Similarly in the tumour landscape, Sialoadhesin^{+} macrophages were involved in regulating immunosuppression in triple negative breast cancer (TNBC) (Jing et al., 2020).

Several Siglec family members demonstrate immune-specific expression across multiple cell types including B-cells, myeloid progenitor cells, mast cells, oligodendrocytes, T-cells, monocytes and neutrophils (Büll et al., 2021). As mentioned above, the intracellular motif denotes Siglec function and inhibitory Siglec proteins are largely correlated with immunosuppression that prevents the activation of neighbouring immune cells. Thus, enabling tumour cells to evade the immune system (Chen et al., 2018; Zheng et al., 2020). Many of the inhibitory Siglec proteins including Siglec-7 and Siglec-9, have upregulated expression profiles in multiple cancer types and have been implicated in tumour development (Stanczak et al., 2022). Siglec-15 is also implicated in multiple cancer types; the immune checkpoint protein that will be the focus of this PhD project is typically expressed on the surface of cancer cells and facilitates tumour progression (Angata et al., 2007).

1.1.6 The role of Siglec-15 in cancer

Siglec-15 is a recently emerging checkpoint protein that plays a role in suppressing the immune system and is capable of promoting cancer progression (Figure 7) (Wang et al., 2019). Whilst the expression of Siglec-15 was first identified in osteoclasts, Siglec-15 expression is predominantly on the surface of myeloid cells (Angata et al., 2007; Pan et al., 2020), and commonly overexpressed in various cell types, including TAMs in the TME and on the surface of cancer cells.

Osteoclasts are commonly regarded as bone resorption cells that play a crucial role in skeletal development and are characterised by their function as effector cells in bone remodelling (Kobayashi et al., 2024). During bone remodelling, osteoblasts can trigger osteoclast differentiation which is mediated by the nuclear factor-kappa B (NF-κB) (RANK) signalling pathway through RANKL ligand binding (Suda et al., 1999). Induction of RANK signalling can stimulate the activation of NFAT2, a transcription factor that mediates *SIGLEC15* expression (Ishida-Kitagawa et al., 2012). Osteoclast precursor molecules that express RANK recognise and internalise RANKL, which induces osteoclast differentiation and maturation through DAP12 and/or FcRγ adapter proteins in the presence of macrophage colony stimulating factor (M-CSF) (Angata, 2020; Huang et al., 2023). The involvement of Siglec-15 in this pathway has demonstrated the expression of Siglec-15 on bone giant tumour cells, which morphologically resemble osteoclasts (Hiruma et al., 2011). Upregulated Siglec-15 expression plays a role in osteoclast differentiation and cellular fusion upon binding with its V-set binding domain (Kameda et al., 2013). Through its binding, Siglec-15 increased the phosphorylation of ERK/AKT and PI3K which are downstream targets of the RANK signalling pathway (Kameda et al., 2013; Stuible et al., 2014). This suggested that Siglec-15 is a potential target for therapeutic strategies for osteoclast-mediated diseases such as osteoporosis (Angata, 2020).

Siglec-15 is a conserved member of the Siglec family and shares homology with sialoadhesin (Siglec-1), CD22 (Siglec-2) and myelin-associated glycoprotein (MAG; Siglec-4) (Angata et al., 2007). Furthermore, the *SIGLEC15* gene is located on 18q12.3 and contains two exons, unlike most other *SIGLEC* genes (Angata et al., 2007). One of the exons responsible for transcribing the second Ig-like domain can also encode the transmembrane domain. This can differ from many other Siglecs, which emphasise the encoding of the transmembrane region from separate exons (Angata et al., 2007; Von Gunten & Bochner, 2008). From a structural

view, the extracellular domain is composed of a variable set (V-set) domain (IgV) containing a binding pocket essential for sialoglycan ligand binding and one constant set (C-set) domain (IgC_2) (Von Gunten & Bochner, 2008). A notable difference in the Siglec-15 structure is the presence of an intracellular ITAM motif in place of an intracellular ITIM motif. This change in motif facilitated interactions with neighbouring 12 kDa DNAX-activating protein-12 (DAP12) for immunoregulation against infections and pathological diseases (Ali et al., 2014; Büll et al., 2016). It is well known that Siglecs are involved in the recognition and binding of sialylated glycans. In the case of Siglec-15, there is preferential recognition for α2,6 sialylated glycan structures (Neu5Ac α2,6 GalNAc) such as the STn antigen, the putative ligand of Siglec-15 (Huang et al., 2023). Other sialylated glycans on T-cells have also been proposed, including MUC5B, CD11b, CD18 and CD44, although the latter is more commonly associated as a ligand on RAW264.7-derived osteoclasts (Boelaars & Van Kooyk, 2024). Mechanistically, recognition and engagement of the STn antigen is via direct salt bridge formation with R143 (R, Arginine). From this, initiation of the signalling pathway is mediated by a transmembrane K274 (K-Lysine) residue interaction with DAP10/DAP12 adaptor proteins facilitating downstream recruitment of spleen tyrosine kinase (Syk) (Ishida-Kitagawa et al., 2012).

Within the tumour landscape, Siglec-15 can inactivate the T-cell response and immune activation via the binding with the STn antigen, its canonical ligand via the R143 residue and salt bridge formation (Crocker et al., 2007). The Siglec-15/sialic acid (Sia) axis is outlined as a regulatory pathway for immune function that enables tolerance to the body's own cells (Läubli et al., 2022). Although Siglec-15 has a high binding affinity for the STn antigen, post-translational modifications, including N-glycosylation, can effectively resolve its immunosuppressive capabilities. One study highlighted potential N-glycosylation modification deficiency, particularly on the N172 residue, which was vital for Siglec-15 function, reduced tumour progression in murine models (Wang et al., 2021). Similarly, a recent study identified the crystal structure of the Siglec-15 V-set binding domain demonstrated effective binding with the STn antigen alongside α2,3- and α2,6-linked sialoglycans in association with its CD11b binding partner (Lenza et al., 2023). The repercussions of these Siglec-15/Sia interactions can result in immunosuppression and immune evasion (Gianchecchi et al., 2021).

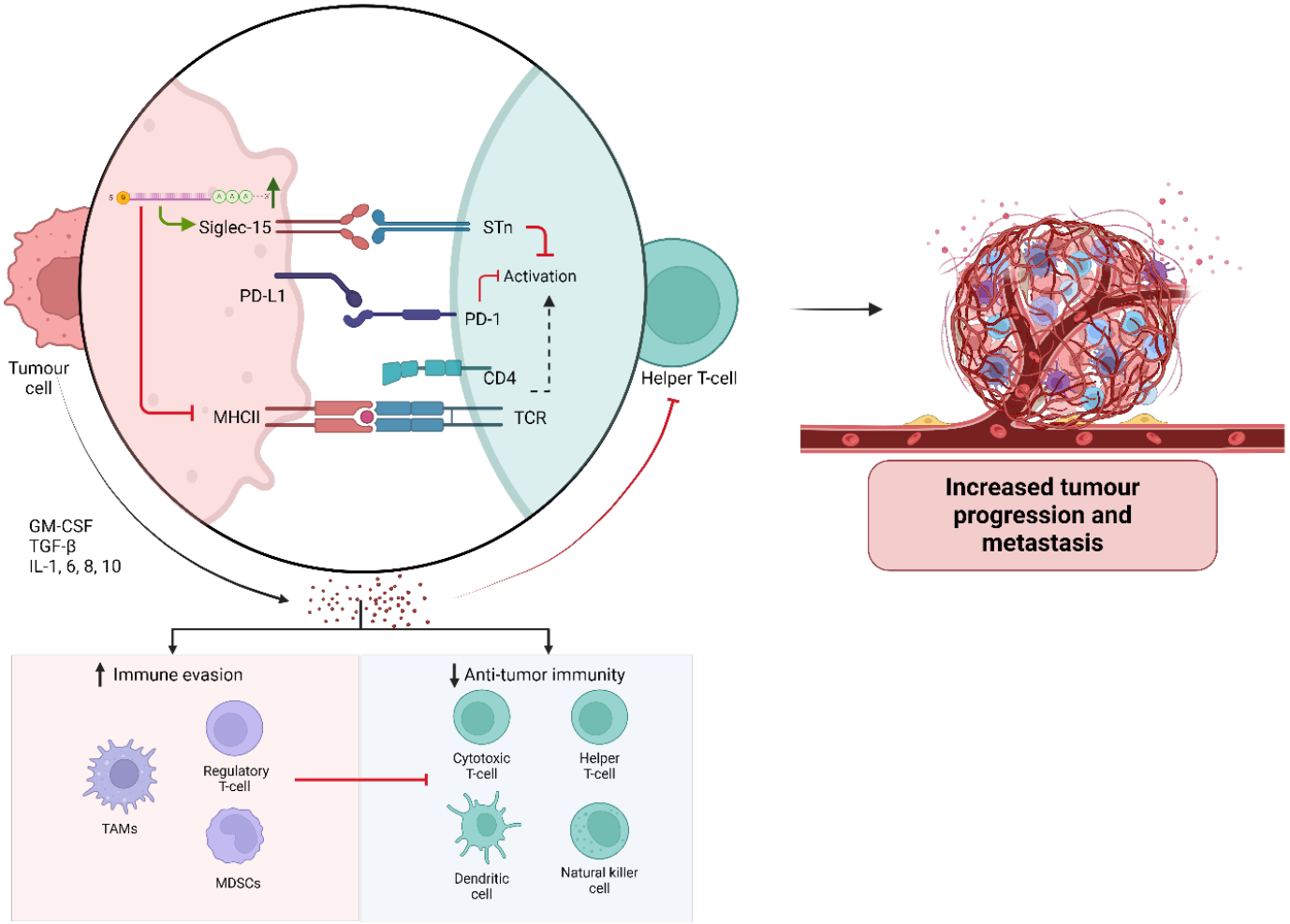

Figure 7: Increased interactions of Siglec-15/Sia binding within the TME, consequently resulting in immunosuppression. Following initial T-cell receptor binding with tumour cells**,** inhibitory Siglec molecules such as Siglec-15 prevent T-cell activation upon engagement with the STn antigen causing immune evasion of cancer cells. Simultaneously, the interactions of the Siglec-15 with STn induce polarisation of macrophages to the M2 tumorigenic phenotype, induce T_{reg} activity and stimulate myeloid derived suppressor cells (MDSCs) to promote cancer progression (Bärenwaldt & Läubli, 2019) [created with BioRender].

1.1.6.1 Siglec-15 interactions in the tumour microenvironment

The overexpression of Siglec-15 has been observed in multiple cancers, such as CRC, NSCLC, lung squamous cell carcinoma (LSCC), head and neck squamous cell carcinoma (HNSCC), ovarian cancer (OV), etc. (Li et al., 2020; Liang et al., 2022; Van Houtum et al., 2021). It is also important to note that high Siglec-15 expression has also been associated with MSI-H type tumours in CRC patients (Du et al., 2021), suggesting the involvement of deregulated Siglec-15 expression in CRC tumour progression. Previous studies have also highlighted the interplay of interleukins and cytokines on Siglec-15 expression particularly in the M2 polarised tumorigenic macrophage phenotype, thus promoting tumour onset and progression (Stanczak et al., 2022, Figure 8). Furthermore, downstream signalling via SYK and DUSP1 emphasises significant inhibitory signalling and vastly enhances TME immunosuppression (Büll et al., 2021; Fan et al., 2021; Wang et al., 2019). Moreover, transcriptomics analysis of Siglec-15 in pre-metastatic CRC sentinel lymph nodes identified *SIGLEC15* as one of the most significantly upregulated genes and was also associated with enriched signalling pathways associated with cellular proliferation, including MYC signalling and the G2/M phase checkpoint (Du et al., 2021). Under matched conditions with non-sentinel lymph nodes, immune function signalling was also enriched, including TGF-β signalling and TNF-α/NF-κB signalling, both of which drive tumour progression when deregulated (Du et al., 2021). However, literature evidence of Siglec-15 functional activity in CRC remains limited and highlights potential investigation.

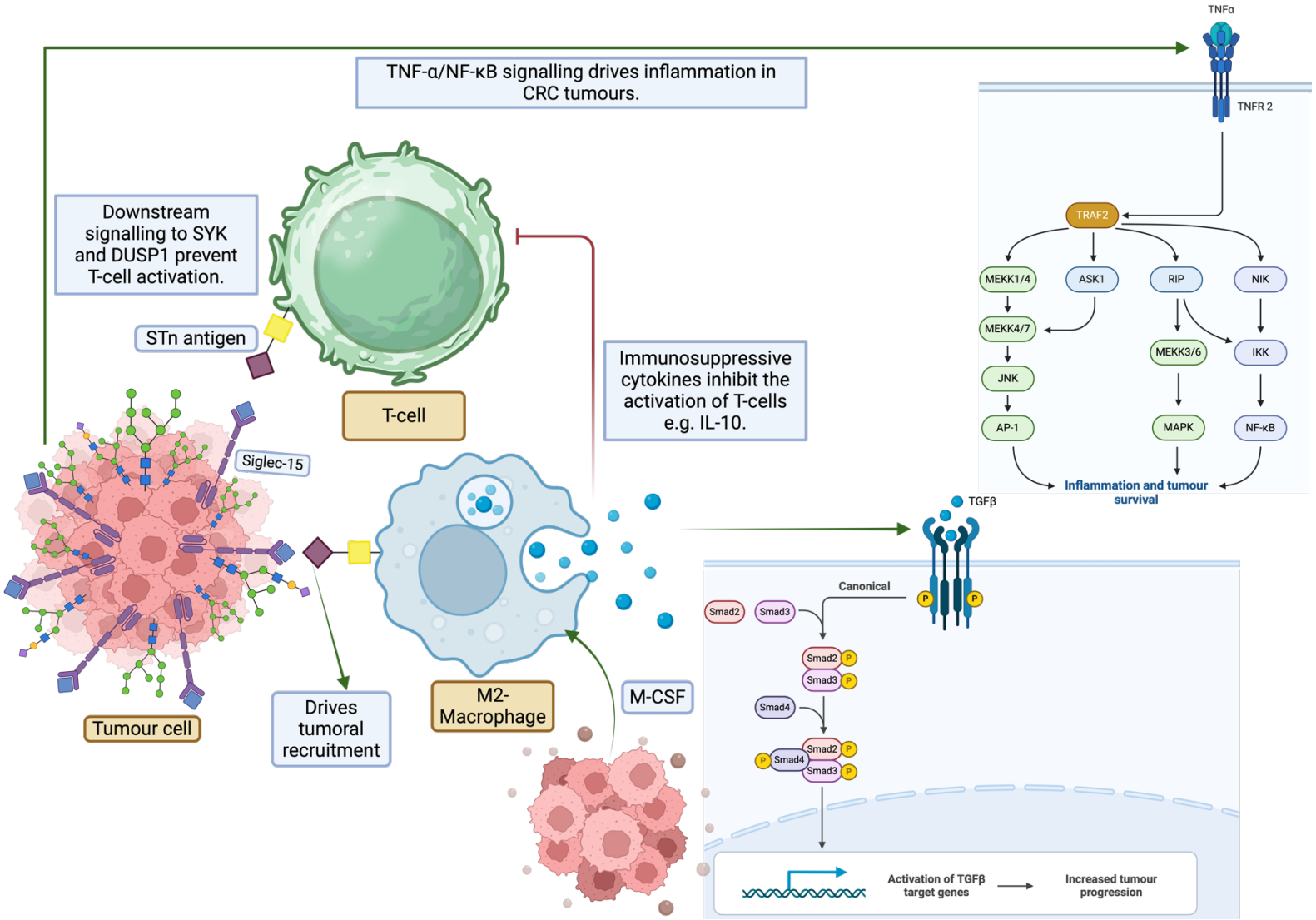

Figure 8: Siglec-15 interactions in the TME drives oncogenic signalling. Downstream signalling following the engagement with the STn antigen drive tumoral recruitment of M2 polarised macrophages which stimulate signalling pathways related to tumour progression and

inflammation. M2 polarised macrophages also stimulate the release of immunosuppressive cytokines which dampens the immune response [created with Biorender].

Additionally, it is important to note that Siglec-15, in conjunction with the immune checkpoint protein PD-L1, exhibits mutually exclusive expression profiles on tumour cells (Fudaba et al., 2021). One recent study identified greater Siglec-15 expression was present in 48.3% of tumour cells and 33.4% of tumour-associated stromal cells in contrast to PD-L1 expression via immunohistochemistry analysis (Lu et al., 2023). Furthermore, Siglec-15 expression correlated to advanced TNM stage and poor immune infiltration (Lu et al., 2023). By inhibiting the expression of one immune checkpoint protein via therapeutic intervention, the presence of the remaining immune checkpoint presents the possibility of rescuing the cancer phenotype. Dual targeting of both immune checkpoint proteins utilising both Siglec-15 and PD-L1 antagonists may present a possible approach as a treatment alternative to current immunotherapy treatment strategies. Prior Siglec-15 targeting approaches have been established particularly through the usage of monoclonal blocking antibodies in the treatment of solid tumours. The monoclonal blocking antibody NC318 (NCT03665285) has been clinically developed to target Siglec-15 expression in Siglec-15^{+} tumours, providing a potential therapeutic approach (Gutierrez et al., 2020; Shum et al., 2021). In addition to this, Siglec-15 has been found to be negatively associated with immunomodulatory drug response, tumour-infiltrating immune cells, and cancer immunity cycles in various cancer types (Hu et al., 2021). It has also been linked to hyper-progression and non-sensitivity to immunotherapy (Hu et al., 2021). Therefore, the development of alternative treatment approaches for Siglec-15 targeting, such as small molecule inhibitors, will allow for better tumour penetration and subsequent inhibition of cancer progression. Our investigation of small molecule inhibitors highlighted the synthesis and cytotoxic evaluation of an organic β-amino carbonyl compound (3-(4-bromophenyl)-1-phenyl-3-(phenylamino)propan-1-one) for Siglec-15 targeting (Ahmad et al., 2023).

More specifically, Siglec-15 is the only Siglec family member that is expressed on the surface of tumour cells (Wang et al., 2024). Although Siglec-15 shares similarities with other Siglec members, a key research question arises. Is there a redundancy mechanism that can rescue the tumour phenotype following the inhibition of Siglec-15?

From the current literature, Siglec-15's expression profile appears highly distinct in contrast to other Siglec proteins, particularly in cell type, their immune signalling pathways and the interactions with neighbouring myeloid cells (Cao et al., 2019). Thus, it is indicated from the literature that Siglec-15 loss of function cannot be fully compensated by other Siglecs. However, the role of PD-L1 may underline possibilities in rescuing the tumour phenotype due

to similar functional roles (Huang et al., 2023). It is the hope that a transition to combination therapeutic approaches will share synergistic effects and simultaneously inhibit both PD-L1 and Siglec-15. Moreover, the role of Siglec-15 in Siglec-15^{+} CRC tumours remains poorly understood. Hence further characterising Siglec-15's oncogenic role in cellular signalling and its subsequent inhibition through therapeutic alternatives is suggested to provide further insights to immune checkpoint blockade approaches.

There is a large amount of evidence within the literature underlining role of Siglec-15 mediated tumour development and poor clinical outcomes in cancer patients. Siglec-15 is portrayed as a valuable diagnostic and prognostic biomarker in the tumour landscape; thus, it will prove beneficial as a therapeutic target in treatment approaches. Moreover, there have been several instances of therapeutic approaches employed in blocking the Siglec-15/Sia axis. Blocking antibodies such as NC318 are in clinical trials (Ding et al., 2023), whilst another blocking antibody, 1-15D1 has shown significant binding to Siglec-15 and enhanced the T-cell response *in vitro* (Wu et al., 2023). Similarly, the utilisation of directed protein aptamers in immune checkpoint blockade demonstrated high binding affinities to Siglec-15 (Stanczak et al., 2022). Thus, suggesting another approach in Siglec-15/Sia axis disruption. Since the identification of Siglec-15 as a possible therapeutic target, there has been less of a focus on the STn antigen and possible therapeutic targets involved in its production.

1.1.7 The role of Siglecs in immune function

Siglec-15's role in immune function has highlighted key involvement in immunosuppression. Upon binding with the STn antigen, a lysine residue in the transmembrane domain allows coupling with the ITAM domains of both DAP12 and FcRγ adapter proteins prompting inhibitory downstream signalling to target proteins (Pillsbury et al., 2023). Within a heterogeneous TME, inhibitory signalling pathways are also stimulated in a similar fashion in TAMs via TGF-β secretion (Takamiya et al., 2013), TGF-β translocation to the nucleus suppresses transcription of tumour suppressor genes (Baba et al., 2022). Moreover, other stimulated pathways following upregulated Siglec-15 activity include the PI3K/AKT and MAPK pathways (Kameda et al., 2013). However, these are primarily involved in osteoclast differentiation.

Separately, under normal homeostasis, sialoglycan ligands act as self-associated molecular patterns (SAMPs) and, provide self-recognition against the body's cells and modulate cell-cell interactions upon Siglec engagement (Egan et al., 2023). However, cancer cells are able to hijack this machinery, and in the context of the tumour landscape, sialoglycans directly bind to respective inhibitory Siglecs with preferential binding on immune cells, dampening immune activation (Rodrigues & Macauley, 2018). Immune cell populations, including NK cells and T-lymphocytes, have impaired functional activity due to interference in antigen recognition via binding with sialoglycans, reducing immune activation and NK cell mediated cytotoxicity (Perdicchio et al., 2016). Due to this phenomenon, the surface of tumour cells exhibits hypersialylation (increased sialylation) and demonstrates increased Siglec-sia binding, masking the glycan epitopes of tumour cells, thus driving tumour onset and progression (Dobie & Skropeta, 2021). Moreover, hypersialylation is not only associated with immune evasion. Sialoglycan accumulation is also involved in reducing sensitisation to therapeutics (Bordron et al., 2018), EMT, angiogenesis, tumour invasion and the inhibition of Fas-mediated apoptosis (Purushothaman et al., 2023). α2,6 sialylation of the Fas receptor via ST6GalI glycosyltransferase activity inhibits effective binding with the Fas ligand (FasL) and prevents activation of apoptotic caspases (Swindall & Bellis, 2011). This is also further exacerbated by the presence of Siglec-15 on cancer cells interacting with the STn antigen. Disrupting the Siglec/Sia axis and preventing the occurrence of hypersialylation in the tumour phenotype presents a novel approach to treatment strategies.

The interactions of Siglec-15/Sia binding also contribute to the development and immunosuppressive capabilities of the TME, primarily relating to affected myeloid populations, with T-cell exhaustion playing a key role in tumour progression (Zhang, Shi, et al., 2024). Overstimulation of T-cell activity and exhausted release of cytokines following antigen recognition reduces the likelihood of a generated effective immune response (Chow et al., 2022). Due to this occurrence, sensitisation to chemotherapeutic treatment is reduced and may promote treatment resistance in patients (Chow et al., 2022). This was observed in a study that identified hypersialylation to be causally linked to T-cell exhaustion and increased Siglec receptor binding (Egan et al., 2023). Other inhibitory Siglecs, such as Siglec-9^{+} TAMs, exhibited the same effect on $CD8^{+}$ T-lymphocytes (Wang et al., 2023).

It is important to note that altered functionality of NK cell mediated cytotoxicity is also affected by aberrant Siglec expression. The role of Siglec-7 sialoglycan binding has been heavily implicated in influencing the activation of NK cells (Rosenstock & Kaufmann, 2021). Similarly, the role of deregulated Siglec-9 expression in solid tumours also plays a role in mediating the activation of NK cells (Belisle et al., 2010). Inversely, dual targeting of both Siglec-9 and Siglec-7 via antibody blockade stimulated NK cell-mediated cytotoxicity, thus exhibiting Siglec modulation on immune cell populations (Jandus et al., 2014). Dysregulated expression of other Siglecs has also been associated with reduced NK cell activity, namely Siglec-10^{+} NK cells demonstrated cellular dysfunction and correlated with poor survival (Zhang et al., 2015). Additionally, Siglec-3 has also been implicated in inhibiting the activation of NK cells and their functionality (Freud & Caligiuri, 2006; Hernández-Caselles et al., 2019). There is also a greater impact of sialylation in myeloid cell mediated antigen recognition; NK cell engagement with its CD48 ligand requires N-glycosylation for functional binding. However, upon desialylation, NK cell activity and activation are substantially increased (Margraf-Schönfeld et al., 2011). Further characterisation of deregulated sialoglycan expression may elucidate particular regulatory effects in tumour progression.

Other myeloid populations affected by the Siglec/Sia axis in the TME include myeloid-derived suppressor cells (MDSCs), which also drive tumour heterogeneity. The presence of MDSCs within the TME decreases sensitisation to immunotherapeutic treatment and contributes to immunosuppression against immune checkpoint proteins, including PD-1 (Safari et al., 2019; Weber et al., 2018). One Siglec protein primarily identified as an MDSC marker is Siglec-3, and it highlights the interplay of Siglec-3 activity on immunosuppression-mediated MDSC

function (Cheng et al., 2022). This was similarly observed in another study that demonstrated $CD33^+$ MDSCs are potential prognostic biomarkers in survival predictions (Ni et al., 2020). Moreover, subsequent targeting with CD33-blocking antibodies has shown decreased MDSC populations *in situ* and concurrently reduced the tumour burden (Cheng et al., 2022).

1.1.8 Sialoglycan deregulation in cancer progression

Inhibitory Siglecs, including Siglec-7/-9 and Siglec-15 on tumour cells have favoured binding to their respective sialoglycan ligands. Upon engagement with the corresponding ligand, the receptor-ligand binding interactions induce immunosuppression and facilitate immune evasion of tumour cells (Gianchecchi et al., 2021; Sun et al., 2021). Sialoglycan ligands are nine-carbon monosaccharide structures linked to membrane-bound and/or glycoproteins and glycolipids (Macauley et al., 2014). In addition to this, sialoglycans display heterogeneity based on the type of glycosidic bond available, including α2,3, α2,6, and α2,8 binding for Siglec recognition (Brinkman-Van Der Linden & Varki, 2000). Moreover, Siglec recognition for binding is also dependent on the negative charges that are present in sialoglycan residues (Van Houtum et al., 2021; Zhou et al., 2020). Sialoglycans are present in one of two isoforms categorised as isoforms N-acetylneuraminic acid (Neu5Ac) and N-glycolylneuraminic acid (Neu5Gc), both of which are distinguished via the hydroxylation of Neu5Ac at the N-acetyl group forming the N-glycolyl group of Neu5Gc (Soares et al., 2021). However, it is important to note that the latter isoform is not expressed in humans due to the mutations observed in the cytidine monophospho-N-acetylneuraminic acid hydroxylase (*CMAH)* gene (Soares et al., 2021). Sialoglycans are involved in several biological processes including cellular signalling, proliferation and adhesion. Nonetheless, the deregulation of sialoglycan expression patterns is implicated in cancer progression, promoting angiogenesis, immunosuppression and metastasis (Pinho & Reis, 2015).

Glycans play a pivotal role in fundamental biological processes via mediating cell-cell interactions in both normal homeostatic and pathological disease states (Smith & Bertozzi, 2021). The functional roles of these glycans are determined by their structure, with conjugation present on proteins and lipids with their construction derived from ten possible monosaccharides within humans (Spiro, 2002). The highly controlled development and extension of these monosaccharides are primarily in the endoplasmic reticulum (ER) and the cis-, medial- and trans- compartments of the Golgi body (Fuster & Esko, 2005). Moreover, they are linked together via a covalent glycosidic bond from an anomeric carbon of one monosaccharide to the hydroxyl group of the second. Additionally, the orientation of the glycosidic bond upon binding to the anomeric carbon (α vs β) can also modify and determine the overall structure of the glycan (Smith & Bertozzi, 2021). Broadly speaking, glycosylation has three main functional roles. Those are, the synthesis of glycan structures with unique

properties, cellular regulation such as protein stability and dimerisation, and lastly, serving as ligands. The defects in these ligands can greatly contribute to a variety of diseases, including cancer (Riley et al., 2020). In addition to this, glycan biosynthesis requires the interplay of multiple proteins and protein families. Hence, the pathway cannot be easily targeted for cancer therapies, limiting the number of therapeutic strategies that are available for patients (Costa et al., 2020). There are several types of glycosylation modifications, but the main focus of this thesis will emphasise the roles of N-linked and O-linked glycosylation and specifically on the role of sialylation in relation to tumour progression in Chapter 2.

1.1.8.1 The role of sialyltransferases in sialylation

Normal homeostasis is maintained through adequate regulation of sialylation post-translational modifications. However, in a tumour phenotype, sialylation expression profiles demonstrate tumour onset and are a driver in tumour progression and metastasis (Lee & Wang, 2020). As mentioned previously, frequent occurrences of hypersialylation (increased production of sialoglycan residues) exhibit enhanced total coverage of 40% - 60% of the tumour cells' surface (Rodrigues & Macauley, 2018). This is further manifested by the deregulation of enzymes involved in sialoglycan synthesis (Table 1), including sialyltransferases and sialidases (neuraminidases). In tumours, typical expression patterns associated with these differing functional proteins involve upregulated sialyltransferase expression and downregulation of neuraminidase activity (Peixoto et al., 2019). The disparity in their expression profiles is further emphasised by the transcriptional regulation of oncogenes such as *RAS* and *MYC*, which modulate sialyltransferase expression, leading to poor clinical outcomes and reduced immune infiltration (Smith et al., 2023). This has been similarly observed in upregulated site-specific N-glycosylation of tumour cells, contributing to immune evasion (Chen et al., 2023). A previous study; highlighted sialyltransferase KO reduced hypersialylation in the TME and reduced tumour progression (Han et al., 2022). Thereby demonstrating significant involvement of sialylation in tumour progression. Multiple sialyltransferases show upregulated expression patterns in the tumour phenotype, mediating the role of sialylation (Macauley et al., 2014). ST6GalI, a prime example of a key enzyme involved in sialoglycan synthesis, typically exhibits increased expression in tumours inducing α2,6 sialylation (Gc et al., 2022; Lu & Gu, 2015; Rodrigues & Macauley, 2018). *ST6GAL1* expression also correlated to *RAS* upregulation, with *RAS* mutations demonstrating a 10-fold increase in ST6GalI protein expression via RalGEF signalling (Dalziel et al., 2004). Similarly, other sialyltransferases (ST3GalII, ST3GalIII,

ST3GalIV, ST3GalV and ST3GalVI) all have correlated with tumour onset by preventing antigen recognition and T-cell activation (Burchell et al., 1999). In addition, several common mutations identified in deregulated sialoglycan expression patterns include O-glycan truncation and modifications to O- and N- glycan binding at the post-transcriptional level (Munkley, 2022).

Table 1: Localisation and function of key sialyltransferases involved in the glycan biosynthesis pathway.

Protein	*Subcellular localisation*	*Function*
ST6GalNAc1	Localised to the Golgi apparatus and nucleoplasm.	Conjugates sialic acids with an α2-6 linkage to N-acetylgalactosamine (GalNAc) glycan chains linked to serine/threonine residues in glycoproteins/glycolipids.
ST6GalNac2	Localised to the Golgi apparatus	Catalysis of transferred N-acetylneuraminyl groups onto glycan chains in glycoproteins/glycolipids.
ST6GalI	Localised to the Golgi apparatus. Can also be present in a soluble form that is secreted into the bloodstream	Transfers sialic acids from CMP-sialoglycans to galactose containing acceptor substrates for antigen generation.
ST3GalIV	Localised to the Golgi apparatus. May also exhibit proteolytic cleavage and secretion into the bloodstream	Terminal sialylation of glycoproteins/glycolipids through catalysis of transferred Neu5Ac from the donor CMP-Neu5Ac onto acceptor glycoconjugates via an α2-3 linkage. Also involved in the biosynthesis of sialyl-lewis epitopes.

1.1.8.2 The involvement of the STn antigen in immune function

The STn antigen has been found to have an upregulated expression in several cancer types and is an effective prognostic biomarker (Munkley, 2016). The STn antigen is structurally composed of a truncated O-glycan with an α2,6-linked Neu5Ac-GalNAc residue (Stowell et al., 2015). Furthermore, STn production may stem from the loss of function and mutation from the molecular chaperone COSMC, allowing for ST6GalNAc1 to sialylate the Tn antigen (Ju et al., 2014). Typically, the deregulated sialylation patterns of the STn antigen are a consequence of multiple factors relating to the synthesis and production of the STn antigen by ST6GalNAc1 and ST6GalNAc2 sialyltransferases and associated molecular chaperones (Figure 9) (Angata et al., 2007; Büll et al., 2021; Takamiya et al., 2013). However, it is also possible for the overexpression of sialyltransferases and increased function to outcompete T-synthase enzyme activity for producing the STn antigen directly (Ikehara et al., 1999). Furthermore, the activity of both sialyltransferases allows several Siglecs, including Siglec-15, to have an enhanced binding affinity for O-glycans and also results in upregulated production of the STn antigen (Angata et al., 2007; Büll et al., 2021; Takamiya et al., 2013). Factors associated with the upregulated production of the STn antigen include the deregulated expression of sialyltransferases and the downregulation of sialidase activity (Rodrigues & Macauley, 2018).

Sialoglycan deregulation plays a pivotal role in tumour progression by affecting various cellular processes linked to tumour invasion, angiogenesis, metastasis, and immune evasion. Furthermore, the aberrant expression of the STn antigen is a unique driver that further facilitates tumour onset upon recognition with Siglec-15. Possible therapies may outline targeting sialyltransferases involved in STn production through blockade or knockdown approaches *in vitro* and *in vivo* (Perez et al., 2021).

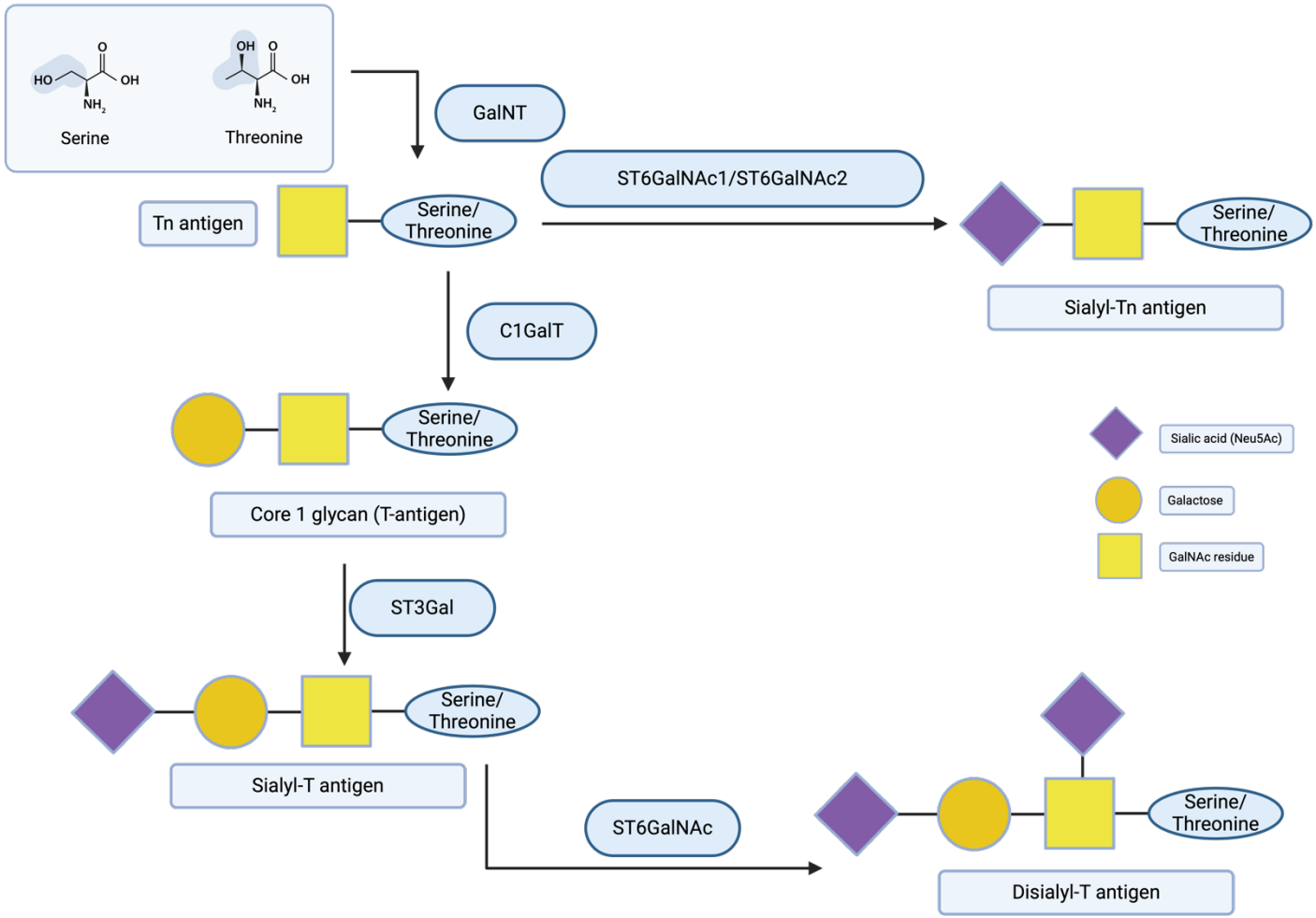

Figure 9: Sequential biosynthesis of the STn antigen and O-glycan synthesis pathway. Truncated O-glycans are expressed on the surface of tumour cells and exhibit many tumour hallmarks. Production of the STn antigen stems from the synthesis and transfer of core GalNAc glycan residues present on glycoproteins/glycolipids, specifically on a serine/threonine residue. Processing of the core glycan with subsequent enzymatic O-glycosylation reactions incorporate sugar residues in a specific order to produce the precursor Tn antigen. Sialylation of the Tn antigen by

sialyltransferases ST6GalNAc1 and ST6GalNAc2 places a terminal sialic acid to the overall glycan structure, the key characteristic of the STn antigen [created with BioRender].

1.1.9 Therapeutic intervention of targeting the Siglec-15/Sia axis

The Siglec/Sia axis presents a promising approach in therapeutic intervention (Figure 10), due to its involvement in multiple biological processes associated with tumour hallmarks and total disruption of the Siglec/Sia axis may outline profound effects for immune normalisation. Additionally, exploring preclinical and clinical evidence for the development of novel approaches could provide insights into possible avenues against Siglec-15 positive tumours.

Whilst there has been significant progress in disrupting the Siglec-15/Sia axis such as the NC318 antibody, several challenges remain, and current methods targeting Siglec-15 positive tumours require further development for easier transition for clinical use. Novel approaches that elucidate Siglec-15 gene regulation through miRNA therapeutics remain unclear, and there is little evidence in the literature of miRNA therapeutics targeting possible Siglec proteins (Yao et al., 2020). However, a previous study identified Siglec-15 expression was dependant on the long non-coding RNA LINC00973/miR-7109 axis at the transcriptional level (Liu, Li, et al., 2020). Moreover, due to the role of PD-L1 in cancer progression, it may be helpful to develop combination therapies to inhibit the tumour phenotype. Supplemental *in vitro* and *in vivo* work is warranted to validate the efficacy and potency of miRNA mimic/inhibitors in target gene regulation against Siglec-15 and allow for an easier transition to the clinic. Similarly, small molecule inhibitors may prove useful in Siglec-15 targeting and are currently not being studied in the literature. The utilisation of small molecule inhibitors as treatment alternatives may exhibit greater tumour penetration due to their small nature in comparison to blocking antibodies.

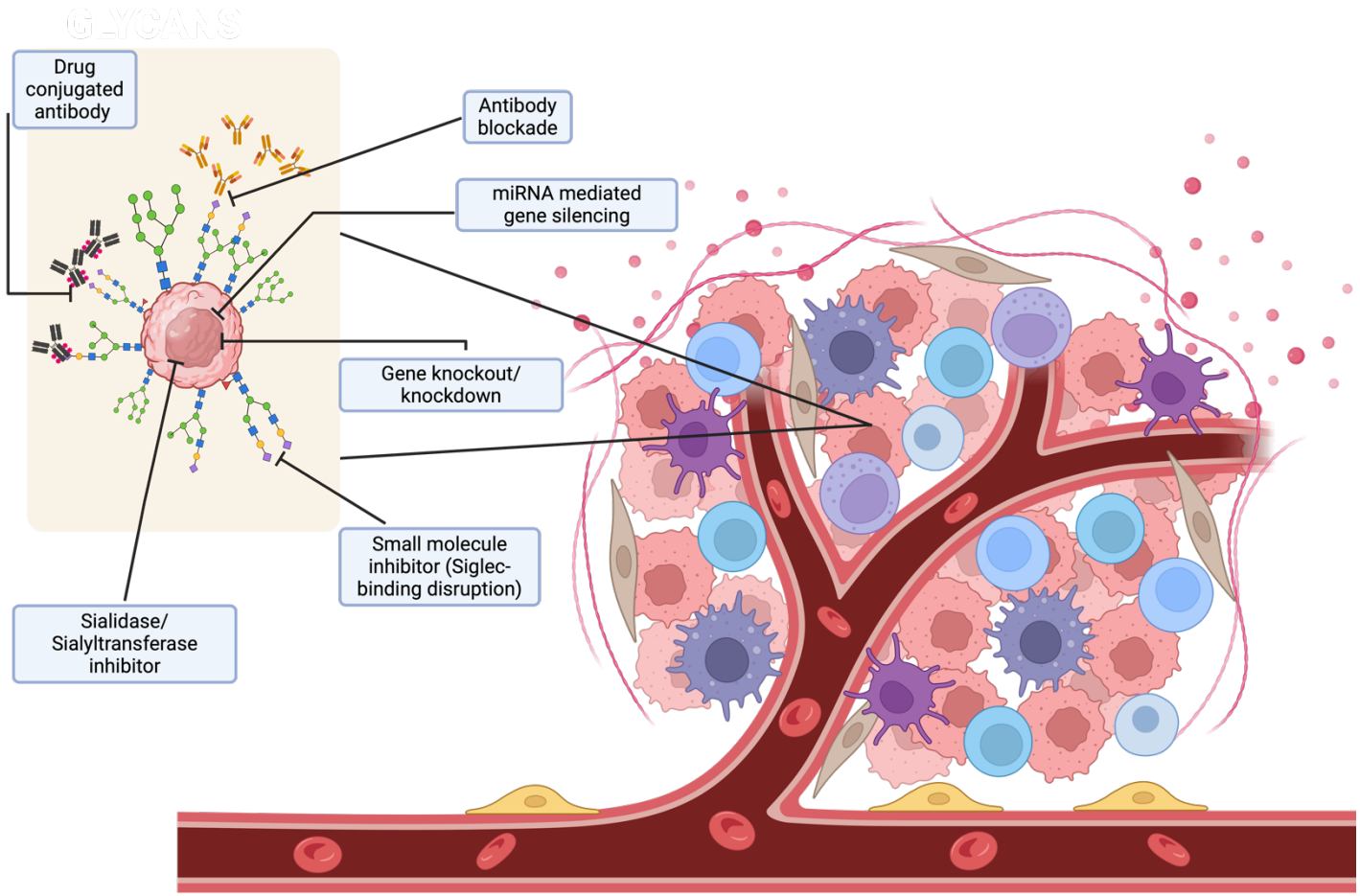

Figure 10: Possible therapeutic interventions that can be implemented in the disruption of the Siglec-15/Sia axis. Blocking antibodies and small molecule inhibitors that are designed to bind to Siglecs with high specificity can block sialoglycan binding; this can prevent downstream inhibitory signalling and potentiate an effective immune response. Similarly, inhibitors that target key enzymes involved in glycan synthesis, such as sialidases and sialyltransferases, can prevent hypersialylation and inhibit sialoglycan cleavage, enabling ligand availability for antigen recognition by immune cells. Gene silencing/knockout methods could regulate *SIGLEC* expression patterns thereby *SIGLEC*s will not exhibit deregulated expression profiles in tumours [created with BioRender].

1.1.10 The role of microRNAs in cancer

In brief, microRNAs (miRNAs) are short, single-stranded non-coding RNA molecules, typically 20-25 nucleotides in length. The introduction and discovery of miRNAs were dated back to 1993, which was first identified in *Caenorhabditis elegans* (Wightman et al., 1993). These miRNAs play significant roles in various cellular pathways related to homeostasis, metabolism, cell growth and development. They are also known to have particular involvement in the modulation of diseases and malignancies, including cancer (Saliminejad et al., 2019). Within normal homeostasis, the key functional roles of miRNAs are to negatively regulate gene expression by mitigating the expression profiles of oncogenes. However, they are frequently altered at the transcriptional level (MacFarlane & Murphy, 2010). Within CRC, the expression of tumour suppressor miRNAs are frequently inhibited, preventing their targeting of oncogenes and facilitating the overexpression of oncogenes including *KRAS*.

The canonical biogenesis of miRNA development is a conserved mechanism that originates from intronic/intergenic transcripts encoded by RNA polymerase II/III, which are involved in the transcription of a miRNA primary precursor (pri-miRNA) characterised by a hairpin loop (Hayes et al., 2014). RNA polymerase II is thought to have the central involvement in pri-miRNA transcription, typically pri-miRNA transcripts are 1kb longer in size in comparison to RNA polymerase III, and the pri-miRNA comprises of uridine residues terminating polymerase III transcription (Chen et al., 2004). Cleavage of the pri-miRNA precursor stem loop by the Drosha/DGCR8 complex releases the pre-miRNA (Westholm & Lai, 2011), producing a miRNA strand with a staggered cut at the 5' phosphate group and a two-nucleotide overhang at the 3' end (Lee et al., 2003). Exporting the pre-miRNA transcript from the nucleus into the cytosol is mediated by the exportin-V and Ran-GTP complex (Yi et al., 2003). Following nuclear export into the cytosol, pre-miRNA maturation and processing is undertaken by RNA pol III Dicer in conjunction with the cofactor TRBP2, which recognises the cleavage of the terminal loop at the 3' and 5' end of the strand forming the miRNA:mRNA duplex (Lagos-Quintana et al., 2002). The duplex comprises both a passenger strand, which is degraded by cellular machinery and a mature strand that is thermodynamically stable. Preferential loading of the mature strand is placed onto Ago proteins, later forming the RNA induced silencing complex (RISC) (Sanghvi & Steel, 2011). The mature strand guides target recognition and has a functional role in the complementarity binding of mRNA target sequences primarily on the 3' untranslated region (UTR) (Figure 11) (Bhaskaran & Mohan, 2014; Zhang et al., 2021).

However, miRNA binding has also been reported at separate binding sites, including the coding sequence, gene promoter and the 5' UTR (Broughton et al., 2016). Interference with the mature mRNA target sequence can inhibit translation and the production of the respective target protein. Reduced translation of the target mRNA strand and degradation of the mRNA transcript is dependent on the complementary binding of the mRNA molecule and the seed region of the miRNA located at the 5' end (Krol et al., 2010). In addition, the non-canonical pathway for miRNA biogenesis relies on the production of pre-miRNA transcripts from Drosha-independent mechanisms from a variety of sources, including alternative splicing events and small nucleolar RNA (snoRNA) (Havens et al., 2012).

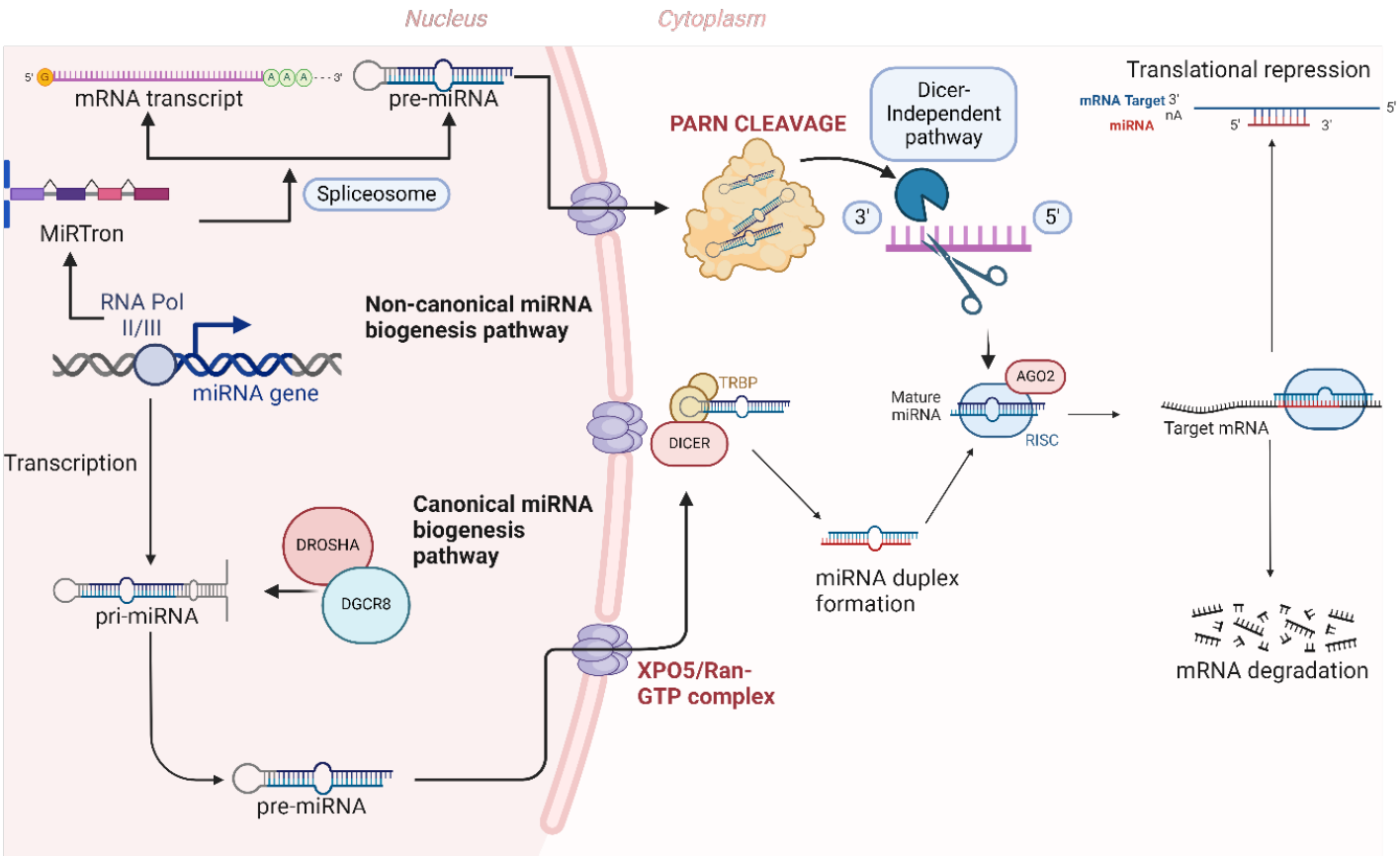

Figure 11: Canonical and non-canonical biogenesis of miRNAs in the nucleus and translational repression of target mRNA strands upon miRNA binding of the 3' UTR. Non-canonical miRNA biogenesis occurs within the introns of protein coding genes which produce miRtron derived pri-miRNA transcripts and are excised through splicing events. Similar to canonical biogenesis, the resultant pre-miRNA is exported from the nucleus for processing. Cleavage of the pre-miRNA occurs through a dicer-independent pathway due to short sequence recognition from the dicer. In contrast, cleavage by the PARN ribonuclease can trim excess nucleotides from the 3' end, generating the miRNA duplex for Ago2 loading and RISC complex formation. The mature miRNA will bind to the target regions of the mRNA strand resulting in translational repression or target degradation [created with BioRender].

It is important to note that miRNAs have tumour-specific expression patterns that are distinct from normal tissues localised in the same region and other tumour types (Lu et al., 2005). These changes in expression profiles are typically highlighted through genomic deregulation, including chromosomal rearrangement and base deletion/amplification, which impact miRNA activity (Calin & Croce, 2006). Due to these factors, miRNA expression profiles outline a prognostic value associated with tumour grade and classification and can serve as valuable tools for diagnosis or prognosis when extrapolated from tissues, such as the usage of liquid biopsies (Sharma & Gupta, 2020). A recent study highlighted the aberrant expression of several miRNAs and was able to predict metastatic CRC progression (Stang et al., 2021). Furthermore, it was also reported that several oncomirs, including miR-21 and miR-29, were overexpressed in CRC patients with high-risk adenomas (To et al., 2018). Particularly in CRC, miRNAs demonstrate tissue specific differential expression in a variety of tumours, underlined by several mechanisms that affect their transcriptional regulation (Lee et al., 2018). Several signalling pathways including MAPK, PI3K/AKT, Wnt/β-catenin and SMAD all affect the activity of transcription factors that are capable of driving the expression of miRNA genes following the binding to their respective promoter regions (Lee et al., 2016). Thus, this highlights miRNA expression profiles as either oncomirs or tumour suppressor miRNAs. In addition, methylation of the promoter regions prevent the binding of several transcription factors which are unable to facilitate enhanced transcription of the miRNA genes (Lila & Martha, 2019). Similarly, histone deacetylation constricts the DNA sequence producing a much more compact chromatin structure which reduces the availability of access sites for RNA polymerase binding and subsequent transcription (Lee et al., 2020). Furthermore, the sponging of miRNAs by long non-coding RNAs and circular RNA (circRNA) molecules prevent the complementarity engagement of the miRNA to the target mRNA strand (Ebert & Sharp, 2010). Thus, typically highlighting the overexpression of oncogenes and the reduced expression of tumour suppressor genes.

With regard to CRC, several miRNAs have shown deregulated expression profiles, including miR-1207/miR-1225/miR-445/miR-21/miR-29 and were correlated with tumour progression (Buhagiar et al., 2021; Stang et al., 2021; To et al., 2018). Moreover, miRNAs have displayed critical roles in CRC progression alongside tumour onset and metastasis (Wang, 2020). MiRNA activity directly targeting the modulation of key tumour suppressor genes such as phosphatase and tensin homolog (*PTEN)* were able to promote PI3K/AKT signalling leading

to tumour progression. With numerous studies highlighting miRNAs as effective diagnostic and prognostic biomarkers, functional studies have elucidated several signalling pathways linked to cancer progression, EMT and metastasis (Elrebehy et al., 2022).

One signalling pathway commonly associated with tumour development includes Wnt/β-catenin signalling. The accumulation of cytosolic β-catenin and movement to the nucleus induced via Wnt signalling modulates the transcription of genes related to cellular proliferation, differentiation and survival (Slattery et al., 2018). From this, oncomirs miR-135b and miR-494 inhibited the expression of tumour suppressor genes, including *APC* by 3' UTR binding and induced Wnt signalling, β-catenin accumulation and tumour progression (Zhang et al., 2021). Similarly, the oncomir miR-410 demonstrated an upregulated expression profile in CRC and was shown to target DKK1, an inhibitor of Wnt (Wang et al., 2018). Furthermore, the role of tumour suppressor miRNAs in Wnt/β-catenin signalling was also identified. MiR-185 targeted Wnt1 and reduced its expression in CRC *in vitro*, thus inhibiting tumour proliferation (Zhang et al., 2021). In a similar fashion, CRC cellular migration and EMT were reduced upon the overexpression of miR-377 targeting of Zinc finger E-box-binding homeobox (*ZEB2*) negatively regulating Wnt/β-catenin signalling (Shayimu et al., 2020).

As one of the deregulated genes in canonical CRC development, *KRAS* can account for approximately 40% of CRC diagnoses (Zenonos, 2013). MiRNA expression patterns have identified tumour suppressor miRNAs, including miR-30b-5p, that, when overexpressed, can inhibit the activity of *KRAS* and inversely, its downregulation induced *KRAS* activity and tumour progression (Ibrahim & Lim, 2020). Simultaneously, oncomirs can significantly impact tumour progression and have been associated with *KRAS* modulation. MiR-31 upregulation in CRC demonstrated an increase in the half-life of GTP in *KRAS* signalling, promoting cellular proliferation and inhibiting apoptosis (Pugh et al., 2017). Likewise, the miR-200c/*KRAS* signalling axis was associated with high tumour grade and was also observed *in vitro* (Roh et al., 2018).

Moreover, miRNAs can also regulate cellular properties linked to immune function. The overexpression of miR-27a and dysregulated MHC-I molecules can cause defects in tumour cell antigen recognition, resulting in cancer development. Both factors were associated with unfavourable patient prognosis (Di Martino et al., 2021). Furthermore, one study has shown that several miRNAs, including miR-21 and miR-124, were able to enhance the maturation of

cytotoxic T-lymphocytes within the tumour microenvironment (Xing et al., 2021). Similarly, miR-150 was also highly involved in the maturation and development of NK cells (Pesce et al., 2020). This, therefore, supports the idea of utilising miRNAs to bolster immunotherapeutic approaches and may prove to be a feasible strategy in boosting/normalising immune cell populations to target Siglec-15 induced CRC tumours.

MiRNA-based cancer therapeutic approaches have entered clinical trials showing positive patient response, and low adverse effects and are well-tolerated in phase I and transitioned to phase II clinical trial for advanced tumour treatment. MRX34 (miR-34 mimic) conducted phase I clinical trials for the treatment of various solid tumours via an IV based liposomal delivery strategy (Bader, 2012). Upon adherence to tumour cells, MRX34 was involved in the direct regulation of multiple oncogenes associated with tumour progression, chemoresistance and metastasis (Bouchie, 2013). Additionally, *in vivo* delivery of xenografted liver cancer murine models observed reduced tumour growth and affecting signalling pathways, including Wnt/β-catenin and induced p53 activity (Daige et al., 2014). However, immune associated serious adverse effects prompted the discontinuation of MRX34 at phase I clinical trial (NCT01829971, NCT02862145). Alternatively, TargomiRs (miR-16 mimic) has shown successful phase I clinical trial data (NCT02369198) (Hanna et al., 2019). The incorporation of the mimic in conjunction with a viable delivery method and anti-EGFR bispecific antibody ensured successful delivery and targeting of Bcl-2 and CCND1, inhibiting tumour progression (Reid et al., 2013). Furthermore, a dose-dependent open label phase I clinical trial highlighted high efficacy and tolerance to treatment when added to conventional chemotherapies (Van Zandwijk et al., 2017). Whilst the utilisation of miRNA-based therapeutics has shown efficacy and selectivity against target genes, several obstacles limit translation of miRNA-based therapeutics to the clinic, including immune related adverse effects and off-target effects. Additionally, delivery methods that are novel and provide high efficacy and tumour specificity require ample pharmacodynamic and pharmacokinetic parameters capable of tumour penetration which still need to be addressed (Kara et al., 2022). Identifying novel miRNA candidates for oncogenes/tumour suppressors, including *SIGLEC15*, may outline potential miRNA mimics for clinical applications in Siglec-15^{+} tumours and normalise the immune response and introduce immunotherapies, treatment alternatives and combination therapies.

1.1.11 Rationale, Aim and Research questions

To date, many of the immune checkpoint inhibitors targeting PD-1, PD-L1, CTLA-4 and LAG-3 that are commercially available are blocking antibodies, which block the binding of immune checkpoint proteins on T-lymphocytes with ligands expressed on tumour cells. However, patients who acquire treatment resistance and demonstrate poor treatment response emphasise the presence of other immune checkpoint proteins, such as Siglec-15. To underline possible therapeutic approaches in the inhibition of Siglec-15 in CRC tumours, a combination of multiomics and *in vitro* approaches utilising CRC cell models will be undertaken to illustrate the key research questions listed below. Additionally, miRNAs involved in regulating the *SIGLEC15*/STn axis are unclear, and the literature surrounding *SIGLEC15*/STn axis in relation to CRC progression is poorly understood. Elucidating candidate miRNAs involved in regulating oncogenes associated with CRC progression and subsequent inhibition of Siglec-15 expression will underline therapeutic targets in Siglec-15^{+} tumours. Hence, it will provide pre-clinical data that will enable the transition of Siglec-15 targeted small molecule inhibitors in combination with PD-L1 antagonists. A combination approach between several compounds may possess synergistic effects and greatly tackle the highly heterogenous nature of CRC tumours themselves, inhibiting both Siglec-15 and PD-L1 immune checkpoint proteins. Thereby, preventing the rescue of the tumour phenotype (Figure 12).

This disruption of the Siglec-15/STn axis overall represents an avenue that can be focussed on the inhibition of the Siglec-15 protein itself and the reduced sialylation of the Tn antigen, rendering its inability to bind to the V-set binding domain of the Siglec-15 protein. Thus, this study will highlight key sialyltransferases in the glycan biosynthesis pathway (Chapter 2) as therapeutic targets for the disruption of the Siglec-15/STn axis. For this, a multiomics approach outlining miRNA target prediction tools that identifies the most frequent miRNA element involved in sialyltransferase expression will be conducted. Furthermore, their expression in CRC tumours and their roles in tumour hallmarks and the TME will be determined to highlight their involvement in tumour heterogeneity. Lastly, immunohistochemical analysis will reveal the expression of ST6GalNAc1 and ST6GalNAc2 and the part they play in STn production, particularly in CRC tumours.

Moving on from this, the development and characterisation of the β-amino carbonyl compound SHG-8 will be synthesised as a small molecule Siglec-15 inhibitor, primarily responsible for

the direct blocking of the Siglec-15 V-set binding domain (Chapter 3). Elucidating the cytotoxic profile of SHG-8 will be primarily focused on *in vitro* cell models SW480, HCT116, HcoEPiC, U937 and THP-1. Prior to the experimental work, an *in silico* molecular docking simulation will provide information relating to the binding affinity between the compound ligand and the Siglec-15 protein structure. From this, the experimental work will underline the characteristics associated with tumour progression such as proliferation, migration and colonisation following SHG-8 treatment. In particular, small-RNA (sRNA) sequencing analysis will identify the most significantly differentially expressed (DE) miRNAs and subsequent gene targets following SHG-8 exposure determining potential mechanisms of action and signalling pathways that are associated with CRC progression.

As currently available small molecule inhibitors already have characterised safety profiles, it will prove beneficial to repurpose therapeutic agents for anti-cancer targeting for Siglec-15 inhibition. An initial *in silico* high-throughput screening analysis utilising MTiOpenScreen (https://bioserv.rpbs.univ-paris-diderot.fr/services/MTiOpenScreen/; accessed 24th March 2024) software has provided docking simulations to a screening library that is composed of over 1500 (drug-lib) compounds and determine their binding affinity towards the R143 residue and V-set binding domain. Following on from this, the compound with the highest binding affinity would then be characterised as an anti-cancer therapeutic agent with similar experimental assays as highlighted in the approach for Chapter 3. Furthermore, RNA illumina sequencing methods will ascertain the most significantly DE gene targets and their association with candidate miRNAs, signalling pathways and mechanisms of action in relation to CRC progression.

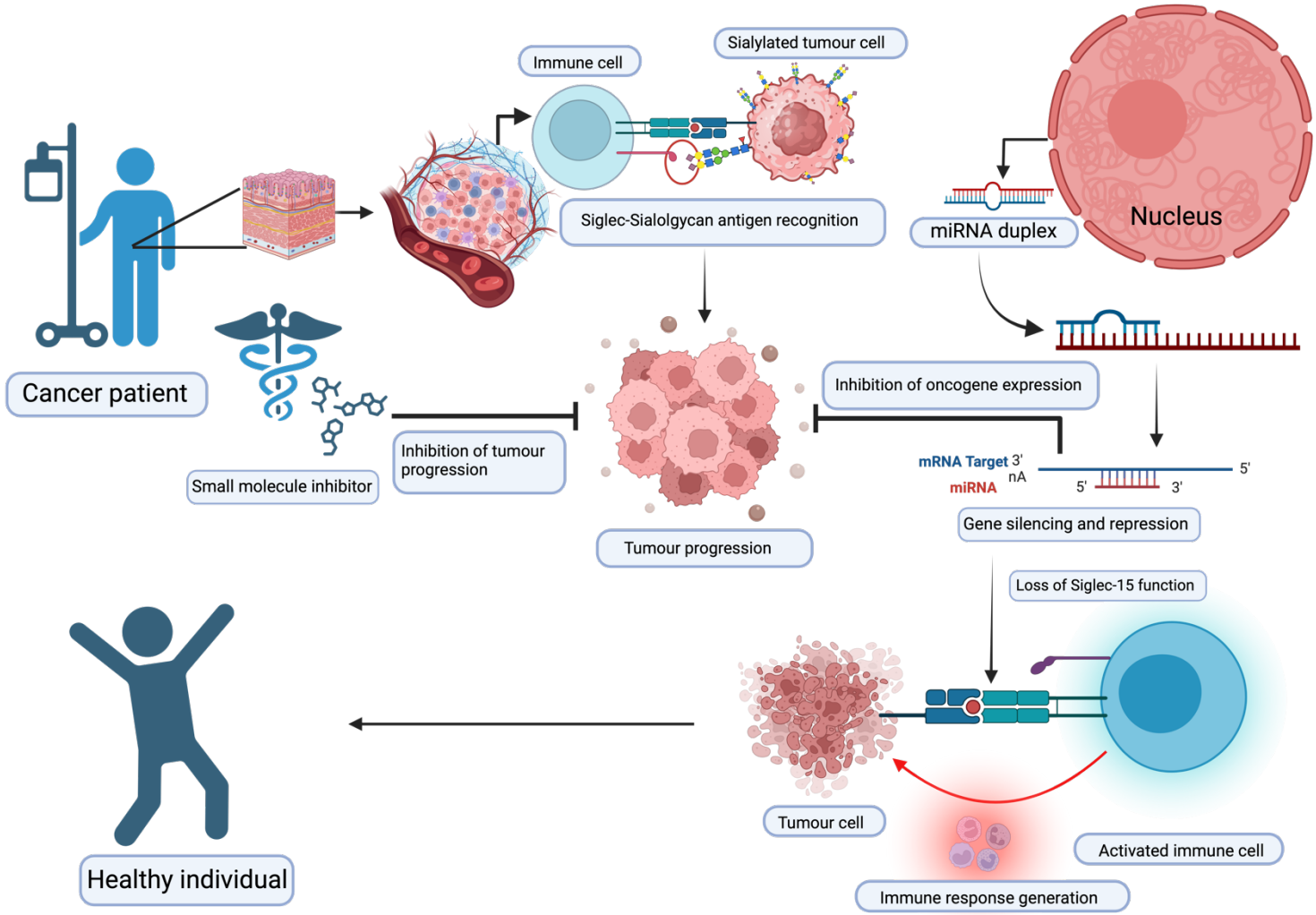

Figure 12: Schematic of Siglec-15 targeting with small molecule inhibitors and its expression regulated by miRNAs. Aberrant Siglec-15 expression in the TME induces immunosuppression and tumour progression through STn antigen binding and T-cell inactivation. Incorporation of miRNAs exerting SIGLEC15 gene downregulation in conjunction with competitive binding on its V-set binding domain via small molecule inhibitors may exhibit Siglec-15 loss of function and present the generation of an effective immune response [created with BioRender].

This PhD project hypothesises the direct targeting of Siglec-15 will inhibit STn antigen binding and subsequent protein receptor-ligand interactions relating to the Siglec-15/Sia axis. Thus, significantly impacting tumour cell viability and proliferation. Based on the present literature, miRNAs involved in modulating the Siglec-15/Sia axis in CRC remains to be elucidated. In addition to this, we previously mentioned that Siglec-15 shares mutually exclusive expression on cancer cell populations with regard to the immune checkpoint protein PD-L1, possibly suggesting future combination therapies with PD-L1 antagonists. This project proposes the novel utilisation of small molecule inhibitors for Siglec-15 targeting and to identify differentially expressed miRNAs involved in the expression of oncogenes and possible gene targets to characterise their clinical relevance to CRC as a therapeutic strategy.

To ascertain the miRNAs and mechanisms of action involved in the regulation/disruption of the Siglec-15/Sia axis, several outlined project questions were set to test the hypothesis listed below:

1. Utilising a bioinformatics approach, which predicted miRNAs exhibit the highest binding affinities for sialyltransferase targeting and how are they involved in CRC progression and in the production of tumour associated glycans?
2. Can the characterisation of the newly synthesised compound SHG-8 be utilised for Siglec-15 competitive inhibition towards its V-set binding domain and what are the implications of SHG-8 exposure towards miRNA activity?
3. From a high-throughput screening approach of 1500 compounds from the MTiOpenScreen drug library software, is it possible for aleplasinin to be repurposed and exhibit cytotoxic activity against CRC *in vitro* cell models?
4. Can small molecule inhibitors SHG-8 and aleplasinin induce the differential expression of miRNAs and identified gene targets, and what is their clinical relevance in CRC progression?
5. Overall, do these compounds serve as possible treatment alternatives to current blocking antibodies in Siglec-15 inhibition and disrupt the Siglec-15/STn axis?

Chapter 2 - Differential expression of sialyltransferases in CRC progression and elucidation of their regulatory mechanisms in glycan biosynthesis

2.1.1 Post-translational mechanisms

There are a number of post-translational modifications that can affect the function and expression of modified proteins (Figure 13). Thus, these modifications are characterised by the deregulation of normal biological processes and consequently contribute to pathological diseases. However, the role of glycans and their clinical impact on tumours via glycosylation modifications was only briefly covered in the previous chapter of this thesis and shall be covered in greater depth as part of this chapter.

2.1.2 N-linked glycosylation

N-linked glycosylation is the addition of N-acetylglucosamine (GlcNAc) towards a nitrogen atom within the asparagine (Asn, N) side chain of a β-1N linkage. Further to this, Asn-linked glycoconjugates also comprise of a distinct $GlcNAc_2$ mannose core where a flexible number of monosaccharides may be added/removed, which can determine its final structure (Reis et al., 2010). Firstly, for N-glycan synthesis initiation, the process is dependent on the $GlcNAc_2$ mannose core to form a branched structure attached to the formation of lipid precursor molecules (dolichopyrophosphate)-linked oligosaccharides) which occur on the cytosolic side of the ER and serve as donors for N-glycosylation substrates (Reis et al., 2010). Additional structural and subsequent processing, such as protein folding is later implemented in the ER. Following this, the lipid precursor molecules are later flipped towards the luminal ER; this is the location where further mannose, and glucose subunits are incorporated to produce the final $Glc_3Man_9GlcNAc_2$ structure (Helenius & Aebi, 2001). The matured glycan structure is recognised by oligosaccharyltransferase protein complexes and positions the glycan chain to an N- Asn-X-serine/threonine (Ser/Thr) site (X is signified as any amino acid residue excluding proline (Pro, P)) of nascent proteins (Schjoldager et al., 2020). The N-glycan protein will undergo quality control processing in the cis- compartment of the Golgi body, which can cleave several mannose residues from the structure via mannosidase activity prior to transferal to the medial-Golgi for nascent maturation and modification. Here, and within the trans-compartment of the Golgi body, oligomannosidic, hybrid and complex N-glycan structures are synthesised (Figure 14) (Ramírez et al., 2022).

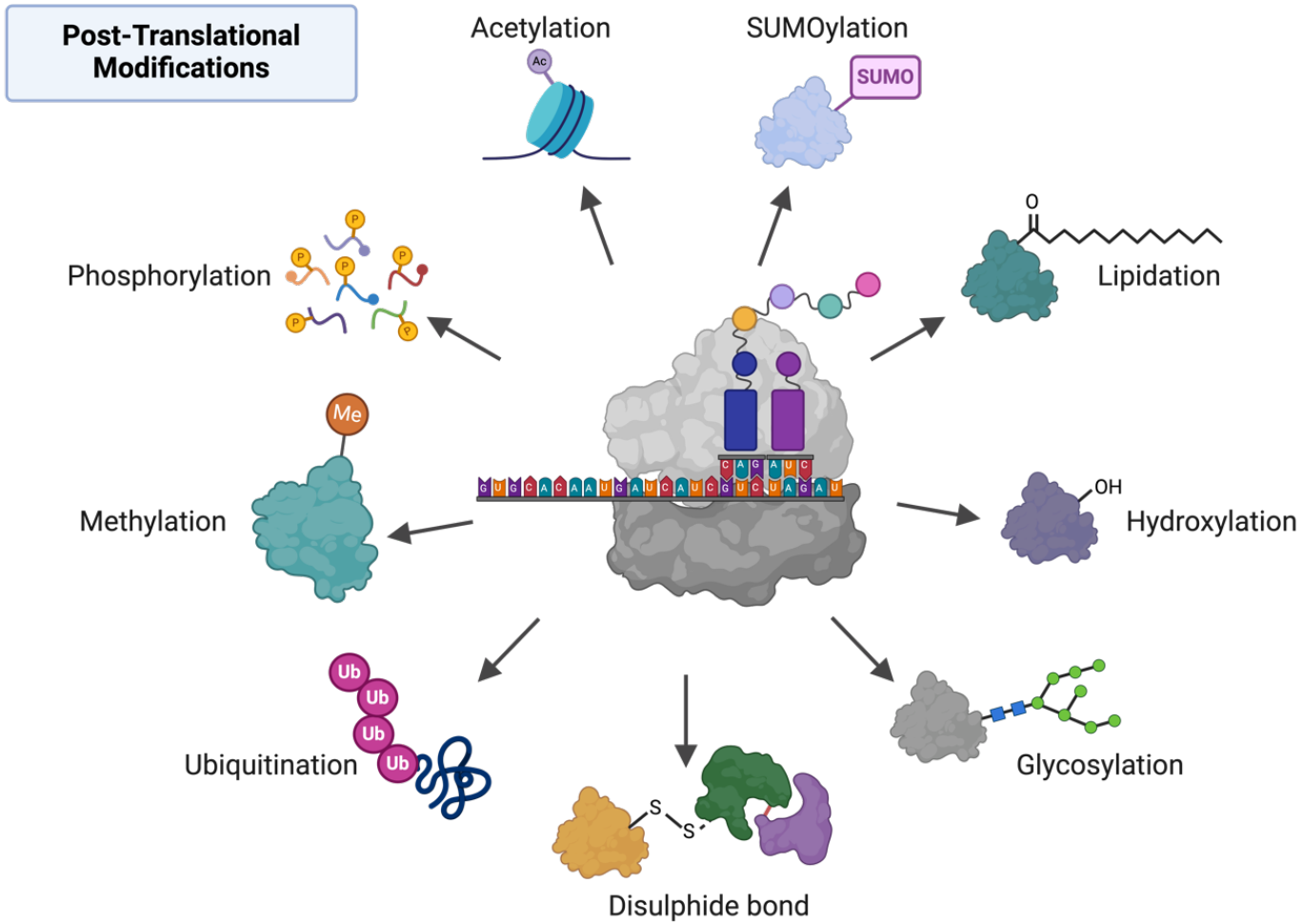

Figure 13: The variety of protein post-translational modifications available following ribosomal translation. Glycosylation is biochemical process that emphasises the covalent bonding of sialoglycans to proteins and lipids. Glycosylation is involved in several processes that can impact homeostasis including protein folding and stability, cellular communication and molecular trafficking. Dysregulation of these post-translational modifications promote the onset of tumour malignancies [created with BioRender].

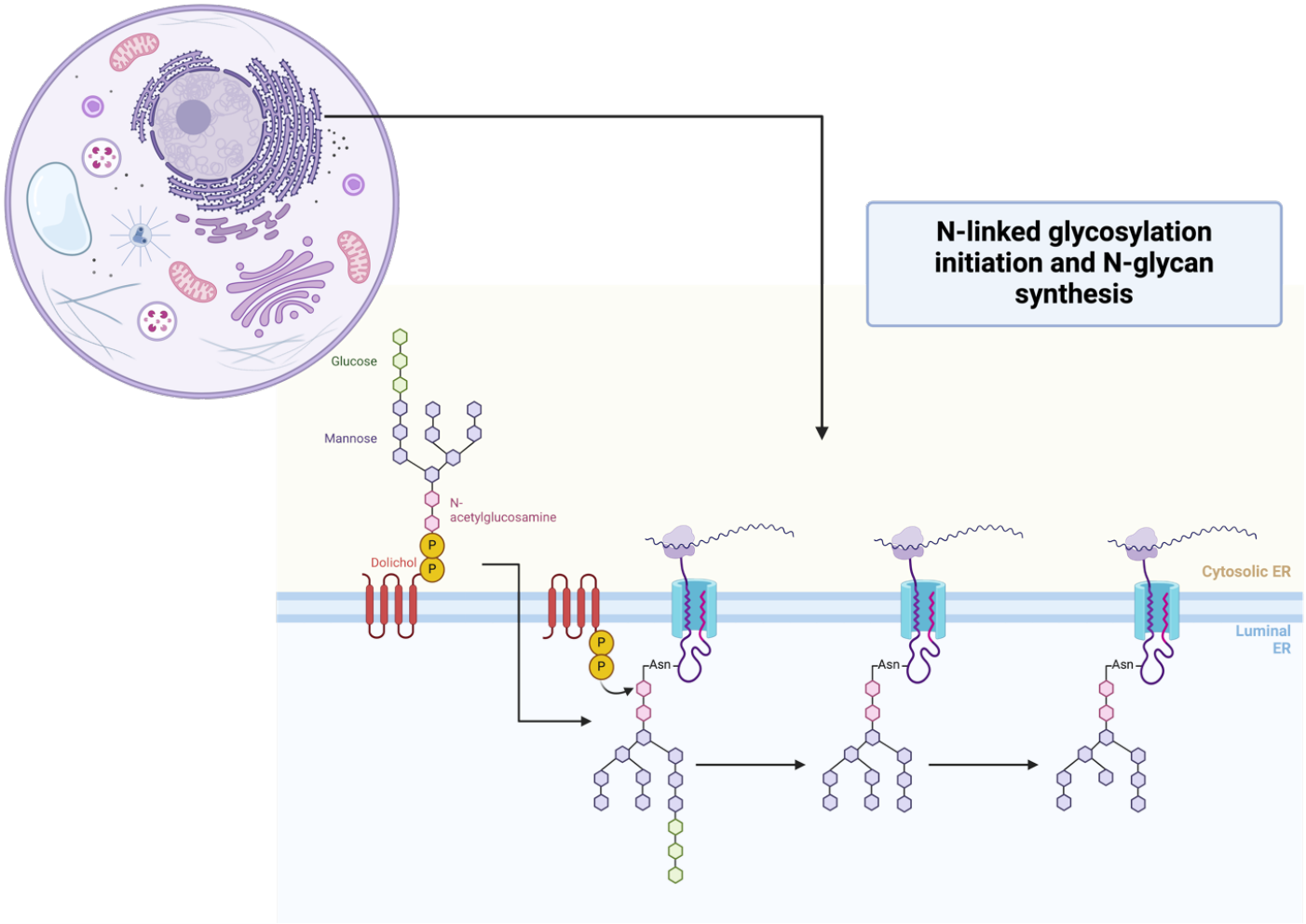

Figure 14: Initiation of N-glycan biosynthesis and glycosylation within the ER prior to maturation in the medial- and trans- compartments of the Golgi body. N-glycans are crucial in the regulation of both intracellular and extracellular functions. Their synthesis is enabled through the post-translational modifications through $Glc_3Man_9GlcNAc_2$ binding at specific Asn-X-Ser/Thr glycosylation sites. The production of complex primary and hybrid N-glycan structures is developed through several additions of GlcNAc, galactose, sia and fucose residues [created with BioRender].

2.1.3 O-linked glycosylation

O-linked glycosylation occurs frequently on serine/threonine hydroxyl groups which predominantly link GlcNAc and N-acetylgalactosamine (GalNAc) (Figure 15). The most common of those (mucin type-O glycosylation) is highly abundant on the surface of many glycoproteins (Bennett et al., 2012). Mucin proteins are comprised of a large number of tandem repeats within their structure, which contain a high content of Pro, Ser and Thr residues that are necessary O-glycosylation sites (Hu et al., 2010). These types of O-glycans possess six major core structures however cores 1-4 are exhibited much more frequently. Initiation and development of mucin O-linked glycosylation structures occur within the Golgi body and are performed by GalNAc transferases or (GalNAcT; GALNT) proteins that provide overlapping regulation of the glycan structure (Nielsen et al., 2022). This regulation is determined by a ricin-like lectin domain within GALNT sialyltransferases that recognise GalNAc several residues away from the acceptor site and control the speed of glycosylation and processing (De Las Rivas et al., 2019). As the protein moves across the different Golgi compartments, unlike N-linked glycosylation, pre- and post-processing of existing sugar molecules do not occur. In place of this, these O-glycans are modified to include residues such as galactose and Sias (Nielsen et al., 2022). However, within the instance of GlcNAc residue addition, the glycan chain is prevented from elongation and the addition/removal of currently available residues occurs by the activity of (O-GlcNAc) transferases taking place outside the Golgi body (Wandall et al., 2021).

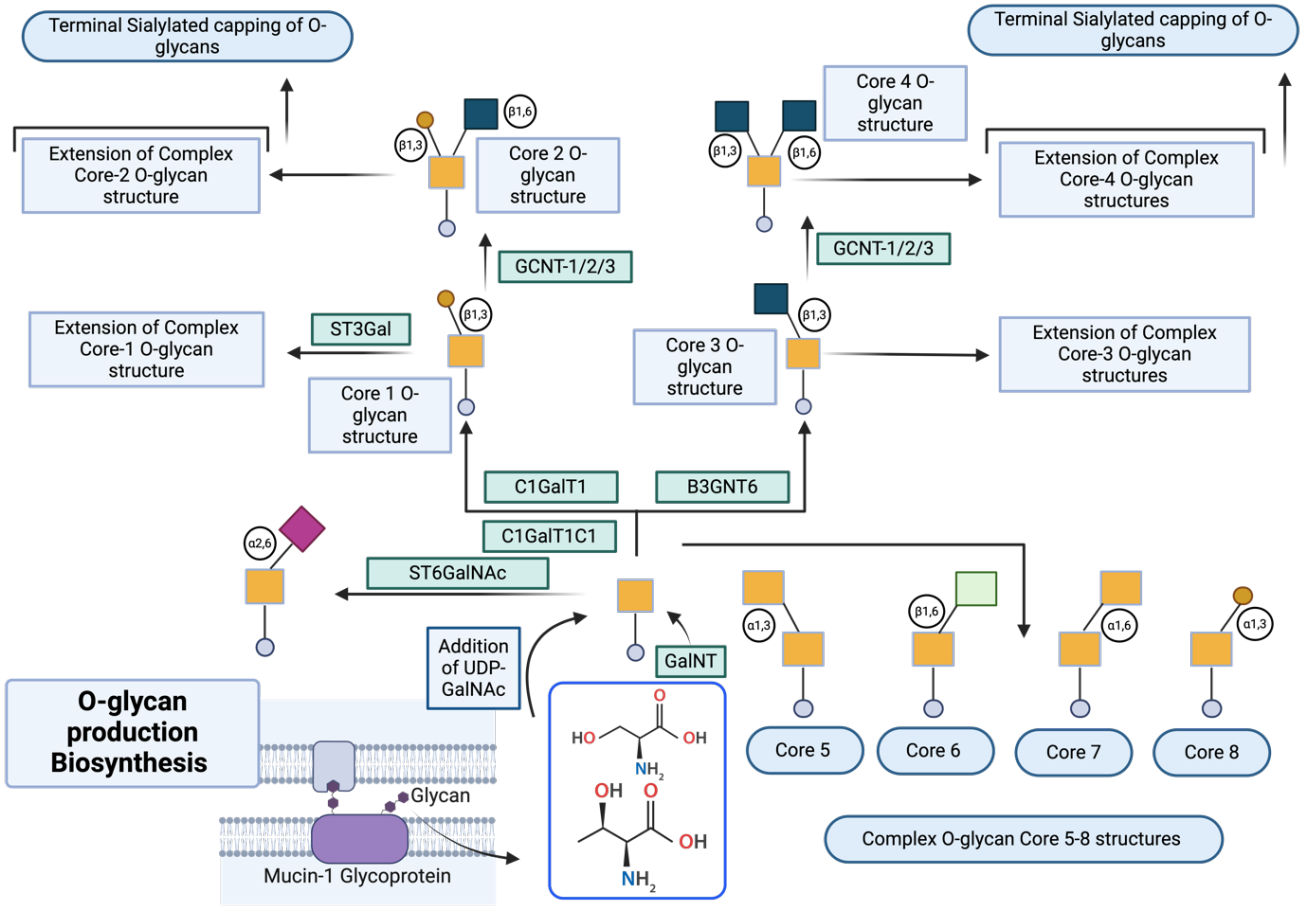

Figure 15: Initiation and biosynthesis of O-glycan chains of proteins through the Golgi body. O-glycans are developed through the activity of GALNT proteins that incorporate various sugar molecules as the protein moves through the Golgi compartments. Synthesis and glycan assembly occur on serine/threonine residues of glycoproteins like mucins within the Golgi body. Following the addition of N-acetyl-galactosamine, several core O-glycan structures can be produced via chain complex extension, and capping occurs by sialylation at the terminal end of the glycan chain. Synthesis of the T, Tn and STn antigens are produced via several sialyltransferases [created with BioRender].

2.1.4 The role of sialylation and its impact on tumour progression

One type of glycosylation modification is sialylation, which enables the introduction of Sia for terminal capping of key glycans (Varki, 2008). Sias are structured with a nine-carbon backbone that will be modified through enzymatic function. Neu5Ac is commonly present in humans. Hence, sialylated glycan synthesis requires the activity of sialyltransferases located within the Golgi body to conduct the catalytic formation of glycosidic linkages. Mechanistically, the linkages stem from C2 of the Sia from the CMP-Neu5Ac donor to either a C3, C6 or C8 hydroxyl group of the glycan acceptor. These interactions can then determine the categorisation of sialyltransferases respectively (Varki, 2008). Each of the subtypes is further classified based on the glycan acceptor, which is more frequently galactose (Gal) or GalNAc (Szabo & Skropeta, 2017). ST3Gal processes linkages that occur between C2-C3, C2-C6 are processed by ST6Gal and ST6GalNAc and C2-C8 by ST8Sia, all of which result in the formation of either α2,3-, α2,6-, or α2,8-linked sialoglycans, respectively (Büll et al., 2014). The production of the variously linked sialoglycans and their organisation vastly contributes to the diversity of glycan structures that are available and is referred to as the Sialome.

Within tumour progression, the abnormal distribution of sialylated glycans becomes apparent, and key mechanisms are thought to be involved. As mentioned previously in Chapter 1, the deregulation of sialyltransferases and sialidases resulted in the enhanced sialylation of tumour-associated antigens such as STn (Häuselmann & Borsig, 2014). In addition, the deregulation of oncogenes *RAS* and *MYC* alongside dysregulated sialyltransferase activity modulated the activity of ST3Gal and ST6Gal sialyltransferases at the transcriptional level. MYC dependent regulation was also reported to bind to the promoter regions of several sialyltransferases by the deregulation of several key glycosylation mechanisms (Smith et al., 2023). Through overexpression, hypersialylation becomes a common phenomenon that results in reduced antigen recognition by myeloid cells and dysregulated immune regulation and immune response generation. Another proposed mechanism has indicated that metabolic flux (increased metabolite turnover via metabolic pathways) through sialoglycan biosynthesis can be enhanced in tumour cells. This is largely due to increased substrate availability and upregulation of genes in glycan biosynthesis (Scheper et al., 2023). One report indicated that the enhancement of sialylated glycoproteins was due to the increase in metabolic flux by increasing the number of sialoglycan precursor molecules in tumour cells (Almaraz et al., 2012). Furthermore, glycopeptides that received high levels of sialoglycan precursor molecules, such as 1,3,4-O-

Bu3ManNAc, demonstrated greater tumour associated cellular signalling and adhesion (Saeui et al., 2020). Therefore, metabolic activity changes may contribute to tumour heterogeneity and emphasise the roles of metabolic precursors and substrates readily available which can contribute to enhanced sialylation.

2.1.5 Sia expression patterns and the role of the STn antigen in tumour progression

Upregulated Sia expression patterns have been observed in tumour malignancies and have largely correlated with cancer-specific glycosylation modifications that serve as unique drivers in tumour progression (Stanczak et al., 2022). Some of the Siglec family members, including Siglec-4/-7/-15 have preferential binding affinities for sialylated GalNAc-type O-glycans; however, there is unique selectivity based on specific protein sequences (Büll et al., 2021). For instance, Siglec-15 binding exhibits a high binding affinity for the Neu5Ac α2,6-GalNAc STn antigen, which is synthesised by glycosyltransferases/sialyltransferases including α-N-acetylgalactosaminide α-2,6-sialyltransferase 1 (ST6GalNAc1). The process by which this occurs can involve ST6GalNAc1 catalysing the addition of the sialic acid in an α2,6- dependent linkage to GalNAc linked Ser/Thr residues (Sewell et al., 2006). Deregulation of these sialyltransferases has been associated with tumour development (Angata et al., 2007). Moreover, ST6GalNAc1's role in STn antigen biosynthesis is upregulated in cancer and can reduce poor clinical survival in CRC patients (Munkley, 2016; Ogawa et al., 2017). Similarly, α-N-acetylgalactosaminide α-2,6-sialyltransferase 2 (ST6GalNAc2), plays a role in STn production, albeit to a lesser extent, which has exhibited increased expression profiles in CRC and other tumour malignancies (Miao & Zhao, 2016; Schneider et al., 2001).

There are additional sialyltransferases that are associated with tumour onset through abnormal sialylation. The role of ST3 β-galactoside α-2,3-sialyltransferase 4 (ST3GalIV) is heavily involved in N-glycan synthesis via the terminal capping of Neu5Ac (α2,3) Gal (Isaji et al., 2020). Moreover, the ST3GalIV protein can also play a significant role in the biosynthetic production of sialyl-lewis antigen (sLE^a and sLE^x) precursor molecules, both of which are commonly associated with tumour development (Dall'Olio et al., 2021). However, *ST3GAL4* KO studies have revealed no significant change in the production of sLE^x but led to a significant decrease in the expression of sLE^a antigens in CRC *in vitro*, which suggested ST3GalIV as a major player in sLE^a biosynthesis (Costa et al., 2023). Previous reports have indicated abnormal ST3GalIV expression patterns in several tumour types, significantly affecting both

survival outcomes and treatment resistance to therapies (Guerrero et al., 2020). However, the role of ST3GalIV-dependent sialylation in CRC remains relatively limited and would require further elucidation. The activity of β-galactoside α-2,6-sialyltransferase 1 (ST6Gal1), which is involved in the catalysis of α2,6-linked sialic acids towards the terminal regions of N-glycans, has played a role in tumour progression and metastasis (Hsieh et al., 2017; Park & Lee, 2013; Wei et al., 2016). As with many sialyltransferases, the upregulation of ST6Gal1 is also directly proportional to an increase in the level of α2,6-linked sialylation exhibited on tumour cells within the TME and responsible for the large majority of α2,6-linked sialylation that is generated (Lu et al., 2014). This is further emphasised by the development of advanced tumour grade and metastasis of solid tumours, enhanced tumour burden, recurrence and poor clinical survival outcomes (Garnham et al., 2019). To ascertain how these proteins are regulated in STn production and their role in CRC progression may highlight sialyltransferases as possible therapeutic targets to disrupt the Siglec-15/Sia axis. Furthermore, the impact of miRNAs in sialyltransferase regulation remains limited and may contribute to the production of the STn antigen, and identifying mechanistic signalling pathways could also display their clinical relevance to CRC progression. In addition, targeting sialyltransferases may exhibit positive treatment responses in patients undergoing immune checkpoint blockade therapies.

2.1.6 Rationale, Aim and Research questions

This chapter of my thesis aimed to adopt a multiomics approach that explores the regulatory mechanisms of the main sialyltransferases ST6GalNAc1, ST6GalNAc2, ST3GalIV and ST6Gal1 in glycan biosynthesis to underline the roles they play in STn production and other glycans. Thus, underlining their relevance to CRC progression. It is also worth noting possible regulatory mechanisms involved in their expression profiles including the impact of miRNA activity, to ascertain their potential as therapeutic targets. Moreover, the role of each sialyltransferase and its association with myeloid cells and immune checkpoint proteins will be determined to highlight potential interactions in the TME, outlining their contribution to tumour heterogeneity.

For this to be undertaken, both interactive gene and protein partners of the chosen sialyltransferases will be identified to elucidate glycosylation mechanisms and pathways. Furthermore, an independent analysis of miRNA target prediction software tools will be utilised to identify the common miRNA elements involved in sialyltransferase regulation. From

this, further analysis of the most common miRNA hits will generate specific binding sites on their respective target mRNA strands via Sfold prediction software and subsequent expression profiles in CRC tumours using the UALCAN omics database. Gene set enrichment analysis (GSEA) will correlate the sialyltransferase expression profiles to known cancer hallmarks associated with tumour progression. Additionally, sialyltransferase expression and their correlation to the abundance of myeloid cells and prevalent immune checkpoint proteins will be determined using TISIDB and TIMER databases.

Several research questions have been highlighted to underline the sialyltransferases ST6GalNAc1, ST6GalNAc2, ST3GalIV and ST6GalI as potential therapeutic targets in CRC progression.

1. Using bioinformatics transcriptomics tools, are sialyltransferases differentially expressed in CRC tumours and what are the implications in glycan biosynthesis and their respective interactive partners as a result?
2. Upon conducting gene enrichment analysis, are any sialyltransferases associated with known tumour hallmarks that are commonly associated with CRC progression and how are they correlated with sialyltransferase expression?
3. Utilising miRNA prediction software, can miRNAs be predicted to be involved in regulating sialyltransferase expression and what is their role in CRC progression?
4. Do sialyltransferases play any role in interacting with myeloid cells or prevalent immune checkpoint proteins and what is their relevance to CRC tumour heterogeneity?
5. What are the roles of sialyltransferases in the production of the STn antigen and other tumour associated glycans at the protein level?
6. Are sialyltransferases suitable therapeutic targets in CRC tumours and is their inhibtion sufficient for the disruption of the Siglec-15/STn axis?

2.2 Methodology

The large proportion of models utilised for this chapter will incorporate *in silico* multiomics database tools to highlight deregulated sialyltransferase expression and their relevance to CRC progression and tumour heterogeneity, as listed in the previous section. Although the STn antigen is often overexpressed in malignancies including CRC, the protein expression of ST6GalNAc1 and ST6GalNAc2 in CRC patient tissues are often limited. Hence, histological staining of CRC patient tissues will reveal the protein levels of ST6GalNAc1 and ST6GalNAc2.

2.2.1 GeneMANIA

The GeneMania predictive database exhibits functional information relating to queried genes based on specific gene datasets and interactions from several criteria. The genes of *ST6GALNAC1*, S*T6GALNAC2*, *ST3GAL4* and *ST6GAL1* were uploaded to the GeneMania predictive database (https://genemania.org/; accessed 26 July 2023), and predictive gene targets were determined with a high degree of association (Warde-Farley et al., 2010).

2.2.2 Search Tool for the Retrieval of Interacting Genes/Proteins (STRING) Analysis

STRING analysis identified protein-protein interactions (PPI) with defined parameters upon the queried protein. The STRING 11.0 (https://version-11-0b.string-db.org/cgi/input?sessionId=brxKfZgAG9Au&input_page_show_search=on; accessed 2 August 2023) software highlighted PPI relationships between ST6GalNAc1, ST6GalNAc2, ST3GalIV and ST6Gal1. The established PPI network highlighted functional and physical protein associations with an initial 5 protein targets. Expansion of the PPI framework with the queried protein exhibits a further 5 interactive protein targets with a high confidence interval of ≥ 0.900.

2.2.3 UALCAN transcriptomics

The UALCAN transcriptomics database outlined corresponding to TCGA genomic expression data for the query genes *ST6GALNAC1* (ENSG00000070526), *ST6GALNAC2* (ENSG00000070731), *ST3GAL4 (*ENSG00000110080) and *ST6GAL1* (ENSG00000073849) following comparisons between normal tissue (N=41) and CRC tumour (colon

adenocarcinoma; COAD) (N=286) cohorts. Similarly, identified miRNA candidates obtained from the *in silico* GeneMANIA and STRING analyses that were predicted to regulate the expression of the chosen query genes were determined between normal tissue (N=7) and COAD (N=251) tumours. Furthermore, expression data was presented as transcript per million (TPM), with box plots constructed using GraphPad Prism 9.0 software and Welch's t-test PERL script statistical analysis encoded onto the UALCAN software to identify differences in clinicopathological features between cohorts (Chandrashekar et al., 2022). Additionally, methylation of DNA promoter regions between normal (N=37) and tumour (N=313) cohorts was compared for all query genes and was presented as β-values (Weinhold et al., 2016). The resulting data with $P< 0.05$ was considered as statistically significant.

2.2.4 MiRNA candidate prediction analysis

A series of miRNA-target predictive software databases were utilised to determine novel candidate miRNAs involved in the regulation of *ST6GALNAC1*, *ST6GALNAC2*, *ST3GAL4* and *ST6GAL1*. The most common miRNAs across each of the chosen databases: TargetScan (https://www.targetscan.org/vert_80/; accessed 28 July 2023), miRSystem (http://mirsystem.cgm.ntu.edu.tw/index.php; accessed 28 July 2023), miRWalk (http://mirwalk.umm.uni-heidelberg.de/; accessed 28 July 2023 and miRDB (https://mirdb.org/; accessed 28 July 2023) were determined and presented in Venn diagrams using Venny 2.0 (https://bioinfogp.cnb.csic.es/tools/venny/). These databases integrates several prediction software algorithms by utilising validated experimental data that identified interactions between miRNAs and their target genes ($P <0.05$). Similarly, all of the miRNA targets that appeared in all four databases were cross-referenced for identified protein targets from the STRING and GeneMANIA prediction analyses. The criteria for miRNA candidate selection were determined in a score prediction hierarchy with those chosen with a cut-off value of 0.900. However, if no miRNAs were observed in the query search across all four chosen databases, the number of databases required were less constringent. In addition, any number of miRNAs were chosen for further prediction if their score prediction was above the cut-off value. Conversely, the most frequent miRNA 'hits' that were identified out of all four databases that was associated with the sialyltransferase query search were further explored, and possible gene binding sites were determined using statistical folding of nucleic acids and studies of regulatory RNAs (Sfold) software (https://sfold.wadsworth.org/cgi-bin/starmir.pl; accessed 13 September 2023).

2.2.5 Gene Set Enrichment Analysis (GSEA)

Enrichment analysis of gene sets related to specific cancer hallmarks associated with tumour progression including oncogenic signalling pathways, EMT, angiogenesis and inflammation were conducted for *ST6GALNAC1, ST6GALNAC2, ST3GAL4* and *ST6GAL1* using the TCGA dataset (TCGA, PanCancer Atlas) from the cBioPortal open access omics repository (http://cbioportal.org/ accessed on 19 September 2023). The selected dataset for CRC comprised a total of 524 patient samples (280 female, 312 male) with an age range of 35yrs – 90yrs for omics analysis. Each queried gene was modified to include only differentially expressed (DE) genes in relation to the normal tissue cohort with a z-score threshold of ± 2.0. Each queried gene dataset has a varied number of DE genes for analysis, and only statistically significant were chosen. A total of 6667 genes for the *ST6GALNAC1* dataset, 4331 genes for the S*T6GALNAC2* dataset, 6348 genes for the *ST3GAL4* dataset and 707 genes for the *ST6GAL1* dataset were identified for enrichment analysis, respectively. The resultant datasets were then sorted to include only the Log2 expression level in a ranked hierarchy. Following this, all queried gene datasets were uploaded into the GSEA v4.3.2 software as rnk files (.csv to .rnk file type change) (https://www.gsea-msigdb.org/ accessed on 19 January 2023). Specific parameters of each dataset were set at 1000 permutations, no collapse (all DE genes were utilised). Upregulated and downregulated pathways and biological processes were identified relating to tumour progression (FDR <0.25 and P <0.05 were considered as statistically significant).

2.2.6 TISIDB immune infiltration analysis

TISIDB is an integrated repository (http://cis.hku.hk/TISIDB/index.php; accessed on 26 July 2023) that outlines connections between 20 different tumour types (N= >8000 tumours) and the abundance of 28 different myeloid cell populations, which are correlated via the Spearman's rank correlation coefficient. Additionally, the relative abundance of each myeloid cell population was determined via gene set variation analysis (GSVA) based on the expression profiles of the query genes. The selected myeloid cell populations chosen are those that are consistently associated with the development of the TME and were analysed as follows: macrophages, activated $CD4^+$ T-cells, activated $CD8^+$ T-cells, T_{regs} and interactions with the sialyltransferase genes *ST6GALNAC1*, *ST6GALNAC2*, *ST3GAL4* and *ST6GAL1* and their clinical relevance to CRC tumours (Ru et al., 2019).

2.2.7 Tumour IMmune Estimation Resource (TIMER) analysis

TIMER analysis (https://cistrome.shinyapps.io/timer/, accessed on 1 August 2023) determined the correlation between the queried genes *ST6GALNAC1*, *ST6GALNAC2*, *ST3GAL4* and *ST6GAL1* and the abundance of chosen prevalent immune checkpoint proteins relating to CRC malignancies (N=457) including *SIGLEC15, PDCD1, CD274, CTLA4, TIGIT,* and *LAG3*. Spearman's rank correlation coefficient analysis determined the statistical significance of COAD tumours via $P< 0.05$ for log2 TPM (T. Li et al., 2017).

2.2.8 Kaplan-Meier (KM-plot)

Kaplan-Meier plots (https://kmplot.com/analysis/, accessed on 26 July 2023) were constructed to outline the prognostic value of high (red) and low (black) expression of the queried genes *ST6GALNAC1*, *ST6ALNAC2*, *ST3GAL4* and *ST6GAL1* and COAD patient survival outcomes over an extended period of time. Parameters relating to overall survival criteria (OS) (N=1061), relapse-free survival (RFS) (N=1336), post-progression survival (PPS) (N=311), hazard ratio (HR), 95% confidence interval (CI), and Log-rank $P <0.05$ were also determined (Győrffy, 2021).

2.2.9 Immunohistochemistry staining

To determine the protein expression of ST6GalNAc1 and ST6GalNAc2 in malignant tumour tissues, histological staining was conducted on normal colon and CRC tissues. The CRC tissue array (Reference code: BC05023a) was obtained from Biomax (TissueArray.Com LLC, Maryland, USA) and contained a total of 18 patient samples (54 cores) outlined as (18 COAD, 18 cancer adjacent colon tissue (AT), and 18 adjacent normal colon tissue (NAT)). Information pertaining to patient age, gender, pathology diagnosis and TNM stage are provided (Appendix 2).

Deparaffinisation of the tissue array was achieved by submerging the sections with a combination of histoclean/ethanol and varied ethanol concentrations (50%, 70%, 95% and 100%) for 3 min wash steps. Following deparaffinisation, antigen retrieval was conducted via treatment with sodium citrate (2.94g/L, 500µL Tween-20, pH 6.0) heated to a temperature of 75°C for 10 min, with 30s cooling intervals, before subsequent washes with 0.025% triton-x/PBS and incubation with 3% hydrogen peroxide:PBS for a total of 15 min. Following incubation, additional wash steps were performed with Triton-X100/PBS for 5 min. Before

primary antibody incubation, non-specific binding sites were blocked using 5% BSA/PBS (2.5g BSA/50mL PBS) followed by an incubation step in an encased humidity chamber with parafilm for 1h at room temperature (RT). The tissue arrays were then incubated with the primary antibodies of ST6GalNAc1 (1:50 dilution; recommended by the manufacturer) (Proteintech Group, Inc., Manchester, UK) and ST6GalNAc2 (1:100 dilution; recommended by the manufacturer) (Life Technologies Limited, Renfrewshire, UK) overnight at 4°C. Following overnight incubation, the tissue arrays were washed with Triton-X100/PBS prior to a 1h incubation with a biotin-labelled anti-rabbit secondary antibody at RT. Following this, the tissue arrays were further washed with 0.025% Triton X-100/PBS and incubated within a humidity chamber with a streptavidin-HRP conjugate for 1h at RT. Additionally, visualisation of the antibody staining was determined following addition of DAB solution (Zytomed Systems GmBH, Berlin, Germany) and haematoxylin nuclear staining for 10 min at RT. The tissue arrays were stained with 0.1% sodium bicarbonate solution (1.0g/L dH_2O) for 30s and rehydrated with the histoclean/ethanol and varied ethanol concentrations for 3 min. Coverslips were mounted onto the tissue arrays with DPX mountant (Sigma-Aldrich, Gillingham, UK) solution. Quantification and imaging of the tissue cores were performed using an AxioCam Hrc (Zeiss Microscopy, Oberkochen, Germany) microscope set at x4 and x10 magnifications. Analysis of the overall staining and staining intensity was conducted by three independent people to prevent subjective bias following scoring criteria (Table 2, Figure 16). Statistical analysis of the staining compared the expression of ST6GalNAc1 and ST6GalNAc2 in normal colon tissues and malignant tumour tissues via unpaired student's t-test.

Table 2: Staining criteria for ST6GalNAc1 and ST6GalNAc2 in normal and malignant CRC tissues. Cellular and core staining was determined under a light microscope position and was compared between three independent people. Scores based on the following criteria were tabulated and averages determined the level of protein staining.

	Cellular intensity staining of antibody	Overall core staining
0	No staining	<10% of cells
1	Only a few number of cells stained with primary antibody	10%-25% of total core stained
2	Up to 10% of cells stained with primary antibody	25%-50% of total core stained
3	10%-50% of cells stained with primary antibody	50%-75% of total core stained

4	>50% of cells stained with the primary antibody	>75% of total core stained

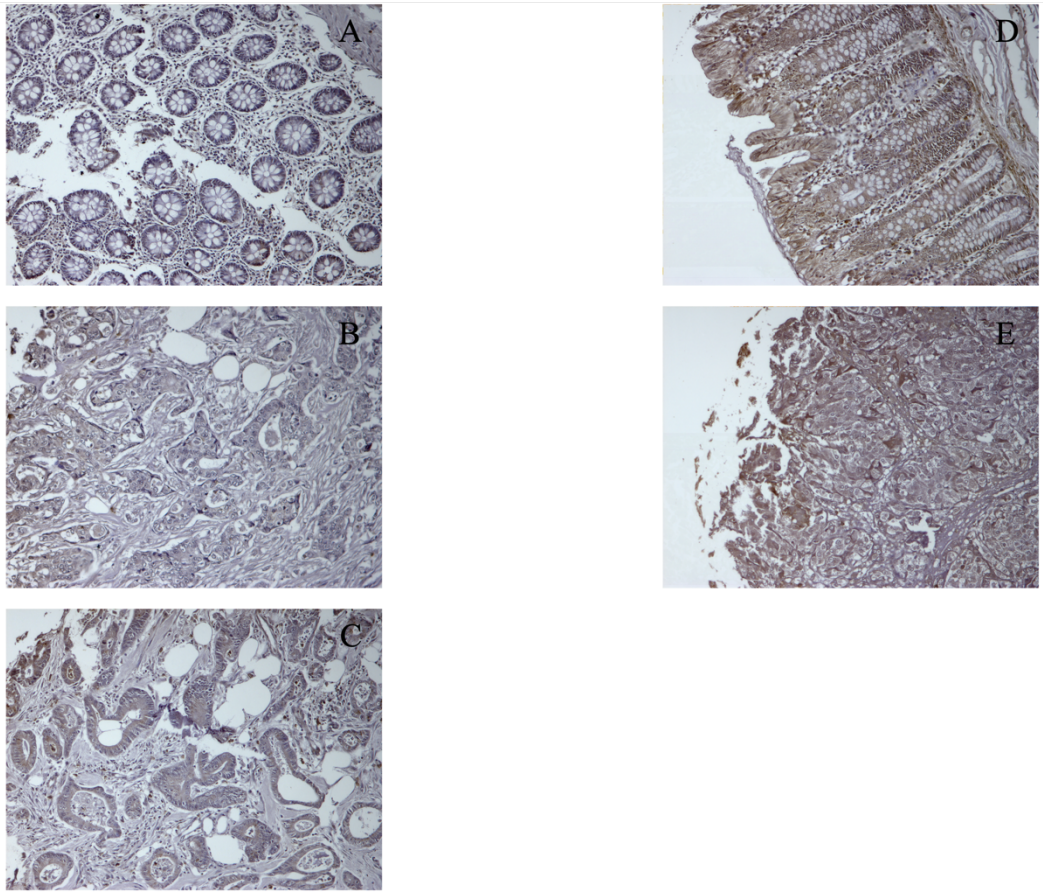

Figure 16: Core images representing the staining criteria of sialyltransferase ST6GalNAc1 and ST6GalNAc2. (**A**) Tissue has very little staining of the antibody and less than <10% of cells are stained providing a score of 0. (**B**) Only a small proportion of cells are stained with the primary antibody with only 10%-25% of the total tissue core providing an adequate staining providing a score of 1. (**C**) A larger proportion of cells are now stained in comparison to the previous score with almost 25%-50% of the tissue core stained providing a score of 2. (**D**) Approximately 50% of all cells are stained with the primary antibody and greater than 50% of the tissue is subsequently stained providing a score of 3. (E) Greater than 50% of cells are adequately visibly stained with the primary antibody and more than 75% of the total tissue core is stained with the brown pigmentation providing a score of 4.

2.3 Results

2.3.1 Sialyltransferase predicted interactions and molecular networks

The utilisation of gene and protein databases such as STRING and GeneMANIA predicted PPI and gene interactions associated with the queried genes.

The predictions exhibited by the GeneMANIA database for the *ST6GALNAC1* gene constructed a framework that incorporated a varied collection of sialyltransferases that are involved mainly throughout the glycan biosynthesis pathway. The framework highlighted a large predictive co-expression (purple) with the gene anterior gradient 2 (*AGR2*) and a minor co-expression prediction with fellow sialyltransferase *ST6GALNAC6* (Figure 17A). Upon inspection of the STRING analysis, the ST6GalNAc1 PPI framework was built with important sialyltransferases related to glycan synthesis. In particular, ST6GalNAc1 was emphasised to share PPI with Core 1 synthase glycoprotein-N-acetylgalactosamine 3-β -galactosyltransferase (C1GALT1), C1GALT1 specific chaperone 1 (C1GALT1C1; COSMC), UDP-GlcNAc:βGal β-1,3-N-acetylglucosaminyltransferase 6 (B3GNT6), glucosaminyl (N-acetyl) transferase 1 (GCNT1) and polypeptide N-acetylgalactosaminyltransferase 6 (GALNT6) Figure 17B). Furthermore, quantitative analysis of the STRING framework determined an average local clustering coefficient (ALCC) of 0.837 indicating a high association with the predicted protein targets (Table 3). Similarly, the analysis has also shown a significant PPI enrichment score upon normalization of $1.87e^{-10}$ at the confidence interval ≥0.900.

Similarly, the GeneMANIA database constructed a genetic framework for *ST6GALNAC2,* which was characterised by a large prediction of physical interactions (red) with a collection of mucin proteins (Figure 18A). Moreover, *ST6GALNAC2* was predicted to be co-expressed with ST8 α-N-Acetyl-Neuraminide α-2,8-Sialyltransferase 5 (*ST8SIA5*). However, STRING analysis exhibited no protein interactions at the ≥0.900 confidence interval. Hence, developing a PPI framework established at a lower confidence interval of ≥0.700 outlined initial interactions with C1GALT1, C1GALTC1, mucin-1 (MUC1), α-2-HS-glycoprotein (AHSG) and eukaryotic translation elongation factor 1α-2 (EEF1A2) (Figure 18B). Furthermore, the ST6GalNAc2 ALCC was recorded as 0.749 and the PPI enrichment score as $3.11e^{-8}$, suggesting a significant correlation to the predicted proteins that were identified (Table 3).

Upon constructing the gene framework for *ST3GAL4* via the GeneMANIA database, predicted physical interactions dominated a large proportion of the overall framework (Figure 19A). In addition, *ST3GAL4* displayed co-expression with the genes *ST3GAL1*, *ST6GALNAC6* and *ST8SIA5*. Furthermore, there were also genetic interactions (green) that were associated with *ST6GALNAC3*. Similarly, the development of the PPI framework from the STRING database outlined interactions with fucosyltransferase-1/-2/-3 (FUT1, FUT2, FUT3) proteins in addition to β-1,3-galactosyltransferase-2/-5 (B3GAL2, B3GAL5) (Figure 19B). Furthermore, ST3GalIV displayed the highest ALCC score of 0.900 and a PPI enrichment of $3.00e^{-15}$ (Table 3), emphasising significant correlation between the predicted proteins.

Similarly to *ST6GALNAC2*, the GeneMANIA framework for the *ST6GAL1* query gene established a large number of physical interactions with several mucin genes alongside further predicted communication (orange) with *FUT1*, *CD22* and SRY-related HMG box 2 (*SOX2*) transcription factor. In addition, the framework also exhibited pathway interactions (light blue) of POU class 2 homeobox transcription factor 1 (*POU2F1*) (Figure 20A). Moreover, ST6GalI STRING analysis predicted several interactions with β-1,4-galactosyltransferase enzymes (B4GALT1, B4GALT2, B4GALT3) alongside interactions with ST6GalII (Figure 20B). In addition, quantitative analysis of the STRING framework established an ALCC score of 0.858 and a PPI enrichment value of $3.51e^{-7}$ (Table 3).

Lastly, framework constructions of all queried genes and proteins from the GeneMANIA database characterised physical interactions with mucin genes and sialyltransferases present in glycan synthesis (Figure 21A). Additionally, *FUT1* was predicted to interact with *ST6GAL1* and also be co-expressed with *ST6GALNAC2*. Furthermore, *ST6GAL1* also shared genetic interactions with one of the query genes, *ST3GAL4*. In contrast, at the confidence interval ≥0.900, the PPI STRING analysis exhibited several interactions with protein targets for ST6GalNAc1 (Figure 21B), which correlated previously in its own STRING analysis, including B3GNT6 and also GALNT8 and C1GALT1C1L (identified as part of the second expansion of the PPI framework) (Figure 21B). In addition to this, ST3GalIV also displayed interactions with B3GALT1 and B3GALT2 but as a separate interactive cluster. However, both ST6GalNAc2 and ST6GalI displayed no common interactions with other proteins. Furthermore, quantitative analysis revealed an ALCC score of 0.750 and an enrichment PPI of 0.0146, demonstrating a significant association of currently available protein targets (Table 3).

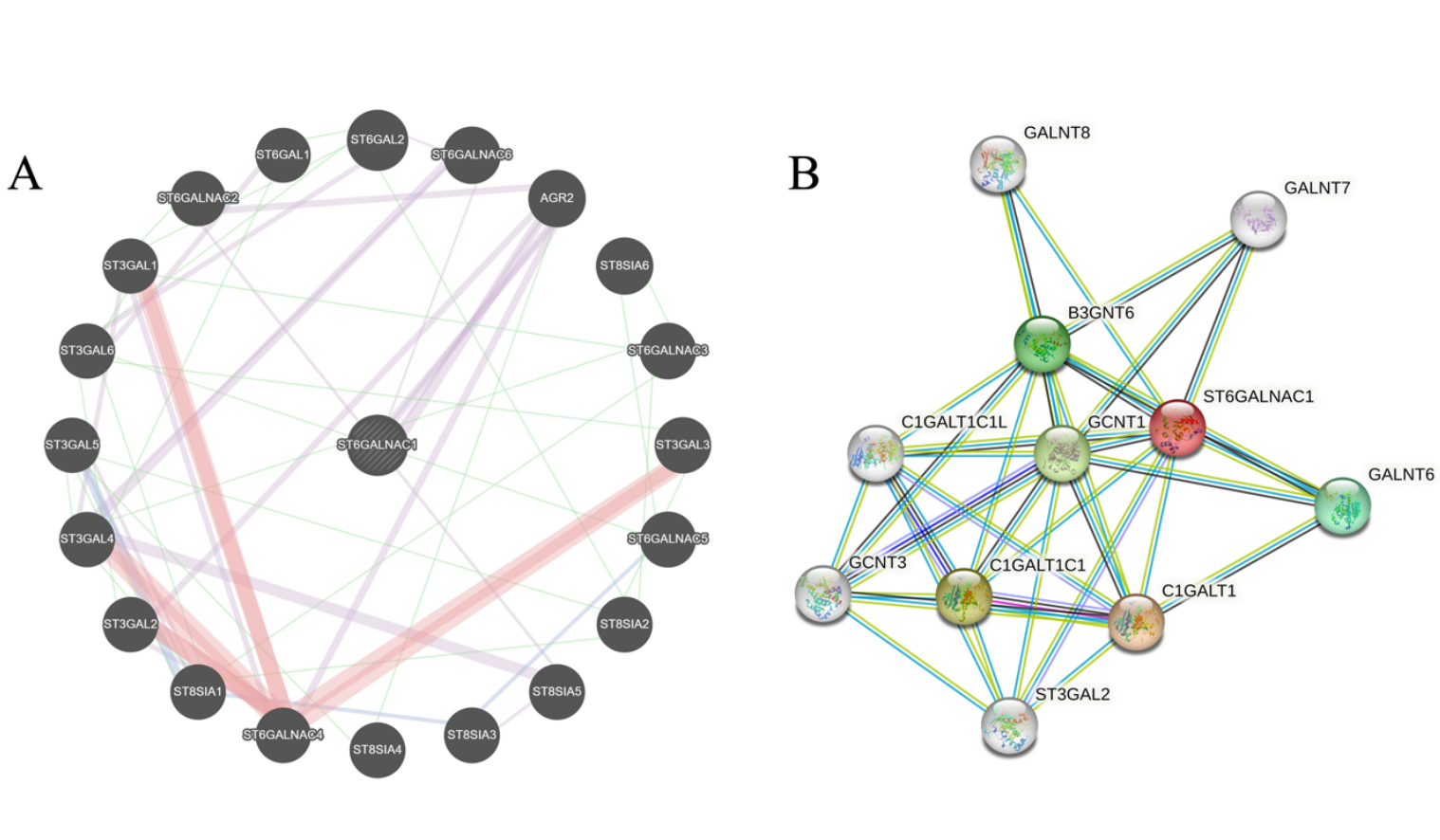

Figure 17: *ST6GALNAC1* shares significant gene communication with other sialyltransferases within the sialoglycan biosynthesis pathway and PPI interactions alongside proteins involved in the production of complex mucin type O-glycans. (**A**) *ST6GALNAC1* gene framework predicts functional information based on corresponding genes and gene datasets. (**B**) ST6GalNAc1 STRING framework highlighting possible PPI from interacting proteins and direct associations via computational data mining. The framework is developed with a confidence interval of ≥ 0.900.

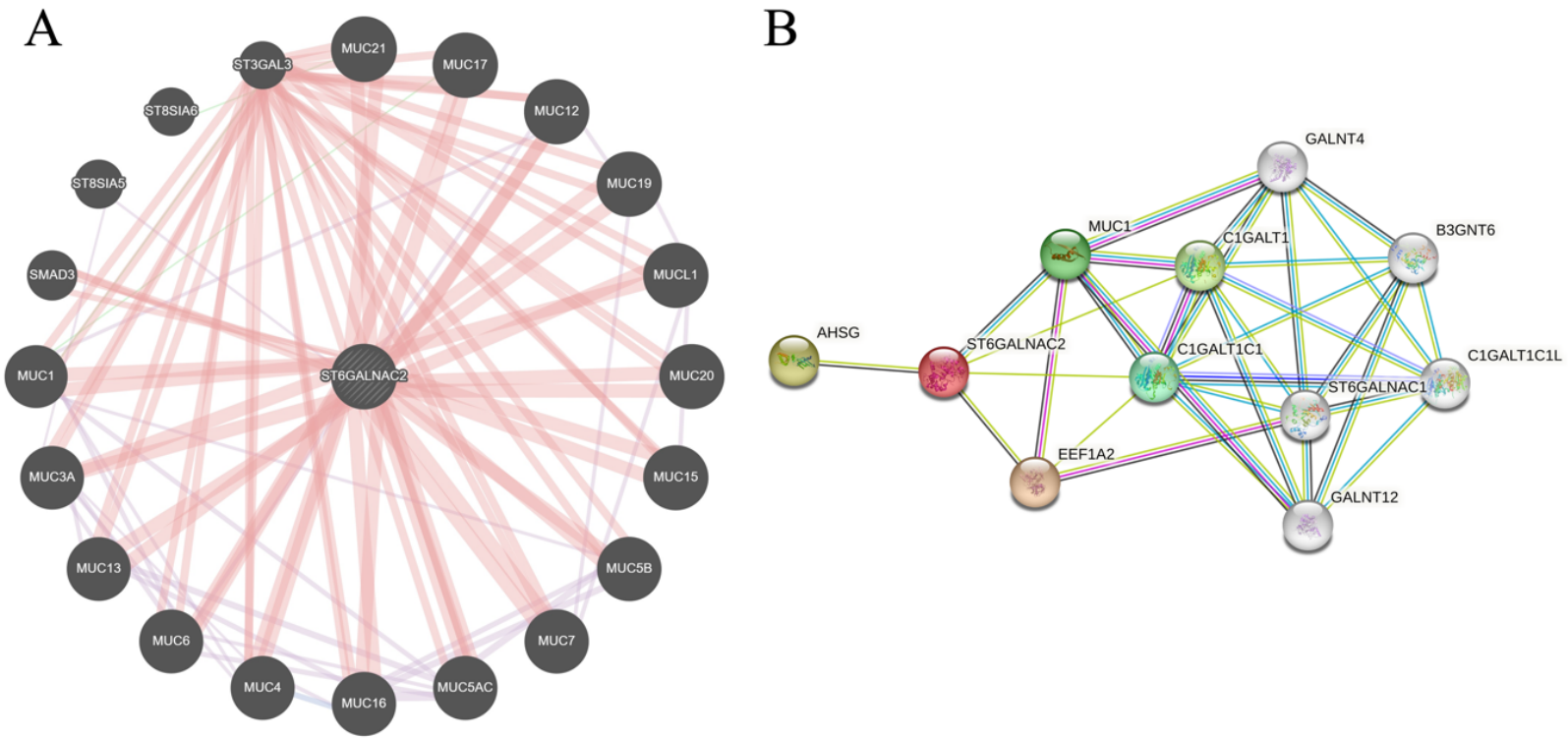

Figure 18: *ST6GALNAC2* shares significant gene communication with mucin genes and PPI interactions with AHSG and EEF1A2. (**A**) *ST6GALNAC2* gene framework predicts functional information based on corresponding genes and gene datasets. (**B**) ST6GalNAc2 STRING framework highlighting possible PPI from interacting proteins and direct associations via computational data mining. The framework is developed with a confidence interval of ≥ 0.700.

Table 3: Predicted sialyltransferase STRING PPI relationship and association analysis. Computational analysis of query proteins ST6GalNAc1, ST6GalNAc2, ST6GalI and ST3GalIV following construction of the PPI framework.

	Number of nodes	Number of edges	Average node degree	Average local clustering coefficient	Expected number of edges	PPI enrichment p-value
ST6GalNAc1	11	36	6.55	0.837	10	$1.87e^{-10}$
ST6GalNAc2	11	32	5.82	0.749	10	$3.11e^{-8}$
ST3GalIV	11	44	8	0.900	10	$3.00e^{-15}$
ST6GalI	10	28	5.6	0.858	9	$3.51e^{-7}$
Combination	14	18	2.57	0.750	10	0.0146

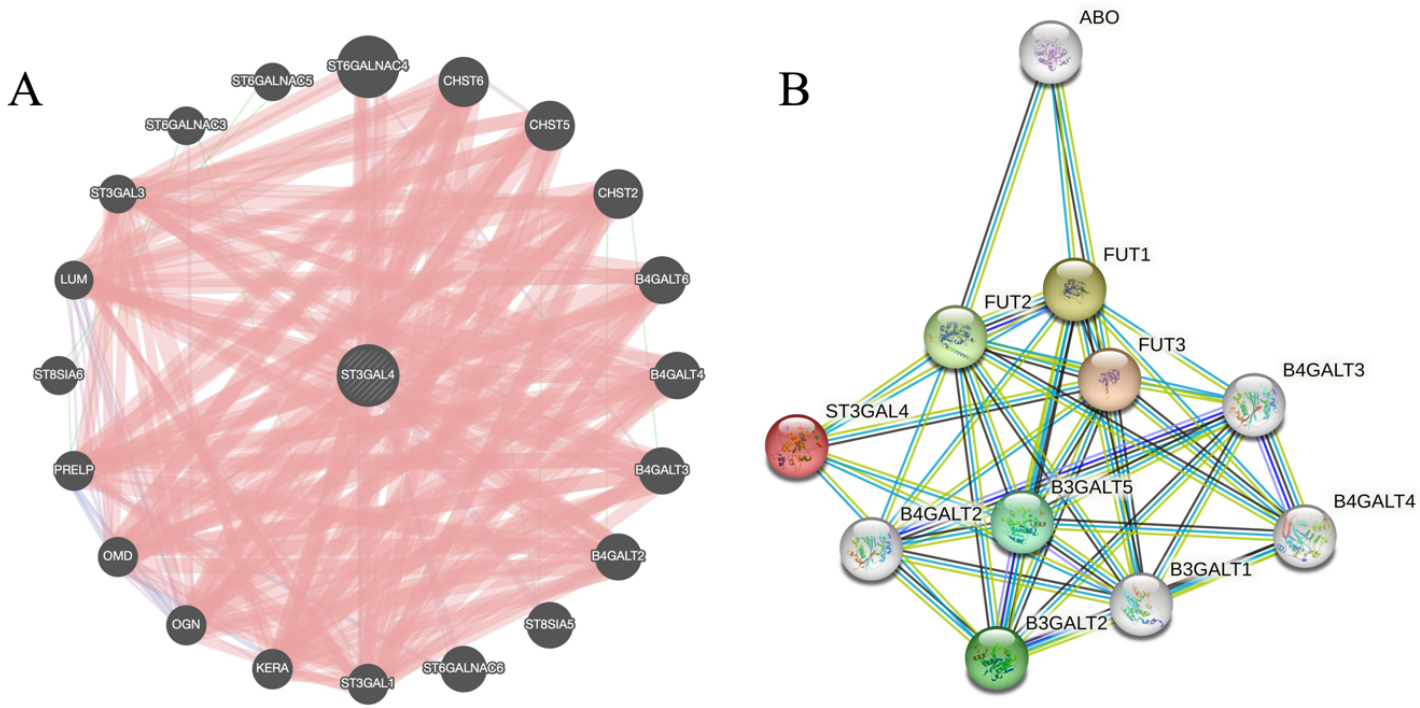

Figure 19: *ST3GAL4* shares significant physical gene interactions with sialyltransferases and with β-1,3-galactosyltransferases and fucosyltransferase proteins, highlighting key targets. (**A**) *ST3GAL4* gene framework predicts functional information based on corresponding genes and gene datasets. (**B**) ST3GalIV STRING framework highlighting possible PPI from interacting proteins and direct associations via computational data mining. The framework is developed with a confidence interval of ≥ 0.900.

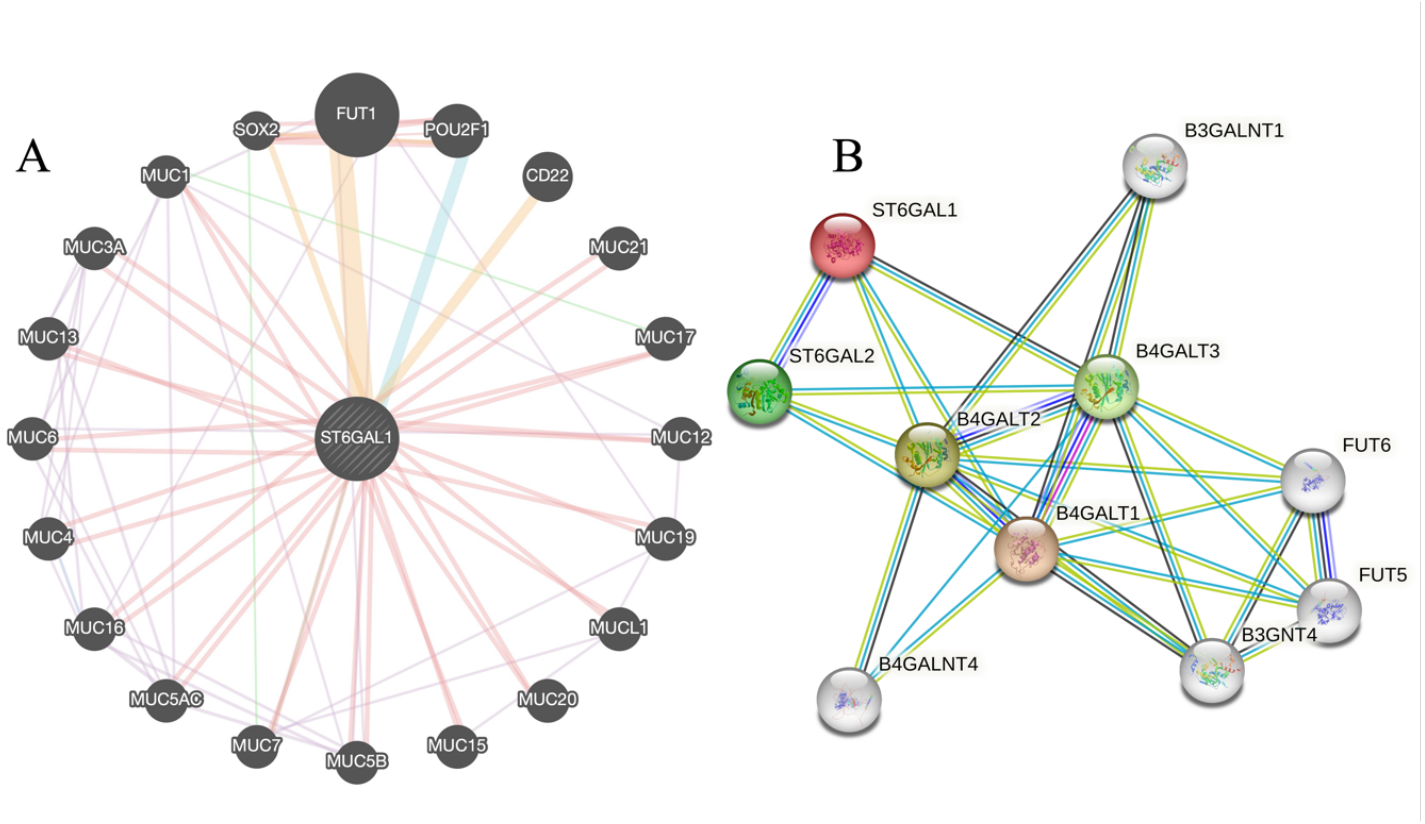

Figure 20: *ST6GAL1* shares significant gene and protein-protein interactions with sialyltransferases and may highlight key targets. (**A**) *ST6GAL1* gene framework predicts functional information based on corresponding genes and gene datasets. (**B**) ST6Gal1 STRING framework highlighting possible PPI from interacting proteins and direct associations via computational data mining. The framework is developed with a confidence interval of ≥ 0.900.

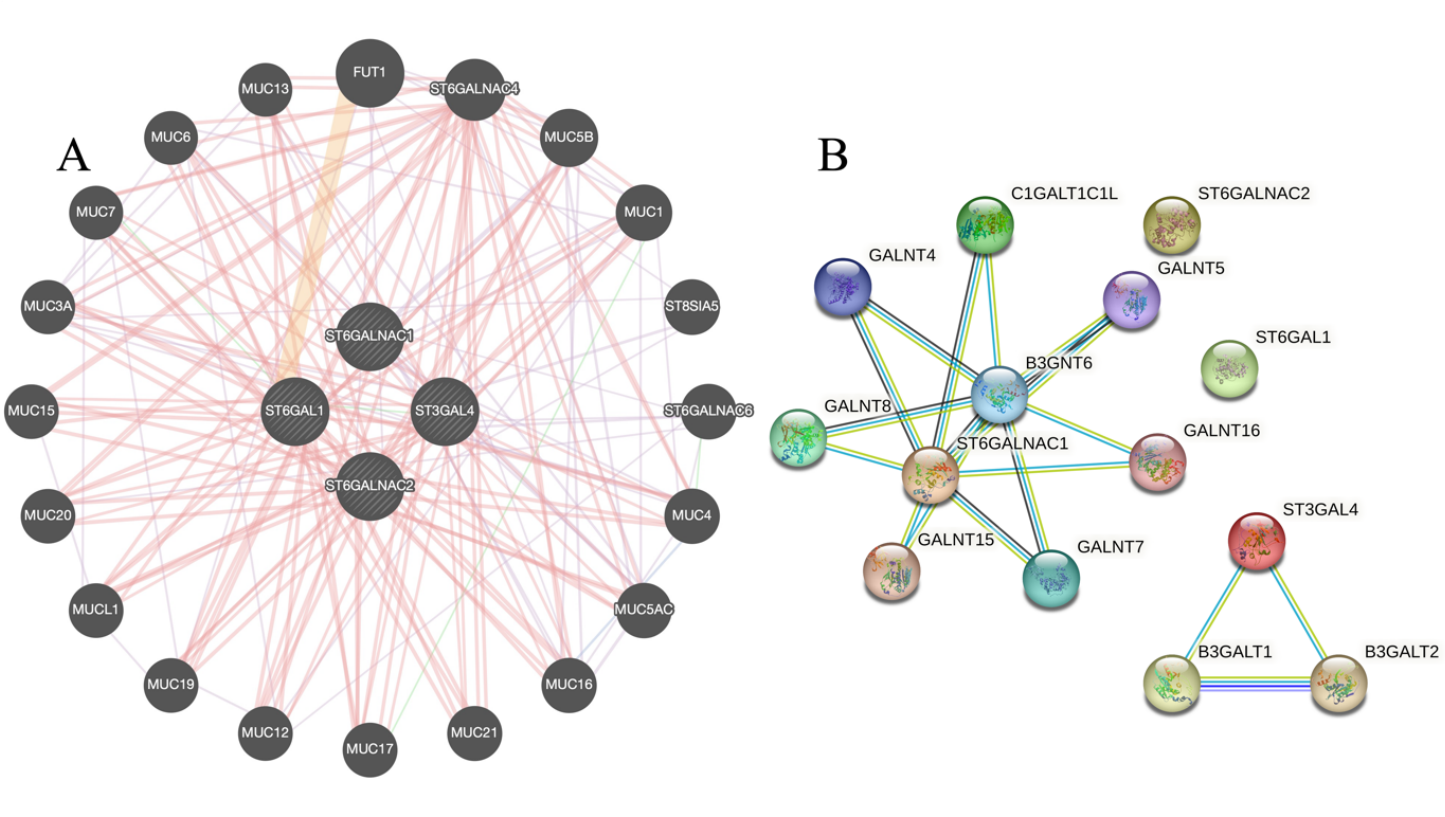

Figure 21: Sialyltransferases share significant gene and protein-protein interactions with sialyltransferases and may highlight key novel targets. (**A**) Combinative network of all query genes *ST6GALNAC1*, *ST6GALNAC2*, *ST3GAL4* and *ST6GAL1* were all integrated into the GeneMANIA database, which identified any communication between genes and interaction partners. (**B**) Combinative network of all query genes *ST6GALNAC1*, *ST6GALNAC2*, *ST3GAL4* and *ST6GAL1*, which characterised protein interactions and PPI relationships via computational STRING software. The confidence interval between interaction proteins was set as ≥ 0.900.

2.3.2 Transcriptomics analysis of sialyltransferase expression profiles in normal and COAD tumours

To determine whether the query sialyltransferase genes have differential expression in CRC tumours, expression data comparing normal (N=41) and COAD (N=286) tissues were performed utilising TCGA transcriptomics data mining which constructed box plots (Figure 22). *ST6GALNAC1* demonstrated significantly downregulated expression in the COAD tumour cohort with a mean TPM of 46.056 in comparison to the recorded TPM expression value of 173.703 TPM ($P< 0.0001$) in normal colon tissues (Figure 22A). This was also similarly observed in the expression of *ST3GAL4*, which exhibited reduced expression in the tumour cohort, having recorded a TPM expression of 41.021 in normal tissues and 17.917 TPM in malignant tissues ($P< 0.01$), respectively (Figure 22C). In contrast, *ST6GALNAC2* exhibited no significant difference in gene expression between the normal colon tissue (3.509 TPM) and tumour (1.813 TPM) cohorts (Figure 22B). However, *ST6GAL1* was demonstrated as the only gene to display upregulated expression in the tumour cohort with a mean expression of 38.457 TPM in normal tissues and 45.813 TPM in COAD tumours, respectively ($P< 0.001$) (Figure 22D).

Similarly, expression analysis of identified interactive targets of sialyltransferases was also determined between comparing normal (N=41) and COAD (N=286) tissues (Figure 23). GALNT proteins play a crucial role in the initial synthesis of the Tn antigen upon O-linked glycosylation of mucin-type glycoproteins, thus, are heavily involved in the production of the STn antigen precursor molecule (Beaman et al., 2022). Hence, the expression of *GALNT6* was elucidated in COAD tumours. *GALNT6* expression analysis displayed a mean expression of 6.198 TPM in normal colon tissues in contrast to a significant mean expression of 25.816 TPM in malignant tissues ($P< 0.0001$) (Figure 23A). Similarly, the expression of other GALNT proteins identified in the combination network (Figure 23B) was also elucidated to determine their correlation to CRC progression. *GALNT4* exhibited a similar expression to *GALNT6* by displaying significantly upregulated expression in the tumour cohort with a mean expression of 30.451 TPM ($P< 0.0001$) (Figure 23B). In contrast, *GALNT8* revealed no significant difference in gene expression between both normal and tumour cohorts (Figure 23C), whilst *GALNT7* exhibited significantly downregulated expression in the tumour cohort (32.805 TPM) when compared to the normal tissue cohort ($P< 0.0001$) (Figure 23D).

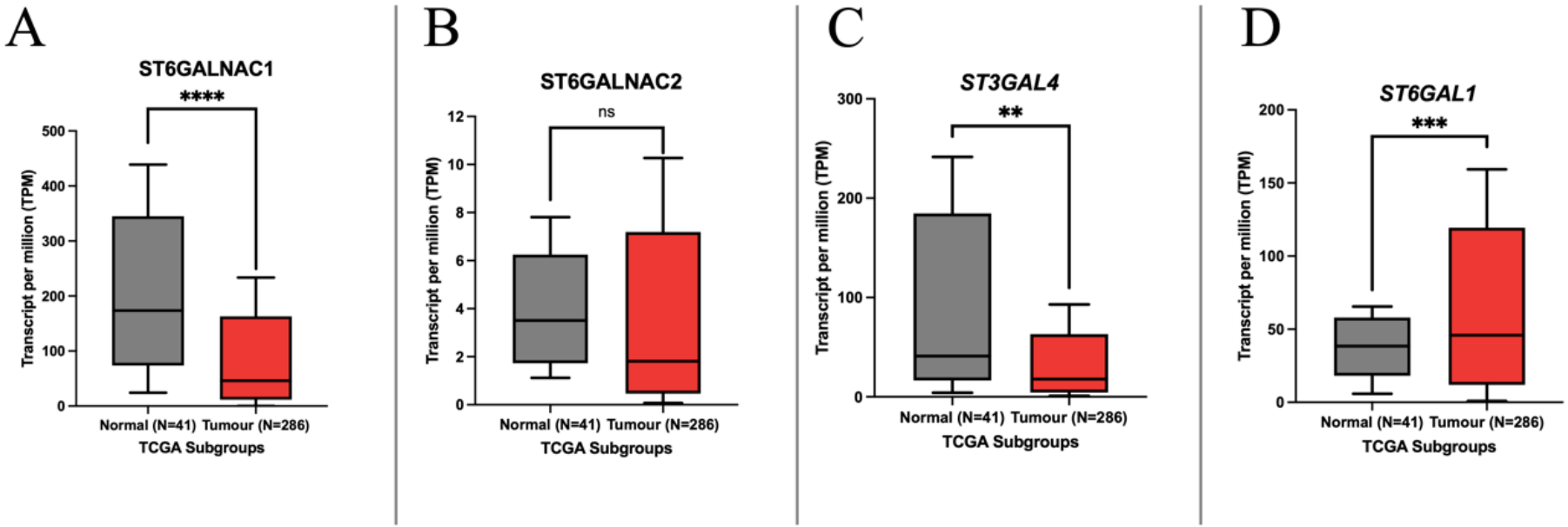

Figure 22: *In silico* UALCAN transcriptomics analysis revealed sialyltransferase expression is downregulated in tumour cohorts. (**A**) TCGA genomic data exhibiting mRNA expression of *ST6GALNAC1* in normal (grey) and COAD (red) cohorts, error bars ± SD. Welch's t-test PERL script. **** P <0.0001. (**B**) TCGA genomic data exhibiting mRNA expression of *ST6GALNAC2* in normal (grey) and COAD (red) cohorts, error bars ± SD. Welch's t-test PERL script. (ns). (**C**) TCGA genomic data exhibiting mRNA expression of *ST3GAL4* in normal (grey) and COAD (red) cohorts, error bars ± SD. Welch's t-test PERL script. ** P < 0.01. (**D**) TCGA genomic data exhibiting mRNA expression of *ST6GAL1* in normal (grey) and COAD (red) cohorts, error bars ± SD. Welch's t-test PERL script. *** P < 0.001.

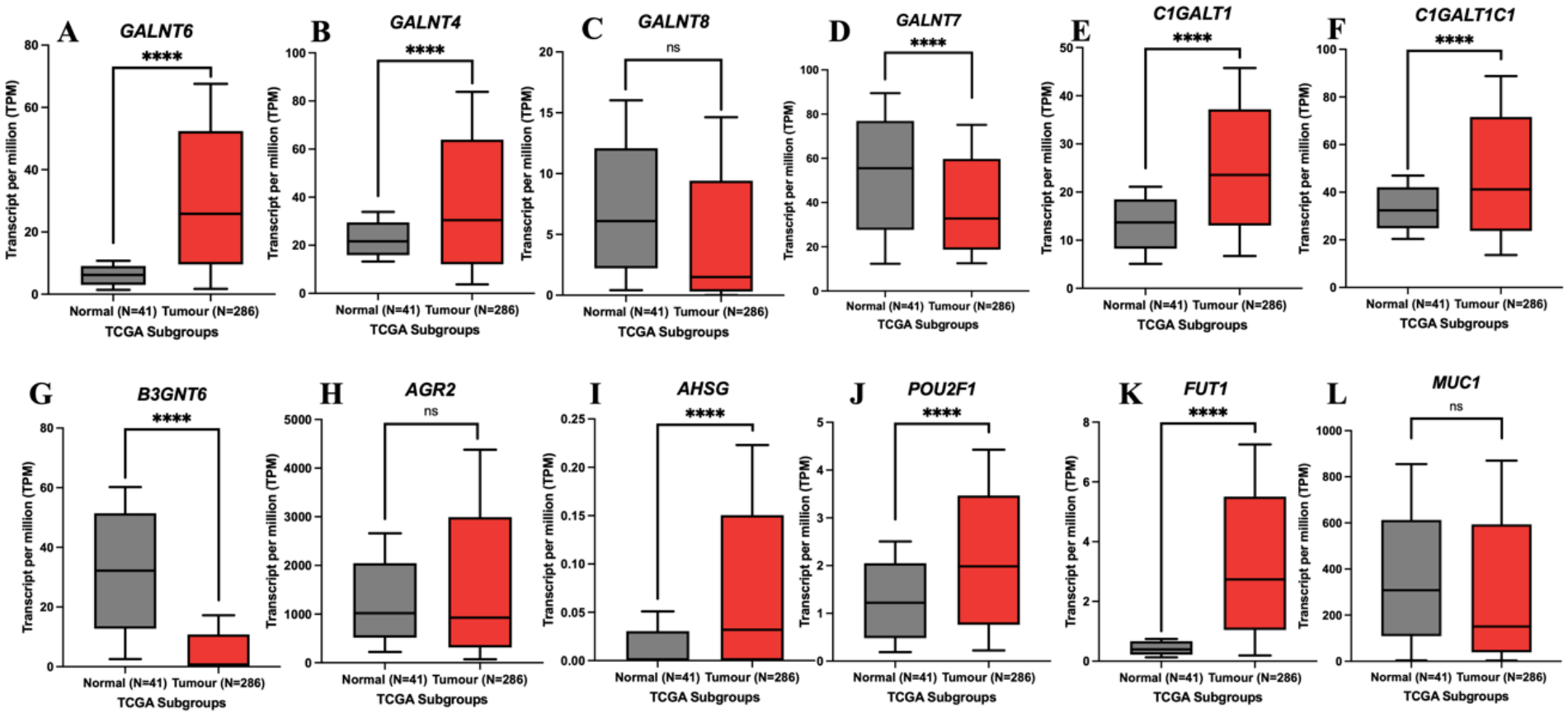

Figure 23: *In silico* UALCAN transcriptomics analysis revealed sialyltransferase expression patterns are dysregulated in COAD tumours. (**A-L**) Expression analysis comparing normal (N=41) and COAD (N=286) tissues was determined for interactive targets that were identified following GeneMANIA and STRING analyses which revealed *GALNT6, GALNT4, GALNT8, GALNT7, G1GALT1, C1GALTC1, B3GNT6, AGR2, AHSG, POU2F1, FUT1* and *MUC1* and all were compared between normal (grey) and COAD tumours (red) cohorts via UALCAN transcriptomics analysis, error bars ± SD. Welch's t-test PERL script statistical analysis. ns, **** $P < 0.0001$.

Likewise, C1GALT1, C1GALT1C1 and C1GALT1C1L were all identified across multiple STRING analyses, all of which dictate the level of Tn antigen that is present. C1GALT1 is directly involved in the generation of the core-1 O-glycan T-antigen structure (Galβ-1-3GalNAc-R) from the Tn antigen via transferring galactose from UDP-Gal to GalNAc-α-1-R (Liu et al., 2014), whilst assisted by the COSMC molecular chaperone exclusive to complex O-glycosylation (Erger et al., 2023). In addition, very little is known about the functional capability of C1GALT1C1L within the literature, but it is possible to be involved in the processing of O-glycans similar to COSMC. The lack of either C1GALT1 or the molecule chaperone leads to enhanced expression of both Tn and STn antigens (Xiang et al., 2022). Therefore, expression analysis of *C1GALT1* and *COSMC* is crucial to determine the role they play in the generation of the STn antigen. Both *C1GALT1* and *COSMC* exhibited significantly upregulated expression in COAD tumours with a mean expression of 13.699 TPM (normal tissues) and 23.550 TPM (COAD tissues) ($P< 0.0001$) and 37.216 TPM (normal tissues) and 54.406 TPM (COAD tissues) ($P< 0.0001$), respectively (Figure 23E-F).

Other sialyltransferases highlighted across the STRING analyses identified B3GALT and B4GALT proteins interacting with the original query proteins. Both groups of proteins result in the biosynthesis of sLE^a and sLE^x by supplementing galactose residues in β1,3 or β1,4 linkages to a GlcNAc residue present at the non-reduced terminus of oligosaccharides (Chachadi et al., 2015). Additionally, they are categorised as lactosamine chains and later catalysed by ST3Gal proteins for incorporation of sialic acids prior to the addition of fucose residues for the final synthesis of these sialoglycans (Chachadi et al., 2015). Due to the function these proteins play, it is very unlikely for these proteins to be involved in a significant role in STn production. Therefore, further study of these targets is not required. Moreover, the role of ST8Sia proteins is largely involved in the catalytic extension of PSA, in particular, *ST8SIA5,* which has shown co-expression with *ST6GALNAC2* is primarily involved in the synthesis of gangliosides and sialylated glycolipids (Hugonnet et al., 2021). Hence, it would not be highly involved in STn production.

Furthermore, B3GNT6 has also appeared in STRING PPI networks of ST6GalNAc1 and ST6GalNAc2 which could also affect the level of production for the STn antigen. Within glycan synthesis, B3GNT6 plays a role in synthesising core-3 O-glycan structures from the Tn precursor antigen (Doi et al., 2020; McVeigh et al., 2018). *B3GNT6* expression analysis

outlined downregulated expression in the CRC tumour group. *B3GNT6* demonstrated a mean expression of 32.203 TPM in the normal cohort in comparison to a substantially lower mean expression of 0.750 TPM in the tumour cohort ($P< 0.0001$) (Figure 23G).

Furthermore, expression analysis of co-expressed genes that are not sialyltransferases may highlight possible regulatory mechanisms that enable the differential expression of sialyltransferases. *AGR2* revealed no significant difference in the expression between normal and tumour cohorts (Figure 23H). However, *AHSG* exhibited significant upregulation in COAD tumours with a mean expression of 0.032 TPM in malignant tissues in contrast to 0.00 TPM expression in the normal tissue cohort ($P< 0.0001$) (Figure 23I).

Additionally, expression analysis of the pathway interactions with the *POU2F1* gene revealed in the *ST6GAL1* geneMANIA framework exhibited significant upregulation in the tumour group with a mean expression of 1.983 TPM in comparison to a mean expression of 1.223 TPM in normal colon tissues ($P< 0.0001$) (Figure 23J). Moreover, *FUT1* was predicted to interact with *ST6GAL1* and appeared in both combination and *ST6GAL1* GeneMANIA frameworks alongside exhibiting co-expression with *ST6GALNAC2* in the combination framework (Figure 21B), which may suggest a significant likelihood of interactions. Therefore, expression analysis revealed a mean expression of 0.393 TPM in normal tissues in comparison to a significantly increased mean expression of 2.738 TPM in malignant tissues ($P< 0.0001$) (Figure 23K).

MUC1 is a glycoprotein frequently displayed as having O-type glycosylation sites, where the addition of α-O-linked GalNAc occurs at the many tandem repeats located throughout its structure (Kudelka et al., 2015). Within the tumour landscape, tumour-associated MUC1 exhibits abnormal distribution over cellular surfaces due to changes in apical-basal polarity (Chugh et al., 2015). Moreover, enhancement of glycosylation on the N-terminal domains results in truncations of branched core 1 O-glycans (Burchell et al., 1999). These truncations can exhibit greater Sia capping when α2,6- and α2,3-sialyltransferases are significantly upregulated in tumours (Häuselmann & Borsig, 2014; Lu & Gu, 2015). From this, there is a greater production of tumour-associated antigens derived from incomplete glycan synthesis, including STn, Tn, TF and T antigens, all of which have been demonstrated as poor prognostic biomarkers (Beckwith & Cudic, 2020). Underlining the expression of MUC1 in CRC tumours

could correlate with the impact of MUC1-derived STn antigens in CRC progression and metastasis. MUC1 has shown no significant difference in its expression profile between normal tissue (308.004 TPM) and COAD (151.125 TPM) cohorts (Figure 23L).

Additionally, it is also worth noting the Pearson correlation analysis between the expression of the sialyltransferase query genes in CRC (N= 9736 tumour tissues, 8587 normal tissues; taken from the TCGA and GTEx repositories) revealed significant correlations among them (Figure 24). Comparisons between *ST6GALNAC1* and *ST6GALNAC2* expression suggested a low positive correlation among both genes. However, the exhibited relationship was shown to be significant (Figure 24A). Similarly, this was also observed from a positive correlation between *ST6GALNAC2* and *ST3GAL4* genes (Figure 24D). Moreover, there was a strong correlative relationship shown between the *ST6GALNAC1* and *ST3GAL4* gene with a regression value of 0.64 (Figure 24B). In contrast, *ST6GALNAC1* and *ST6GAL1* have shown a significantly negative correlation possibly indicting little to no interaction (Figure 24C). This was also similarly observed via a significantly negative correlation between *ST6GALNAC2* and *ST6GAL1* with a -0.29 regression (Figure 24E), and also alongside the TPM expression between *ST3GAL4* and *ST6GAL1* highlighting a regression value of -0.22, respectively (Figure 24F).

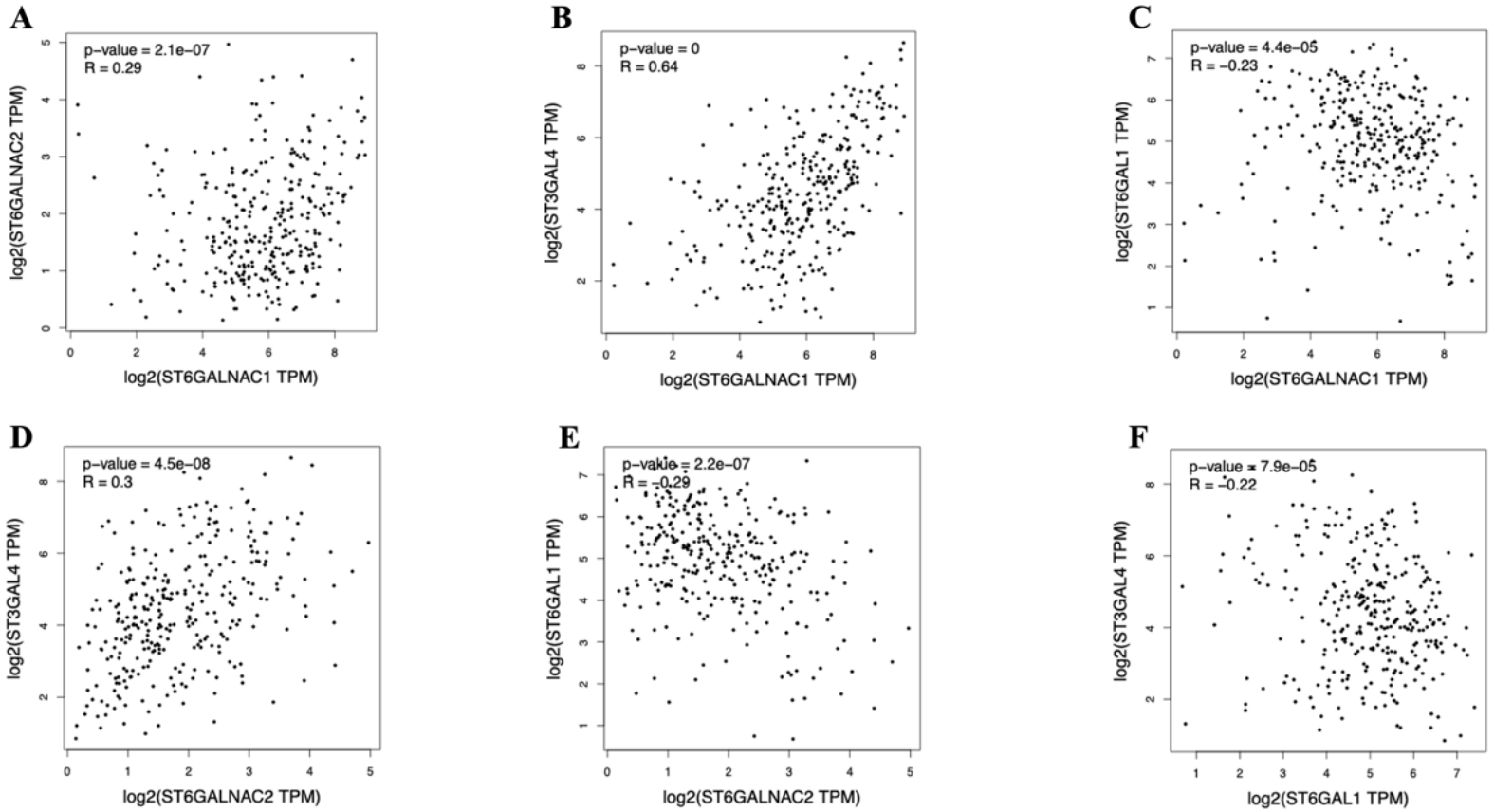

Figure 24: Pearson correlation analysis revealed a significant relationship between sialyltransferase genes. Pearson correlation analysis was conducted to determine the correlative relationship between the sialyltransferase query genes and their relevance to CRC progression (N= 9736 tumours, 8587 normal tissues; taken from the TCGA and GTEx repositories) utilising GEPIA software. (**A**) Pearson correlation coefficient analysis between Log_2 *ST6GALNAC1* expression TPM compared against Log_2 *ST6GALNAC2* expression TPM. (**B**) Pearson correlation coefficient analysis between Log_2 *ST6GALNAC1* expression TPM compared against Log_2 *ST3GAL4* expression TPM. (**C**) Pearson correlation coefficient analysis between Log_2 *ST6GALNAC1* expression TPM compared against Log_2 *ST6GAL1* expression TPM. (**D**) Pearson correlation coefficient analysis between Log_2 *ST6GALNAC2* expression TPM compared against Log_2 *ST3GAL4* expression TPM. (**E**) Pearson correlation coefficient analysis between Log_2 *ST6GALNAC2* expression TPM compared against Log_2 *ST6GAL1* expression TPM. (**F**) Pearson correlation coefficient analysis

between Log_2 *ST6GAL1* expression TPM compared against Log_2 *ST3GAL4* expression TPM. $P < 0.05$ was considered as statistically significant for all Pearson correlation analyses

2.3.3 Candidate miRNAs involved in the regulation of sialyltransferase expression

To underline the identities of miRNAs that are capable of modulating sialyltransferase expression, several miRNA target prediction databases were utilised to compare across *ST6GALNAC1*, *ST6GALNAC2*, *ST3GAL* and *ST6GAL1* and other identified interactive targets (Figure 25-29). The filtering of the miRNAs were produced by the software algorithms compiling bulk experimental datasets which provided score predictions for mRNA target binding to their target and ranked their binding probability ($P< 0.05$). With regard to *ST6GALNAC1*, there were no identified miRNAs that were predicted to regulate the gene across all four databases (Table 4). Hence, it was determined to reduce the constraints of the query search and thus reduce the number of databases to identify any possible targets. Additionally, due to the downregulated expression associated with *ST6GALNAC1* that was observed in the transcriptomics analysis, commonly deregulated miRNAs that are also downregulated were filtered out. The remaining candidate miRNAs that were overexpressed in relation to CRC progression were determined. Of those multiple miRNAs cross-referenced, a total of 16 common miRNAs were identified (Figure 25A) between miRSystem and TargetScan databases. It was revealed from that cluster that miR-21-5p, miR-30e-5p and miR-26b-5p could act as potential modulators of *ST6GALNAC1* and exhibit significantly upregulated expression in the tumour cohorts ($N=251$) ($P< 0.0001$) when compared to normal colon tissues ($N=7$) (Figure 25B). Furthermore, it is essential to determine possible binding sites among the *ST6GALNAC1* gene. MiRNA binding and resultant activity primarily occur at the 3' UTR region of the target mRNA strand. Therefore, this formed the basis of the Sfold predictive software. MiR-21-5p demonstrated a high binding affinity of -18.700 kcal/mol towards the seed region of the target *ST6GALNAC1* mRNA strand at position 2441-2458 (Figure 25C). In addition, both miR-30e-5p and miR-26b-5p revealed high binding affinities to the *ST6GALNAC1* gene with -22.200 kcal/mol and -17.600 kcal/mol, respectively. It was revealed that miR-30e-5p could potentially bind at position 2331-2348, whilst miR-25b-5p demonstrated a predicted binding site at position 2085-2113 of the target mRNA. Therefore, all identified miRNAs denoted a significant association with the nucleotide bases on the target strand.

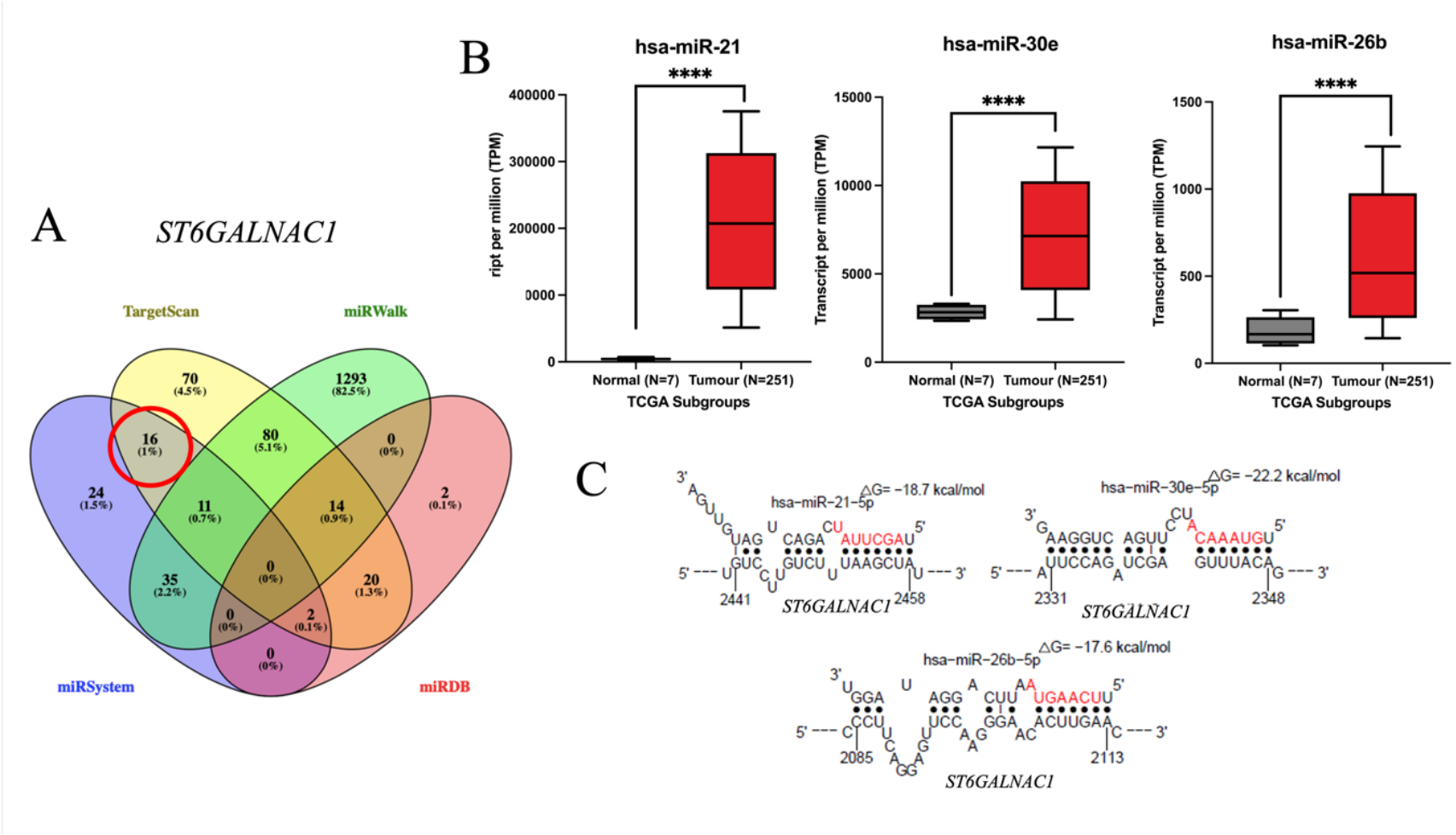

Figure 25: MiR-21, miR-30e and miR-26b all displayed significantly high binding affinities and upregulated expression in COAD tumours to regulate *ST6GALNAC1* expression. (**A**) Cross-referenced miRNAs from TargetScan, miRSystem databases demonstrated "16 hits" for *ST6GALNAC1* regulation. (**B**) Expression analysis was determined for predicted miRNAs and was compared between normal (grey) and COAD tumours (red) cohorts via UALCAN transcriptomics analysis, error bars ± SD. Welch's t-test PERL script statistical analysis. ****P <0.0001. (**C**) Predicted positional binding sites of the upregulated miRNAs were conducted, revealing high binding affinities for the *ST6GALNAC1* seedless region via Sfold predictive software.

When comparing all four databases to highlight common miRNA elements in *ST6GALNAC2* regulation, only hsa-miR-588 was identified across all miRNA predictive tools (Table 4, Figure 26A). Further expression analysis revealed no expression data available in the UALCAN transcriptomics database for both cohorts and there was no apparent difference in the expression of the miRNA in relation to CRC progression (Figure 26B). However, *ST6GALNAC2* displayed no significant difference in expression via transcriptomics analysis, and its protein only plays a role in STn production to a lesser extent in regard to ST6GalNAc1. Therefore, further study to determine miRNA regulation is warranted.

ST3GAL4 reported 2 common miRNAs across all four miRNA prediction databases (Figure 27A). They revealed hsa-miR-193a-3p and hsa-miR-370-3p as potential regulators of the gene (Table 4). However, the two miRNAs also exhibited downregulated expression in CRC progression, emphasising the need to reduce the number of databases in the query search similar to *ST6GALNAC1*. Based on this information, a total of 34 common elements were highlighted between three databases, miRSystem, TargetScan and miRWalk, which demonstrated significant upregulation of two possible miRNA candidates in the tumour cohor (N=251). They are revealed as hsa-let7g-5p and hsa-miR-98-5p (Figure 27B) ($P< 0.01$, $P< 0.0001$). Upon further analysis with the Sfold predictive software to determine key binding sites, it was revealed that both hsa-let7g-5p and hsa-miR-98-5p were predicted to bind to the *ST3GAL4* mRNA strand on a seedless region of the 3' UTR, indicating only partial complementarity binding (Figure 27C). Additionally, both miRNAs displayed high binding affinities towards their predicted target with -15.600 kcal/mol and -18.400 kcal/mol, respectively. Moreover, hsa-let7g-5p was predicted to bind at position 959-976, whilst in comparison, hsa-miR-98-5p binding was located at position 899-920 (Figure 27C).

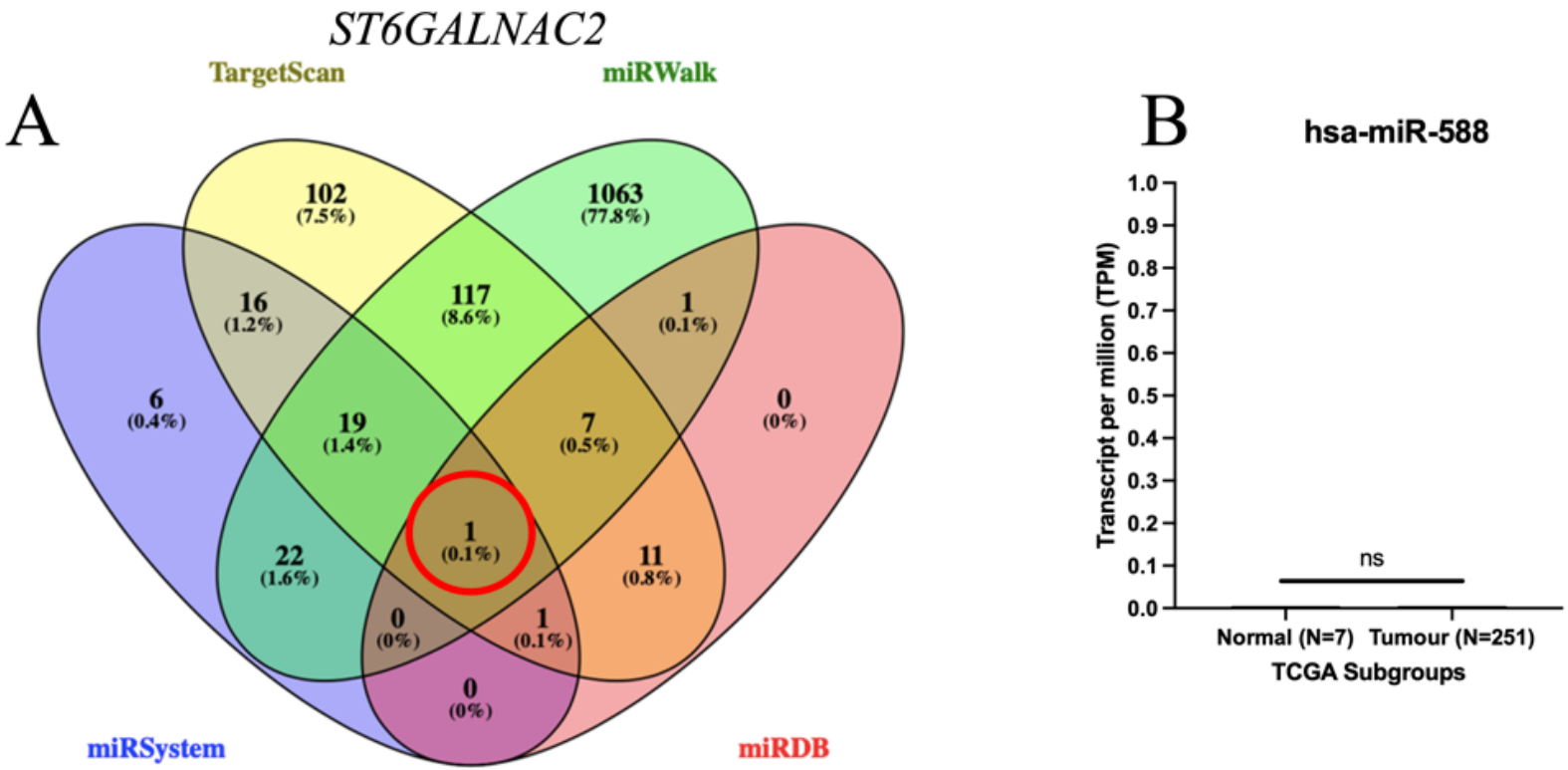

Figure 26: MiR-588 was predicted to regulate *ST6GALNAC2* expression but no expression profiles were present within the UALCAN database. (**A**) Cross-referenced miRNAs from TargetScan, miRSystem, miRWalk and miRDB databases demonstrated "1 hit" for *ST6GALNAC2* regulation. (**B**) Expression analysis was determined for miR-588 and was compared between normal (grey) and COAD tumours (red) cohorts via UALCAN transcriptomics analysis. Welch's t-test PERL script statistical analysis. ns $P > 0.05$.

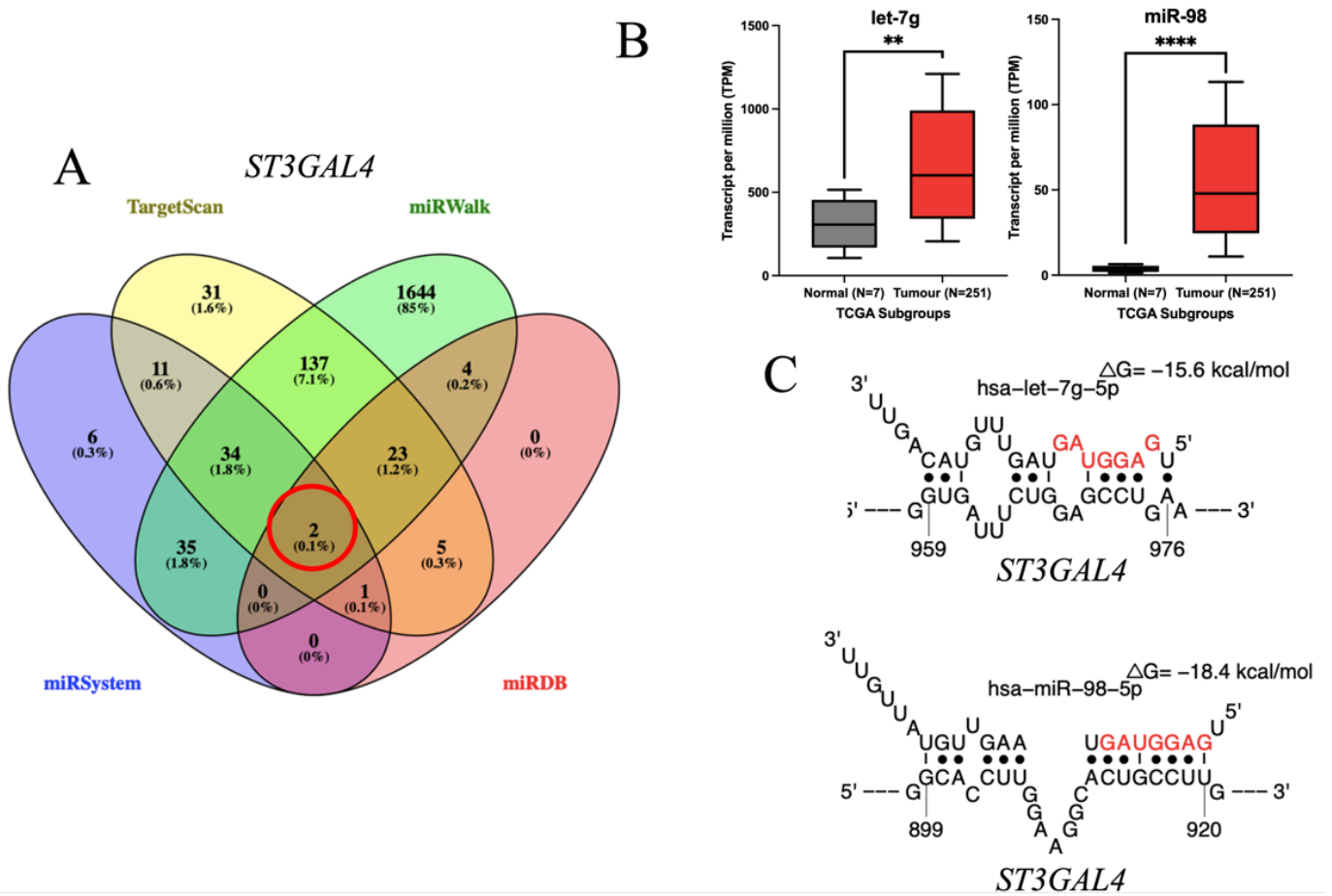

Figure 27: Let-7g and miR-98 were predicted to regulate *ST3GAL4* expression after exhibiting upregulated expression in COAD tumours. (**A**) Cross-referenced miRNAs from TargetScan, miRSystem, miRWalk and miRDB databases demonstrated "2 hits" for *ST3GAL4* regulation. (**B**) Expression analysis was determined for both predicted miRNAs and was compared between normal (grey) and COAD tumours (red) cohorts via UALCAN transcriptomics analysis, error bars ± SD. Welch's t-test PERL script statistical analysis. ** P< 0.01, **** P< 0.0001. (**C**) Predicted positional binding sites of the upregulated miRNAs were conducted, revealing high binding affinities for the *ST3GAL4* seedless region via Sfold predictive software.

ST6GAL1 was revealed to have the highest number of common miRNA elements across all of the predictive databases (Table 4, Figure 28A). Of the total 17 miRNAs identified, a total of 10 miRNAs displayed significantly downregulated expression in the tumour cohort (Figure 28B). They were identified as hsa-miR-1228-3p, hsa-miR-125a-5p, hsa-miR-125b-5p, hsa-miR-150-5p, hsa-miR-324-3p, hsa-miR-328-3p, hsa-miR-370-3p, hsa-miR-484, hsa-miR-500a-5p and hsa-miR-501-5p (not all data shown). Predicted binding sites for these miRNAs revealed the highest binding affinities towards the *ST6GAL1* seed region were miR-484, miR-125a-5p and miR-125b-5p. MiR-484 was recorded with a binding affinity of -28.900 kcal/mol at position 950-976. In contrast, miR-125a-5p and miR-125b-5p were predicted to have the same binding site with binding affinities of -22.600 kcal/mol and -17.800 kcal/mol, respectively (Figure 28C).

To identify common miRNA elements across the STRING and GeneMANIA interactive targets, the miRSystem database was utilised (Figure 29). When comparing across several *GALNT* genes, no singular miRNA was determined to be involved in their regulation (Table 5, Figure 29A). This was also similarly observed for comparisons made between *ST6GALNAC1*, *ST6GALNAC2*, *AGR2* and *AHSG* (Table 5, Fig 29C). However, several miRNAs correlated between *ST6GALNAC1, GALNT6, GALNT7* and *B3GNT6* revealing hsa-miR-140-5p, hsa-miR-30a-5p, hsa-miR-30b-5p, hsa-miR-30c-5p, hsa-miR-30d-5p, hsa-miR-30e-5p and hsa-miR-526b-5p (Table 5, Figure 29B). Other miRNA targets that were also identified were hsa-miR-199a-5p and hsa-miR-665 between the sialyltransferases *ST6GALNAC1, ST6GALNAC2, ST3GAL4* and *ST6GAL1* (Table 5, Figure 29D) and hsa-miR-147a when compared against the targets *C1GALT1, C1GALTC1, FUT1* and *POU2F1* (Table 5, Figure 29E). Additionally, two common miRNA elements were identified as hsa-miR-541-3p and hsa-miR-96-5p between targets *ST6GALNAC1*, *ST6GAL1*, *ST3GAL4* and *MUC1* (Table 5, Figure 29F).

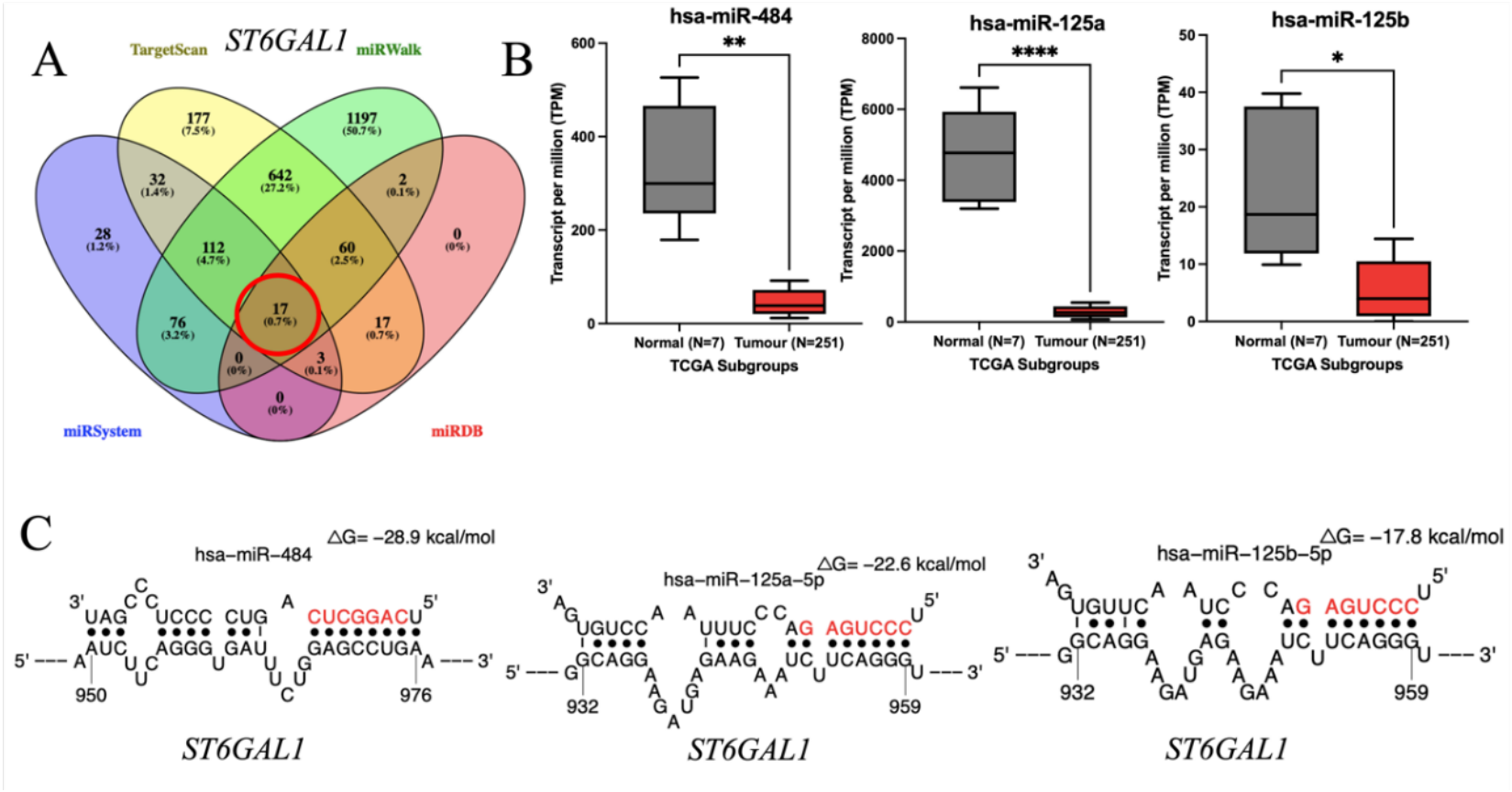

Figure 28: MiR-484, miR-125a and miR-125b were all predicted to have a high binding affinity for *ST6GAL1* regulation. (**A**) Cross-referenced miRNAs from TargetScan, miRSystem, miRWalk and miRDB databases demonstrated "17 hits" for *ST6GAL1* regulation. (**B**) Expression analysis was determined for several miRNAs (not all data shown for downregulated miRNAs) and compared between normal (grey) and COAD tumours (red) cohorts via UALCAN transcriptomics analysis, error bars ± SD. Welch's t-test PERL script statistical analysis. *P< 0.05, **P< 0.01, **** P < 0.0001. (**C**) Predicted positional binding sites of all downregulated miRNAs were conducted, revealing only miRNAs with the highest binding affinities for the *ST6GAL1* seed region via Sfold predictive software.

Table 4: Predicted miRNA binding targets for sialyltransferase gene regulation. *In silico* analysis tools utilising miRNA prediction databased were used to determine common miRNA targets predicted to modulate *ST6GALNAC1*, *ST6GALNAC2*, *ST3GAL4* and *ST6GAL1* expression via Venn diagrams.

Query genes	Predicted candidate miRNAs
ST6GALNAC1	hsa-miR-21-5p, hsa-miR-30e-5p and hsa-miR-26b-5p
ST6GALNAC2	hsa-miR-588
ST3GAL4	hsa-miR-193a-3p, hsa-miR-370-3p
ST6GAL1	hsa-miR-103a-3p, hsa-miR-107, hsa-miR-1178-3p, hsa-miR-1228-3p, hsa-miR-125a-5p, hsa-miR-125b-5p, hsa-miR-150-5p, hsa-miR-155-5p, hsa-miR-21-5p, hsa-miR-324-3p, hsa-miR-328-3p, hsa-miR-370-3p, hsa-miR-484, hsa-miR-492, hsa-miR-500a-5p, hsa-miR-501-5p, hsa-miR-628-5p

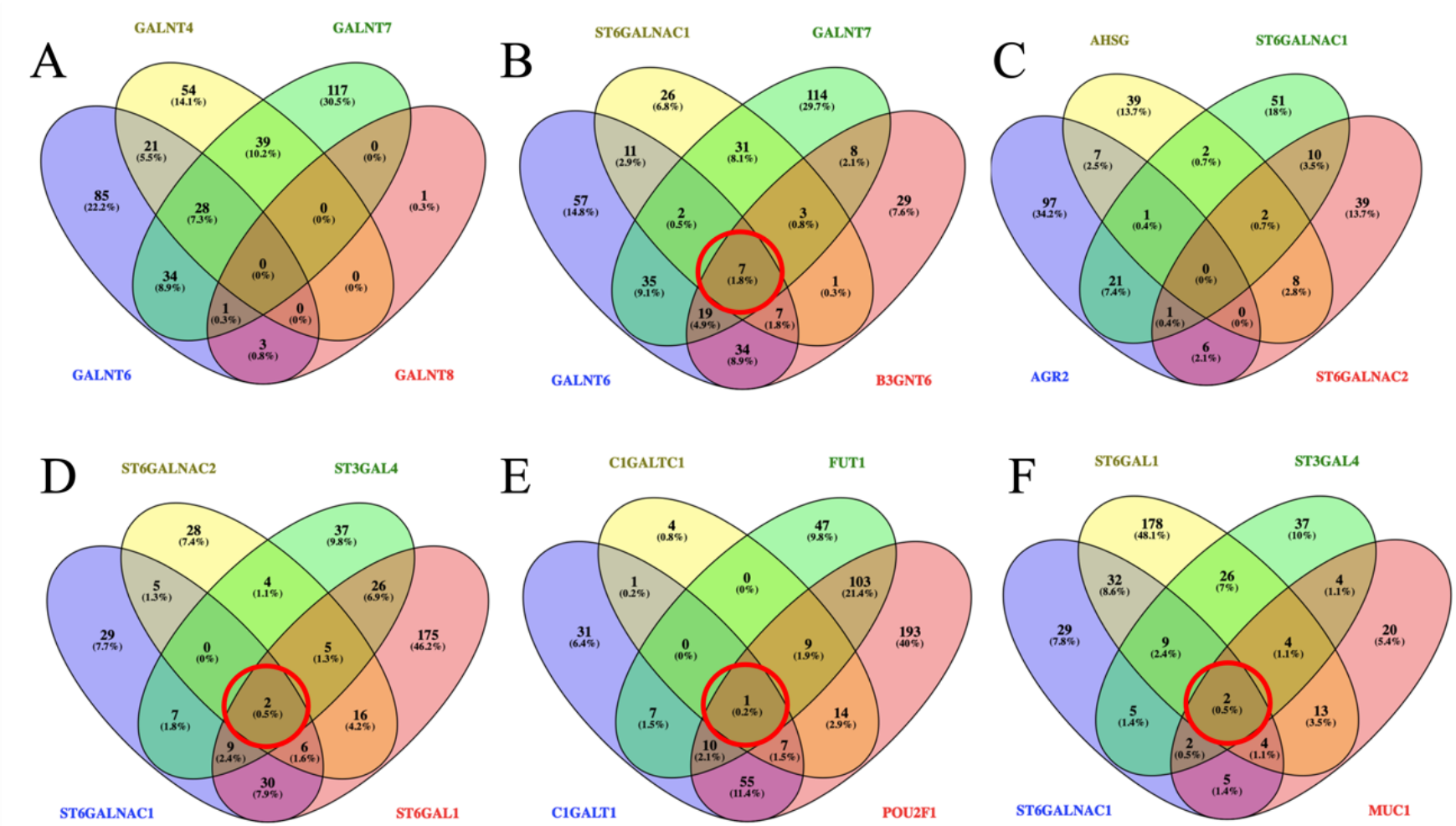

Figure 29: Common miRNA elements between sialyltransferases in glycan biosynthesis were discovered and predicted to regulate gene expression. The miRSystem database was utilised to identify common miRNA target candidates predicted to be involved in regulating interactive targets obtained from GeneMANIA and STRING analyses. Cross-referenced miRNAs were presented in Venn diagrams.

Table 5: Predicted miRNA binding candidates for identified interactive targets. *In silico* analysis tools utilising the miRNA prediction database miRSystem to determine common miRNA targets predicted to modulate various identified interactive genes and proteins obtained from STRING and GeneMANIA analysis.

Query genes	Predicted candidate miRNAs
GALNT4, GALNT6, GALNT7, GALNT8	N/A
ST6GALNAC1, GALNT6, GALNT7, B3GNT6	hsa-miR-140-5p, hsa-miR-30a-5p, hsa-miR-30b-5p, hsa-miR-30c-5p, hsa-miR-30d-5p, hsa-miR-30e-5p, hsa-miR-526b-5p
AHSG, AGR2, ST6GALNAC1, ST6GALNAC2	N/A
ST6GALNAC1, ST6GALNAC2, ST3GAL4, ST6GAL1	hsa-miR-199a-5p, hsa-miR-665
C1GALT1, C1GALTC1, FUT1, POU2F1	hsa-miR-147a
ST6GALNAC1, ST6GAL1, ST3GAL4, MUC1	hsa-miR-541-3p, hsa-miR-96-5p

Additionally, miRNA activity may not only modulate the expression of sialyltransferases. Other epigenetic modifications may pose an effect on gene expression including promoter methylation. Hence, promoter methylation of the sialyltransferases was determined (Figure 30). There was no significant change in the promoter methylation of *ST6GALNAC1* between normal and COAD tumour cohorts (Figure 30A). In comparison, *ST6GALNAC2, ST3GAL4* and *ST6GAL1* all demonstrated a significantly enhanced promoter methylation in malignant tissues when compared to the normal tissue control cohort (Figure 30B-D) ($P < 0.001$, $P < 0.0001$).

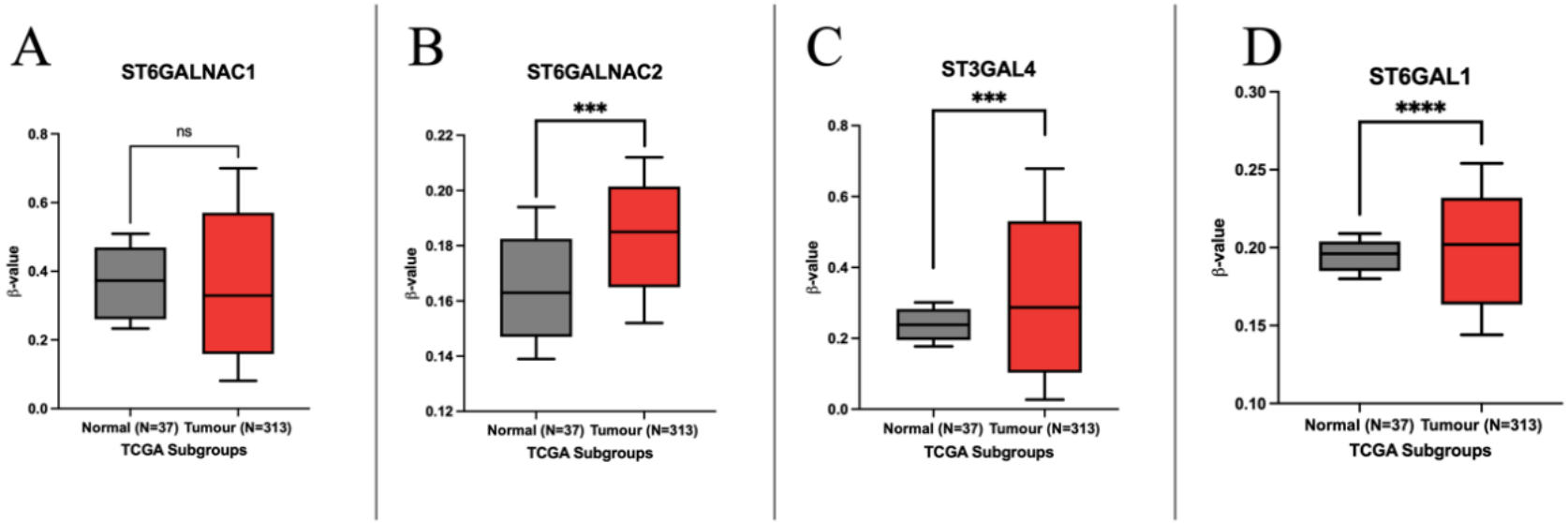

Figure 30: The promoter regions of sialyltransferase DNA sequences excluding *ST6GALNAC1* are significantly methylated in COAD tumours. UALCAN transcriptomics analysis was conducted to determine the methylation of the promoter regions of sialyltransferase query genes between normal tissue (grey) and COAD tumour (red) cohorts, error bars ± SD. Methylation data is presented as box plots. Welch's t-test PERL script statistical analysis. ***P< 0.001, ****P< 0.0001.

2.3.4 GSEA analysis of sialyltransferase expression in CRC and their association with known cancer hallmarks

Determining the clinical relevance of sialyltransferases and underlying enriched pathways associated with common cancer hallmarks may provide insights into possible regulatory mechanisms associated with deregulated sialyltransferase expression. Therefore, focusing only on the subset of DE genes in association with the CRC phenotype was elucidated (Figure 31-37). *ST6GALNAC1* revealed a total of 47 gene sets in conjunction with the CRC phenotype. Of those identified, three of those gene sets were significantly upregulated, and seven gene sets were significantly downregulated in association with CRC progression (Table 6, Figure 31-32) (FDR< 0.25 and P< 0.05). Furthermore, it highlighted the significantly upregulated enrichment of EMT, MYC targets and myogenesis hallmarks (Table 6, Figure 31). In comparison, downregulated enrichment highlighted the inflammatory response, IL-6 mediated JAK/STAT3 signalling, and deregulated *KRAS* signalling and various other biological processes (Table 6, Figure 32).

ST6GALNAC2 GSEA analysis revealed a total of 42 possible gene sets related to the CRC phenotype (Figure 33-34). Of those identified, *ST6GALNAC2* demonstrated an increase in the number of enriched gene sets. A total of 10 upregulated gene sets were shown to be enriched, which included cancer hallmarks such as E2F targets, MYC targets, the G2M checkpoint, mTOR signalling, and other various pathways (FDR< 0.25 and P< 0.05) (Figure 33). Similarly to *ST6GALNAC1*, seven enriched gene sets were shown as downregulated, highlighting biological processes and signalling pathways related to *KRAS* signalling, allograft rejection, EMT, inflammatory response, IFNγ response and others (FDR< 0.25 and P< 0.05) (Table 7, Figure 34).

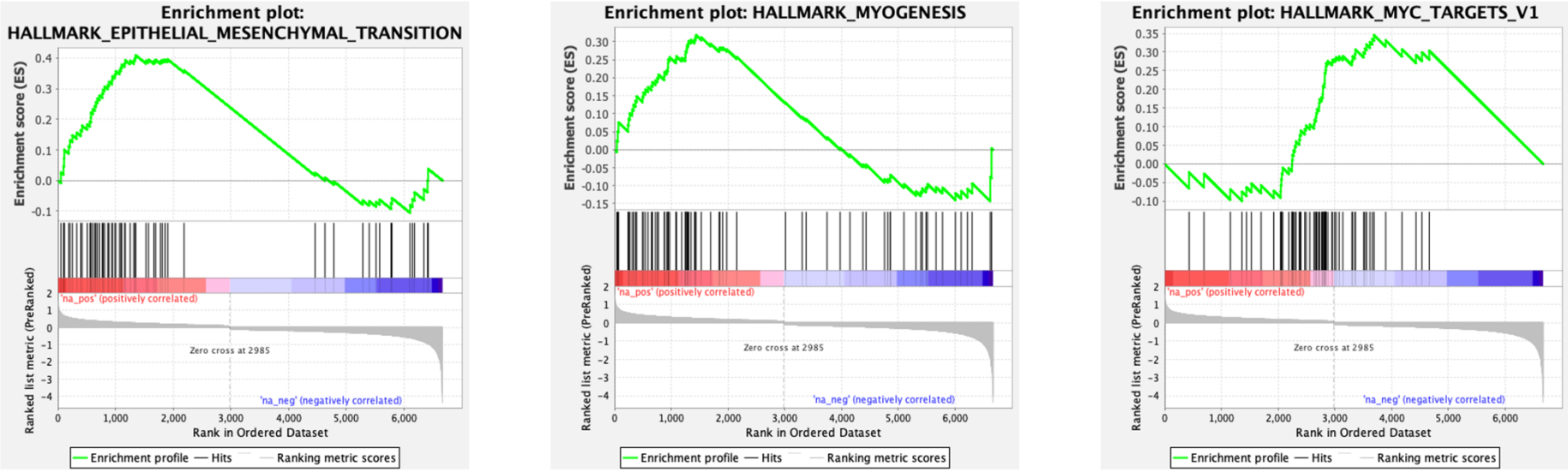

Figure 31: *ST6GALNAC1* GSEA analysis revealed only EMT, MYC targets and myogenesis pathways were enriched. GSEA analysis was conducted utilising the TCGA, PanCancer Atlas dataset for omics analysis (N=524). Significantly DE genes in COAD and commonly associated cancer hallmarks were determined in relation to *ST6GALNAC1* expression. FDR< 0.25 and P< 0.05.

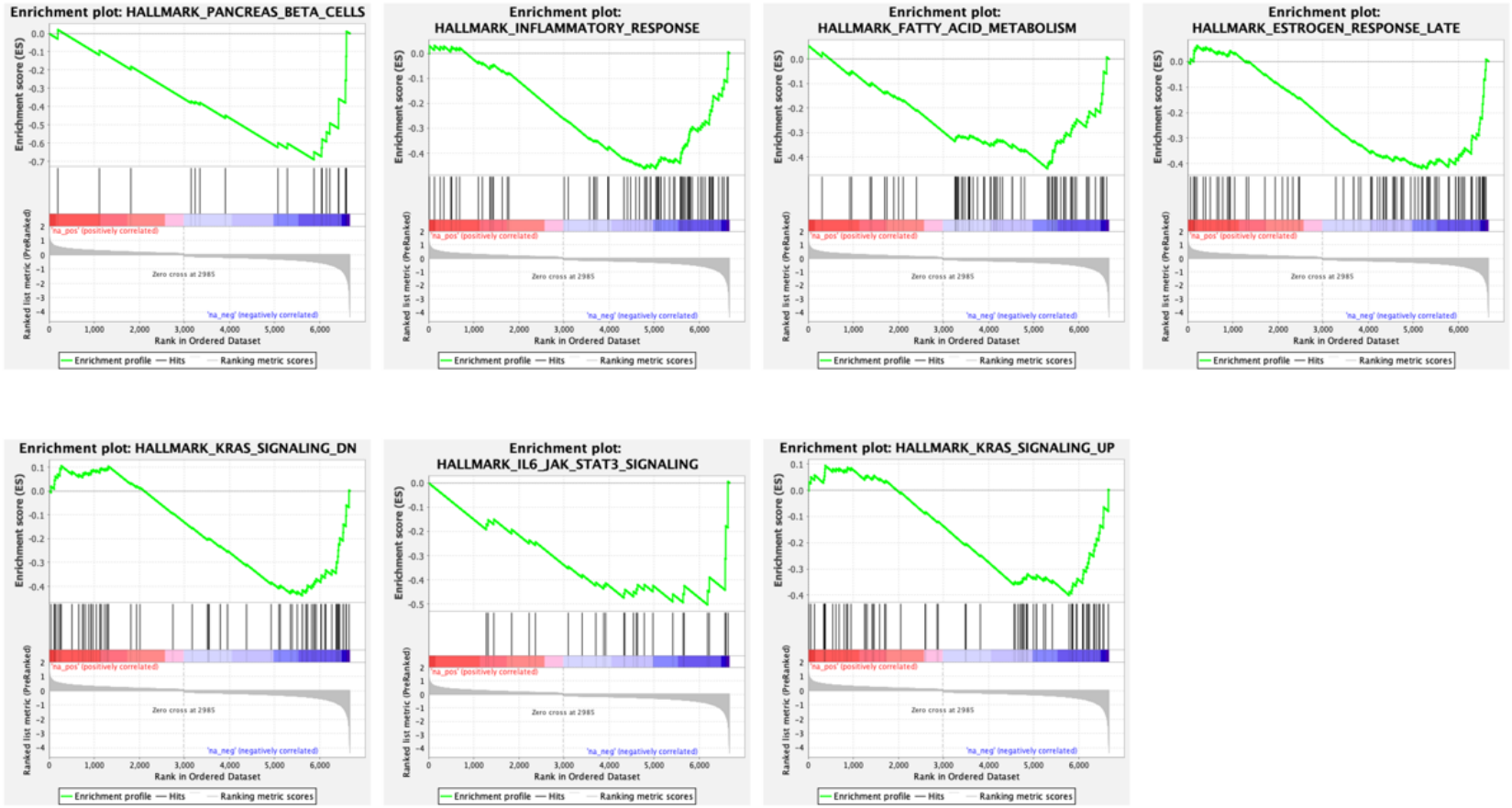

Figure 32: *ST6GALNAC1* GSEA analysis revealed inflammatory response, IL-6 mediated JAK/STAT3 signalling, and deregulated *KRAS* signalling were all significantly downregulated. GSEA analysis was conducted utilising the TCGA, PanCancer Atlas dataset for omics analysis (N=524). Significantly, DE genes in COAD and commonly associated cancer hallmarks were determined in relation to *ST6GALNAC1* expression. FDR< 0.25 and P< 0.05.

Table 6: GSEA analysis underlined enriched signalling pathways corresponding to *ST6GALNAC1* expression and its clinical relevance to CRC progression. GSEA enrichment scores for the association of *ST6GALNAC1* with cancer hallmarks. NES scores are provided as Log2FC changes (N=524) (FDR< 0.25 and P< 0.05).

	ENRICHED PATHWAY	EFFECT ON GENE REGULATION	NORMALISED ENRICHMENT SCORE (NES)	FDR Q-VALUE
ST6GALNAC1	Epithelial-Mesenchymal transition	Upregulated	2.14	0.00240
	Myogenesis	Upregulated	1.74	0.0246
	MYC targets V1	Upregulated	1.79	0.0260
	Pancreas - β cells	Downregulated	-2.01	0.00342
	Inflammatory response	Downregulated	-1.76	0.0741
	Fatty acid metabolism	Downregulated	-1.70	0.0871
	Late Oestrogen response	Downregulated	-1.63	0.122
	KRAS signalling - downregulation	Downregulated	-1.61	0.115
	IL-6/JAK/STAT3 signalling	Downregulated	-1.56	0.150
	KRAS signalling - upregulation	Downregulated	-1.49	0.215
	HEME metabolism	Downregulated	-1.45	0.248

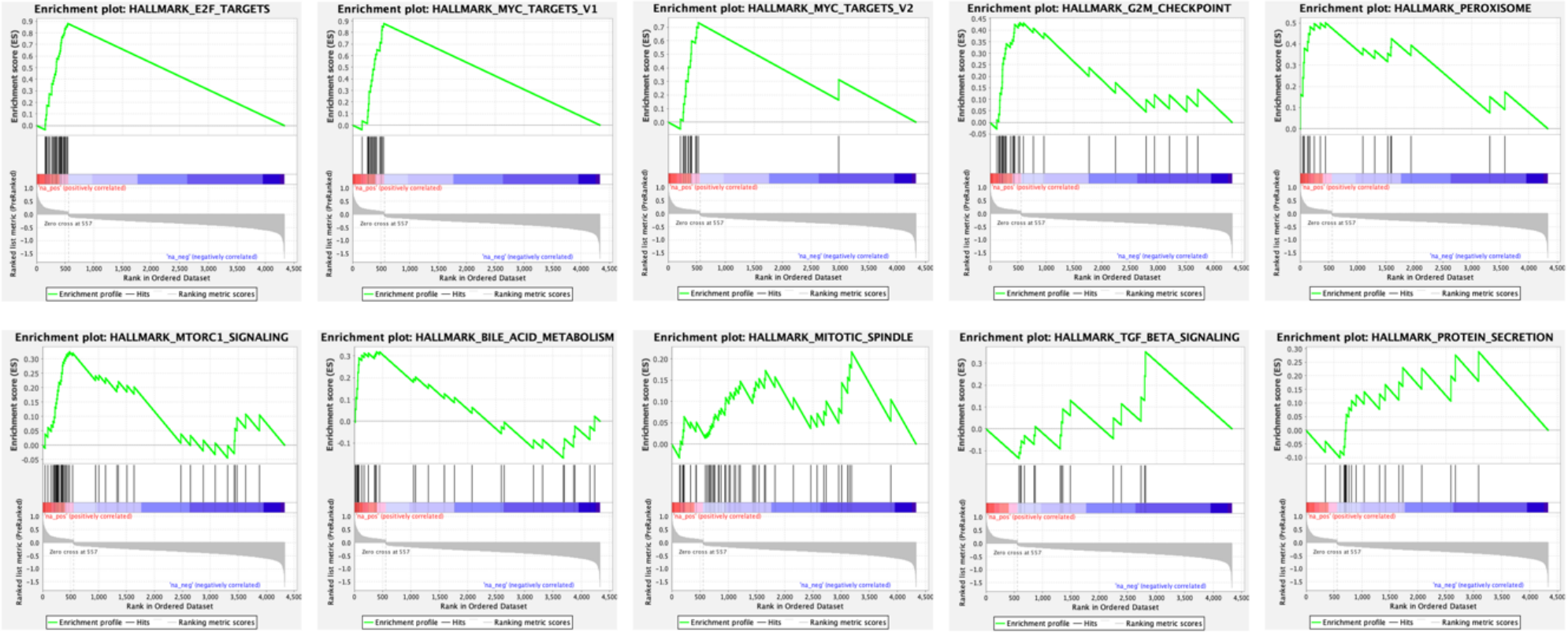

Figure 33: *ST6GALNAC2* GSEA analysis revealed multiple hallmarks related to tumour progression were enriched including E2F targets, MYC targets and mTOR signalling. GSEA analysis was conducted utilising the TCGA, PanCancer Atlas dataset for omics analysis (N=524). Significantly, DE genes in COAD and commonly associated cancer hallmarks were determined in relation to *ST6GALNAC2* expression. FDR< 0.25 and P< 0.05.

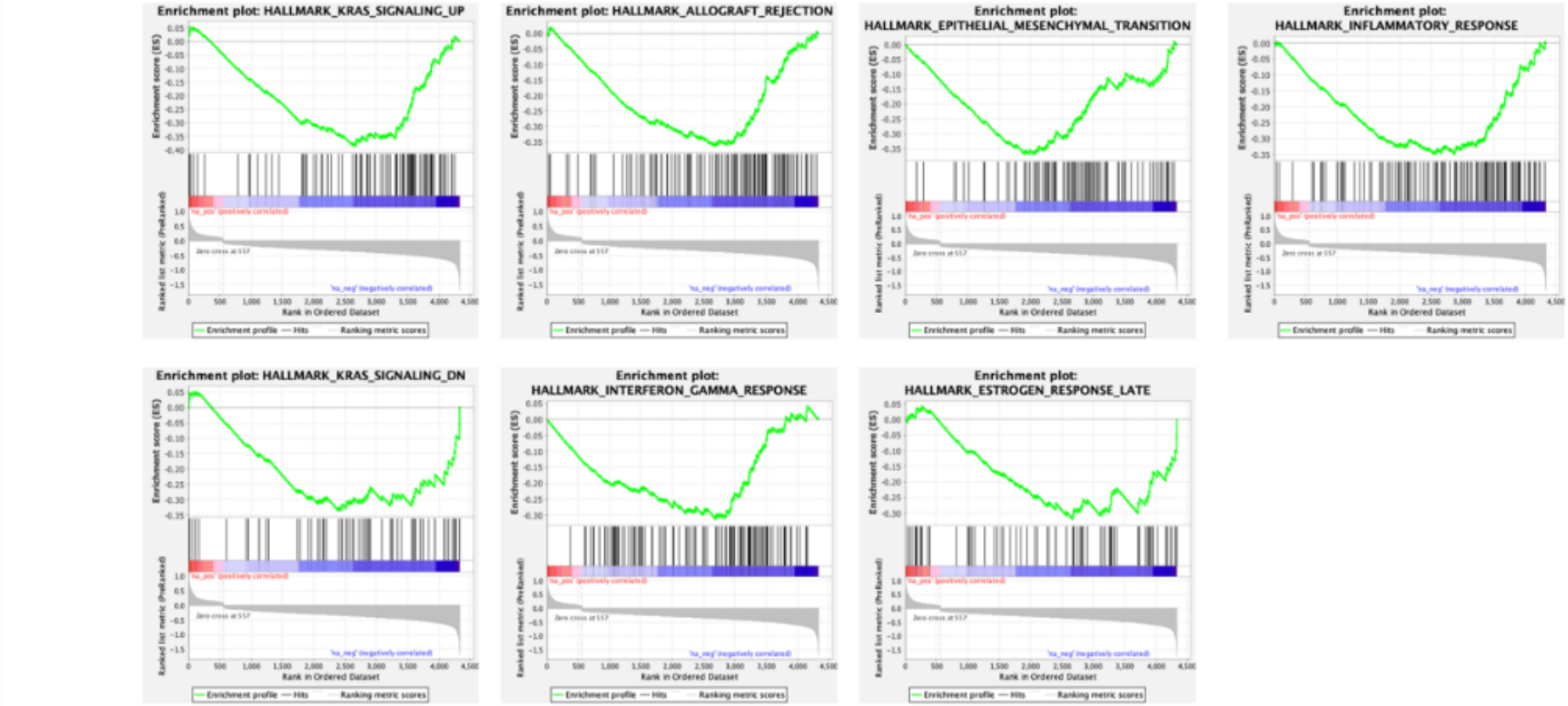

Figure 34: *ST6GALNAC2* GSEA analysis revealed downregulated enrichment of multiple hallmarks, including *KRAS* signalling, allograft rejection, EMT, inflammatory response and IFNγ response. GSEA analysis was conducted utilising the TCGA, PanCancer Atlas dataset for omics analysis (N=524). Significantly, DE genes in COAD and commonly associated cancer hallmarks were determined in relation to *ST6GALNAC2* expression. FDR< 0.25 and P< 0.05.

Table 7: GSEA analysis underlined enriched signalling pathways corresponding to *ST6GALNAC2* expression and its clinical relevance to CRC progression (N=524). GSEA enrichment scores for the association of *ST6GALNAC1* with cancer hallmarks. NES scores are provided as Log2FC changes (FDR< 0.25 and P< 0.05).

	ENRICHED PATHWAY	EFFECT ON GENE REGULATION	NORMALISED ENRICHMENT SCORE (NES)	FDR Q-VALUE
ST6GALNAC2	E2F Targets	Upregulated	5.91	0.000
	MYC targets V1	Upregulated	4.56	0.000
	MYC targets V2	Upregulated	3.54	0.000
	G2M checkpoint	Upregulated	2.94	0.000
	Peroxisome	Upregulated	2.56	0.000
	mTORC1 Signalling	Upregulated	2.45	0.000
	Bile Acid metabolism	Upregulated	1.99	0.00296
	Mitotic signalling	Upregulated	1.70	0.0244
	TGF-β Signalling	Upregulated	1.64	0.0292
	Protein secretion	Upregulated	1.48	0.0451
	KRAS signalling - Up	Downregulated	-1.67	0.166
	Allograft Rejection	Downregulated	-1.64	0.109

EMT	Downregulated	-1.60	0.103
Inflammatory response	Downregulated	-1.58	0.102
KRAS signalling -DN	Downregulated	-1.41	0.306
Interferon gamma response	Downregulated	-1.40	0.284
Late Oestrogen response	Downregulated	-1.37	0.290

Upon performing GSEA analysis for the *ST3GAL4* gene and its clinical relevance to cancer hallmarks in relation to CRC progression, a total of 46 gene sets were identified (Figure 35-36). Seventeen gene sets were demonstrated as upregulated, and from those, only 9 gene sets displayed significant upregulated enrichment (Table 8). Those identified included TNFα signalling via NFkβ, IFNγ response and upregulated *KRAS* signalling and other commonly associated hallmarks. Some of the biological processes identified also appeared in the previous GSEA analyses of *ST6GALNAC1* and *ST6GALNAC2*, including MYC targets, E2F targets, IL-6/JAK/STAT and mTOR1 signalling, among others (FDR< 0.25 and P< 0.05) (Figure 35). However, some of the mentioned processes have shown different levels of regulation with respect to the other genes. For example, MYC targets and E2F targets have shown downregulation for *ST3GAL4* but were significantly enriched for *ST6GALNAC2*. Similarly, the inflammatory response was upregulated with respect to *ST3GAL4* in contrast to *ST6GALNAC1*, which revealed this cancer hallmark was downregulated with respect to its expression. Furthermore, of the 29 gene sets that were downregulated, only 11 gene sets exhibited significantly enriched downregulation (FDR< 0.25 and P< 0.05) (Table 8, Figure 36). These identified hallmarks included oxidative phosphorylation, DNA repair, mTOR signalling and other commonly associated pathways.

When conducting the GSEA analysis for *ST6GAL1*, the number of genes identified as DE was lowered considerably, revealing only 707 genes for the total analysis. This revealed a singular enriched gene set significantly upregulated as the early oestrogen response (FDR< 0.25 and P< 0.05) (Table 9, Figure 37). Inversely, this identified a pathway not mentioned for the other sialyltransferase query genes, as both *ST6GALNAC1* and *ST6GALNAC2* were emphasised to exhibit downregulated enrichment of the late oestrogen response, whilst this was shown to be an upregulated hallmark for *ST3GAL4* (Table 6-9). However, no enriched gene sets were identified as downregulated.

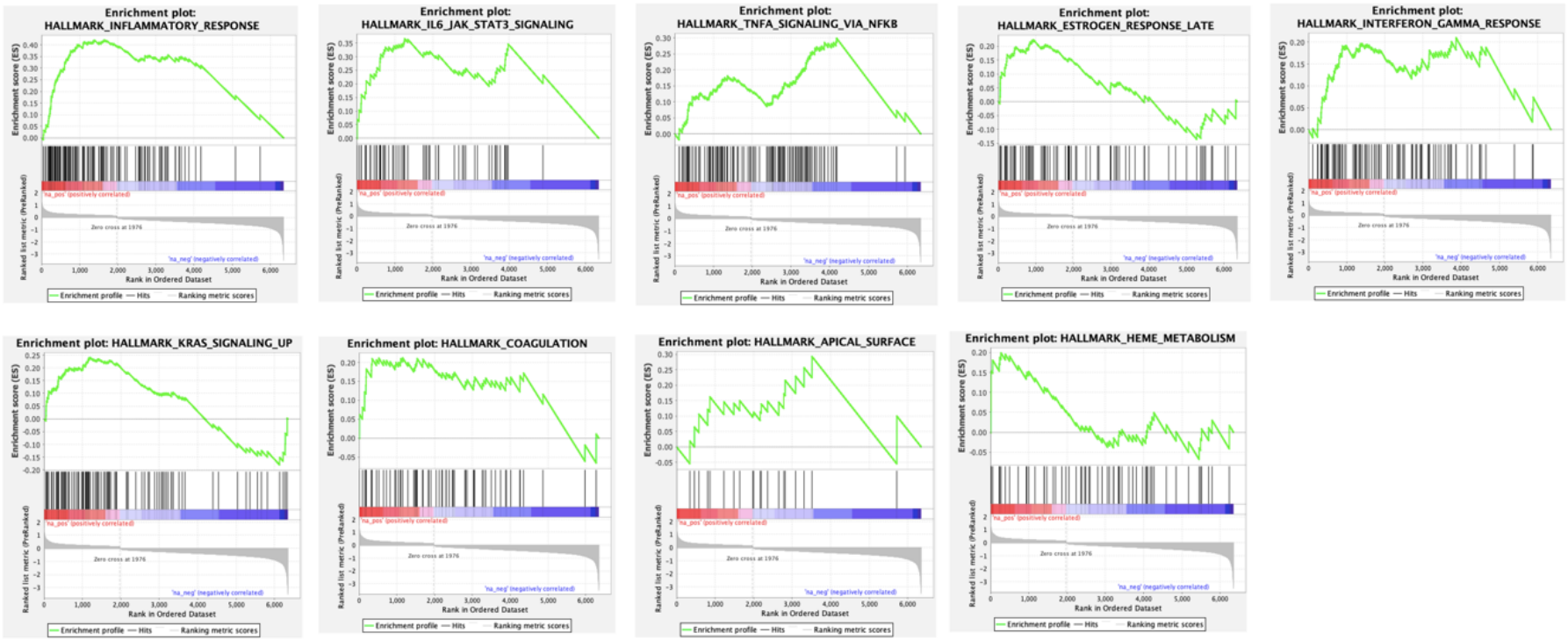

Figure 35: *ST3GAL4* GSEA analysis revealed the upregulated enrichment of multiple biological processes relating to tumour progression, including TNFα signalling via NFkβ, IFNγ response and upregulated *KRAS* signalling. GSEA analysis was conducted utilising the TCGA, PanCancer Atlas dataset for omics analysis (N=524). Significantly, DE genes in COAD and commonly associated cancer hallmarks were determined in relation to ST3GAL4 expression. FDR< 0.25 and P< 0.05

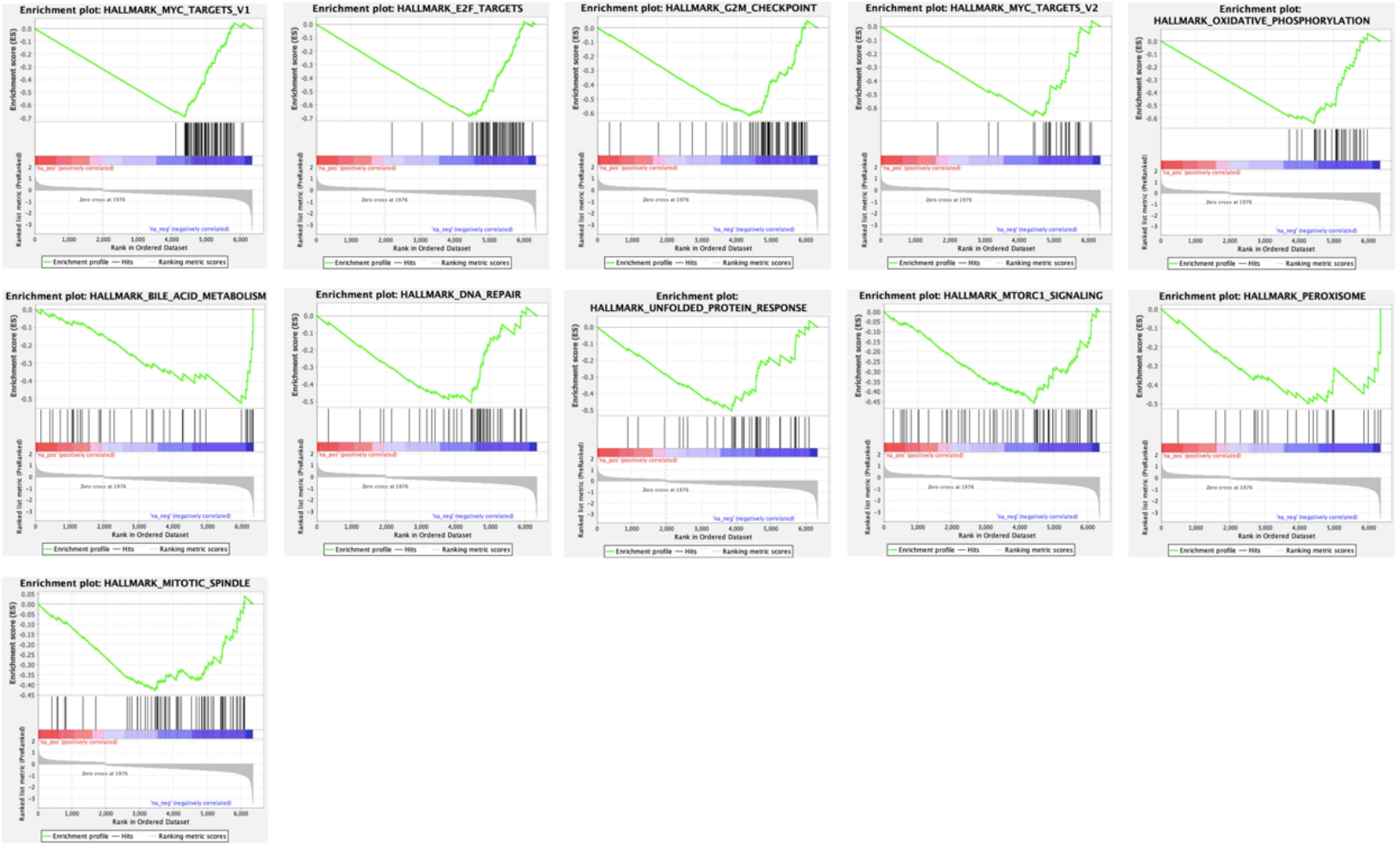

Figure 36: *ST3GAL4* GSEA analysis revealed the enrichment of multiple biological processes and pathways, including oxidative phosphorylation, DNA repair and mTOR signalling, were significantly downregulated. GSEA analysis was conducted utilising the TCGA, PanCancer Atlas dataset for omics analysis (N=524). Significantly, DE genes in COAD and commonly associated cancer hallmarks were determined in relation to *ST3GAL4* expression. FDR< 0.25 and P< 0.05.

Table 8: GSEA analysis underlined enriched signalling pathways corresponding to *ST3GAL4* expression and its clinical relevance to CRC progression. GSEA enrichment scores for the association of *ST6GALNAC1* with cancer hallmarks. NES scores are provided as Log2FC changes (N=524) (FDR< 0.25 and P< 0.05).

	ENRICHED PATHWAY	EFFECT ON GENE REGULATION	NORMALISED ENRICHMENT SCORE (NES)	FDR Q-VALUE
ST3GAL4	Inflammatory response	Upregulated	4.95	0.000
	IL-6/JAK/STAT signalling	Upregulated	2.56	0.000
	TNFα via NFkβ	Upregulated	2.29	0.000
	Late oestrogen response	Upregulated	1.78	0.0365
	IFNγ response	Upregulated	1.60	0.0560
	KRAS signalling - Up	Upregulated	1.59	0.0566
	Coagulation	Upregulated	1.43	0.125
	Apical surface markers	Upregulated	1.33	0.166
	HEME metabolism	Upregulated	1.29	0.181
	MYC targets V1	Downregulated	-2.53	0.000
	E2F targets	Downregulated	-2.47	0.000

G2M checkpoint	Downregulated	-2.27	0.000
MYC target V2	Downregulated	-2.14	0.000
Oxidative phosphorylation	Downregulated	-2.10	0.000
Bile acid metabolism	Downregulated	-1.78	0.00154
DNA repair	Downregulated	-1.77	0.00252
Unfolded protein response	Downregulated	-1.71	0.00474
mTOR1 signalling	Downregulated	-1.66	0.00872
Peroxisome hallmarks	Downregulated	-1.59	0.0181
Mitotic spindles	Downregulated	-1.54	0.0257

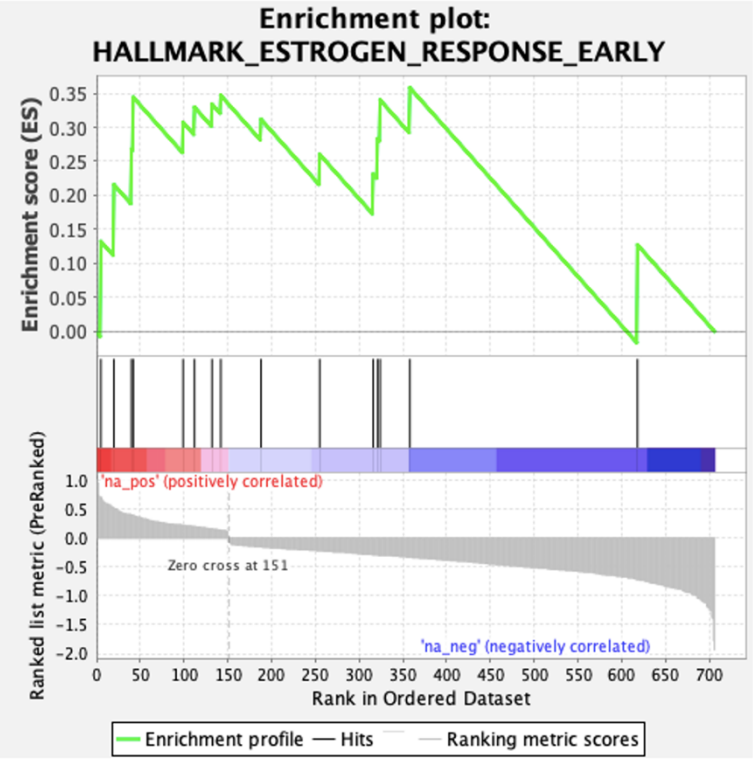

Figure 37: *ST6GAL1* GSEA analysis revealed only the enrichment of the early oestrogen response as significantly upregulated. GSEA analysis was conducted utilising the TCGA, PanCancer Atlas dataset for omics analysis (N=524). Significantly, DE genes in COAD and commonly associated cancer hallmarks were determined in relation to *ST6GAL1* expression. FDR< 0.25 and P< 0.05.

Table 9: GSEA analysis underlined enriched signalling pathways corresponding to *ST6GAL1* expression and its clinical relevance to CRC progression. GSEA enrichment scores for the association of *ST6GALNAC1* with cancer hallmarks. NES scores are provided as Log2FC changes (N=524) (FDR< 0.25 and P< 0.05).

	ENRICHED PATHWAY	EFFECT ON GENE REGULATION	NORMALISED ENRICHMENT SCORE (NES)	FDR Q-VALUE
ST6GAL1	Early oestrogen response	Upregulated	1.56	0.0363

2.3.5 Sialyltransferase predicted interactions and molecular networks

The correlation between sialyltransferase expression and the abundance of myeloid cells within the TME could underline the likelihood of STn production and subsequent masking against antigen recognition. Hence, identifying the relative expression of sialyltransferases in association with immune-related signatures was determined via TISIDB analysis (Figure 38-41). *ST6GALNAC1* expression exhibited a low Spearman's rank correlation coefficient (SRCC) with all myeloid populations that were analysed. However, there was a significant correlation between the expression of the query gene and the abundance of activated $CD4^+$ T-lymphocytes and monocyte cell populations (Figure 38). In comparison, *ST6GALNAC2* displayed a weak causal relationship with macrophages, indicating a significant correlation between the two parameters (Figure 39). Moreover, there was a significant association with the other myeloid populations, which included activated $CD4^+$ T-lymphocytes, activated $CD8^+$ T-lymphocytes, T_{regs} and monocytes alongside the observed macrophage immune signature that was mentioned. TISIDB analysis of *ST3GAL4* expression has shown a weak SRCC correlation with the abundance of monocyte cells (Figure 40). There was a significant association with both monocytes and macrophages. However, *ST6GAL1* analysis revealed significant negative SRCC correlations with several myeloid cell populations, including macrophages, activated $CD4^+$ T-lymphocytes, activated $CD8^+$ T-lymphocytes, Tregs and monocytes (Figure 41).

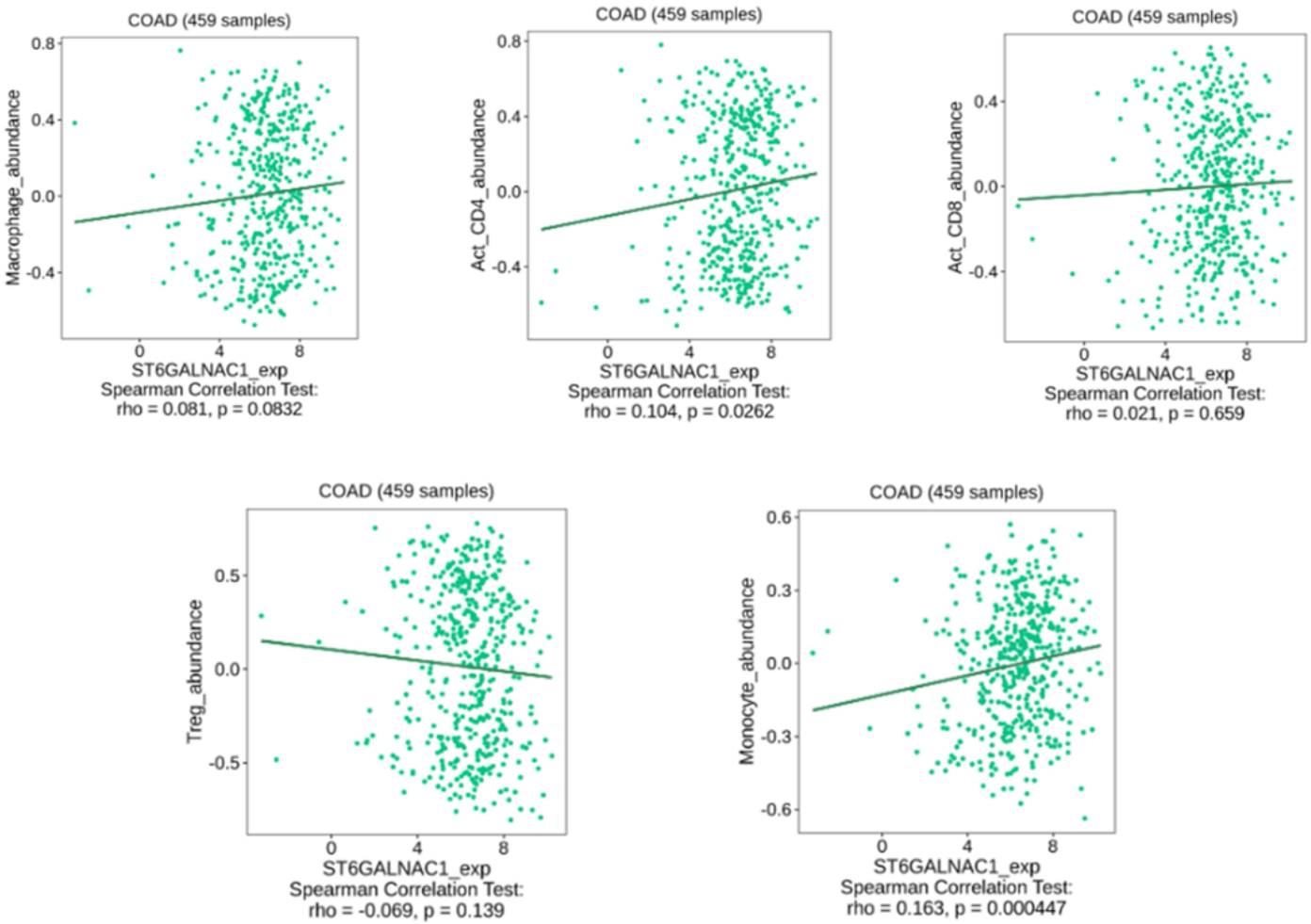

Figure 38: *ST6GALNAC1* exhibits only a significant relationship with the abundance of activated CD4$^+$ T-lymphocytes and monocyte cells. SRCC analysis was executed to correlate the role of *ST6GALNAC1* expression and the abundance of several immune-related signatures in COAD tumours (N= >8000 tumours). Myeloid populations that were assessed included macrophages, activated CD4$^+$ T-cells, activated CD8$^+$ T-cells, Tregs and monocytes. P< 0.05 was considered statistically significant.

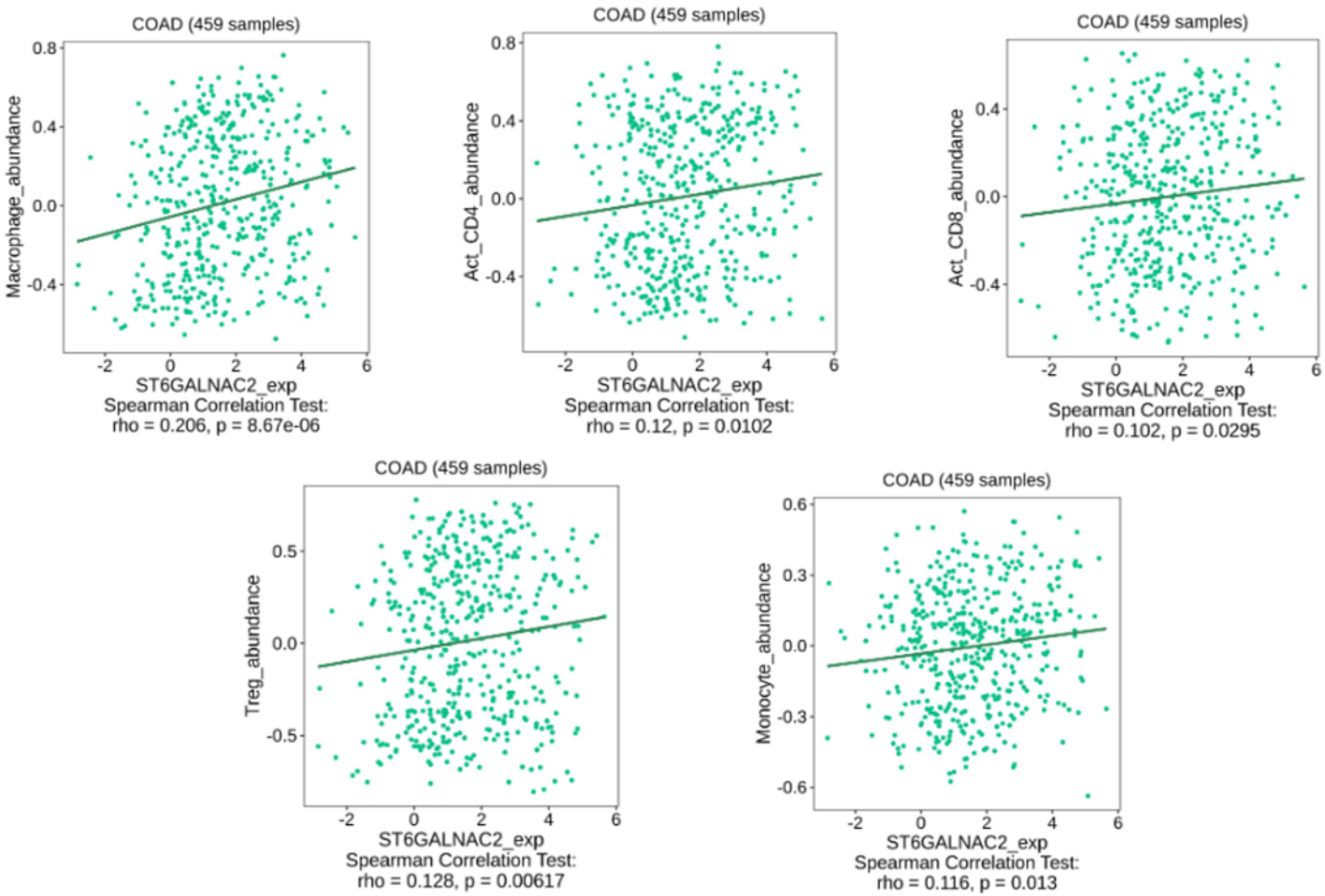

Figure 39: *ST6GALNAC2* exhibits a significant relationship with the abundance of all myeloid cell populations. SRCC analysis was executed to correlate the role of *ST6GALNAC2* expression and the abundance of several immune-related signatures in COAD tumours (N= >8000 tumours). Myeloid populations that were assessed included macrophages, activated $CD4^+$ T-cells, activated $CD8^+$ T-cells, Tregs and monocytes. $P< 0.05$ was considered statistically significant.

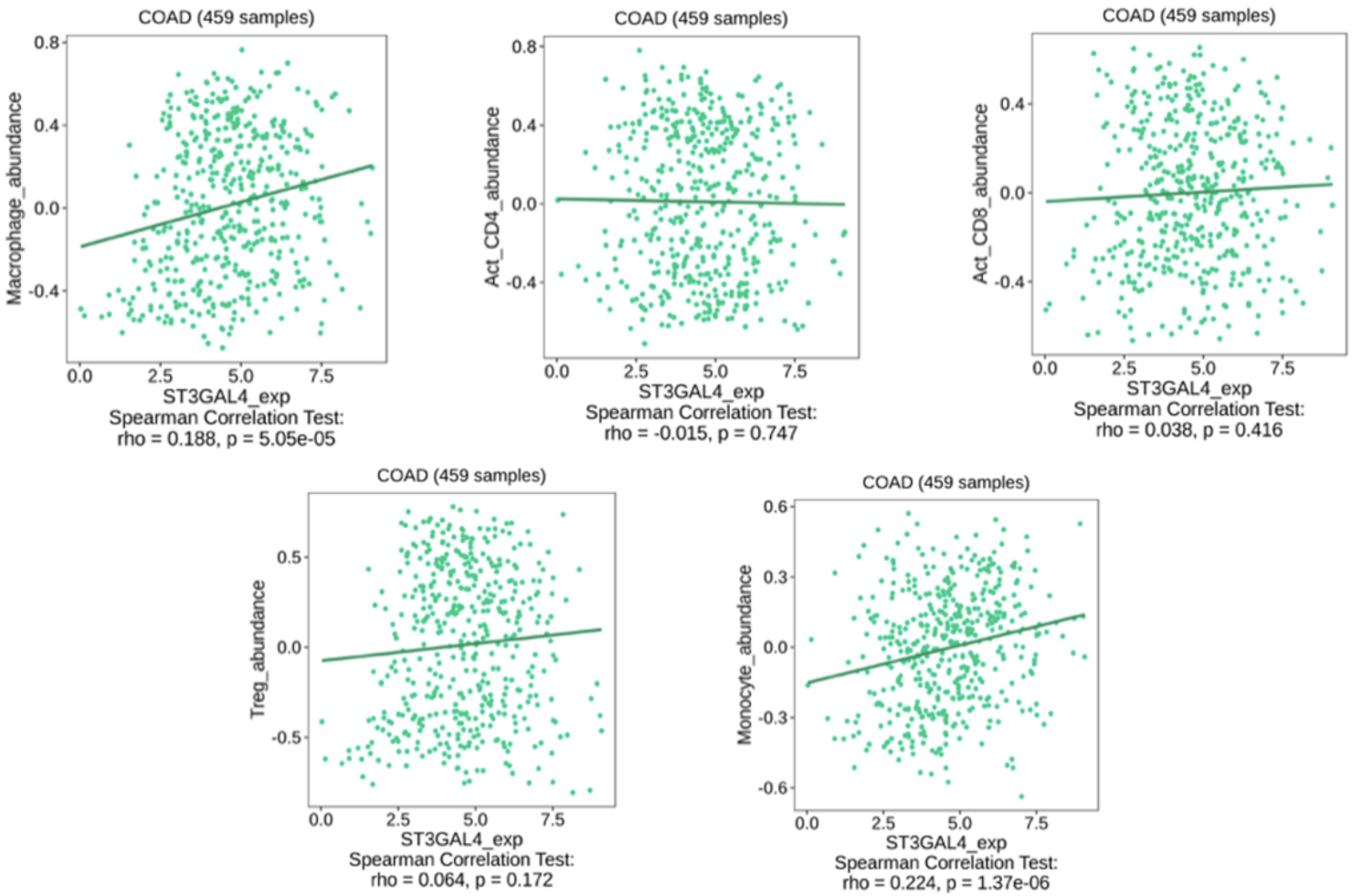

Figure 40: *ST3GAL4* exhibits a weak association with the abundance of monocytic cellular populations. SRCC analysis was executed to correlate the role of *ST3GAL4* expression and the abundance of several immune-related signatures in COAD tumours (N= >8000 tumours). Myeloid populations that were assessed included macrophages, activated $CD4^+$ T-cells, activated $CD8^+$ T-cells, Tregs and monocytes. P< 0.05 was considered statistically significant.

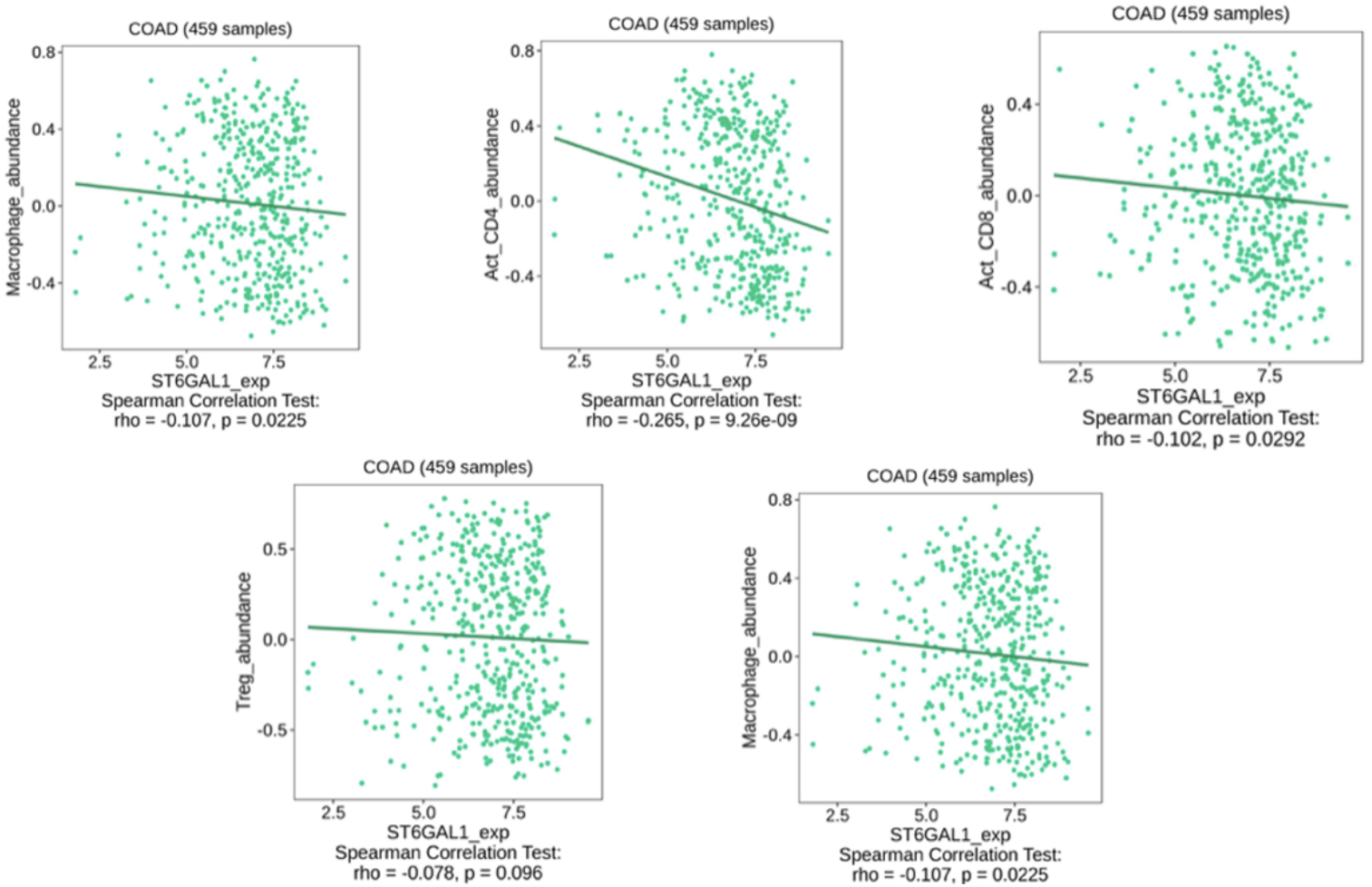

Figure 41: *ST6GAL1* exhibits negative correlations with the abundance of several myeloid cell populations. SRCC analysis was executed to correlate the role of *ST6GAL1* expression and the abundance of several immune-related signatures in COAD tumours (N= >8000 tumours). Myeloid populations that were assessed included macrophages, activated $CD4^+$ T-cells, activated $CD8^+$ T-cells, Tregs and monocytes. $P< 0.05$ was considered statistically significant.

2.3.6 The correlative relationship between sialyltransferases and immune checkpoint proteins

The TIMER analysis could indicate the correlative relationships between deregulated sialyltransferase expression and the abundance of prevalent immune checkpoint genes that are heavily associated with malignancies (Figure 42-45). The immune checkpoints that were analysed as part of this analysis have been associated with tumour progression over a variety of cell types. Thus, any correlative relationship may indicate factors contributing to CRC tumour heterogeneity and their roles in the TME. *ST6GALNAC1* has indicated a non-significant poor correlative relationship with all of the pro-tumorigenic immune checkpoint genes that were queried (Figure 42). In contrast, *ST6GALNAC2* displayed an SRCC that was associated with the abundance of most immune checkpoints, excluding both *CTLA4* and *SIGLEC15*, with the highest abundant expression relating to *CD274* (Figure 43). However, of the two checkpoint proteins that were mentioned, there was only a significant association with *CTLA4*. Similar to *ST6GALNAC1*, *ST3GAL4* expression exerted no correlative relationship across all analysed immune checkpoint genes as part of the TIMER analysis (Figure 44). However, *ST3GAL4* expression was characterised by significant association with the immune checkpoints *TIGIT, LAG3, CD274, CTLA4* and *SIGLEC15*, underlining low expression levels are associated with the abundance of the queried immune checkpoints. Lastly, *ST6GAL1* expression analysis has shown limited correlative relationships to the abundance of immune checkpoint genes, similar to the other query genes. However, there is a significant association with immune checkpoint genes *CD274* and *SIGLEC15*, both of which are frequently associated with tumour progression (Figure 45).

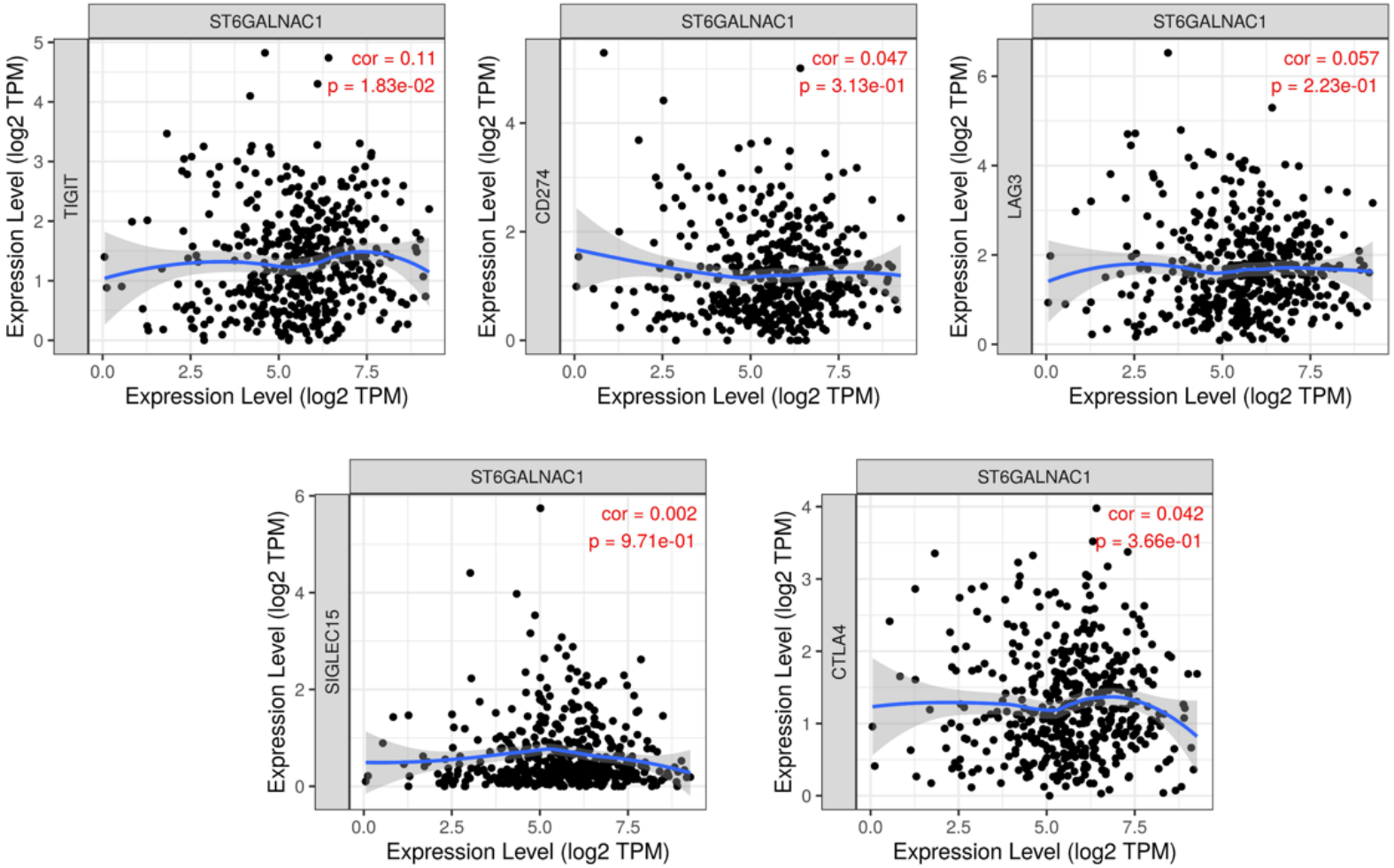

Figure 42: *ST6GALNAC1* shares a poor correlation with pro-tumorigenic immune checkpoint proteins. The correlative relationship between the query gene *ST6GALNAC1* and the abundance of pro-tumorigenic immune checkpoint proteins *SIGLEC15*, *CD274*, *CTLA4*, *TIGIT*, and *LAG3* was determined via the TIMER database.

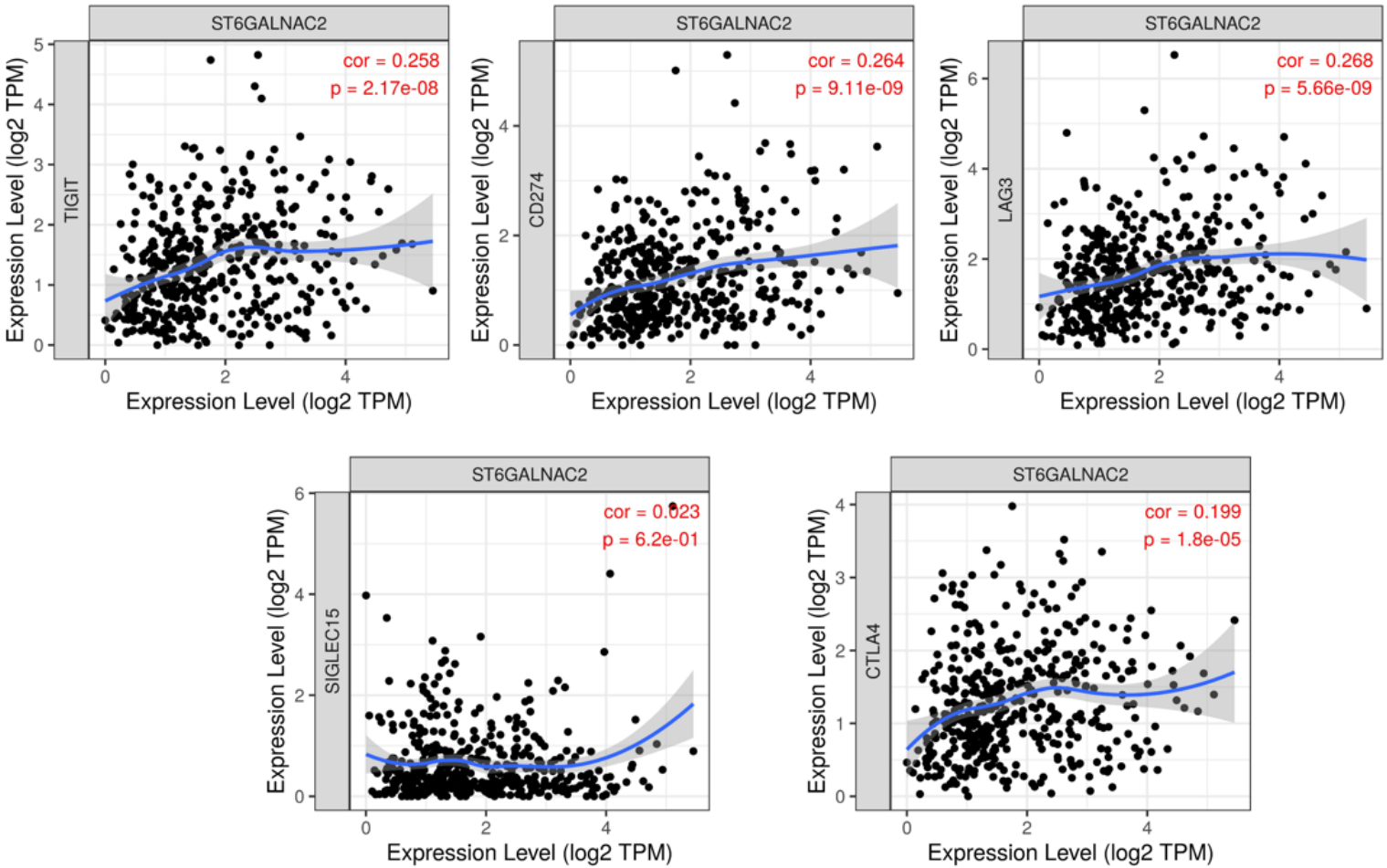

Figure 43: *ST6GALNAC2* expression shares a significant correlation with pro-tumorigenic immune checkpoint proteins excluding *SIGLEC15*. The correlative relationship between the query gene *ST6GALNAC2* and the abundance of pro-tumorigenic immune checkpoint proteins *SIGLEC15*, *CD274*, *CTLA4*, *TIGIT*, and *LAG3* was determined via the TIMER database.

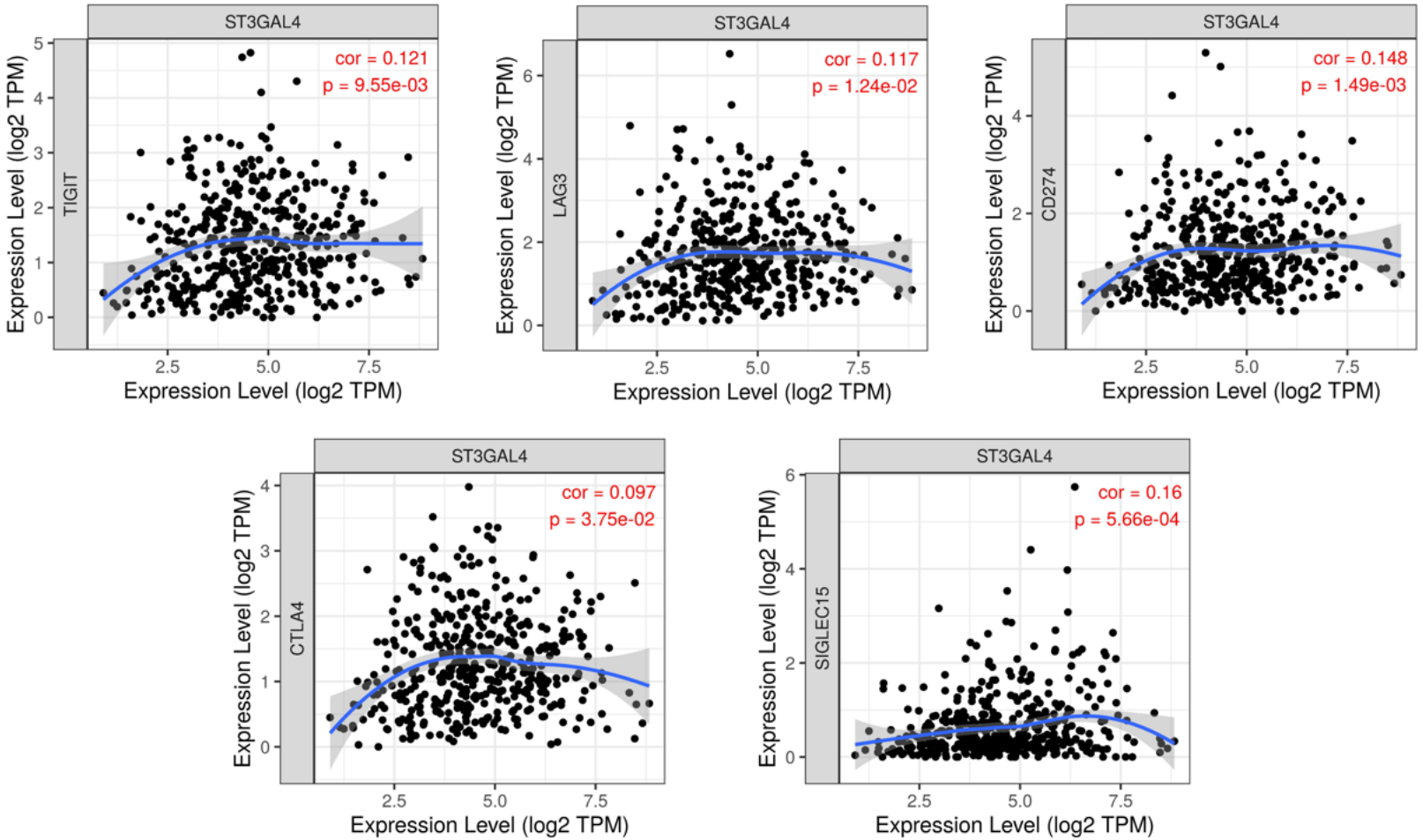

Figure 44: *ST3GAL4* expression shares a significant correlation with pro-tumorigenic immune checkpoint proteins. The correlative relationship between the query gene *ST3GAL4* and the abundance of pro-tumorigenic immune checkpoint proteins *SIGLEC15*, *CD274*, *CTLA4*, *TIGIT*, and *LAG3* was determined via the TIMER database.

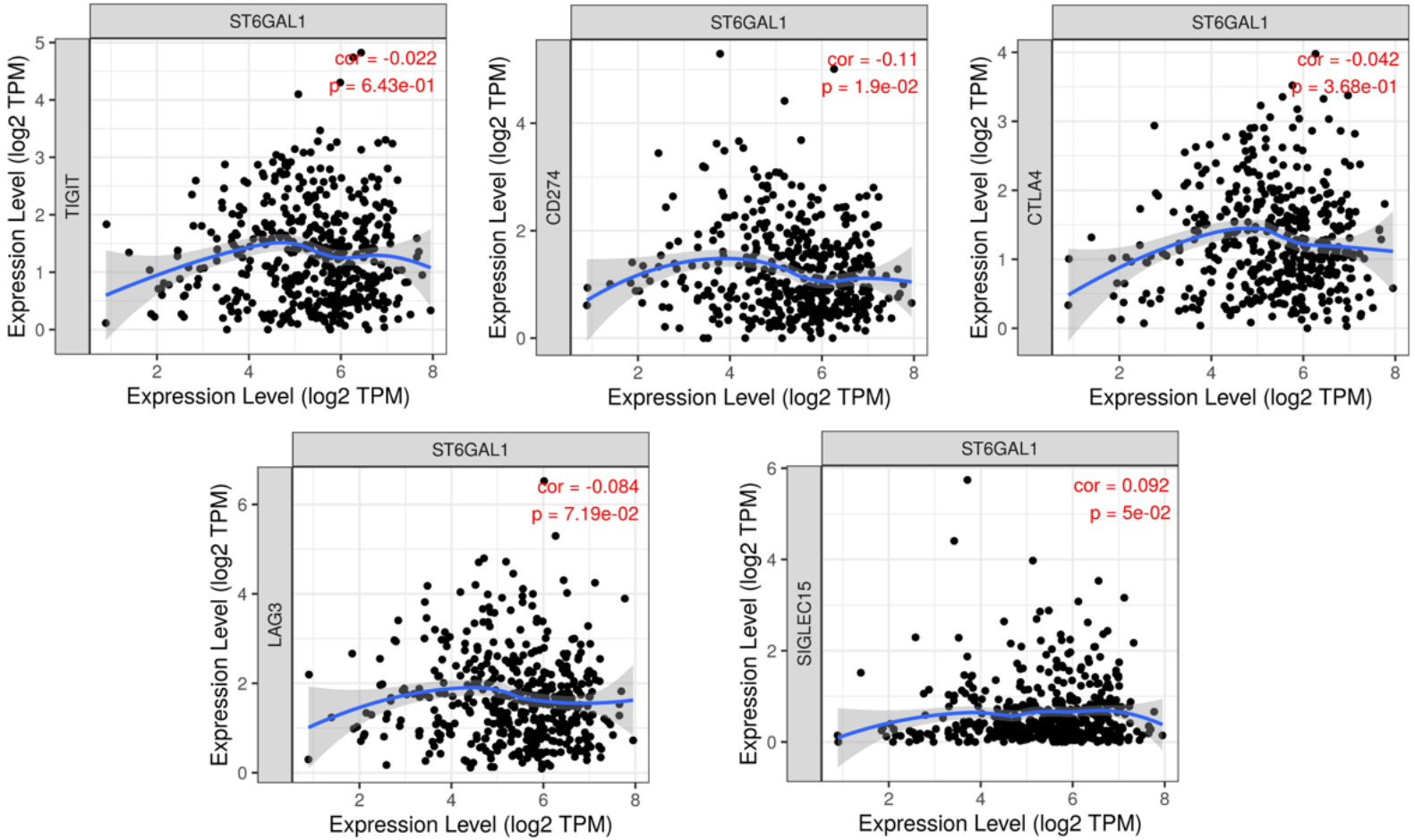

Figure 45: *ST6GAL1* expression shares a significant correlation with only *CD274* and *SIGLEC15*. The correlative relationship between the query gene *ST6GAL1* and the abundance of pro-tumorigenic immune checkpoint proteins *SIGLEC15*, *CD274*, *CTLA4*, *TIGIT*, and *LAG3* was determined via the TIMER database.

2.3.7 Deregulated sialyltransferase expression denoting CRC patient survival outcomes

As glycan synthesis is one of the biological processes that become deregulated within tumour malignancies, it is worth characterising the role of deregulated expression profiles of sialyltransferases on prognostic clinical survival outcomes (Figure 46-49). Low *ST6GALNAC1* expression exhibited poor prognostic outcomes in all survival criteria ($P < 0.05$) (Figure 46). Inversely, *ST6GALNAC2* has shown the complete opposite, emphasising that high deregulated expression was correlated to reduced survival outcomes in OS criteria ($P < 0.05$), the RFS criteria ($P < 0.05$), and PPS criteria ($P < 0.05$) (Figure 47). Similarly, survival curves demonstrated that higher *ST3GAL4* expression correlated greater to poor clinical survival in OS and RFS survival criteria ($P < 0.05$). Moreover, PPS criteria characterised low expression was associated with poor survival outcomes. However, over the extended period, the prognostic value of high *ST3GAL4* expression also displayed similar survival outcomes as low *ST3GAL4* expression in PPS survival (Figure 48). Similar to observed survival data of *ST6GALNAC1*, *ST6GAL1* survival demonstrated low expression was associated with poor survival outcomes of CRC patients across all survival parameters ($P < 0.05$) (Figure 49).

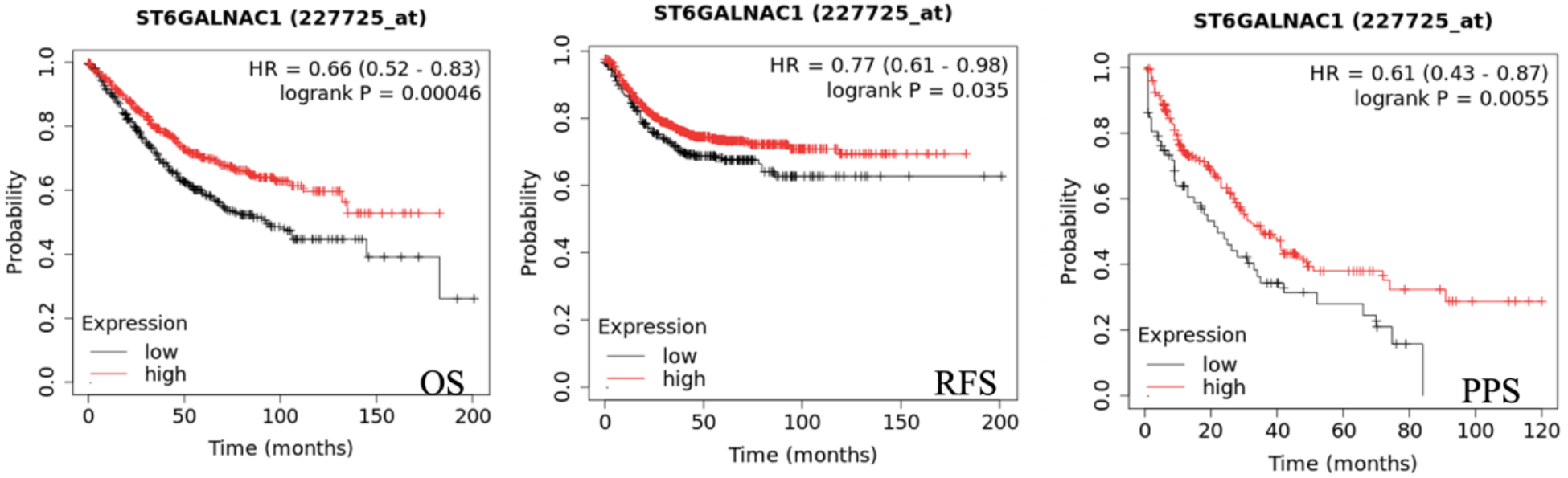

Figure 46: Low ST6GALNAC1 expression is associated with poor survival outcomes. Comparisons between high *ST6GALNAC1* expression (red) and low *ST6GALNAC1* expression (black) were conducted to elucidate the relationship between query gene expression and the prognostic factor in COAD patients. Survival curves were constructed to outline ST6GALNAC1 expression with survival criteria: overall survival (OS), post-progression survival (PPS), and relapse-free survival (RFS) criteria. P< 0.05 was considered statistically significant.

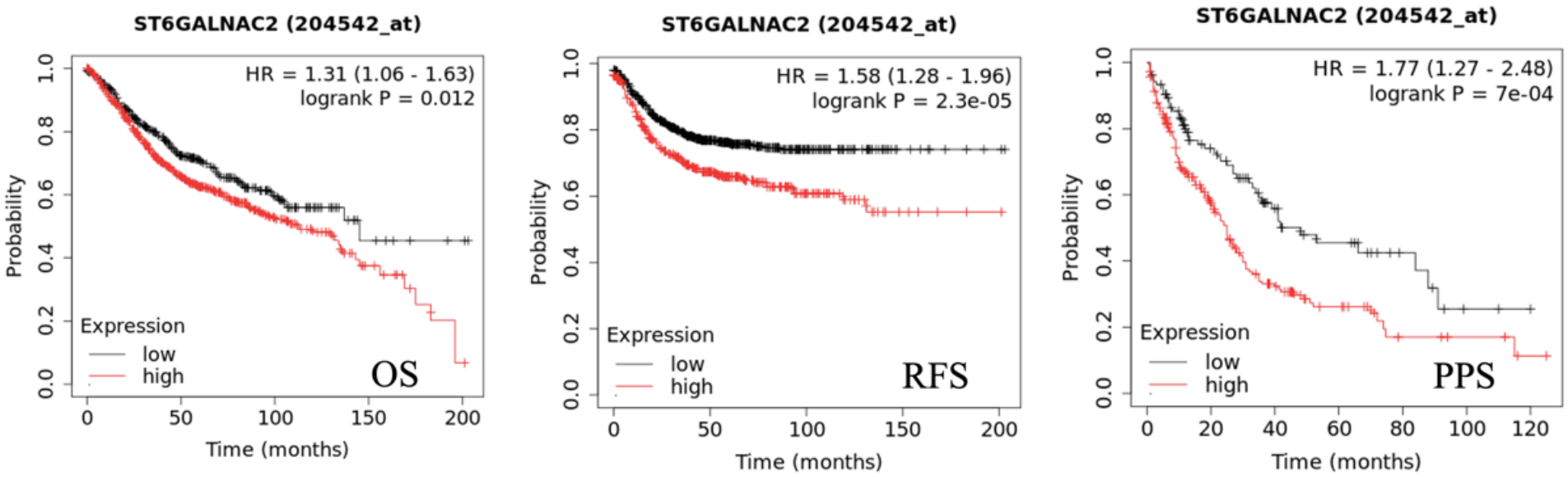

Figure 47: High *ST6GALNAC2* expression is associated with poor survival outcomes in all survival criteria. Comparisons between high *ST6GALNAC2* expression (red) and low *ST6GALNAC2* expression (black) were conducted to elucidate the relationship between query gene expression and the prognostic factor in COAD patients. Survival curves were constructed to outline *ST6GALNAC2* expression with survival criteria: overall survival (OS), post-progression survival (PPS), and relapse-free survival (RFS) criteria. $P < 0.05$ was considered statistically significant.

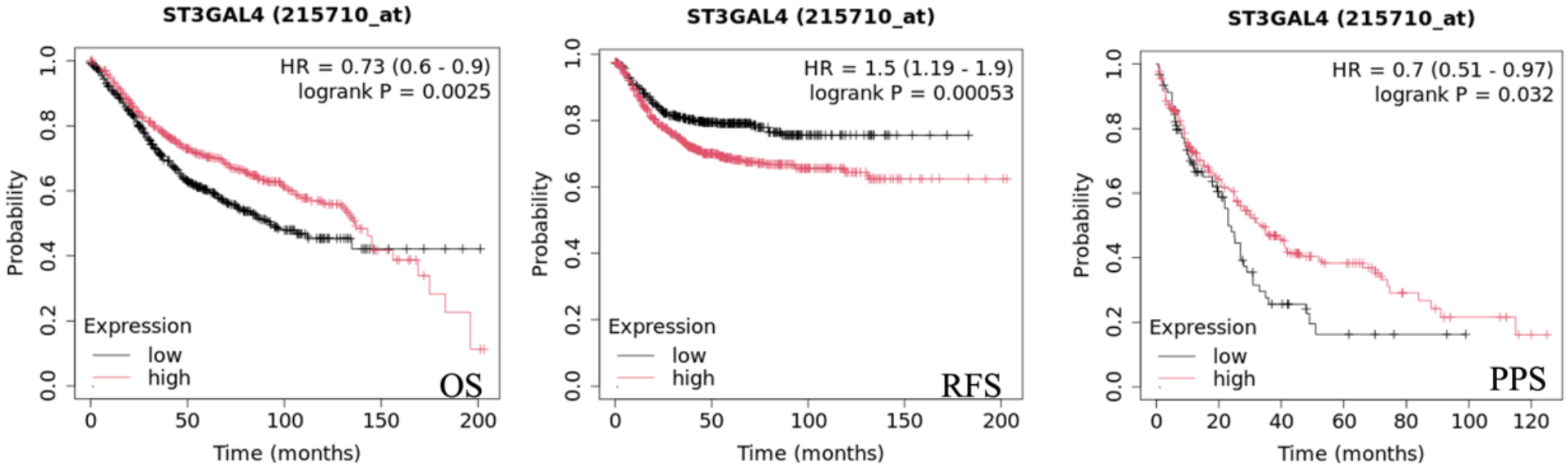

Figure 48: High *ST3GAL4* expression is associated with poor survival outcomes in OS and RFS criteria. Comparisons between high *ST3GAL4* expression (red) and low *ST3GAL4* expression (black) were conducted to elucidate the relationship between query gene expression and the prognostic factor in COAD patients. Survival curves were constructed to outline *ST3GAL4* expression with survival criteria: overall survival (OS), post-progression survival (PPS), and relapse-free survival (RFS) criteria. $P < 0.05$ was considered statistically significant.

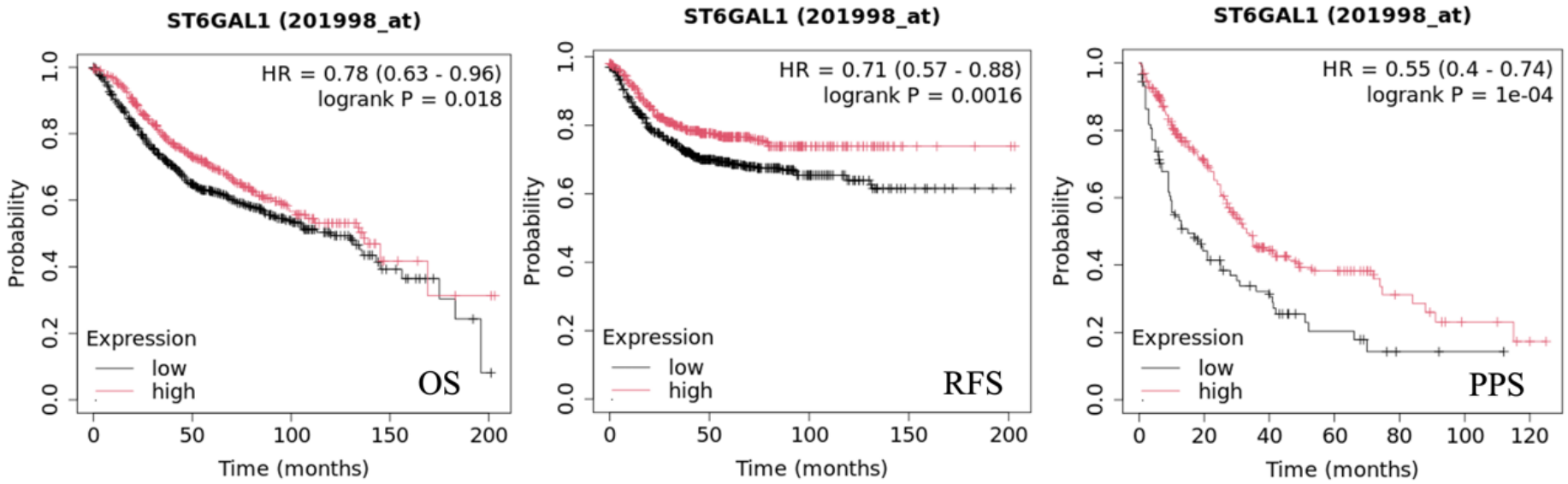

Figure 49: Low *ST6GAL1* expression is associated with poor survival outcomes in COAD patients. Comparisons between high *ST6GAL1* expression (red) and low *ST6GAL1* expression (black) were conducted to elucidate the relationship between query gene expression and the prognostic factor in COAD patients. Survival curves were constructed to outline *ST6GAL1* expression with survival criteria: overall survival (OS), post-progression survival (PPS), and relapse-free survival (RFS) criteria. $P < 0.05$ was considered statistically significant.

2.3.8 ST6GalNAc1 exhibited lower expression in CRC patient tissues

The *in silico* analysis obtained via UALCAN transcriptomics required experimental validation to confirm the deregulation of sialyltransferase ST6GalNAc1 and ST6GalNAc2, which are both directly involved in STn production. Therefore, immunohistochemistry staining was performed on tissue microarrays (N=18) (Figure 50). The transition from NAT to COAD tissues indicated greater changes in tissue morphology, particularly the standard epithelial cell structure which forms epithelial crypts in normal epithelial colon tissues have lost their arrangement due to their irregular morphology. In addition, the presence of goblet cells have been reduced in the tumour tissues, indicating a reduction in the mucin layer. Conversely, there are greater fibrous connective tissue in the tumour cores which are largely clustered around the tumour cells, a prominent feature that is not present in normal epithelial tissue cores. Furthermore, ST6GalNAc1 exhibited greater staining intensity in the normal colon patient tissues in comparison to the malignant tissue cores (enhanced brown staining in NAT and AT tissues with respect to COAD), with respective images of the tissue cores shown (Figure 50A). This was further emphasised by quantitative analysis of the staining, which revealed decreased levels of staining were present in the malignant tumour tissues ($P < 0.05$) (Figure 50C). However, ST6GalNAc2 exhibited no significant differences between NAT, AT and COAD tissue cores, similar to the data observed from UALCAN transcriptomics (Figure 50B).

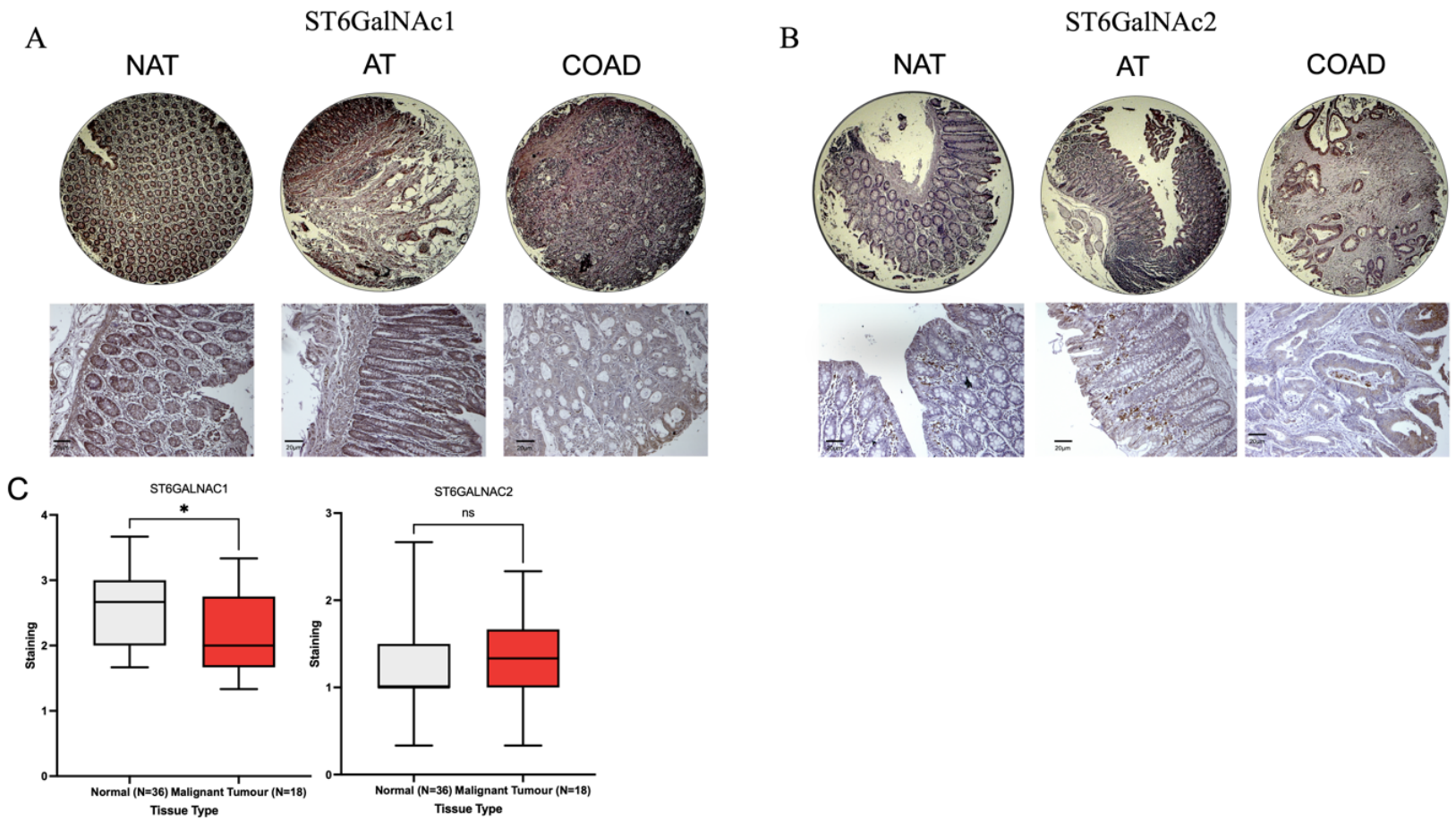

Figure 50: ST6GalNAc1 has low expression in CRC tissues. (A) IHC was performed on the CRC tissue array (BC05023a) with a primary ST6GalNAc1 antibody. Representative images of core tissues were visualised at x4 and x10 magnification. (B) IHC was performed on the CRC tissue array (BC05023a) with a primary ST6GalNAc2 antibody. Representative images of core tissues were visualised at x4 and x10 magnification. (C) Scoring analysis of CRC tissue array cores for ST6GalNAc1 and ST6GalNAc2 staining intensity to outline expression. Data was presented as box plots for NAT and AT as the normal cohort (grey) compared against malignant (COAD) tissues (red), error bars ± SD. Unpaired student's t-test. * $P < 0.05$.

2.4 Discussion

This chapter has demonstrated the multifaceted roles of deregulated sialyltransferase expression patterns of ST6GalNAc1, ST6GalNAc2, ST3GalIV and ST6Gal1. It also shows their possible role in STn production and the clinical relevance associated with CRC progression. By elucidating miRNA targets and regulatory mechanisms that modulate their expression, we can provide some insights that determine the effectiveness of sialyltransferases as therapeutic targets in cancer treatment. Furthermore, this chapter aimed to answer several questions that were outlined in this project. Thus, we believe we have identified miRNAs that can disrupt the Siglec-15/Sia axis by affecting the production of the STn antigen.

2.4.1 *In silico* target prediction analysis

Prediction analysis of interactive partners identified *ST6GALNAC1* to be co-expressed with the *AGR2* gene via GeneMANIA. AGR2 proteins are primarily localised to the ER, which plays a role in the organelles' homeostasis through the formation, breakage and subsequent isomerisation of disulphide bonds that are involved in nascent protein maturation (Moidu et al., 2020). Additionally, *AGR2* is characterised as a prominent oncogene that has correlated with tumour onset and progression in multiple tumour malignancies, including CRC (Tian et al., 2022; Xiu et al., 2019). However, there is evidence of extracellular AGR2 secretion (Fessart et al., 2016), that initiates disparate O-glycosylation patterns in comparison to ER-resident AGR2 (Pirro et al., 2021). Other interactive partners that were identified included C1GALT1, COSMC, B3GNT6 and GALNT6 from STRING analysis. C1GALT1 and COSMC are responsible for the biosynthesis of core 1 O-glycans. High energy exertion from an α-GalNAc-Thr conformational structure is recognised by C1GALT1, and by assisting 3D structural rearrangement with α-GalNAc-Ser peptide chains, C1GALT1 enables glycosylation of both acceptor molecules (González-Ramírez et al., 2022). Furthermore, C1GALT1 overexpression in CRC tumours has promoted tumour pathophysiological properties, including growth, survival and migration. Conversely, siRNA-mediated KO suppressed *C1GALT1* expression, repressing the tumour phenotype *in vitro* and *in vivo* (Hung et al., 2014). C1GALT1 function in core-1 O-glycan physiology retains greater sialylation in tumour cells, prompting reduced antigen recognition from myeloid cells via the production of the (Galβ1,3GalNAc) T antigen. Moreover, a lack of core-1 and core-3 O-glycan murine models suggested higher levels of Tn antigen present (Bergstrom et al., 2016). Furthermore, higher levels of Tn antigen were

indicative of greater instances of spontaneous chronic colitis-associated CRC (Bergstrom et al., 2016). This could suggest that the production of the tumour-associated T antigen could impact the availability of the Tn antigen substrate and negatively impact the production of the STn antigen in colitis-associated CRC. In solid CRC tumours, the literature reported the downregulation of B3GNT6 as a prognostic factor for reduced survival outcomes following downregulated expression profiles in tumour cohorts (Xiao et al., 2022), supporting our multiomics findings. Furthermore, lower B3GNT6 expression profiles were correlated to a higher proportion of CIN type tumours and *KRAS* mutations (Xiao et al., 2022). In association with ST6GalNAc1, B3GNT6 functions in O-glycan biosynthesis (Sun et al., 2023), primarily in the production of core-3 and core-4 O-glycans but also adopts a secondary function in the extension of core-1 O-glycans without the assistance of B3GALT5 or ST6Gal1 (Cherian et al., 2015). Downregulated expression of B3GNT6 in COAD tumours may suggest a reduced number of core-3 and core-4 O-glycans are synthesised from the extension of the Tn antigen, which enables the availability of the Tn antigen to remain high. This could emphasise dual roles within the glycan biosynthesis pathway and provide insights for producing several Siglec ligands.

ST6GalNAc2 indicated co-expression with AHSG from the STRING analysis, a pro-tumorigenic gene often associated with dysregulated metabolic processes and is upregulated in several tumours (Xing et al., 2023). Furthermore, *AHSG* possesses two differing human alleles that can result in three separate genotypes, including *AHSG*1*, *AHSG*2*, and heterozygous *AHSG1/2*. The resultant genotypes are contrasted by only two amino acids, which change O-glycosylation sites at position 256 (Lin et al., 2019). Changes in the *AHSG* genotype were shown to affect glycosylation patterns and exhibited greater fucosylation in patient samples (Lin et al., 2019). The diversity of glycosylation sites and O-glycan structures may emphasise possible sialylated capping of the glycoprotein by the ST6GalNAc2 protein. Furthermore, there is a greater emphasis on gene communication with MUC genes. Collectively, mucin genes produce tumour-associated truncated O-glycans, including the Tn and STn antigens (Sanz-Martinez et al., 2023). There are several reports which indicate the overexpression of MUC1 in the development of CRC tumours alongside advanced tumour stage and greater tumour invasion and metastasis (Li et al., 2019). Spatial analysis also revealed an intercellular crosstalk between $MUC1^{+}$ tumour cells and myofibroblasts that stimulated mucinous COAD tumour development (Zhou et al., 2024). A previous report has identified four tandem repeat domains within MUC1 that displayed glycosylation preferences for ST6GalNAc2, ST6GalNAc3 and

ST6GalNAc4 and underlined the importance of a lectin domain for glycosylation site selection following the addition of GalNAc (Coelho et al., 2023). As ST6GalNAc2 is dependent on particular glycosylation sites for MUC1 sialylation, this could provide insights into *ST6GALNAC2's* physical interactions with other mucin genes in a similar manner. This may suggest ST6GalNAc2 having initial interactions with glycoproteins prior to sialylated capping of STn by ST6GalNAc1. Furthermore, although MUC1 revealed no significant difference in expression between normal and COAD tumours and is contradicted within the literature. It is suggested that terminal sialylation of mucins is independent of the available glycoproteins that are present due to other deregulated sialyltransferases.

Protein analysis depicted several fucosyltransferases, such as FUT1, FUT2 and FUT3, interacting with ST3GalIV. FUT1 exhibited enhanced expression in the tumour cohort as part of our findings. Similarly, within the literature, FUT1 displayed upregulated expression in CRC *in vitro* and has been associated with poor clinical survival in CRC patients (Wu et al., 2021). Terminal fucosylation modifications are elevated in tumours due to greater FUT1 activity. FUT1 function in CRC remains limited, but it could suggest similar mechanisms in CRC for the formation of fucosylated sLE antigens following interactions with ST3GalIV. Similarly, galactosyltransferases, including B3GALT and B4GALT proteins, are involved in O-glycan and N-glycan biosynthesis, respectively, by functionally adding galactose residues for complex O-glycan and N-glycan extension via β1,3 and β1,4-linkages (Hassinen et al., 2019; Lee et al., 2011). Additionally, it has been shown that B4GALT proteins stimulated AKT activation-induced β-catenin translocation following downregulated expression profiles (Zhang et al., 2024). However, the role of galactosyltransferases in the context of CRC largely remains unexplored. A previous report, however, identified liver metastases of CRC murine models displayed higher levels of sialylation. It also demonstrated upregulated expression profiles of both B3GALT and B4GALT type proteins alongside other glycan biosynthesis pathway enzymes (Lee et al., 2011). This could suggest that greater galactosyltransferase activity could be responsible for tumour invasion and metastasis to secondary organ locations such as the liver. Interestingly, *ST3GAL4* gene communication revealed physical interactions with carbohydrate sulphotransferase proteins (*CHST2*, *CHST5*, *CHST6*) as part of the GeneMANIA analysis. CHST proteins catalyse proteoglycan biosynthesis via sulphation of hydroxyl and amine constituent groups of glycan substrates from the 3'-phosphoadenosine-5'-phosphosulphate donor molecule (Begolli et al., 2023). A previous study identified the

overexpression of *CHST4* in CRC cells. In contrast, *CHST5* exhibited greater prevalence in normal epithelial cells, and *CHST2* has shown no significant difference between normal and CRC (Yu et al., 2018). Moreover, it has been suggested that overexpression of CHST1, CHST2 and CHST4 may contribute to the sulphation modifications of Siglec ligands that can enhance receptor-ligand binding (Jung et al., 2021). From the overexpression of CHST1, Siglec-15 demonstrated significantly greater binding in HEK293 and U937 cells (Büll et al., 2021; Jung et al., 2021). Although *CHST1* was not observed to have physical interactions with the *ST3GAL4* gene, it may provide possible insights into the role of CHST proteins in the biosynthesis of Siglec ligands, including the STn antigen.

ST6GAL1 GeneMANIA analysis revealed pathway interactions with the *POU2F1* transcription factor. The transcription factor is part of the DNA-binding POU domain family and has been shown to regulate tumour onset and progression (Tantin, 2013). Further to this, *POU2F1* in CRC has demonstrated upregulated in tumours and correlated with oxaliplatin treatment resistance by stimulating glycolysis and pentose phosphate pathways (Lin et al., 2022). Moreover, a recent report identified the ubiquitination at K272 (Lysine residue, position 272) of the POU2F1 transcription factor having shown evidence of suppressing CRC via reduced PI3K/AKT signalling (Xia et al., 2024). *POU2F1* may regulate the expression of *ST6GAL1* in the glycan biosynthesis pathway. The overexpression of both *ST6GAL1* and *POU2F1* could, therefore, suggest an increase in α2,6 sialylation. Other interactions that were highlighted from our findings revealed predicted interactions with *SOX2*, *FUT1* and *CD22* (Siglec-2). SOX-2 is another transcription factor that utilises its HMG domain to directly bind to DNA sequences for transcriptional modulation (Mirzaei et al., 2022). Preferential ligands for CD22 are usually presented as α2,6 sialylated glycans (Crocker et al., 2007). This could suggest the direct involvement of ST6Gal1 in the production of CD22 preferential ligands following assisted fucosylation by FUT1 and transcription factors SOX2 and POU2F1 facilitating enhanced transcriptional *ST6GAL1* expression.

2.4.2 *In silico* expression analysis

Previous evidence within the literature demonstrated the abnormal overexpression of sialyltransferases in tumour malignancies and tumour progression, with an emphasis on the overproduction of the STn antigen and hypersialylation (Munkley, 2016; Sanz-Martinez et al.,

2023). However, UALCAN transcriptomics analysis identified significant downregulation of *ST6GALNAC1*, and *ST3GAL4* and no significant difference in the expression of *ST6GALNAC2* in the tumour cohort when compared against the normal tissue control group. A previous report indicated that enhanced *ST6GALNAC1* expression was dependent on the deregulation of M2 pro-tumorigenic phenotype macrophages and the progression of CRC cells *in vitro*. Furthermore, stimulation in STn production was also observed (Kvorjak et al., 2020). Moreover, a recent study reported the overexpression of GALNT6 in CRC tissues, an important glycosyltransferase in glycan biosynthesis (Peng et al., 2021). Additionally, the deregulation of *GALNT6* stimulated pro-tumorigenic characteristics of CRC cells *in vitro*, which increased the production of the Tn antigen. GALNT6 has been shown as an interactive partner in the STRING analysis. Its upregulated expression profiles in CRC tumours indicated the increased production of the Tn antigen precursor, which may underline the STn antigen's overexpression and its production. In addition, both pro-tumorigenic antigens Tn and STn are prevalent in CRC tumours, both of which have strongly suggested poor survival outcomes in patients (Sun et al., 2018; Tian et al., 2024). Thus, this could infer the enhanced expression of the Tn antigen and STn production is independent of ST6GalNAc1 expression. Additionally, ST6GalNAc1 may require intercellular signalling with myeloid cells to facilitate STn production within the TME. Moreover, interactions with pro-tumorigenic TAMs could also drive these observed expression patterns and promote tumour heterogeneity. *ST3GAL4* expression suggested downregulated expression in COAD tumours from the transcriptomics analysis. This correlated with evidence from the literature, which demonstrated reduced *ST3GAL4* expression in inflammation mediated colitis-associated CRC murine models (Bernard et al., 2023). Furthermore, ST3GalIV is an important player in the production of sLE^x antigens via N-glycan α2,3-sialylation, and its KO greatly impacted the production of sLE^x. However, there was not a complete abolishment of sLE^x expression until dual KO with *ST3GAL6* was conducted (Costa et al., 2023). However, downregulated expression in CRC may emphasise the role of other ST3Gal, such as ST3GalVI, to rescue the sLE^x phenotype. In addition to this, a previous report identified the roles of both ST3GalI and ST3GalIV, which contributed to the synthesis of ligands for Siglec-7 and Siglec-9 binding. Interestingly, both of these are pro-tumorigenic and are associated with poor clinical survival (Rodriguez et al., 2021). It could suggest ST3GalIV involvement in possible ligand synthesis for pro-tumorigenic Siglecs, such as Siglec-15 binding, although it has not been implicated in STn production. Furthermore, upregulated expression of *ST6GAL1* is associated with CRC progression and tumour onset (Venturi et al., 2019). Its expression profile exhibited profound transcriptomic changes in SW948 cells which

were related to chromosomal instability type tumours (Venturi et al., 2019). Moreover, *ST6GAL1* expression was associated with reduced sensitisation to chemo-radiation therapies in organoids (Smithson et al., 2024). A previous report also demonstrated enhanced ST6Gal1 expression resulted in increased α2,6-sialylation at N-glycosylation sites, showing heightened resistance to Cetuximab-based therapies (Rodrigues et al., 2021). ST6Gal1 is a known modulator of N-glycans with α2,6-sialylated linkages. Hence, greater sialylation could contribute to hypersialylation and reduced antigen recognition from myeloid cell populations. Similarly, there are also a number of other pro-tumorigenic characteristics that are also enhanced by increased α2,6-sialylation. These included reduced sensitisation of therapeutic approaches, sialylation of EGFR and the activation of the PI3K/AKT pathway mediating gefitinib resistance (Chang et al., 2018). Moreover, adhesion molecules including intercellular adhesion molecule-1 (ICAM-1) and nectin-like molecule 2 (Necl-2) are also α2,6-sialylated (Minami et al., 2013; L. Zhou et al., 2019). This suggested adhesion proteins are likely substrates of ST6Gal1 activity and induced cellular adhesion via α2,6-sialylation can stimulate tumour progression. The predominant function of ST6Gal1 is the α2,6-sialylation of N-glycans. However, our findings highlighted the downregulated expression of ST6GalNAc1 which sialylated the Tn antigen to form STn in a α2,6-sialylated linkage. This inferred ST6Gal1 activity rescues the sialylated STn phenotype leading to its overproduction. To determine the differing expression profiles that were reported, it could infer the roles of epigenetic mechanisms such as miRNAs manipulating sialyltransferase expression and activity.

2.4.3 Epigenetic regulation of sialyltransferases

UALCAN transcriptomics also characterised epigenetic regulation in the expression profiles of *ST6GALNAC2*, *ST3GAL4* and *ST6GAL1* by exhibiting significantly increased promoter methylation in the tumour cohort. It is common in CIMP molecular CRC subtype tumours to illicit greater CpG island methylation on the promoter regions of tumour-specific genes, significantly impacting tumour progression and metastasis (Nishiyama & Nakanishi, 2021). Furthermore, sialyltransferase expression can become heterogenous. *GALNT* genes that are part of the initial glycan biosynthesis pathway share abnormal expression in tumours following the hypermethylation of promoter regions (Vojta et al., 2016). Moreover, in a clinical trial conducted, findings identified promoter methylation of *ST6GALNAC3* and zinc-finger protein 660 (*ZNF660*) as diagnostic biomarkers in prostate cancer (Haldrup et al., 2018). As the hypermethylation of gene promoter regions controls tumour progression and also genes

involved in cell cycle regulation, targeting methylation sites of tumour suppressor genes may normalise gene expression. The use of DNA methyltransferase inhibitors, including 5-AZA-2′-deoxycytidine and 5-AZAcytidine, both FDA-approved, have shown positive responses in clinical trials by inducing DNA hypomethylation on DNA sequences (Greville et al., 2016). Consequently, promoter methylation can inhibit gene expression by preventing available binding sites for transcription factors, which may impact the expression of sialyltransferases across tumours. This could be the reason why *ST6GALNAC2* and *ST3GAL4* displayed downregulated expression in COAD tumours. Furthermore, it could also infer that the expression of these sialyltransferases is tumour specific. This suggests the interplay of miRNAs that regulate gene expression at the post-transcriptional level and other epigenetic modification mechanisms in solid CRC tumours. Moreover, it has been reported that the deacetylation of histone proteins can repress gene transcription (Erfani et al., 2022).

As part of the epigenetic modifications that are associated with manipulating sialyltransferase expression. The identification of novel candidate miRNAs that are predicted to be involved in the regulation of the chosen sialyltransferases were determined and the roles they play in CRC progression. In particular, the expression profiles of oncomirs and subsequent tumour suppressor miRNAs that were identified may play a direct role in the regulation of oncogenes/tumour suppressor genes such as the sialyltransferases chosen for this study and their role in CRC progression. The identification of predicted miRNAs involved in modulating gene expression and the binding affinities of predicted binding sites for the 3’ UTR region of the target mRNAs have suggested a high likelihood of gene silencing (Wang et al., 2021). For complementarity binding with target mRNA sequences, the Ago proteins are directed by the guide strand of the miRNA duplex. In addition, the complementarity between the mRNA-miRNA sequences can also dictate targeting efficiency (Hiers et al., 2024). Conversely, upon engagement with the target mRNA strand, full complementarity binding between nucleotide bases will lead to directed degradation of the target, whilst in contrast, only partial complementarity between the miRNA and target mRNA demonstrates translational repression (Shang et al., 2023). Following the binding of the RISC complex to the target mRNA strand, further scaffolding proteins, including TNRC6, facilitate the binding of transcriptional factors such as CCR4-NOT deadenylase complex to stabilise the overall structure (Rehwinkel et al., 2005). The stabilisation of the complex assists in target degradation or translational repression of the mRNA strand.

To determine that the role of sialyltransferases in STn production is affected by miRNA activity, *ST6GALNAC1* was predicted to be regulated by miR-21, miR-30e and miR-26b. As our findings suggested a tumour suppressor role of *ST6GALNAC1* in COAD tumours, all three miRNAs were demonstrated to have significant upregulation in the tumour cohorts. Previous reports have correlated miR-21 as a pro-tumorigenic oncomir that exhibits upregulated expression in multiple cancer types, including CRC, serving as a tumour biomarker (Li et al., 2023). Within the CRC tumour landscape, the synergistic effect of miR-21 and miR-335 was reported in advanced stage and MSI type CRC tumours, with the interplay of both miRNAs correlating to reduced survival outcomes in CRC patients (Calvo-López et al., 2022). Several tumour associated signalling pathways have also been suggested as a result of enhanced miR-21 activity, including greater PI3K/AKT and TGF-β signalling following deregulated expression profiles in tumour malignancies (Despotovic et al., 2021; Lai et al., 2021). Similar mechanisms have also been suggested to induce CRC progression. The role of miR-30e displayed upregulated expression in solid tumours and serves as a potential biomarker for CRC malignancies (Peng et al., 2020). Moreover, miR-30e expression profiles induced the CXCL12 axis, which facilitated CRC tumour progression (Wei et al., 2023). Previous reports have suggested that deregulated expression profiles of miR-26b correlated with CRC tumours and the modulation of MMP-9 (Farouk et al., 2023). However, the evidence in the literature of miR-26b's oncogenic properties remains limited and would require experimental validation to elucidate its role in CRC tumours. Evidence in the literature has shown that dysregulated expression patterns of miRNAs can drive tumour onset (Hussen et al., 2021). The significance between miRNA binding on the 3' UTR seed region and downregulated *ST6GALNAC1* expression may address the observations that we have witnessed.

The profile of *ST6GALNAC2* is not differentially expressed between normal and tumour cohorts. Therefore, the effect of miRNA activity to modulate its expression remains unnecessary. Similarly, the role of miR-588 also exhibited no significant difference and information regarding its expression was not available within the UALCAN database. This could suggest that the role of epigenetic modifications, such as promoter methylation has a greater impact in regulating *ST6GALNAC2* expression in comparison to the other sialyltransferases.

Of the two miRNAs identified for regulating *ST3GAL4* expression, let-7g and miR-98 demonstrated high expression in the tumour cohort that was obtained via transcriptomics analysis. Both miRNAs have only shown partial complementarity binding with the *ST3GAL4* gene sequence, suggesting translational repression. Within the tumour landscape, let-7g exhibited significant expression in CRC tumours and reduced patient survival, signifying its role as an oncomir following *ST3GAL4* downregulation (Cho et al., 2021). *In silico* analysis from a previous study has also supported these findings, which largely correlated to progression free survival and OS independent of tumour grade and patient age (Yang et al., 2017). One study suggested the inhibition of let-7g has a significant effect on CRC migration, invasion and modulation of the influx of Ca^{2+} via calcium channels (Chang et al., 2019). Typically, signal transduction mechanisms are activated through an increase of intracellular Ca^{2+} which can activate transcription factors and DNA regulatory elements in promoter regions necessary for transcriptional regulation. Thus, controlling the rate of transcription of regulatory genes (Johnson et al., 1997). Interestingly, the expression of miR-98 was shown to exhibit higher expression within high grade intra-epithelial dysplastic polyps of human orthologous familial *APC* porcine models (Stachowiak et al., 2017). The deregulation of the *APC* tumour suppressor gene is involved in the initial stages of CRC tumour onset due to somatic mutations and loss of heterozygosity in 80% of sporadic CRC tumour diagnoses (Zhang & Shay, 2017). This may indicate the role of miR-98 as a predictive biomarker of CRC development. A suggested pathway from the literature proposed miR-98 as a tumour suppressor via directed targeting of frizzled receptor 3 (*FZD3*) inhibiting Wnt signalling and CRC cellular proliferation (Kenneth et al., 2023).

ST6GAL1 regulation was characterised by the reduction of activity in tumour suppressor miRNAs miR-484, miR-125a and miR-125b in COAD tumours. Within the literature, miR-484 has typically expressed reduced expression in CRC (Jia et al., 2022). Other studies have also corroborated miR-484 expression and identified it as a tumour suppressor miRNA, particularly in MSI type CRC tumours that display distinct hypermethylation on its promoter regions (Mei et al., 2015). Furthermore, the role of long non-coding RNA (lncRNA) molecules (LINC01315) has also shown competitive binding to miR-484 to negatively impact its expression in tumours through ‘sponging’, thus promoting CRC progression and metastasis (Li et al., 2022). In addition to this, a recent study reported that miR-484 expression in the serum of CRC patients was downregulated in lower tumour grade (grade I-II) in comparison to

expression profiles in normal tissues. In contrast, miR-484 expression reported elevated levels in advanced CRC tumour grade (III-IV) (Lu & Lu, 2015). This may suggest that miR-484 expression profiles are stage dependent in CRC. Possible targets may have also been identified, both *CD137* (co-stimulatory ligand expressed on activated $CD8^+$ T-cells for antitumour response induction) and pro-inflammatory cytokine IL-8 have shown downregulated expression inhibiting MSI type CRC when miR-484 was overexpressed (Jia et al., 2022; Mei et al., 2015). Therefore, miR-484 downregulation could suggest a greater presence of an immunosuppressive TME, likely due to ineffective antitumour response generation and stimulated tumour progression following chronic inflammation. Possible elucidation of signalling pathways affected by miR-484 downregulation in CRC remains limited and would require further investigation. A previous study has elucidated that the expression of miR-125a was reduced in CRC *in vitro* (Zhang et al., 2020). Furthermore, it was reported that miR-125a has established downregulation in CRC tissues and *in vitro* cell lines. Conversely, its overexpression in functional studies suggested tumour reduction in several criteria, including migration, invasion and EMT, following the direct targeting of tafazzin (*TAZ*), a transcriptional regulator in hippo signalling (Tang et al., 2019). Therefore, this could suggest greater emphasis on regulation across N-glycan biosynthesis following ST6GalI mediated sialylation. Moreover, suggested pathways have indicated that miR-125a was responsible for the direct targeting of regulators in the PI3K/AKT and mTOR signalling pathways (Li et al., 2020; Liang et al., 2017). Similar to its counterpart, miR-125b has been reported with low expression in CRC tumour cells and tissues. However, when overexpressed, miR-125b improved tumour sensitivity to chemotherapy treatment (Zeng et al., 2021). Inversely, another thorough study also reported that repressed miR-125b expression led directly to greater chemoresistance in cells to oxaliplatin and 5-FU-based therapies (Park et al., 2020). A suggested pathway could involve the direct targeting of STAT3 and the regulation of JAK/STAT signalling, which ensures effective regulation of pro-tumorigenic genes related to cellular proliferation and apoptosis (Johnston & Grandis, 2011; Zhang et al., 2022). Upon elucidating the role of both miR-125a and miR-125b clustered expression in CRC, a previous study reported significant CpG hypermethylation on their promoter regions in CRC tissues, resulting in their inactivation (Chen & Xu, 2015).

Interestingly, miR-30e identified for *ST6GALNAC1* was revealed as a predictive miRNA candidate in the regulation of *GALNT6*, *GALNT7* and *B3GNT6*. The function may indicate a

dual role in the regulation of multiple sialyltransferases in glycan biosynthesis. *GALNT7* has shown significant downregulation in the tumour cohort, suggesting miR-30e as a probable oncomir. Similarly, a previous study reported direct targeting of *GALNT7* by miR-30e in cervical cancer cells repressed its expression profile. Thus, miR-30e could play a similar role in CRC progression (Wu et al., 2017). These findings also infer predicted binding with *B3GNT6*, indicating a similar function. Interestingly, *GALNT6* was overexpressed in tumour tissues (Peng et al., 2021). This could imply other members of the miR-30 family involved in further regulation of multiple genes particularly in the case of *GALNT6*. Evidence from the literature has suggested that genes from the same miRNA family possess similar functions to one another due to conserved sequence and structural similarities (Kamanu et al., 2013). Therefore, the likelihood of other miRNAs, including hsa-miR-30a-5p, hsa-miR-30b-5p, hsa-miR-30c-5p, hsa-miR-30d-5p could be involved separately for *GALNT6* regulation and subsequent Tn antigen production. In contrast, hsa-miR-199a-5p and hsa-miR-665 were predicted to regulate the four main sialyltransferase query genes *ST6GALNAC1*, *ST6GALNAC2*, *ST3GAL4* and *ST6GAL1*. However, both miRNAs were not observed in the individual prediction analysis of each of the aforementioned genes. Further experimental validation could underline complex disease mechanisms related to tumour progression (Dou et al., 2023). The role of hsa-miR-147a in the regulation of *C1GALT1, C1GALTC1, FUT1* and *POU2F1* suggested its role as a possible tumour suppressor miRNA. Indeed, the downregulated expression profile of miR-147a has been observed in CRC tumours (Tan et al., 2022). Correspondingly, it has also been shown to target LINC00263 to suppress the lncRNA's oncogenic properties, and its knockdown promoted tumour progression (Lee et al., 2021). The role of miR-147a in glycan biosynthesis has not been reported, albeit it is suggested that the formation of the T antigen is possible due to regulating both *C1GALT1* and *COSMC*. Lastly, both hsa-miR-541-3p and hsa-miR-96-5p were predicted for *ST6GALNAC1, ST6GAL1, ST3GAL4* and *MUC1* regulation. Evidence from the literature detailing miR-541 in CRC remains limited but was suggested to have downregulated expression in both prostate and CRC tumours (Fu et al., 2024; Pashaei et al., 2017). Based on the evidence from the literature, it could highlight a tumour suppressor role in *ST6GAL1* regulation. However, this may not fully describe its role in the other genes. In comparison, miR-96 displayed enhanced expression patterns in CRC correlating with poor clinical survival in CRC patients (Chen et al., 2022; Ge et al., 2020). Furthermore, based on the evidence from the literature, it may emphasise a direct role in regulating both *ST6GALNAC1* and *ST3GAL4*, as both exhibited decreased expression profiles in CRC. MUC1-derived STn is a tumour associated glycopeptide that has

demonstrated abnormal expression in tumours (Marchiori et al., 2020). As our findings demonstrated no significant difference in the expression of *MUC1* between normal and tumour cohorts, it is possible that sialylation, other post-translational modifications and epigenetic factors contributed to the production of overexpressed MUC1-derived sialylated glycans. The intensity of O-glycosylation for glycan biosynthesis is independent of the number of glycosylation sites available. This was observed following an increase in MUC1 tandem repeats, which did not proportionally increase the production of sialylated glycans (Syrkina et al., 2019). Therefore, miR-541 and miR-96 may regulate *MUC1*. However, this would not significantly impact its expression profile, and a greater emphasis would be placed following *MUC1* sialylation and other epigenetic factors in a CRC context-dependent environment. In addition to sialyltransferases, including *ST3GAL4*, directed targeting by miR-96 may influence its expression and synthesis of sialylated glycans. Furthermore, the role of miRNAs in relation to *ST6GALNAC1*, which is the major player in STn production, could underline miR-98 mediated regulation in STn production is independent of ST6GalNAc1 activity. Hypermethylation of *ST6GALNAC1* and the loss of heterozygosity has been observed in a prior study but still contributed to significant tumour progression in oesophageal squamous cell carcinomas (Iwaya et al., 2017). Another study reported that the biosynthesis of the STn antigen could also be a result of mutations and the loss of heterozygosity of COSMC (Munkley, 2016). Hence, the overexpression of STn could be independent of CRC progression and would not require ST6GalNAc1 activity. However, this also may only be possible due to external factors including sialylation and hypermethylation controlling expression and function. Moreover, experimental validation utilising miRNA mimics/antagomirs and post-translational modification studies will be required for further elucidation of the glycan biosynthesis pathway.

2.4.4 Associated tumour hallmark enrichment analysis and their correlation with sialyltransferase expression

Elucidating the relevance of regulatory signalling pathways and the expression of *ST6GALNAC1, ST6GALNAC2*, *ST3GAL4*, and *ST6GAL1* highlighted several frequently associated tumour hallmarks related to CRC progression (Figure 51).

Based on our GSEA analysis findings, the positive enrichment of EMT and MYC targets were identified in relation to *ST6GALNAC1* expression. This suggested the possible involvement of

these targets and key signalling mechanisms driving CRC progression (Gao et al., 2023; Shin et al., 2023). Additionally, downregulation of IL-6-mediated JAK/STAT3 signalling was observed. The pro-inflammatory stimulation and release of IL-6 and subsequent JAK/STAT3 signalling were associated with the induced EMT in multiple solid tumours (Huang et al., 2022). Through this pathway, the activation of EMT is directly mediated by a collection of tyrosine and serine/threonine kinases (Huang et al., 2022). A previous study has reported a direct correlation between the development of EMT and CRC metastasis, which occurred through crosstalk between CRC tumour cells and TAMs (Wei et al., 2019). Therefore, *ST6GALNAC1* is suggested to facilitate TME heterogeneity via signalling with myeloid cell populations and tumour associated EMT pathways. However, from our findings, the downregulated enrichment of the inflammatory response and IL-6 mediated JAK/STAT3 signalling could infer EMT is likely mediated through another mechanism. Thus, this suggested the upregulation of MYC targets could facilitate EMT in CRC progression. Dishevelled-3, a key protein in Wnt signalling, has been shown to induce EMT in CRC progression through enhanced MYC signalling and Wnt/β-catenin translocation (Yang, et al., 2023). Moreover, other MYC targets, including syntrophin β1 (SNTB1), enhanced EMT associated CRC progression via similar signalling pathways when silenced in knockdown studies (Zhang et al., 2023). In addition, another MYC target may also be highly involved, including Zinc finger protein SNAI1 (SNAIL), a key modulator of EMT. A previous study demonstrated MYC induced *SNAIL* transcription promoted EMT through TGF-β signalling (Meškytė et al., 2020). Therefore, the deregulation of *ST6GALNAC1* and its relevance to CRC progression could be characterised by the MYC/Wnt/β-catenin crosstalk as a possible axis in solid tumours.

ST6GALNAC2 GSEA analysis identified the enrichment of E2F and MYC targets. There has been evidence that E2F enhanced expression profiles correlate with tumour onset and progression from being involved in transcriptional regulation (He et al., 2023). Moreover, a large proportion of CRC *KRAS* mutant and CIN type tumours have also exhibited high expression levels of E2F (Chong et al., 2022). Furthermore, enhanced E2F expression was directly associated with clinicopathological characteristics of CRC tumours and reduced patient survival outcomes (Xu et al., 2022). Another common pro-tumorigenic signalling pathway that was highlighted by GSEA analysis revealed upregulated TGF-β signalling. TGF-β is a multifaceted cytokine that is implicated in tumorigenesis and is known to frequently regulate immune function between normal self-cells and tumour cells via promoting the

activation and production of tumour associated neutrophils (Shang et al., 2020). Moreover, TGF-β has been implicated in several pathophysiological characteristics associated with the CRC phenotype, including EMT, angiogenesis, cellular stemness, tumour invasion and metastasis (Papavassiliou et al., 2023). Deregulation of the TGF-β isoforms can affect downstream effectors, including SMAD, which can induce pro-tumorigenic signalling towards the nucleus (Attisano & Wrana, 2002). Activation of these TGF-β1 and TGF-β3 isoforms occur through the presence of avβ6 or avβ8 integrin molecules that facilitate the binding of TGF-β ligands to their complementary receptors forming a hetero-tetrameric complex between TGF-β receptor 1 and TGF-β receptor 2 (TGFβR1 and TGFβR2), respectively (Li et al., 2022). The kinase domain of TGFβR2 phosphorylates TGFβR1 at glycine (Gly, G) and Serine-rich domains, thus activating TGFβR1 to subsequently phosphorylate SMAD2/SMAD3. These proteins then form complexes with SMAD4, followed by a nuclear translocation that modulates the transcription of pro-tumorigenic genes (Colak & Ten Dijke, 2017). Interestingly, *SMAD3* was identified as part of the GeneMANIA analysis for *ST6GALNAC2*, suggesting a high likelihood of signal transduction following *ST6GALNAC2* deregulation. Identifying mTOR and TGF-β enriched hallmarks in relation to *ST6GALNAC2* could suggest the activation of both PI3K/AKT/mTOR and TGF-β/SMAD signal transduction mechanisms that promote CRC progression. Moreover, downregulated enrichment revealed tumour hallmarks that were related to EMT, the inflammatory response and the IFNγ response. This suggested that CRC tumours were not mediated by inflammation. As such deregulated *ST6GALNAC2* expression is less likely to be implicated in tumours such as colitis-associated CRC, which promotes tumour progression following large intestinal tissue damage as a result of sustained chronic inflammation (Zhou et al., 2023). Moreover, this specific type of CRC is mediated by underlying health conditions, including IBD and UC (Dan et al., 2023). Conversely, the role of the IFNγ cytokine typically modulates immunological responses to infection and inflammation and plays a role in anti-tumour activity (Coelho et al., 2023). The identification of the IFNγ response as negatively enriched may emphasise a reduction in IFNγ mediated signalling, particularly related to the downstream effector JAK/STAT pathway (P. Sharma et al., 2017). Furthermore, missense mutations in the IFNγ DNA sequence alongside reported mutations in JAK1/JAK2 have inhibited the expression of genes involved in encoding proteins for antigen recognitions (Patel et al., 2017). Thus suggesting increased resistance to immune checkpoint blockade therapies.

GSEA enrichment analysis of *ST3GAL4* revealed contradictory findings compared to *ST6GALNAC1* and *ST6GALNAC2,* which identified the enrichment of the inflammatory response, IL-6 mediated JAK/STAT3 signalling and the IFNγ response. The inflammatory response and elevated levels of IL-6 are both observed under chronic inflammatory states, and the hyperactivation of both pathways is associated with reduced patient survival (Hirano, 2021; Johnson et al., 2018; Lin et al., 2019). Interestingly, chronic inflammation from conditions including UC and CD have implications associated with CRC development, which see greater instances of inflammation prior to the development of polyps and CRC tumours (Rogler, 2014). As previously mentioned, the activity of miR-98 has shown higher levels of expression in APC mutant polyps, which are also correlated to greater inflammation and inflammatory cytokine production (Klampfer, 2011). This may emphasise that *ST3GAL4* downregulated expression is more commonly associated with inflammation mediated conditions that lead to sporadic CRC tumours. Additionally, *KRAS* signalling was revealed as positively enriched. Deregulated *KRAS* is a common oncogene identified in CRC tumour onset and is a known driver of CRC development (Sameer, 2013). Thus, this suggested that *ST3GAL4* is associated with tumour onset rather than tumour progression. Moreover, IFNγ response was shown to induce PD-L1 expression via the modulation of the PI3K/AKT signalling pathway (Gao et al., 2018). Furthermore, *ST3GAL4* GSEA analysis identified the enriched hallmark TNFα signalling via NFkβ, an inflammatory pro-tumorigenic signalling mechanism involving the activation and induction of NFkβ for transcriptional regulation, similar to STAT signalling (De Simone et al., 2015). Furthermore, in response to stimuli, deregulation of the NFkβ pathway could illicit the activation and polarisation of macrophages to the M2 tumorigenic phenotype and stimulate the release of anti-inflammatory cytokines, including IL-10 (Liu et al., 2017). As *ST3GAL4* expression is downregulated in CRC tumours, this suggested an immunomodulatory role that stimulates TAMs mediated immunosuppression, possibly through NFkβ. Downregulated enrichment of tumour hallmarks identified MYC, E2F, mTOR signalling and DNA repair. In contrast to *ST6GALNAC1* and *ST6GALNAC2*, the downregulated enrichment of these pathways may infer that *ST3GAL4* expression has a greater emphasis on inflammatory mediated signalling in CRC progression. Based on these findings, *ST3GAL4* may play a pre-emptive role in CRC development and could be utilised as a significant diagnostic biomarker and therapeutic target.

ST6GAL1 GSEA analysis revealed the enrichment of the early oestrogen response as being significantly relevant to the CRC phenotype. However, due to the low number of DE genes involved in the analysis, it is difficult to draw conclusions relating to signalling pathways and cancer hallmarks associated with CRC tumour progression. Nevertheless, previous evidence has correlated the role of the early oestrogen response via premature oestrogen receptor activation in positive breast cancer cases (Skriver et al., 2020). Typically, neoadjuvant endocrine therapy is used in the treatment of oestrogen receptor (ER^+) $HER2^-$ breast cancer tumours, inhibiting the deregulation of oestrogen within the body (López-Velazco et al., 2024). Although it is difficult to speculate, these findings suggested the likelihood of CRC metastases to breast tissues. A previous study demonstrated that there is a possibility of primary CRC tumours metastasising to breast tissues (Hsieh & Hsu, 2019). However, the occurrence of breast metastases originating from CRC tumours is extremely rare. Further elucidation of the query genes could underline specific pro-tumorigenic signalling pathways related to the CRC phenotype. Moreover, these findings, have suggested the activity of each sialyltransferase is context-dependent with specific CRC molecular subtypes.

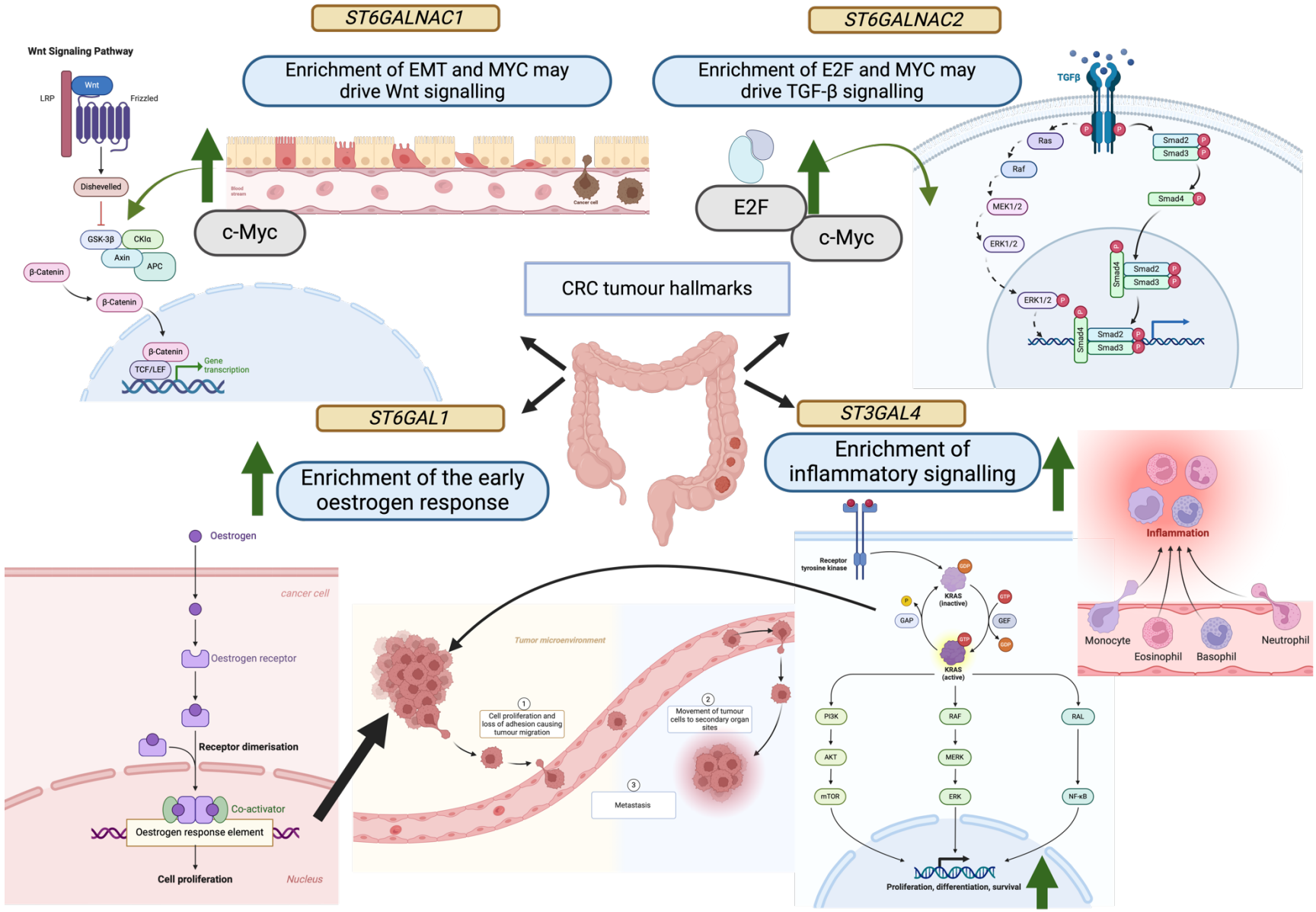
ST6GALNAC1
Enrichment of EMT and MYC may drive Wnt signalling
Wnt Signaling Pathway
Wnt
LRP
Frizzled
Dishevelled
GSK-3β
CKIα
Axin
APC
β-Catenin
β-Catenin
β-Catenin
TCF/LEF
Gene transcription
c-Myc
ST6GALNAC2
Enrichment of E2F and MYC may drive TGF-β signalling
E2F
c-Myc
TGFβ
Ras
Raf
MEK1/2
ERK1/2
Smad2
Smad3
Smad4
CRC tumour hallmarks
ST6GAL1
Enrichment of the early oestrogen response
ST3GAL4
Enrichment of inflammatory signalling
Oestrogen
cancer cell
Oestrogen receptor
Receptor dimerisation
Co-activator
Oestrogen response element
Cell proliferation
Nucleus
Tumor microenvironment
1 Cell proliferation and loss of adhesion causing tumour migration
2 Movement of tumour cells to secondary organ sites
3 Metastasis
Receptor tyrosine kinase
KRAS (inactive)
KRAS (active)
GAP
GEF
GTP
GDP
PI3K
AKT
mTOR
RAF
MERK
ERK
RAL
NF-κB
Proliferation, differentiation, survival
Inflammation
Monocyte
Eosinophil
Basophil
Neutrophil

Figure 51: Summary of the GSEA enrichment analysis of the queried sialyltransferases *ST6GALNAC1*, *ST6GALNAC2*, *ST3GAL4* and *ST6GAL1* and their association with tumour hallmarks that are frequently manifested in CRC progression. GSEA enrichment analysis revealed the positive enrichment of several signalling pathways associated with CRC progression including EMT, inflammation, and Wnt signalling. The deregulation of key pathways that are highlighted drives tumour progression and tumour heterogeneity, emphasising the correlation between sialyltransferase expression and their potential as therapeutic targets.

2.4.5 The role of sialyltransferases and myeloid cell populations

Sialyltransferase expression and the abundance of immune related signatures may emphasise intercellular signalling that enhances TME heterogeneity. The SRCC quantitative analysis exhibited a non-correlative relationship between myeloid cells and *ST6GALNAC1* expression. However, it did report significance between the query gene and $CD4^+$ T-lymphocytes and monocytes. A previous study revealed that monocytes and macrophages would account for a significant proportion of tumour infiltrating myeloid cells via a pan-cancer transcriptomics analysis (Cheng et al., 2021). Therefore, pro-tumorigenesis of myeloid cell populations, including $CD4^+$ T-lymphocytes, could enhance TME heterogeneity (Zhao et al., 2021). Furthermore, a pan-cancer study revealed tumour stromal heterogeneity predicted naïve $CD4^+$ T-lymphocyte response to efficacious immunotherapeutic treatment (Qian et al., 2020). Additionally, the depletion of monocyte populations in tumours also correlated to an immunosuppressive tumour phenotype in patients (Ortiz-Muñoz et al., 2023). At the gene level, a previous report identified DE *ST6GALNAC1,* and miRNAs involved in *ST6GALNAC1* regulation stimulated intra-tumour heterogeneity upon the occurrence of CRC metastasis (Urh et al., 2022). Conversely, another study identified STn engagement with Siglec-15 induced TGF-β secretion from monocytes and macrophages (Hugonnet et al., 2021). This suggested possible tumoral recruitment and greater tumour heterogeneity from *ST6GALNAC1* expression. It has been shown that immunotherapeutic treatment approaches elicit a positive response in a small subset of patients. However, targeting pro-tumorigenic myeloid cells in conjunction with the specific targeting of therapeutic targets may further enhance the clinical effectiveness of treatment strategies. Monocytes demonstrate plasticity in a tumorigenic environment and can contribute to tumour heterogeneity when differentiated into pro-tumorigenic M2 macrophages. Direct blocking of M2 polarisation and stimulating monocyte differentiation to anti-tumorigenic M1 macrophages could prevent TAM formation (Olingy et al., 2019). Hence, this suggests improvements to current immunotherapeutic approaches. Additionally, stimulating $CD4^+$ T-cells to Th_1 cells and inducing $CD8^+$ T-cell activation could significantly improve anti-tumour activity (Speiser et al., 2023).

TISIDB analysis revealed several correlations of multiple myeloid cell populations with *ST6GALNAC2* expression. Several interactions with myeloid cells and components related to the TME could regulate immune tolerance and tumour metastasis (Bai et al., 2023). Moreover, solid CRC tumours have displayed an immunogenic phenotype that is characterised by

immune-induced inflammation which contributed to TME heterogeneity (Chen & Mellman, 2017). Thus, this suggested possible targets for increasing therapeutic efficacy. Additionally, this may infer a broader immunomodulatory role associated with ST6GalNAc2 activity. Observable changes in sialylation of cell surface antigens may alter the antigen recognition of tumour cells and macrophages, modulating their activation and polarisation. A previous study reported the crosstalk between tumour cells and macrophages, which stimulated *ST6GALNAC1* and STn antigen production in colitis-associated CRC (Kvorjak et al., 2020). Therefore, this could infer the crosstalk between *ST6GALNAC2* expression and macrophages in a similar fashion. Furthermore, *ST6GALNAC2* expression correlating with activated T-cell lymphocytes is intriguing. Following the terminal capping of sialoglycan ligands for Siglec receptors and upon engagement, studies have shown reduced activation of effector myeloid cells, including $CD4^+$ and $CD8^+$ T-lymphocytes (Wang et al., 2022). Hence, this suggests that *ST6GALNAC2* expression has little effect on the activation of myeloid cells, as there was no significant difference in *ST6GALNAC2* expression between normal and tumour cohorts. Additionally, a reduction in sialylated glycans on plasma membranes will enable further antigen recognition and stimulation of anti-tumour activity (Munkley, 2022).

ST3GAL4 demonstrated a significant correlative relationship with macrophages and monocytes, albeit only the monocyte cell population revealed an SRCC of greater than >0.2. A previous study demonstrated that the early stages of chronic inflammation were characterised by monocytic adhesion to the endothelium following the recruitment by pro-inflammatory cytokines such as TNFα (Ingersoll et al., 2011). Furthermore, IFNγ was also shown to increase the adhesive capabilities of monocytes through the upregulation of pro-tumorigenic immune checkpoint proteins inducing PD-L1 (Cai et al., 2023). The identification of the IFNγ response as enriched suggested a possible mechanism for driving chronic inflammation mediated tumour progression. Correspondingly, Sialoadhesin, a monocytic and macrophage marker, interacts with α2,3-sialylated glycan structures synthesised by ST3GalIV, thus promoting tumour progression (Singh & Choi, 2019). Similarly, cancer-associated fibroblasts that display N-glycan ligands produced by ST3GalIV activity can serve as Siglec ligands that prevent antigen recognition and drive tumoral recruitment of M2 macrophages (Boelaars et al., 2024). The terminal capping by ST3Gals may emphasise greater tumoral recruitment towards the tumour stroma, leading to heterogenous immunosuppression. However, reduced expression of

ST3GAL4 in CRC tumours could suggest that other sialyltransferases rescue the inflammatory phenotype and infer the inhibition of myeloid cells via ST3GalIV activity as tumour specific.

ST6GAL1 TISIDB analysis revealed similar correlative relationships as *ST3GAL4*, possibly indicating myeloid regulation in a similar mechanism. A previous study reported ST6Gal1 activity modulated monocyte and macrophage activity in association with NFkβ nuclear translocation and phosphorylation of ERK and AKT (Rusiniak et al., 2022). Furthermore, greater α2,6 sialylation induced by ST6Gal1 activity significantly impacted immune signalling pathways in chronic inflammatory immune cell models (Holdbrooks et al., 2020). Furthermore, prolonged TNFα mediated NFkβ nuclear translocation was reduced in *ST6GAL1* knockdown studies, indicating a significant role in modulating tumour associated inflammation. Other sialylated targets that were also reported to influence immune cells included tumour necrosis factor receptor 1 (TNFR1) stimulated via TNFα activity, preventing phorbol-12-myristate-13-acetate (PMA) mediated apoptosis of macrophages (Liu et al., 2011). Thus, increased α2,6 sialylation of TNFR1 may underline desensitisation to TNFα mediated apoptosis and inducing M2 macrophage polarisation. As α2,6 sialylated glycans are predominantly synthesised by ST6Gal1 activity, it may signify its role in mediating a hypersialylated TME via preventing antigen recognition. Additionally, it suggested an immunomodulatory role in myeloid tumoral recruitment, inducing tumour heterogeneity and greater immunosuppression.

2.4.6 The role of sialyltransferases and pro-tumorigenic immune checkpoint proteins

ST6GALNAC1 exhibited a significant association with *TIGIT*, a pro-tumorigenic immune checkpoint protein, via TIMER analysis (Urh et al., 2022). *TIGIT* expression has been associated with tumour progression and has demonstrated the regulation of myeloid cell exhaustion, including $CD8^+$ T-cells (Liang et al., 2021). Furthermore, deregulated TIGIT expression has emphasised reduced overall survival in CRC patients (Liang et al., 2021). This suggested the involvement of other immune checkpoint related pathways that facilitated tumour progression via deregulated sialoglycan biosynthesis.

In contrast, *ST6GALNAC2* TIMER analysis revealed distinct relationships with most immune checkpoint proteins, excluding *SIGLEC15*. ST6GalNAc2 is involved in STn antigen production to a lesser extent (Miao & Zhao, 2016; Schneider et al., 2001). However, this suggested that *ST6GALNAC2* expression is more associated with the synthesis of other glycan

ligands. Hence, *ST6GALNAC2* expression is not correlated to the abundance of *SIGLEC15*. ST6GalNAc2 expression altered the abundance of other O-glycans on the cellular surface, such as promoting galectin-3 binding and inducing tumour progression (Ferrer & Reginato, 2014). Furthermore, there were greater levels of core-1 O-glycans, including the T antigen, that were produced (Ferrer & Reginato, 2014). Additionally, another study demonstrated the role of ST6GalNAc2 in the synthesis of the disialyl-T antigen (Fuseya et al., 2023). Therefore, this suggests that ST6GalNAc2 exhibits a complex role in the synthesis of multiple glycan structures.

ST3GAL4 exhibited no correlative relationship with all the queried immune checkpoint genes. However, *ST3GAL4* did demonstrate a significant association with several immune checkpoints, including *TIGIT, LAG3, CD274, CTLA4* and *SIGLEC15*. One study reported the synthesis of Siglec ligands mediated by ST3GalIV activity for Siglec-7^+ and Siglec-9^+ tumour cells and is associated with the synthesis of both N- and O- glycan structures (Rodriguez et al., 2021). Moreover, ST4GalIV has shown to be the major contributor of E-, P- and L- selectin ligands in comparison to its ST3GalIII and ST3GalVI counterparts (Mondal et al., 2015). Targeting P-selectin glycoprotein ligand-1 (PSGL-1) demonstrated positive responses in PD-1/PD-L1 resistant melanomas (DeRogatis et al., 2022). Thus, this suggested possible treatment strategies upon ST3GalIV and PSGL-1 dual targeting for patients who responded poorly to immune checkpoint blockade therapy. Conversely, *ST3GAL4* expression may be associated with the production of other pro-tumorigenic immune checkpoint proteins and is possibly not solely limited to the production of Siglec ligands.

ST6GAL1 expression analysis exhibited only a significant association with immune checkpoints *CD274* and *SIGLEC15*. Siglec ligands mediated by ST6Gal1 have been suggested in tumour progression. The regulation of ST6Gal1 activity corresponded to the development and characterisation of cis-ligands for Siglec-7^+ NK cells (Jame-Chenarboo et al., 2024). Moreover, CD33 was capable of recognising both α2,3 and α2,6 sialylated glycan structures, which suggested a possible functionality of ST6Gal1 activity (Rodrigues et al., 2020). Similarly, PD-L1 is a highly glycosylated protein that is upregulated in cancer. PD-L1 exhibited several N-glycosylation sites at residues N192, N200 and N219 (Asn192, Asn200, Asn219), stabilising the protein structure and inhibiting T-cell activity (Li et al., 2016). Another study has also reported that PD-L1 glycosylation helped in the stability and maturation of the PD-L1 ligand, which was necessary for immune evasion (Shi et al., 2022). Therefore, N-

glycosylation of PD-L1 and possible synthesis of Siglec ligands has emphasised the tumorigenicity of ST6Gal1 in glycan biosynthesis. Furthermore, sialyltransferases associated with multiple immune checkpoint proteins could suggest a potential introduction for combination therapies that target sialyltransferases alongside current immune checkpoint blockade approaches.

2.4.7 The role of sialyltransferases and patient survival

Several reports have demonstrated the enhanced expression of *ST6GALNAC1* in multiple malignancies, including lung adenocarcinoma (LUAD), lung squamous cell carcinoma (LUSC), and ccRCC (Alabiad et al., 2021; Bai et al., 2018). However, based on the findings from our multiomics approach, patient survival data correlated with low *ST6GALNAC1* expression with reduced survival in all queried parameters ($P < 0.05$). These findings also supported both transcriptomics and IHC findings, exhibiting a lower prevalence of *ST6GALNAC1* in tumour tissues. Similarly, reduced expression of *ST6GALNAC1* was shown to promote tumour progression in patient samples and *in vitro* cell lines in oesophageal squamous cell carcinoma, another epithelial tumour malignancy (Iwaya et al., 2017). Additionally, the silencing of other O-linked glycosyltransferases impacted the expression of *ST6GALNAC1*. A recent study reported that *C1GALT1* knockdown also downregulated the expression of *ST6GALNAC1* and *B3GNT6*, both of which are heavily involved in O-linked glycan biosynthesis (Khiaowichit et al., 2022). Therefore, this highlighted that low expression of *ST6GALNAC1* is a significant contributor to tumour progression and subsequent reduced patient survival, possibly in CRC tumours.

High levels of *ST6GALNAC2* expression were associated with poor survival outcomes in all patient survival criteria. A previous study has indicated the activity of miR-135b and miR-182 mediated abnormal *ST6GALNAC2* expression in CRC *in vitro*, prompting greater treatment resistance to 5-FU-based approaches (Liu et al., 2017). Similarly, another study reported the direct targeting of *ST6GALNAC2* by miR-182/-135b activity inhibited pro-tumorigenic characteristics, including migration, adhesion and invasion in CRC cells (Jia et al., 2017). However, the expression of *ST6GALNAC2* may be context-dependent. In breast cancer tumours, *ST6GALNAC2* was identified as a tumour suppressor and was correlated to improved survival (Murugaesu et al., 2014). Other pathological diseases, such as acute coronary syndrome, have also reported reduced *ST6GALNAC2* expression (Hadžibegović et al., 2014).

Suggesting the possibility of *ST6GALNAC2* expression as context-dependent with regard to CRC progression.

In comparison, *ST3GAL4* displayed high expression that correlated only with OS and RFS criteria. Conversely, *ST3GAL4* expression demonstrated significantly reduced expression in tumour cohorts identified from our transcriptomics data. This discrepancy suggests the involvement of other factors which determine the differential expression of *ST3GAL4* in CRC. One study reported that the presence of IFNγ induced the expression profile of ST3GalIV, stimulating pro-tumorigenic pathways, including NFkβ nuclear translocation and PI3K/AKT signalling (Templeton et al., 2021). However, the role of *ST3GAL4* in CRC survival remains to be elucidated. Nevertheless, based on the mechanisms provided as part of our findings, it suggests possible implications of external factors that modulate the differential expression of *ST3GAL4*. Thus, impacting patient survival outcomes.

Similarly to *ST6GALNAC1*, low *ST6GAL1* expression in CRC patients has correlated with decreased survival across all criteria, albeit exhibiting higher expression in CRC tumours obtained from UALCAN transcriptomics. Inversely, ST6Gal1 overexpression in CRC was identified and has shown higher expression in lower grade tumours (grade I-II), in contrast to advanced grade (grade III-IV) (Zhang et al., 2017). Therefore, this suggested *ST6GAL1* may play a role in the initial stages of tumour development compared to the development and metastasis of more advanced CRC tumours. Furthermore, due to the genetic heterogeneity of CRC tumours, *ST6GAL1* expression may also be dependent on the molecular subtype and therapeutic intervention. A previous study demonstrated MSI type tumours exhibited lower levels of *ST6GAL1*, whilst CIN tumours revealed high expression of the *ST6GAL1* gene (Pérez et al., 2020). Similarly, *ST6GAL1* expression was upregulated in CRC patients following chemoradiation therapies, possibly inferring *ST6GAL1* as a major player in tumours that developed treatment resistance (Smithson et al., 2022). Hence, it suggested the differential expression of *ST6GAL1* across CRC molecular subtypes, malignancies and before and after receiving treatment. As such, from the collective evidence as part of this chapter, our findings have outlined possible mechanisms that are involved in the observable discrepancies between the sialyltransferase genes, transcriptomics analysis and patient survival data. Furthermore, to better understand the differential expression of these sialyltransferase genes, *in silico* tools would require certain parameters to be more constringent for data curation and analysis.

2.4.8 Possibilities of other sialyltransferases involved in the production of the STn antigen

The present multiomics approach identified miRNAs involved in sialyltransferase expression. However, other sialyltransferases may impact STn production and play a pivotal role in CRC progression. It is well known that the STn antigen displays a high binding affinity for the engagement with the Siglec-15 protein, the putative ligand synthesised by ST6GalNAc1 and ST6GalNAc2 (Murugesan et al., 2021). However, it has also been reported that other sialylated glycans can also display high binding affinities for Siglec-15, particularly when modulated via upregulated sialyltransferases *ST3GAL4* and *ST6GAL1* (Briard et al., 2018). Moreover, we have emphasised the role of GALNT proteins involved in the initial stages of GalNAc type-O glycosylation. Furthermore, several GALNT genes have deregulated expression profiles in CRC (Lavrsen et al., 2018; Liao et al., 2023). Thus, this suggests that upregulated GALNT proteins such as GALNT4 and GALNT6 could facilitate sialylation, increasing the production of the T antigen. Consequently, this could enhance the production of the STn antigen independently of ST6GalNAc1 and ST6GalNAc2 expression. Similarly, other post-translational modifications, including the sulphation of sialoglycans, can play a pivotal role in tumour onset and immune evasion. The overexpression of carbohydrate sulfotransferases such as CHST1 and CHST2 can stimulate the occurrence of hypersialylation (Jung et al., 2021). Thus promoting Siglec binding. Additionally, *CHST1* overexpression exhibited a greater effect on sialoglycan binding and heavily impacted the preferential binding of Siglecs for specific O-glycans. Elucidating the roles of these proteins may provide further information on the production of the STn antigen in glycan biosynthesis within CRC. Contrary to the present literature, the multiomics approach that was adopted to elucidate the inner workings of sialyltransferases in glycan biosynthesis and STn production has underlined the production of the STn antigen is independent of ST6GalNAc1/ST6GalNAc2 expression. However, based on the evidence from the literature and our *in silico* data mining analysis, their interactions with other possible gene targets underline their potential as therapeutic targets in CRC progression. Furthermore, it has been demonstrated that the interplay of other sialyltransferases that are involved in glycan biosynthesis, including ST3GalIV, ST6Gal1 and possibly sulphotransferases such as CHST1, may rescue STn production. Additionally, epigenetic modifications that were identified alongside the differential expression of sialyltransferases may work in conjunction and achieve a synergistic effect on their respective expression profiles.

2.4.9 Limitations and future directions

This chapter characterised the crosstalk of interactive gene and protein targets and elucidated several regulatory pathways associated with CRC progression by integrating the data of key databases. However, it is worth mentioning that there are several limitations that would need to be addressed when utilising a one-method approach. Power calculations of the patient cohort tissue samples for the UALCAN database was not incorporated into the analysis as the algorithms for expression profiles are pre-generated with sample parameters and sample sizes not solely fixed. The addition of a power calculation can determine the minimum sample size required for a sample cohort to illicit an effect and any significant relationship between two variables (Burgess, 2014). Therefore, implementing power calculations within the algorithms to underline expression profiles will greatly enhance any significance that is identified. Although well-defined pathways and predictive targets were identified, it may not fully grasp the interplay of complex sialylation networks without experimental validation to confirm their significant impact on cellular behaviour and tumorigenesis (Kaur et al., 2021; Subramanian et al., 2020). Similarly, differences in methodological approaches, including data compilation, distinct computational models across studies, and variations in data selection and normalisation, all present challenges for data comparability (Ye & Vakhrushev, 2021). These can accentuate varied data processing algorithms, affecting final data outcomes and evaluation metrics. Particularly, in the case of miRNA target prediction, the variance of candidate miRNAs that were chosen to regulate the sialyltransferases are varied among each of the databases that were used. This highlighted that the algorithms provide different score predictions for creating a hierarchy of predicted miRNAs, underlining the difficulty in replicating a meta-analysis of available experimental data. Furthermore, limited sample size, sample availability and the requirement of specific computational tools and algorithms generated difficulties, which require sophisticated data mining tools and specialist software that limits reproducibility. Experimental validation can also present significant challenges. There are difficulties in the histological staining of truncated O-glycans, particularly in the histological staining of the STn antigen, especially as antibodies exhibit low target specificity, initiating cross-reactive staining of similar glycans (Loureiro et al., 2018). However, addressing these challenges can introduce robust data interpretation without the generation of false positive results. Further improvements to the chapter would involve characterising the identified miRNAs involved in sialyltransferase gene regulation. From this, transfection studies incorporating antagomirs/mimics will normalise the expression of miRNAs capable of

effective mRNA targeting. Hence, determining the expression profiles of these sialyltransferases in the presence of positively transfected cell lines would underline the direct binding of miRNA-mRNA strands. Although IHC analysis elucidated the expression of ST6GalNAc1 and ST6GalNAc2 at the protein level, it would be greatly beneficial to determine the expression profiles of the other query sialyltransferases, ST3GalIV and ST6GalI as well. Additionally, increasing the sample size of stained patient samples would reduce the variation between normal and malignant tissues. Furthermore, evidence from the literature has shown the overexpression of the STn antigen in CRC malignancies (Dombek et al., 2022). Hence, it would prove beneficial to elucidate the expression analysis of the STn antigen by IHC analysis and infer other sialyltransferases are involved in rescuing STn production upon observing the downregulation of ST6GalNAc1 and ST6GalNAc2.

2.5 Conclusion

To conclude, this chapter has predicted possible oncomirs and tumour suppressor miRNAs involved in regulating the sialyltransferases of interest that were identified utilising the miRNA prediction database software tools (Table 10). MiRNAs were chosen based on a score prediction algorithm and were cross-referenced across four possible databases and the most frequent hits that appeared were chosen for further analysis. Moreover, the further analysis of these candidate miRNAs revealed only a certain proportion of miRNAs with high binding affinities towards their respective target genes. One key example that underlined miRNA targeting is the tumour associated oncomirs miR-21 that is overexpressed in several malignancies including CRC and was demonstrated as targeting *ST6GALNAC1* expression. Furthermore, physical interactions and communications with neighbouring genes/proteins highlighted by GeneMANIA and STRING analysis tools also revealed common miRNA elements, indicating that miRNAs are involved in the regulation of multiple sialyltransferases in the glycan biosynthesis pathway. Thus, this suggested possible regulatory mechanisms for the production of tumour associated glycans including the STn, Tn and T antigens. When associating sialyltransferase expression to commonly associated tumour hallmarks in relation to CRC progression, several prominent signalling pathways were revealed including TGF-β and Wnt/β-catenin signalling. Both of these pathways are commonly deregulated in CRC progression. In addition, *ST3GAL4* expression underlined the enrichment of inflammatory signalling responses which possibly indicate its role in inflammation mediated CRC development, possibly stemming from pathologies including IBD, CD and UC. In relation to the tumour heterogeneity CRC tumour possess and the possible involvement in the TME, the association between sialyltransferase expression alongside myeloid cell populations and immune checkpoint proteins have suggested sialyltransferase expression is correlated to multiple facets of CRC tumour progression. In particular, the role of *ST6GAL1* overexpression in the prevalence of PD-L1^{+} and Siglec-15^{+} tumours, both of which are capable of inducing immunosuppression and driving CRC progression. Upon elucidating the protein expression of ST6GalNAc1 and ST6GalNAc2 at the protein level, it was surmised that the production of the STn antigen is independent of sialyltransferase activity. Therefore, this inferred the interplay of other sialyltransferases that could rescue the production of the STn antigen. Moreover, one the project's objectives referred to the disruption of the Siglec-15/Sia axis through various mechanisms and its impact on miRNA activity. Hence, this chapter has emphasised the roles of sialyltransferases as potential therapeutic targets and identified several miRNAs that may

prove useful in miRNA-mediated therapies. However, further elucidation and experimental validation of these identified miRNAs and gene targets are required to gain further insights into the regulation of the Siglec-15/Sia axis.

Table 10: Summary of the expression profiles of sialyltransferases and their respective miRNAs in CRC.

Query genes	Sialyltransferase expression in CRC tumours	Identified miRNAs predicted for sialyltransferase expression	miRNA expression profile in CRC tumours
ST6GALNAC1	Downregulated	hsa-miR-21-5p	Overexpressed
		hsa-miR-30e-5p	Overexpressed
		hsa-miR-26b-5p	Overexpressed
ST6GALNAC2	Not differentially expressed	hsa-miR-588	N/A
ST3GAL4	Downregulated	hsa-miR-193a-3p	Overexpressed
		hsa-miR-370-3p	Overexpressed
ST6GAL1	Upregulated	hsa-miR-125a-5p	Under expressed
		hsa-miR-125b-5p	Under expressed
		hsa-miR-484	Under expressed

Chapter 3 - Characterisation of a novel small molecule Siglec-15 inhibitor and its effect on miRNA regulation as a treatment alternative for CRC progression

3.1 Introduction

3.1.1 Siglec-15 as a therapeutic target in CRC progression

As mentioned in Chapter 1, Siglec-15 is also a recently discovered pro-tumorigenic immune checkpoint protein (Figure 52), that was identified in immunosuppression and correlated to tumour progression in several malignancies (Figure 53) (Wang et al., 2019). Typically, it is expressed as a plasma membrane receptor on solid tumours, which has demonstrated an abnormal expression of Siglec-15 in various tumour types. Further to this, its overexpression is also contributed to by enhanced N-glycosylation at N172 (N, Asparagine), which stabilised the protein structure and stimulated transport to the plasma membrane (Chen et al., 2020). Of note, a pan-cancer analysis reported the overexpression of Siglec-15 in OV, LSCC, NSCLC, CRC and many others (Li et al., 2020). Furthermore, particularly in the CRC tumour landscape, significantly enhanced *SIGLEC15* expression was associated with MSI type tumours (Du et al., 2021). In addition to this, Siglec-15 is associated with having sequence similarity with PD-L1 (a pro-tumorigenic immune checkpoint protein ligand), with approximately 30% of the extracellular domain possessing homology (Huang et al., 2023). The functional role of PD-L1 is associated with the activation of the PD-1 pathway. However, sequence homology may infer shared immunoregulatory functions with Siglec-15. What is also interesting is that the expression of PD-L1 and Siglec-15 have exhibited mutually exclusive expression on the surface of tumour cell populations (Sun et al., 2021). However, a recent study reported a greater proportion of tumour and tumour stromal cells exhibited higher levels of Siglec-15 in comparison to PD-L1 (Lu et al., 2023). This underlines Siglec-15 as an ideal candidate for targeted therapeutic approaches, particularly in PD-L1^{-} Siglec-15^{+} and dual positive cancer patients. As part of this study, we primarily focused on the characterisation of a newly synthesised organic β-amino carbonyl compound for Siglec-15 targeting and elucidating downstream regulatory mechanisms that are affected in CRC progression, namely the involvement of miRNAs. Although Siglec-15 has been identified as a pan-cancer associated therapeutic target, we have utilised CRC *in vitro* cell models to investigate the oncogenic role of Siglec-15 following Siglec-15 targeted inhibition. Characteristics of CRC tumours provide a well-established model system for studying the cytotoxic profile of therapeutic agents for treating epithelial tumours. However, it is emphasised that by targeting CRC tumours, there are much broader applications in the treatment of other Siglec-15^{+} tumours. Moreover, following preliminary characterisation of the β-amino carbonyl compound, the next steps

would follow in a combination approach with PD-L1 antagonists for improved clinical effectiveness (Sun et al., 2021).

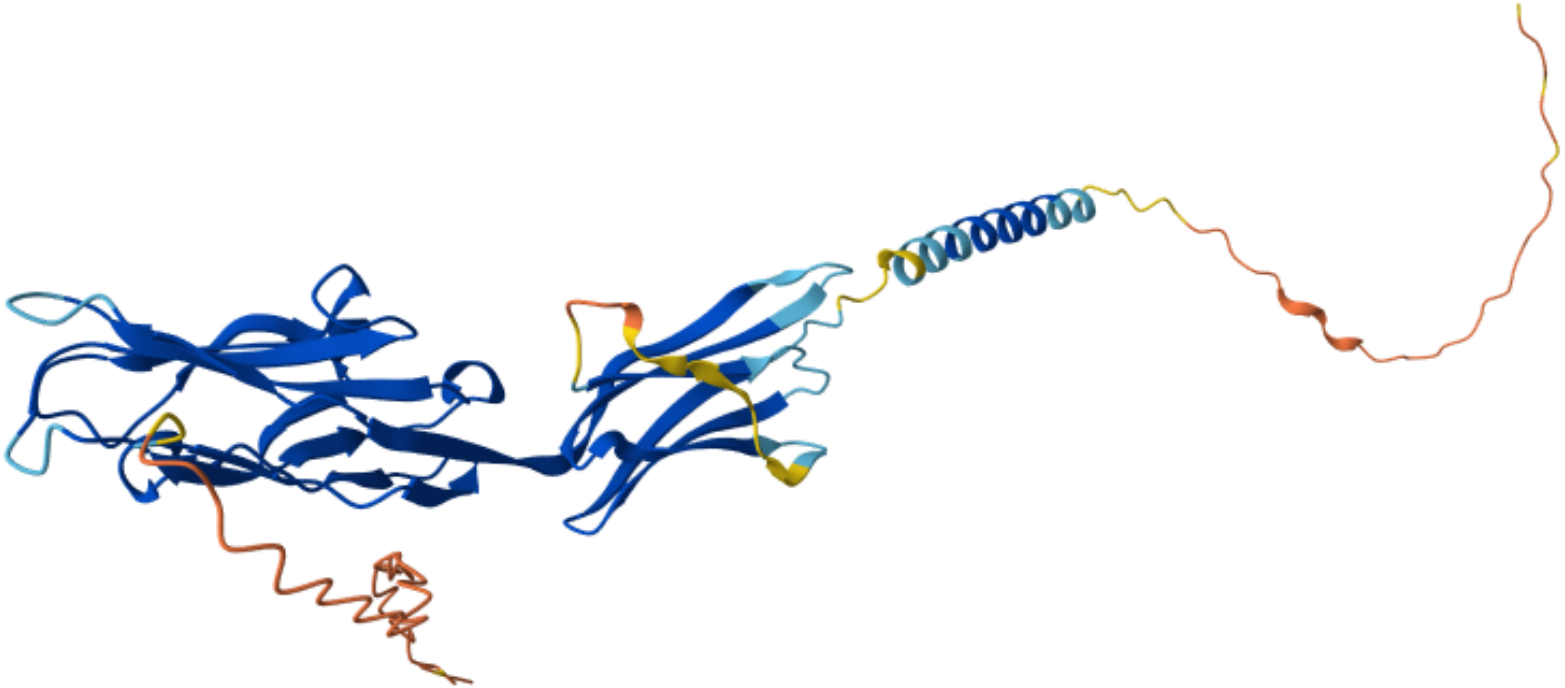

Figure 52: AlphaFold model (Q6ZMC9) of the tertiary structure of the Siglec-15 protein. Siglec-15 is a type-I transmembrane protein that comprises of several distinct extracellular structural domains, a single ITAM intracellular domain and a transmembrane region. Furthermore, the Siglec-15 protein structure possesses a V-set binding domain located on the N-terminus and serves as the primary region for sialoglycan ligand binding. Obtained from the AlphaFold PBD (https://alphafold.ebi.ac.uk/entry/Q6ZMC9; accessed 4th Dec 2021),

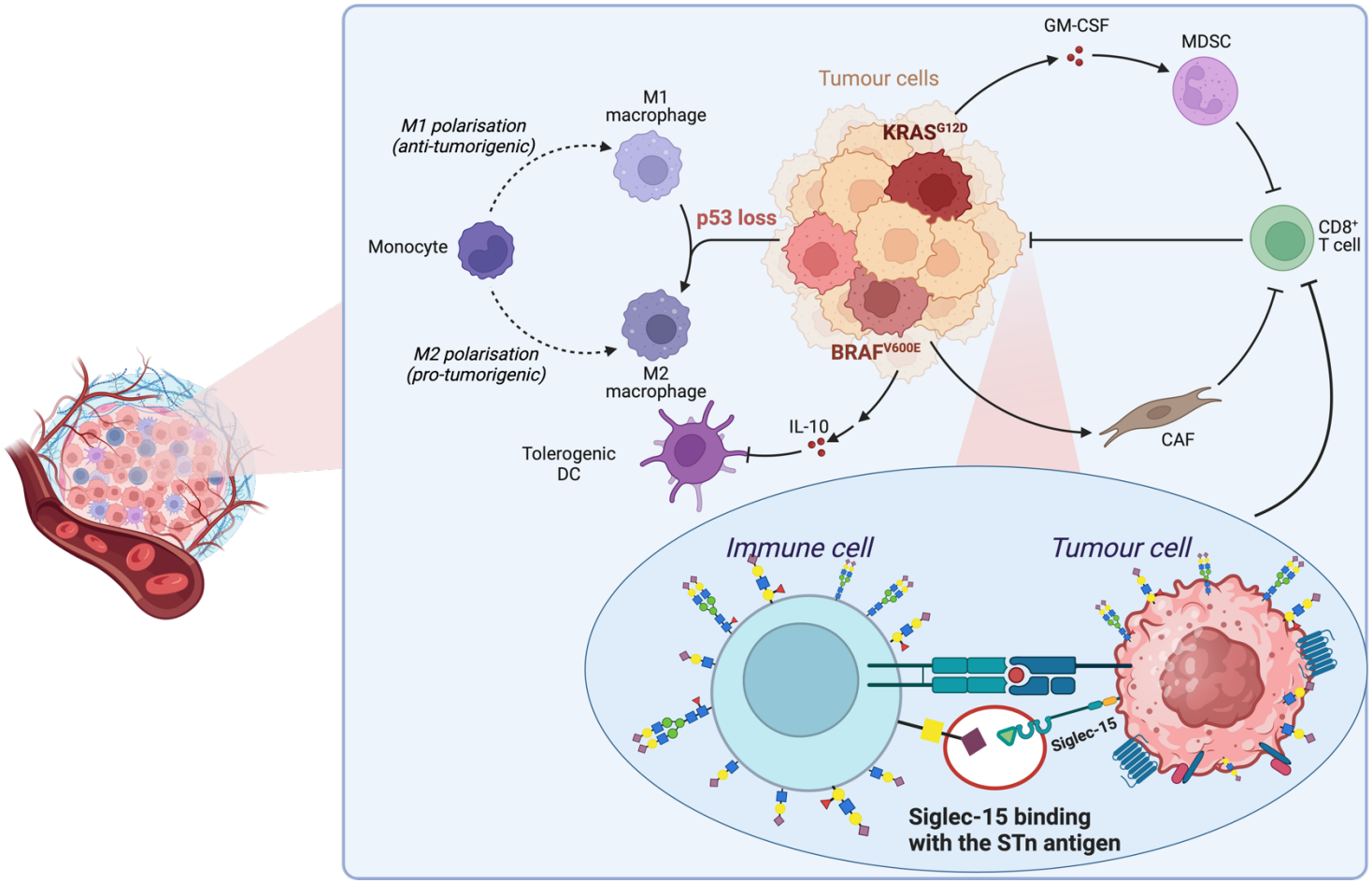

Figure 53: Siglec-15 interactions in the tumour microenvironment. Increased interactions of Siglec-15/STn antigen binding within the TME. Consequently, these interactions induce significant immunosuppression. Inhibitory Siglec molecules such as Siglec-15 enable tumour cells to evade recognition by immune cells, preventing T-cell activation and generation of an effective immune response. Additionally, there is greater polarisation of monocytes to the pro-tumorigenic macrophage phenotype. Thus, the interactions of Siglec-15 enhance tumour progression [created with BioRender].

3.1.2 The role of miRNAs in the Siglec-15/Sia axis

Several miRNAs have been elucidated to impact the Siglec-15/Sia axis (Table 11). A recent report has identified *SIGLEC15* as a target of miR-4786 in bladder cancer. However, the molecular sponging of miR-4786 by BTB domain and CNC homolog 1 intrinsic transport 2 (*BACH1-IT2*) has prevented miRNA-mRNA target binding, which induced *SIGLEC15* expression (Li et al., 2024). However, the identification of miRNAs associated with CRC progression in relation to the Siglec-15/Sia axis remains generally unclear, with the exception of miR-6715b-3p, which we have elucidated as part of this chapter (Ahmad et al., 2023; Mustafov et al., 2024). This chapter aimed to investigate the effects of a β-amino carbonyl compound utilised for Siglec-15 targeting and the subsequent effects on miRNA regulation and their gene targets in association with CRC progression. In particular, a small-RNA sequencing method analysis will be utilised to profile miRNAs within CRC *in vitro* cell models following treatment exposure. Through this high-throughput approach, comparisons between the untreated and treated condition will reveal the top 5 most significantly upregulated and downregulated miRNAs that have substantial changes in their expression profiles. From this, it is hypothesised that these miRNAs may act as downstream effectors following Siglec-15 inhibition and outline targets associated with various CRC tumour hallmarks including proliferation, invasion and several oncogenic signalling pathways. In addition,

Table 11: Summary of miRNAs linked to *SIGLEC15* regulation.

	Observed cell type expression	**MiRNAs linked to directly target *SIGLEC15***	**Reference**
SIGLEC15	Tumour cells, osteoclasts, TAMs	miR-6715b-3p, miR-4786, miR-582-5p, miR-7109	(Ahmad et al., 2023; Boelaars & Van Kooyk, 2024; Läubli, 2024; Lenza et al., 2023; Li et al., 2024; Liu et al., 2020; Ren et al., 2022)

3.1.3 β-amino carbonyl compounds as possible treatment therapies in CRC

β-amino ketones, a class of carbonyl compounds, are structured with an amine group of a β-carbon to a ketone functional group is a key pharmacophore typically synthesised in natural products, environmentally derived medication and bioactive molecules. There have been

numerous strategies that have enabled the synthesis of β-amino ketones with the focus of generating significantly high yields whilst maintaining low costs (Sun et al., 2015). Structurally, these compounds behave as biological scaffolds which can exhibit a variety of pharmacological properties including anticancer, anti-inflammatory and anti-viral (Figure 54) (Roman, 2015). Moreover, several derived β-amino carbonyl compounds are already clinically available for treating pathological diseases (Farzaneh et al., 2018). The chemical synthesis of β-amino carbonyls including 3-(4-bromophenyl)-1-phenyl-3-(phenylamino)propan-1-one (SHG-8) is primarily produced through a Mannich reaction which is a standardised carbon-carbon bond reaction utilised for organic synthesis (Shi et al., 2021). A classical reaction synthesised carbonyl compounds through reacting acetophenone, aromatic aldehydes and aromatic amines via an amine exchange reaction and the addition of ketones to Schiff bases (ligands that contain nitrogen and oxygen donors) (Craig et al., 1964). Furthermore, later approaches incorporated HCl/EtOH mediated catalysis for the condensation reaction to further improve the reaction rate (Wu et al., 2007). Other approaches are available for β-amino ketone synthesis; however, the components can differ. Another approach utilised the reduction of enaminone molecules, involving the direct reduction and hydroamination of carbonyl alkynes to synthesise enamines with terminal alkynes that are hydro-aminated (Hammouda & Elattar, 2022). The selection of the SHG-8 compound for characterising its cytotoxic profile in CRC was aimed to demonstrate treatment efficacy in Siglec-15 inhibition following specific binding to the Siglec-15 V-set binding domain. Preliminary testing of SHG-8 highlighted favourable cytotoxicity (data not shown) and underlined significant inhibition of tumour viability with minimal off-target effects. In addition, the literature highlighted SHG-8 possesses efficient pharmacokinetic properties including suitably reduced toxicity and improved bioavailability, suggesting SHG-8 has an ideal therapeutic profile for *in vitro* applications (Mustafov et al., 2024). Thus, this provided a strong case for elucidating its cytotoxic profile as a Siglec-15 small molecule inhibitor. Furthermore, small-RNA sequencing approaches will elucidate differentially expressed miRNAs in the presence of SHG-8 and underline the direct targeting of specific oncogenes associated with CRC progression. The top targets for analysis will be the gene target with the highest score prediction and whether the gene target is differentially expressed between normal and tumour cohorts. From this, prediction binding software will outline key binding sites on the target mRNA strand. Hence, this would highlight potential gene targets associated with CRC progression.

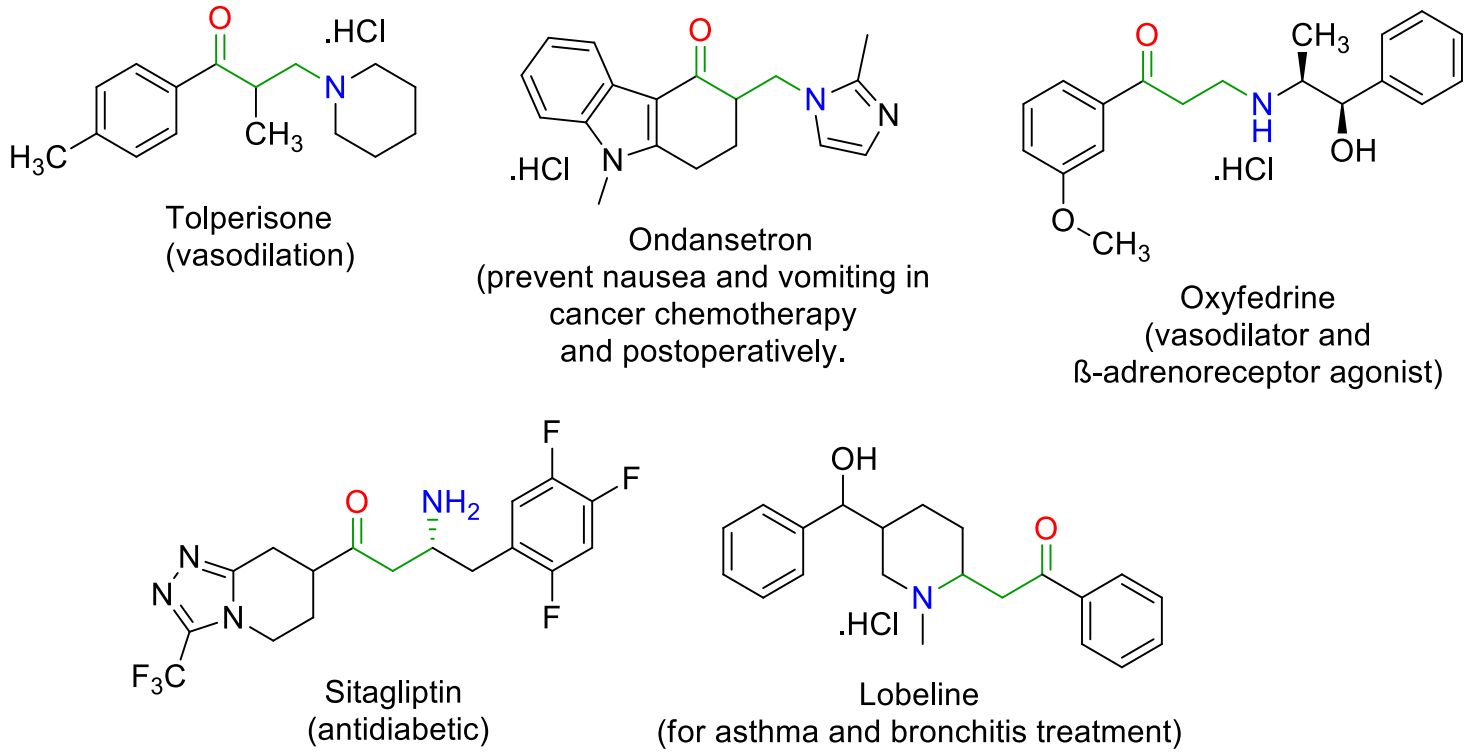

Figure 54: β-amino carbonyl compound derivatives of diphenyl-3-(phenylamino)propan-1-one used for various treatments. β-amino carbonyl compounds are important in the development of synthetic molecules used for various treatments and can be found in natural products and bioactive molecules. They can possess high levels of drug potency. The β-amino carbonyl Tolperisone has been developed for use in improving vasodilation. Ondansetron is another example of a β-amino carbonyl compound; this molecule is typically used as an antiemetic agent to prevent nausea, vomiting and other adverse side effects and is frequently given to cancer patients. Oxyfedrine, another β-amino carbonyl compound, has been developed as a β-adrenoreceptor agent for use as a therapeutic treatment in coronary diseases. Lobeline, an identified alkaloid has been used as a cholinesterase inhibitor and also in the treatment of asthma and bronchitis. Fluoroalkyl compounds, including Sitagliptin, are also derivatives of β-amino carbonyl compounds and are used in the treatment of diabetes (Doggrell & Hancox, 2013; Hammouda & Elattar, 2022; Remya et al., 2023) [created with Chemdraw].

3.1.4 The use of experimental cell lines

For the experimental work as part of this Chapter, *in vitro,* CRC cell lines must exhibit the positive expression of Siglec-15. Therefore, from this, we determined the feasibility of the SHG-8 compound as a Siglec-15 small molecule inhibitor and alternative to current therapeutic treatments. A greater proportion of CRC tumours are diagnosed in adult patients (typically 45-50+ years). In addition, it was highlighted in chapter 1 that the large proportion of diagnoses for CRC tumours typically were presented in males. Thus, appropriate cell lines are required to accurately represent the larger target population (Briggs et al., 2022). Some of the more frequently used CRC cell lines utilised in cancer studies are the SW480 and HCT116 cell lines due to their extensively characterised molecular profiles. The origin of the SW480 cell line was established in the lab of Albert Leibovitz and later characterised and authenticated by the work of Jørgen Fogh alongside its more metastatic cell line SW620 (Leibovitz et al., 1979). The SW480 (ATCC designation: CCL-228) cell line is an adherent cell line originating from primary COAD tumours. The cell line isolated from the large intestine/colon of a 50-year-old male presented with an epithelial morphology, which is unable to differentiate and comprises of flat polygonal shaped cells forming clusters of epithelial cells (colonies) (Capes-Davis, 2018; Duranton et al., 2003; Tomita et al., 1992). Additionally, ultrastructural analysis of the cell line identified that SW480 cells contained large glycogen stores and displayed deep cellular protrusions when grown *in vitro* (Biazik, 2010). Conversely, the origin of the HCT116 (ATCC designation: CCL-247) cell line was established from colorectal carcinoma colon tissues of a 48-year-old male alongside its clonal cell line HCT116b and also displaying an adherent epithelial morphology similar to SW480 cells. Furthermore, both SW480 and HCT116 cells are also able to develop spheroids with a diameter that can range from 150µm - 400µm (Butler et al., 2017; Heck et al., 2023). Both cell lines have differing metastatic potentials; HCT116 was characterised as a significant proliferative cell line. In contrast, SW480 cells demonstrated a low metastatic potential (Butler et al., 2017; Depciuch et al., 2020). The molecular profile of SW480 cells positively expresses several oncogenes associated with CRC progression, including *KRAS, MYC*, *MYB* and *TP53*, although the latter is characterised by mutant p53 and is not present in HCT116 cells (McCoy et al., 1984). By comparing two cell lines with differing molecular characteristics, it enabled the exploration of varying tumour associated characteristics associated with CRC.

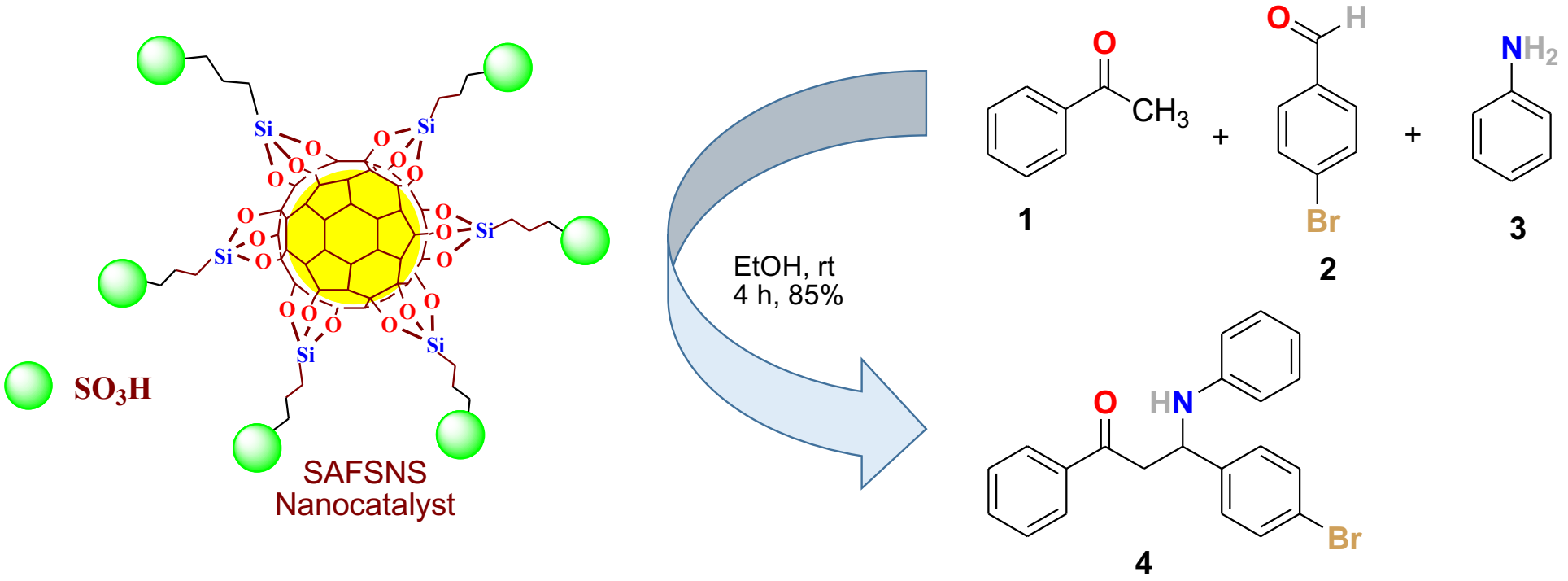

Figure 55: Synthesis of 3-(4-bromophenyl)-1-phenyl-3-(phenylamino)propan-1-one (SHG-8) via the sulfonic acid functionalised silica nanospheres (SAFSNS) nano-catalyst. The reaction incorporated the use of acetophenone, benzaldehyde and 4-bromo benzaldehyde precursor molecules in the presence of ethanol at room temperature (RT). Completion of the reaction was confirmed with thin layer chromatography (TLC). The product was purified and recrystallised to a yellow solid with a generated yield of 85%. Characterisation of the 3-(4-bromophenyl)-1-phenyl-3-(phenylamino)propan-1-one (SHG8) was performed using spectroscopic techniques including IR, mass spectrometry, ^{1}HNMR and ^{13}C NMR. Synthesis and characterisation of the SHG-8 compound via the Mannich reaction were performed by collaborators at the American University of Ras Al Khaimah, Ras Al Khaimah, UAE.

3.1.5 Rationale, Aim and Research questions

Small molecule inhibitors used in the normalisation of the immune response have targeted immunomodulatory signalling pathways to stimulate positive responses to immunotherapeutic treatment methods (Van Der Zanden et al., 2020). However, as far as the literature is concerned, the utilisation of small molecule inhibitors targeting Siglec-15 has not been explored in treating Siglec-15^+ tumours. Understanding the clear impact for the environmental and clinical benefit of β-amino carbonyl compounds and their biological significance, the compound 3-(4-bromophenyl)-1-phenyl-3-(phenylamino)propan-1-one (referred to as SHG-8, as part of this thesis) was synthesised via an environmentally stable nano-catalyst in a one-step mediated reaction (Figure 55) (Shi et al., 2021). A collection of synthesised b-amino carbonyl compounds and other organic compounds were first developed in house at the University of Ras Al Khaimah via the Mannich reaction. Initial screening of the cytotoxic properties for each compound revealed SHG-8 as the most cytotoxic compound that was developed by our collaborators. It was hypothesised that SHG-8 may prove to be an effective anti-cancer agent in CRC tumours and its mechanism of action was to be elucidated *in vitro*. Following this, the role of SHG-8 as a small molecular inhibitor against Siglec-15 was investigated. It was hypothesised that the nature of the SHG-8 compound could interact with the V-set binding domain of the Siglec-15 target and possibly indicate treatment alternatives for CRC treatment and management. In addition to this, β-amino carbonyl compounds may affect miRNA expression patterns and pathways associated with CRC progression following treatment, and the regulation of *SIGLEC15* through these mechanisms is largely unclear. Therefore, we aimed to characterise the anti-tumorigenic properties of the β-amino carbonyl compound SHG-8 on CRC *in vitro* cell models SW480 and HCT116. In addition, we emphasised the possible mechanisms of action relating to cellular death and aimed to elucidate deregulated miRNAs via small-RNA sequencing analysis following treatment exposure. Thus, we proposed a possible axis relating to CRC progression.

This chapter poses several research questions for the utilisation of small molecule inhibitors in the treatment of Siglec-15^+ tumours, which will be addressed below:

1. With molecular docking simulations of the AlphaFold Siglec-15 protein, does SHG-8 exhibit a high binding affinity for the V-set binding domain for competitive inhibition?

2. What comparisons can be made by the cytotoxic effects of SHG-8 against *in vitro* cell models SW480 and HCT116 when used against conventional anti-cancer agents such as cisplatin?
3. What is the mechanism of action for the induction of apoptosis pathways that are stimulated in CRC cells following SHG-8 exposure?
4. What is the relevance of the differentially expressed miRNAs following SHG-8 treatment exposure in relation to CRC progression and how are they directly affecting their identified gene target?

3.2 Methodology

3.2.1 Reagents, synthesis and characterisation of 3-(4-bromophenyl)-1-phenyl-3-(phenylamino)propan-1-one

Materials, reagents and solvents required for one-step nano-catalyst mediated synthesis of the SHG-8 compound were obtained from Merck (Merck, Feltham, UK) and Spectrochem (Spectrochem, Mumbai, India). Previous synthesis and characterisation data of the environmentally benign developed nano-catalyst (sulfonic acid-functionalised silica nanospheres; SAFSNS) was conducted based on the recent publication (Ahmad et al., 2021). Progression of the SHG-8 synthesis reaction was directly monitored via thin-layer chromatography (TLC) on silica gel plates, with the separated dots visualised with ultraviolet light (UV, λ254 nm). In addition, the infrared spectra and mass spectrum of the SHG-8 compound were measured by a PerkinElmer FTIR spectrophotometer (PerkinElmer, Connecticut, USA) and electrospray (ESI-MS) Shimadzu LCMS-spectrophotometer (Shimadzu, Milton Keynes, UK). ^{1}H and ^{13}C NMR spectra to determine the molecular weight of the SHG-8 compound were recorded with Bruker AV-400 NMR spectrometer (Bruker, Coventry, UK) with tetramethylsilane used as an internal standard. The high-resolution mass spectrum was also recorded with an Agilent 6540 HD Accurate Mass QTOF/LC/MS (Agilent Technologies, Loughborough, UK), which was determined with an electrospray ionisation (ESI) technique.

Synthesis of the SHG-8 compound was prepared with the SAFSNS nano-catalyst (0.03g) through direct mixing of acetophenone (1.1 mmol), 4-Bromo benzaldehyde (1 mmol), and aniline (1 mmol) in 1mL volume of ethanol at RT. Following the addition of all the constituents, the reaction mixture was stirred for a period of 4h. Completion of the synthesis reaction was indicated by TLC, then subsequently left to air dry at RT to evaporate excess ethanol and H_2O. The resultant process obtained a yellow solid. Purification of the synthesised SHG-8 compound to remove the SAFSNS catalyst required dissolution via dichloromethane (5mL) at 35°C, followed by gradual filtering. Further purification of the product involved recrystallisation using an ethanol solvent, producing an 85% yield from the initial individual reagents and a compound purity of 96%.

3.2.2 Molecular docking

The Siglec-15 protein structure (Uniprot ID: Q6ZMC9) was downloaded from the AlphaFold protein structure database (https://alphafold.ebi.ac.uk, accessed 4th Dec 2021). The reasoning behind this was due to no unbound Siglec-15 protein structures available to the protein databank (PDB), as only the crystal Siglec-15 bound with a Fab structure was available (Varadi et al., 2022). In addition, the COACH server (https://zhanggroup.org/COACH/, accessed 11th February 2022), predicted several protein binding sites of protein receptor-ligand interactions (Yang et al., 2013). For docking analysis, an SDF file of the chemical structure of the SHG-8 ($C_{21}H_{18}BrNO$) compound was uploaded alongside the Siglec-15 AlphaFold model onto the Webina 1.0.5 software (https://durrantlab.pitt.edu/webina/, accessed 12th February 2022), and converted to PDBQT files prior to blind docking (Siglec-15 AlphaFold structure as protein model and SHG-8 as binding ligand) via AutoDock Vina. The grid box was centred at the ARG143 residue, the main residue responsible for ligand binding (Crocker et al., 2007), with the following parameters: centre_x = -23, center_y = 6, center_z = 13.272 and size_x = 28, size_y =21, size_z = 22. Additionally, further parameters included 2 CPU usage and exhaustiveness for the global search was set at 8 for high confidence prediction. The molecular docking simulation of SHG-8 binding towards the V-set binding domain of the Siglec-15 protein structure was conducted in December 2021. This approach utilised structural data available at the time and provided an effective bases for highlighting SHG-8's binding affinity and any subsequent binding sites on the protein structure. Following on from this, the current modelling software has undergone significant updates which included greater model accuracy and predictions for ligand-receptor binding interactions and the incorporation of post-translational modifications. Although SHG-8 has not been remodelled with the updated AlphaFold software, it is worth mentioning that further enhancements could further refine the binding dynamics regarding SHG-8 and Siglec-15 and expand from our initial findings.

3.2.3 UALCAN transcriptomics data mining

The UALCAN transcriptomics database (http://ualcan.path.uab.edu, accessed on 2nd February 2023) outlined corresponding TCGA genomic expression data for query genes *SIGLEC15* (ENSG00000197046) and *PTTG1IP* (ENSG00000183255) following comparisons between normal tissue and CRC COAD cohorts. Furthermore, expression data was presented as TPM, with box plots constructed using GraphPad Prism 9.0 software and Welch's t-test PERL script

statistical analysis encoded onto the UALCAN software to identify differences in clinicopathological features between cohorts (Chandrashekar et al., 2022). In addition, methylation of the *SIGLEC15* gene was also determined alongside the expression profile of PTTG1IP at the protein level and its promoter methylation.

3.2.4 Cell culture and treatments

Human CRC cell lines SW480 and HCT116 were utilised in association with glioblastoma (GB) cell line U87MG, all of which were obtained from ATCC (ATCC, Virginia, USA). The adherent SW480, HCT116 and U87MG cell lines were cultivated using high glucose (4.5g/L D-glucose, 0.11g/L sodium pyruvate) DMEM (Gibco, Bleiswijk, Netherlands) and MEM (Gibco, Bleiswijk, Netherlands) media, respectively. Followed by supplementation with 10% FBS (Gibco, Bleiswijk, Netherlands), 1% penicillin/streptomycin (10,000U/mL) (Gibco, Bleiswijk, Netherlands) and 1% L-glutamine (200mM) (Gibco, Bleiswijk, Netherlands).
In addition, both human monocytic cell lines THP-1 and U937 were also obtained from ATCC (ATCC, Virginia, USA). Similarly, the THP-1 and U937 suspension cell lines were grown with the following conditions: high glucose (4.5h/L D-glucose, 0.11g/L sodium pyruvate) DMEM (Gibco, Bleiswijk, Netherlands) media, and supplemented with 10% FBS (Gibco, Bleiswijk, Netherlands) and 1% penicillin/streptomycin (10,000U/mL) (Gibco, Bleiswijk, Netherlands). Furthermore, prior to experimental work, both monocytic cell lines were differentiated into macrophages 48h post-PMA treatment (50ng/mL). For SHG-8 evaluation on normal epithelial cells, the human normal colonic epithelial tissue HcoEPiC primary cell line was obtained from iXcells Biotechnologies (iXcells Biotechnologies, San Diego, USA). To support its growth and maintenance, the HcoEPiC cell line was maintained using epithelial cell growth media (iXcells Biotechnologies, San Diego, USA) supplemented with 1% antibiotic-antimycotics (iXcells Biotechnologies, San Diego, USA). All experimental cell lines were placed for incubation at 37°C, 5% CO_2 and experimental work was performed for each cell line upon reaching an 80% confluency. To determine the cytotoxic profile of SHG-8 on tumour cells *in vitro*, the SHG-8 compound was solubilised in dimethyl sulfoxide (DMSO) at a concentration of 10 mM.

3.2.5 Immunofluorescence staining

To confirm the chosen CRC *in vitro* cell lines were indeed Siglec-15^+, the U87MG cells were proposed to have the highest Siglec-15 expression, as indicated from the Human Protein Atlas

database (https://www.proteinatlas.org; accessed 4th November 2021), which provided comprehensive expression profiles across various human cell lines and tissues. Hence, based on this information, U87MG cells were used as a positive control to confirm positive Siglec-15 expression in CRC *in vitro* cell lines HCT116 and SW480. CRC cells HCT116 and SW480 alongside GB U87MG cells were seeded onto coverslips within 12 well plates at a density of $3x10^5$ cells/well and were left to adhere overnight. Following cellular adherence, DMEM media was removed via three consecutive PBS wash steps at 5 min at RT prior to cellular fixation with 4% paraformaldehyde (PFA) for a fixation period of 40 min. The fixation was subsequently removed by a further three consecutive wash steps, and all wells were treated with 1% BSA/PBS (5g BSA/500mL PBS) blocking buffer for 1h. This was followed by incubation with a primary Siglec-15 antibody (Life Technologies Limited, Renfrewshire, UK) (1:500 dilution, recommended by the manufacturer) at 4°C overnight. Following the antibody incubation, an excess antibody was removed with three consecutive PBS wash steps before all wells were treated with an anti-rabbit Alexa-488 secondary antibody (Life Technologies Limited, Renfrewshire, UK) (1:500 dilution, recommended by the manufacturer) for 1h on a rocker at RT in the dark. The coverslips were then mounted onto microscope slides and submerged in DAPI Antifade Mounting Medium (2Bscientific, Hatfield, UK) before visualisation with an EVOS XL Core Imaging system (Fisher Scientific, Hemel Hempstead, UK) at 40x magnification with the DAPI (blue) and GFP (green) filters.

3.2.6 MTT cell viability assay

CRC cell lines HCT116 and SW480 alongside normal epithelial cell line HcoEPiC cells were seeded onto 96 well plates at cellular densities of $2.5x10^4$ cells/well and were placed to adhere in the incubator at conditions 37°C, 5% CO_2 (N=5). Following cellular adherence, all wells were treated with different SHG-8 concentrations: 20µM, 40µM, 60µM, 80µM and 100µM to determine the compounds' IC_{50} value and were left to incubate for 24h at 37°C, 5% CO_2. Following the treatment period, all wells were treated with 20µL MTT (0.5mg/mL) and placed into the incubator for 2h at 37°C for formazan crystals to develop. Subsequently, the MTT was removed by inverting the excess solution and the remaining formazan crystals were solubilised with isopropanol in the dark for 30 min on a shaker at RT. Absorbance values were recorded at 540nm via a CLARIOstar plus multi-mode microplate reader (BMG LABTECH, Aylesbury, UK). The average percentage of cellular viability was calculated based on the following equation:

$$\frac{(\text{Treatment} - \text{Background})}{(\text{Average treatment control})} = \text{x}$$

$$\frac{\text{x}}{\text{no. of replicates (N = 3)}} = (\text{cell viability x } 100) = \ \% \text{ cell viability}$$

Equation 1: Used to determine % cell viability of SW480, HCT116 and HcoEPiC cells following 24h SHG-8 exposure in the MTT viability assay.

3.2.7 Wound healing migration assay

SW480 cells were seeded at a density of $4x10^5$ cells/well onto 12 well plates and were placed to incubate at 37°C, 5% CO_2 (N=3). Upon reaching cellular adherence and total well coverage, a 2µL tip was used to create scratches in vertical and horizontal directions, with an overlap of both in the epicentre. The detached cells were washed off with several PBS washes before well treatment with the SHG-8 10µM and 40µM concentrations and control conditions DMSO and cisplatin 100µM. Images that pertained to the wound were taken at separate time intervals at: 0h, 24h and 48h using an Olympus CKX41 inverted microscope (Olympus Life Science Solutions, Stansted, UK) at 4x magnification. All images that were taken of the wound area were analysed through ImageJ analysis software (ImageJ bundled with Java8, https://imagej.net/ij/download.html, accessed 20th February 2023). In addition, installed macro plugins for wound healing analysis studies (Wound_healing_size_tool.ijm) were obtained and implemented based on the following study (Suarez-Arnedo et al., 2020). Further to this, wound healing parameters included: variance window radius set at 20, threshold value set at 100, percentage of saturated pixels remained at a default of 0.001, and a global scale was set.

3.2.8 Colonisation assay

SW480 cells were seeded at a total of $1x10^3$ cells/well onto 12 well plates and were left to adhere at 37°C, 5% CO_2 (N=3). Following adherence of the tumour cells, all wells were treated with the conditions: SHG-8 10µM and 40µM concentrations and control conditions DMSO and cisplatin 100µM for a 24h treatment period. Subsequently, the treatment was replaced with supplemented high glucose DMEM media and was placed in an incubator at 37°C, 5% CO_2

for a total of 7 days. The colonisation was determined by the total number of observable colonies in the DMSO control condition (colonies were determined as a cluster of cells totalling larger than 30-50 cells) (Niyazi et al., 2007). Following the 7-day incubation protocol, all wells were fixed with 4% PFA for 40 min at RT and then removed by three consecutive PBS wash steps at 5 min. The wells were stained with 0.1% crystal violet (Pro-Lab Diagnostics, Wirral, UK) for 45 min on a rocker at RT. The wells were then washed with a further three consecutive PBS wash steps at 5 min to remove excess crystal violet, and images of the colonies were taken at both 4x and 10x magnifications using an Olympus CKX41 inverted microscope (Olympus Life Science Solutions, Stansted, UK).

3.2.9 Nuclear fragmentation staining via DAPI

For determining cell death, SW480 cells were seeded onto circular coverslips within 12 well plates at a density of ($4x10^5$ cells/well) and placed for adhering at 37°C, 5% CO_2 (N=3). The wells were treated with the following conditions: DMSO, 10µM and 40µM SHG-8 and 100µM cisplatin for a treatment period of 24h. Following the treatment period, all wells were washed with PBS and fixed with 4% PFA for 40 minutes at RT. The fixation was removed by consecutive PBS wash steps for 3 min at RT on a rocker. The coverslips were placed onto microscope slides containing DAPI Antifade Mounting Medium (2Bscientific, Hatfield, UK). Fluorescent images of the microscope slides were then taken using an EVOS XL Core Imaging system (Fisher Scientific, Hemel Hempstead, UK) at 40x magnification with the DAPI (blue) filter.

3.2.10 Cell death determination via Annexin-V/ propidium iodide staining

To determine apoptosis occurrence post treatment, SW480 cells were seeded at $3x10^6$ cells/well onto 6 well plates and were left to adhere at 37°C, 5% CO_2 (N=3). The wells were subsequently treated with DMSO, 10µM SHG-8, 40µM SHG-8 and 100µM cisplatin for a treatment period of 24h. Following the treatment period, all wells underwent cold shock with 1mL ice-cold PBS and a density of $1x10^6$ cells was harvested to 100µL suspensions. The SW480 treated cell suspensions were treated with 1µL RNase A (10mg/mL) prior to labelling with Annexin-V FITC (5µL) and propidium iodide (PI) (100µg/mL) via the dead cell apoptosis kit with Annexin-V FITC and propidium iodide for flow cytometry (Invitrogen, Inchinnan, UK), as per the manufacturer's instructions. 400µL of 1x binding buffer was added to all

treated cell suspensions following a 15 min incubation at RT and then placed on ice to maintain cellular viability. Fluorescent analysis was conducted via the Guavasoft 3.1.1 software and Guava easyCyte HT system (Merck Millipore, Watford, UK).

3.2.11 Reactive Oxygen Species stimulation assay

To determine reactive oxygen species (ROS) production as a possible mechanism of action, SW480 cells were seeded at a density of $1.5x10^4$ cells/well onto clear bottom black opaque 96 well plates and were left for cellular adherence overnight at 37°C, 5% CO_2 (N=3). ROS production was determined via the ROS Detection Assay Kit (Abcam, Cambridge, UK), as per the manufacturer's instructions. Following adherence, all wells were treated with 20µL ROS red dye and placed to incubate at 37°C, 5% CO_2 for 1h. Following incubation, all wells were treated with 20µL of each treatment condition: DMSO, 10µM and 40µM SHG-8, 100µM cisplatin, H_2O_2 (internal positive control), PBS (internal negative control), DMEM media (background) at 11x concentrations following the manufacturer's protocol. Fluorescence readings were taken at separate time intervals scheduled at 15-, 30-, 45-, 60- and 75-minutes at 37°C, 5% CO_2 with the following emission/excitation wavelengths Ex/Em = 520/605 nm using a CLARIOstar plus multi-mode microplate reader (BMG LABTECH, Aylesbury, UK).

$$ROS\ generation = \frac{(Treatment - Average\ background)}{no.of\ replicates}$$

Equation 2: Used to determine ROS production of SW480 cells following 24h SHG-8 exposure with the ROS assay kit.

3.2.12 Quantitative analysis of Siglec-15 protein expression via flow cytometry

The CRC SW480 cell line was seeded at a cellular density of $3x10^6$ cells/well onto 6 well plates for overnight adherence at 37°C, 5% CO_2 (N=3). All wells were treated with the following conditions: DMSO, 10µM and 40µM SHG-8 and 100µM cisplatin for a 24h treatment period. Following the treatment protocol, all wells were cold shocked with ice-cold PBS and were later harvested with 10mM disodium ethylenediaminetetraacetic acid (EDTA) (3.7g of disodium EDTA dihydrate in 950ml dH_2O) and resuspended with 2% BSA:PBS (10g BSA:500mL PBS) flow cytometry buffer. Each harvested cell suspension was washed with ice-cold PBS and

placed in a microfuge at 200xg for 5 min. The samples were then later resuspended with a primary mouse Siglec-15 antibody (R&D Systems, Minneapolis, USA) (0.25µg/10^6 cells) diluted in flow cytometry buffer and were placed on ice to incubate for a total of 1h. Following antibody incubation, all cell suspensions were washed with ice-cold PBS and placed in a microfuge at 200xg for 5 min before resuspension with an anti-mouse Alexa-488 secondary antibody (Life Technologies Limited, Renfrewshire, UK) (1:500 dilution, as recommended by the manufacturer) in flow cytometry buffer and were placed on ice to incubate for a further 45 min in the dark. Following incubation of the secondary antibody, all cell suspensions were placed in a microfuge at 200xg for 5 min and resuspended in flow cytometry buffer. Fluorescent analysis was recorded via the Guava easyCyte HT system (Merck Millipore, Watford, UK) and Guavasoft 3.1.1 software and fluorescence intensity was recorded. Furthermore, mean fluorescence intensity (MFI) was determined from the obtained raw fluorescent emission data.

3.2.13 Cytokine expression determination via enzyme-linked immunosorbent assay

Pro-inflammatory cytokine secretion of TNFα and IL-1β was determined following SHG-8 treatment in THP-1 and U937 differentiated macrophages via enzyme-linked immunosorbent assay (ELISA) methods (N=2). Both monocytic cell lines were differentiated with PMA (50ng/mL, solubilised in ethanol) for a period of 48h before treatment with SHG-8 at 40µM and lipopolysaccharide (LPS) (50ng/mL) stimulation for 24h. The treatment conditions were as follows: untreated control, LPS stimulation 50ng/mL only, LPS 50ng/mL + SHG-8 40µM combination and SHG-8 40µM only. Centrifugation of the differentiated macrophages allowed the harvesting of the treatment supernatant and was placed on microwell strips in duplicate at a concentration of 200µg/mL alongside internal standards via cytokine human ELISA kit (Life Technologies Limited, Renfrewshire, UK), following several wash steps as per the manufacturers' protocol. Following this, 50µL of biotin conjugate was added to the tagged strips, which were incubated for 2h using a microplate shaker. Subsequently, the strips were then washed, and all strips were treated with 100µL of streptavidin-HRP for 1h. Following this, the strips were washed, and 100µL of TMB substrate solution was added to all treatment wells for 10 min at RT or until a noticeable colour change was detected. Upon reaching a discernible colour change, 100µL of stop solution was added to each well strip and later measured at 620nm via a CLARIOstar microplate reader (BMG LABTECH, Aylesbury, UK).

3.2.14 RNA extraction, sample purification and reverse transcription quantitative polymerase chain reaction

To elucidate the expression profiles of genes and miRNAs following SHG-8 treatment, reverse transcription quantitative polymerase chain reaction (RT-qPCR) methods were conducted (N=3).

3.2.14.1 RNA extraction

Total RNA was obtained from the cellular lysis of SW480 CRC treated cells 24h post-treatment with the following conditions: DMSO, 10µM and 40µM SHG-8 and 100µM cisplatin using the TRIzol method (Life Technologies Limited, Renfrewshire, UK). Following cell lysis, the RNA quality and quantity of all treated samples for mRNA and miRNA expression analyses were recorded using Nanodrop ND-1000 spectrophotometer UV-Vis Nanogen Inc. (Marshall Scientific, Hampton, USA). Expression analysis was only conducted with samples with a 260/280 purity of >2.0.

3.2.14.2 Sample purification

Following sample quantification, all treated samples were subjected to DNase treatment (removal of DNA contaminants) with the RNase-free DNase kit (Qiagen, Hilden, Germany). In contrast, miRNA expression analyses required further purification and miRNA enrichment which was aided with the miRvana miRNA Isolation Kit (Life Technologies Limited, Renfrewshire, UK) as per the manufacturer's instructions.

3.2.14.3 Reverse transcription quantitative polymerase chain reaction

Samples designated for gene expression analysis undertook cDNA synthesis protocols for reverse transcription, which was performed using the high-capacity cDNA reverse transcription kit (Applied Biosystems, Massachusetts, USA), with final products at a concentration of 100ng/µL. In addition to this, reverse transcription protocols are listed in Table 12. Subsequently, cDNA samples ready for gene expression analyses were then processed as part of SYBR green reverse transcription-quantitative polymerase chain reaction (RT-qPCR) methods using the corresponding cDNA template samples and master mix reagent PowerUp SYBR Green Master mix (Applied Biosystems, Massachusetts, USA). In addition, SYBR green primers were used as *GAPDH* forward (GGAGCGAGATCCCTCCAAAAT) and

reverse (GGCTGTTGTCATACTTCTCATGG), *PTTG1IP* forward (GTCTGGACTACCCAGTTACAAGC) and reverse (CGCCTCAAAGTTCACCCAA) and *SIGLEC15* forward (CGCGGATCGTCAACATCTC) and reverse (GTTCGGCGGTCACTAGGTG) which were used at 10µM concentrations following primer solubility with RNase-free H_2O with the following setup (Table 13).

After miRNA expression analysis sample purification, all treated samples were subjected to miRNA quantification before reverse transcription methods with the TaqMan MicroRNA Reverse Transcription kit (Applied Biosystems, Massachusetts, USA) with the following experimental setup (Table 14). RT-qPCR for miRNA expression analyses was conducted using the TaqMan Universal Master mix II, no UNG (Applied Biosystems, Massachusetts, USA), in addition to TaqMan primers and cDNA sample templates with the following experimental setup (Table 15).

All samples were analysed in mechanical triplicate via QuantStudio 7 Flex Real-Time PCR System (Applied Biosystems, Massachusetts, USA). GAPDH and U47 gene primers were used as housekeeping controls for gene and miRNA analyses, respectively. Furthermore, the relative expression of *SIGLEC15*, gene targets and candidate miRNAs was performed via the **$2^{-\Delta\Delta Ct}$ method.**

Table 12: Experimental protocol for mRNA reverse transcription.

Protocol Step	Temperature	Time
Reverse transcription	25°C	10 min
	37°C	120 min
Stop Reaction	85°C	5 min
Hold	4°C	Hold

Table 13: Experimental protocol for RT-qPCR gene expression method.

Protocol Step	Temperature	Time	No. of cycles
Enzyme activation	95°C	20 s	1
Denaturation	95°C	1 s	40
Annealing/Extension	60°C	20 s	

Table 14: Experimental protocol for miRNA reverse transcription.

Protocol Step	Temperature	Time
Reverse transcription	16°C	30 min
	42°C	30 min
Stop Reaction	85°C	5 min
Hold	4°C	Hold

Table 15: Experimental protocol for RT-qPCR miRNA expression method.

Protocol Step	Temperature	Time	No. of cycles
Enzyme activation	95°C	10 min	1
Denaturation	95°C	15 s	40
Annealing/Extension	60°C	60 s	

3.2.15 Extraction, library preparation and small RNA-sequencing

To elucidate the differential expression of specific miRNAs following SHG-8 treatment, small RNA-sequencing (sRNA-seq) analysis was conducted by Biomarker technologies (Biomarker Technologies Inc., California, USA) to correlate DE miRNAs to possible gene targets and their relevance to CRC progression (N=4). Please find the available data posted in the Mendeley repository: doi: 10.17632/r2xdf868k9.1.

3.2.15.1 RNA extraction

Total RNA was obtained from the cellular lysis of SW480 CRC treated cells 24h post-treatment with the following conditions: DMSO and 40μM SHG-8 using the TRIzol method (Life Technologies Limited, Renfrewshire, UK). Following cell lysis, the RNA quality and quantity of all treated samples for miRNA expression analyses were recorded via Nanodrop ND-1000 spectrophotometer UV-Vis Nanogen Inc. (Marshall Scientific, Hampton, USA) and 4150 TapeStation System (Agilent Technologies, California, USA). All samples displayed RIN numbers >7.0, indicating good RNA integrity and expression analysis was only conducted with samples with a 260/280 purity of >2.0.

3.2.15.2 Library preparation for RNA sequencing

Preparation of the sequencing sample library required a 1.5μg RNA sample as the input material and was performed using the NEBNext® small RNA library prep set for Illumina (New England Biolabs, Hitchen, UK) as per the manufacturer's instructions, with index codes linking sequences to each sample. Initially, ligation of the 3' SR adaptor was produced via the addition of the 3' SR Illumina adaptor, RNA sample and nuclease-free H_2O. The resulting reaction mixture was placed into a preheated thermal cycler for 2 min at 70°C and later transferred to cool on ice. Subsequently, the addition of 3' ligation reaction mixture (2X) and 3' ligation enzyme mix to the 3' SR adaptor reaction mixture was performed, followed by 1h incubation in a preheated thermal cycler at 25°C. Additionally, the hybridisation of the SR RT primer to excess 3' SR adaptor strands transforms single stranded DNA molecules to double stranded DNA, thus preventing the dimerisation of adaptor molecules. Following this, the ligation of the 5' SR adaptor was conducted prior to synthetic reverse transcription and PCR amplification. The resulting PCR amplicons were purified via AMPure XP (Beckman Coulter, High Wycombe, UK) and the quality of purification was determined via the Agilent Bioanalyser 2100 instrument (Agilent Technologies, California, USA).

3.2.15.3 Data clustering

The samples tagged with index codes were clustered with a cBot Cluster Generation System (Illumina, Cambridge, UK) alongside a TruSeq 110 PE Cluster Kit v4-cBot-HS (Illumina, Cambridge, UK) kit, following the manufacturer's standard pipeline. Following the generated clustering, the libraries were later sequenced using an Illumina Hiseq 2500 instrument

(Illumina, Cambridge, UK), and subsequent paired-end reads were generated based on the input data.

3.2.15.4 Paired end data analysis

The obtained raw data was presented in a fastq format and processed through PERL script software. Removal of adapters, ploy-N, exhibited low-quality reads, and sequences <18 nucleotides and >30 nucleotides were filtered to produce clean reads. Additionally, several parameters, including Q20, Q30, GC-content and sequence duplication, were all determined from the remaining data.

3.2.15.5 MiRNA prediction

Imputing the clean reads dataset to the Bowtie software (https://www.bowtiexp.com/downloads/) and implementing several databases for prediction analysis including Silva (https://www.arb-silva.de), GtRNAdb (https://gtrnadb.ucsc.edu), Rfam (https://rfam.org) and Repbase (https://www.girinst.org/repbase/), filtered out all non-coding RNAs excluding miRNAs. The remaining clean reads were utilised to correlate currently known miRNAs and predictions of possible miRNA targets via comparisons with miRbase. In addition, Randfold tools (https://bio.tools/randfold) were used to assist in predictions for calculating secondary structures of non-coding RNA sequences.

3.2.15.6 MiRNA expression

MiRNA expression was determined for each sequenced sample (four control groups vs four sample groups). Small RNAs were mapped to the original sequences, and the read count for individual miRNAs was constructed based on mapping.

3.2.15.7 Differential miRNA expression via computational programming R methods

The differential expression of treated and untreated conditions was compared using the DESeq R package (1.10.1) (R-4.4.1-arm64.pkg, followed by install - macro package). The software provides DE of miRNA expression data via negative binomial distribution models. Adjusted P-values of P >0.05 were incorporated using Benjamini and Hochberg's false discovery rate method, which selected out DE miRNAs. Moreover, DE of samples was also performed using IDEG6 software, which characterised P-value adjustment with Q-values (Storey & Tibshirani,

2003). Q-value< 0.05, and Log2 foldchange ≥ 1 was used as the parameter threshold that determined the significance of DE miRNAs (Mustafov et al., 2024).

3.2.15.8 GO and KEGG enrichment analysis via computational programming R methods

Enrichment analysis for GO utilised DE genes as the input dataset for comparisons using the GOseq R package, which has been derived from Wallenius non-central hyper-geometric distribution (Mustafov et al., 2024). Furthermore, KEGG pathway analysis of biological processes, molecular function and cellular components was generated via the KEGG database (https://www.genome.jp/kegg/) alongside the KOBAS statistical software (Kanehisa et al., 2007; Mao et al., 2005).

3.2.16 Statistical analysis

Statistical analyses of all experiment work were performed. Several *in vitro* assays, including MTT, colonisation, IF, Siglec-15 MFI following SHG-8 treatment and RT-qPCR of *SIGLEC15*, *PTTG1IP* and miRNA candidates were compared using one-way ANOVA followed by Dunnett's multiple comparison post-hoc tests. In addition, migration distance was statistically compared using Welch's one-way ANOVA followed by Dunnett's multiple comparison post-hoc test. Pro-inflammatory TNFα and IL-1β cytokine secretion from differentiated macrophages were compared via one-way ANOVA followed by Tukey's multiple comparison post-hoc tests. Furthermore, statistical analysis for ROS production was determined using two-way ANOVA followed by Dunnett's multiple comparison post-hoc tests. UALCAN transcriptomics analysis detailing genomic miRNA and gene target expression data, promoter methylation, and proteomics expression were all compared using an unpaired student's t-test. Determination of the IC_{50} for SHG-8 activity was identified through technical and biological replicates (N=5). Other experimental assays were performed with (N=3) biological and technical replicates, unless stated otherwise. SRNA-sequencing analysis was performed with (N=4) biological replicates. Statistical significance was denoted in the form of asterisks as provided: *P <0.05, **P <0.01, *** P<0.001, ****P <0.0001. All constructed graphs were produced via GraphPad Prism 10.

3.3 Results

3.3.1 Synthesis and characterisation of 3-(4-bromophenyl)-1-phenyl-3-(phenylamino)propan-1-one

Synthesis and structural characterisation of the SHG-8 compound via the one-step Mannich reaction were performed by collaborators at the American University of Ras Al Khaimah, Ras Al Khaimah, UAE.

Synthesis of the 3-(4-bromophenyl)-1-phenyl-3-(phenylamino)propan-1-one (SHG-8) compound was conducted using the environmentally friendly SAFSNS nano-catalyst at RT, which had produced a high yield from the addition of initial products. Characterisation of the SHG-8 was further performed by spectroscopy methods including IR, Mass, ^{1}H NMR and ^{13}C NMR and recorded a melting point of 122-126°C that is representative of the literature (123–127°C) (Kidwai et al., 2008). In addition, IR spectroscopy methods revealed sharp peaks at 3391 cm^{-1} and 1667 cm^{-1}, indicating the presence of an amine (-NH) and ketone (C=O) functional group (Figure 56).

Moreover, the ^{1}H NMR spectra identified two $COCH_2$ protons within the structure appearing as a multiplet at δ 3.41-3.3.45 and the singular NH proton as a singlet δ 4.56. The proton of the CH group adjacent to NH appeared as a triplet at δ 4.96. A total of fourteen aromatic protons were identified highlighted as the following: two protons as a doublet at δ 6.53, one proton exhibited as a triplet at δ 6.68, two further protons as a multiplet at δ 7.07-7.11, two protons exhibited as a doublet at δ 7.31, multiplet of four protons at δ 7.42-7.57, a multiplet of a singular proton at δ 7.55-7.57 and lastly two protons as a doublet at δ 7.79 (Figure 57). In contrast, ^{13}C NMR analysis revealed a total of fifteen peaks recorded at δ 45.9, 54.1, 113.8, 118.6, 121.3, 128.2, 128.3, 128.8, 129.4, 132.0, 133.7, 136.7, 142.3, 146.3, 197.9 (Figure 58).

Further to this, the mass spectroscopy ESI method revealed a mass-to-charge ratio (m/z) of 380 at an $[M+H]^+$ peak (Figure 59). In addition to this, HRMS ESI spectroscopy also correlated with an m/z peak of 380.0643 matching a structural formula of $C_{21}H_{19}BrNO$ $[M+H]^+$ with an associated mass of 380.0645, with Δ 0.0002 (Figure 60).

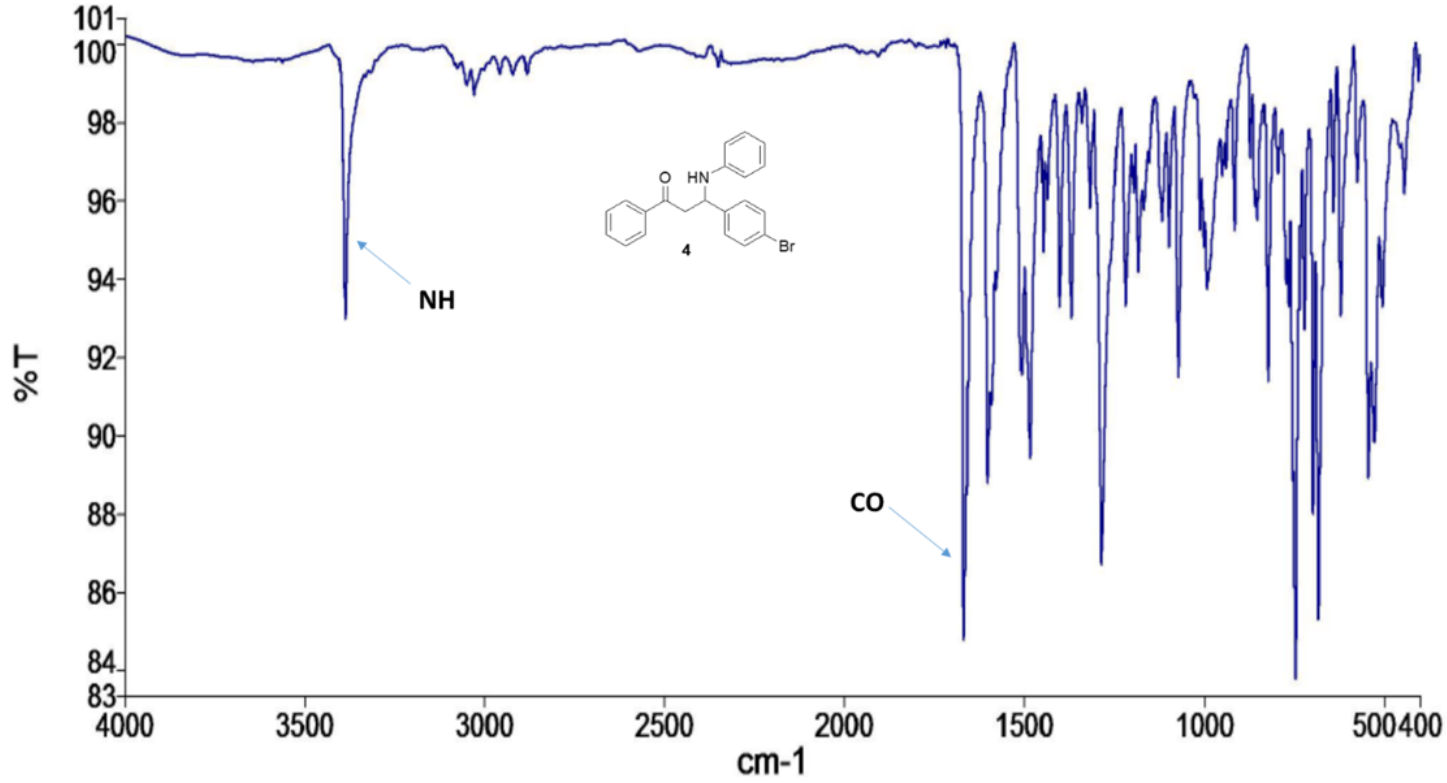

Figure 56: FTIR spectrum of the SHG-8 compound revealed functional groups present within the structure. Fourier Transform Infrared Spectroscopy (FTIR) method to identify certain functional groups across an infrared spectrum to elucidate SHG-8's structural profile.

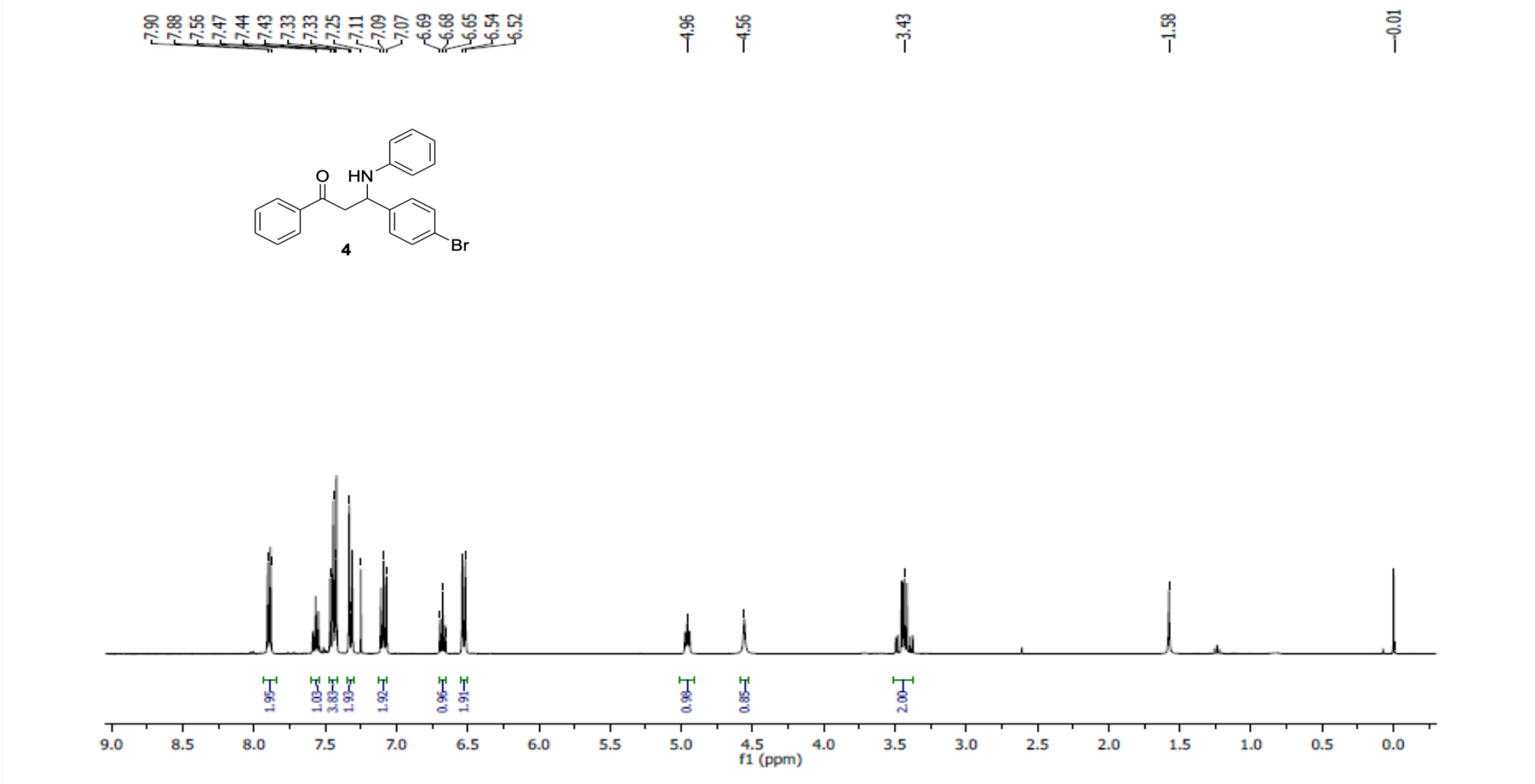

Figure 57: ^{1}H NMR spectrum of the SHG-8 compound in a CDCl3 solvent confirmed SHG-8 structure. ^{1}H NMR methods are used in the identification/confirmation of unknown structures by determining the magnetic resonance of protons localised across the molecule and the different types of resonance emitted as a result of the final SHG-8 compound.

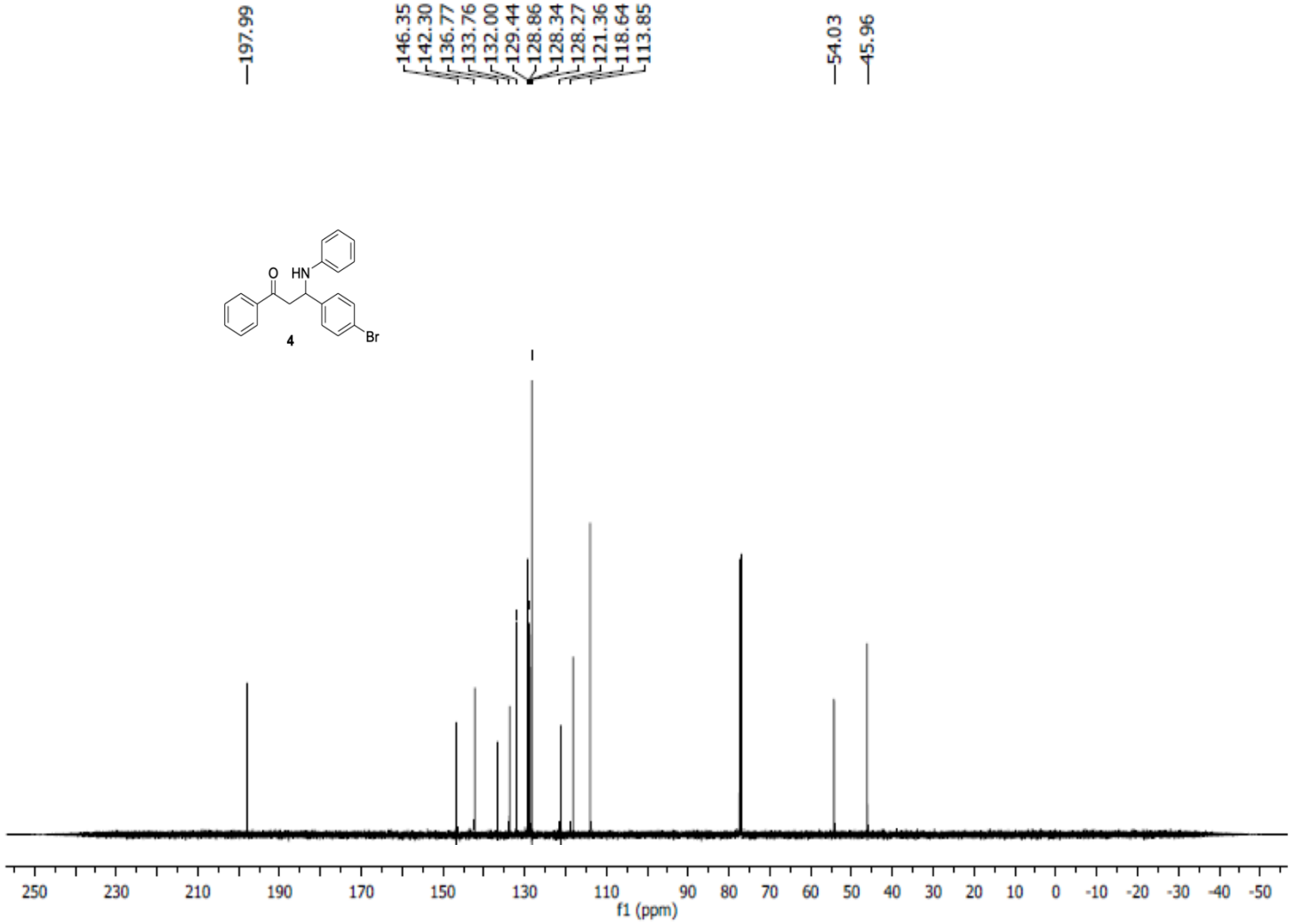

Figure 58: ^{13}C NMR spectrum of the SHG-8 compound in a CDCl3 solvent confirmed SHG-8 structure. The^{13}C NMR method utilises the magnetic resonance of carbon atoms localised within a given structure to assist in structural identification and connectivity to other organic molecules

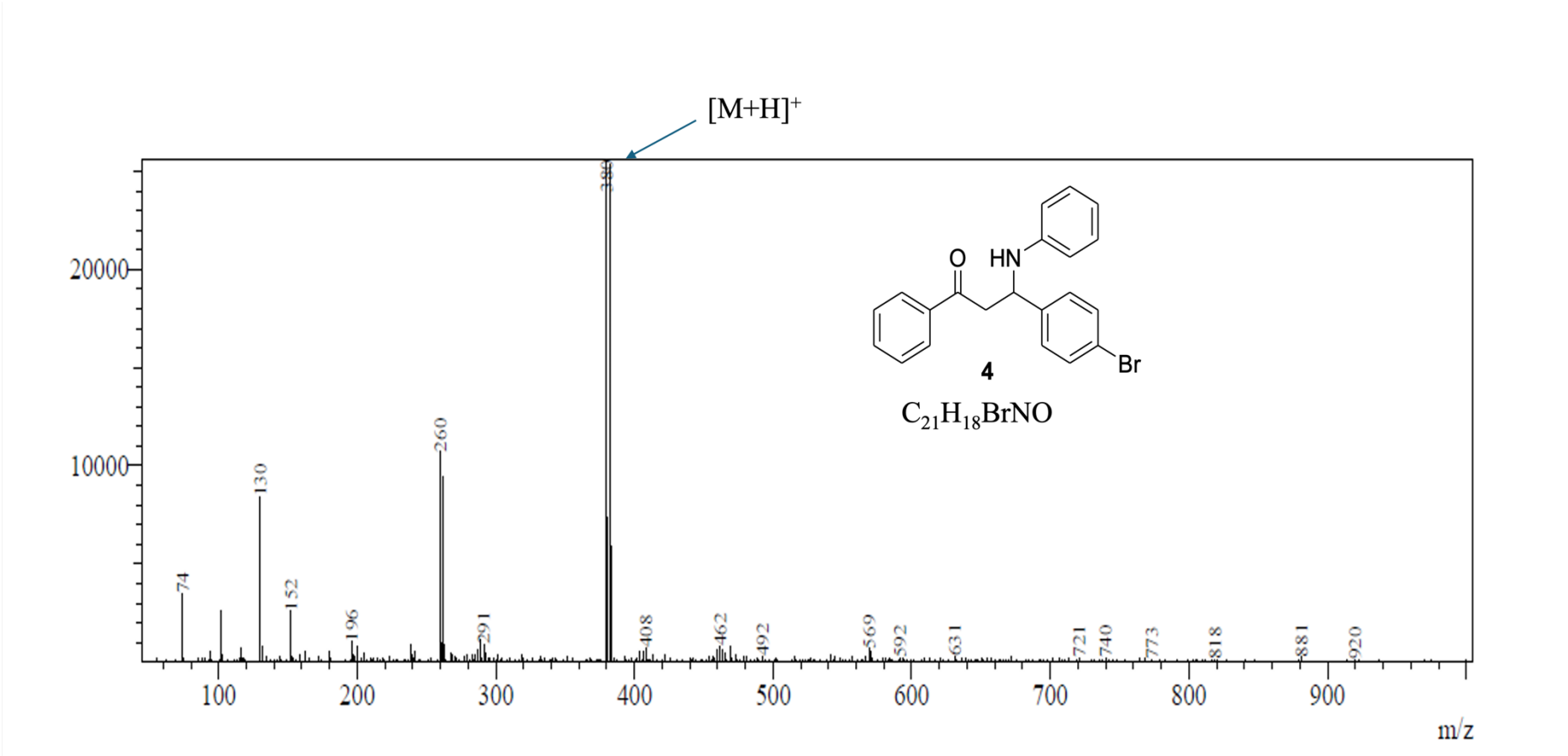

Figure 59: ESI-MS spectrum of the SHG-8 compound revealed the molecule weight of the compound. Electrospray ionisation is utilised to determine the molecular weight of polar structural molecules whilst minimising structural fragmentation.

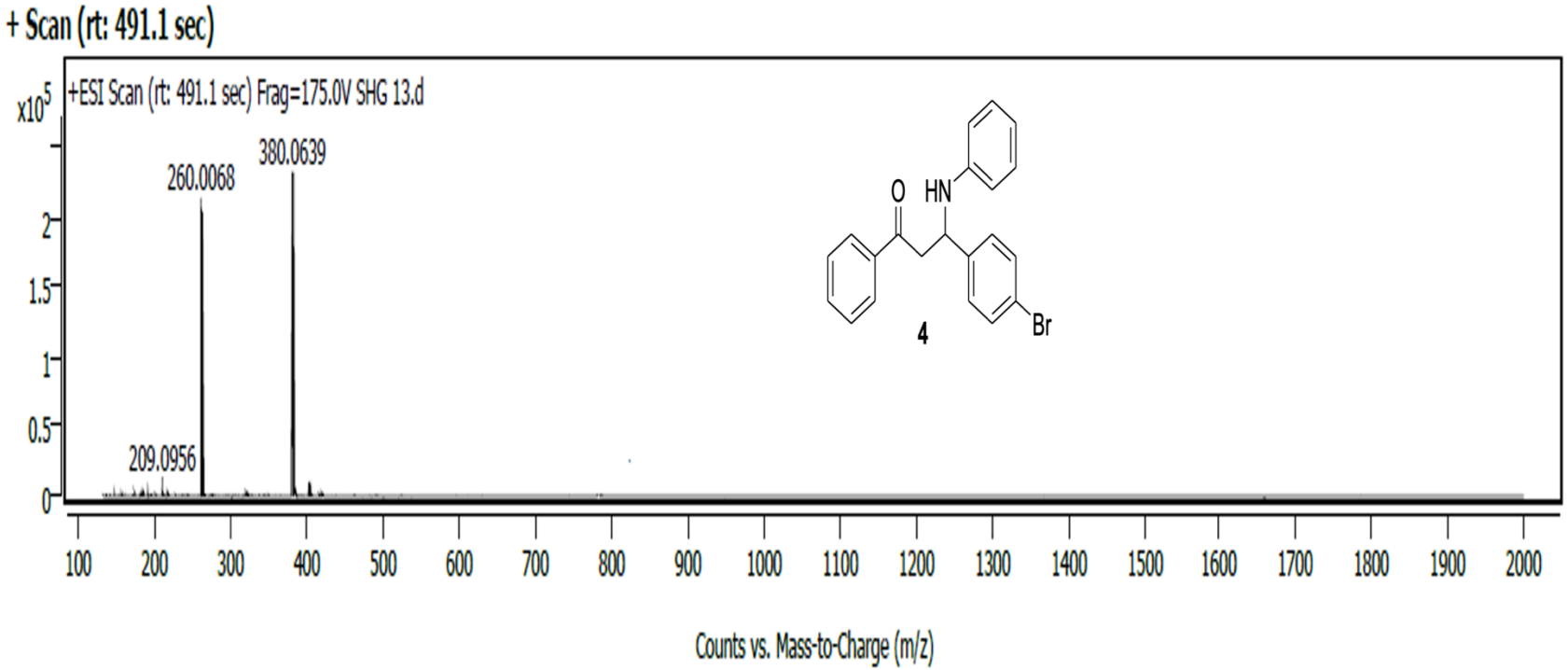

Figure 60: High-resolution mass spectrum (HRMS) of the SHG-8 compound confirming a molecular weight of 380.0645 and structural formula as $C_{21}H_{18}BrNO$. HRMS methods distinguished the identification of compounds that are presented with the same molecular mass through interactions with halides.

3.3.2 Molecular docking analysis prediction and *in silico* Siglec-15 expression in CRC tumours

COACH prediction analysis revealed several amino acid residues of the Siglec-15 protein structure to interact with the SHG-8 molecule as a ligand (Table 16). Of those identified, amino acid residues involved in binding were at positions: 44, 70, 143, 152, 153, 154, 155 and 157. Furthermore, the binding affinity of the predicted protein receptor-ligand interactions was recorded at -5.2 kcal/mol with direct binding to the V-set binding domain and the target site was exhibited at high confidence (Figure 61A). In addition, the interactions within the V-set binding domain revealed amino acid residues that are structurally part of the protein structure and within 5.0 Å of SHG-8 binding were revealed as Trp44, Tyr87, Tyr154, Arg143, Asp152, Arg153 (Figure 61A). Additionally other structural conformations of the bound SHG-8 ligand in association with the Siglec-15 protein revealed predicted localisation of the R143 within the protein structure (Figure 61B). In addition, the updated software of AlphaFold modelling comprises of greater modelling accuracy and also incorporates post-translational modifications which may impact the tertiary structure of the Siglec-15 protein structure. For Siglec-15, it is worth highlighting that any modifications such as glycosylation and phosphorylation could alter the conformational structure of the binding pocket or prevent the availability of key residues from binding.

To determine if Siglec-15 is in fact deregulated in CRC progression, UALCAN transcriptomics analysis revealed enhanced *SIGLEC15* expression in the tumour cohort in comparison to the normal tissue cohort with the mean expression of 0.232 TPM and 0.107 TPM, respectively ($P< 0.001$) (Figure 62A). Moreover, *SIGLEC15* expression was significantly hypomethylated in COAD tumours in contrast to normal colon tissues ($P< 0.0001$) (Figure 62B).

To confirm the CRC cell lines HCT116 and SW480 cells express Siglec-15 on the plasma membranes, Siglec-15 antibody staining in comparison to the GB U87MG cell line was conducted. When compared against U87MG cells, both cell lines were shown to fluorescently express Siglec-15 at the protein level (Figure 63).

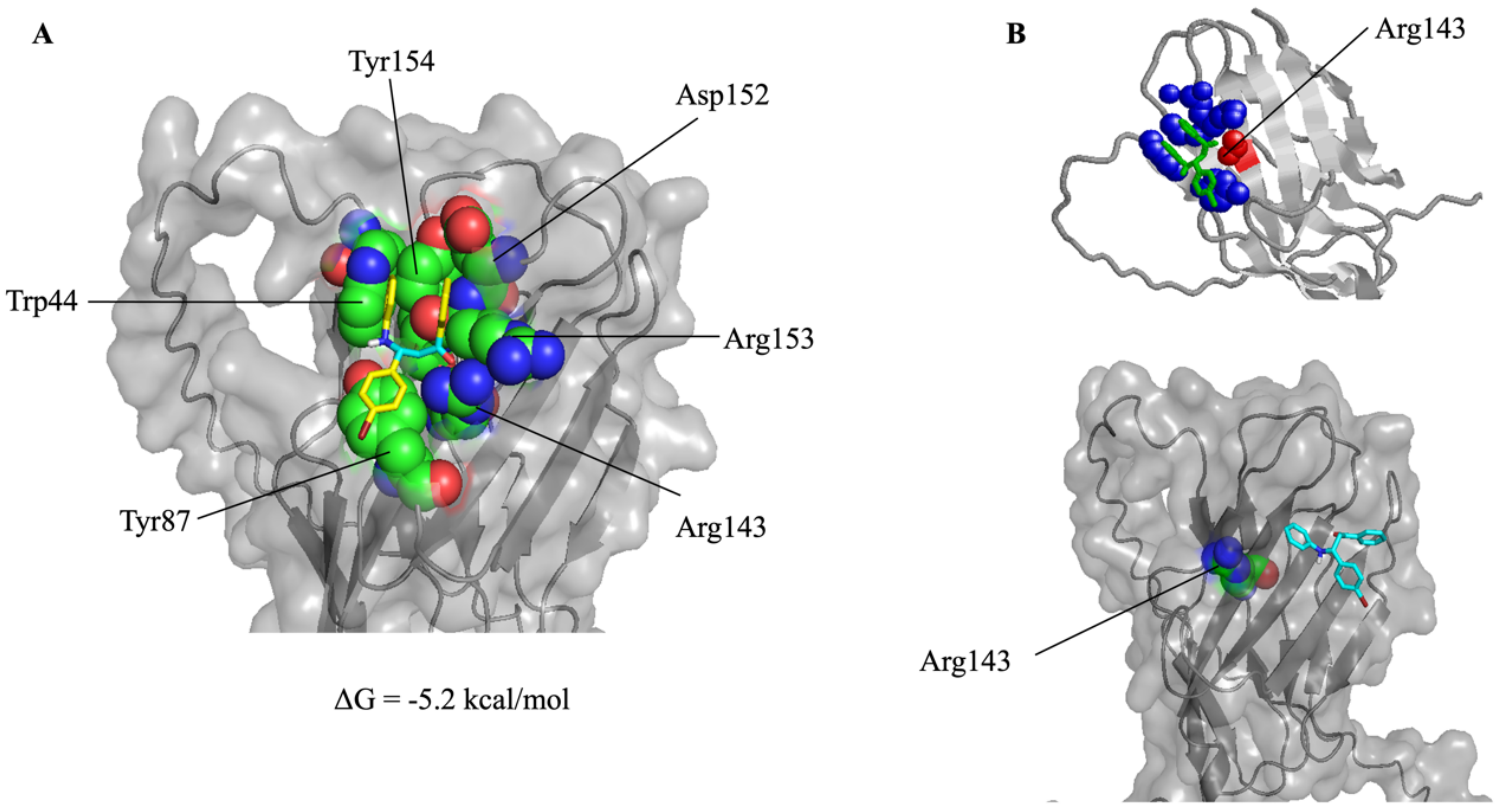

Figure 61: Molecular docking analysis revealed possible amino acid residues contact with SHG-8 binding. (**A**) Protein docking analysis of the AlphaFold Siglec-15 protein structure identified amino acid residues predicted to be within 5.0 Å of the SHG-8 compound ligand and possible interactions via Autodock Vina software. (**B**) Changes in Siglec-15 structural conformation highlighted the localisation of the R143 residue, which is critical in salt bridge formation and ligand binding.

Table 16: COACH prediction revealed Sia binding sites. COACH prediction analysis exhibited possible amino acid residues in contact between the Siglec-15 protein structure and the binding of the SHG-8 compound.

Rank	**C-score**	**Cluster size**	**Ligand Name**	**Consensus binding residues**
1	0.12	7	SIA	44, 70, 143, 152, 153, 153, 155, 157
2	0.05	3	UNL	50, 159, 161
3	0.03	2	FMT	48, 140, 141, 142, 156, 159, 160
4	0.03	2	MAN	236, 247, 248, 249
5	0.02	1	2E9WA00	234, 247, 249, 251
6	0.02	1	N/A	134, 137, 138, 217, 219, 220
7	0.02	1	N/A	22, 23, 24, 25, 26, 28, 49, 51, 52, 53, 55, 58, 59
8	0.02	1	2EC8A00	19, 56. 57. 58
9	0.02	1	N/A	83, 110, 113, 114, 135, 136, 140

10	0.02	1	2JLKA01	178, 179, 225, 227

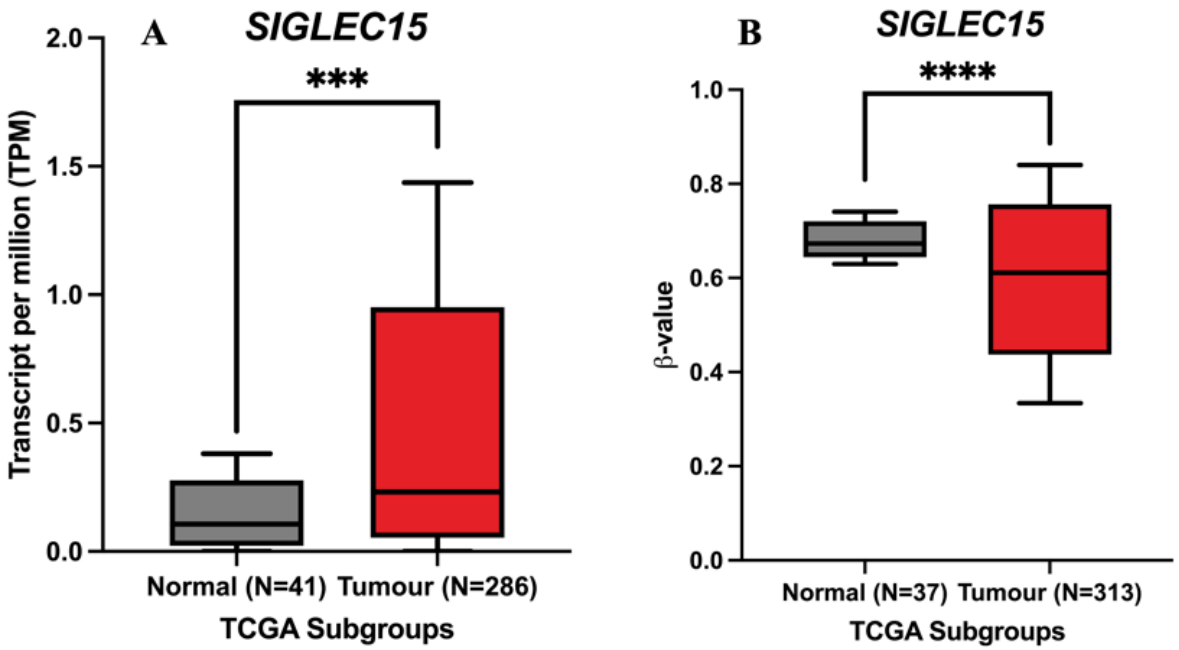

Figure 62: *SIGLEC15* is overexpressed and hypomethylated in COAD tumours. (**A**) UALCAN TCGA genomic data exhibiting mRNA expression of *SIGLEC15* in normal (grey) (N=37) and COAD (red) (N=313) cohorts. Welch's t-test PERL script. *** P<0.001. (**B**) UALCAN transcriptomics analysis was conducted to determine the methylation of the promoter regions of *SIGLEC15* between normal tissue (grey) and COAD tumour (red) cohorts. error bars ± SD. Welch's t-test PERL script. **** P<0.0001.

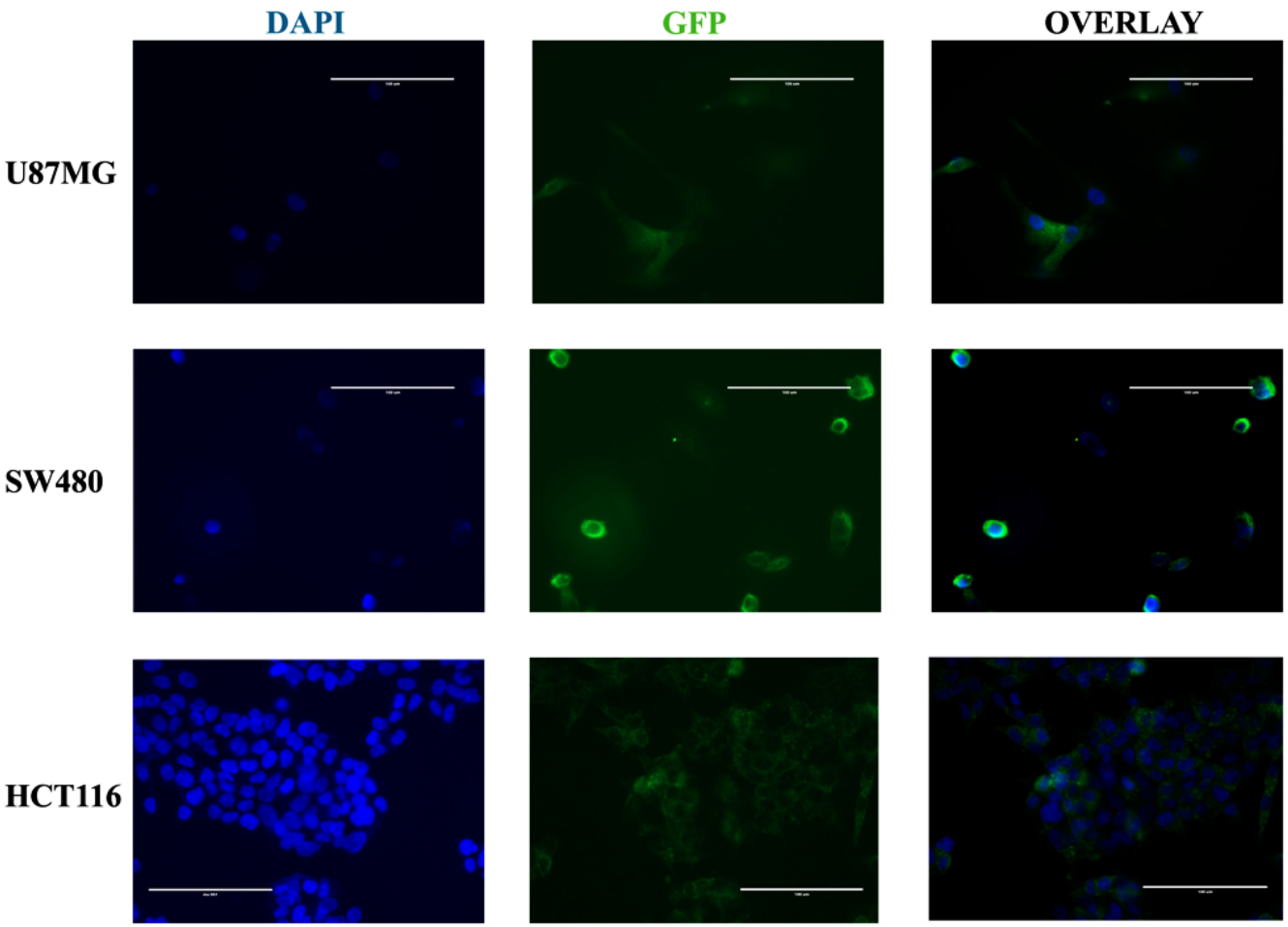

Figure 63: Expression of Siglec-15 was validated within *in vitro* CRC cell lines SW480 and HCT116. IF staining analysis was conducted to determine if Siglec-15 is expressed in CRC cell lines HCT116 and SW480 (N=3).

3.3.3 Determining the cytotoxicity profile of the SHG-8 compound *in vitro*

The cytotoxicity of the SHG-8 compound at varying concentrations (20µM, 40µM , 60µM, 80µM and 100µM) was elucidated on SW480 cells *in vitro* via several functional assays (Figure 64). Conventional anti-cancer therapies such as cisplatin were used as a positive control for the experimental work to draw significant comparisons between the functionality of both compounds. In addition, the negative control DMSO was utilised at a concentration of 1%. Cytotoxicity assays revealed significant cytotoxic profiles in both HCT116 and SW480 cell lines with IC_{50} values of 17.75µM and 20.78µM, respectively ($P< 0.0001$). Additionally, at the highest concentration of 100µM, there was significant cell death, reaching as high as 95.412% and 95.339% in SW480 and HCT116 cells ($P< 0.0001$). In contrast, normal epithelial HcoEPiC cells have shown no significant difference in cellular viability at 20µM. In addition, the observed IC_{50} value for this cell line was recorded as 92.34µM ($P< 0.0001$), which is significantly greater than the recorded IC_{50} values for both HCT116 and SW480 cell lines. Thus, indicating SHG-8 activity induced reduced toxicity in normal epithelial cells. Moreover, SHG-8 demonstrated a dose-dependent cytotoxicity upon reaching higher concentrations, with cellular viability decreasing from 77.18% at 40µM to 45.26% at 100µM concentration ($P< 0.0001$).

Wound healing analysis of SW480 cells treated with the SHG-8 compound revealed the inhibition of cellular migration of 15.37% at 24h following SHG-8 exposure with the 40µM treatment ($P< 0.05$, $P< 0.01$) (Figure 65A). In addition to this, comparative images taken of the wound healing area also supported observations of reduced migration of the treatment conditions across a 48h treatment period when compared against the DMSO control (Figure 65B). Moreover, both SHG-8 treatment conditions at 10µM and 40µM has shown similar anti-migration at 48h recorded an open wound area of 13.22% and 13.28% in comparison to the DMSO control condition, respectively.

Furthermore, all treatment conditions resulted in reduced cellular colonisation (N=3), indicated by quantitative colonisation assay data with both 10µM and 40µM concentrations, resulting in the formation of no colonies alongside the cisplatin control ($P< 0.0001$) (Figure 66A). This was also similarly observed via comparative images of the well plate and brightfield images of the colonies present in the DMSO control condition at 4x and 10x magnification (Figure 66B, 66C).

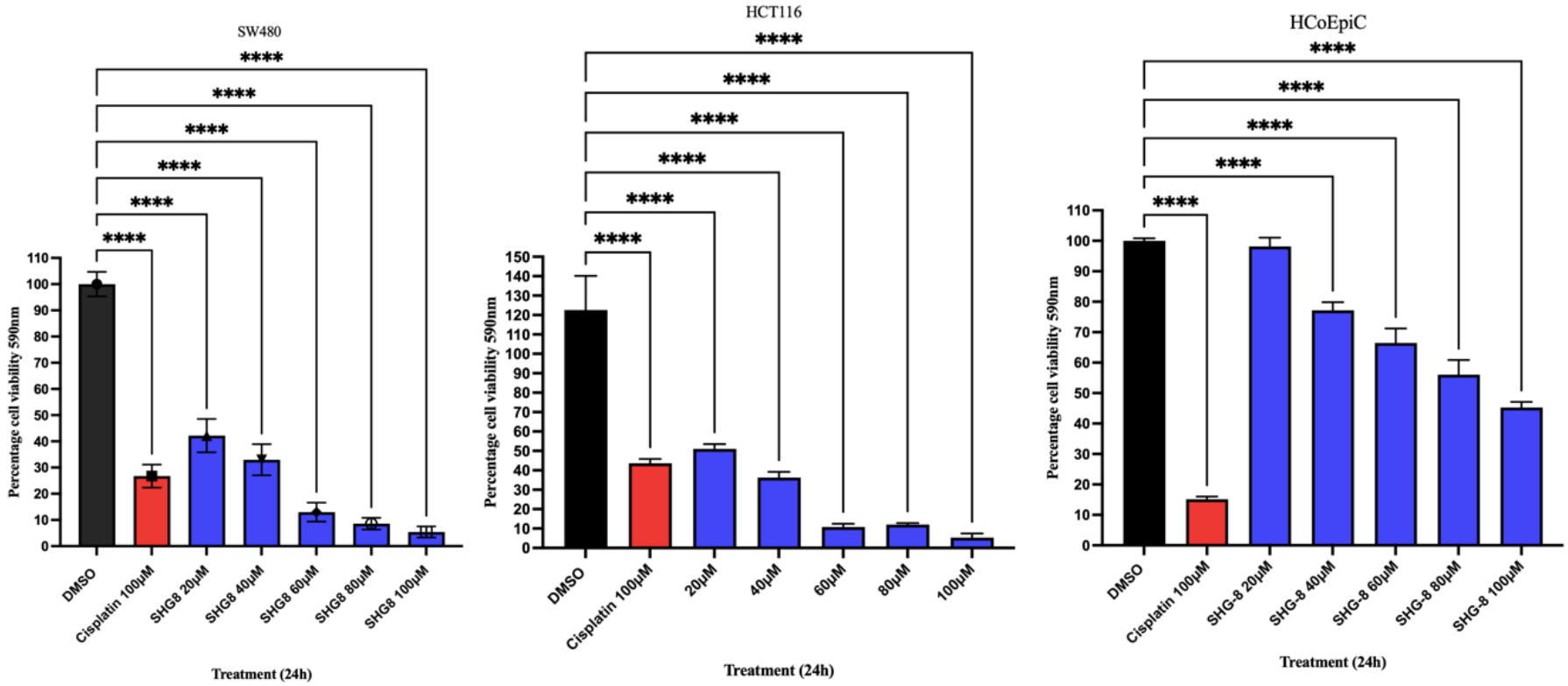

Figure 64: SHG-8 exhibited a dose-dependent cytotoxicity against tumour and epithelial cells *in vitro*. The MTT cytotoxicity assay was performed to elucidate the SHG-8 cytotoxic profile in normal epithelial and tumour cell lines following 24h SHG-8 exposure. Additionally, the IC_{50} of the SHG-8 compound was determined in the three HCT116 (N=5), SW480 (N-5) and HcoEPiC (N=3) cell lines. Data is presented as mean ± SD. One-Way ANOVA statistical test followed by Dunnett's multiple comparison post-hoc test. **** P<0.0001.

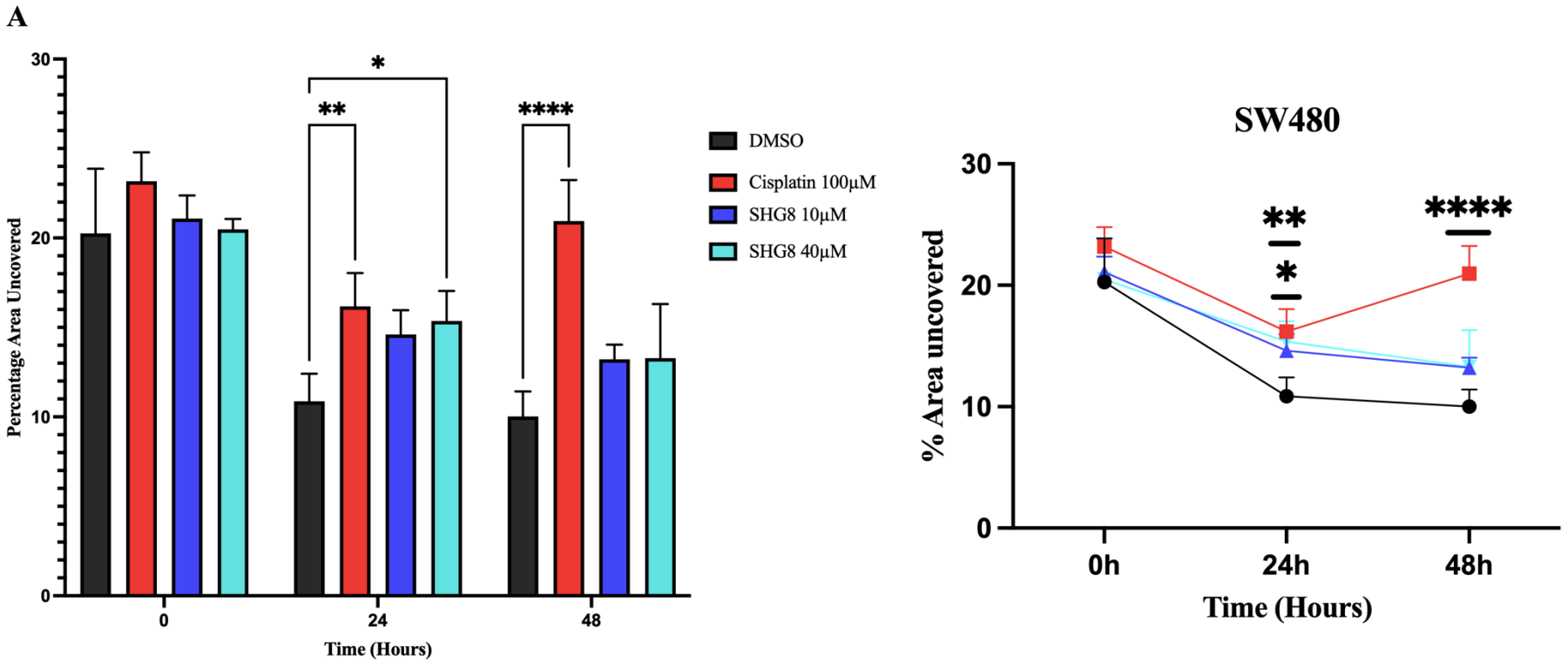
A
Percentage Area Uncovered
30
20
10
0
0
24
48
Time (Hours)
*
**
****
DMSO
Cisplatin 100µM
SHG8 10µM
SHG8 40µM
SW480
% Area uncovered
30
20
10
0
0h
24h
48h
Time (Hours)
**
*
****

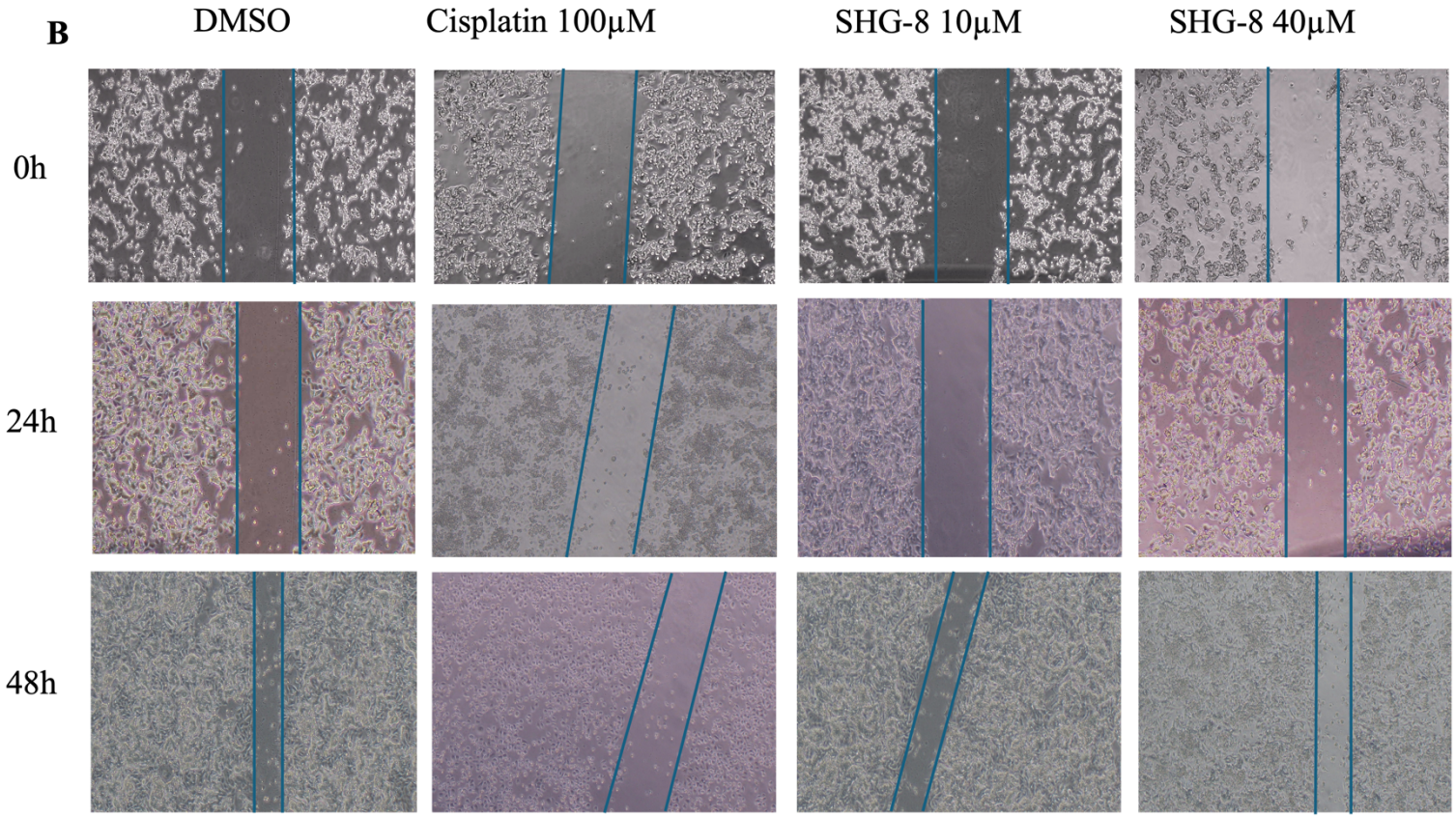

`

Figure 65: SHG-8 reduced tumour migration in SW480 cells following a 24h treatment period. (**A**) The migration assay was performed to determine the effect of the SHG-8 compound on tumour cell migration across 48h (N=3). Data is presented as mean ± SD. Welch's One-Way ANOVA followed by Dunnett's multiple comparison post-hoc test. *P<0.05, **P<0.01, ***P<0.001, **** P<0.0001. (**B**) Comparative images of migration distance taken at 4x magnification of SW480 cells treated with SHG-8 at 10µM and 40µM condition across a 48h treatment period. Image analysis was conducted using ImageJ software with plugins outlined by (Suarez-Arnedo et al., 2020).

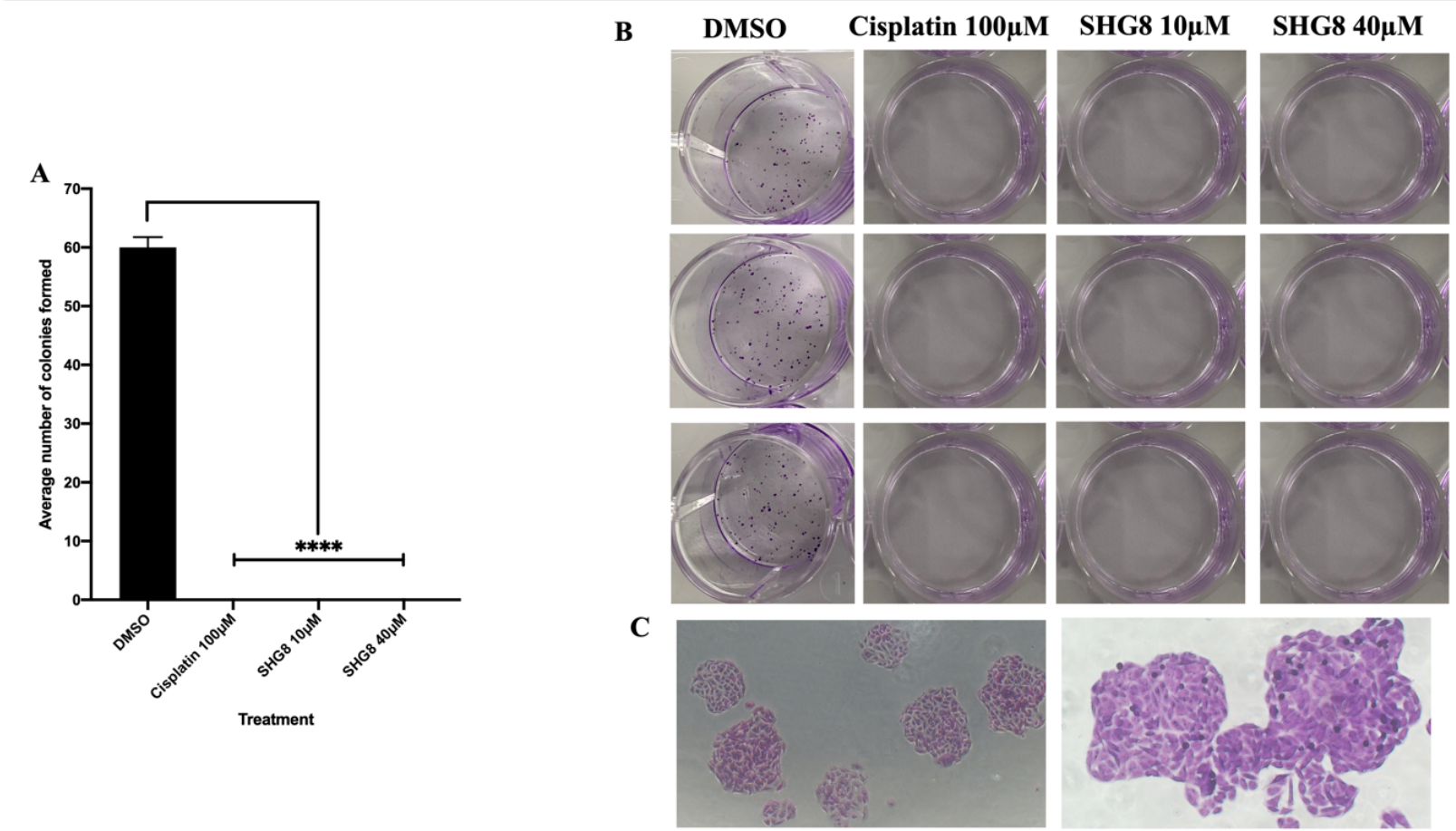

Figure 66: SHG-8 inhibited tumour cell colonisation following 24h SHG-8 treatment exposure. (**A**) Colonisation assays determined the effect of SHG-8 treatment on SW480 colonisation post 24h treatment period and proliferation across 7 days post-treatment (N=3). Data is presented as mean ± SD. One-way ANOVA statistical analysis followed by Dunnett's multiple comparison post-hoc test. **** P<0.0001. (**B**) Visualisation of the 12-well plate utilised for 24h treatment of SW480 colonisation assay following 0.1% crystal violet staining. (**C**) Comparative images taken of the colonies of the DMSO control condition following 24h SHG-8 treatment period at 4x and 10x magnification stained with 0.1% crystal violet staining. Colonies were determined in the DMSO control condition of cellular clusters that are greater than >30 cells.

3.3.4 SHG-8-mediated cellular death

To determine the likelihood of apoptotic cell death induced in SW480 cells following SHG-8 treatment, DAPI nuclear staining; a marker of apoptotic death, was conducted (Figure 67). Fluorescent images taken of the DAPI filter at 40x magnification revealed apoptotic induction following SHG-8 treatment in a dose-dependent manner. This indicated greater instances of nuclear fragmentation at 10µM and 40µM conditions in comparison to the DMSO control (Figure 67). Additionally, cells treated with SHG-8 had undergone structural changes to their morphology presenting with irregular shapes; a possible effect of nuclear fragmentation (shown by white arrows).

Moreover, flow cytometry staining of cellular death was performed to give a quantitative view of the effect of SHG-8 on SW480 cells (Figure 68). Annexin-V and PI dual staining revealed a significant proportion of cells undergoing apoptosis at 100µM cisplatin, 10µM and 40µM SHG-8 conditions in contrast to DMSO (Figure 68A). Furthermore, cisplatin demonstrated a larger proportion of cells undergoing early apoptosis (lower left quadrant) of 13.88%. In contrast, both 10µM and 40µM conditions exhibited a higher proportion of cells undergoing late apoptosis (upper right quadrant), shown at 15.74% and 17.75%, respectively. In addition, all conditions have shown minute cell populations exhibiting necrosis (upper left quadrant). Following on from this, cell cycle arrest analyses via PI staining demonstrated SHG-8 induced greater cell cycle arrest at the G2/M phase at higher concentrations, demonstrating populations of 13.31% and 16.17% cells in comparison to 10.97% in DMSO, respectively (Figure 68B). Interestingly, the cisplatin condition exhibited the greatest proportion of cells arresting at the S phase (12.80%), when compared against SHG-8 demonstrating 5.95% and 5.96% of cells at 10µM and 40µM correspondingly. Moreover, the DMSO control condition exhibited the largest proportion of cells in the G0/G1 phase with 80.94% of cells arrested. However, only a small subset of the cell population had undergone cellular arrest at the sub-G0 phase of the cell cycle.

ROS production was hypothesised as a possible stimulant for apoptosis induction in CRC cells following SHG-8 treatment. Measuring ROS production via fluorescence emission demonstrated no significant difference between SHG-8 treatments and the control conditions (Figure 69). Further to this, only the positive control H_2O_2, a known stimulant in ROS production, exhibited significant ROS production ranging from 0 min to 120 min. Hence, it is

inferred that ROS production is independent of SHG-8-mediated cytotoxicity and is not the mechanism of action for which cellular death occurs.

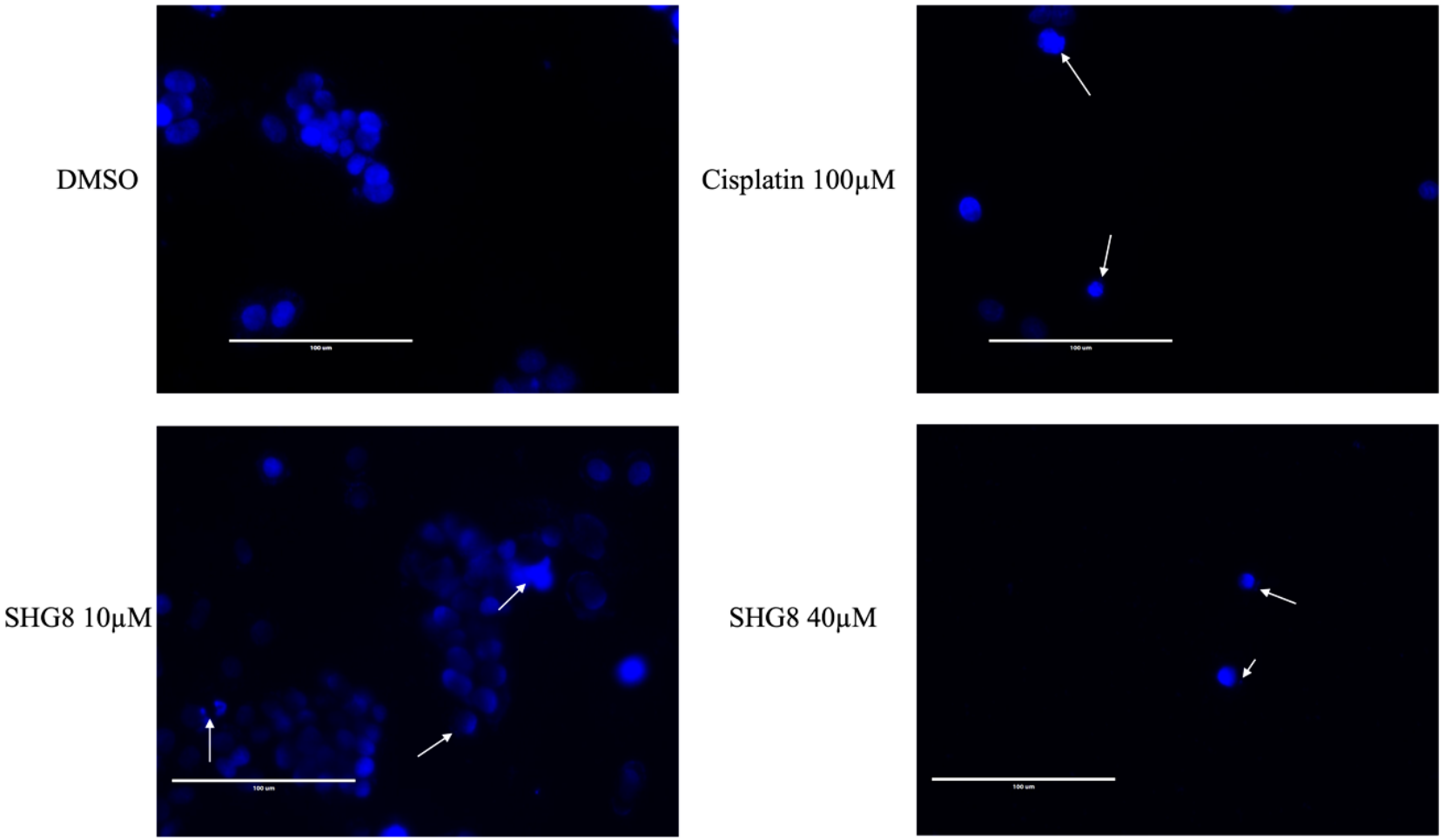

Figure 67: SHG-8 activity stimulated dose-dependent apoptosis in SW480 CRC cells. Nuclear fragmentation via DAPI staining was conducted to elucidate the apoptosis induction following SHG-8 10µM and 40µM treatment on SW480 cells. Morphological irregularities and nuclear fragments are indicated by white arrows (N=3).

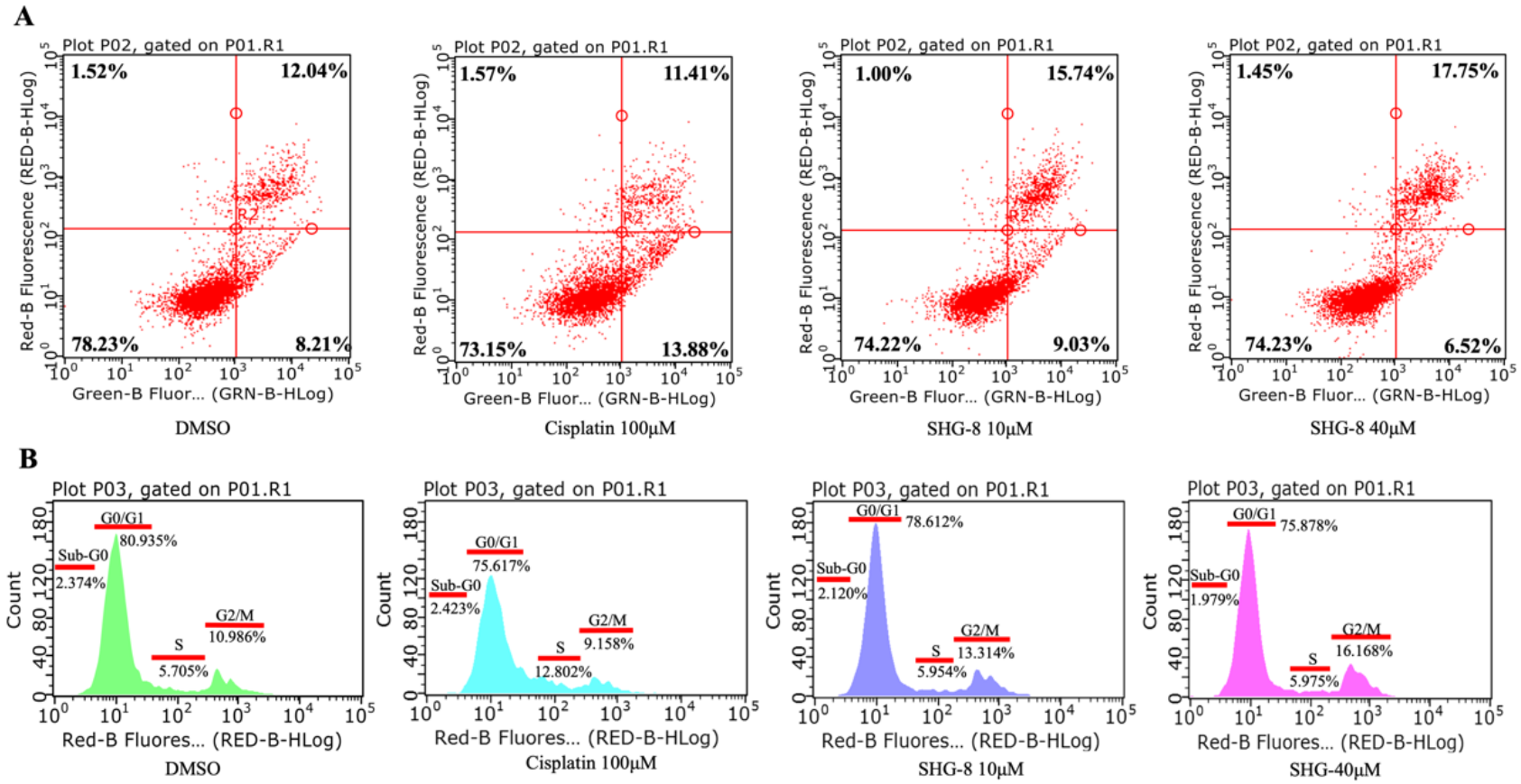

Figure 68: Annexin-V and PI dual staining revealed SHG-8 stimulated late apoptosis activation at higher concentrations and cell cycle arrest at the G2/M phase. (**A**) Annexin-V/propidium iodide dual staining of CRC cells following 24h treatment 10µM and 40µM SHG-8 treatment condition. Quadrats are divided into four sections. $FITC^-$ and PI^+ (upper left quadrant) represented SW480 cells undergoing necrosis. $FITC^+$ and PI^+ (upper right quadrant) represented SW480 cells undergoing late apoptosis. $FITC^-$ and PI^- (lower left quadrant) represented SW480 live cells. $FITC^+$ and PI^- (lower right quadrant) represented SW480 cells undergoing early apoptosis. (**B**) Cell cycle arrest of G1/S/G2/M determined via PI staining of SW480 cells treated with SHG-8 24h treatment period. Conditions are presented as DMSO (green), cisplatin 100µM (light blue) and SHG-8 at 10µM (dark blue) and 40µM (pink) conditions.

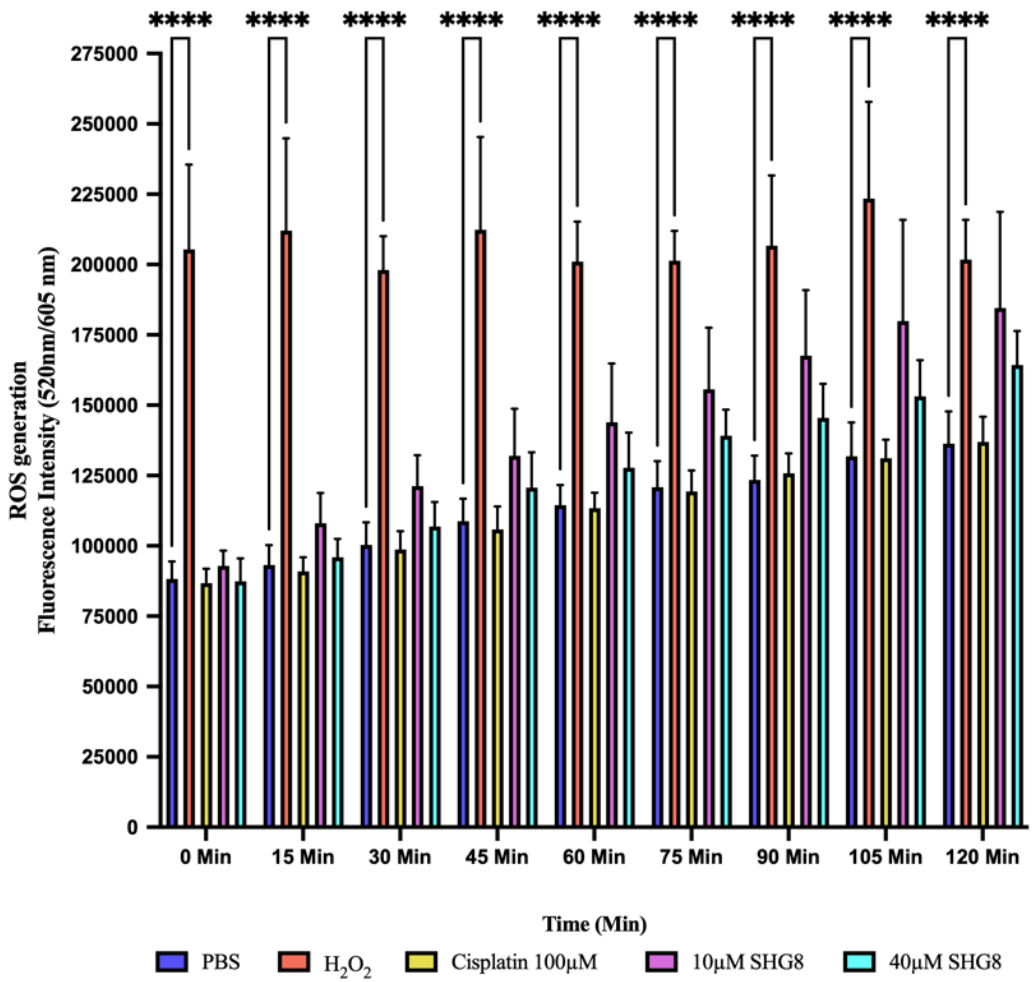

Figure 69: SHG-8 apoptosis induction is not mediated by ROS production in SW480 cells. ROS production was determined in SW480 cells following 24h SHG-8 exposure as a possible mechanism of action. Fluorescence intensity was taken at several time intervals at excitation/emission 520/605nm (N=4). Data is presented as mean ± SD. Two-way ANOVA followed by Dunnett's multiple comparison post-hoc test was conducted. ****P< 0.0001.

3.3.5 Siglec-15 expression following SHG-8 treatment exposure

Determining the expression of Siglec-15 at the gene and protein level, several methods, including IF, RT-qPCR and flow cytometry methods, were performed (Figure 70). RT-qPCR expression analysis exhibited *SIGLEC15* gene expression at 10µM and 40µM treatment conditions with 24h exposure of SHG-8 versus the cisplatin positive and DMSO negative control conditions ($P< 0.05$, $P< 0.01$) (Figure 70A). *SIGLEC15* exhibited significantly downregulated expression, highlighted by a two-fold decrease in expression at 10µM and 40µM conditions. Two differing methodologies were utilised to illustrate Siglec-15 protein expression to underline the variance and reliability of the experiemntal data that was collated between flow cytometry and immunofluorescence approaches. Flow cytometry image and quantitative analysis of Siglec-15 expression indicated no significant difference in protein expression following SHG-8 treatment at both 10µM and 40µM conditions when compared against the DMSO control (Figure 70B). Moreover, quantitative image analaysis of IF images underlined the mean GFP intentisty via the ImageJ software, which demonstrated significant downregulation of Siglec-15 at the protein level following 24h SHG-8 exposure ($P< 0.01$, $P< 0.001$) (Figure 70C, 70D).

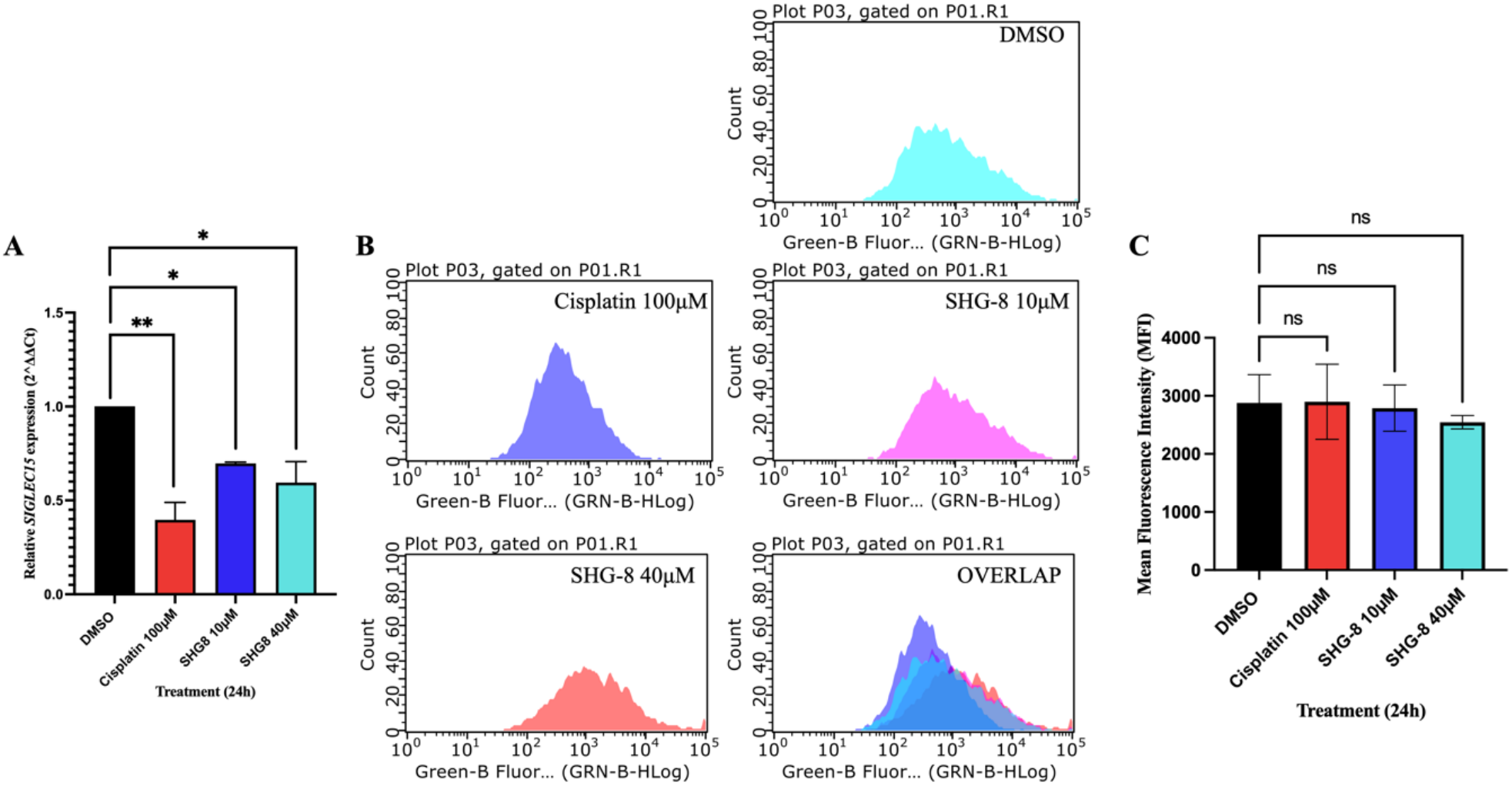
A
Relative SIGLEC15 expression (2^-ΔΔCt)
1.5
1.0
0.5
0.0
*
*
**
DMSO
Cisplatin 100μM
SHG8 10μM
SHG8 40μM
Treatment (24h)
B
Plot P03, gated on P01.R1
DMSO
Count
Green-B Fluor... (GRN-B-HLog)
Cisplatin 100μM
SHG-8 10μM
SHG-8 40μM
OVERLAP
C
Mean Fluorescence Intensity (MFI)
4000
3000
2000
1000
0
ns
ns
ns
DMSO
Cisplatin 100μM
SHG-8 10μM
SHG-8 40μM
Treatment (24h)

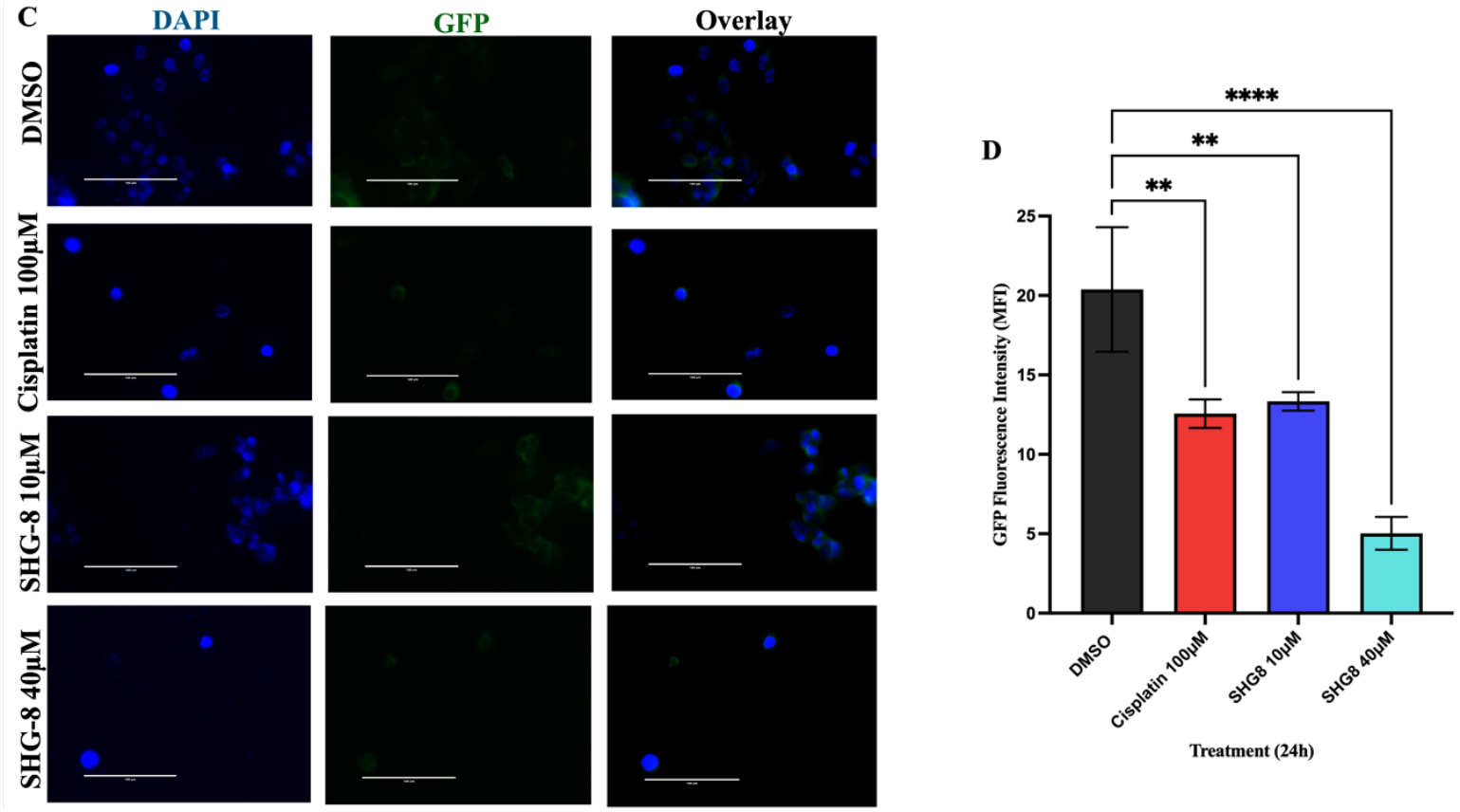

Figure 70: RT-qPCR methods underline SHG-8 activity plays a role in downregulating *SIGLEC15* gene expression. (**A**) RT-qPCR expression analysis of *SIGLEC15* in SW480 cells following 24h SHG-8 treatment exposure (N=3). One-way ANOVA statistical test followed by Dunnett's multiple comparison post-hoc test, *P<0.05, **P<0.01. (**B**) Flow cytometry analysis of Siglec-15 expression, following treatment of SHG-8 in SW480 cells (N=3). Treatment conditions are as follows: DMSO (light blue), cisplatin 100µM (dark blue), SHG-8 10µM (pink) and 40µM (red) conditions. In addition, mean fluorescence intensity (MFI) was also calculated based on the flow cytometry expression peaks. Data is presented as mean ± SD. One-way ANOVA followed by Dunnett's multiple comparison post-hoc test was conducted. (**C**) IF image visualisation of SW480 cells stained with a primary Siglec-15 antibody following 24h SHG-8 exposure taken at 40x magnification with DAPI and GFP filters

(N=3). (**D**) Quantitative analysis of mean green fluorescence intensity of IF image visualisation following SHG-8 treatment (N=3). Data is presented as mean ± SD. One-way ANOVA followed by Dunnett's multiple comparison post-hoc test was conducted. ** P <0.01, *** P <0.001.

3.3.6 Pro-inflammatory cytokine secretion in differentiated macrophages via ELISA

Determining the role of cytokine expression and possible stimulation of myeloid cells within the TME, pro-inflammatory cytokine expression of TNFα and IL-1β was determined following 24h SHG-8 exposure and LPS (50ng/mL) mediated activation (Figure 71). Stimulation by LPS had resulted in the activation of both THP-1 and U937 differentiated macrophages and significantly induced the secretion of both TNFα and IL-1β, in comparison to the untreated control condition ($P< 0.001$) (Figure 71A-D). Furthermore, the 40μM SHG-8 treatment condition inhibited LPS stimulation and pro-inflammatory cytokine secretion of TNFα and IL-1β in all observable treatment conditions ($P< 0.001$) (Figure 71A-D). In addition, the 40μM SHG-8 only treatment condition had significantly inhibited pro-inflammatory cytokine secretion of TNFα secreted in U937 (7.731ng/mL) and IL-1β in THP-1 cells (11.52ng/mL) in comparison to the control condition (Figure 71B, 71C).

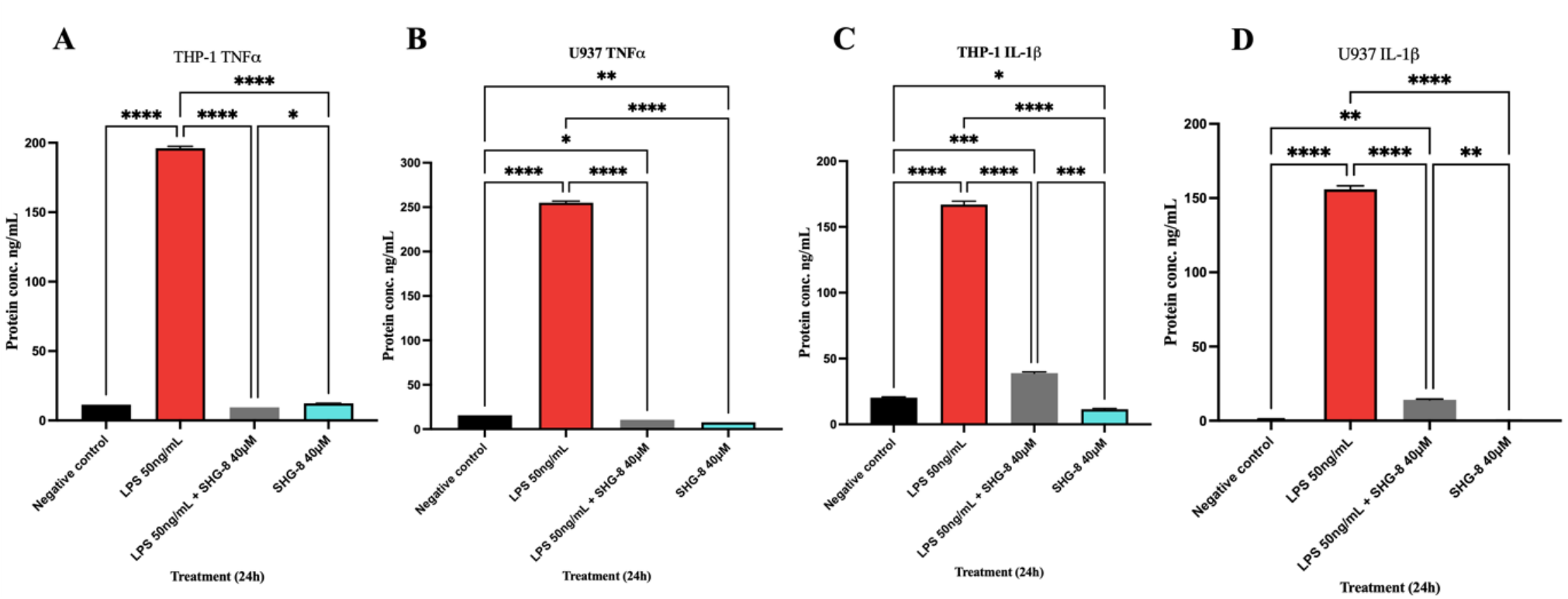

Figure 71: SHG-8 inhibited the secretion of pro-inflammatory cytokines in differentiated macrophages. (**A**) Elucidation of TNFα cytokine secretion following LPS stimulation and SHG-8 exposure of THP-1 differentiated macrophages via ELISA method. Data is presented as mean ± SD. One-way ANOVA statistical test followed by Tukey's multiple comparison post-hoc test. *P< 0.05, ****P< 0.0001. (**B**) Elucidation of TNFα cytokine secretion following LPS stimulation and SHG-8 exposure of U937 differentiated macrophages via ELISA method. Data is presented as mean ± SD. One-way ANOVA statistical test followed by Tukey's multiple comparison post-hoc test. *P< 0.05, **P< 0.01, ****P< 0.0001. (**C**) Elucidation of IL-1β cytokine secretion following LPS stimulation and SHG-8 exposure of THP-1 differentiated macrophages via ELISA method. Data is presented as mean ± SD. One-way ANOVA statistical test followed by Tukey's multiple comparison post-hoc test. * P< 0.05, ***P< 0.001, ****P< 0.0001. (**D**) Elucidation of IL-1β cytokine secretion following LPS stimulation and SHG-8 exposure of U937 differentiated macrophages via ELISA method. Data is presented as mean ± SD. One-way ANOVA statistical test followed by Tukey's multiple comparison post-hoc test. **P< 0.01, ****P< 0.0001.

3.3.7 sRNA-seq analysis

Elucidation of DE miRNAs was determined via sRNA sequencing analysis of SHG-8 treated for 24h and untreated conditions (Figure 72). The constructed heatmap identified multiple DE miRNAs following SHG-8 exposure, indicated by a shift in expression profiles from the untreated DMSO condition to the treatment group (Figure 72A). Furthermore, the correlation analysis revealed a positive correlation between both treatment groups, hinting that cellular exposure to SHG-8 has a profound effect on miRNA expression profiles (Figure 72B). Moreover, a total of 185 DE miRNAs were identified as part of the volcano plot analysis. Of those DE miRNAs that were identified, 106 miRNAs were classified as significantly downregulated, and 79 miRNAs were classified as significantly upregulated following a two-fold change in expression as the cut-off (Figure 72C). In addition to this, the top five most significantly downregulated miRNAs were all revealed to be novel miR-1031, novel miR-1130, novel miR-308, novel miR-503 and novel miR-993. In contrast, the top five significantly upregulated miRNAs were revealed as novel miR-1401, novel miR-1065, novel miR-233, novel miR-1431 and hsa-miR-6715b-3p (Table 17). Additionally, the DE of miRNAs revealed signalling transduction mechanisms and functional activity relating to translation, ribosomal structure and biogenesis. These were all enriched functional terms in the cluster of orthologous genes (COG) classification of consensus analysis (Figure 72D).

KEGG and GO classification analysis was also conducted on the sRNA-seq data to elucidate enriched biological processes and signalling pathways following SHG-8 treatment (Figure 73). KEGG analysis revealed several enriched biological processes that possibly indicate signalling pathways related to inhibiting tumour progression (Figure 73A). This revealed autophagy, hippo signalling and lysosomes were all significantly enriched. Furthermore, GO classification analysis also exhibited the enrichment of biological processes, such as the regulation of myeloid cell apoptotic processes, including neutrophils, regulation of oxidative stress, response to IL-6, regulation of IFNβ production and regulation of cellular components and cellular response (Figure 73B). Interestingly, enrichment of lysosomes, cytoplasmic vesicle membranes and vesicle membranes all showed the highest enrichment for cellular components (Figure 73C). Moreover, determining the molecular function associated with DE miRNAs revealed GTP binding, nucleic acid binding and protein domain specific binding as the most enriched molecular functional terms (Figure 73D).

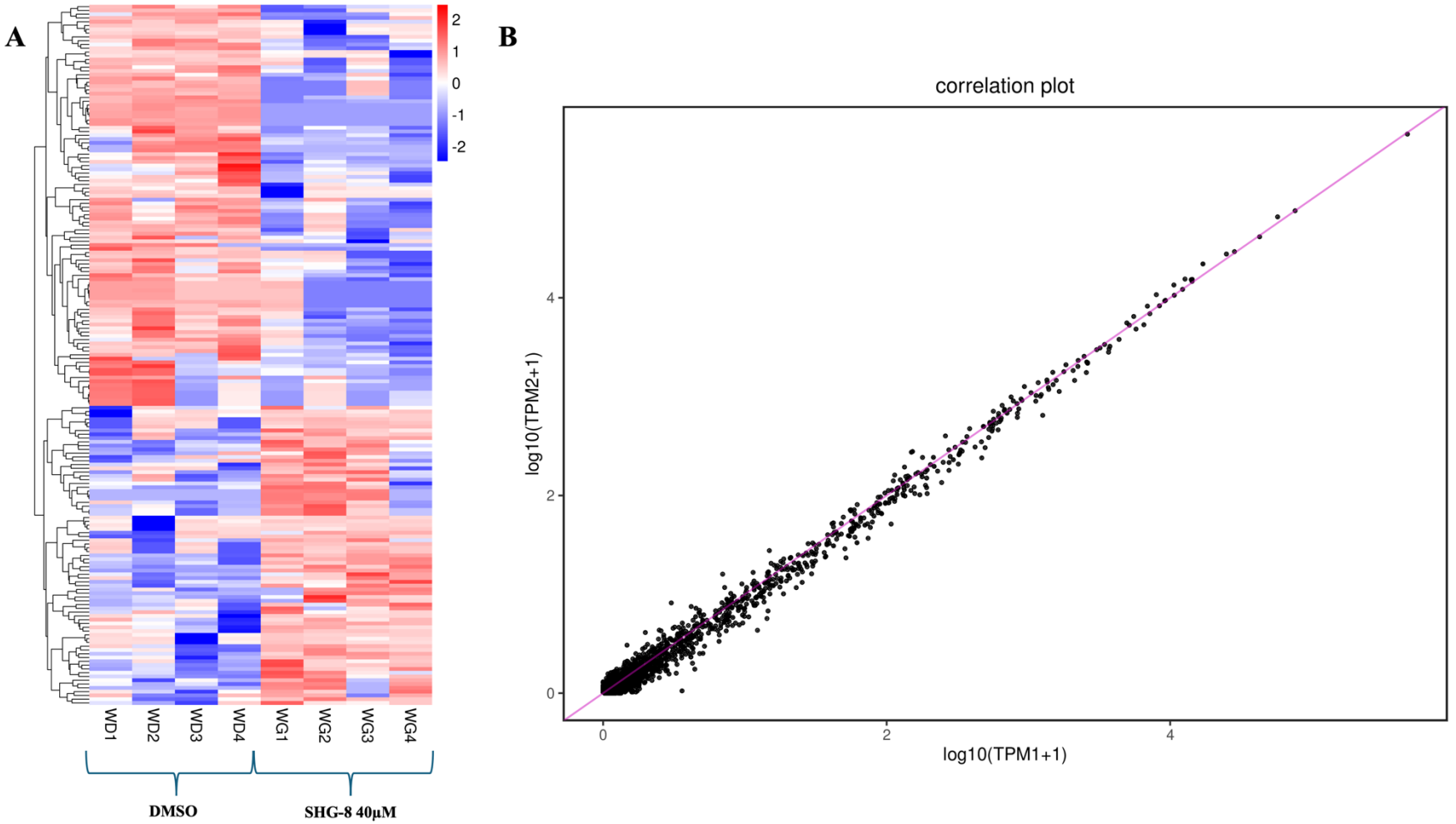
A
2
1
0
-1
-2
WD1
WD2
WD3
WD4
WG1
WG2
WG3
WG4
DMSO
SHG-8 40µM
B
correlation plot
log10(TPM2+1)
log10(TPM1+1)
0
2
4
0
2
4

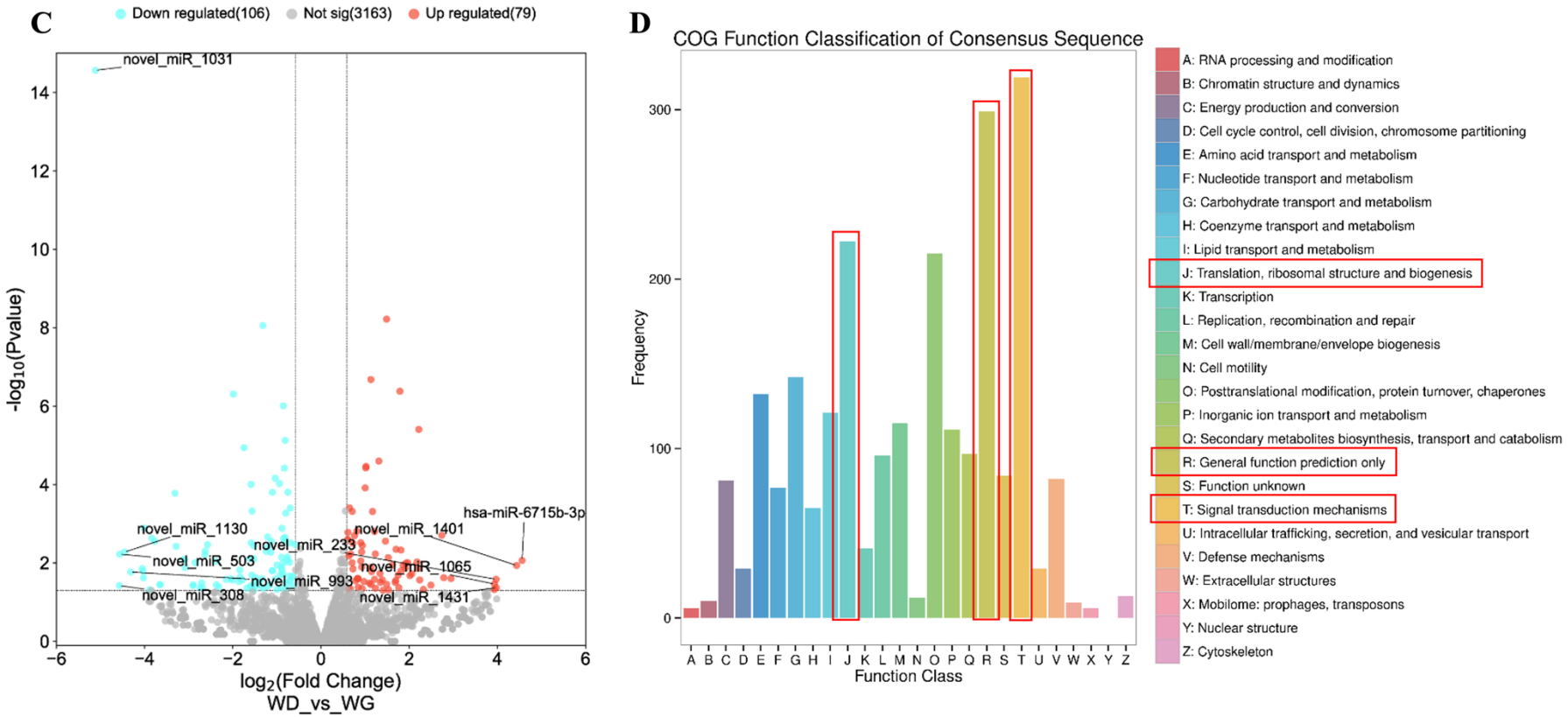

Figure 72: SHG-8 stimulated the DE of miRNAs following 24h treatment at 40µM condition. (**A**) SRNA-seq analysis revealed DE miRNAs between SHG-8 treated and untreated conditions. (**B**) Correlation analysis for DE miRNAs between untreated control condition groups and SHG-8 treatment condition group. (**C**) Constructed volcano plot illustrating the top deregulated miRNAs following SHG-8 treatment. (**D**) COG functional classification of consensus sequence analysis was conducted to elucidate possible enriched deregulated mechanisms.

Table 17: List of the top five differentially expressed miRNAs that are significantly upregulated and downregulated following 24h SHG-8 exposure.

	MIRNA NAME	DIFFERENTIAL EXPRESSION	LOG_2FC
SMALL-RNA SEQUENCING ANALYSIS	hsa-miR-6715b-3p	Upregulated	4.559
	novel_miR_1401	Upregulated	4.435
	novel_miR_1431	Upregulated	3.975
	novel_miR_233	Upregulated	3.970
	novel_miR_1065	Upregulated	3.934
	novel_miR_1031	Downregulated	-5.113
	novel_miR_308	Downregulated	-4.571
	novel_miR_503	Downregulated	-4.563
	novel_miR_1130	Downregulated	-4.456
	novel_miR_993	Downregulated	-4.316

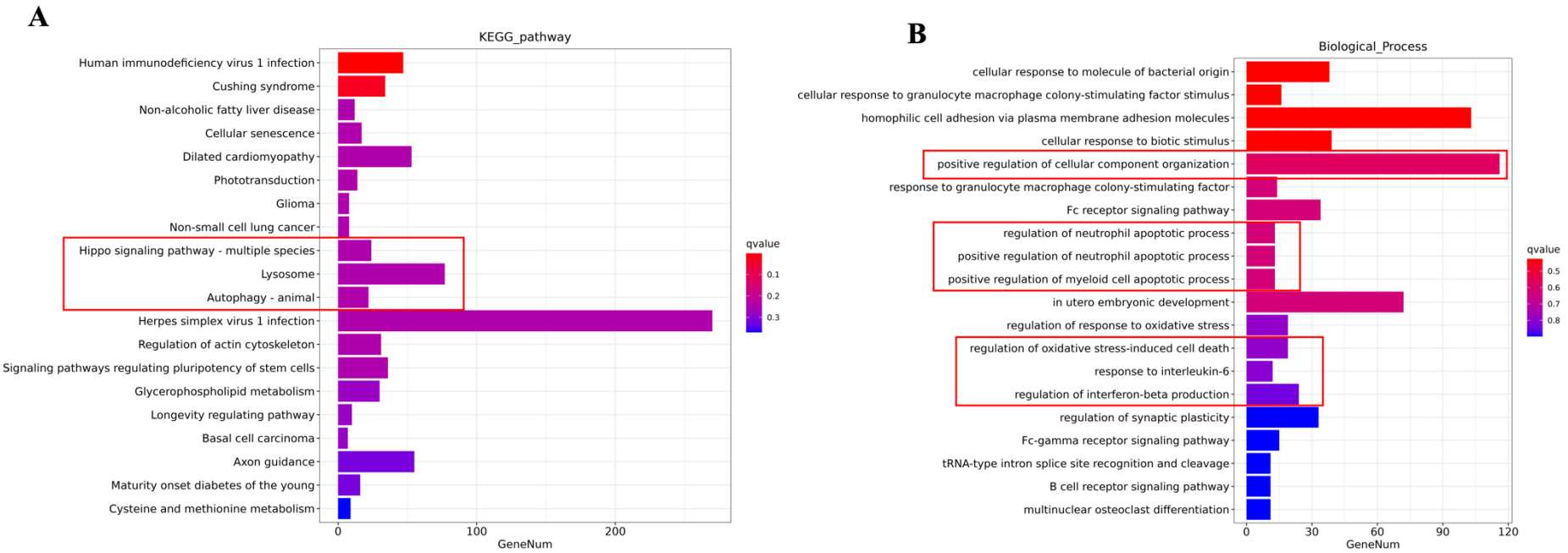
A
KEGG_pathway
Human immunodeficiency virus 1 infection
Cushing syndrome
Non-alcoholic fatty liver disease
Cellular senescence
Dilated cardiomyopathy
Phototransduction
Glioma
Non-small cell lung cancer
Hippo signaling pathway - multiple species
Lysosome
Autophagy - animal
Herpes simplex virus 1 infection
Regulation of actin cytoskeleton
Signaling pathways regulating pluripotency of stem cells
Glycerophospholipid metabolism
Longevity regulating pathway
Basal cell carcinoma
Axon guidance
Maturity onset diabetes of the young
Cysteine and methionine metabolism
0
100
200
GeneNum
qvalue
0.1
0.2
0.3
B
Biological_Process
cellular response to molecule of bacterial origin
cellular response to granulocyte macrophage colony-stimulating factor stimulus
homophilic cell adhesion via plasma membrane adhesion molecules
cellular response to biotic stimulus
positive regulation of cellular component organization
response to granulocyte macrophage colony-stimulating factor
Fc receptor signaling pathway
regulation of neutrophil apoptotic process
positive regulation of neutrophil apoptotic process
positive regulation of myeloid cell apoptotic process
in utero embryonic development
regulation of response to oxidative stress
regulation of oxidative stress-induced cell death
response to interleukin-6
regulation of interferon-beta production
regulation of synaptic plasticity
Fc-gamma receptor signaling pathway
tRNA-type intron splice site recognition and cleavage
B cell receptor signaling pathway
multinuclear osteoclast differentiation
0
30
60
90
120
GeneNum
qvalue
0.5
0.6
0.7
0.8

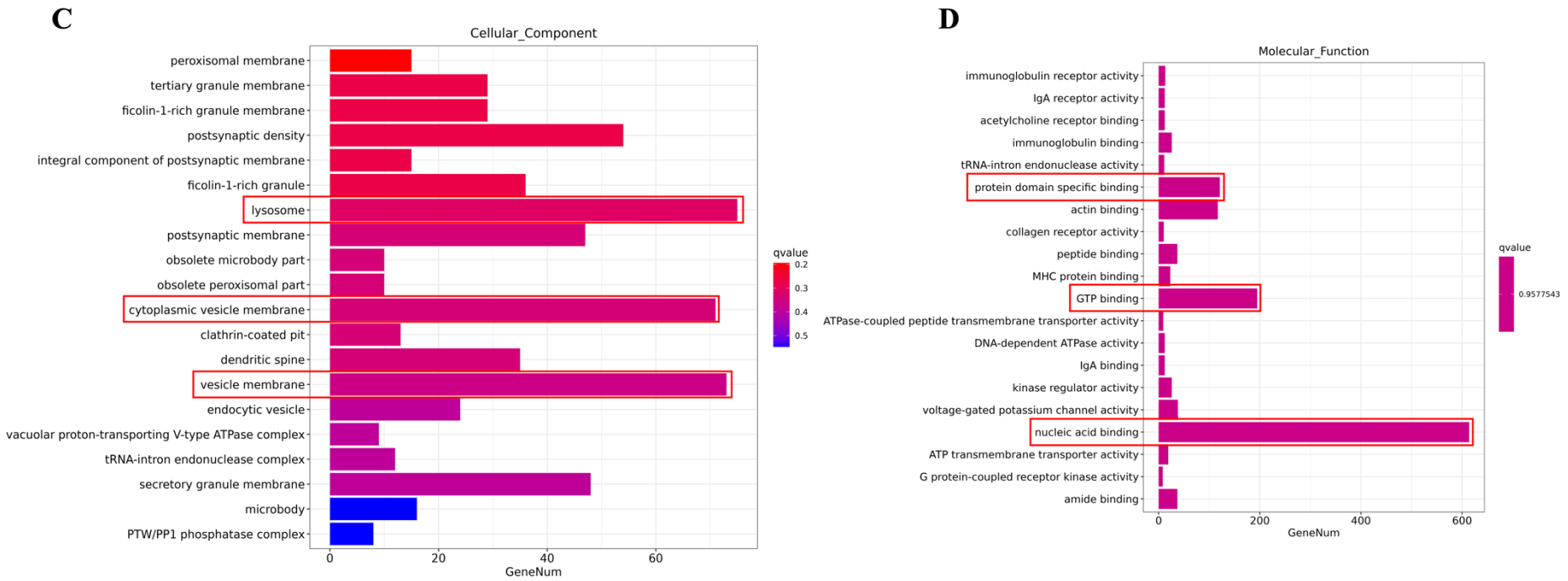

Figure 73: SHG-8 activity induced several biological processes relating to cell death and hints of miRNA dysregulation. (**A**) KEGG pathway enrichment depicting the possible enrichment of molecular pathways between SHG-8 treated and untreated conditions. (**B**) GO classification analysis reveals enriched biological processes between SHG-8 treated and untreated conditions. (**C**) GO classification analysis reveals enriched cellular components between SHG-8 treated and untreated conditions. (**D**) GO classification analysis revealing enriched molecular functions between SHG-8 treated and untreated conditions.

3.3.8 Experimental validation of sRNA-seq findings

Validation of the hsa-miR-6715b-3p expression profile was investigated via UALCAN transcriptomics and RT-qPCR analyses methods (Figure 74). Indeed, *in silico* analysis revealed significant downregulation in the expression of miR-6715b-3p in the tumour cohort with a mean expression of 0.655 TPM. In comparison, the significant expression of the miRNA was recorded at 6.949 TPM ($P< 0.05$) in normal tissues (Figure 374A). Moreover, experimental validation of the expression profile identified a significantly enhanced expression pattern following SHG-8 treatment at both 10µM and 40µM conditions in contrast to the DMSO control (Figure 74B). Thus, this confirms the results of the sRNA-seq analysis.

Furthermore, sRNA-seq analysis revealed pituitary tumour-transforming 1 protein interacting protein (*PTTG1IP*) as a possible target of miR-6715b-3p and seemed to be involved in regulating its gene expression. Due to the downregulated expression of miR-6715b-3p before treatment and enhanced expression post-SHG-8 activity, it could indicate *PTTG1IP* as a possible oncogene in CRC tumours. To investigate the possibilities of PTTG1IP expression and its relevance to CRC progression, *in silico* analyses characterised *PTTG1IP*'s gene expression, protein expression and the level of promoter methylation observed in CRC progression (Figure 75). Subsequently, data analysis demonstrated that the *PTTG1IP* gene is significantly downregulated in COAD tumours, exhibiting mean expression of 242.052 TPM and 169.849 TPM in normal tissue and COAD tumour cohorts, respectively ($P< 0.001$) (Figure 75A). Further analysis has also revealed no significant difference in the promoter methylation of both cohorts (Figure 75B). However, transcriptomics analysis at the protein level corresponded with significant translation of the PTTG1IP protein in the tumour cohort with an expression of 0.00 in comparison to a recorded expression value of -0.554 in normal tissues ($P< 0.05$) (Figure 375C). Additionally, *in vitro* validation via RT-qPCR methods indicated that *PTTG1IP* expression profiles were significantly reduced following SHG-8 exposure in both 10µM and 40µM conditions demonstrating a relative mean expression of 0.525 TPM and 0.449 TPM, respectively ($P< 0.001$, $P< 0.0001$) (Figure 75D). In addition to this, *PTTG1IP* expression identified a 1.12 lower fold change in the treatment conditions following SHG-8 treatment, inferring an SHG-8 mediated effect on *PTTG1IP* regulation in SW480 cells *in vitro*. As all of the experimental data have indicated *PTTG1IP* as a possible target of miR-6715b-3p, further *in silico* predictions have revealed possible binding sites on the target mRNA strand (Figure 75E). Sfold software predictions illustrated a possible binding site on the *PTTG1IP*

gene at position 1-23 on the 5' UTR seedless region, exhibiting a high binding affinity towards the target. Furthermore, high levels of *PTTG1IP* expression has demonstrated poor prognostic outcomes in RFS and PPS survival criteria ($P< 0.05$) (Figure 75F). In comparison, OS survival criteria suggested low *PTTG1IP* expression has a significantly greater impact on poor clinical survival outcomes ($P< 0.05$) (Figure 75F).

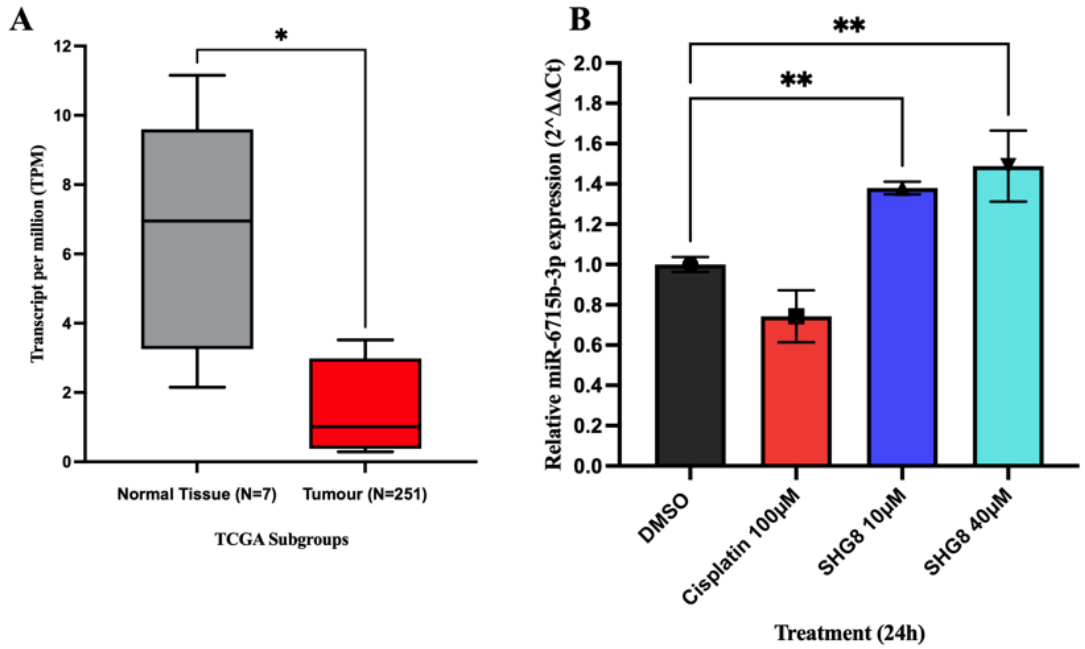

Figure 74: Validation of miR-6715b-3p reveals tumour suppressor activity following SHG-8 mediated cytotoxicity in SW480 cells. (**A**) UALCAN TCGA genomic data exhibiting miRNA expression of miR-6715b-3p in normal (grey) and COAD (red) cohorts. Welch's t-test PERL script. *P < 0.05. (**B**) RT-qPCR expression analysis of miR-6715b-3p in SW480 cells following 24h SHG-8 treatment exposure (N=3). One-way ANOVA statistical test followed by Dunnett's multiple comparison post-hoc test. **P<0.01.

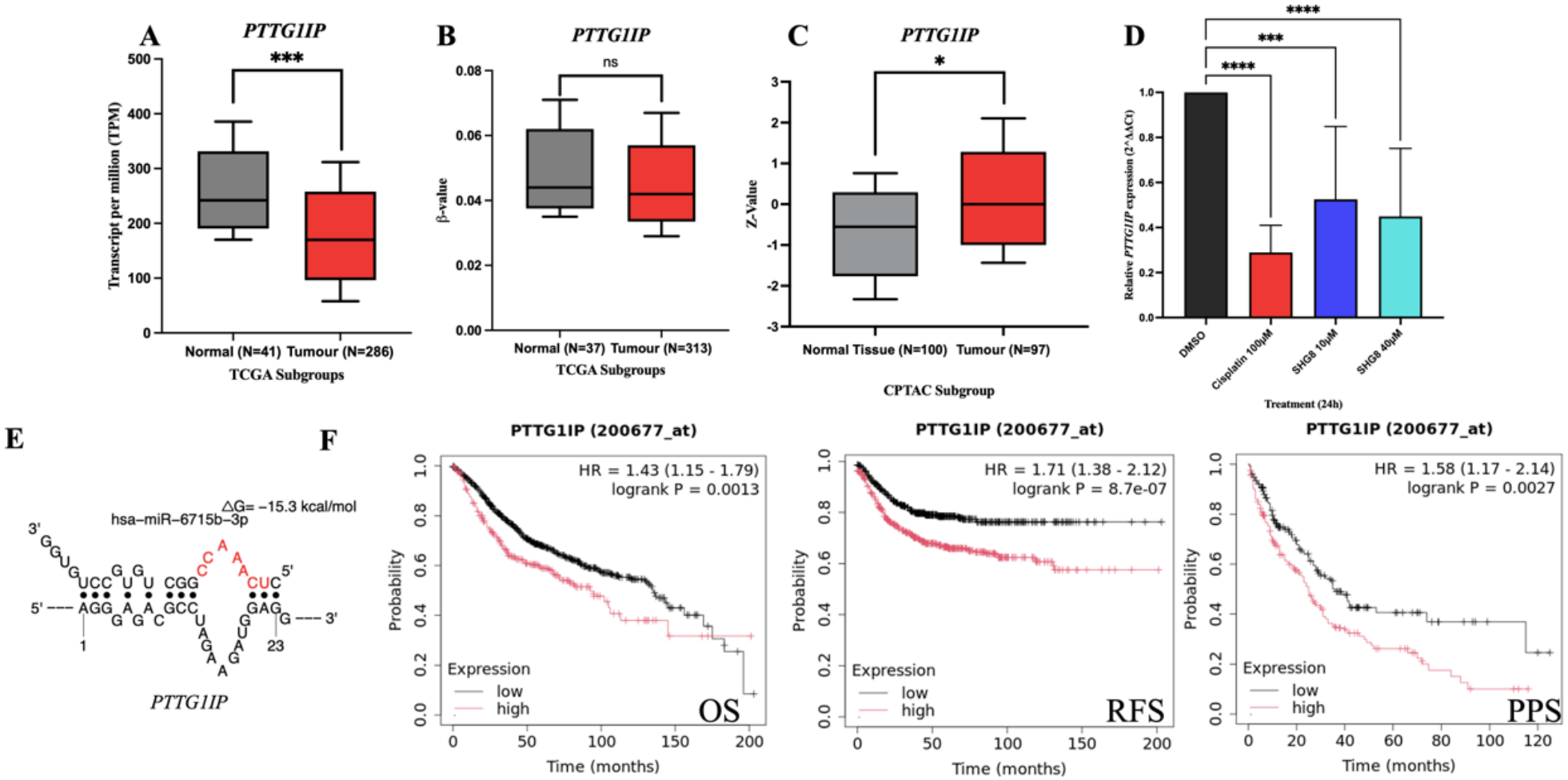

Figure 75: Following SHG-8 treatment, expression analysis revealed *PTTG1IP;* a possible oncogene in CRC progression, may be a target of miR-6715b-3p. (**A**) TCGA genomic data exhibiting mRNA expression of *PTTG1IP* in normal (grey) and COAD (red) cohorts, error bars ± SD. Welch's t-test PERL script. ***P< 0.001. (**B**) UALCAN transcriptomics analysis was conducted to determine the methylation of the promoter regions of *PTTG1IP* between normal tissue (grey) and COAD tumour (red) cohorts. Methylation data is presented as box plots, error bars ± SD.

Welch's t-test PERL script statistical analysis. (**C**) UALCAN proteomics analysis was conducted to determine the protein expression of PTTG1IP between normal tissue (grey) and COAD tumour (red) cohorts, error bars ± SD. Welch's t-test PERL script statistical analysis. *P< 0.05. (**D**) RT-qPCR expression analysis of *PTTG1IP* in SW480 cells following 24h SHG-8 treatment exposure (N=3). One-way ANOVA statistical test followed by Dunnett's multiple comparison post-hoc test. ***P< 0.001, ****P< 0.0001. (**E**) Predicted positional binding sites of miR-6715b-3p on the target PTTGIP mRNA strand were conducted via Sfold prediction software, revealing high binding affinities. (**F**) Comparisons between high *PTTG1IP* expression (red) and low *SIGLEC15* expression (black) were conducted to elucidate the relationship between *SIGLEC15* and the prognostic factor in COAD patients. Survival curves were constructed to outline *SIGLEC15* expression with survival criteria: overall survival (OS), post-progression survival (PPS), and relapse-free survival (RFS) criteria. P< 0.05 was considered statistically significant.

3.4 Discussion

The treatment of diagnosed CRC tumours with conventional front-line therapeutic approaches entails clinical regimens that focus on chemotherapies, radiotherapies and surgical resection of the tumour or a combination of these approaches that improve the likelihood of patient remission (Johdi & Sukor, 2020). Nevertheless, the prevalence of CRC malignancies has steadily shown an increase despite the advancements made in tumour diagnosis, prognosis and disease management (Piawah & Venook, 2019). In recent years, the development of targeted anti-tumour drug molecules including small molecule inhibitors and blocking antibodies, has shown positive patient response. This is partly due to their pharmacological characteristics, exhibiting high specificity for their therapeutic target, high clinical efficacy and low toxicity to surrounding tissues/organs (Zhai et al., 2019). In contrast to macromolecular therapeutic agents like targeted antibodies, small molecule inhibitors possess several key advantages, including lower cost, improved pharmacokinetics, simple storage, transportation and patient tolerance (Zhong et al., 2021). Thus, these factors underline the significant potential of small molecule therapeutic agents for anti-cancer development. In particular, they have emerged as potential therapies in several tumour malignancies, including CRC, which inhibited tumour progression (He et al., 2021). With reference to the prevalence of CRC worldwide, the development and characterisation of the β-amino carbonyl compound (SHG-8) was elucidated to target the Siglec-15/Sia axis.

This chapter emphasised the unique role of the SHG-8 compound as a treatment alternative to current therapeutic approaches, as being the first small molecule inhibitor for targeting the pro-tumorigenic Siglec-15 protein. Additionally, miRNAs involved in *SIGLEC15* regulation remained limited within the literature, and we aimed to elucidate the clinical relevance of these miRNAs to CRC progression as outlined in this project. Thus, we believe we have identified deregulated miRNAs in CRC progression following the disruption of the Siglec-15/Sia axis via SHG-8 binding to the V-set binding domain. Thus preventing engagement of the STn antigen.

3.4.1 Synthesis and characterisation of the SHG-8 compound

The SHG-8 structure is comprised of three aromatic rings that are connected by a β-amino ketone group. Additionally, the introduction of a halide constituent to the aromatic ring

enhances the structures' hydrophobicity and lipophilicity capabilities. The chemical synthesis of 3-(4-bromophenyl)-1-phenyl-3-(phenylamino)propan-1-one compounds and their derivatives are accomplished through a one-step Mannich reaction involving the key constituents: an aromatic amine, aromatic aldehyde and ketone in the presence of a catalyst (Iwanejko et al., 2018). There have been several iterations for the synthesis of these compounds, but there are a number of limiting factors that prevent their applicability, some of which can include long reaction time, excessive temperature, low recyclability and challenges in product purification (Cai & Xie, 2013). Furthermore, the incorporation of some catalysts used for chemical synthesis may pose environmental risks due to their corrosive and toxic properties. Hence, it would prove substantial for the development of a catalyst that is both recyclable and effective in the Mannich reaction, which resulted in the heterogenous SAFSNS nano-catalyst, as synthesised in a previous study (Ahmad et al., 2021).

3.4.2 Molecular docking simulations for SHG-8:Siglec-15 interactions

Previous reports have suggested that Siglec-15 activity upon engagement of the STn antigen requires canonical ligand binding (Crocker et al., 2007). For this to occur, interactions between arginine residues and sialoglycan carboxylate groups are required for salt bridge formation (Crocker et al., 2007). Molecular docking analysis elucidated the V-set binding pocket capable of ligand interaction, in particular, amino acid residues within 5.0 Å of ligand binding identified R143, a key residue in glycan ligand binding (Murugesan et al., 2021). Further supporting this, another study demonstrated sialidase treatment prevented Siglec-15-Fc binding. Additionally, the study has also reported the mutation of R143 to an alanine residue greatly impacted Siglec-15-Fc binding (Ding et al., 2023). Hence, SHG-8 binding to R143 with a high binding affinity may suggest specificity towards the Siglec-15 protein. Furthermore, binding to the V-set domain may underline competitive binding and possibilities for outcompeting the STn antigen. Moreover, the expression profile of key sialyltransferases, including ST6GalNAc1, is responsible for STn production and is commonly deregulated in CRC tumours (Kvorjak et al., 2020). Our findings from Chapter 2 suggested that the production of the STn antigen maybe context-dependent, inferring that low availability of the STn substrate ligand will be unable to outcompete the SHG-8 molecule. Similarly, glycan sulphation has been shown to play a role in mediating Siglec-15/STn antigen interactions (Boelaars & Van Kooyk, 2024). Affecting the production of the STn antigen in conjunction with SHG-8 treatment may significantly inhibit the Siglec-15/Sia axis. However, it is also understood that the STn antigen is not the only ligand

capable of Siglec-15 binding. Glycan microarrays elucidated Siglec-15 specific for α2,6-linked glycan structures produced from GlcNAc (Murugesan et al., 2020). Additionally, activation of the Siglec receptor may require binding partners to enable ligand engagement. In particular, a recent study characterised CD11b (macrophage marker) as a binding partner on activated T-cells (Lenza et al., 2023). Thus, the interactions between protein receptor-ligand binding remains highly complex. However, whilst the molecular docking simulations utilised the previous Siglec-15 AlphaFold protein model, it is important to underline the role of post-translational modifications that are implicated in the overall protein structure. Modifications including glycosylation, methylation and phosphorylation which is limited in the literature could influence the binding affinity of the SHG-8 compound due to unavailable binding sites and the orientation of the structure preventing access to the V-set binding domain. Future studies could incorporate either validated/predicted modified sites into structural modelling to further refine docking simulation providing a greater understanding of protein receptor-ligand binding interactions. Furthermore, it would also illustrate the binding of SHG-8 with Siglec-15 in its native and modified structural conformations, which could possibly identify mechanisms for inhibitor binding and any changes to efficacy.

3.4.3 Abnormal *SIGLEC15* expression is hypomethylated in CRC tumours

In silico tools correlated the upregulated expression of *SIGLEC15* in tumours as indicated within the literature. Dysregulated transcriptional regulation may provide a possible indication of abnormal *SIGLEC15* expression in COAD tumours. For instance, CpG island methylation on the promoter regions of gene sequences is a common occurrence of CRC CIMP molecular subtype tumours (Nishiyama & Nakanishi, 2021). However, in the case of *SIGLEC15*, which exhibited significant hypomethylation in COAD tumours, this has suggested that *SIGLEC15* expression is independent of promoter methylation. Moreover, a recent study reported high *SIGLEC15* expression was observed following a negative correlation of CpG methylation sites in thyroid carcinomas (Lan, et al., 2022). Furthermore, transcriptional regulation may also be affected through interactions with STn at the protein level, primarily through the release of TGF-β (Flavell et al., 2010). A previous study highlighted the interaction of Siglec-15 with the STn antigen-stimulated TGF-β following the activation of its downstream target Syk (Takamiya et al., 2013). Typically observed within the literature, the secretion of an immunosuppressive cytokine such as TGF-β is mediated by TAMs in advanced tumour grade stages, which also exhibited high levels of Siglec-15 expression (Takamiya et al., 2013).

Secretion of TGF-β interacts with receptor kinases, leading to a phosphorylation-mediated signalling cascade of SMAD proteins (SMAD2 and SMAD3). Upon activation, SMAD proteins associate with SMAD4, forming a trimeric complex that is translocated to the nucleus, facilitating transcriptional modulation (Tzavlaki & Moustakas, 2020). Conversely, a previous study has suggested elevations of Siglec-15 expression are dependent on the immune status of the tumour, with the heterogenous TME an important contributor to Siglec-15 expression (Mutka et al., 2023). However, the mechanism by which that occurred remains unclear. Additionally, transcriptional regulation may also imply the interplay of miRNAs on *SIGLEC15* expression. As such, due to the expected overexpression typically seen of *SIGLEC15* in solid tumours, the deregulation of tumour suppressor miRNAs involved in *SIGLEC15* gene regulation could be inferred. Furthermore, only complementarity binding between miRNAs and their target mRNA strands is able to fully degrade the target strand or induce translational repression (Shang et al., 2023). Thus, the deregulation of a number of transcriptional mechanisms is related to abnormal *SIGLEC15* expression.

3.4.4 SHG-8's cytotoxic profile *in vitro*

The findings that explored the cytotoxic profile of the SHG-8 compound identified a significant dose-dependent cytotoxicity in CRC cell lines. With a recorded IC_{50} value of 17.75μM and 20.78μM in SW480 and HCT116 cells, respectively, this demonstrated a higher efficacy in comparison to the conventional anticancer agent cisplatin. A previous report indicated cisplatin exhibited an IC_{50} of 23.61μM in CRC (Zhang et al., 2019). Hence, it has been suggested that SHG-8 is a more effective inhibitor in promoting anti-tumorigenic properties. Additionally, there has also been reports of combination therapies that are able to enhance the efficacy of cisplatin treatment, possibly due to acquired therapeutic resistance (Hoffmeister et al., 2012). Therefore, a possibility of a combination approach utilising both SHG-8 and cisplatin may prove effective in reducing tumour progression. Furthermore, the role of SHG-8 on epithelial cells indicated a substantially higher IC_{50} of 92.34μM and lower treatment efficacy in comparison to the SW480 and HCT116 cell lines. A key characteristic of targeted approaches is preventing the likelihood of off-target effects and adverse cytotoxicity against normal cellular tissues. Similar to the action of SHG-8, another small molecule inhibitor, actein, a triterpene glycoside, has demonstrated significant inhibition of SW480 and HT-29 CRC cells in contrast to reduced efficacy in HCoEPiC cells (Yan et al., 2021). Additionally, the concentration-dependent cytotoxicity observed in HCoEPiC cells has indicated increased

sensitisation to SHG-8 treatment. Ultimately, the cytotoxic profile of SHG-8 on tumour and normal epithelial cells has highlighted the potential for SHG-8 treatment alternatives in comparison to conventional anti-cancer treatments that are currently available.

Other functional assay data revealed significantly reduced cellular migration following 40μM SHG-8 exposure and 100μM cisplatin at 24h. However, SHG-8 treatment demonstrated no significant difference in the reduction of cellular migration at the 48h interval at both 10μM and 40μM concentrations. Various mechanisms and signalling pathways could be involved to rescue cellular migration and drive cellular movement and metastasis (Stuelten et al., 2018). In osteosarcomas, Siglec-15 stimulated the activation of autophagy through interactions with beclin-1, an autophagic protein which induced EMT and tumour migration (Zheng et al., 2022). Another possible protein target that has been suggested is the overexpression of dual specificity phosphatase 1 (DUSP1), which rescued the tumour phenotype following *SIGLEC15* knockdown stimulating tumour proliferation, migration and invasion (Fan et al., 2021). A pre-clinical study reported the immunoregulation of the PD-1/PD-L1 pathway can work independently to the functional role of Siglec-15 (Wang et al., 2019). Moreover, the interactions of the PD-1/PD-L1 axis in CRC modulated cellular migration through signalling transduction mechanisms that promoted the activation of the ERK/MAPK signalling pathway and EMT (Cao et al., 2022). Additionally, a recent study demonstrated that high levels of IFNγ were required for stimulating PD-L1 expression, which negatively affects Siglec-15 expression (Zhou et al., 2023). Thus, mutually exclusive expression of both pro-tumorigenic immune checkpoints on tumour cell populations could suggest dual targeting is necessitated for inhibiting cellular migration.

Moreover, all treatment conditions exhibited a profound effect on cellular colonisation as no colonies were present in comparison to the DMSO control condition. Similarly, other reports have highlighted several small molecule inhibitors and combination therapy approaches that significantly inhibited CRC proliferation *in vitro* (Chen et al., 2020). Siglec-15 has been a known contributor to cellular proliferation in several malignancies (Chen et al., 2024). Inversely, the targeting and KO of *SIGLEC15* had shown reduced cellular proliferation and stimulated apoptosis following reduced STAT3 signalling (He, et al., 2022). This was also similarly observed in another study that observed *SIGLEC15* KO in osteosarcomas (Song et al., 2022). Hence, there is a direct correlation between the blocking of Siglec-15 with SHG-8

treatment and its effect on the capability of tumour cells undergoing cellular proliferation and colonisation. These findings have, therefore, suggested that SHG-8 is a suitable therapeutic agent to target Siglec-15 and exert its cytotoxic effects on tumour cells. However, the impact of PD-L1 to rescue several pro-tumorigenic characteristics like cellular migration may highlight the need for combination therapies with PD-L1 antagonists.

3.4.5 SHG-8 mediated apoptosis in CRC cells

Elucidation of the SHG-8's possible mechanism of action was performed. Greater instances of apoptosis induction were elucidated at higher SHG-8 treatment conditions. This has also been previously reported with several anti-tumour compounds, including cisplatin, which has stimulated apoptosis in several tumour types (Singh & Lim, 2022). Additionally, comparative images (highlighted by white arrows) are indicative of apoptotic like features, including nuclear fragmentation, abnormal cellular morphology and reductions in cellular size (Majtnerová & Roušar, 2018). It has been extensively studied that p53 is a key regulator of the apoptotic process. When cells have undergone significant amounts of stress, p53's functional role inhibits cellular differentiation of DNA sequences that appear 'damaged' (Wang et al., 2023). However, the cell line utilised for the experimental work, SW480, possesses several missense mutations on the *TP53* gene. In particular, 237G>A mutation (R273H) changes the codon from CGT TO CAT, resulting in the substitution of arginine to histidine residues. In addition, the 309C > T (P309S) mutation changes the codon from CCG to TCG, resulting in the substitution of proline to serine residues (Schroy et al., 1995). Both of which have resulted in p53 loss of function. Therefore, this would typically lead to tumour development (Zhang et al., 2020).

However, in the case of SW480 cells treated with SHG-8, cellular death is suggested to have occurred via a p53-independent pathway. It has been suggested that the presence of DNA damage was associated with the inhibition of p53 translation via reduced ribosomal activity (Boon et al., 2024), only then could p53 independent apoptosis take place. A suggested pathway is the role of Fas-mediated apoptosis. Fas receptors act as death receptors, which recognise and internalise Fas ligands (FasL) into a dimeric complex (Nikoletopoulou et al., 2013). Following this, adapter molecules, including FAS-associated death domain protein (FADD), are coupled with the Fas/FasL complex, inducing the activation of caspase-8 and subsequent cascade into the cleavage and activation of caspase-3 and caspase-7 (Cao et al.,

2021). The Fas/FasL pathway is also further stimulated through the activation of TNF and IFNγ in a p53 independent manner (Porta et al., 2005). There are also other p53 independent apoptotic pathways that have been studied. Ferroptosis, as one example could induce apoptosis from the accumulation of iron and lipid peroxidation of cells (Li et al., 2020). This is unlikely the mechanism of SHG-8 action as there is no iron present within its biological structure. In addition, morphological characteristics commonly associated with conventional apoptotic pathways are not observed (Xie et al., 2016). Our findings have elucidated the inhibition of pro-inflammatory cytokines TNFα and IL-1β production from differentiated macrophages following SHG-8 treatment, which will be discussed further below. Therefore, this suggests that inflammation-mediated apoptosis is highly unlikely to occur as a mechanism of action. This also rules out the induction of tumour necrosis factor-related apoptosis-inducing ligand (TRAIL) mediated apoptosis as TNFα is required for activating the signalling cascade (Pimentel et al., 2023).

Quantitative analysis via Annexin-V/PI dual staining revealed a greater proportion of cells undergoing late apoptosis following SHG-8 exposure. Thus, this demonstrated SHG-8 mediated cell death is unlikely to be through necrosis and necrotic signalling. Moreover, the cell cycle arrest at the G2/M phase was also made evident via PI staining. A previous study reported CIN type CRC tumours displayed reduced cellular arrest at the G2/M checkpoint, emphasising greater mutation and cellular proliferation of damaged DNA sequences (Fernando et al., 2021). Primarily, the G2 checkpoint halts entry to mitosis upon the identification of damaged DNA sequences (Fernando et al., 2021). However, cellular arrest within the cell cycle could indicate double-stranded breaks within the DNA helical structure, thus stimulating, in this case, p53 independent apoptosis (Sunada et al., 2021). Furthermore, it was also reported that cisplatin-induced cellular arrest at the S phase of the cell cycle, which was also identified in our findings (Pian et al., 2022).

It was also hypothesised that the role of ROS production could be a stimulus for apoptosis induction. It has been reported that high levels of ROS in the TME can significantly damage DNA sequences and protein structures, thus inducing the activation of apoptosis (Redza-Dutordoir & Averill-Bates, 2016). However, this doesn't seem to be the case, as only H_2O_2 displayed significantly high levels of ROS production following SHG-8 exposure. Hence, this

suggested a similar signalling pathway modulating apoptosis induction. However, the mechanism of action remains unclear.

3.4.6 *SIGLEC15* expression in CRC cells following SHG-8 treatment

The therapeutic potential of *SIGLEC15* in tumour onset and progression has been emphasised in several tumour types and is not solely limited to CRC progression (Du et al., 2021; Hu et al., 2021; Li et al., 2020). Comprehensive analyses have reported that *SIGLEC15* mRNA expression is frequently associated with tumour tissues in comparison to normal tissues (Wang et al., 2023). Thus, RT-qPCR expression analysis highlighted that SHG-8 treatment conditions inhibited *SIGLEC15* expression in SW480 cells. Transcriptional regulation of *SIGLEC15* was previously mentioned above. Other epigenetic modifications have also been suggested to play a role in *SIGLEC15* expression. Chromatin remodelling factor AT-rich interaction domain 1A (Arid1a) stimulated the transcription factor Jun/Fos, enhancing chromatin access of the *SIGLEC15* promoter regions, resulting in overexpression (Sun, et al., 2024). Conversely, deacetylation of histone proteins has also been reported to repress gene transcription by preventing transcription factors from binding to the *SIGLEC15* mRNA strand (Erfani et al., 2022). Moreover, the role of non-coding RNAs such as miRNAs was also shown to directly target *SIGLEC15* to modulate its expression profile *in vitro* in several malignancies, including miR-4786, miR-582-5p and miR-7109 (Li et al., 2024; Li et al., 2020; Ren et al., 2022). Thus, it is suggested that SHG-8 induced significant epigenetic modifications that negatively impacted *SIGLEC15* expression in tumour cells, and further clarification could shed insights into possible transcriptional elements involved in its regulation. However, there was no significant difference in Siglec-15 expression at the protein level from flow cytometry analysis. Although affecting Siglec-15 protein expression is unlikely, the main goal was to competitively block the V-set binding domain and change its conformational structure upon SHG-8 binding (Li & Ji, 2019). Thus, SHG-8 could theoretically outcompete the binding of the STn antigen, although binding assays are required to confirm (Hunter & Cochran, 2016). Additionally, several limiting factors can also contribute to the ligand binding ability to protein targets, including availability of binding sites, concentration of competing ligands, protein and ligand concentration and external stimuli including temperature and pH (Hunter & Cochran, 2016). However, our findings have also shown reduced Siglec-15 expression following SHG-8 treatment via IF intensity analysis. It is possible that quantitative analysis obtained directly from IF images is unreliable as it largely depends on the chosen fields of view. The number of

cells emitting fluorescence and the resolution of quantified IF images are important to determining accurate MFI (Shihan et al., 2021). Additionally, acquisition parameters relating to exposure times, gains and binning are all factors that can affect MFI variation. Furthermore, image acquisition using advanced confocal imaging, high stability of the fluorophore probe and mounting media are required to prevent variations in brightness, all of which could affect reproducibility (Datta et al., 2020). In addition to this, differences in gating and threshold methods using analysis software such as ImageJ or FIJI to remove the background noise may prove difficult and could retain traces of background fluorescence, thereby affecting quantification (Gómez et al., 2019). Hence, a transition to more standardised protein expression methods is required. Several methods include flow cytometry as seen from our findings, ELISA and quantification of bands obtained via western blotting for quantifying protein expression (Barkovits et al., 2021). The differing findings from both methodologies can also be explained by the turnover rate for Siglec-15. Changes in protein homeostasis is heavily regulated to ensure proteins are not damaged or misfolded and their function remains intact following protein disruption (Ross et al., 2021). If Siglec-15 does possess a slower turnover rate, then any effect of SHG-8 on Siglec-15 protein expression will take more than 48h to illicit an effect. Based on these findings, inhibiting *SIGLEC15* expression with SHG-8 has suggested the interplay of miRNAs and other epigenetic modifications which impacted its transcription.

3.4.7 SHG-8 inhibited pro-inflammatory cytokine secretion

CRC development and progression have been associated with chronic inflammation, particularly with pathologies associated with an inflammatory state, such as UC-associated CRC, IBD and CD (Muthusami et al., 2021). Enhanced secretion of pro-inflammatory cytokines, including TNF-α and IL-1β, are commonly associated with the development of the TME via the stimulation of pro-tumorigenic immune cells, including TAMs (Wen et al., 2022). Therefore, this suggests that increased levels of both cytokines can lead to the development of chronic inflammation and facilitate tumour progression. Inflammation-related signalling is typically associated with the detection of foreign pathogens, which are presented with specific molecular signatures that are recognised by specific recognition receptors (Li & Wu, 2021). These recognition receptors later stimulate the activation of adaptor proteins, leading to a signalling cascade event that results in the cleavage and release of pro-inflammatory cytokines such as IL-1β (Sharma & Kanneganti, 2023). SHG-8 treatment suppressed the stimulation of pro-inflammatory cytokines in both differentiated macrophage cell lines THP1 and U937.

Moreover, a correlative link has been suggested between ROS production and the secretion of pro-inflammatory cytokines (Singh & Manna, 2022). Hence, it could indicate low levels of ROS production are unable to induce the release of TNF-α and IL-1β as seen from our findings. Therefore, it has been inferred that SHG-8 may play a role as a feasible treatment in inflammation-mediated CRC tumours.

3.4.8 DE of miRNAs revealed several enriched signalling pathways and biological processes

SHG-8 mediated DE of miRNAs has suggested its compatibility in the treatment of CRC tumours to reduce tumour proliferation. To determine if *SIGLEC15* expression is mediated by interacting miRNAs, sRNA seq analysis was performed and compared SHG-8 treated and untreated conditions, which has shown a direct correlative relationship. Although a large number of miRNAs were revealed to be significantly DE following treatment, no miRNAs that were significantly regulating *SIGLEC15* were revealed. Therefore, it could be inferred that reduced *SIGLEC15* expression is likely a result of other epigenetic modifications that have transcriptional control over the *SIGLEC15* gene. Albeit, the significant upregulation of miR-6715b-3p was identified via constructed volcano plot analysis. One thing that requires consideration is that a number of novel miRNAs have exhibited no identified profile in the miRDB database upon classification. Also, there is very little in the literature regarding miR-6715b-3p, which was the most deregulated miRNA in our sRNA-seq data. Nevertheless, a previous report has suggested its role in regulating the activation of autophagy through its direct target sestrin 1 (*SESN1*), in Huntington's disease (Anderson et al., 2022; Martínez-González et al., 2021). Additionally, in the tumour landscape, miR-6715b-3p has demonstrated reduced expression in prostate adenocarcinomas (Anderson et al., 2022; Martínez-González et al., 2021). Possibly suggesting its role as a tumour suppressor miRNA, as observed in our data. Validation findings from *in silico* and RT-qPCR methods further confirmed miR-6715b-3p expression as a tumour suppressor miRNA following SHG-8 treatment. Furthermore, a recent study reported a synergistic effect between miR-6715b-3p and miR-34a in inhibiting tumour progression (Orellana et al., 2019). Hence, this miRNA would indicate the regulation of possible oncogenes related to CRC progression.

COG functional classification revealed significant enrichment of translation, ribosomal structure and biogenesis alongside signal transduction mechanisms. MiRNAs can play an

important role in modulating protein translation by directly targeting mRNA target strands. Primarily, the inhibition of signal transduction molecules like the tyrosine kinase c-Met by miR-146a targeting can inhibit the stimulation of cellular proliferation pathways, including PI3K/AKT and Wnt/β-catenin pathways (Bleau et al., 2018; Y. Zhang et al., 2018). Moreover, another study which conducted sRNA-seq analysis revealed miR-6715b-3p induced the activation of the tyrosine kinase ErbB2, MAPK and PI3K/AKT signalling. In addition to this, the study also demonstrated significantly decreased p53 signalling (Ingelson-Filpula & Storey, 2023). Thus, this has suggested the role of miR-6715b-3p in stimulating p53-independent apoptosis and inhibition of signal transduction mechanisms relating to translation.

SRNA-seq KEGG pathway analysis revealed several biological processes and functions enriched following SHG-8 treatment. Of the number of pathways exhibited, the enrichment of cellular senescence, autophagy, lysosomal enrichment and hippo signalling were all of interest. These pathways are highly regulated, and multiple miRNAs would be involved in regulating the genes involved in cellular death pathways, such as senescence and autophagy. Autophagy is a recycling mechanism that designates cellular proteins and organelles for lysosomal degradation for recycling these components (Debnath et al., 2023). During the autophagic process, several autophagy-related genes are stimulated and subsequently encode and transcribe the production of double membrane-bound vesicles (autophagosomes). The initiation occurs via a mTOR mediated signalling cascade triggered by kinases such as UNC-51-like kinase 1 (ULK1). The function of this is to engulf cellular organelles and proteins, which are internalised following interactions with neighbouring lysosomes. The contents are then ultimately degraded by lysosomal hydrolysis (Nishimura & Tooze, 2020). In addition to this, it has also been referred to as another programmed cell death mechanism. Based on the literature search, miR-6715b-3p may function as an autophagic modulator in CRC progression. Furthermore, it has been suggested that the baseline levels of p53 can repress the activation of autophagy. However, at times of cellular stress, upregulated p53 can promote its activation, and inversely, independent mechanisms can trigger autophagy to degrade mutant p53 (Kenzelmann Broz et al., 2013; Tasdemir et al., 2008). Hence, it could be hypothesised that the role of p53-independent apoptosis is associated with the induction of autophagy and miR-6715b-3p may serve as a potential regulator of the process. If autophagy is a likely process that is stimulated following SHG-8 treatment, it could also emphasise the enrichment of lysosomes, lysosomal cellular components and the positive regulation of cellular components that are

found in both KEGG and GO analysis. The other interesting pathway observed was the hippo signalling pathways following SHG-8 treatment. Hippo signalling is involved in regulating the size of organs and is an important tissue homeostatic pathway that is frequently deregulated in malignancies (Yu et al., 2015). The hippo signalling pathway relies on the phosphorylation of hippo kinases (MST1, MST2) and large tumour suppressor kinases (LATS1, LATS2) which trigger the inactivation of transcription activator proteins yes-associated protein (YAP) and transcriptional co-activator with PDZ-binding motif (TAZ) (Harvey et al., 2013). Under a hypomethylated structural conformation, these transcription activator proteins are translocated to the nucleus and bind with neighbouring transcription factors to modulate gene expression (Harvey et al., 2013). However, dysregulation of the hippo signalling pathway or the loss of protein function from those mentioned above can lead to tumour onset and progression (Wan et al., 2020). Furthermore, the crosstalk of autophagy and hippo signalling has been previously reported, particularly initiated by metabolic stress (Gwinn et al., 2008). Therefore, the role of autophagy in SHG-8 treated tumours may infer metabolic stress as a possible mechanism of action via hippo signalling.

GO analysis of biological processes revealed the regulation of immune cell apoptosis, regulation of oxidative stress and IFNβ and response to IL-6. IL-6 is a known pro-inflammatory cytokine that is associated with CRC progression via the STAT3 signalling pathway (Sharma et al., 2022). Additionally, several cell types within the colon have exhibited inflammatory receptors for cytokines, including TNFα, IL-1β and IL-6, in inflammation mediated pathologies including IBD, UC and CD (Muthusami et al., 2021). As seen in our ELISA findings, pro-inflammatory cytokines, including TNFα and IL-1β secretion, were inhibited following SHG-8 exposure, possibly suggesting the inhibition of IL-6 responses in a similar fashion. In addition, IFNβ production is typically produced in the TME and is found to have an anti-tumour functional role upon inhibiting tumoral recruitment of angiogenic neutrophils (Kumaran Satyanarayanan et al., 2019). Moreover, it was reported to also regulate pro-tumorigenic differentiation of myeloid cells (Dunn et al., 2006). However, it was revealed that the interplay of IFNβ in JAK/STAT signalling could induce apoptosis and cell cycle arrest (Xiang et al., 2022). This could suggest the stimulated production of IFNβ in CRC progression as a possible route to induce apoptosis via SHG-8 treatment. The sRNA-seq findings revealed the positive regulation of myeloid cell apoptosis, particularly in regard to neutrophils. It has been reported that the stimulation of IFNβ production inhibits the tumoral recruitment of

neutrophils upon blocking pro-tumorigenic mechanisms related to angiogenesis and immunosuppression (Wu et al., 2020).

GO enrichment analysis revealed significant enrichment of nucleic acid binding as the main molecular function following SHG-8 treatment. As seen with the constructed heat map, the DE of miRNAs is highly involved in regulating several biological processes relating to the inhibition of CRC progression. Direct binding of the miRNA to the 3' UTR region involves displaying a complementarity sequence to a length of approximately 6-8 nucleotides referred to as the seed region (Shukla et al., 2011). Following the engagement with the target mRNA strand, full complementarity binding between nucleotide bases will lead to directed degradation of the target, whilst only partial complementarity between the miRNA and target mRNA demonstrates translational repression (Shang et al., 2023). It is also important to note that mRNA regulation via direct targeting with miRNAs revealed functional binding sites on the 5' UTR and coding regions, however transcriptional efficiency may be affected as a consequence (Shukla et al., 2011).

3.4.9 Validation studies of *PTTG1IP* as a target of miR-6715b-3p

The identification of DE miRNAs following SHG-8 exposure revealed *PTTG1IP*, a possible CRC oncogene, as a predicted target of miR-6715b-3p. Additionally, *in silico* proteomics analysis indicated higher levels of PTTG1IP expression in tumours. Furthermore, RT-qPCR methods demonstrated significantly downregulated expression following treatment, suggesting an oncogenic role. Hence, *in silico* and experimental validation confirmed sRNA-seq findings. However, it was found interesting that *PTTG1IP* exhibited a reduced expression profile between normal and tumour cohorts at the gene level. This has suggested its overexpression may be a result of other post-translational modifications since promoter methylation exhibited no significant difference between normal and tumour cohorts. A previous report highlighted phosphorylation at Y174 (Tyrosine; Y) can inhibit its expression profile (Smith et al., 2013). A more recent study also demonstrated that the transmembrane domain of PTTG1IP is palmitoylated (addition of saturated fatty acid to cysteine residues via thioester side chain), which prevents domain cleavage by γ-secretase, enabling enhanced functional activity (Aßfalg et al., 2024). In CRC progression, increased hypermethylation at the protein level may potentiate PTTG1IP functional activity. However, following SHG-8 exposure, increased transcriptional regulation by miR-6715b-3p and other epigenetic modifications may inhibit its

expression profile. Previous reports have demonstrated the overexpression of *PTTG1IP* in several malignancies including CRC (Hsueh et al., 2013; Read et al., 2016; Watkins et al., 2010). However, there are also contradictions of low *PTTG1IP* expression associated with reduced clinical survival (Tan et al., 2019). As seen from our patient survival data, low *PTTG1IP* expression correlated to lower OS outcomes in contrast to RFS and PPS survival criteria. Particularly in the CRC landscape, the expression of *PTTG1IP* abundance was found to be commonly associated with genetic instability, somatic *TP53* mutation, and extramural vascular invasion (Read et al., 2016). Furthermore, it was also reported that PTTG1IP function involves binding to both p53 wild type and mutants, and its overexpression can modulate the activity of effector genes, including MDM2 proto-oncogene (*MDM2*), cyclin dependent kinase inhibitor 1A (*p21*) and stratifin (*SFN*) (Read et al., 2016). The overexpression of PTTG1IP in solid tumours may be presented as a unique driver of tumour progression, and its expression seems to be context dependent (Imruetaicharoenchoke et al., 2017). Particularly in the case of SHG-8 treated SW480 cells, PTTG1IP overexpression following treatment may impact the functional ability of mutant p53 and promote the activation of p53 independent apoptosis pathways. As mentioned previously, miRNAs have been reported to exert transcriptional regulation of target genes upon binding at uncommon complementary binding sites, namely the coding and 5' UTR regions. MiR-6715b-3p binding at the 5' UTR may impact transcriptional efficiency and underline its inability to effectively regulate the *PTTG1IP* gene. However, full complementarity between the miRNA and nucleotide bases is suggestive of complete degradation of the target, which may be stimulated following SHG-8 activity (Shang et al., 2023; Shukla et al., 2011). Thus, our findings suggest that although PTTG1IP is an oncogene and is commonly overexpressed in CRC. Further mechanistic studies would underline its role in CRC tumour progression and metastasis. Moreover, the role of *PTTG1IP* in CRC progression is limited, further experimental validation could provide insights into the crosstalk between the miR-6715b-3p/*PTTG1IP* and Siglec-15/Sia axes as targets for SHG-8 treatment approaches in CRC.

3.4.10 Future directions

Subsequent follow-up studies are required to further elucidate SHG-8's mechanism of action and thus offer a complete outlook on SHG-8 as a treatment alternative for CRC. Additional parameters within the study design could implement power calculations to ensure there is statistical significance between variables, particularly changes in miRNA and gene target

expression profiles. A key objective is particularly in relation to the induction of extrinsic apoptosis pathways. Determining the expression profiles of autophagic markers, Fas/FasL, caspases and cleaved caspase counterparts may underline the role of Fas-mediated apoptosis or autophagy as possible mechanisms for cellular death (Sena et al., 2022). Moreover, reduced *SIGLEC15* expression following SHG-8 treatment would likely require *in vitro SIGLEC15* KO and knockdown studies to further elucidate the interplay of miRNAs and any off-target effects of SHG-8 treatment. In addition to this, due to the pro-tumorigenic nature of PD-L1, a combination approach with PD-L1 antagonists may share possible synergism in Siglec-15^+ PD-$L1^+$ tumours and prevent both immune checkpoints from rescuing the tumour phenotype. Ligand binding assays would characterise the interaction of SHG-8 to Siglec-15 and help determine the binding affinity to the R143 residue when competing against the STn antigen ligand. Additionally, treatment with sialidases in a co-culture environment would explore the competitive binding of SHG-8 against STn. Lastly, patient derived xenografted (PDX) murine models may outline the clinical efficacy of SHG-8 *in vivo*, thus determining its therapeutic window and identifying adverse effects before the transition to clinical settings (Pothuraju et al., 2024). Similarly, *in vivo* models can help ascertain drug pharmacokinetics that are currently unknown with SHG-8. In particular, determining SHG-8's half-life is key for establishing dosing regimens. Additionally, expanding on differing drug delivery routes may enhance the efficacy of SHG-8, either through intravenous or intraperitoneal can achieve varying effective drug potencies that can induce tumour cell death. Undertaking these methods could enhance SHG-8's potential as a prospective treatment alternative in Siglec-15^+ tumours.

3.5 Conclusion

To conclude, molecular docking analysis revealed SHG-8 binding with R143, a critical amino acid residue required for canonical glycan binding with the STn antigen. Subsequently, functional data analyses revealed SHG-8 exerted dose-dependent cytotoxicity *in vitro* against CRC cell lines. In addition, further mechanistic studies revealed late apoptosis induction following SHG-8 exposure and cell cycle arrest at the G2/M phase. Conversely, the enrichment of autophagy and the role of Fas-mediated apoptosis are possible p53 independent mechanisms of action due to p53 mutant cell lines utilised for this experimental work. SHG-8 was shown to inhibit the pro-inflammatory cytokine secretion of TNFα and IL-1β suggesting SHG-8 is a potential inhibitor of inflammation-mediated CRC tumours. Moreover, sRNA-seq analysis identified 185 DE miRNAs following SHG-8 treatment, highlighting miR-6715b-3p as the most significantly upregulated miRNA and its target *PTTG1IP* as a possible oncogene in CRC progression. MiR-6715b-3p is a novel miRNA that has not been previously associated with CRC progression and has shown downregulated expression in other pathologies. Hence, due to its downregulated expression profile, it has warranted further investigation for oncogenes as direct targets of miR-6715b-3p activity. Validation of PTTGIP demonstrated a higher prevalence in tumour adjacent normal tissues. Hence, the context-dependent expression of *PTTG1IP* in malignant tumours may underline its potential as a prognostic marker. Although the crosstalk between the miR-6715b-3p/*PTTG1IP* and Siglec-15/Sia axes requires further elucidation, we believe we have elucidated possible ways to disrupt the Siglec-15/Sia axis and the impact of SHG-8 on miRNA regulation as per the project objectives. This Chapter has elucidated novel β-amino carbonyl compounds such as Siglec-15 small molecule inhibitors as a therapeutic alternative in CRC progression.

Chapter 4 - Repurposing a currently available small molecule inhibitor for the specific targeting of Siglec-15 in colorectal cancer

4.1 Introduction

4.1.1 Background overview

As mentioned in chapter 1, CRC tumours display a high level of tumour heterogeneity due to frequently occurring sporadic mutations in DNA sequences, which results in increased treatment resistance (Molinari et al., 2018). This has highlighted significant limitations of current therapeutic approaches which are associated with poor patient response and reduced clinical survival (Molinari et al., 2018). It is now crucial to improve upon these approaches for better clinical response and inhibit tumour recurrence.

Recent immunotherapeutic approaches predominantly rely on immune checkpoint blockade strategies against targets such as PD-1 and PD-L1 for immune normalisation and stimulating the activation of immune responses for effective inhibition of tumours (Gou et al., 2020). However, only a small subset of treated patients exhibit positive treatment response and full remission, emphasising reduced sensitisation to therapies and poor overall survival (Sun et al., 2020). Hence, this underlines the involvement of other immune checkpoint proteins, such as Siglecs.

4.1.2 The role of Siglec-15 and the STn antigen as therapeutic targets

Abnormal Siglec-15 expression has been associated with tumour progression in several malignancies due to its involvement in the development of the TME and immunosuppression (Lu et al., 2023). As mentioned in chapters 2 and 3, Siglec-15 and PD-L1 are both expressed by different clones of tumour cells that are mutually distinct from one another (Fudaba et al., 2021). This has suggested a significant role in modulating immune evasion in PD-L1^{-} patients and rescuing the tumour phenotype. As seen in other malignancies, a higher proportion of cancer patients were reported to have high expression of PD-L1 in tumour tissues. 30.3% of PDAC and 70.3% of nasopharyngeal tumours all exhibited PD-L1^{+} status, in comparison to 18.6% of PDAC and 37.9% in nasopharyngeal tumours exhibiting Siglec-15^{+} status, respectively (Chen et al., 2022; Zhao et al., 2022). However, only a small proportion of tumour cells exhibited dual positive expression in both malignancies. Furthermore, a greater proportion of stromal immune cells were reported to have higher Siglec-15 expression. The report indicated 83% of myeloid cells in lung malignancies, 70.1% in breast tumours, 95.2% in head and neck squamous cell carcinoma tumours and 89% in bladder malignancies all exhibited

upregulated Siglec-15 expression (Shafi et al., 2022). For Siglec-15 to induce an immunosuppressive tumour microenvironment, activation of the receptor only occurs through canonical glycan ligand binding with the STn antigen, the putative ligand of Siglec-15 (Crocker et al., 2007; Fan et al., 2021; Wang et al., 2019). On a molecular level, the binding of receptor-ligand interactions is determined via R143 (R, Arginine) interactions with the carboxyl group of glycan structures forming salt bridges (Crocker et al., 2007; Fan et al., 2021; Wang et al., 2019). These interactions prevent T-cell activation and the inability to trigger an immune response (Lenza et al., 2023). Inversely, the inhibition of Siglec-15 demonstrated the opposite effect. Siglec-15 downregulation stimulated the levels of TNFα pro-inflammatory cytokines, inducing a pro-inflammatory TME (Wang et al., 2019). Simultaneously, dual targeting with PD-L1 antagonists enhanced patient responses to therapy, in comparison to monotherapies that targeted either immune checkpoint protein (Wang et al., 2022). Highlighted by a melanoma murine model, the knockdown of *SIGLEC15* stimulated T-cell response, enhancing tumour inhibition and overall survival (He et al., 2021). Thus, this underlines the importance of Siglec-15 targeting as a therapeutic approach in PD-L1 therapy-resistant patients.

4.1.3 Rationale, Aim and Research questions

Within the literature, the development and characterisation of small molecule inhibitors targeting Siglec-15 remains largely unknown. However, the characteristics of these inhibitors may underline enhanced tumour infiltration in comparison to currently available blocking antibodies used in immune checkpoint blockade approaches. The previous chapter emphasised the characterisation of synthesised small molecule inhibitors targeting Siglec-15 as a therapeutic strategy in CRC tumours (Ahmad et al., 2023). Nevertheless, currently, existing small molecule inhibitors may be repurposed and exhibit better binding affinity to Siglec-15, suggesting a therapeutic approach for Siglec-15^{+} tumours. The high throughput screening of 1500 currently available small molecule inhibitors via MTiOpenScreen (https://bioserv.rpbs.univ-paris-diderot.fr/services/MTiOpenScreen/; accessed 24th March 2024) integrated drug library software (drug-lib) was utilised for preliminary analysis. Custom parameters were applied for establishing the grid coordinates for the V-set binding domain before a hierarchy was generated. The custom grid coordinates were stated as the following: X=-23, Y=6, Z=13.272. In addition, the size of the V-set binding domain grid was set to identify residues at: X=30, Y=24, Z=24. The initial screening revealed aleplasinin with the highest binding affinity to the Siglec-15 protein structure. There is limited information in the

literature regarding the usage of aleplasinin in treatment. Albeit, clinically, aleplasinin was previously utilised as an inhibitor of plasminogen activator inhibitor-1 (PAI-1/SERPINE1) for the treatment of Alzheimer's disease (Kellici et al., 2021; Stevenson et al., 2022). Furthermore, the inhibition of SERPINE1 via aleplasinin exposure was suggested as a possible treatment approach for COVID-19 (Kellici et al., 2021). In the tumour landscape, a recent study reported that aleplasinin exposure inhibited $HER2^{+}$ normal and resistant breast cancer progression *in vitro* (Boz Er & Er, 2024). In this chapter, we aimed to highlight the binding site of aleplasinin to the Siglec-15 protein structure via the V-set binding domain and elucidate the cytotoxic profile of aleplasinin on SW480 and HCT116 cells for Siglec-15 targeting. In addition, the elucidation of mRNA targets was determined through Illumina RNA sequencing methods following the impact of aleplasinin exposure on gene expression.

This chapter highlighted several key research questions, which are listed below:

1. Using molecular docking simulations, can aleplasinin be able to bind to the Siglec-15 protein structure at the V-set binding domain?
2. Experimental utilising *in vitro* cell lines, can aleplasinin exert anti-tumorigenic properties in SW480 and HCT116 *in vitro* cell models with cytotoxicity assays?
3. Utilising apoptotic staining assays, what are possible mechanisms of action that induce apoptosis *in vitro*?
4. Can sequencing methods underline whether aleplasinin exposure can induce the differential expression of target genes and what are their relevance to CRC progression?
5. Can a combination of multiomics and gene expression analyses determine the impact of miRNAs in CRC cell models following aleplasinin exposure and what is the impact of these identified miRNAs on identified gene targets?

4.2 Methodology

4.2.1 Molecular docking

Aleplasinin was revealed as the highest binding affinity ligand towards the V-set binding domain of the Siglec-15 protein structure using the MTiOpenScreen prediction software. Incorporating the Siglec-15 AlphaFold structure (Q6ZMC9) into the integrated drug library of over 1500 compounds, a custom parameter predictive modelling was performed with the following grid coordinates: X = -23, Y = 6, Z = 13.272, for all drug compounds. Following this, the search grid to identify interacting ligands were performed with the following parameters: X = 30, Y = 24, Z = 24. The AlphaFold Siglec-15 structure (Q6ZMC9) was utilised for docking analysis with the CB-DOCK2 (https://cadd.labshare.cn/cb-dock2/index.php; accessed 23rd April 2024) software for predicting binding interactions. Amino acid residues that interacted with the aleplasinin ligand were determined. The aleplasinin ligand chemical structure ($C_{28}H_{27}NO_3$) was uploaded to the CB-DOCK2 software as an SDF file, and blind docking was performed with the parameters set by default. Interactions were verified using Biolip (Version 2021.09.15) (Yang et al., 2012).

4.2.2 *SIGLEC15* GSEA enrichment analysis

Enrichment analysis of gene sets related to specific cancer hallmarks was conducted for *SIGLEC15* using the TCGA dataset (TCGA, PanCancer Atlas) from the cBioPortal open access omics repository (http://cbioportal.org/ accessed on 19 September 2023). The selected dataset for CRC comprised a total of 524 patient samples for omics analysis. The *SIGLEC15* query gene was modified to include only DE genes in relation to the normal tissue cohort with a z-score threshold of ± 2.0. Only the 3416 significant DE genes relating to the *SIGLEC15* dataset were chosen for enrichment analysis. The resulting datasets were then sorted to include only the Log2 expression level in a ranked hierarchy. Following this, the *SIGLEC15* dataset was uploaded into the GSEA v4.3.2 software as a rnk file (.csv to .rnk file type change) (https://www.gsea-msigdb.org/ accessed on 12 January 2024). Specific parameters of each dataset were set at 1000 permutations, no collapse (all DE genes were utilised). Upregulated and downregulated pathways and biological processes were identified relating to tumour progression (FDR< 0.25 and P< 0.05 were considered as statistically significant).

4.2.3 Cell culture and treatments

Human CRC cell lines SW480 and HCT116 were obtained from ATCC (ATCC, Virginia, USA). Both adherent SW480 and HCT116 cell lines were cultivated using high glucose (4.5g/L D-glucose, 0.11g/L sodium pyruvate) DMEM (Gibco, Bleiswijk, Netherlands) media. Followed by supplementation with 10% FBS (Gibco, Bleiswijk, Netherlands), 1% penicillin/streptomycin (10,000U/mL) (Gibco, Bleiswijk, Netherlands) and 1% L-glutamine (200mM) (Gibco, Bleiswijk, Netherlands). All experimental cell lines were placed for incubation at 37°C, 5% CO_2 and experimental work was performed for each cell line upon reaching an 80% confluency. To determine the cytotoxic profile of aleplasinin on tumour cells *in vitro*, the aleplasinin compound was solubilised in dH_2O at a concentration of 10mM.

4.2.4 MTT cell viability assay

CRC cell lines HCT116 and SW480 were seeded onto 96 well plates at cellular densities of $2.5x10^4$ cells/well and were placed to adhere in the incubator at conditions 37°C, 5% CO_2. Following cellular adherence, all wells were treated with an aleplasinin concentration range of 20µM - 100µM to determine the IC_{50} value and were left to incubate at 48h at 37°C, 5% CO_2. Following the treatment period, all wells were treated with 20µL MTT (0.5mg/mL) and placed into the incubator for 2h at 37°C for formazan crystals to develop. Subsequently, the MTT was removed by inverting the excess solution and the remaining formazan crystals were solubilised with isopropanol in the dark for 30 min on a shaker at RT. Absorbance values were recorded at 540nm via a CLARIOstar plus multi-mode microplate reader (BMG LABTECH, Aylesbury, UK). The average percentage of cellular viability was calculated based on the following equation, as shown in Chapter 3.

4.2.5 Wound healing migration assay

SW480 and HCT116 cells were seeded at a density of $4x10^5$ cells/well onto 12 well plates and were placed to incubate at 37°C, 5% CO_2. Upon reaching cellular adherence and total well coverage, a 2µL tip was used to create scratches in vertical and horizontal directions, with an overlap of both in the epicentre. The detached cells were washed off with several PBS washes prior to well treatment with the following conditions: DMSO, Cisplatin 100µM, aleplasinin 30µM and aleplasinin 60µM. Images that pertained to the wound were taken at separate time intervals at: 0h, 24h, and 48h using an Olympus CKX41 inverted microscope (Olympus Life

Science Solutions, Stansted, UK) at 4x magnification. All images that were taken of the wound area were analysed through ImageJ analysis software (ImageJ bundled with Java8, https://imagej.net/ij/download.html, accessed 20th February 2023). In addition, installed macro plugins for wound healing analysis studies and parameters are outlined in Chapter 3.

4.2.6 Colonisation assay

SW480 and HCT116 cells were seeded at a total of $1x10^3$ cells/well onto 12 well plates and were left to adhere at 37°C, 5% CO_2. Following adherence of the tumour cells, all wells were treated with DMSO, cisplatin 100µM, aleplasinin 30µM and aleplasinin 60µM for a 48h treatment period. Subsequently, the treatment was replaced with supplemented high glucose DMEM media and was placed in an incubator at 37°C, 5% CO_2, for a total of 5 days. The colonisation was determined by the total number of observable colonies in the DMSO control condition control (colonies were determined as a cluster of cells totalling larger than 30-50 cells) (Niyazi et al., 2007). Following the 5-day incubation protocol, all wells were fixed with 4% PFA for 40 min at RT and then removed by three consecutive PBS wash steps at 5 min. The wells were then stained with 0.1% crystal violet (Pro-Lab Diagnostics, Wirral, UK) for 45 min on a rocker at RT. The wells were then washed with a further three consecutive PBS wash steps at 5 min to remove excess crystal violet, and images of the colonies were taken at both 4x and 10x magnifications using an Olympus CKX41 inverted microscope (Olympus Life Science Solutions, Stansted, UK).

4.2.7 Nuclear fragmentation staining via DAPI

For determining cell death, SW480 and HCT116 cells were seeded onto circular coverslips within 12 well plates at a density of ($4x10^5$ cells/well) and placed for adhering at 37°C, 5% CO_2. The wells were treated with the following conditions: DMSO, cisplatin 100µM, aleplasinin 30µM and aleplasinin 60µM for a treatment period of 48h. Following the treatment period, all wells were washed with PBS and fixed with 4% PFA for a period of 40 minutes at RT. The fixation was removed by consecutive PBS wash steps for 3 min at RT on a rocker. The coverslips were placed onto microscope slides containing DAPI Antifade Mounting Medium (2Bscientific, Hatfield, UK). Fluorescent images of the microscope slides were then taken using an EVOS XL Core Imaging system (Fisher Scientific, Hemel Hempstead, UK) at 40x magnification with the DAPI (blue) filter.

4.2.8 Acridine orange/ Ethidium bromide staining

SW480 and HCT116 cells were seeded at a density of $2x10^6$ cells/well and placed into an incubator overnight for adherence at 37°C, 5% CO_2 conditions. Subsequently, the wells were treated with the following conditions: DMSO, cisplatin 100µM, aleplasinin 30µM and aleplasinin 60µM for a 48h treatment period. All cell treatments were harvested following trypsinisation and centrifuged at 1000rpm (170xg) for 5 min prior to resuspension with ice-cold PBS and a further centrifugation step at 1000rpm (170xg) for 5 min. The cell pellets were resuspended with PBS, and a cellular density of $1x10^5$ was taken for analysis in 25µL volumes. Staining of the resuspended cells was performed with 1µL acridine orange (AO) (100ug/mL) and 1µL ethidium bromide (EB) (100ug/mL), respectively, and incubated at RT and in the dark for 3 min. Following the incubation period, 20µL of the treated, stained cells were placed onto microscope slides, and visualisation was determined at 10x magnification using the EVOS XL Core Imaging system (Fisher Scientific, Hemel Hempstead, UK) with the GFP and RFP filters.

4.2.9 Immunofluorescence staining

HCT116 and SW480 cells were seeded at a density of $3x10^5$ cells/well onto coverslips and incubated at 37°C, 5% CO_2 conditions. Subsequently, all wells were treated with the following conditions: DMSO, cisplatin 100µM, aleplasinin 30µM and aleplasinin 60µM for a 48h treatment period. IF staining was determined following the protocol as mentioned in chapter 3, and visualisation was performed via EVOS XL Core Imaging system (Fisher Scientific, Hemel Hempstead, UK) at 10x magnification.

4.2.10 Illumina RNA sequencing

RNA-seq analysis was conducted on SW480 treated cells with aleplasinin 60µM and compared against DMSO untreated cells following a 48h treatment period. Extraction, sample purification and sequence library preparation were performed following the protocols as mentioned in Chapter 3. Please find attached the available data posted in the Mendeley repository: doi:10.17632/frb7ss9n92.1. The DE expression of genes was determined following aleplasinin treatment alongside KEGG and GO enrichment analysis to elucidate enriched signalling mechanisms and possible gene targets.

4.2.11 UALCAN transcriptomics

The UALCAN transcriptomics database outlined corresponding to TCGA genomic expression data for the query genes: *ASCL6* (ENSG00000164398) and *SPRR2D* (ENSG00000163216) following comparisons between normal tissue and CRC COAD cohorts. Similarly, identified miRNA candidates predicted for *ASCL6* regulation were also determined between normal tissue and COAD tumours. Welch's t-test PERL script statistical analysis was encoded onto the UALCAN software to identify differences in clinicopathological features between cohorts (Chandrashekar et al., 2022). The resulting data with $P < 0.05$ was considered as statistically significant.

4.2.12 RT-qPCR

Total RNA extraction and gene expression methods were conducted, as mentioned in Chapter 3, for the following treatment conditions: DMSO, cisplatin 100µM, aleplasinin 30µM and aleplasinin 60µM. SYBR green primer sequences are as follows: *SIGLEC15* forward (CGCGGATCGTCAACATCTC) and reverse (GTTCGGCGGTCACTAGGTG), *ACSL6* forward (GCACGGCGATCTGTGATTG) and reverse (GGCGGAACACCTGGTACAT) and *SPRR2D* forward (GCCTCTCCTGCAAGTGTGA) and reverse (TCCTCATTTATGACATTTTCAGTCTC). Gene expression analysis of HCT116 and SW480 cells following aleplasinin treatment was normalised to the DMSO control and all samples were amplified at 100ng/µL for reverse transcription prior to cDNA amplification. In addition, fold change expression was determined via the $2^{-\Delta\Delta Ct}$ method.

4.2.13 KM survival plots

KM-plots (https://kmplot.com/analysis/, accessed on 26 July 2023) were constructed to outline the prognostic value of high (red) and low (black) expression of the *ACSL6* query gene in COAD patient survival outcomes over an extended period of time. Parameters relating to OS, RFS, PPS, HR, 95% CI, and Log-rank P-value were also determined (Győrffy, 2021).

4.2.14 *In silico* predictive miRNA data mining

A series of miRNA-target predictive software databases were utilised to determine candidate miRNAs involved in the gene regulation of ACSL6 and SPRR2D. Common miRNAs across each of the chosen databases: TargetScan (https://www.targetscan.org/vert_80/; accessed 28

July 2023), miRSystem (http://mirsystem.cgm.ntu.edu.tw/index.php; accessed 28 July 2023), miRWalk (http://mirwalk.umm.uni-heidelberg.de/; accessed 28 July 2023 and miRDB (https://mirdb.org/; accessed 28 July 2023) were determined and presented in Venn diagrams (https://bioinfogp.cnb.csic.es/tools/venny/). In addition to this, frequent miRNA 'hits' associated with gene expression were further explored and possible gene binding sites were determined using Sfold software (https://sfold.wadsworth.org/cgi-bin/starmir.pl; accessed 13 September 2023).

4.2.15 GeneMANIA

The GeneMania predictive database (https://genemania.org/; accessed 26th July 2024) exhibits functional information relating to the queried gene *ACSL6*. Parameters and protocols were followed, as mentioned in Chapter 2.

4.2.16 Search Tool for the Retrieval of Interacting Genes/Proteins analysis

Search Tool for the Retrieval of Interacting Genes/Proteins (STRING) analysis identified PPI with defined parameters upon queried proteins. The STRING 11.0 (https://version-11-0b.string-db.org/cgi/input?sessionId=brxKfZgAG9Au&input_page_show_search=on; accessed 17th July 2024) software highlighted PPI relationships between ACSL6. Construction of the framework was conducted with protocols as mentioned in Chapter 2.

4.2.17 Statistical analysis

Statistical analysis of aleplasinin cytotoxicity on cellular viability, colonisation, migration, and gene expression analyses were all determined by a one-way ANOVA statistical test followed by Dunnett's multiple comparison post-hoc test. Quantitative apoptotic staining by AO/EB was determined by the two-way ANOVA statistical test followed by Dunnett's multiple comparisons post-hoc tests. Unpaired student's t-test was conducted on UALCAN transcriptomics analysis comparing gene and miRNA expression between normal and malignant tumour cohorts. Data presented with $P < 0.05$ was considered statistically significant. Graphs were produced with GraphPad Prism 10 software.

4.3 Results

4.3.1 Aleplasinin docking analysis

High-throughput screening using MTiOpenscreen (https://bioserv.rpbs.univ-paris-diderot.fr/services/MTiOpenScreen/) of currently available inhibitors identified aleplasinin as an inhibitor of Siglec-15 via R143 receptor-ligand binding with a binding affinity of -7.8 kcal/mol (Figure 76A). Molecular docking analysis also revealed amino acid residues within contact of the aleplasinin compound at a distance of 3Å. They amino acids were identified as ASN30, ALA41, GLN42, ARG43, TRP44, SER45, MET46, GLN47, VAL48, PRO49, PRO50, GLU51, VAL52, PRO63, CYS64, THR65, PRO86, TYR87, ASP124, SER126, ARG143, HIS151, ASP152, ARG153, TYR154, GLU155, SER156, ARG157 and HIS158 (Table 18). It is well understood that Sigle-15 canonical binding occurs through the V-set binding domain, but it was unclear if the binding of aleplasinin was solely focused on the localised binding pocket. Therefore, blind docking of the aleplasinin ligand to the Siglec-15 protein was performed. Molecular docking analysis revealed a total of five possible binding sites, which included the V-set binding domain at various locations of the Siglec-15 structure (Figure 76B). Of those other four possible allosteric binding sites, only one exhibited a higher binding affinity to the Siglec-15 V-set domain with a binding affinity of -9.1 kcal/mol (Figure 76C). These interactions revealed a larger cavity volume and identified key amino acid residues within direct contact were: SER19, PHE20, VAL21, ARG22, THR23, LYS24, ILE25, ASP26, THR27, THR28, GLU29, VAL48, PRO49, PRO50, GLU51, VAL52, SER53, ALA54, GLU55, ASP58, ALA59, VAL61, PRO63, CYS64, LEU117, GLY118, ASP124, SER126, HIS163, THR165 and LEU243 (Figure 76C, Table 18). The other three allosteric sites exhibited a range of binding affinities from -6.7 kcal/mol to -6.9 kcal/mol with different amino acid residues responsible for binding (Figure 76D-1F, Table 18).

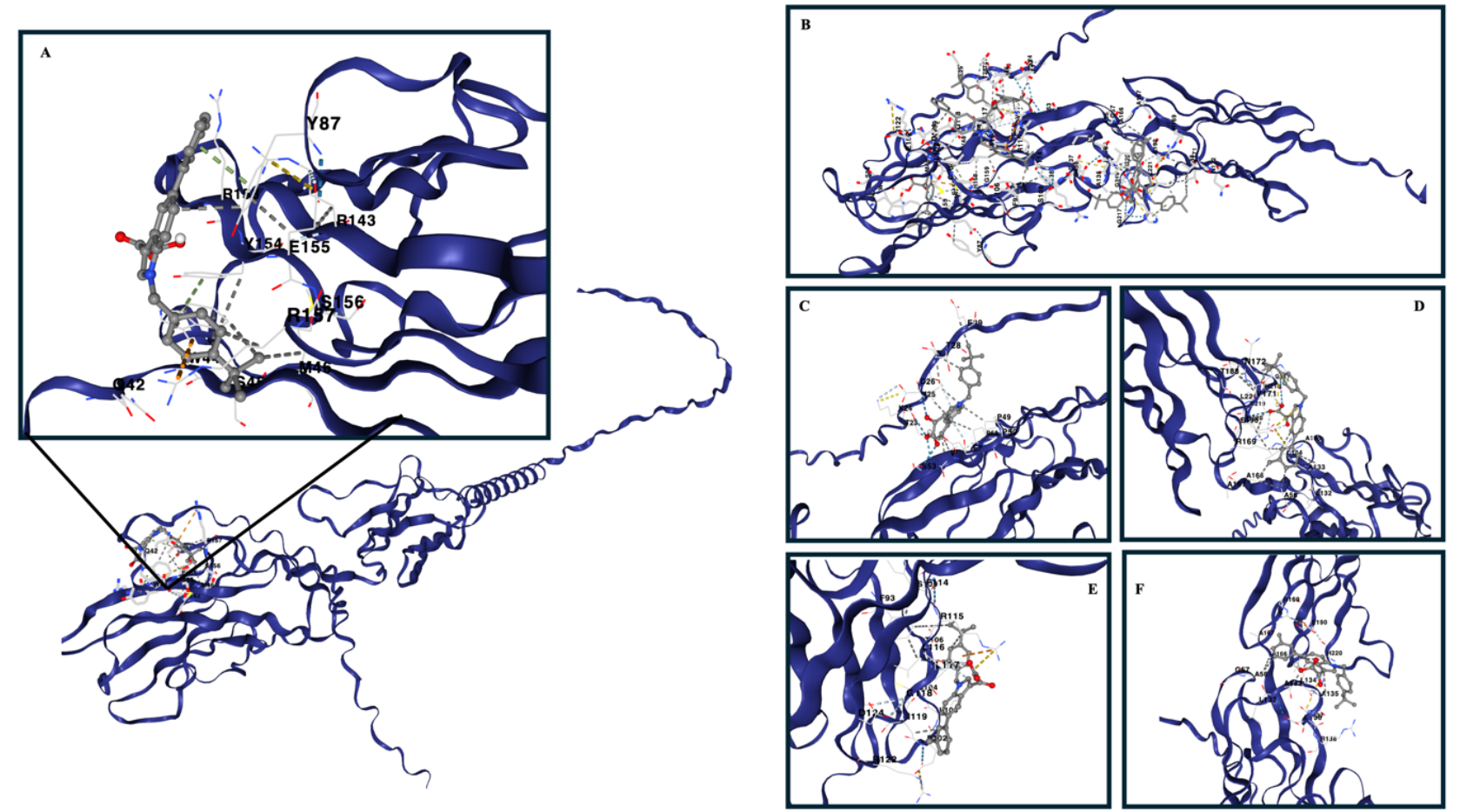

Figure 76: Aleplasinin was capable of binding to Siglec-15 at the V-set binding domain through R143 interactions. (A) Protein docking analysis of the AlphaFold Siglec-15 protein structure identified amino acid residues predicted to be within 3.0 Å of the aleplasinin compound ligand and possible interactions with the V-set binding domain via CB-DOCK2 software. (**B**) Protein docking analysis of the AlphaFold Siglec-15 protein with all possible binding sites via CB-DOCK2 software. (**C-F**) Protein docking analysis of the AlphaFold Siglec-15 protein structure identified amino acid residues predicted to be within 3.0 Å of the aleplasinin compound ligand and possible interactions with allosteric binding sites via CB-DOCK2 software.

Table 18: Molecular docking analysis between the aleplasinin contact ligand and the Siglec-15 protein structure revealed several binding sites. Information regarding amino acid residues in contact with the aleplasinin compound ligand is listed below, with respective binding affinities and the size of the binding pocket via CB-DOCK2 software.

	VINA SCORE (BINDING AFFINITY) KCAL/MOL	CAVITY VOLUME ($Å^3$)	CENTRE (X, Y, Z)	DOCKING SIZE	CONTACT RESIDUES
BINDING SITE 1	-9.1	571	-8, -11, 4	24, 24, 24	SER19, PHE20, VAL21, ARG22, THR23, LYS24, ILE25, ASP26, THR27, THR28, GLU29, VAL48, PRO49, PRO50, GLU51, VAL52, SER53, ALA54, GLU55, ASP58, ALA59, VAL61, PRO63, CYS64, LEU117, GLY118, ASP124, SER126, HIS163, THR165, LEU243
BINDING SITE 2	-7.8	331	-12, 1, 20	24, 24, 24	ASN30, ALA41, GLN42, ARG43, TRP44, SER45, MET46, GLN47, VAL48, PRO49, PRO50, GLU51, VAL52, PRO63, CYS64, THR65, PRO86, TYR87, ASP124, SER126, ARG143, HIS151, ASP152, ARG153, TYR154, GLU155, SER156, ARG157, HIS158
BINDING SITE 3	-6.9	145	3, 2, -1	24, 24, 24	ALA56, GLY57, ALA83, GLY84, GLU85, PRO90, VAL92, LEU110, HIS111, ARG113, PHE114, ARG131, LEU132, ALA133, LEU134, ALA135, ASP136, ASP137, ARG138, TYR140, ARG161,

					ALA166, ALA167, PRO168, ARG169, VAL171, ASN172, THR188, GLU190, GLY217, HIS218, GLY219, HIS220, LEU221
BINDING SITE 4	-6.8	104	-24, 0, 0	24, 24, 24	PHE93, CYS95, GLU102, LEU103, CYS104, GLN105, THR106, ALA107, LEU108, SER109, GLY112, ARG113, PHE114, ARG115, LEU116, LEU117, GLY118, ASN119, PRO120, ARG122, ASP124, GLU130
BINDING SITE 5	-6.7	155	-8, 8, 3	24, 24, 24	ALA56, GLY57, ALA83, GLU85, ALA88, GLY89, PRO90, GLN91, VAL92, LEU108, LEU110, HIS111, ARG113, PHE114, GLU130, ARG131, LEU132, ALA133, LEU134, ALA135, ASP136, ASP137, ARG138, TYR140, ALA166, ALA167, ARG169, GLU190, HIS218, HIS220, LEU221

4.3.2 *SIGLEC15* GSEA enrichment analysis revealed positive enrichment of EMT

SIGLEC15 GSEA analysis revealed a total of 39 possible gene sets related to the CRC phenotype (Figure 77-78). Of those identified, *SIGLEC15* demonstrated an increase in the number of enriched gene sets. A total of 11 upregulated gene sets were shown to be enriched, which included cancer hallmarks such as EMT, myogenesis, adipogenesis, p53 and dysregulated *KRAS* signalling (FDR< 0.25 and P< 0.05) (Figure 77, Table 19). In contrast, only 8 gene sets were shown as downregulated, highlighting biological processes and targets including MYC, E2F, IFNγ response, G2/M checkpoint, protein secretion and mitotic spindles (FDR< 0.25 and P< 0.05) (Table 19, Figure 78).

Table 19: GSEA analysis underlined enriched signalling pathways corresponding to *SIGLEC15* expression and its clinical relevance to CRC progression. GSEA enrichment scores for the association of *SIGLEC15* with associated cancer hallmarks. NES scores are provided as Log2FC changes (N=524) (FDR< 0.25 and P< 0.05).

	ENRICHED PATHWAY	EFFECT ON GENE REGULATION	NORMALISED ENRICHMENT SCORE (NES)	FDR Q-VALUE
SIGLEC15	Epithelial-Mesenchymal transition	Upregulated	3.08	0.000
	Myogenesis	Upregulated	2.87	0.000
	Apical junction	Upregulated	2.53	0.000
	Coagulation	Upregulated	2.25	0.000
	KRAS signalling – Up	Upregulated	2.15	0.000365
	Late Oestrogen response	Upregulated	2.14	0.000637
	Early Oestrogen response	Upregulated	2.07	0.000137
	KRAS signalling – Downregulation	Upregulated	1.93	0.00670

p53 pathway	Upregulated	1.80	0.0176
Hypoxia	Upregulated	1.73	0.0292
Adipogenesis	Upregulated	1.60	0.0686
EF2 Targets	Downregulated	-3.76	0.000
G2/M checkpoint	Downregulated	-3.35	0.000
MYC targets V1	Downregulated	-2.71	0.000
Mitotic spindles	Downregulated	-2.38	0.000622
MYC targets V2	Downregulated	-2.14	0.00118
IFNγ response	Downregulated	-1.71	0.0366
Protein Secretion	Downregulated	-1.66	0.0394
Spermatogenesis	Downregulated	-1.47	0.106

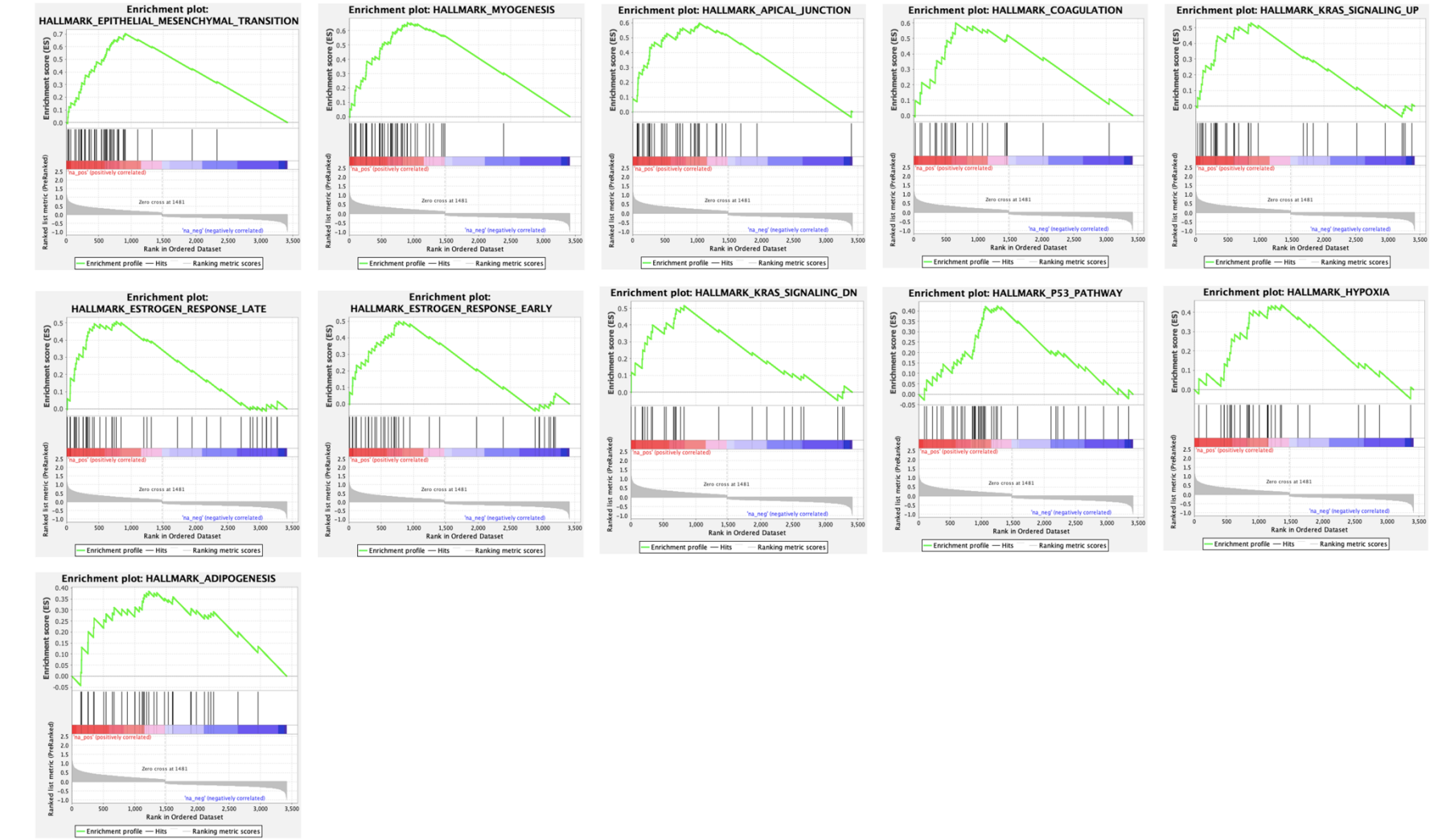

Figure 77: *SIGLEC15* GSEA analysis revealed EMT, myogenesis, adipogenesis and p53 pathways were all significantly upregulated. GSEA analysis was conducted utilising the TCGA, PanCancer Atlas dataset for omics analysis. Significantly, DE genes in COAD and commonly associated cancer hallmarks were determined in relation to *SIGLEC15* expression. FDR< 0.25 and P< 0.05.

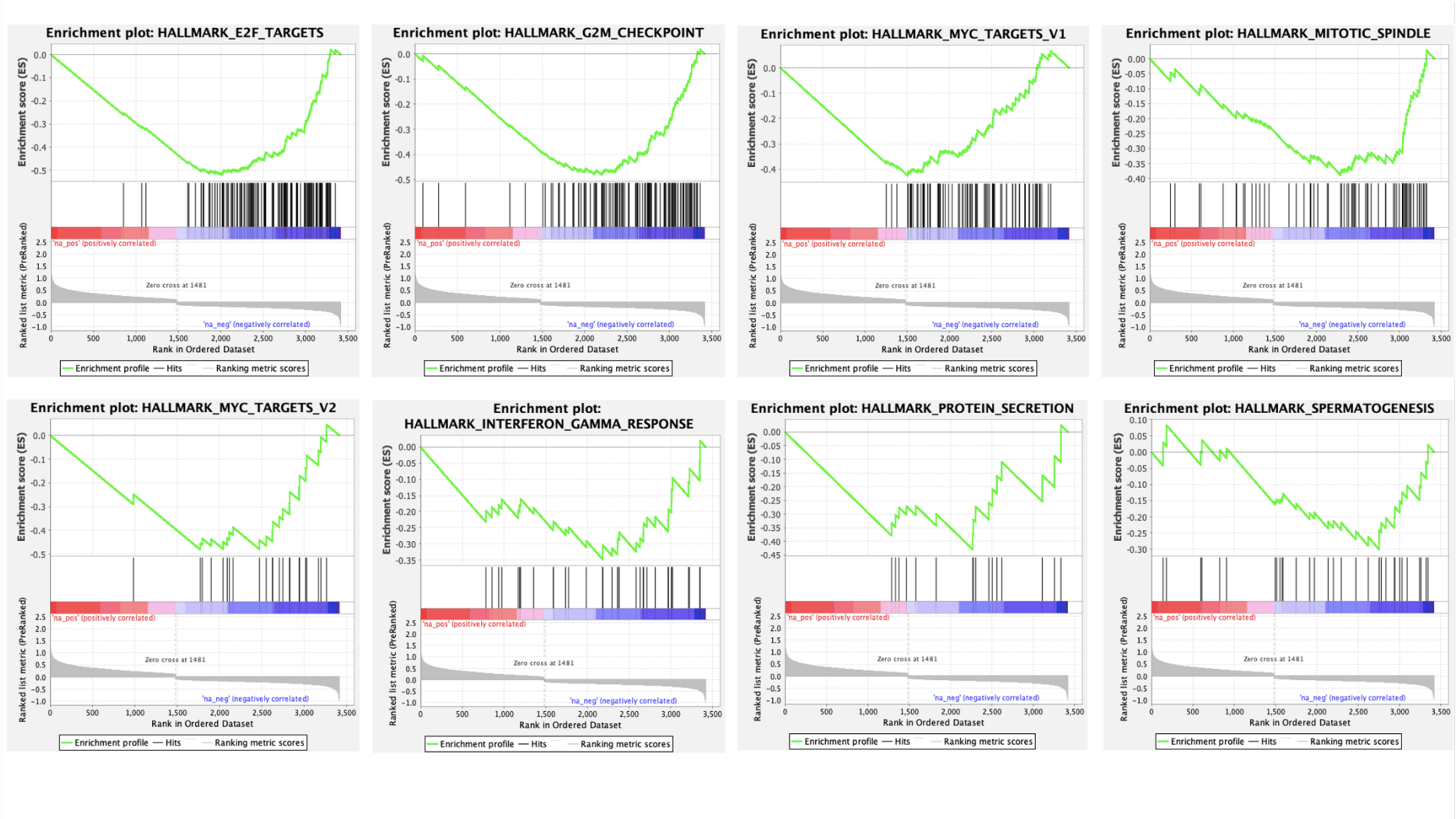

Figure 78: *SIGLEC15* GSEA analysis revealed MYC, E2F, IFNγ response, G2/M checkpoint and protein secretion all significantly downregulated. GSEA analysis was conducted utilising the TCGA, PanCancer Atlas dataset for omics analysis. Significantly, DE genes in COAD and commonly associated cancer hallmarks were determined in relation to *SIGLEC15* expression. FDR< 0.25 and P< 0.05.

4.3.3 Characterisation of aleplasinin cytotoxicity *in vitro*

The cytotoxicity of the aleplasinin compound was elucidated on SW480 and HCT116 cells *in vitro* (Figure 79). Conventional anti-cancer therapies such as cisplatin were used as a positive control for the experimental work to draw significant comparisons with the functionality of aleplasinin. Aleplasinin exhibited significant dose-dependent cytotoxicity on both respective cell lines, achieving 91.4% and 92.6% cell death in SW480 and HCT116 cells at the highest concentration of 100µM. In addition, aleplasinin demonstrated greater efficacy than cisplatin, which only induced cellular death of 44.9% and 74.3% in SW480 and HCT116 cells at 100µM, respectively ($P< 0.0001$) (Figure 79A, 79C). Dose response curves revealed significant cytotoxic profiles in both HCT116 and SW480 cell lines with IC_{50} values of 38.31µM and 57.38µM, respectively (Figure 79B, 79D).

Wound healing analysis of SW480 and HCT116 cells following 48h aleplasinin exposure was conducted (Figure 80). Quantitative analysis of the wound area identified significant reduction of cellular migration only at the 60µM aleplasinin condition with 41.07% and 42.32% in SW480 and HCT116 cells at 48h, respectively ($P< 0.05$, $P< 0.01$) (Figure 80A, 80B). Both 60µM and cisplatin conditions were shown to gradually decrease the rate of cellular inhibition in both cell lines ($P< 0.05$, $P< 0.01$) (Figure 80C). In addition, only cisplatin treatment was shown to inhibit cellular migration only in HCT116 cells following 48h treatment at 38.2% ($P< 0.05$) (Figure 80B). In contrast, the 30µM aleplasinin treatment demonstrated no significant difference in the inhibition of cellular migration across all recorded time intervals when compared against the control condition. Following this, comparative images pertaining to the wound area also indicated similar inhibition at the 60µM condition affecting tumour cell migration (Figure 80D, 80E).

In the colonisation assay, both HCT116 and SW480 CRC cells exhibited a significant reduction in cell colonisation at the 60µM condition ($P< 0.0001$), similar to the cisplatin positive control (Figure 81A, 81B), which is also highlighted by the low number of colonies present in the stained plate images (Figure 81C, 81D). Additionally, there was significantly less colonies formed in the HCT116 cells. In contrast, aleplasinin at the 30µM condition has no effect on cellular colonisation following 24h treatment exposure. Images relating to the colonies present are also forming a greater number of colonies in comparison to same assay for SHG-8 treatment. There may be differences that could arise from variations in experimental

conditions which contributed to colony growth including cell seeding, DMSO concentration and assay time and also passage number of the cell line that were used.

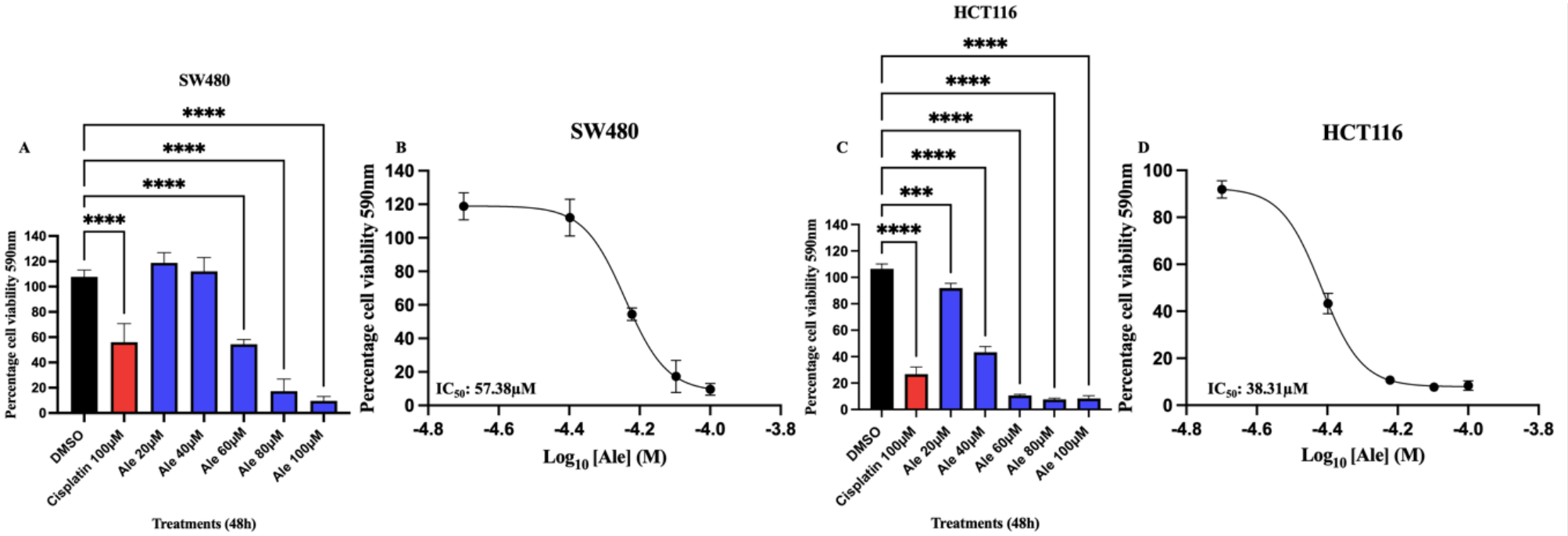

Figure 79: SHG-8 exhibited a dose-dependent cytotoxicity against tumour cells *in vitro*. (**A**) Dose-dependent cytotoxicity was determined via MTT cytotoxicity assay for the aleplasinin compound at varying concentrations following 48h treatment in SW480 cells. (N=5) Data is presented as mean ± SD. One-way ANOVA statistical test followed by Dunnett's multiple comparison post-hoc test. **** P< 0.0001. (**B**) Dose-response curve of SW480 cells following 48h aleplasinin treatment for determining the IC_{50} profile. (**C**) Dose-dependent cytotoxicity was determined via MTT cytotoxicity assay for the aleplasinin compound at varying concentrations following 48h treatment in HCT116 cells. (N=5) Data is presented as mean ± SD. One-way ANOVA statistical test followed by Dunnett's multiple comparison post-hoc test. ****P< 0.0001. (**D**) Dose-response curve of SW480 cells following 48h aleplasinin treatment for determining the IC_{50} profile.

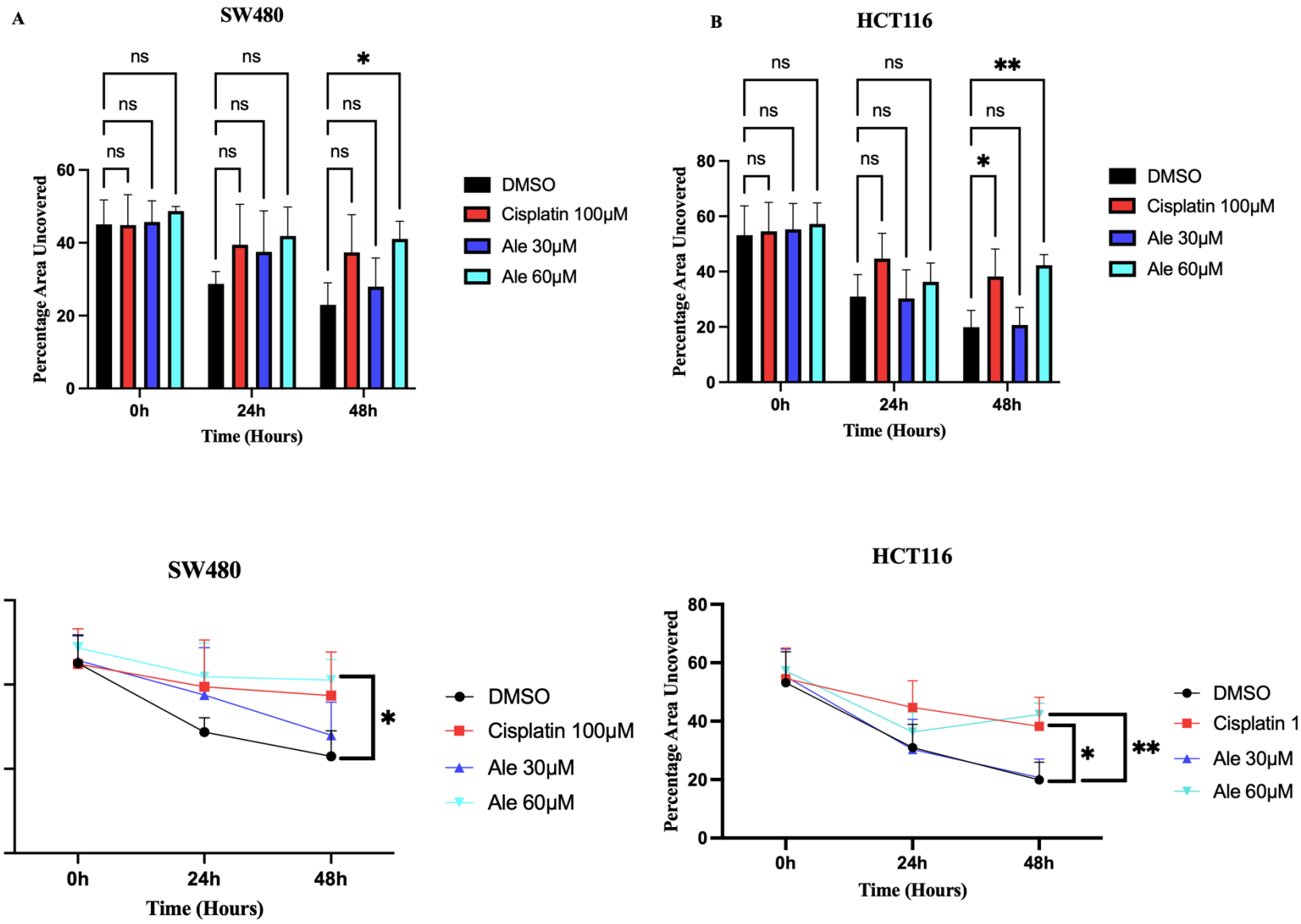
A
SW480
ns
ns
ns
ns
ns
ns
*
Percentage Area Uncovered
0
20
40
60
0h
24h
48h
Time (Hours)
DMSO
Cisplatin 100μM
Ale 30μM
Ale 60μM
B
HCT116
ns
ns
ns
ns
ns
ns
**
*
Percentage Area Uncovered
0
20
40
60
80
0h
24h
48h
Time (Hours)
DMSO
Cisplatin 100μM
Ale 30μM
Ale 60μM
C
SW480
Percentage Area Uncovered
0
20
40
60
*
0h
24h
48h
Time (Hours)
DMSO
Cisplatin 100μM
Ale 30μM
Ale 60μM
HCT116
Percentage Area Uncovered
0
20
40
60
80
*
**
0h
24h
48h
Time (Hours)
DMSO
Cisplatin 100μM
Ale 30μM
Ale 60μM

SW480

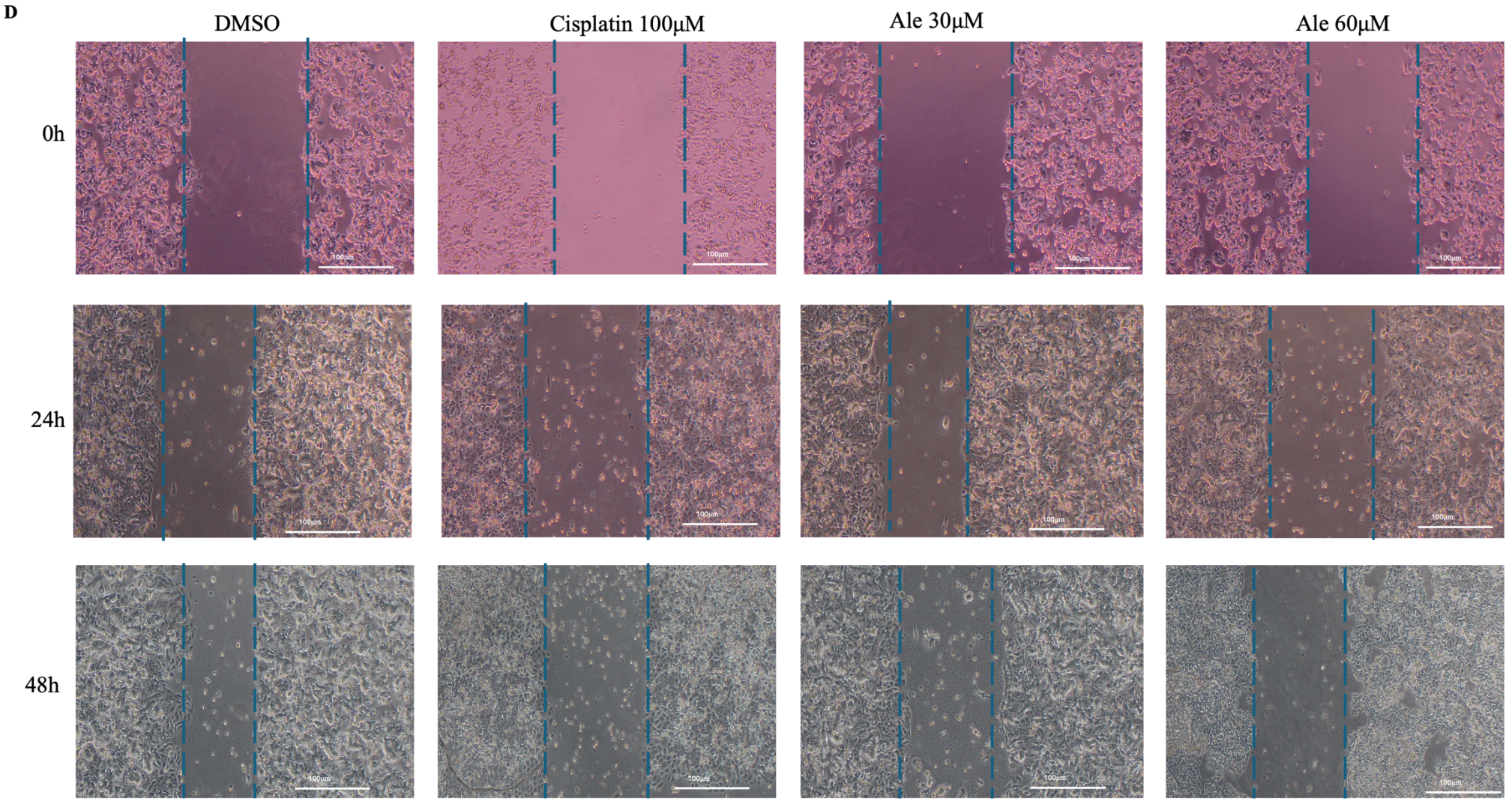

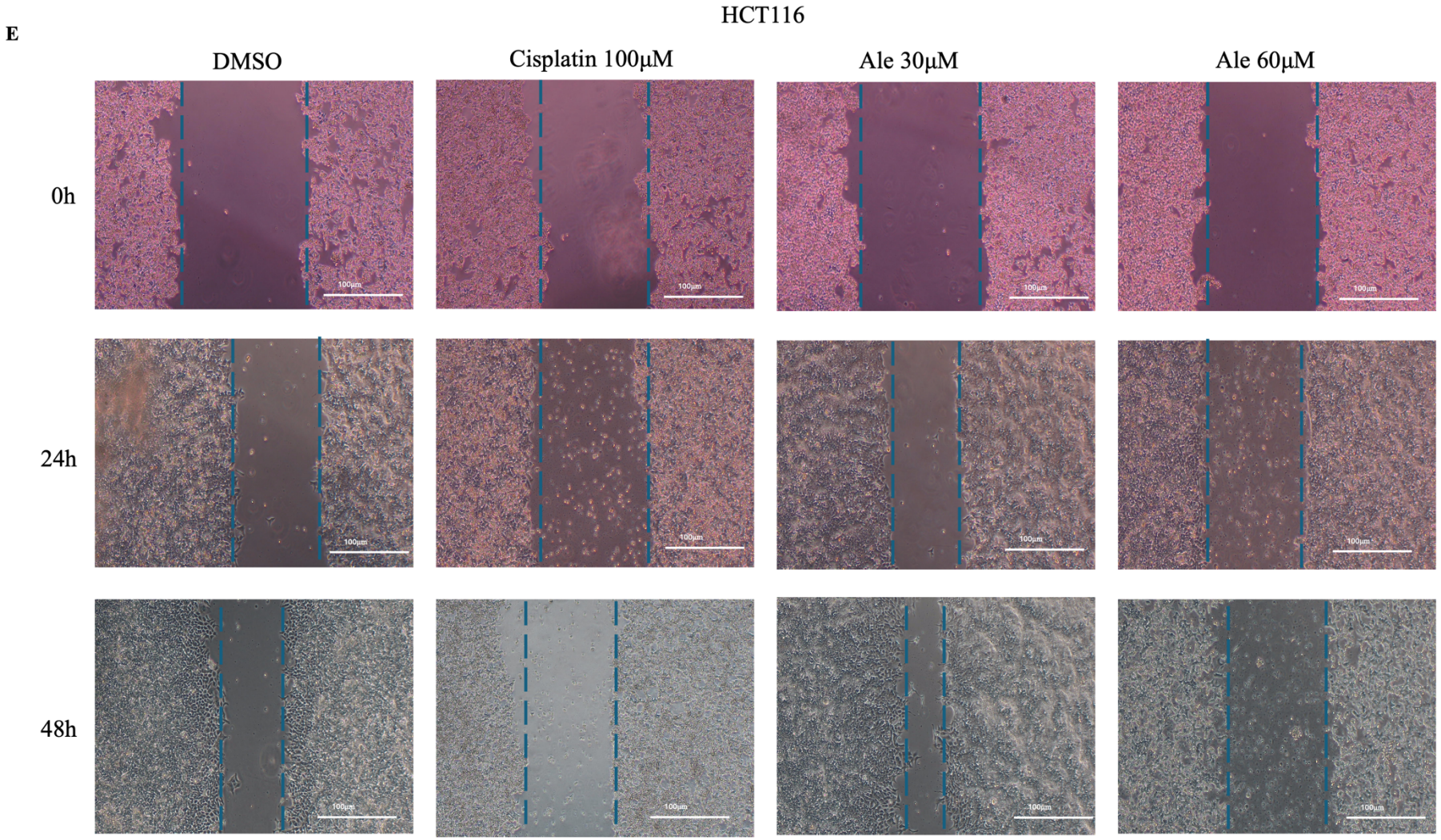
E
HCT116
DMSO
Cisplatin 100µM
Ale 30µM
Ale 60µM
0h
24h
48h

Figure 80: Aleplasinin reduced tumour migration in SW480 cells following 48h exposure in SW480 and HCT116 cells. (**A**) The migration assay was performed to determine the effect of the aleplasinin compound on SW480 tumour cell migration across 48h (N=3). Data is presented as mean ± SD. Welch's One-Way ANOVA followed by Dunnett's multiple comparison post-hoc test. *P<0.05. (**B**) The migration assay was performed to determine the effect of the aleplasinin compound on HCT116 tumour cell migration across 48h (N=3). Data is presented as mean ± SD. Welch's One-Way ANOVA followed by Dunnett's multiple comparison post-hoc test. *P<0.05, **P<0.01. (**C**) Line graphs of the quantitative migration assay analysis to illustrate the effect of aleplasinin and cisplatin treatments on cellular migration following 48h exposure. *P<0.05, **P<0.01. (**D**) Comparative images of migration distance taken at 4x magnification of SW480 cells treated with aleplasinin at 30µM and 60µM conditions across a 48h treatment period. Image analysis was conducted using ImageJ software with plugins outlined by (Suarez-Arnedo et al., 2020). (**E**) Comparative images of migration distance taken at 4x magnification of HCT116 cells treated with aleplasinin at 30µM and 60µM conditions across a 48h treatment period. Image analysis was conducted using ImageJ software with plugins outlined by (Suarez-Arnedo et al., 2020).

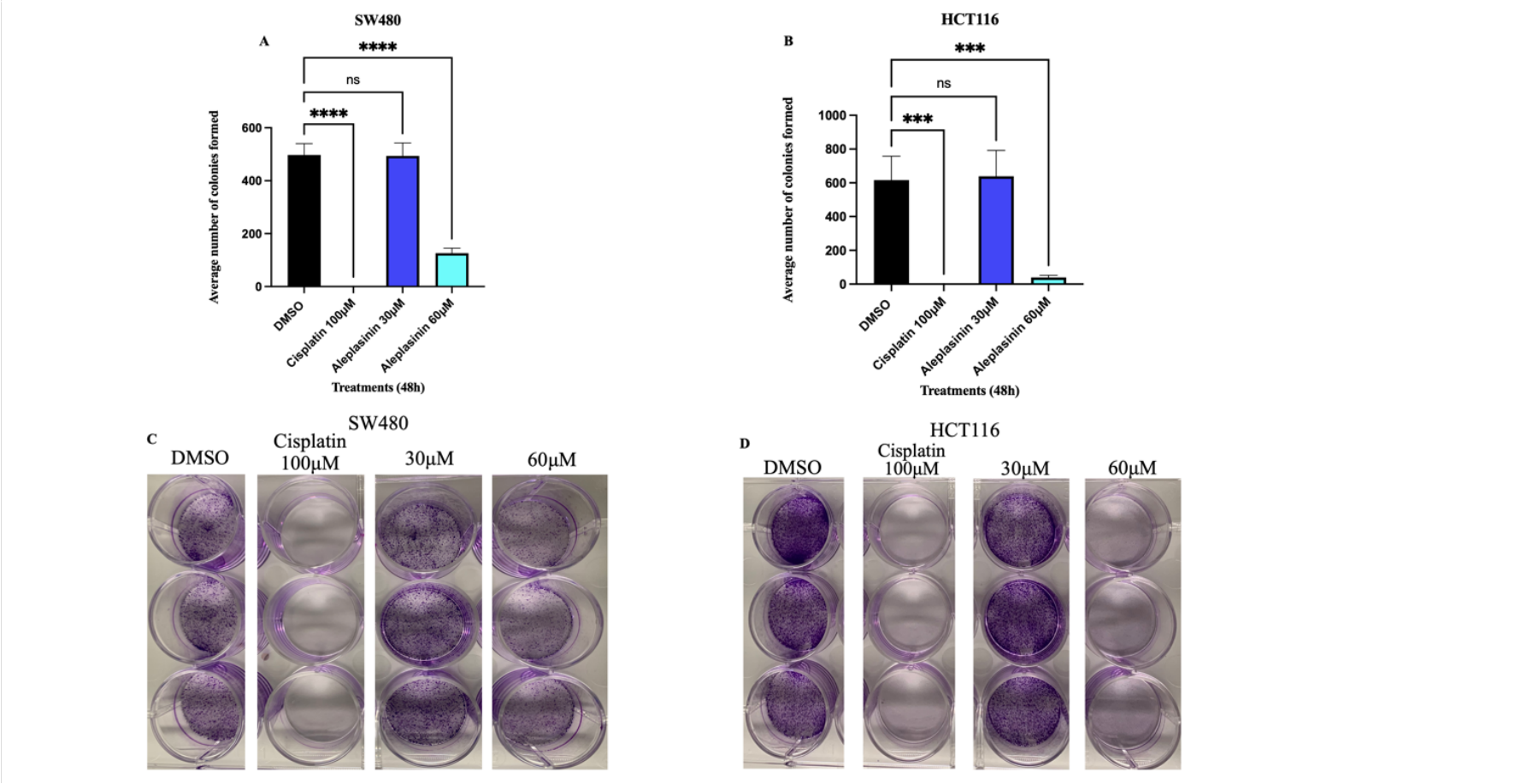

Figure 81: Aleplasinin inhibited tumour cell colonisation following 48h treatment period. (**A**) Colonisation assays determined the effect of aleplasinin treatment on SW480 colonisation post 48h treatment period and proliferation across 5 days post-treatment (N=3). Data is presented as mean ± SD. One-way ANOVA statistical analysis followed by Dunnett's multiple comparison post-hoc test. ****P< 0.0001. (**B**) Colonisation assays determined the effect of aleplasinin treatment on HCT116 colonisation post 48h treatment period and proliferation across 5 days post-treatment (N=3). Data is presented as mean ± SD. One-way ANOVA statistical analysis followed by Dunnett's multiple comparison post-hoc test. ***P< 0.001. (**C**) Visualisation of the 12-well plate utilised for 48h treatment of SW480 colonisation assay following 0.1% crystal violet staining. (**D**) Visualisation of the 12-well plate utilised for 48h treatment of HCT116 colonisation assay following 0.1% crystal violet staining.

4.3.4 Apoptosis staining of CRC cells following aleplasinin treatment

To determine the likelihood of aleplasinin-mediated cellular death induced in SW480 and HCT116 cells, DAPI nuclear staining, a marker of apoptotic death, was performed (Figure 82). Fluorescent images taken at the DAPI filter of both treated cell lines at 40x magnification revealed cellular death in only 60µM and cisplatin conditions, possibly suggesting apoptotic induction in a dose-dependent manner (Figure 82A, 82B). Additionally, there was very little cellular death at the 30µM aleplasinin treatment condition when compared against the DMSO control. Features commonly associated with apoptotic induction were present in both mentioned conditions, including abnormal morphological changes, irregular cellular size and fragmentation of the nucleus (shown by red arrows).

Moreover, AO/EB staining of cellular death was performed to give a quantitative view of the effect of aleplasinin on SW480 and HCT116 cells (Figure 83). Qualitative images of AO/EB staining on SW480 and HCT116 cells following 48h aleplasinin exposure revealed dose-dependent cytotoxicity and a significant proportion of cells undergoing apoptosis across all treated conditions (Figure 83A). In addition, both aleplasinin 60µM and cisplatin treatment conditions has shown a higher proportion of cells dual stained, suggesting late apoptosis induction. Indeed, quantitative analysis of stained cells following exposure revealed there was a significant reduction in healthy viable cells in all treated conditions in both SW480 and HCT116 cell lines ($P< 0.01$, $P< 0.0001$) (Figure 83B, 83C). Indeed, quantitative analysis of stained cells following exposure revealed there was a significant reduction in healthy viable cells in all treated conditions in both SW480 and HCT116 cell lines ($P< 0.01$, $P< 0.0001$) (Figure 83B, 83C). In addition, the significant presence of cells undergoing early apoptosis (47.2%) was observed in SW480 cells induced via 30µM aleplasinin treatment ($P< 0.05$) (Figure 83B). However, this wasn't the case in HCT116 cells as there was no significant difference in the proportion of cells undergoing apoptosis (Figure 83C). In comparison to the DMSO control condition, cisplatin and aleplasinin 60µM treatment conditions demonstrated a greater proportion of cells undergoing late apoptosis at 53.73% and 47.51% in SW480 cells and 29.41% and 47.51% in HCT116 cells, respectively ($P< 0.05$, $P< 0.01$, $P< 0.001$). Interestingly, there was also a significant increase in the number of cells undergoing necrosis, particularly in HCT116 cells following 48h cisplatin (37.99%) and aleplasinin 60µM (37.15%) treatment exposure when compared against the DMSO control ($P< 0.01$) (Figure 83C).

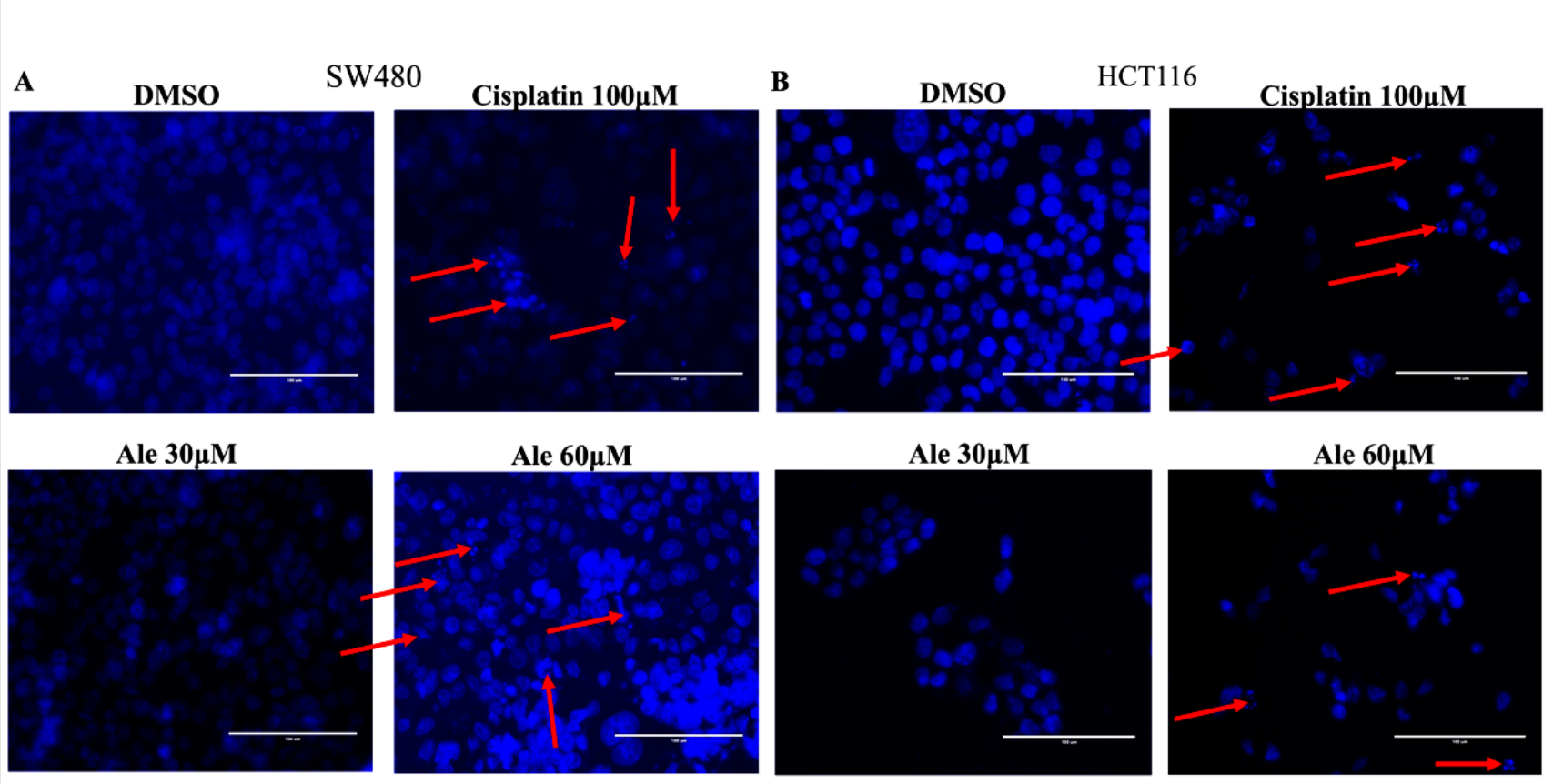

Figure 82: Aleplasinin activity stimulated apoptosis at the 60µM in CRC cells. (**A**) Nuclear fragmentation via DAPI staining was conducted to elucidate the apoptosis induction following aleplasinin 30µM and 60µM treatment on SW480 cells. The morphological irregularities and nuclear fragments are indicated by red arrows (N=3). (**B**) Nuclear fragmentation via DAPI staining was conducted to elucidate the apoptosis induction following aleplasinin 30µM and 60µM treatment on HCT116 cells. The morphological irregularities and nuclear fragments are indicated by red arrows (N=3).

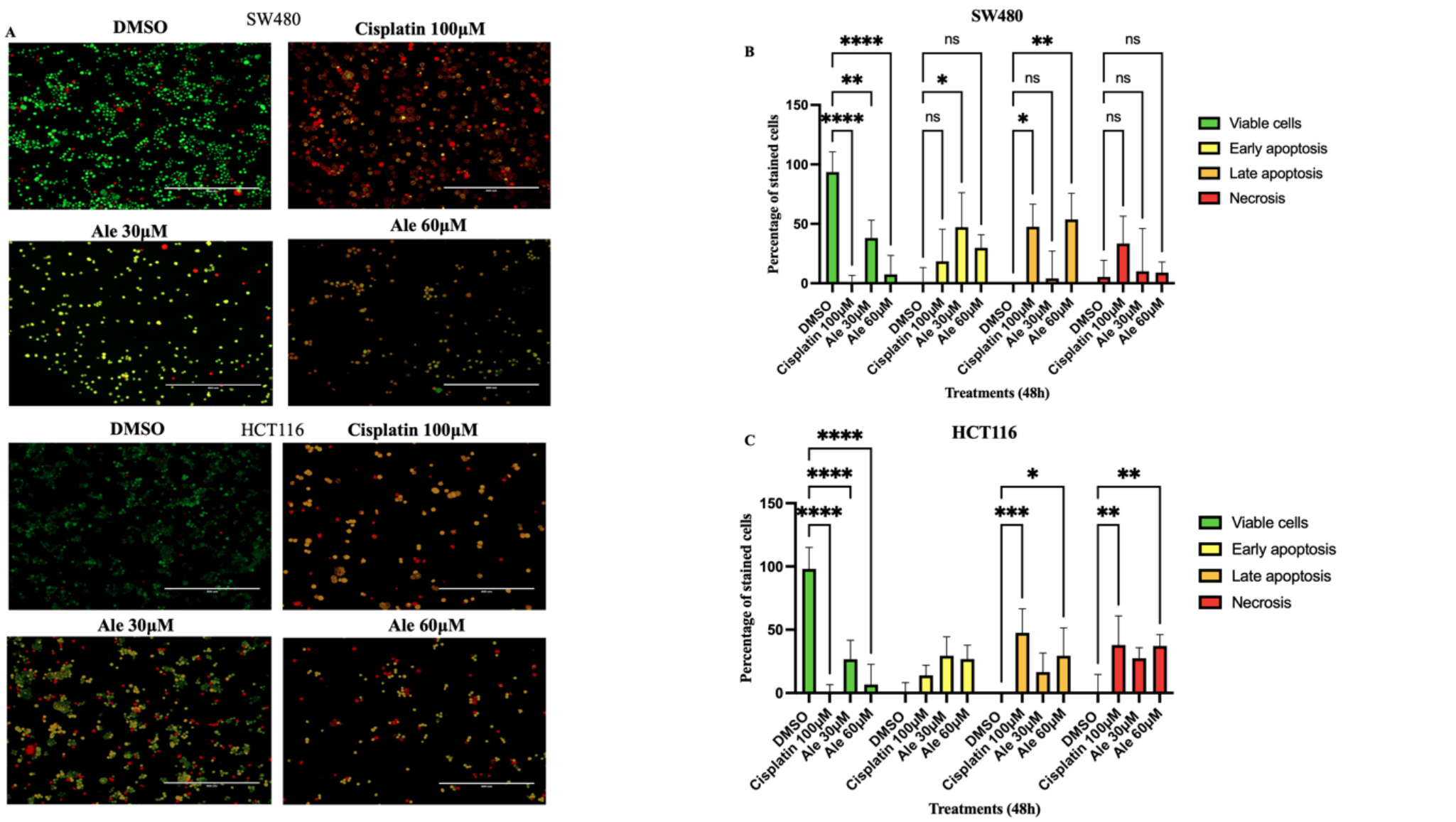
A
SW480
DMSO
Cisplatin 100µM
Ale 30µM
Ale 60µM
HCT116
DMSO
Cisplatin 100µM
Ale 30µM
Ale 60µM
B
SW480
Percentage of stained cells
Treatments (48h)
Viable cells
Early apoptosis
Late apoptosis
Necrosis
C
HCT116
Percentage of stained cells
Treatments (48h)
Viable cells
Early apoptosis
Late apoptosis
Necrosis

Figure 83: Aleplasinin exerts dose-dependent apoptotic induction at varying concentrations. (**A**) Qualitative images stained with AO/EB following 48h aleplasinin exposure in SW480 and HCT116 cells. Cellular staining is denoted as follows: Green stained cells represent cells that are healthy and viable. Yellow stained cells represented a proportion of cells undergoing early apoptosis. Orange-stained cells represented a proportion of cells undergoing late apoptosis. Red stained cells represented a proportion of cells undergoing necrosis. (**B**) Quantitative analysis of the number of apoptotic AO/EB stained cells present following 48h aleplasinin treatment in SW480 cells. AO/EB quantification was determined by the two-way ANOVA statistical test followed by Dunnett's multiple comparisons post-hoc tests (N=3). *P< 0.05, **P< 0.01, ****P< 0.0001. (**C**) Quantitative analysis of the number of apoptotic AO/EB stained cells present following 48h aleplasinin treatment in HCT116 cells. AO/EB quantification was determined by the two-way ANOVA statistical test followed by Dunnett's multiple comparisons post-hoc tests (N=3). *P<0.05, **P< 0.01, ****P< 0.0001.

4.3.5 The role of aleplasinin on Siglec-15 expression

To determine the impact of aleplasinin on Siglec-15 expression in SW480 and HCT116 cells, several methods were utilised. In particular, RT-qPCR methods determined *SIGLEC15* gene expression following aleplasinin treatment, whilst IF methods were used to determine the effect of aleplasinin on Siglec-15 protein expression (Figure 84). Gene expression analysis revealed the downregulation of the *SIGLEC15* gene in a dose-dependent manner in both SW480 and HCT116 cell lines in the 60µM condition ($P< 0.01$) (Figure 84A, 84B). In contrast, the 30µM aleplasinin treatment condition only significantly downregulated *SIGLEC15* expression in SW480 cells, and there was no significant difference in its expression in HCT116 cells ($P< 0.05$) (Figure 84A). Similarly, IF visualisation and quantification of aleplasinin treated SW480 and HCT116 cells revealed no significant difference in the expression of the Siglec-15 protein (Figure 84C-F).

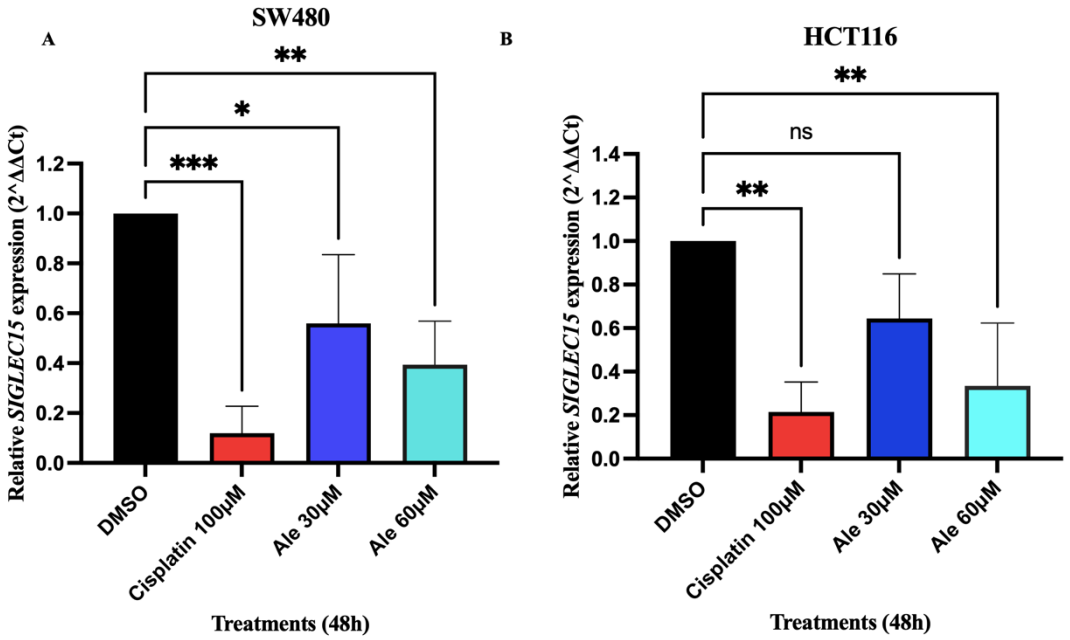
A
SW480
**
*
***
Relative SIGLEC15 expression (2^ΔΔCt)
1.2
1.0
0.8
0.6
0.4
0.2
0.0
DMSO
Cisplatin 100μM
Ale 30μM
Ale 60μM
Treatments (48h)
B
HCT116
**
ns
**
Relative SIGLEC15 expression (2^ΔΔCt)
1.4
1.2
1.0
0.8
0.6
0.4
0.2
0.0
DMSO
Cisplatin 100μM
Ale 30μM
Ale 60μM
Treatments (48h)

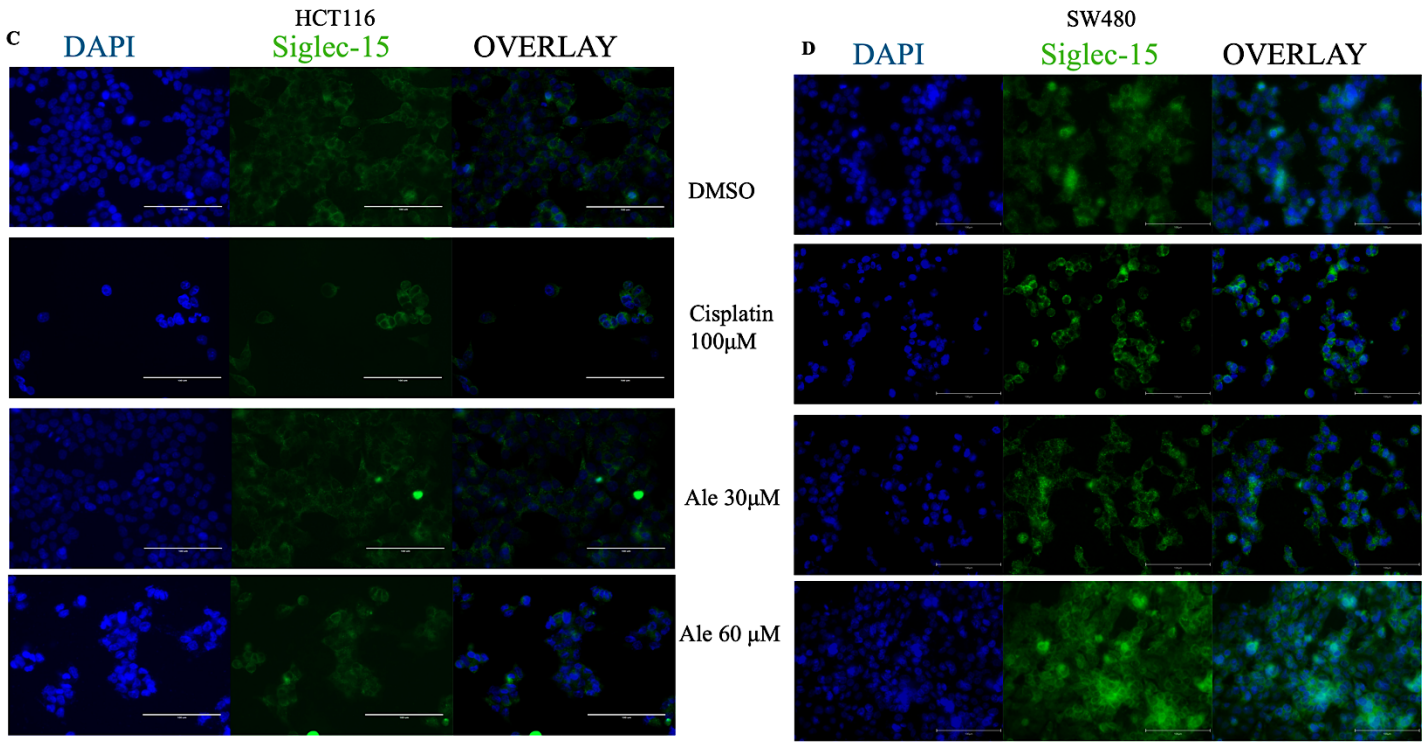
C
HCT116
DAPI
Siglec-15
OVERLAY
D
SW480
DAPI
Siglec-15
OVERLAY
DMSO
Cisplatin 100μM
Ale 30μM
Ale 60 μM

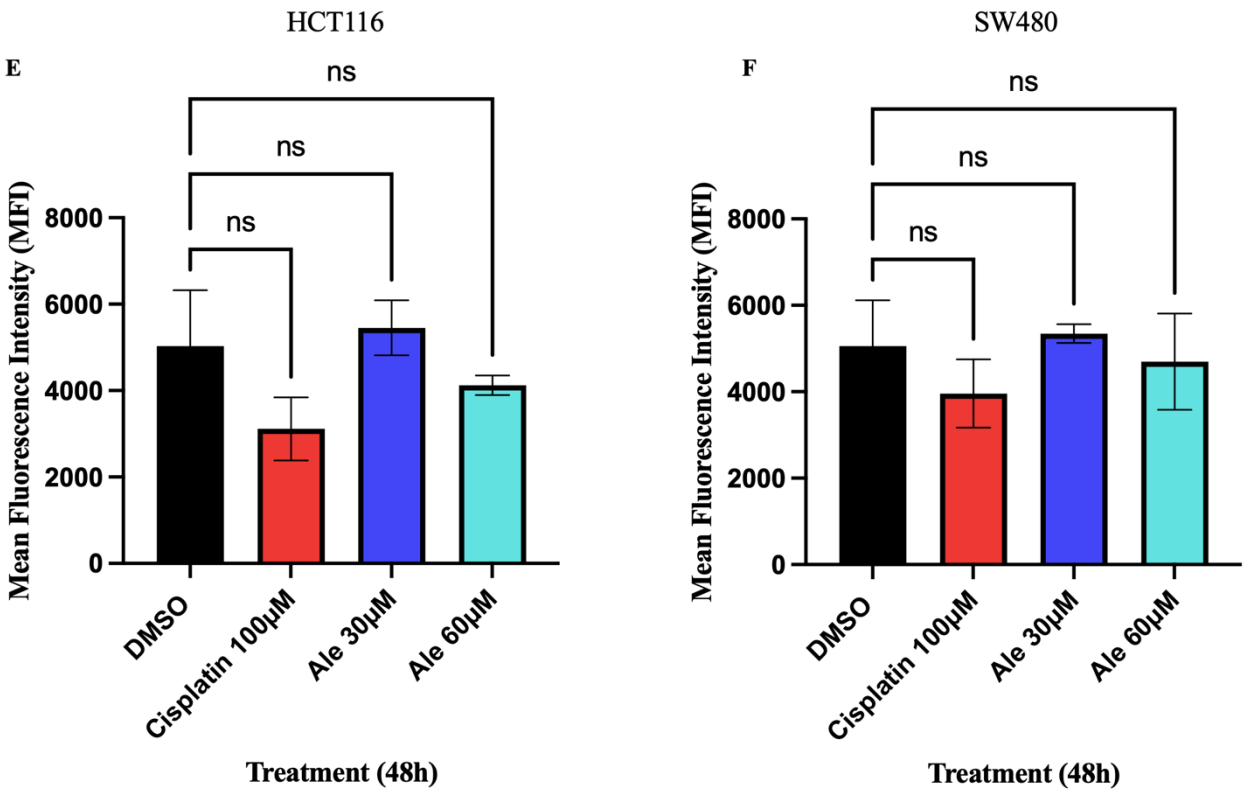

Figure 84: Aleplasinin exposure affects *SIGLEC15* expression in a dose-dependent manner at the gene level. (**A**) RT-qPCR expression analysis of *SIGLEC15* in SW480 cells following 48h aleplasinin treatment exposure (N=3). One-way ANOVA statistical test followed by Dunnett's multiple comparisons post-hoc tests, *P< 0.05, **P< 0.01, **** P< 0.0001. (**B**) RT-qPCR expression analysis of *SIGLEC15* in HCT116 cells following 48h aleplasinin treatment exposure (N=3). One-way ANOVA statistical test followed by Dunnett's multiple comparisons post-hoc tests, **P<0.01. Gene expression analysis of HCT116 and SW480 cells following aleplasinin treatment was normalised to the DMSO control condition and all samples were amplified at 100ng/μL for reverse transcription prior to cDNA amplification. (**C-D**) IF image visualisation of SW480 and HCT116 cells stained with a primary Siglec-15 antibody following 48h aleplasinin exposure taken at 40x magnification with DAPI (blue) and green filters (N=3). (**E-F**) Quantitative analysis of the IF images taken of HCT116 and SW480 cells following 48h aleplasinin exposure (N=3).

4.3.6 Illumina RNA-sequencing

Following 48h aleplasinin 60μM treatment of SW480 and the DMSO control condition, SW480 cells underwent total RNA extraction, upon which RNA Illumina sequencing was conducted to illustrate the effect of aleplasinin of gene expression (Figure 85). The effect of aleplasinin exposure exhibited a profound effect on gene expression, suggested by the change in the DE of genes when compared between the treated and untreated conditions in the constructed heatmap (Figure 85A). In addition, the correlation analysis of DE genes following aleplasinin treatment was revealed to be positively correlated, indicating changes in gene expression due to the aleplasinin compound (Figure 85B). Further analysis of the total number of DE genes identified a total of 5293 with varied expression profiles. Of those, 3482 genes were downregulated, and 1811 were upregulated genes (Figure 85C). The constructed volcano plot also exhibited that the most upregulated and downregulated genes were *SPRR2D* and *ACSL6,* respectively (Figure 85D). The most significantly DE gene targets were determined by a minimum set threshold of a Log2 fold change alongside the significance cut-off at $P< 0.05$. To determine the functional classification related to the DE genes, COG functional classification showed the enrichment of signal transduction mechanisms and post-translational modifications that were related to protein turnover and molecule chaperones (Figure 85E).

Upon conducting KEGG and GO, functional analysis on the DE genes following aleplasinin exposure was performed (Figure 86). Several biological processes were enriched as part of the KEGG analysis. In particular, the enrichment of regulated transcription, regulation of gene expression and the Wnt signalling pathway were all observed (Figure 86A). Additionally, when comparing the molecular functions that were enriched, GO analysis identified several functions related to transcriptional regulation including DNA and nucleic acid binding, DNA binding transcription factors and transcriptional regulator activity alongside Wnt-activated receptor activity as well (Figure 86B). Furthermore, enrichment of cellular components revealed nuclear localisation (Figure 86C).

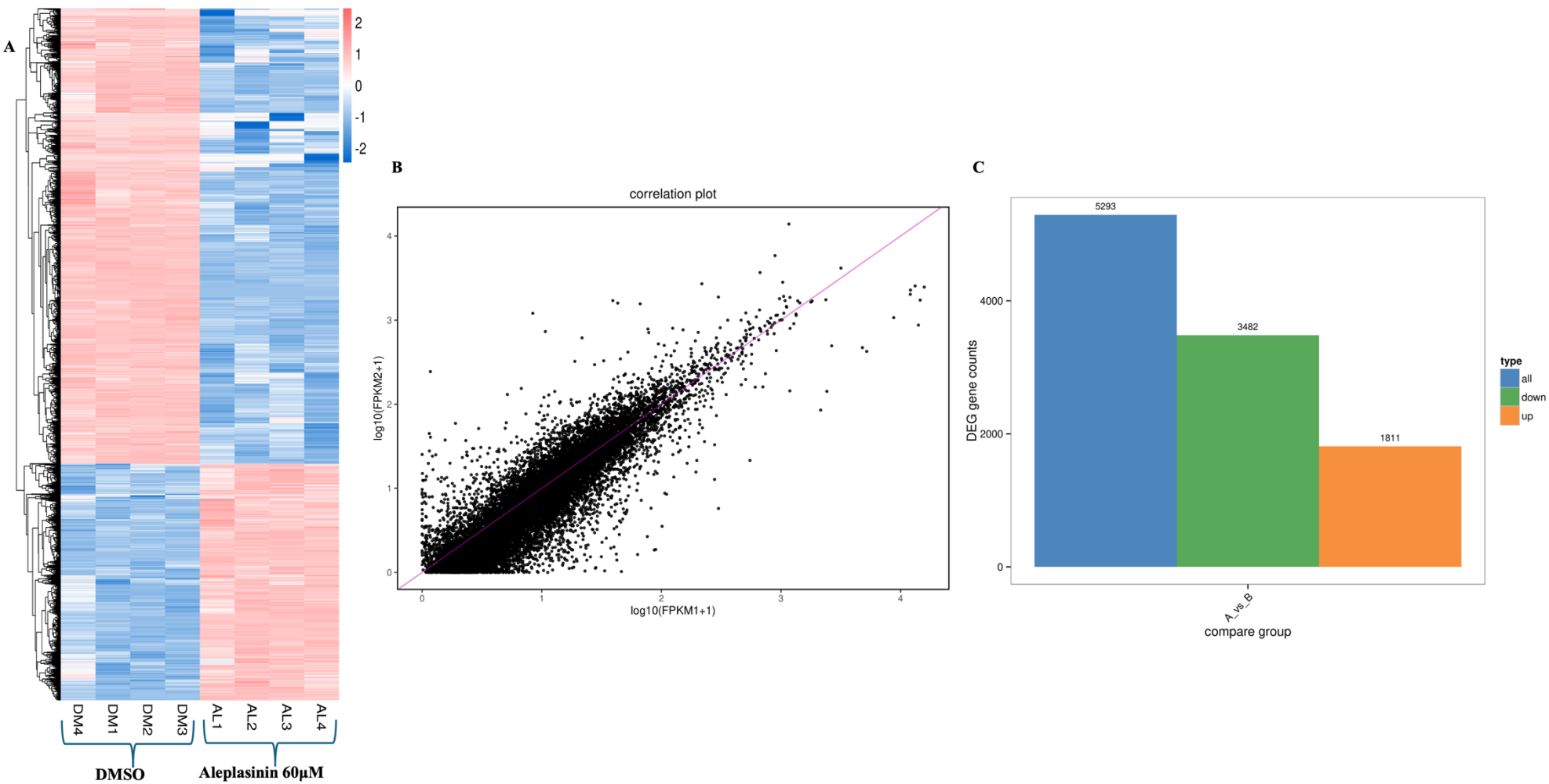
A
2
1
0
-1
-2
DM4
DM1
DM2
DM3
AL1
AL2
AL3
AL4
DMSO
Aleplasinin 60µM
B
correlation plot
log10(FPKM2+1)
log10(FPKM1+1)
C
5293
3482
1811
DEG gene counts
4000
2000
0
A_vs_B
compare group
type
all
down
up

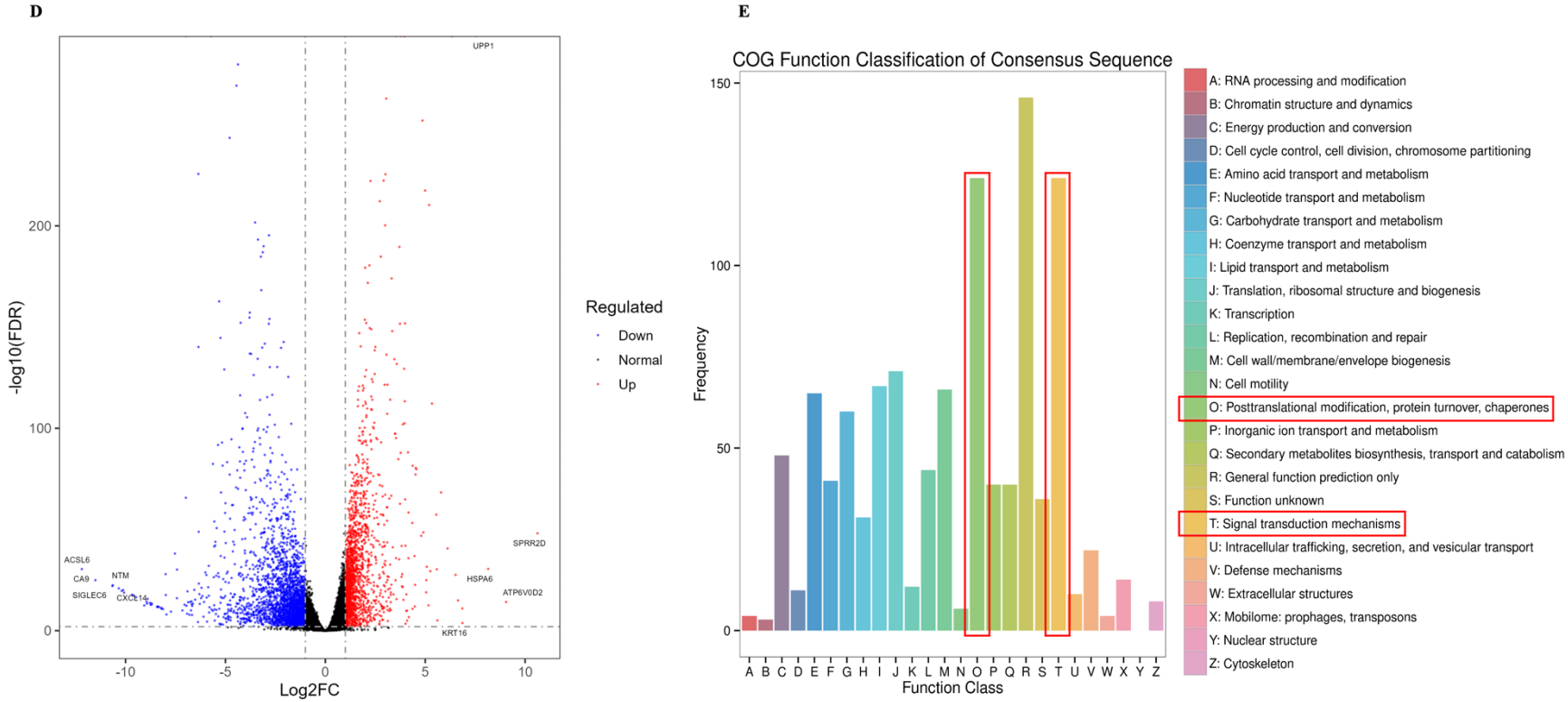
D
UPP1
SPRR2D
HSPA6
ATP6V0D2
KRT16
ACSL6
CA9
NTM
SIGLEC6
CXCL14
-log10(FDR)
Log2FC
Regulated
Down
Normal
Up
E
COG Function Classification of Consensus Sequence
Frequency
Function Class
A: RNA processing and modification
B: Chromatin structure and dynamics
C: Energy production and conversion
D: Cell cycle control, cell division, chromosome partitioning
E: Amino acid transport and metabolism
F: Nucleotide transport and metabolism
G: Carbohydrate transport and metabolism
H: Coenzyme transport and metabolism
I: Lipid transport and metabolism
J: Translation, ribosomal structure and biogenesis
K: Transcription
L: Replication, recombination and repair
M: Cell wall/membrane/envelope biogenesis
N: Cell motility
O: Posttranslational modification, protein turnover, chaperones
P: Inorganic ion transport and metabolism
Q: Secondary metabolites biosynthesis, transport and catabolism
R: General function prediction only
S: Function unknown
T: Signal transduction mechanisms
U: Intracellular trafficking, secretion, and vesicular transport
V: Defense mechanisms
W: Extracellular structures
X: Mobilome: prophages, transposons
Y: Nuclear structure
Z: Cytoskeleton

Figure 85: Aleplasinin stimulated the DE of gene targets following 48h treatment at 60µM. (**A**) Illumina RNA-seq analysis revealed DE genes between aleplasinin-treated and untreated conditions. (**B**) Correlation analysis for the presence of DE genes between untreated control condition group and aleplasinin treatment condition group. (**C**) The number of DE genes based on their expression patterns following 48h aleplasinin exposure. (**D**) Constructed volcano plot illustrating the top deregulated genes that are both upregulated and downregulated following aleplasinin treatment. (**E**) COG functional classification of consensus sequence analysis was conducted to elucidate possible enriched deregulated mechanisms.

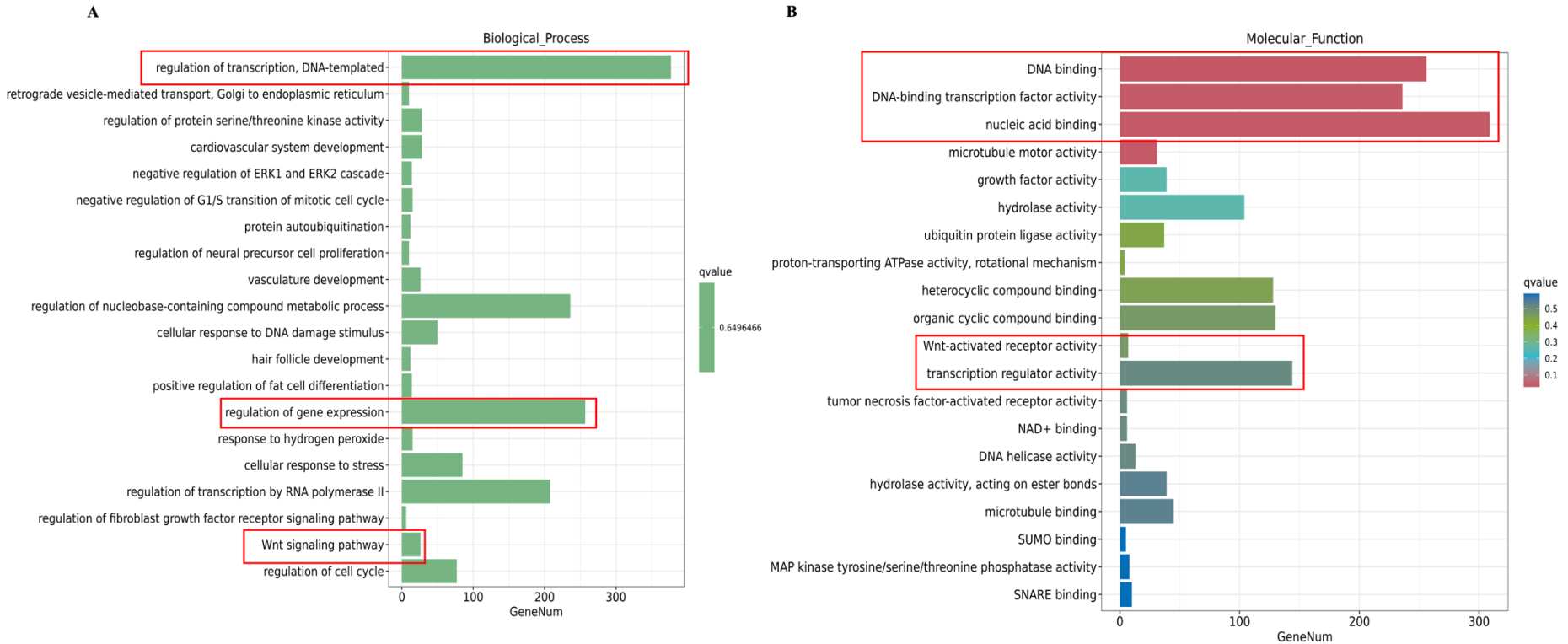
A
Biological_Process
regulation of transcription, DNA-templated
retrograde vesicle-mediated transport, Golgi to endoplasmic reticulum
regulation of protein serine/threonine kinase activity
cardiovascular system development
negative regulation of ERK1 and ERK2 cascade
negative regulation of G1/S transition of mitotic cell cycle
protein autoubiquitination
regulation of neural precursor cell proliferation
vasculature development
regulation of nucleobase-containing compound metabolic process
cellular response to DNA damage stimulus
hair follicle development
positive regulation of fat cell differentiation
regulation of gene expression
response to hydrogen peroxide
cellular response to stress
regulation of transcription by RNA polymerase II
regulation of fibroblast growth factor receptor signaling pathway
Wnt signaling pathway
regulation of cell cycle
0
100
200
300
GeneNum
qvalue
0.6496466
B
Molecular_Function
DNA binding
DNA-binding transcription factor activity
nucleic acid binding
microtubule motor activity
growth factor activity
hydrolase activity
ubiquitin protein ligase activity
proton-transporting ATPase activity, rotational mechanism
heterocyclic compound binding
organic cyclic compound binding
Wnt-activated receptor activity
transcription regulator activity
tumor necrosis factor-activated receptor activity
NAD+ binding
DNA helicase activity
hydrolase activity, acting on ester bonds
microtubule binding
SUMO binding
MAP kinase tyrosine/serine/threonine phosphatase activity
SNARE binding
0
100
200
300
GeneNum
qvalue
0.5
0.4
0.3
0.2
0.1

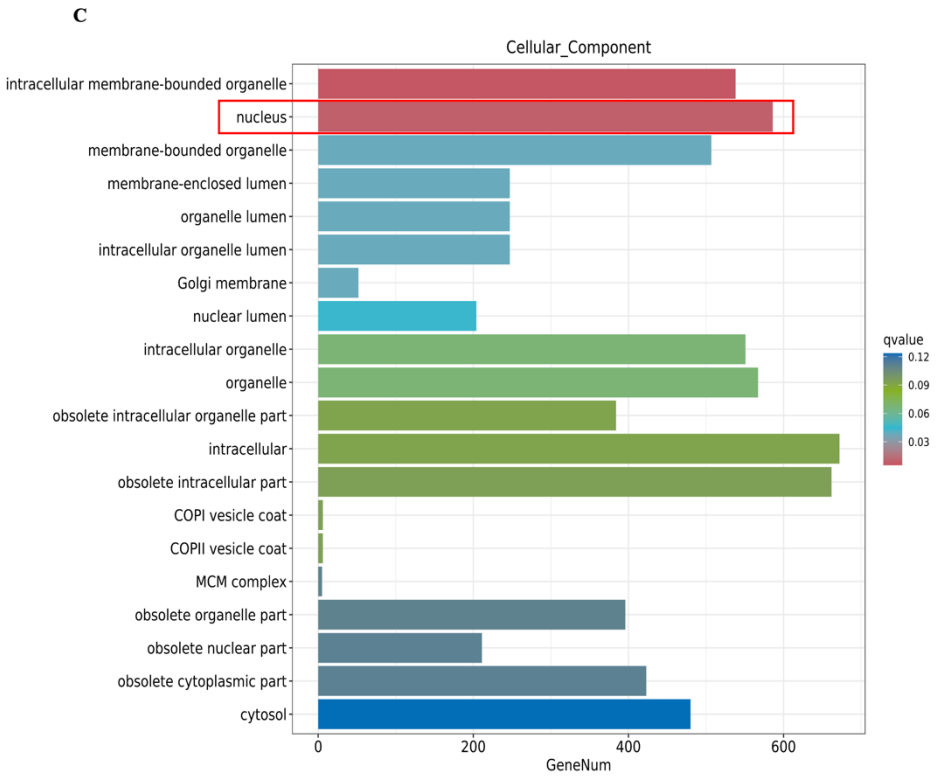

Figure 86: Aleplasinin activity had induced transcriptional regulation via Wnt signalling. (**A**) KEGG pathway enrichment depicts the possible enrichment of molecular pathways between SHG-8 treated and untreated conditions. (**B**) GO classification analysis reveals enriched biological

processes between SHG-8 treated and untreated conditions. (**C**) GO classification analysis reveals enriched cellular components between SHG-8 treated and untreated conditions. (**D**) GO classification analysis reveals enriched molecular functions between SHG-8 treated and untreated conditions.

4.3.7 Validation of RNA Illumina sequencing targets in CRC

To corroborate the reliability of the findings obtained from RNA Illumina sequencing, *in silico* and RT-qPCR methods were conducted to determine the expression profiles of the DE genes in relation to CRC tumours (Figure 87). UALCAN transcriptomics analysis indicated significantly upregulated expression for the *ACSL6* gene in the COAD tumour cohorts with a mean expression of 3.087 TPM ($P< 0.001$) (Figure 87A). For *SPRR2D*, there was no significant difference in its expression profile between normal and malignant tumour cohorts which exhibited a mean expression of 0.079 TPM (Figure 87B). These findings underlined *ACSL6* as a possible oncogene in CRC progression. Gene expression analysis of *ACSL6* demonstrated significant downregulation of the gene at both 30µM and 60µM aleplasinin treatment conditions, with greater downregulation observed at higher concentrations ($P< 0.05$, $P< 0.01$) (Figure 87C). In contrast, *SPRR2D* expression was shown to have no significant difference in its expression profile following aleplasinin treatment (Figure 87D). Furthermore, the clinical role of *ACSL6* and CRC prognosis was determined via Kaplan-meier plot (Figure 87E). The survival plot analysis revealed high *ACSL6* expression was associated with lower OS outcomes over an extended period of time ($P< 0.05$).

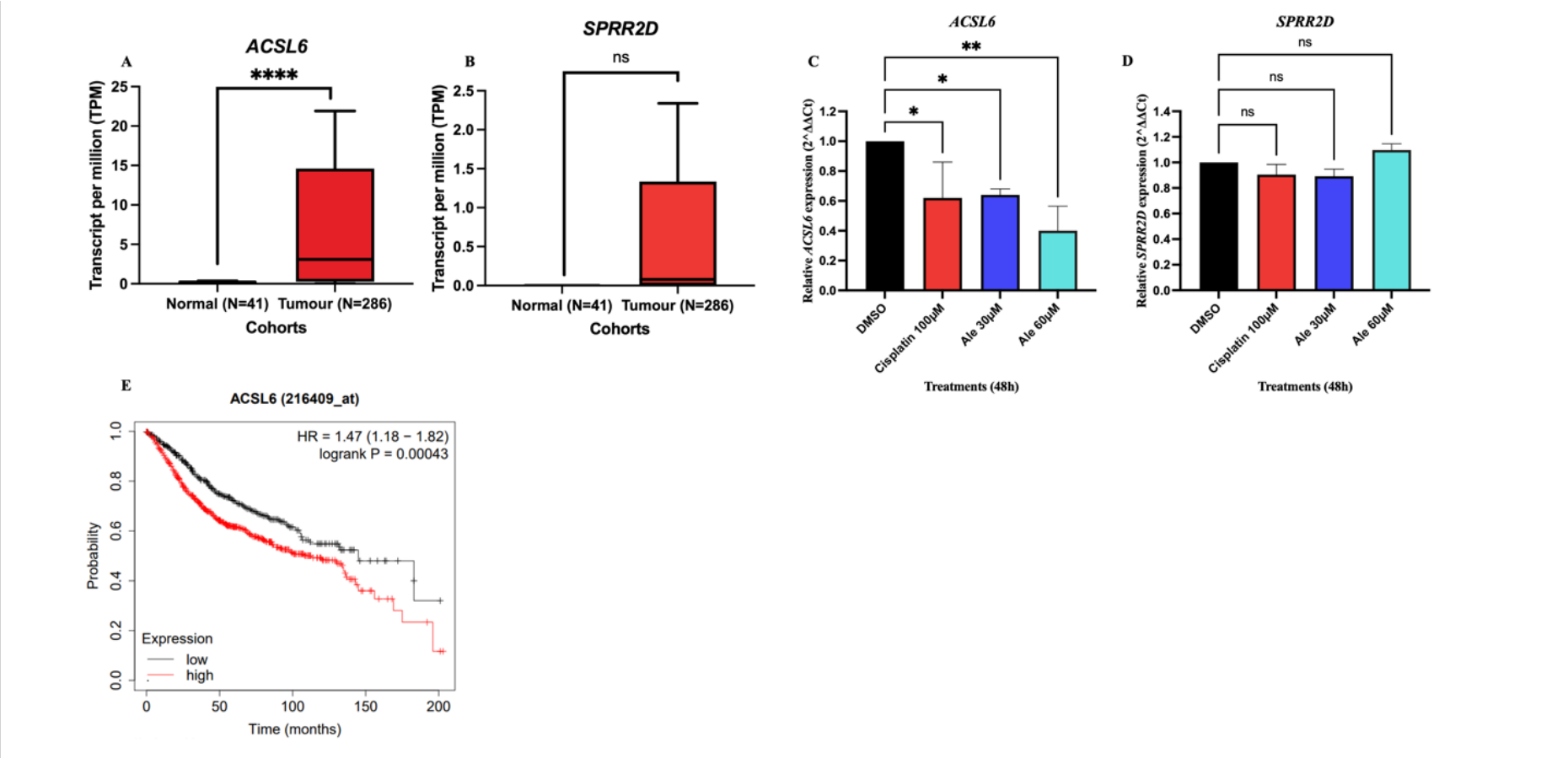

Figure 87: *In silico* and RT-qPCR methods validated the role of *ACSL6* oncogenic activity following aleplasinin exposure in SW480 cells. (**A**) UALCAN TCGA genomic data exhibiting mRNA expression of *ACSL6* in normal (grey) and COAD (red) cohorts, error bars ± SD. Welch's t-test PERL script. ****P< 0.0001. (**B**) UALCAN TCGA genomic data exhibiting mRNA expression of *SPRR2D* in normal (grey) and COAD (red) cohorts, error bars ± SD. Welch's t-test PERL script. (**C**) RT-qPCR expression analysis of *ACSL6* in SW480 cells following 48h aleplasinin treatment exposure (N=3). One-way ANOVA statistical test followed by Dunnett's multiple comparison post-hoc test. *P< 0.05, **P< 0.01. (**D**)

RT-qPCR expression analysis of *SPRR2D* in SW480 cells following 48h aleplasinin treatment exposure (N=3). One-way ANOVA statistical test followed by Dunnett's multiple comparison post-hoc test. (**E**) Survival curves were constructed by Kmplot software (N=1061) to outline *ACSL6* expression with overall survival (OS) criteria. The cut-off between the illustrated low and high expression levels were based on the distribution of *ACSL6* expression values that were within the dataset. The thresholds were defined on quartiles at the 25th percentile as low expression and 75th percentile classified as high expression, and values were later stratified based on the group classifications into low and high expression groups. P< 0.05 was considered statistically significant.

4.3.8 Impact of miRNAs in regulating *ACSL6* and *SPRR2D* gene targets following aleplasinin treatment and possible binding partners

Elucidating the impact of miRNAs involved in the regulation of *ACSL6* and *SPRR2D* following aleplasinin treatment could emphasise regulatory mechanisms associated with CRC progression (Figure 88). Cross-referencing several miRNA prediction databases for common miRNA "hits" revealed a possible 2 and 37 predicted miRNAs involved in the regulation of *ACSL6* and *SPRR2D*, respectively (Figure 88A, 88B). Upon further *in silico* analysis, predicted binding sites were identified. The miRNAs associated with the highest binding affinity for the *ACSL6* mRNA strand were revealed as hsa-let-7a-5p with -20.1 kcal/mol at position 7-27 on the seed region of the 3' UTR. In addition, hsa-miR-527 was identified as the miRNA with the highest binding affinity with -21.5 kcal/mol to the *SPRR2D* gene at position 612-629 at the seedless region of the 3' UTR (Figure 88C). Moreover, both hsa-let-7a-5p and hsa-miR-527 were shown to have partial complementarity and full complementarity to their respective genes. From these predictions, UALCAN transcriptomics analysis exhibited the expression profile of let-7a-5p as significantly downregulated in the tumour cohort with a mean expression of 5848.54 TPM in comparison to the normal tissue group with a mean TPM of 14,802.93 (Figure 88D). Hence, this suggested a tumour suppressor expression profile of this miRNA. For elucidating possible binding partners for the role of *ACSL6* in CRC progression, GeneMANIA and STRING analyses were utilised. At the gene level, *ACSL6* interactions suggested significant interactive prediction (orange) with phytanoyl-CoA 2-hydroxylase (*PHYH*) and acyl-CoA synthetase short chain family member 2 (*ACSS2*) (Figure 88E). In addition, the *ACSL6* framework demonstrated co-expression (purple) with acyl-CoA synthetase family member 2 (*ACSF2*) and retinoid X receptor β (*RXRB*) genes. Furthermore, *ACSL6* was predicted to be co-localised (light blue) with a number of carnitine palmitoyl transferase 1 (*CPT1*) genes and physical interactions (red) with zinc finger protein 16 (*ZNF16*). From the STRING PPI analysis, the ACSL6 protein interactions revealed direct interactions with fatty acid synthase (FASN) and carnitine palmitoyl transferase 1A (CPT1A), which was also previously identified in the GeneMANIA framework (Figure 88F). Similarly, secondary expansion of the PPI framework also revealed interactions with multiple other acyl-CoA synthetase long chain family member with an ALCC score of 0.00 via STRING analysis at a confidence interval of ≥ 0.900 (Figure 88F, Table 20).

Table 20: Predicted ACSL6 STRING PPI relationship and association analysis. Computational analysis of the query ACLS6 protein following construction of the PPI framework.

	Number of nodes	Number of edges	Average node degree	Average local clustering coefficient	Expected number of edges	PPI enrichment P-value
ACSL6	8	12	3	0.00	7	0.0539

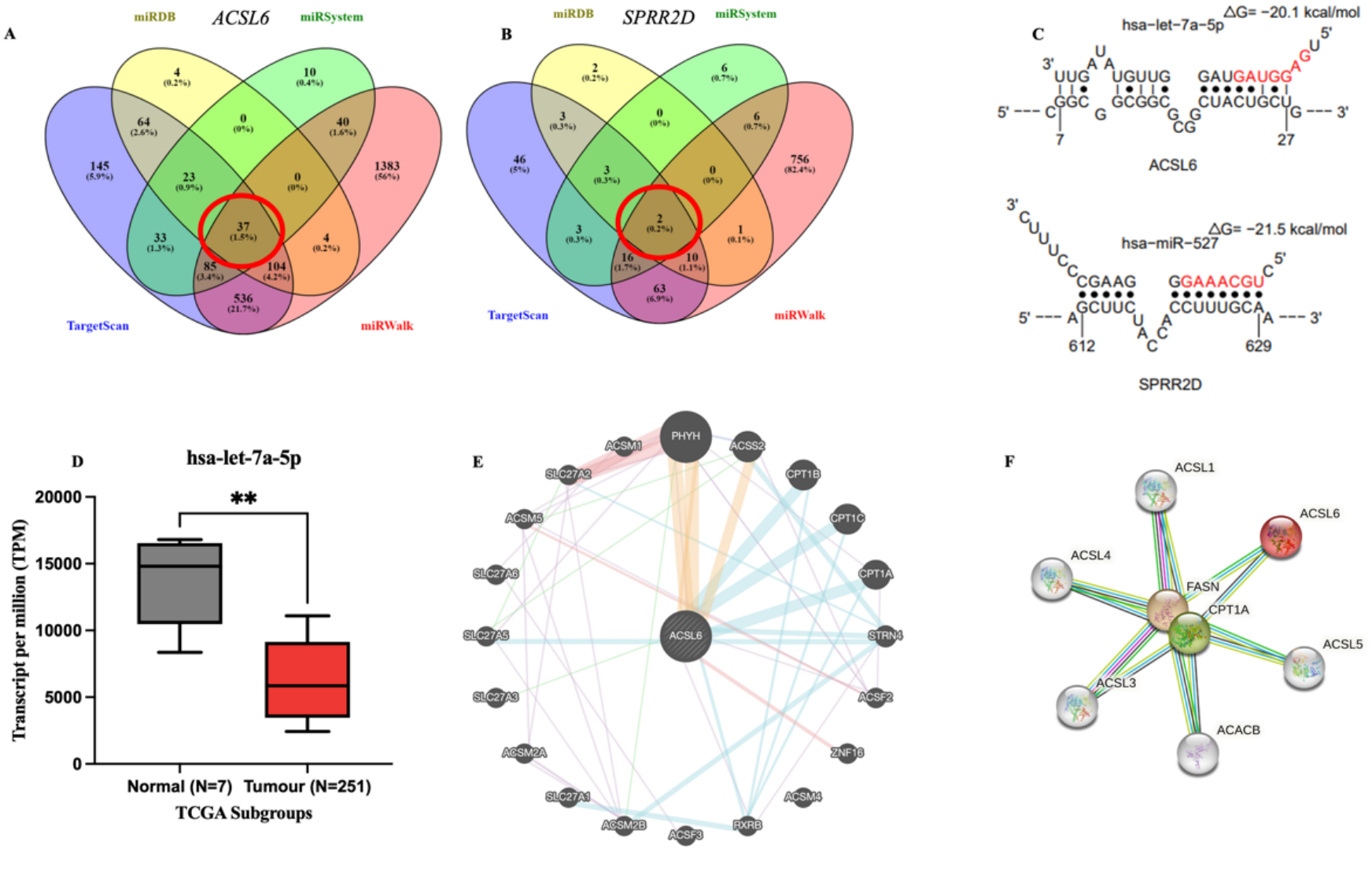
A
miRDB
ACSL6
miRSystem
4 (0.2%)
10 (0.4%)
64 (2.6%)
0 (0%)
40 (1.6%)
145 (5.9%)
23 (0.9%)
0 (0%)
1383 (56%)
37 (1.5%)
33 (1.3%)
4 (0.2%)
85 (3.4%)
104 (4.2%)
536 (21.7%)
TargetScan
miRWalk
B
miRDB
SPRR2D
miRSystem
2 (0.2%)
6 (0.7%)
3 (0.3%)
0 (0%)
6 (0.7%)
46 (5%)
3 (0.3%)
0 (0%)
756 (82.4%)
3 (0.3%)
2 (0.2%)
1 (0.1%)
16 (1.7%)
10 (1.1%)
63 (6.9%)
TargetScan
miRWalk
C
ΔG= −20.1 kcal/mol
hsa-let-7a-5p
5'
3'
UUG
UGUUG
GAUGAUGG
GGC
GCGGC
CUACUGCU
5' --- C
G
G G
CG
G --- 3'
7
27
ACSL6
3'
ΔG= −21.5 kcal/mol
hsa-miR-527
5'
CGAAG
GGAAACGU
GCUUC
CCUUUGCA
5' --- A
A --- 3'
612
629
SPRR2D
D
hsa-let-7a-5p
**
20000
15000
10000
5000
0
Transcript per million (TPM)
Normal (N=7)
Tumour (N=251)
TCGA Subgroups
E
PHYH
ACSM1
ACSS2
SLC27A2
CPT1B
ACSM5
CPT1C
SLC27A6
CPT1A
SLC27A5
ACSL6
STRN4
SLC27A3
ACSF2
ACSM2A
ZNF16
SLC27A1
ACSM4
ACSM2B
ACSF3
RXRB
F
ACSL1
ACSL6
ACSL4
FASN
CPT1A
ACSL5
ACSL3
ACACB

Figure 88: Let-7a-5p and miR-527 were predicted as miRNA candidates involved in *ACSL6* and *SPRR2D* regulation. (**A**) Cross-referenced miRNAs from miRNA prediction databases demonstrated "37 hits" for *ACSL6* regulation. (**B**) Cross-referenced miRNAs from miRNA prediction databases demonstrated "2 hits" for *SPRR2D* regulation. (**C**) Predicted positional binding sites of the miRNAs were conducted, revealing high binding affinities for the *ACSL6* and *SPRR2D* target genes via Sfold predictive software. (**D**) Expression analysis was determined for predicted miRNA hsa-let-7a-5p and was compared between normal (grey) and COAD tumours (red) cohorts via UALCAN transcriptomics analysis. Welch's t-test PERL script statistical analysis. **P<0.01. (**E**) *ACSL6* gene framework predicted functional information based on corresponding genes and gene datasets via the GeneMANIA database. (**F**) ACSL6 STRING framework highlighting possible PPI from interacting proteins and direct associations via computational data mining. The framework is developed with a confidence interval of ≥ 0.900.

4.4 Discussion

From this chapter, the repurposing and utilisation of currently available small molecule inhibitors that were previously used in disease treatment may underline an approach for Siglec-15 targeting. The characterisation of aleplasinin, a drug compound previously used in Alzheimer's disease, and its application as a possible anti-cancer agent was elucidated (Vashchenko et al., 2023). It is important to mention that the specificity of repurposed therapeutic agents is key for Siglec-15 targeting, largely due to the necessity for minimising any potential off-target effects to healthy cells/tissues. Furthermore, repurposing drug compounds provides a cheaper alternative with already characterised safety profiles that have been used in targeting specific tumour markers in CRC progression and treatment resistance (Ma et al., 2023). In particular, chemoresistance plays a major role in CRC progression due to the heterogenous nature of the tumours themselves, stemming from various somatic mutations including *APC* or *KRAS* (Ma et al., 2023). Hence, specifically targeting CRC tumours with repurposed drug compounds presents a feasible approach for molecular targets such as Siglec-15.

4.4.1 Aleplasinin as a Siglec-15 Inhibitor

A high-throughput screening analysis of many currently available small molecule inhibitors used in clinical trials was identified based on their binding affinities to the V-set binding domain of the Siglec-15 protein structure. From these screened candidates, aleplasinin was revealed as a possible protein inhibitor with the highest binding affinity of -7.8 kcal/mol to the R143 residue, which is responsible for canonical glycan ligand binding via salt bridge formation (Crocker et al., 2007). Competitively inhibiting the STn antigen could provide insights for preventing subsequent immunosuppression. Typical strategies for Siglec-15 blocking are the development of blocking antibodies characterised by a high binding affinity to disrupt the Siglec-15/Sia axis (He et al., 2021). However, the large size of the antibody prevents efficient infiltration into the tumour and requires high specificity for targeting. In contrast, the nature of small molecule inhibitors is better equipped for tumour penetration and may offer inherent advantages over traditional monoclonal antibodies, including pharmacokinetics (Zhong et al., 2020). Repurposing clinically available therapeutic agents like aleplasinin may require less development for transitioning to an approved drug within a clinical setting. One study suggested this was an ideal approach for developing compounds with

reduced overall costs and shorter timelines required for clinical settings than *de novo* drug development (Fu et al., 2022). Additionally, although this was the first instance of repurposing aleplasinin for its possible therapeutic potential as an anti-cancer agent in CRC, repurposing available drug compounds for anti-cancer targeting is not new. The therapeutic potential of drug compounds that are not anti-cancer agents has shown success in patient response and are either FDA-approved or are in clinical trials for treating various malignancies (Sleire et al., 2017). Some examples included Pitavastatin (NCT05977738), a cholesterol inhibitor, and Posaconazole (NCT04825275), an antifungal medication that was both repurposed for treating glioblastomas. In contrast, drug compounds such as metformin, a diabetic therapeutic agent, reported successful patient response as an adjunct therapy in several tumour types (Schein, 2021), and utilised in several clinical trials (NCT01529593, NCT05929495, NCT01632020) for multiple malignancies including CRC. Thus, characterising the therapeutic potential of aleplasinin on CRC progression may pave the way for its transition as an anti-cancer therapeutic agent.

4.4.2 Enrichment analysis of *SIGLEC15* in CRC progression

Elucidating the relevance of signalling pathways associated with CRC progression and the expression of *SIGLEC15* identified the enrichment of several tumour hallmarks.

Upregulated enrichment of tumour hallmarks revealed EMT, myogenesis, adipogenesis and p53. Adipogenesis is referred to as the process by which mesenchymal stem cells are differentiated into adipocytes through a series of signalling transduction pathways (Ambele et al., 2020). Particularly relating to CRC progression, the increased lipid storage of adipocytes is utilised as energy storage sites for the metabolic regulation of solid tumours (Han et al., 2023). Moreover, it was reported that the interplay between adipogenesis related genes stimulated EMT and enhanced glycolytic metabolism, both of which were associated with CRC metastasis (Holowatyj et al., 2020). Our findings, which also highlighted EMT and adipogenesis in the enrichment analysis, suggested CRC progression is facilitated by enhanced EMT and the interplay of adipogenesis related genes. Additionally, myogenesis is referred to as the process of the formation of skeletal muscle tissue from the fusion of precursor myoblasts (Bentzinger et al., 2012). However, the correlation between myogenesis and CRC development remains limited. Nevertheless, previous reports have suggested myogenesis plays a role in cachexia-associated CRC development (Ruan et al., 2023). Cachexia-associated CRC is defined as a metabolic syndrome that is characterised by increased skeletal muscle loss and/or

loss of fat deposits in CRC patients (Dunne et al., 2024). In particular, cachexia-associated CRC was correlated with chronic inflammation induced via stimulated pro-inflammatory cytokine IL-6 production (Chovsepian et al., 2023). It was previously reported that Siglec-15 induced genes related to the tumoral recruitment of TAMs via a pro-inflammatory TME, emphasising IL-6 to play a key role in the differentiation and activation of the polarised tumour associated phenotype (Wang et al., 2023). Hence, it may be inferred that Siglec-15 activity stimulated IL-6-mediated tumoral recruitment in cachexia-associated CRC and signalling pathways, including myogenesis. Conversely, the role of p53 and *SIGLEC15* in CRC development is unclear. However, a previous report identified low *SIGLEC15* expression correlated with upregulated p53 signalling in breast cancer (Cao et al., 2022). As PD-L1 and Siglec-15 share mutually exclusive expression in cancer cell populations, Siglec-15^- tumour cells may experience greater intracellular p53 signalling (Cho et al., 2020). In contrast, tumour hallmarks that were downregulated in CRC progression with regard to *SIGLEC15* expression demonstrated enrichment of MYC, E2F and other biological processes. MYC is a deregulated oncogene in several malignancies and a promising therapeutic target in CRC (Tan et al., 2022). In particular, MYC was identified as one of the oncogenes capable of regulating glycosylation of tumour cells. MYC regulates the production of Siglec ligands responsible for suppressing myeloid cell activation and stimulating immunosuppression (Gabay et al., 2014). As MYC is associated with downregulated genes in the enrichment analysis, this suggested that another oncogene, such as *KRAS,* could rescue the glycosylation and synthesis of Siglec ligands. One previous study reported that $KRAS^{G12D}$ mutations stimulate the levels of protein glycosylation and activate pro-tumorigenic signalling pathways, including MAPK and MYC (Zhang et al., 2023). Furthermore, *KRAS* deregulation is a key predictor in CRC onset and progression (Jančík et al., 2010). Additionally, it was previously reported that MYC also stimulated N-glycan branching in COAD tumours (Sakuma et al., 2012). However, in this context, MYC is a driver of ST6GalNAc4 expression, a key sialyltransferase responsible for the production of the disialyl-T antigen, a ligand for Siglec-7 (Smith et al., 2023). The key difference between both the disialyl-T antigen and the STn antigen is the further addition of a Neu5Ac residue to the already sialylated STn antigen (Dimitroff, 2015). However, the downregulated enrichment of MYC suggests decreased production of sialoglycan ligands such as disialyl-T antigen following abnormal *SIGLEC15* expression. It may infer that oncogenes such as MYC are reduced in Siglec-15^+ tumours, and the overexpression of *KRAS* is more likely to synthesise the STn antigen. It was also reported that sialylation pathways were negatively associated with E2F targets (Wu et al., 2023). Several malignancies, including CRC, have demonstrated E2F

transcription factors regulate downstream pro-tumorigenic signalling pathways, including the AKT/PI3K signalling pathway (Xu et al., 2021). However, the direct correlation between Siglec-15 and E2F has not been elucidated. It could suggest that other transcription factors/oncogenes are likely involved in transcriptional regulation, such as *KRAS*, a prominent oncogene in CRC progression and also in dysregulated glycosylation, as mentioned in chapter 2.

4.4.3 Aleplasinin cytotoxicity on tumour cell characteristics *in vitro*

Aleplasinin demonstrated a dose-dependent cytotoxicity in reducing cellular viability in both *in vitro* cell lines, highlighted by the IC_{50} values of 57.38μM and 38.31μM. Aleplasinin also demonstrated greater efficacy of 90.4% and 91.6% cellular death than the positive control cisplatin. It was reported that Siglec-15 expression is highly prevalent in CRC progression, suggesting aleplasinin may be capable of disrupting the Siglec-15/Sia axis in tumour proliferation and progression (Lu et al., 2023). Additionally, further elucidation of the role of aleplasinin on normal epithelial cells would highlight its safety profile as a potential treatment alternative when compared to conventional anti-cancer agents such as cisplatin. In recent years, FDA-approved chemotherapeutic agents, including cisplatin and oxaliplatin, have been heavily used in CRC, which suffers from significant consequences such as adverse effects on neighbouring cells/tissues (Wu et al., 2022). Furthermore, there was significant inhibition of cellular migration and colonisation following aleplasinin treatment over 48h. These are key clinicopathological characteristics commonly associated with tumour progression and advanced clinical tumour stage (Chen et al., 2020). Hence, aleplasinin demonstrated its effectiveness in limiting CRC metastasis. There are subtle differences between HCT116 and SW480 cells in their pathological characteristics. Whilst SW480 cells are categorised as COAD tumours, HCT116 cells have a colorectal carcinoma morphology, which exhibits greater metastatic and proliferative potential (Depciuch et al., 2020). Furthermore, HCT116 cells were reported to have the highest migratory behaviour in comparison to other metastatic cell lines, including SW620 cells (Brás et al., 2022). Similarly, another study demonstrated SW480 and HCT116 cells to have significant migratory activity over 72h due to both cell lines possessing enhanced EMT states (Druzhkova et al., 2020). This suggested that regardless of the metastatic potential of possible CRC tumours that are diagnosed, aleplasinin can exert significant inhibition on the migratory and colonisation ability of malignant tumour cells. Conversely, *SIGLEC15* GSEA analysis revealed the enrichment of EMT in relation to CRC tumour

hallmarks, suggesting a possibility of inducing CRC progression and migration. Significantly impacting *SIGLEC15* expression via aleplasinin exposure may be a consequence of reduced migration by 48h and inhibiting EMT. Typically, EMT plays a significant role in wound healing and restoring epithelial cell integrity upon responding to cellular damage and inflammation (Mittal, 2018). To highlight this, EMT is discerned through the activity of several EMT translational factors, including SNAIL, the activity of miRNAs as well as other epigenetic modifications (Hong et al., 2022). In the context of tumour progression, EMT promotes metastatic properties, enabling tumour cells to exhibit characteristics that are epithelial and mesenchymal in a transition state for better cellular survival and induce migration to secondary organ sites (Hong et al., 2022). Exploring the impact of EMT markers following *SIGLEC15* inhibition may underline specific pathways related to Siglec-15 mediated CRC progression.

4.4.4 Aleplasinin induced apoptosis in CRC cells

As observed in the functional assays, cellular death analyses via AO/EB and nuclear fragmentation staining suggested that aleplasinin treatment stimulated apoptotic signalling pathways similar to other anti-cancer agents and possibly induced the production of apoptotic markers (Ranasinghe et al., 2022). Several other compounds have initiated the activation of apoptosis in CRC following treatment. A small molecule inhibitor targeting karyopherin β1 (Kpnβ1) stimulated apoptosis in cancer cells and induced cell cycle arrest (Ajayi-Smith et al., 2021). Thus suggesting aleplasinin is a potent small molecule inhibitor. In addition, AO/EB staining revealed a larger proportion of red-stained cells following aleplasinin treatment, possibly indicating the occurrence of necrosis. The differences between AO/EB staining could suggest variations in apoptotic signalling pathways between both cell lines, underlined by molecular and pathophysiological characteristics between HCT116 and SW480 cells (Galluzzi et al., 2018). As previously mentioned in Chapter 3, SW480 cells have persistent p53 mutant characteristics, which are not observed in HCT116 cells. Additionally, HCT116 differs from SW480 cells by exhibiting positive expression for induced TGFβ1 and TGFβ2 expression (Yeung et al., 2010). There is a greater likelihood of p53 independent apoptosis pathways occurring in SW480 cells, as mentioned in Chapter 3. However, within HCT116 cells, p53 dependent apoptosis activation is possible. There are two distinct pathways of p53-mediated apoptosis induction. Firstly, the intrinsic pathway is regulated by the activity of Bcl-2 that triggers the activation of cell death effectors Bcl-2 associated X, apoptosis regulator (BAX)

and Bcl-2 antagonist/killer 1 (BAK), which permeabilise the outer membrane of mitochondria for cell death by caspases (Aubrey et al., 2018). This pathway primarily becomes activated upon external stress conditions. In contrast, the extrinsic pathway involves the activation of TNF receptors that possess an intracellular death domain (Czabotar et al., 2014). The initiation of the extrinsic pathway relies on the recruitment of caspase-8, which triggers a signalling cascade with other caspases (caspase-3, caspase 7) for effective apoptosis (Jost et al., 2009). As seen in our findings, aleplasinin exerts a concentration-dependent effect on nuclear fragmentation, an indication of DNA damage and a stress stimulus that consequently resulted in cellular death (Borges et al., 2008). Thus, this suggested that the activation of the intrinsic pathway may be the mechanism for apoptotic initiation. However, to confirm this, experimental validation of the expression of key proteins associated with the intrinsic pathway may underline some mechanistic insights. Key intrinsic apoptotic markers that would be evaluated for this pathway could include BH3-domain proteins (BH3 domains are short peptide motifs that trigger mitochondrial associated apoptosis) such as Bcl-2 interacting mediator of cell death (BIM) and Bcl-2 associated agonist of cell death (BAD) (Czabotar et al., 2014). Additionally, the activation of caspases such as caspase-9 can trigger the activation of other caspases that are also involved in the permeabilisation of the mitochondria (Li et al., 2017). Therefore, it may be worth considering the expression of known caspases and their inactivated non-cleaved counterparts following aleplasinin exposure.

4.4.5 RNA Illumina sequencing analysis revealed DE genes

Comparisons between aleplasinin treated and untreated conditions following 48h treatment period emphasise numerous DE genes, including *ACSL6* and *SPRR2D,* as the most significantly downregulated and upregulated. It was previously reported that *ACSL6* has been documented as a potential oncogene in CRC progression (Angius et al., 2019; Huang et al., 2018). Moreover, *in silico* analysis revealed its upregulated expression profile in the CRC tumour cohort and high expression is associated with reduced overall survival outcomes. It was demonstrated that *ACSL6* plays a key role in the stimulation of lipid biosynthesis, facilitating both cancer metabolism and cell proliferation (Quan et al., 2021). Cellular exposure to aleplasinin could underline the regulation of key metabolic pathways associated with tumour metabolism and outline *ACSL6* as a therapeutic target in CRC progression. Conversely, the other gene target that displayed the most significantly upregulated expression via RNA Illumina sequencing was *SPRR2D.* The role of *SPRR2D* in CRC progression remains limited

within the literature. Additionally, *in silico* and RT-qPCR methods revealed no significant difference in the expression of *SPRR2D* between normal and malignant tissues alongside treated and untreated conditions. Further investigation into the role of *SPRR2D* is warranted to elucidate its role in aleplasinin-mediated cytotoxicity.

4.4.6 RNA Illumina sequencing analysis revealed the enrichment of Wnt signalling

Enrichment of biological processes from KEGG analysis identified transcriptional regulation and Wnt signalling pathways following aleplasinin exposure. Additionally, GO associated molecular functions also revealed the enrichment of DNA binding, transcriptional factor activity, nucleic acid binding and Wnt receptor activity. Thus, suggesting Wnt signalling and transcriptional regulation as promising mechanisms of action mediated by aleplasinin treatment. The canonical Wnt/β-catenin is heavily characterised by the binding of the Wnt ligand to LDL receptor related protein 5 and protein 6 (LRP5/6) core receptors and frizzled (FZD) proteins (Shi et al., 2017). Under normal homeostasis, β-catenin is phosphorylated by a protein complex comprised of glycogen synthase kinase 3β (GSK3β), casein kinase I (CKI) and APC. This complex is also further structurally supported by the role of axin (Tewari et al., 2021). The phosphorylation of β-catenin by GSK3β and the activity of APC directs the β-catenin protein to ubiquitin mediated proteolysis in the cytoplasm (Zhao et al., 2022). The dysregulation of the Wnt signalling pathway is also reported in the development of multiple malignancies, including CRC (Bian et al., 2020). Moreover, the signalling pathway is reliant on over-accumulated β-catenin nuclear translocation and stimulation of Wnt target genes via the binding with transcription factor T cell factor/lymph enhancer factor 1 (TCF/LEF1) (Bugter et al., 2021). Furthermore, it was suggested that the deregulation of specific genes in the Wnt/β-catenin pathway, including GSK3β and APC, play a significant role in the development of colitis-associated CRC (Foersch & Neurath, 2014). Several genes display a loss of function, including APC in CRC progression, and Wnt/β-catenin signalling could be viewed as a possible regulatory mechanism for CRC onset. In particular, Axin2 and ring finger protein 43 (RNF43) that functionally prevent the binding of Wnt ligands have downregulated expression in IBD-related CRC tumours. Additionally, the crosstalk with NFkB may also play a role in colitis-associated CRC progression. The dishevelled segment polarity protein 2 (Dvl2) is a key adapter molecule in Wnt/β-catenin signalling, and upon binding with the c-terminal side of TNFR1, can induce TNFR1 endocytosis inhibiting NFkB (Tang et al., 2022). This led to the stimulation of colitis-associated CRC. Our findings suggested the stimulation of Wnt tumour

suppressor genes following aleplasinin exposure as a possible regulatory axis in inhibiting CRC progression, particularly relating to inflammation-mediated CRC tumours. However, no specific inflammatory markers were experimentally elucidated. It may provide further insights into the role of aleplasinin treatment in CRC tumours.

4.4.7 Induced lipid metabolism via Wnt signalling is a possible mechanism in CRC progression

Further elucidation of ACSL6's role in lipid metabolism may outline further targets involved in functional regulation. The development of the GeneMANIA gene and STRING PPI frameworks revealed direct interactions with CPT1A and FASN. It was demonstrated that FASN plays a key role in *de novo* lipogenesis and is important in the production of palmitate derived from acetyl-coenzyme A (CoA) and malonyl-CoA in the presence of NADPH (Fhu & Ali, 2020). Particularly in the CRC landscape, abnormal expression patterns of FASN have correlated with tumour onset, playing a role in reduced sensitisation to treatment (Han et al., 2023; Jin et al., 2021). The interactions between FASN and ACSL6 in lipid metabolism pathways are suggested to facilitate the activation of fatty acids for stimulating metabolic activity and enhancing cellular energy efficiency. Thus, this suggested the stimulation of cellular survival and proliferation of tumour cells. In addition, the role of FASN activity was identified in regulating CRC metastasis via modulation of the Wnt signalling pathway (Fhu & Ali, 2020). Similarly, this was also demonstrated in another study, which reported that upregulated FASN expression was associated with enhanced CDK8 and β-catenin activity (Firestein et al., 2010). This may underline a possible regulatory mechanism that is directed through downregulated *ACSL6* mediated Wnt signalling. As part of lipid metabolism, CPT1A was shown to play an important role in the transport and oxidation of fatty acid chains (Wang et al., 2018). Similarly to *ACSL6*, the expression profile of *CPT1A* is upregulated in CRC tumours by facilitating the enhanced growth of adipocytes (Xiong et al., 2020). Moreover, it was reported that CPT1A overexpression in cervical cancer tumours enhanced Wnt signalling and subsequent β-catenin nuclear translocation (Liu et al., 2024). Hence, this suggests a similar mechanism may be involved in CRC tumour onset. From these findings, the CPT1A/ACSL6/FASN axis is possibly implicated in CRC progression via deregulated lipid metabolism pathways that are essential for enhanced tumour proliferation and cellular survival.

4.4.8 Future directions

The findings from chapter 4 provided the characterisation of the aleplasinin compound on Siglec-15$^+$ CRC cells. However, further characterisation of aleplasinin is required before its transition to a clinical setting, primarily elucidating its safety profile with regard to normal epithelial cells. From this, it will present a clearer image for feasibly repurposing currently available small molecule inhibitors. Additionally, elucidation of EMT and inflammatory markers may underline mechanistic signalling pathways, including Wnt/β-catenin signalling that are affected by aleplasinin treatment. Highlighting the interactions between the let-7a-5p/*ACSL6* axis through knockdown studies and miRNA mimics for normalised miRNA expression would validate *ACSL6* as a direct target that is implicated in CRC progression. Furthermore, the ASCL6/CPT1A/FASN crosstalk may provide insights into the role of ACSL6 and lipid metabolism to play a role in CRC progression, but further experimental validation is required to emphasise the roles of CPT1A and FASN in the lipid metabolism pathway. These interactions may outline the enhanced synthesis, storage, uptake and breakdown of lipids in facilitating tumour progression (Fu et al., 2021). The clarification of lipid signatures taken in lipid metabolic panels may prove useful as a diagnostic tool and predictor for CRC tumour onset and progression (Zhou et al., 2022). Similarly, the characterisation of aleplasinin using PDX murine models may underline the clinical efficacy of aleplasinin and highlight its therapeutic window and any adverse systemic effects before transitioning to human patients. In addition, the requirement of CRC *in vivo* data is essential to emphasise aleplasinin's specificity for Siglec-15 targeting in murine models. Comparative studies in other tumour models could also elucidate whether aleplasinin demonstrates selectivity for CRC tumours or provides cytotoxicity for a broader application in various Siglec-15$^+$ tumours. The role of aleplasinin in mediating immune function was not tested. Hence, aleplasinin exposure of immune effector and regulatory cells, including CD4$^+$, CD8$^+$, and M1-polarised macrophages alongside immune response markers, including IL-2, would suggest aleplasinin regulation of immune function (Morad et al., 2021). Furthermore, co-culture experiments may highlight the activation of immune cells in the presence of tumour cells following aleplasinin exposure. Conversely, aleplasinin exposure may play a role in the inhibition of pro-tumorigenic pro-inflammatory markers such as TNFα would be validated by ELISA experiments. Additionally, a large proportion of patients develop resistance to therapies, resulting in reduced patient survival. Utilising aleplasinin against treatment resistant cells may inhibit tumour progression

and can be used alternatively in resistant tumours (Dong et al., 2022). Ultimately, these further studies would significantly improve the characterisation of aleplasinin as an anti-cancer agent.

4.5 Conclusion

In conclusion, this chapter elucidated the primary testing of aleplasinin's cytotoxic profile in CRC cell lines as a possible Siglec-15 inhibitor. Our findings have proven significant dose-dependent cytotoxicity *in vitro* and highlighted the possible involvement of the let-7a-5p/*ACSL6* axis in CRC progression. Additionally, aleplasinin treatment may induce apoptotic signalling in a p53-independent manner. However, there may be variations in signalling pathways due to the characteristic differences associated with SW480 and HCT116 cells. *In silico* prediction targets have elucidated the roles of CPT1A and FASN, both of which are previously implicated in CRC progression. From our *in silico* and RNA Illumina sequencing findings, the ASCL6/CPT1A/FASN crosstalk may play a role in deregulated Wnt signalling and suggested lipid metabolism as a unique driver of CRC tumour progression. Additional experimental validation and *in vivo* studies will further optimise aleplasinin's efficacy and toxicological profile for utilisation as a treatment alternative to currently available anti-cancer agents. Nevertheless, the work in this chapter has addressed a novel approach for repurposing clinically available small molecule inhibitors for Siglec-15 targeting the treatment of solid CRC tumours.

Chapter 5 - Final Discussion

Over the past several decades, the prevalence of CRC has consistently risen worldwide, escalating the number of patient mortalities. CRC has displayed distinct age and sex distribution patterns across each of the molecular CRC subtypes. The accumulation of sporadic mutations appear much more frequently in an aging population, with typical mutations in *APC*, *KRAS* and *TP53* all of which are commonly associated with CRC tumour onset (Zaki et al., 2022). Similarly, delayed diagnosis and late screening of adenomatous polyps and early-stage CRC tumours can allow initial tumours to progress over a number of years to advanced disease stages leading to high mortality rates. Although most CRC diagnoses are commonly associated with older patients, increased trends in EO-CRC and the highly heterogeneous nature of the tumours themselves pose a substantial risk. In particular, males have more frequent diagnoses in comparison to their female counterparts in MSI type tumours (Massat et al., 2013). Similarly, anatomical distribution of CRC tumours can vary between males and females. In males, the distribution of CRC tumours are more likely to be present in the rectum and distal colon, whilst females are more prone to tumours manifesting in the proximal region of the colon (White et al., 2018). Hence, are often left misdiagnosed/undiagnosed. Although this study has greatly focused on the greater population of patients that are typically diagnosed with CRC, and the *in vitro* cell models utilised as part of the experimental work to reflect this. The future studies implementing this work would greatly benefit from the inclusion of other cell models that stem from patients such as those that are derived from EO-CRC patients and female patients as well. From this inclusion, there can be a better understanding of the age and sex distribution of CRC tumours following the alternative Siglec-15 targeting treatment approaches as proposed in this study.

The current literature has emphasised the targeting of immune checkpoint proteins, including PD-1, PD-L1, LAG-3 and CTLA-4 for effective anti-cancer immune response. As the emerging immune checkpoint protein in cancer, Siglec-15 has demonstrated abnormal expression in malignancies as observed in the literature and our findings (Mustafov, Ahmad, et al., 2024). However, very little is known about the oncogenic role of Siglec-15 and the Siglec-15/Sia axis in CRC as a whole. For current conventional immunotherapeutic treatments, it is typically comprised of monoclonal blocking antibodies that prevent Siglec-15 interaction with the STn antigen. However, there is now an unmet clinical need for the development of novel targeted therapeutic strategies that effectively treat CRC tumours. To address this aspect, this study has primarily focused on elucidating oncogenic cellular signalling pathways that are involved in CRC progression and how they are affected following Siglec-15 targeting. By

highlighting the mechanisms that are potentially involved, it would identify new therapeutic targets that may operate independently or synergistically with Siglec-15 in CRC tumours. The rationale for this study emphasised targeting Siglec-15 with novel, effective therapies and the disruption of the Siglec-15/Sia axis in CRC tumours. This disruption aimed to also elucidate miRNA activity following treatment exposure and explore these compounds as treatment alternatives (Mustafov, Ahmad et al., 2024). Inhibiting the binding of the STn antigen would effectively enable T-cell activation and generation of an immune response in an immunological capacity whilst its inhibiting its oncogenic function will prevent tumour proliferation and progression in CRC tumours.

Firstly, a multiomics approach characterised the multifaceted roles of sialyltransferases involved in the production of the STn antigen, the putative ligand of Siglec-15, as part of the findings in chapter 2 (M. S. Ahmad et al., 2024). Engagement of the STn antigen with Siglec-15 inhibits the activation of T-cells, preventing the generation of an effective immune response against the tumour cells. The sialyltransferases ST6GalNAc1 and ST6GalNAc2, key enzymes in the glycan biosynthesis pathway, synthesise the STn antigen upon sialylation of the Tn antigen. Moreover, the roles of ST3GalIV and ST6GalI also play significant roles in the synthesis of N- and O-glycans and were suggested to be involved in sialylation modifications. Hence, elucidating the regulatory mechanisms of key sialyltransferases to inhibit the production of the STn antigen suggested a possible therapeutic approach in inhibiting Siglec-15^{+} CRC tumours. Thus, this would highlight their potential as therapeutic targets. Herein, we established the expression profiles of the investigated sialyltransferases in CRC and elucidated the impact of miRNAs on their regulation, a key research question that was posed as part of this investigation. From our investigation, we established candidate miRNAs miR-21, miR-30e and miR-26b to be involved in regulating *ST6GALNAC1* expression. Similarly, miR-588 was identified for *ST6GALNAC2* regulation, albeit the transcriptomics database utilised for this study contained no information regarding the miRNA expression profile. In addition, let-7g and miR-98 was predicted to regulate *ST3GAL4*, whilst miR-484, miR-125a and miR-125b was highlighted for *ST6GAL1* regulation. These miRNAs all displayed various oncogenic and tumour suppressor expression profiles and were predicted to have a high binding affinity towards their corresponding target gene. Furthermore, the common miRNA candidates were demonstrated to relate with other interacting sialyltransferases and also exhibited high binding affinities including hsa-miR-199a-5p and hsa-miR-665 for the four sialyltransferases that were investigated and miR-147 for *C1GALT1* and *COSMC*, both of which are influential in the

synthesis of the precursor molecule of the STn antigen. We also established the role of the sialyltransferases in their contribution to CRC tumour heterogeneity. Immunohistochemistry analysis revealed low ST6GalNAc1 expression in CRC patient tissues, indicating STn production is independent of ST6GalNAc1 activity, which may be rescued by the activity of other sialyltransferases. Thus, our findings suggested that inhibiting these sialyltransferases could inhibit the production of the STn antigen. Ultimately, it is believed that with further development, validation and exploration of these miRNAs and their regulatory mechanisms of the query sialyltransferases, there is a greater potential of targeting sialyltransferases for overall disruption of the Siglec-15/Sia axis.

The interaction of Siglec-15 and the STn antigen relies on direct binding with the R143 residue located in the V-set binding domain. However, the development of small molecule inhibitors for Siglec-15 targeting is currently unexplored, and existing conventional treatments, such as cisplatin, exhibit significant adverse effects on cells/tissues throughout the body. Therefore, the utilisation of β-amino carbonyl compounds as treatment alternatives for Siglec-15^{+} tumours was suggested as an effective therapeutic option for investigation. Herein, we aimed to elucidate the cytotoxic profile of the SHG-8 compound on CRC cell lines as a potential small molecule inhibitor for Siglec-15, as part of the findings in chapter 3 (Ahmad et al., 2023). Our findings emphasised the dose-dependent cytotoxicity of SHG-8 *in vitro* and is ability to induce apoptosis. Conversely, sRNA-seq analysis following SHG-8 treatment revealed the DE of 185 miRNAs, particularly the most significant miRNA upregulation as miR-6715b-3p and the direct targeting of *PTTG1IP*, a possible oncogene in CRC. Further analysis demonstrated the miR-6715b-3p/*PTTG1IP* axis as a potential mechanism in CRC progression. Our research questions stemmed from the possibility of SHG-8 binding to the V-set domain, and our findings suggested that SHG-8 could act as a Siglec-15 small molecule inhibitor. Moreover, compared to conventional anti-cancer agents, SHG-8 displayed reduced cytotoxicity against normal colonic epithelial cells, emphasising its potential as a treatment alternative to platinum-based therapeutic agents. The evidence presented in chapter 3 highlighted the impact of SHG-8 as an anti-cancer agent, showing sufficient promise as a therapeutic strategy. This paves the way for the novel development of small molecule inhibitors targeting Siglec-15 following the development and characterisation of β-amino carbonyl compounds. As discussed in Chapter 3, future directions for SHG-8 as a Siglec-15 inhibitor will focus on further characterising its

efficacy and safety profiles prior to transitioning to clinical settings. It is hoped that there will be a shift from conventional agents to more optimised therapies.

Similarly, other approaches for developing inhibitors targeting Siglec-15 were also evident. Repurposing available small molecule inhibitors for off-label treatment has proven effective in various pathologies and, therefore, poses as a feasible strategy for Siglec-15^+ tumours due to their already characterised safety profiles. In addition, several advantages signify small molecule inhibitors as effective anti-cancer agents, including their small size and pharmacokinetic profiles. Moreover, repurposing available therapeutic agents reduces costs and timelines compared to *de novo* drug development. Our virtual screening of therapeutic compounds revealed aleplasinin as having significant binding affinity to the V-set domain of Siglec-15, highlighting its potential as a small molecule inhibitor. Hence, we aimed to repurpose aleplasinin, an Alzheimer's disease therapeutic agent, as a treatment alternative in cancer and as a potential small molecule inhibitor of Siglec-15, as part of the findings in chapter 4 (Ahmad et al., 2024b, *in press*). Our research focused on characterising the cytotoxicity of aleplasinin *in vitro*, which demonstrated low IC_{50} values in SW480 and HCT116 cells. Furthermore, aleplasinin exposure induced the DE of gene targets, particularly the oncogene *ACSL6* and the enrichment of the Wnt/β-catenin signalling pathway, the latter being frequently associated with CRC progression. Further analysis revealed *ACSL6* as a target of let-7a-5p alongside the interplay of CPT1A and FASN, key proteins involved in lipid metabolism. These findings suggested that the tumour suppressor let-7a-5p becomes deregulated in CRC progression, highlighting the relevance of lipid metabolism pathways in CRC development. The CPT1A/ACSL6/FASN crosstalk and the let-7a-5p/*ACSL6* axis highlighted possible mechanisms associated with CRC progression identifying let-7a-5p and these proteins as potential therapeutic targets. In addition, the cytotoxic profile of aleplasinin supported its feasibility as a treatment alternative targeting Siglec-15, reinforcing the likelihood of repurposing existing therapeutic agents for cancer treatment. Ultimately, we provided evidence for the development of novel, effective therapies against Siglec-15^+ CRC tumours while also identifying other possible therapeutic targets associated with CRC progression.

Our research illustrated the use of alternative treatments for Siglec-15 targeting, and the impact of miRNAs in gene regulation, as established in our findings. The evidence presented here opens new avenues for Siglec-15 inhibitors and aids in the identification of new therapeutic

strategies. As previously mentioned, the expression of Siglec-15 is mutually exclusive with PD-L1 expression, and the inhibition of one could allow the other to rescue the tumour phenotype. We anticipate that SHG-8 and aleplasinin may exhibit synergistic effects with PD-L1 antagonists in Siglec-15^+ PD-$L1^+$ tumours. The future impact of these approaches will highlight Siglec-15 inhibition for potential immune checkpoint blockade and facilitate their transition towards clinical trials for CRC tumours and other malignancies.

To conclude, the current study has emphasised the targeting of Siglec-15 with small molecule inhibitors aleplasinin and SHG-8 in CRC tumours and the overall disruption of the Siglec-15/Sia axis. Through extensive *in vitro* experimentation and in line with the literature, this study underlined the oncogenic role of Siglec-15, primarily its involvement in cellular viability and proliferation. This research has provided further insights into the complexities of Siglec-15 and identified novel therapeutic targets that may work synergistically or independently with Siglec-15 in CRC tumour progression. Through cytotoxic functional assays, the small molecule inhibitors demonstrated the inhibition of pro-tumorigenic characteristics that are frequently associated with Siglec-15 including cellular viability, migration and colonisation with *in vitro* cell models SW480 and HCT116. These findings support their proposed use as viable treatment alternatives to current conventional therapies in CRC management. Moreover, our observations suggested that sialyltransferases involved in STn production may serve as therapeutic targets particularly ST6GalNAc1 and ST6Gal1, and regulatory mechanisms associated with their expression require further exploration. In particular, transfected cell models with antagomirs of identified miRNAs including miR-21 could underline the sialyltransferase gene expression profiles, and confirm whether they are involved in sialyltransferase regulation.

A critical aspect of this study was to explore the role of miRNAs in the Siglec-15/Sia axis and their function in regulating gene expression following treatment. This research elucidated specific miRNAs involved in gene regulation of sialyltransferases functionally active in glycan biosynthesis. Conversely, miRNAs were demonstrated for direct targeting of identified deregulated gene targets in CRC progression such as *PTTG1IP* and *ACSL6*, offering miRNA-based therapeutic strategies for Siglec-15^+ CRC tumours. Thus, this underlined novel targets that also serve as biomarkers for CRC progression. Furthermore, the combination of small molecule inhibitors and PD-L1 antagonists and/or miRNA-based treatments may exhibit synergistic effects and require further investigation. Additional mechanistic studies are needed

to further characterise the efficacy and safety profiles of SHG-8 and aleplasinin before transitioning to clinical trials such as the utilisation of *in vivo* murine models as highlighted previously. Addressing challenges related to dosing and off-target effects in pre-clinical/clinical trials would highlight any long-term implications. Ultimately, this study expanded the therapeutic landscape of Siglec-15^{+} tumours and would help facilitate the development of further inhibitors for Siglec-15 targeting, significantly advancing the field of oncology.

References

Ahmad, I., Shagufta, Dhar, R., Hisaindee, S., & Hasan, K. (2021). An Environmentally Benign Solid Acid Nanocatalyst for the Green Synthesis of Carboxylic Acid Ester. *ChemistrySelect*, *6*(36), 9645–9652. https://doi.org/10.1002/slct.202102230

Ahmad, M. S., Braoudaki, M., Patel, H., Ahmad, I., Shagufta, & Siddiqui, S. S. (2023a). Novel Siglec-15-Sia axis inhibitor leads to colorectal cancer cell death by targeting miR-6715b-3p and oncogenes. *Frontiers in Immunology*, *14*, 1254911. https://doi.org/10.3389/fimmu.2023.1254911

Ahmad, M. S., Braoudaki, M., Patel, H., Ahmad, I., Shagufta, & Siddiqui, S. S. (2023b). Novel Siglec-15-Sia axis inhibitor leads to colorectal cancer cell death by targeting miR-6715b-3p and oncogenes. *Frontiers in Immunology*, *14*, 1254911. https://doi.org/10.3389/fimmu.2023.1254911

Ahmad, M. S., Braoudaki, M., & Siddiqui, S. S. (2024). Differential expression of ST6GALNAC1 and ST6GALNAC2 and their clinical relevance to colorectal cancer progression. *PLOS ONE*, *19*(9), e0311212. https://doi.org/10.1371/journal.pone.0311212

Ajayi-Smith, A., Van Der Watt, P., Mkwanazi, N., Carden, S., Trent, J. O., & Leaner, V. D. (2021). Novel small molecule inhibitor of Kpnβ1 induces cell cycle arrest and apoptosis in cancer cells. *Experimental Cell Research*, *404*(2), 112637. https://doi.org/10.1016/j.yexcr.2021.112637

Alabiad, M., Harb, O., Abozaid, M., Embaby, A., Mandour, D., Hemeda, R., & Shalaby, A. (2021). The Diagnostic and Prognostic Roles of Combined Expression of Novel Biomarkers in Lung Adenocarcinoma (LUAD) and Lung Squamous Cell Carcinoma (LUSC); An Immunohistochemical Study. *Iranian Journal of Pathology*, *16*(2), 162–173. https://doi.org/10.30699/ijp.2020.130944.2452

Alcindor, T., & Beauger, N. (2011). Oxaliplatin: A Review in the Era of Molecularly Targeted Therapy. *Current Oncology*, *18*(1), 18–25. https://doi.org/10.3747/co.v18i1.708

Ali, S. R., Fong, J. J., Carlin, A. F., Busch, T. D., Linden, R., Angata, T., Areschoug, T., Parast, M., Varki, N., Murray, J., Nizet, V., & Varki, A. (2014). Siglec-5 and Siglec-14 are polymorphic paired receptors that modulate neutrophil and amnion signaling responses to group B *Streptococcus*. *Journal of Experimental Medicine*, *211*(6), 1231–1242. https://doi.org/10.1084/jem.20131853

Almaraz, R. T., Tian, Y., Bhattarcharya, R., Tan, E., Chen, S.-H., Dallas, M. R., Chen, L., Zhang, Z., Zhang, H., Konstantopoulos, K., & Yarema, K. J. (2012). Metabolic Flux Increases Glycoprotein Sialylation: Implications for Cell Adhesion and Cancer Metastasis. *Molecular & Cellular Proteomics*, *11*(7), M112.017558-1-M112.017558-12. https://doi.org/10.1074/mcp.M112.017558

Al-Sohaily, S., Biankin, A., Leong, R., Kohonen-Corish, M., & Warusavitarne, J. (2012). Molecular pathways in colorectal cancer. *Journal of Gastroenterology and Hepatology*, *27*(9), 1423–1431. https://doi.org/10.1111/j.1440-1746.2012.07200.x

Ambele, M. A., Dhanraj, P., Giles, R., & Pepper, M. S. (2020). Adipogenesis: A Complex Interplay of Multiple Molecular Determinants and Pathways. *International Journal of Molecular Sciences*, *21*(12), 4283. https://doi.org/10.3390/ijms21124283

Anderson, K. E., Stevenson, M., Varghese, R., Hebron, M. L., Koppel, E., McCartin, M., Kuprewicz, R., Matar, S., Ferrante, D., & Moussa, C. (2022). Alteration of Autophagy and Glial Activity in Nilotinib-Treated Huntington's Disease Patients. *Metabolites*, *12*(12), 1225. https://doi.org/10.3390/metabo12121225

André, T., Shiu, K.-K., Kim, T. W., Jensen, B. V., Jensen, L. H., Punt, C., Smith, D., Garcia-Carbonero, R., Benavides, M., Gibbs, P., De La Fouchardiere, C., Rivera, F., Elez, E., Bendell, J., Le, D. T., Yoshino, T., Van Cutsem, E., Yang, P., Farooqui, M. Z. H., … Diaz, L. A. (2020). Pembrolizumab in Microsatellite-Instability–High Advanced Colorectal Cancer. *New England Journal of Medicine*, *383*(23), 2207–2218. https://doi.org/10.1056/NEJMoa2017699

Angata, T. (2020). Siglec-15: A potential regulator of osteoporosis, cancer, and infectious diseases. *Journal of Biomedical Science*, *27*(1), 10. https://doi.org/10.1186/s12929-019-0610-1

Angata, T., Tabuchi, Y., Nakamura, K., & Nakamura, M. (2007a). Siglec-15: An immune system Siglec conserved throughout vertebrate evolution. *Glycobiology*, *17*(8), 838–846. https://doi.org/10.1093/glycob/cwm049

Angata, T., Tabuchi, Y., Nakamura, K., & Nakamura, M. (2007b). Siglec-15: An immune system Siglec conserved throughout vertebrate evolution. *Glycobiology*, *17*(8), 838–846. https://doi.org/10.1093/glycob/cwm049

Angius, A., Uva, P., Pira, G., Muroni, M. R., Sotgiu, G., Saderi, L., Uleri, E., Caocci, M., Ibba, G., Cesaraccio, M. R., Serra, C., Carru, C., Manca, A., Sanges, F., Porcu, A., Dolei, A., Scanu, A. M., Cossu Rocca, P., & De Miglio, M. R. (2019). Integrated Analysis of miRNA and mRNA Endorses a Twenty miRNAs Signature for Colorectal Carcinoma.

International Journal of Molecular Sciences, *20*(16), 4067. https://doi.org/10.3390/ijms20164067

Arnold, M., Sierra, M. S., Laversanne, M., Soerjomataram, I., Jemal, A., & Bray, F. (2017). Global patterns and trends in colorectal cancer incidence and mortality. *Gut*, *66*(4), 683–691. https://doi.org/10.1136/gutjnl-2015-310912

Aßfalg, M., Güner, G., Müller, S. A., Breimann, S., Langosch, D., Muhle-Goll, C., Frishman, D., Steiner, H., & Lichtenthaler, S. F. (2024). Cleavage efficiency of the intramembrane protease γ-secretase is reduced by the palmitoylation of a substrate's transmembrane domain. *The FASEB Journal*, *38*(2), e23442. https://doi.org/10.1096/fj.202302152R

Attisano, L., & Wrana, J. L. (2002). Signal Transduction by the TGF-β Superfamily. *Science*, *296*(5573), 1646–1647. https://doi.org/10.1126/science.1071809

Aubrey, B. J., Kelly, G. L., Janic, A., Herold, M. J., & Strasser, A. (2018). How does p53 induce apoptosis and how does this relate to p53-mediated tumour suppression? *Cell Death & Differentiation*, *25*(1), 104–113. https://doi.org/10.1038/cdd.2017.169

Baba, A. B., Rah, B., Bhat, Gh. R., Mushtaq, I., Parveen, S., Hassan, R., Hameed Zargar, M., & Afroze, D. (2022). Transforming Growth Factor-Beta (TGF-β) Signaling in Cancer-A Betrayal Within. *Frontiers in Pharmacology*, *13*, 791272. https://doi.org/10.3389/fphar.2022.791272

Bader, A. G. (2012). miR-34 – a microRNA replacement therapy is headed to the clinic. *Frontiers in Genetics*, *3*. https://doi.org/10.3389/fgene.2012.00120

Bai, Q., Liu, L., Xi, W., Wang, J., Xia, Y., Qu, Y., Xiong, Y., Long, Q., Xu, J., & Guo, J. (2018). Prognostic significance of ST6GalNAc-1 expression in patients with non-metastatic clear cell renal cell carcinoma. *Oncotarget*, *9*(3), 3112–3120. https://doi.org/10.18632/oncotarget.11258

Bai, Z., Yan, C., & Chang, D. (2023). Prediction and therapeutic targeting of the tumor microenvironment-associated gene CTSK in gastric cancer. *Discover Oncology*, *14*(1), 200. https://doi.org/10.1007/s12672-023-00821-0

Bärenwaldt, A., & Läubli, H. (2019). The sialoglycan-Siglec glyco-immune checkpoint – a target for improving innate and adaptive anti-cancer immunity. *Expert Opinion on Therapeutic Targets*, *23*(10), 839–853. https://doi.org/10.1080/14728222.2019.1667977

Barkovits, K., Pfeiffer, K., Eggers, B., & Marcus, K. (2021). Protein Quantification Using the "Rapid Western Blot" Approach. In K. Marcus, M. Eisenacher, & B. Sitek (Eds.),

Quantitative Methods in Proteomics (Vol. 2228, pp. 29–39). Springer US. https://doi.org/10.1007/978-1-0716-1024-4_3

Barresi, V., Reggiani Bonetti, L., Ieni, A., Alberto Caruso, R., & Tuccari, G. (2015). Histological grading in colorectal cancer: New insights and perspectives. *Histology and Histopathology*, *30*, 1059–1067. https://doi.org/10.14670/HH-11-633

Beaman, E.-M., Carter, D. R. F., & Brooks, S. A. (2022). GALNTs: Master regulators of metastasis-associated epithelial-mesenchymal transition (EMT)? *Glycobiology*, *32*(7), 556–579. https://doi.org/10.1093/glycob/cwac014

Beckwith, D. M., & Cudic, M. (2020). Tumor-associated O-glycans of MUC1: Carriers of the glyco-code and targets for cancer vaccine design. *Seminars in Immunology*, *47*, 101389. https://doi.org/10.1016/j.smim.2020.101389

Bedard, P. L., Hansen, A. R., Ratain, M. J., & Siu, L. L. (2013). Tumour heterogeneity in the clinic. *Nature*, *501*(7467), 355–364. https://doi.org/10.1038/nature12627

Begolli, G., Marković, I., Knežević, J., & Debeljak, Ž. (2023). Carbohydrate sulfotransferases: A review of emerging diagnostic and prognostic applications. *Biochemia Medica*, *33*(3), 255–265. https://doi.org/10.11613/BM.2023.030503

Belisle, J. A., Horibata, S., Jennifer, G. A., Petrie, S., Kapur, A., André, S., Gabius, H.-J., Rancourt, C., Connor, J., Paulson, J. C., & Patankar, M. S. (2010). Identification of Siglec-9 as the receptor for MUC16 on human NK cells, B cells, and monocytes. *Molecular Cancer*, *9*(1), 118. https://doi.org/10.1186/1476-4598-9-118

Bennett, E. P., Mandel, U., Clausen, H., Gerken, T. A., Fritz, T. A., & Tabak, L. A. (2012). Control of mucin-type O-glycosylation: A classification of the polypeptide GalNAc-transferase gene family. *Glycobiology*, *22*(6), 736–756. https://doi.org/10.1093/glycob/cwr182

Bentzinger, C. F., Wang, Y. X., & Rudnicki, M. A. (2012). Building Muscle: Molecular Regulation of Myogenesis. *Cold Spring Harbor Perspectives in Biology*, *4*(2), a008342–a008342. https://doi.org/10.1101/cshperspect.a008342

Bergstrom, K., Liu, X., Zhao, Y., Gao, N., Wu, Q., Song, K., Cui, Y., Li, Y., McDaniel, J. M., McGee, S., Chen, W., Huycke, M. M., Houchen, C. W., Zenewicz, L. A., West, C. M., Chen, H., Braun, J., Fu, J., & Xia, L. (2016). Defective Intestinal Mucin-Type O-Glycosylation Causes Spontaneous Colitis-Associated Cancer in Mice. *Gastroenterology*, *151*(1), 152-164.e11. https://doi.org/10.1053/j.gastro.2016.03.039

Bernard, J. K., Bucar, E. B., Liu, C. Y., Katada, K., Washington, M. K., Schumacher, M. A., & Frey, M. R. (2023). Deletion of Endogenous Neuregulin-4 Limits Adaptive

Immunity During Interleukin-10 Receptor–Neutralizing Colitis. *Inflammatory Bowel Diseases*, *29*(11), 1778–1792. https://doi.org/10.1093/ibd/izad092

Bhaskaran, M., & Mohan, M. (2014). MicroRNAs: History, Biogenesis, and Their Evolving Role in Animal Development and Disease. *Veterinary Pathology*, *51*(4), 759–774. https://doi.org/10.1177/0300985813502820

Bian, J., Dannappel, M., Wan, C., & Firestein, R. (2020). Transcriptional Regulation of Wnt/β-Catenin Pathway in Colorectal Cancer. *Cells*, *9*(9), 2125. https://doi.org/10.3390/cells9092125

Biazik, J. M. (2010). Unlocking the ultrastructure of colorectal cancer cells *in vitro* using selective staining. *World Journal of Gastroenterology*, *16*(22), 2743. https://doi.org/10.3748/wjg.v16.i22.2743

Bien, S. A., Su, Y.-R., Conti, D. V., Harrison, T. A., Qu, C., Guo, X., Lu, Y., Albanes, D., Auer, P. L., Banbury, B. L., Berndt, S. I., Bézieau, S., Brenner, H., Buchanan, D. D., Caan, B. J., Campbell, P. T., Carlson, C. S., Chan, A. T., Chang-Claude, J., … Peters, U. (2019). Genetic variant predictors of gene expression provide new insight into risk of colorectal cancer. *Human Genetics*, *138*(4), 307–326. https://doi.org/10.1007/s00439-019-01989-8

Bischoff, K. E., Zapata, C., Sedki, S., Ursem, C., O'Riordan, D. L., England, A. E., Thompson, N., Alfaro, A., Rabow, M. W., & Atreya, C. E. (2020). Embedded palliative care for patients with metastatic colorectal cancer: A mixed-methods pilot study. *Supportive Care in Cancer*, *28*(12), 5995–6010. https://doi.org/10.1007/s00520-020-05437-6

Bleau, A.-M., Redrado, M., Nistal-Villan, E., Villalba, M., Exposito, F., Redin, E., De Aberasturi, A. L., Larzabal, L., Freire, J., Gomez-Roman, J., & Calvo, A. (2018). miR-146a targets c-met and abolishes colorectal cancer liver metastasis. *Cancer Letters*, *414*, 257–267. https://doi.org/10.1016/j.canlet.2017.11.008

Blondy, S., David, V., Verdier, M., Mathonnet, M., Perraud, A., & Christou, N. (2020). 5-Fluorouracil resistance mechanisms in colorectal cancer: From classical pathways to promising processes. *Cancer Science*, *111*(9), 3142–3154. https://doi.org/10.1111/cas.14532

Boelaars, K., Rodriguez, E., Huinen, Z. R., Liu, C., Wang, D., Springer, B. O., Olesek, K., Goossens-Kruijssen, L., Van Ee, T., Lindijer, D., Tak, W., De Haas, A., Wehry, L., Nugteren-Boogaard, J. P., Mikula, A., De Winde, C. M., Mebius, R. E., Tuveson, D. A., Giovannetti, E., … Van Kooyk, Y. (2024). Pancreatic cancer-associated fibroblasts

modulate macrophage differentiation via sialic acid-Siglec interactions. *Communications Biology*, *7*(1), 430. https://doi.org/10.1038/s42003-024-06087-8

Boelaars, K., & Van Kooyk, Y. (2024). Targeting myeloid cells for cancer immunotherapy: Siglec-7/9/10/15 and their ligands. *Trends in Cancer*, *10*(3), 230–241. https://doi.org/10.1016/j.trecan.2023.11.009

Bogaert, J., & Prenen, H. (2014). Molecular genetics of colorectal cancer. *Annals of Gastroenterology*, *27*(1), 9–14.

Bonjer, H. J., Deijen, C. L., Abis, G. A., Cuesta, M. A., Van Der Pas, M. H. G. M., De Lange-de Klerk, E. S. M., Lacy, A. M., Bemelman, W. A., Andersson, J., Angenete, E., Rosenberg, J., Fuerst, A., & Haglind, E. (2015). A Randomized Trial of Laparoscopic versus Open Surgery for Rectal Cancer. *New England Journal of Medicine*, *372*(14), 1324–1332. https://doi.org/10.1056/NEJMoa1414882

Boon, N. J., Oliveira, R. A., Körner, P.-R., Kochavi, A., Mertens, S., Malka, Y., Voogd, R., Van Der Horst, S. E. M., Huismans, M. A., Smabers, L. P., Draper, J. M., Wessels, L. F. A., Haahr, P., Roodhart, J. M. L., Schumacher, T. N. M., Snippert, H. J., Agami, R., & Brummelkamp, T. R. (2024). DNA damage induces p53-independent apoptosis through ribosome stalling. *Science*, *384*(6697), 785–792. https://doi.org/10.1126/science.adh7950

Bordron, A., Bagacean, C., Mohr, A., Tempescul, A., Bendaoud, B., Deshayes, S., Dalbies, F., Buors, C., Saad, H., Berthou, C., Pers, J.-O., & Renaudineau, Y. (2018). Resistance to complement activation, cell membrane hypersialylation and relapses in chronic lymphocytic leukemia patients treated with rituximab and chemotherapy. *Oncotarget*, *9*(60), 31590–31605. https://doi.org/10.18632/oncotarget.25657

Borges, H. L., Linden, R., & Wang, J. Y. (2008). DNA damage-induced cell death: Lessons from the central nervous system. *Cell Research*, *18*(1), 17–26. https://doi.org/10.1038/cr.2007.110

Bouchie, A. (2013). First microRNA mimic enters clinic. *Nature Biotechnology*, *31*(7), 577–577. https://doi.org/10.1038/nbt0713-577

Boz Er, A. B., & Er, I. (2024). PAI1 Regulates Cell Morphology and Migration Markers in Trastuzumab-Resistant HER2-Positive Breast Cancer Cells. *Life*, *14*(8), 1040. https://doi.org/10.3390/life14081040

Brandi, G. (2016). Adjuvant chemotherapy for resected colorectal cancer metastases: Literature review and meta-analysis. *World Journal of Gastroenterology*, *22*(2), 519. https://doi.org/10.3748/wjg.v22.i2.519

Brás, M. M., Cruz, T. B., Maia, A. F., Oliveira, M. J., Sousa, S. R., Granja, P. L., & Radmacher, M. (2022). Mechanical Properties of Colorectal Cancer Cells Determined by Dynamic Atomic Force Microscopy: A Novel Biomarker. *Cancers*, *14*(20), 5053. https://doi.org/10.3390/cancers14205053

Bray, F., Ferlay, J., Soerjomataram, I., Siegel, R. L., Torre, L. A., & Jemal, A. (2018). Global cancer statistics 2018: GLOBOCAN estimates of incidence and mortality worldwide for 36 cancers in 185 countries. *CA: A Cancer Journal for Clinicians*, *68*(6), 394–424. https://doi.org/10.3322/caac.21492

Breugom, A. J., Boelens, P. G., Van Den Broek, C. B. M., Cervantes, A., Van Cutsem, E., Schmoll, H. J., Valentini, V., & Van De Velde, C. J. H. (2014). Quality assurance in the treatment of colorectal cancer: The EURECCA initiative. *Annals of Oncology*, *25*(8), 1485–1492. https://doi.org/10.1093/annonc/mdu039

Briard, J. G., Jiang, H., Moremen, K. W., Macauley, M. S., & Wu, P. (2018). Cell-based glycan arrays for probing glycan–glycan binding protein interactions. *Nature Communications*, *9*(1), 880. https://doi.org/10.1038/s41467-018-03245-5

Briggs, S. E. W., Law, P., East, J. E., Wordsworth, S., Dunlop, M., Houlston, R., Hippisley-Cox, J., & Tomlinson, I. (2022). Integrating genome-wide polygenic risk scores and non-genetic risk to predict colorectal cancer diagnosis using UK Biobank data: Population based cohort study. *BMJ*, e071707. https://doi.org/10.1136/bmj-2022-071707

Brinkman-Van Der Linden, E. C. M., & Varki, A. (2000). New Aspects of Siglec Binding Specificities, Including the Significance of Fucosylation and of the Sialyl-Tn Epitope. *Journal of Biological Chemistry*, *275*(12), 8625–8632. https://doi.org/10.1074/jbc.275.12.8625

Broughton, J. P., Lovci, M. T., Huang, J. L., Yeo, G. W., & Pasquinelli, A. E. (2016). Pairing beyond the Seed Supports MicroRNA Targeting Specificity. *Molecular Cell*, *64*(2), 320–333. https://doi.org/10.1016/j.molcel.2016.09.004

Brown, K. G. M., Solomon, M. J., Mahon, K., & O'Shannassy, S. (2019). Management of colorectal cancer. *BMJ*, l4561. https://doi.org/10.1136/bmj.l4561

Brugnera, E., Bhandoola, A., Cibotti, R., Yu, Q., Guinter, T. I., Yamashita, Y., Sharrow, S. O., & Singer, A. (2000). Coreceptor Reversal in the Thymus. *Immunity*, *13*(1), 59–71. https://doi.org/10.1016/S1074-7613(00)00008-X

Bugter, J. M., Fenderico, N., & Maurice, M. M. (2021). Mutations and mechanisms of WNT pathway tumour suppressors in cancer. *Nature Reviews Cancer*, *21*(1), 5–21. https://doi.org/10.1038/s41568-020-00307-z

Buhagiar, A., Seria, E., Borg, M., Borg, J., & Ayers, D. (2021). Overview of microRNAs as liquid biopsy biomarkers for colorectal cancer sub-type profiling and chemoresistance. *Cancer Drug Resistance*. https://doi.org/10.20517/cdr.2021.62

Büll, C., Heise, T., Adema, G. J., & Boltje, T. J. (2016). Sialic Acid Mimetics to Target the Sialic Acid–Siglec Axis. *Trends in Biochemical Sciences*, *41*(6), 519–531. https://doi.org/10.1016/j.tibs.2016.03.007

Büll, C., Nason, R., Sun, L., Van Coillie, J., Madriz Sørensen, D., Moons, S. J., Yang, Z., Arbitman, S., Fernandes, S. M., Furukawa, S., McBride, R., Nycholat, C. M., Adema, G. J., Paulson, J. C., Schnaar, R. L., Boltje, T. J., Clausen, H., & Narimatsu, Y. (2021). Probing the binding specificities of human Siglecs by cell-based glycan arrays. *Proceedings of the National Academy of Sciences*, *118*(17), e2026102118. https://doi.org/10.1073/pnas.2026102118

Büll, C., Stoel, M. A., Den Brok, M. H., & Adema, G. J. (2014). Sialic Acids Sweeten a Tumor's Life. *Cancer Research*, *74*(12), 3199–3204. https://doi.org/10.1158/0008-5472.CAN-14-0728

Burchell, J., Poulsom, R., Hanby, A., Whitehouse, C., Cooper, L., Clausen, H., Miles, D., & Taylor-Papadimitriou, J. (1999). An 2,3 sialyltransferase (ST3Gal I) is elevated in primary breast carcinomas. *Glycobiology*, *9*(12), 1307–1311. https://doi.org/10.1093/glycob/9.12.1307

Burgess, S. (2014). Sample size and power calculations in Mendelian randomization with a single instrumental variable and a binary outcome. *International Journal of Epidemiology*, *43*(3), 922–929. https://doi.org/10.1093/ije/dyu005

Butler, S. J., Richardson, L., Farias, N., Morrison, J., & Coomber, B. L. (2017). Characterization of cancer stem cell drug resistance in the human colorectal cancer cell lines HCT116 and SW480. *Biochemical and Biophysical Research Communications*, *490*(1), 29–35. https://doi.org/10.1016/j.bbrc.2017.05.176

Cai, K., Chen, Q., Shi, D., Huang, S., Wang, C., Ai, Z., & Jiang, J. (2023). Sialylation-dependent interaction between PD-L1 and CD169 promotes monocyte adhesion to endothelial cells. *Glycobiology*, *33*(3), 215–224. https://doi.org/10.1093/glycob/cwad005

Cai, X., & Xie, B. (2013). Recent advances on organocatalysed asymmetric Mannich reactions. *Arkivoc*, *2013*(1), 264–293. https://doi.org/10.3998/ark.5550190.p007.839

Calin, G. A., & Croce, C. M. (2006). MicroRNA signatures in human cancers. *Nature Reviews Cancer*, *6*(11), 857–866. https://doi.org/10.1038/nrc1997

Calvo-López, T., Paz-Cabezas, M., Llovet, P., Ibañez, M. D., Sastre, J., Alonso-Orduña, V., Viéitez, J. Ma., Yubero, A., Vera, R., Asensio-Martínez, E., Garcia-Alfonso, P., Aranda, E., Diaz-Rubio, E., & Perez-Villamil, B. (2022). Association of miR-21 and miR-335 to microsatellite instability and prognosis in stage III colorectal cancer. *Cancer Biomarkers*, *34*(2), 201–210. https://doi.org/10.3233/CBM-210353

Cancer today. (n.d.). Retrieved 26 May 2023, from http://gco.iarc.fr/today/home

Cao, G., Xiao, Z., & Yin, Z. (2019). Normalization cancer immunotherapy: Blocking Siglec-15! *Signal Transduction and Targeted Therapy*, *4*(1), 10. https://doi.org/10.1038/s41392-019-0045-x

Cao, X., Zhou, Y., Mao, F., Lin, Y., Zhou, X., & Sun, Q. (2022). Identification and characterization of three Siglec15-related immune and prognostic subtypes of breast-invasive cancer. *International Immunopharmacology*, *106*, 108561. https://doi.org/10.1016/j.intimp.2022.108561

Cao, Y., Liang, W., Fang, L., Liu, M., Zuo, J., Peng, Y., Shan, J., Sun, R., Zhao, J., & Wang, J. (2022). PD-L1 / PD-L1 signalling promotes colorectal cancer cell migration ability through RAS / MEK / ERK. *Clinical and Experimental Pharmacology and Physiology*, *49*(12), 1281–1293. https://doi.org/10.1111/1440-1681.13717

Capes-Davis, A. (2018). Cell Line Detective Work. *Advances in Molecular Pathology*, *1*(1), 229–238. https://doi.org/10.1016/j.yamp.2018.06.011

Chachadi, V. B., Bhat, G., & Cheng, P.-W. (2015). Glycosyltransferases involved in the synthesis of MUC-associated metastasis-promoting selectin ligands. *Glycobiology*, *25*(9), 963–975. https://doi.org/10.1093/glycob/cwv030

Chakedis, J., & Schmidt, C. R. (2018). Surgical Treatment of Metastatic Colorectal Cancer. *Surgical Oncology Clinics of North America*, *27*(2), 377–399. https://doi.org/10.1016/j.soc.2017.11.010

Chan, G. H. J., & Chee, C. E. (2019). Making sense of adjuvant chemotherapy in colorectal cancer. *Journal of Gastrointestinal Oncology*, *10*(6), 1183–1192. https://doi.org/10.21037/jgo.2019.06.03

Chandrashekar, D. S., Karthikeyan, S. K., Korla, P. K., Patel, H., Shovon, A. R., Athar, M., Netto, G. J., Qin, Z. S., Kumar, S., Manne, U., Creighton, C. J., & Varambally, S.

(2022). UALCAN: An update to the integrated cancer data analysis platform. *Neoplasia*, *25*, 18–27. https://doi.org/10.1016/j.neo.2022.01.001

Chang, C.-M., Wong, H. S.-C., Huang, C.-Y., Hsu, W.-L., Maio, Z.-F., Chiu, S.-J., Tsai, Y.-T., Chen, B.-K., Wan, Y.-J. Y., Wang, J.-Y., & Chang, W.-C. (2019). Functional Effects of let-7g Expression in Colon Cancer Metastasis. *Cancers*, *11*(4), 489. https://doi.org/10.3390/cancers11040489

Chang, T.-C., Chin, Y.-T., Nana, A. W., Wang, S.-H., Liao, Y.-M., Chen, Y.-R., Shih, Y.-J., Changou, C. A., Yang, Y.-C. S., Wang, K., Whang-Peng, J., Wang, L.-S., Stain, S. C., Shih, A., Lin, H.-Y., Wu, C.-H., & Davis, P. J. (2018). Enhancement by Nano-Diamino-Tetrac of Antiproliferative Action of Gefitinib on Colorectal Cancer Cells: Mediation by EGFR Sialylation and PI3K Activation. *Hormones and Cancer*, *9*(6), 420–432. https://doi.org/10.1007/s12672-018-0341-x

Chen, C.-Z., Li, L., Lodish, H. F., & Bartel, D. P. (2004). MicroRNAs Modulate Hematopoietic Lineage Differentiation. *Science*, *303*(5654), 83–86. https://doi.org/10.1126/science.1091903

Chen, D. S., & Mellman, I. (2017). Elements of cancer immunity and the cancer–immune set point. *Nature*, *541*(7637), 321–330. https://doi.org/10.1038/nature21349

Chen, H., Gao, S., Liu, W., Wong, C.-C., Wu, J., Wu, J., Liu, D., Gou, H., Kang, W., Zhai, J., Li, C., Su, H., Wang, S., Soares, F., Han, J., He, H. H., & Yu, J. (2021). RNA N6-Methyladenosine Methyltransferase METTL3 Facilitates Colorectal Cancer by Activating the m6A-GLUT1-mTORC1 Axis and Is a Therapeutic Target. *Gastroenterology*, *160*(4), 1284-1300.e16. https://doi.org/10.1053/j.gastro.2020.11.013

Chen, H., & Xu, Z. (2015). Hypermethylation-Associated Silencing of miR-125a and miR-125b: A Potential Marker in Colorectal Cancer. *Disease Markers*, *2015*, 1–7. https://doi.org/10.1155/2015/345080

Chen, K., Collins, G., Wang, H., & Toh, J. W. T. (2021). Pathological Features and Prognostication in Colorectal Cancer. *Current Oncology*, *28*(6), 5356–5383. https://doi.org/10.3390/curroncol28060447

Chen, M., Assis, D. M., Benet, M., McClung, C. M., Gordon, E. A., Ghose, S., Dupard, S. J., Willetts, M., Taron, C. H., & Samuelson, J. C. (2023). Comparative site-specific N-glycoproteome analysis reveals aberrant N-glycosylation and gives insights into mannose-6-phosphate pathway in cancer. *Communications Biology*, *6*(1), 48. https://doi.org/10.1038/s42003-023-04439-4

Chen, P., Li, X., Zhang, R., Liu, S., Xiang, Y., Zhang, M., Chen, X., Pan, T., Yan, L., Feng, J., Duan, T., Wang, D., Chen, B., Jin, T., Wang, W., Chen, L., Huang, X., Zhang, W., Sun, Y., … Xie, T. (2020). Combinative treatment of β-elemene and cetuximab is sensitive to KRAS mutant colorectal cancer cells by inducing ferroptosis and inhibiting epithelial-mesenchymal transformation. *Theranostics*, *10*(11), 5107–5119. https://doi.org/10.7150/thno.44705

Chen, X., Cai, Q., Wong, K., Shen, X., & Guan, Z. (2024). Bioinformatic analysis reveals prognostic value and immunotherapy potential of Siglec-15 in laryngeal squamous cell carcinoma. *Heliyon*, *10*(3), e25266. https://doi.org/10.1016/j.heliyon.2024.e25266

Chen, X., Dang, X., Song, J., Wang, G., Liu, C., Cui, L., & Huang, Z. (2020). N-glycosylation of Siglec-15 decreases its lysosome-dependent degradation and promotes its transportation to the cell membrane. *Biochemical and Biophysical Research Communications*, *533*(1), 77–82. https://doi.org/10.1016/j.bbrc.2020.08.111

Chen, X., Mo, S., Zhang, Y., Ma, H., Lu, Z., Yu, S., & Chen, J. (2022). Analysis of a novel immune checkpoint, Siglec-15, in pancreatic ductal adenocarcinoma. *The Journal of Pathology: Clinical Research*, *8*(3), 268–278. https://doi.org/10.1002/cjp2.260

Chen, Y., Liu, H., Ning, S., Wei, C., Li, J., Wei, W., & Zhang, L. (2022). The High Ratio of the Plasma miR-96/miR-99b Correlated With Poor Prognosis in Patients With Metastatic Colorectal Cancer. *Frontiers in Molecular Biosciences*, *8*, 799060. https://doi.org/10.3389/fmolb.2021.799060

Chen, Z., Bai, F.-F., Han, L., Zhu, J., Zheng, T., Zhu, Z., & Zhou, L.-F. (2018). Targeting Neutrophils in Severe Asthma via Siglec-9. *International Archives of Allergy and Immunology*, *175*(1–2), 5–15. https://doi.org/10.1159/000484873

Cheng, P., Chen, X., Dalton, R., Calescibetta, A., So, T., Gilvary, D., Ward, G., Smith, V., Eckard, S., Fox, J. A., Guenot, J., Markowitz, J., Cleveland, J. L., Wright, K. L., List, A. F., Wei, S., & Eksioglu, E. A. (2022). Immunodepletion of MDSC by AMV564, a novel bivalent, bispecific CD33/CD3 T cell engager, ex vivo in MDS and melanoma. *Molecular Therapy*, *30*(6), 2315–2326. https://doi.org/10.1016/j.ymthe.2022.02.005

Cheng, S., Li, Z., Gao, R., Xing, B., Gao, Y., Yang, Y., Qin, S., Zhang, L., Ouyang, H., Du, P., Jiang, L., Zhang, B., Yang, Y., Wang, X., Ren, X., Bei, J.-X., Hu, X., Bu, Z., Ji, J., & Zhang, Z. (2021). A pan-cancer single-cell transcriptional atlas of tumor infiltrating myeloid cells. *Cell*, *184*(3), 792-809.e23. https://doi.org/10.1016/j.cell.2021.01.010

Cherian, R., Jin, C., Liu, J., Karlsson, N., & Holgersson, J. (2015). A Panel of Recombinant Mucins Carrying a Repertoire of Sialylated O-Glycans Based on Different Core Chains

for Studies of Glycan Binding Proteins. *Biomolecules*, *5*(3), 1810–1831. https://doi.org/10.3390/biom5031810

Cho, W.-C., Kim, M., Park, J. W., Jeong, S.-Y., & Ku, J.-L. (2021). Exosomal miR-193a and let-7g accelerate cancer progression on primary colorectal cancer and paired peritoneal metastatic cancer. *Translational Oncology*, *14*(2), 101000. https://doi.org/10.1016/j.tranon.2020.101000

Cho, Y.-H., Ro, E. J., Yoon, J.-S., Mizutani, T., Kang, D.-W., Park, J.-C., Il Kim, T., Clevers, H., & Choi, K.-Y. (2020). 5-FU promotes stemness of colorectal cancer via p53-mediated WNT/β-catenin pathway activation. *Nature Communications*, *11*(1). https://doi.org/10.1038/s41467-020-19173-2

Chong, W., Zhu, X., Ren, H., Ye, C., Xu, K., Wang, Z., Jia, S., Shang, L., Li, L., & Chen, H. (2022). Integrated multi-omics characterization of KRAS mutant colorectal cancer. *Theranostics*, *12*(11), 5138–5154. https://doi.org/10.7150/thno.73089

Chovsepian, A., Prokopchuk, O., Petrova, G., Gjini, T., Kuzi, H., Heisz, S., Janssen, K.-P., Martignoni, M. E., Friess, H., Hauner, H., & Rohm, M. (2023). Diabetes increases mortality in patients with pancreatic and colorectal cancer by promoting cachexia and its associated inflammatory status. *Molecular Metabolism*, *73*, 101729. https://doi.org/10.1016/j.molmet.2023.101729

Chow, A., Perica, K., Klebanoff, C. A., & Wolchok, J. D. (2022). Clinical implications of T cell exhaustion for cancer immunotherapy. *Nature Reviews Clinical Oncology*, *19*(12), 775–790. https://doi.org/10.1038/s41571-022-00689-z

Chugh, S., Gnanapragassam, V. S., Jain, M., Rachagani, S., Ponnusamy, M. P., & Batra, S. K. (2015). Pathobiological implications of mucin glycans in cancer: Sweet poison and novel targets. *Biochimica et Biophysica Acta (BBA) - Reviews on Cancer*, *1856*(2), 211–225. https://doi.org/10.1016/j.bbcan.2015.08.003

Ciardiello, D., Vitiello, P. P., Cardone, C., Martini, G., Troiani, T., Martinelli, E., & Ciardiello, F. (2019). Immunotherapy of colorectal cancer: Challenges for therapeutic efficacy. *Cancer Treatment Reviews*, *76*, 22–32. https://doi.org/10.1016/j.ctrv.2019.04.003

Coelho, M. A., Cooper, S., Strauss, M. E., Karakoc, E., Bhosle, S., Gonçalves, E., Picco, G., Burgold, T., Cattaneo, C. M., Veninga, V., Consonni, S., Dinçer, C., Vieira, S. F., Gibson, F., Barthorpe, S., Hardy, C., Rein, J., Thomas, M., Marioni, J., … Garnett, M. J. (2023). Base editing screens map mutations affecting interferon-γ signaling in cancer. *Cancer Cell*, *41*(2), 288-303.e6. https://doi.org/10.1016/j.ccell.2022.12.009

Colak, S., & Ten Dijke, P. (2017). Targeting TGF-β Signaling in Cancer. *Trends in Cancer*, *3*(1), 56–71. https://doi.org/10.1016/j.trecan.2016.11.008

Costa, A. F., Campos, D., Reis, C. A., & Gomes, C. (2020). Targeting Glycosylation: A New Road for Cancer Drug Discovery. *Trends in Cancer*, *6*(9), 757–766. https://doi.org/10.1016/j.trecan.2020.04.002

Costa, A. F., Senra, E., Faria-Ramos, I., Teixeira, A., Morais, J., Pacheco, M., Reis, C. A., & Gomes, C. (2023). ST3GalIV drives SLeX biosynthesis in gastrointestinal cancer cells and associates with cancer cell motility. *Glycoconjugate Journal*, *40*(4), 421–433. https://doi.org/10.1007/s10719-023-10113-y

Costi, R. (2014). Palliative care and end-stage colorectal cancer management: The surgeon meets the oncologist. *World Journal of Gastroenterology*, *20*(24), 7602. https://doi.org/10.3748/wjg.v20.i24.7602

Coughlin, S. S. (2020). Social determinants of colorectal cancer risk, stage, and survival: A systematic review. *International Journal of Colorectal Disease*, *35*(6), 985–995. https://doi.org/10.1007/s00384-020-03585-z

Craig, J. C., Moyle, M., & Johnson, L. F. (1964). Amine Exchange Reactions. Mannich Bases from Aromatic Amines [1]. *The Journal of Organic Chemistry*, *29*(2), 410–415. https://doi.org/10.1021/jo01025a039

Crocker, P. R., & Gordon, S. (1986). Properties and distribution of a lectin-like hemagglutinin differentially expressed by murine stromal tissue macrophages. *The Journal of Experimental Medicine*, *164*(6), 1862–1875. https://doi.org/10.1084/jem.164.6.1862

Crocker, P. R., Kelm, S., Dubois, C., Martin, B., McWilliam, A. S., Shotton, D. M., Paulson, J. C., & Gordon, S. (1991). Purification and properties of sialoadhesin, a sialic acid-binding receptor of murine tissue macrophages. *The EMBO Journal*, *10*(7), 1661–1669. https://doi.org/10.1002/j.1460-2075.1991.tb07689.x

Crocker, P. R., Paulson, J. C., & Varki, A. (2007a). Siglecs and their roles in the immune system. *Nature Reviews Immunology*, *7*(4), 255–266. https://doi.org/10.1038/nri2056

Crocker, P. R., Paulson, J. C., & Varki, A. (2007b). Siglecs and their roles in the immune system. *Nature Reviews Immunology*, *7*(4), 255–266. https://doi.org/10.1038/nri2056

Czabotar, P. E., Lessene, G., Strasser, A., & Adams, J. M. (2014). Control of apoptosis by the BCL-2 protein family: Implications for physiology and therapy. *Nature Reviews Molecular Cell Biology*, *15*(1), 49–63. https://doi.org/10.1038/nrm3722

Daige, C. L., Wiggins, J. F., Priddy, L., Nelligan-Davis, T., Zhao, J., & Brown, D. (2014). Systemic Delivery of a miR34a Mimic as a Potential Therapeutic for Liver Cancer.

Molecular Cancer Therapeutics, *13*(10), 2352–2360. https://doi.org/10.1158/1535-7163.MCT-14-0209

Dall'Olio, F., Pucci, M., & Malagolini, N. (2021). The Cancer-Associated Antigens Sialyl Lewisa/x and Sda: Two Opposite Faces of Terminal Glycosylation. *Cancers*, *13*(21), 5273. https://doi.org/10.3390/cancers13215273

Dalziel, M., Dall'Olio, F., Mungul, A., Piller, V., & Piller, F. (2004). Ras oncogene induces β-galactoside α2,6-sialyltransferase (ST6Gal I) via a RalGEF-mediated signal to its housekeeping promoter. *European Journal of Biochemistry*, *271*(18), 3623–3634. https://doi.org/10.1111/j.1432-1033.2004.04284.x

Dan, W.-Y., Zhou, G.-Z., Peng, L.-H., & Pan, F. (2023). Update and latest advances in mechanisms and management of colitis-associated colorectal cancer. *World Journal of Gastrointestinal Oncology*, *15*(8), 1317–1331. https://doi.org/10.4251/wjgo.v15.i8.1317

Datta, R., Heaster, T. M., Sharick, J. T., Gillette, A. A., & Skala, M. C. (2020). Fluorescence lifetime imaging microscopy: Fundamentals and advances in instrumentation, analysis, and applications. *Journal of Biomedical Optics*, *25*(07), 1. https://doi.org/10.1117/1.JBO.25.7.071203

De Las Rivas, M., Lira-Navarrete, E., Gerken, T. A., & Hurtado-Guerrero, R. (2019). Polypeptide GalNAc-Ts: From redundancy to specificity. *Current Opinion in Structural Biology*, *56*, 87–96. https://doi.org/10.1016/j.sbi.2018.12.007

De Rosa, M., Pace, U., Rega, D., Costabile, V., Duraturo, F., Izzo, P., & Delrio, P. (2015). Genetics, diagnosis and management of colorectal cancer (Review). *Oncology Reports*, *34*(3), 1087–1096. https://doi.org/10.3892/or.2015.4108

De Simone, V., Franzè, E., Ronchetti, G., Colantoni, A., Fantini, M. C., Di Fusco, D., Sica, G. S., Sileri, P., MacDonald, T. T., Pallone, F., Monteleone, G., & Stolfi, C. (2015). Th17-type cytokines, IL-6 and TNF-α synergistically activate STAT3 and NF-kB to promote colorectal cancer cell growth. *Oncogene*, *34*(27), 3493–3503. https://doi.org/10.1038/onc.2014.286

Debnath, J., Gammoh, N., & Ryan, K. M. (2023). Autophagy and autophagy-related pathways in cancer. *Nature Reviews Molecular Cell Biology*, *24*(8), 560–575. https://doi.org/10.1038/s41580-023-00585-z

Deen, K. I., Silva, H., Deen, R., & Chandrasinghe, P. C. (2016). Colorectal cancer in the young, many questions, few answers. *World Journal of Gastrointestinal Oncology*, *8*(6), 481. https://doi.org/10.4251/wjgo.v8.i6.481

Dempke, W. C. M., Uciechowski, P., Fenchel, K., & Chevassut, T. (2018). Targeting SHP-1, 2 and SHIP Pathways: A Novel Strategy for Cancer Treatment? *Oncology*, *95*(5), 257–269. https://doi.org/10.1159/000490106

Deng, Y., Wan, H., Tian, J., Cheng, X., Rao, M., Li, J., Zhang, H., Zhang, M., Cai, Y., Lu, Z., Li, Y., Niu, S., Shen, N., Chang, J., Fang, Z., & Zhong, R. (2020). Cpg-Methylation-Based Risk Score Predicts Progression in Colorectal Cancer. *Epigenomics*, *12*(7), 605–615. https://doi.org/10.2217/epi-2019-0300

Depciuch, J., Klębowski, B., Stec, M., Szatanek, R., Węglarczyk, K., Baj-Krzyworzeka, M., Parlińska-Wojtan, M., & Baran, J. (2020). Similarities in the General Chemical Composition of Colon Cancer Cells and Their Microvesicles Investigated by Spectroscopic Methods-Potential Clinical Relevance. *International Journal of Molecular Sciences*, *21*(5), 1826. https://doi.org/10.3390/ijms21051826

DeRogatis, J. M., Viramontes, K. M., Neubert, E. N., Henriquez, M. L., Guerrero-Juarez, C. F., & Tinoco, R. (2022). Targeting the PSGL-1 Immune Checkpoint Promotes Immunity to PD-1–Resistant Melanoma. *Cancer Immunology Research*, *10*(5), 612–625. https://doi.org/10.1158/2326-6066.CIR-21-0690

Despotovic, J., Dragicevic, S., & Nikolic, A. (2021). Effects of Chemotherapy for Metastatic Colorectal Cancer on the TGF-β Signaling and Related miRNAs hsa-miR-17-5p, hsa-miR-21-5p and hsa-miR-93-5p. *Cell Biochemistry and Biophysics*, *79*(4), 757–767. https://doi.org/10.1007/s12013-021-00980-3

Di Martino, M. T., Riillo, C., Scionti, F., Grillone, K., Polerà, N., Caracciolo, D., Arbitrio, M., Tagliaferri, P., & Tassone, P. (2021). miRNAs and lncRNAs as Novel Therapeutic Targets to Improve Cancer Immunotherapy. *Cancers*, *13*(7), 1587. https://doi.org/10.3390/cancers13071587

Dimitroff, C. J. (2015). Galectin-Binding O-Glycosylations as Regulators of Malignancy. *Cancer Research*, *75*(16), 3195–3202. https://doi.org/10.1158/0008-5472.can-15-0834

Ding, H., Yao, B., Ci, L., Feng, J., Ouyang, P., Chen, G., Hui, X., & Zhou, D. (2023). Enhancing the Anti-tumor Potency of a Novel Siglec-15 Antibody by Engineering its Fc-mediated Effector Functions. *Journal of Immunotherapy*, *46*(5), 161–169. https://doi.org/10.1097/CJI.0000000000000465

Dobie, C., & Skropeta, D. (2021). Insights into the role of sialylation in cancer progression and metastasis. *British Journal of Cancer*, *124*(1), 76–90. https://doi.org/10.1038/s41416-020-01126-7

Doggrell, S. A., & Hancox, J. C. (2013). Cardiac safety concerns for ondansetron, an antiemetic commonly used for nausea linked to cancer treatment and following anaesthesia. *Expert Opinion on Drug Safety*, *12*(3), 421–431. https://doi.org/10.1517/14740338.2013.780026

Doi, N., Ino, Y., Angata, K., Shimada, K., Narimatsu, H., & Hiraoka, N. (2020). Clinicopathological significance of core 3 O-glycan synthetic enzyme, β1,3-N-acetylglucosaminyltransferase 6 in pancreatic ductal adenocarcinoma. *PLOS ONE*, *15*(11), e0242851. https://doi.org/10.1371/journal.pone.0242851

Dombek, G. E., Ore, A. S., Cheng, J., Matsumoto, Y., Glickman, J. N., Fleishman, A., Heimburg-Molinaro, J., Poylin, V. Y., Fabrizio, A., Cataldo, T., Messaris, E., & Cummings, R. D. (2022). Immunohistochemical analysis of Tn antigen expression in colorectal adenocarcinoma and precursor lesions. *BMC Cancer*, *22*(1), 1281. https://doi.org/10.1186/s12885-022-10376-y

Dong, S., Liang, S., Cheng, Z., Zhang, X., Luo, L., Li, L., Zhang, W., Li, S., Xu, Q., Zhong, M., Zhu, J., Zhang, G., & Hu, S. (2022). ROS/PI3K/Akt and Wnt/β-catenin signalings activate HIF-1α-induced metabolic reprogramming to impart 5-fluorouracil resistance in colorectal cancer. *Journal of Experimental & Clinical Cancer Research*, *41*(1), 15. https://doi.org/10.1186/s13046-021-02229-6

Druzhkova, I., Shirmanova, M., Ignatova, N., Dudenkova, V., Lukina, M., Zagaynova, E., Safina, D., Kostrov, S., Didych, D., Kuzmich, A., Sharonov, G., Rakitina, O., Alekseenko, I., & Sverdlov, E. (2020). Expression of EMT-Related Genes in Hybrid E/M Colorectal Cancer Cells Determines Fibroblast Activation and Collagen Remodeling. *International Journal of Molecular Sciences*, *21*(21), 8119. https://doi.org/10.3390/ijms21218119

Du, H., Tang, J., Li, X., Wang, X., Wu, L., Zhang, R., Hu, P., & Yang, Y. (2021). Siglec-15 Is an Immune Suppressor and Potential Target for Immunotherapy in the Pre-Metastatic Lymph Node of Colorectal Cancer. *Frontiers in Cell and Developmental Biology*, *9*, 691937. https://doi.org/10.3389/fcell.2021.691937

Duan, S., & Paulson, J. C. (2020). Siglecs as Immune Cell Checkpoints in Disease. *Annual Review of Immunology*, *38*(1), 365–395. https://doi.org/10.1146/annurev-immunol-102419-035900

Dunn, G. P., Koebel, C. M., & Schreiber, R. D. (2006). Interferons, immunity and cancer immunoediting. *Nature Reviews Immunology*, *6*(11), 836–848. https://doi.org/10.1038/nri1961

Dunne, R. F., Crawford, J., Smoyer, K. E., McRae, T. D., Rossulek, M. I., Revkin, J. H., Tarasenko, L. C., & Bonomi, P. D. (2024). The mortality burden of cachexia or weight loss in patients with colorectal or pancreatic cancer: A systematic literature review. *Journal of Cachexia, Sarcopenia and Muscle*. https://doi.org/10.1002/jcsm.13510

Duranton, B., Holl, V., Schneider, Y., Carnesecchi, S., Gossé, F., Raul, F., & Seiler, N. (2003). Polyamine metabolism in primary human colon adenocarcinoma cells (SW480) and their lymph node metastatic derivatives (SW620). *Amino Acids*, *24*(1), 63–72. https://doi.org/10.1007/s00726-002-0333-5

Eaden, J. (2004). Colorectal carcinoma and inflammatory bowel disease. *Alimentary Pharmacology & Therapeutics*, *20*(s4), 24–30. https://doi.org/10.1111/j.1365-2036.2004.02046.x

Ebert, M. S., & Sharp, P. A. (2010). MicroRNA sponges: Progress and possibilities. *RNA*, *16*(11), 2043–2050. https://doi.org/10.1261/rna.2414110

Egan, H., Treacy, O., Lynch, K., Leonard, N. A., O'Malley, G., Reidy, E., O'Neill, A., Corry, S. M., De Veirman, K., Vanderkerken, K., Egan, L. J., Ritter, T., Hogan, A. M., Redmond, K., Peng, L., Che, J., Gatlin, W., Jayaraman, P., Sheehan, M., … Ryan, A. E. (2023). Targeting stromal cell sialylation reverses T cell-mediated immunosuppression in the tumor microenvironment. *Cell Reports*, *42*(5), 112475. https://doi.org/10.1016/j.celrep.2023.112475

Elrebehy, M. A., Al-Saeed, S., Gamal, S., El-Sayed, A., Ahmed, A. A., Waheed, O., Ismail, A., El-Mahdy, H. A., Sallam, A.-A. M., & Doghish, A. S. (2022). miRNAs as cornerstones in colorectal cancer pathogenesis and resistance to therapy: A spotlight on signaling pathways interplay — A review. *International Journal of Biological Macromolecules*, *214*, 583–600. https://doi.org/10.1016/j.ijbiomac.2022.06.134

ElSherbiney, M., Khawaja, A., Noureldin, K., Issa, M., & Varma, A. (2023). Single incision laparoscopy versus conventional multiport laparoscopy for colorectal surgery: A systematic review and meta-analysis. *The Annals of The Royal College of Surgeons of England*, *105*(8), 709–720. https://doi.org/10.1308/rcsann.2022.0132

Entezar-Almahdi, E., Mohammadi-Samani, S., Tayebi, L., & Farjadian, F. (2020). Recent Advances in Designing 5-Fluorouracil Delivery Systems: A Stepping Stone in the Safe Treatment of Colorectal Cancer. *International Journal of Nanomedicine*, *Volume 15*, 5445–5458. https://doi.org/10.2147/IJN.S257700

Erfani, M., Zamani, M., & Mokarram, P. (2022). Evidence of histone modification affecting ARID1A expression in colorectal cancer cell lines. *Gastroenterology and Hepatology from Bed to Bench*, *15*(1), 32–38.

Erger, F., Aryal, R. P., Reusch, B., Matsumoto, Y., Meyer, R., Zeng, J., Knopp, C., Noel, M., Muerner, L., Wenzel, A., Kohl, S., Tschernoster, N., Rappl, G., Rouvet, I., Schröder-Braunstein, J., Seibert, F. S., Thiele, H., Häusler, M. G., Weber, L. T., … Beck, B. B. (2023). Germline *C1GALT1C1* mutation causes a multisystem chaperonopathy. *Proceedings of the National Academy of Sciences*, *120*(22), e2211087120. https://doi.org/10.1073/pnas.2211087120

Esfahani, K., Roudaia, L., Buhlaiga, N., Del Rincon, S. V., Papneja, N., & Miller, W. H. (2020). A Review of Cancer Immunotherapy: From the Past, to the Present, to the Future. *Current Oncology*, *27*(12), 87–97. https://doi.org/10.3747/co.27.5223

Fan, A., Wang, B., Wang, X., Nie, Y., Fan, D., Zhao, X., & Lu, Y. (2021). Immunotherapy in colorectal cancer: Current achievements and future perspective. *International Journal of Biological Sciences*, *17*(14), 3837–3849. https://doi.org/10.7150/ijbs.64077

Fan, M., Zhang, G., Chen, W., Qi, L., Xie, M., Zhang, Y., Wang, L., & Zhang, Q. (2021). Siglec-15 Promotes Tumor Progression in Osteosarcoma via DUSP1/MAPK Pathway. *Frontiers in Oncology*, *11*, 710689. https://doi.org/10.3389/fonc.2021.710689

Farouk, S., El-Shenawy, R., Khairy, A. M., & Bader El-Din, N. G. (2023). Overexpression of Mirna 26A and 26B with Mmp-9 are Valuable Diagnostic Biomarkers for Colorectal Cancer Patients. *Biomarkers in Medicine*, *17*(3), 159–169. https://doi.org/10.2217/bmm-2022-0861

Farzaneh, S., Shahhosseini, S., Arefi, H., Daraei, B., Esfahanizadeh, M., & Zarghi, A. (2018). Design, Synthesis and Biological Evaluation of New 1,3-diphenyl-3-(phenylamino)propan-1-ones as Selective Cyclooxygenase (COX-2) Inhibitors. *Medicinal Chemistry*, *14*(7), 652–659. https://doi.org/10.2174/1573406414666180525133221

Fearon, E. R., & Vogelstein, B. (1990). A genetic model for colorectal tumorigenesis. *Cell*, *61*(5), 759–767. https://doi.org/10.1016/0092-8674(90)90186-I

Fernando, M., Duijf, P. H. G., Proctor, M., Stevenson, A. J., Ehmann, A., Vora, S., Skalamera, D., Adams, M., & Gabrielli, B. (2021). Dysregulated G2 phase checkpoint recovery pathway reduces DNA repair efficiency and increases chromosomal instability in a wide range of tumours. *Oncogenesis*, *10*(5), 41. https://doi.org/10.1038/s41389-021-00329-8

Ferrer, C. M., & Reginato, M. J. (2014). Sticking to Sugars at the Metastatic Site: Sialyltransferase ST6GalNAc2 Acts as a Breast Cancer Metastasis Suppressor. *Cancer Discovery*, *4*(3), 275–277. https://doi.org/10.1158/2159-8290.CD-14-0075

Fessart, D., Domblides, C., Avril, T., Eriksson, L. A., Begueret, H., Pineau, R., Malrieux, C., Dugot-Senant, N., Lucchesi, C., Chevet, E., & Delom, F. (2016). Secretion of protein disulphide isomerase AGR2 confers tumorigenic properties. *eLife*, *5*, e13887. https://doi.org/10.7554/eLife.13887

Fhu, C. W., & Ali, A. (2020). Fatty Acid Synthase: An Emerging Target in Cancer. *Molecules*, *25*(17), 3935. https://doi.org/10.3390/molecules25173935

Firestein, R., Shima, K., Nosho, K., Irahara, N., Baba, Y., Bojarski, E., Giovannucci, E. L., Hahn, W. C., Fuchs, C. S., & Ogino, S. (2010). CDK8 expression in 470 colorectal cancers in relation to β-catenin activation, other molecular alterations and patient survival. *International Journal of Cancer*, *126*(12), 2863–2873. https://doi.org/10.1002/ijc.24908

Flavell, R. A., Sanjabi, S., Wrzesinski, S. H., & Licona-Limón, P. (2010). The polarization of immune cells in the tumour environment by TGFβ. *Nature Reviews Immunology*, *10*(8), 554–567. https://doi.org/10.1038/nri2808

Flores, R., Zhang, P., Wu, W., Wang, X., Ye, P., Zheng, P., & Liu, Y. (2019). Siglec genes confer resistance to systemic lupus erythematosus in humans and mice. *Cellular & Molecular Immunology*, *16*(2), 154–164. https://doi.org/10.1038/cmi.2017.160

Foersch, S., & Neurath, M. F. (2014). Colitis-associated neoplasia: Molecular basis and clinical translation. *Cellular and Molecular Life Sciences*, *71*(18), 3523–3535. https://doi.org/10.1007/s00018-014-1636-x

Freitas, M., Ferreira, F., Carvalho, S., Silva, F., Lopes, P., Antunes, L., Salta, S., Diniz, F., Santos, L. L., Videira, J. F., Henrique, R., & Jerónimo, C. (2018). A novel DNA methylation panel accurately detects colorectal cancer independently of molecular pathway. *Journal of Translational Medicine*, *16*(1), 45. https://doi.org/10.1186/s12967-018-1415-9

Freud, A. G., & Caligiuri, M. A. (2006). Human natural killer cell development. *Immunological Reviews*, *214*(1), 56–72. https://doi.org/10.1111/j.1600-065X.2006.00451.x

Fu, L., Jin, W., Zhang, J., Zhu, L., Lu, J., Zhen, Y., Zhang, L., Ouyang, L., Liu, B., & Yu, H. (2022). Repurposing non-oncology small-molecule drugs to improve cancer therapy: Current situation and future directions. *Acta Pharmaceutica Sinica B*, *12*(2), 532–557. https://doi.org/10.1016/j.apsb.2021.09.006

Fu, X.-P., Ji, C.-Y., Tang, W.-Q., Yu, T.-T., & Luo, L. (2024). Long non-coding RNA LOXL1-AS1: A potential biomarker and therapeutic target in human malignant tumors. *Clinical and Experimental Medicine*, *24*(1), 93. https://doi.org/10.1007/s10238-024-01355-7

Fu, Y., Zou, T., Shen, X., Nelson, P. J., Li, J., Wu, C., Yang, J., Zheng, Y., Bruns, C., Zhao, Y., Qin, L., & Dong, Q. (2021). Lipid metabolism in cancer progression and therapeutic strategies. *MedComm*, *2*(1), 27–59. https://doi.org/10.1002/mco2.27

Fudaba, H., Momii, Y., Hirakawa, T., Onishi, K., Asou, D., Matsushita, W., Kawasaki, Y., Sugita, K., & Fujiki, M. (2021). Sialic acid-binding immunoglobulin-like lectin-15 expression on peritumoral macrophages is a favorable prognostic factor for primary central nervous system lymphoma patients. *Scientific Reports*, *11*(1), 1206. https://doi.org/10.1038/s41598-020-79742-9

Fujii, S., Tsukamoto, M., Fukushima, Y., Shimada, R., Okamoto, K., Tsuchiya, T., Nozawa, K., Matsuda, K., & Hashiguchi, Y. (2016). Systematic review of laparoscopic vs open surgery for colorectal cancer in elderly patients. *World Journal of Gastrointestinal Oncology*, *8*(7), 573. https://doi.org/10.4251/wjgo.v8.i7.573

Fujiyoshi, K., Väyrynen, J. P., Borowsky, J., Papke, D. J., Arima, K., Haruki, K., Kishikawa, J., Akimoto, N., Ugai, T., Lau, M. C., Gu, S., Shi, S., Zhao, M., Da Silva, A. F. L., Twombly, T. S., Nan, H., Meyerhardt, J. A., Song, M., Zhang, X., … Ogino, S. (2020). Tumour budding, poorly differentiated clusters, and T-cell response in colorectal cancer. *EBioMedicine*, *57*, 102860. https://doi.org/10.1016/j.ebiom.2020.102860

Fuseya, S., Izumi, H., Hamano, A., Murakami, Y., Suzuki, R., Koiwai, R., Hayashi, T., Kuno, A., Takahashi, S., & Kudo, T. (2023). Reduction in disialyl-T antigen levels in mice deficient for both St6galnac3 and St6galnac4 results in blood filling of lymph nodes. *Scientific Reports*, *13*(1), 10582. https://doi.org/10.1038/s41598-023-37363-y

Fuster, M. M., & Esko, J. D. (2005). The sweet and sour of cancer: Glycans as novel therapeutic targets. *Nature Reviews Cancer*, *5*(7), 526–542. https://doi.org/10.1038/nrc1649

Gabay, M., Li, Y., & Felsher, D. W. (2014). MYC Activation Is a Hallmark of Cancer Initiation and Maintenance. *Cold Spring Harbor Perspectives in Medicine*, *4*(6), a014241–a014241. https://doi.org/10.1101/cshperspect.a014241

Gaikwad, S., Agrawal, M. Y., Kaushik, I., Ramachandran, S., & Srivastava, S. K. (2022). Immune checkpoint proteins: Signaling mechanisms and molecular interactions in cancer immunotherapy. *Seminars in Cancer Biology*, *86*, 137–150. https://doi.org/10.1016/j.semcancer.2022.03.014

Galluzzi, L., Vitale, I., Aaronson, S. A., Abrams, J. M., Adam, D., Agostinis, P., Alnemri, E. S., Altucci, L., Amelio, I., Andrews, D. W., Annicchiarico-Petruzzelli, M., Antonov, A. V., Arama, E., Baehrecke, E. H., Barlev, N. A., Bazan, N. G., Bernassola, F., Bertrand, M. J. M., Bianchi, K., … Kroemer, G. (2018). Molecular mechanisms of cell death: Recommendations of the Nomenclature Committee on Cell Death 2018. *Cell Death & Differentiation*, *25*(3), 486–541. https://doi.org/10.1038/s41418-017-0012-4

Ganesh, K., Stadler, Z. K., Cercek, A., Mendelsohn, R. B., Shia, J., Segal, N. H., & Diaz, L. A. (2019). Immunotherapy in colorectal cancer: Rationale, challenges and potential. *Nature Reviews Gastroenterology & Hepatology*, *16*(6), 361–375. https://doi.org/10.1038/s41575-019-0126-x

Gao, F., Li, X., Xu, K., Wang, R., & Guan, X. (2023). C-MYC mediates the crosstalk between breast cancer cells and tumor microenvironment. *Cell Communication and Signaling*, *21*(1), 28. https://doi.org/10.1186/s12964-023-01043-1

Gao, Y., Yang, J., Cai, Y., Fu, S., Zhang, N., Fu, X., & Li, L. (2018). IFN-γ-mediated inhibition of lung cancer correlates with PD-L1 expression and is regulated by PI3K-AKT signaling. *International Journal of Cancer*, *143*(4), 931–943. https://doi.org/10.1002/ijc.31357

Garnham, R., Scott, E., Livermore, K., & Munkley, J. (2019). ST6GAL1: A key player in cancer (Review). *Oncology Letters*. https://doi.org/10.3892/ol.2019.10458

Gc, S., Tuy, K., Rickenbacker, L., Jones, R., Chakraborty, A., Miller, C. R., Beierle, E. A., Hanumanthu, V. S., Tran, A. N., Mobley, J. A., Bellis, S. L., & Hjelmeland, A. B. (2022). A2,6 Sialylation mediated by ST6GAL1 promotes glioblastoma growth. *JCI Insight*, *7*(21), e158799. https://doi.org/10.1172/jci.insight.158799

Ge, T., Xiang, P., Mao, H., Tang, S., Zhou, J., & Zhang, Y. (2020). Inhibition of miR-96 enhances the sensitivity of colorectal cancer cells to oxaliplatin by targeting TPM1. *Experimental and Therapeutic Medicine*. https://doi.org/10.3892/etm.2020.8936

Gianchecchi, E., Arena, A., & Fierabracci, A. (2021). Sialic Acid-Siglec Axis in Human Immune Regulation, Involvement in Autoimmunity and Cancer and Potential Therapeutic Treatments. *International Journal of Molecular Sciences*, *22*(11), 5774. https://doi.org/10.3390/ijms22115774

Gómez, A. I., Cruz, M., & López-Giménez, J. F. (2019). Evaluating the pharmacological response in fluorescence microscopy images: The Δm algorithm. *PLOS ONE*, *14*(2), e0211330. https://doi.org/10.1371/journal.pone.0211330

González-Ramírez, A. M., Grosso, A. S., Yang, Z., Compañón, I., Coelho, H., Narimatsu, Y., Clausen, H., Marcelo, F., Corzana, F., & Hurtado-Guerrero, R. (2022). Structural basis for the synthesis of the core 1 structure by C1GalT1. *Nature Communications*, *13*(1), 2398. https://doi.org/10.1038/s41467-022-29833-0

Gou, Q., Dong, C., Xu, H., Khan, B., Jin, J., Liu, Q., Shi, J., & Hou, Y. (2020). PD-L1 degradation pathway and immunotherapy for cancer. *Cell Death & Disease*, *11*(11), 955. https://doi.org/10.1038/s41419-020-03140-2

Greville, G., McCann, A., Rudd, P. M., & Saldova, R. (2016). Epigenetic regulation of glycosylation and the impact on chemo-resistance in breast and ovarian cancer. *Epigenetics*, *11*(12), 845–857. https://doi.org/10.1080/15592294.2016.1241932

Grigore, A., Jolly, M., Jia, D., Farach-Carson, M., & Levine, H. (2016). Tumor Budding: The Name is EMT. Partial EMT. *Journal of Clinical Medicine*, *5*(5), 51. https://doi.org/10.3390/jcm5050051

Guerrero, P. E., Miró, L., Wong, B. S., Massaguer, A., Martínez-Bosch, N., Llorens, R. D., Navarro, P., Konstantopoulos, K., Llop, E., & Peracaula, R. (2020). Knockdown of α2,3-Sialyltransferases Impairs Pancreatic Cancer Cell Migration, Invasion and E-selectin-Dependent Adhesion. *International Journal of Molecular Sciences*, *21*(17), 6239. https://doi.org/10.3390/ijms21176239

Guinney, J., Dienstmann, R., Wang, X., De Reyniès, A., Schlicker, A., Soneson, C., Marisa, L., Roepman, P., Nyamundanda, G., Angelino, P., Bot, B. M., Morris, J. S., Simon, I. M., Gerster, S., Fessler, E., De Sousa E Melo, F., Missiaglia, E., Ramay, H., Barras, D., … Tejpar, S. (2015). The consensus molecular subtypes of colorectal cancer. *Nature Medicine*, *21*(11), 1350–1356. https://doi.org/10.1038/nm.3967

Guo, J., Yu, Z., Das, M., & Huang, L. (2020). Nano Codelivery of Oxaliplatin and Folinic Acid Achieves Synergistic Chemo-Immunotherapy with 5-Fluorouracil for Colorectal Cancer and Liver Metastasis. *ACS Nano*, *14*(4), 5075–5089. https://doi.org/10.1021/acsnano.0c01676

Gutierrez, M., Hamid, O., Shum, E., Wise, D. R., Balar, A. V., Weber, J. S., LoRusso, P., Shafi, S., Rimm, D. L., Tolcher, A. W., Basudhar, D., Dujka, M. E., & Heller, K. N. (2020). Trial in progress: A phase I/II, open-label, dose-escalation, safety and tolerability study of NC318 in subjects with advanced or metastatic solid tumors. *Journal of Clinical Oncology*, *38*(15_suppl), TPS3166–TPS3166. https://doi.org/10.1200/JCO.2020.38.15_suppl.TPS3166

Gwinn, D. M., Shackelford, D. B., Egan, D. F., Mihaylova, M. M., Mery, A., Vasquez, D. S., Turk, B. E., & Shaw, R. J. (2008). AMPK Phosphorylation of Raptor Mediates a Metabolic Checkpoint. *Molecular Cell*, *30*(2), 214–226. https://doi.org/10.1016/j.molcel.2008.03.003

Győrffy, B. (2021). Survival analysis across the entire transcriptome identifies biomarkers with the highest prognostic power in breast cancer. *Computational and Structural Biotechnology Journal*, *19*, 4101–4109. https://doi.org/10.1016/j.csbj.2021.07.014

Hadžibegović, I., Vrselja, Z., Lauc, G., & Ćurić, G. (2014). Expression of leukocyte adhesion-related glycosyltransferase genes in acute coronary syndrome patients. *Inflammation Research*, *63*(8), 629–636. https://doi.org/10.1007/s00011-014-0735-3

Häfner, M. F., & Debus, J. (2016). Radiotherapy for Colorectal Cancer: Current Standards and Future Perspectives. *Visceral Medicine*, *32*(3), 172–177. https://doi.org/10.1159/000446486

Haldrup, C., Pedersen, A. L., Øgaard, N., Strand, S. H., Høyer, S., Borre, M., Ørntoft, T. F., & Sørensen, K. D. (2018). Biomarker potential of *ST 6 GALNAC 3* and *ZNF 660* promoter hypermethylation in prostate cancer tissue and liquid biopsies. *Molecular Oncology*, *12*(4), 545–560. https://doi.org/10.1002/1878-0261.12183

Hammouda, M. M., & Elattar, K. M. (2022). Recent progress in the chemistry of β-aminoketones. *RSC Advances*, *12*(38), 24681–24712. https://doi.org/10.1039/D2RA03864A

Han, J., Li, S., Zhan, Q., Hu, Y., Zhong, C., Yang, J., & Qiu, Z. (2023). Comprehensive characterization of adipogenesis-related genes in colorectal cancer for clinical significance and immunogenomic landscape analyses. *Lipids in Health and Disease*, *22*(1). https://doi.org/10.1186/s12944-023-01942-9

Han, L., Dai, W., Luo, W., Ye, L., Fang, H., Mo, S., Li, Q., Xu, Y., Wang, R., & Cai, G. (2023). Enhanced De Novo Lipid Synthesis Mediated by FASN Induces Chemoresistance in Colorectal Cancer. *Cancers*, *15*(3), 562. https://doi.org/10.3390/cancers15030562

Han, X., Zhang, Y., Li, Y., Lin, Z., Pei, X., Feng, Y., Yang, J., Li, F., Li, T., Fu, Z., Wang, C., & Li, C. (2022). Pyrotinib Targeted EGFR-STAT3/CD24 Loop-Mediated Cell Viability in TSC. *Cells*, *11*(19), 3064. https://doi.org/10.3390/cells11193064

Hanna, J., Hossain, G. S., & Kocerha, J. (2019). The Potential for microRNA Therapeutics and Clinical Research. *Frontiers in Genetics*, *10*, 478. https://doi.org/10.3389/fgene.2019.00478

Harada, S., & Morlote, D. (2020). Molecular Pathology of Colorectal Cancer. *Advances in Anatomic Pathology*, *27*(1), 20–26. https://doi.org/10.1097/PAP.0000000000000247

Harvey, K. F., Zhang, X., & Thomas, D. M. (2013). The Hippo pathway and human cancer. *Nature Reviews Cancer*, *13*(4), 246–257. https://doi.org/10.1038/nrc3458

Hassinen, A., Khoder-Agha, F., Khosrowabadi, E., Mennerich, D., Harrus, D., Noel, M., Dimova, E. Y., Glumoff, T., Harduin-Lepers, A., Kietzmann, T., & Kellokumpu, S. (2019). A Golgi-associated redox switch regulates catalytic activation and cooperative functioning of ST6Gal-I with B4GalT-I. *Redox Biology*, *24*, 101182. https://doi.org/10.1016/j.redox.2019.101182

Häuselmann, I., & Borsig, L. (2014). Altered Tumor-Cell Glycosylation Promotes Metastasis. *Frontiers in Oncology*, *4*. https://doi.org/10.3389/fonc.2014.00028

Havens, M. A., Reich, A. A., Duelli, D. M., & Hastings, M. L. (2012). Biogenesis of mammalian microRNAs by a non-canonical processing pathway. *Nucleic Acids Research*, *40*(10), 4626–4640. https://doi.org/10.1093/nar/gks026

Hayes, J., Peruzzi, P. P., & Lawler, S. (2014). MicroRNAs in cancer: Biomarkers, functions and therapy. *Trends in Molecular Medicine*, *20*(8), 460–469. https://doi.org/10.1016/j.molmed.2014.06.005

He, F., Wang, N., Li, J., He, L., Yang, Z., Lu, J., Xiong, G., Yu, C., & Wang, S. (2021). High affinity monoclonal antibody targeting Siglec-15 for cancer immunotherapy. *Journal of Clinical and Translational Research*, *7*(6), 739–749.

He, J., Gao, R., Yang, J., Li, F., Fu, Y., Cui, J., Liu, X., Huang, K., Guo, Q., Zhou, Z., & Wei, W. (2023). NCAPD2 promotes breast cancer progression through E2F1 transcriptional regulation of CDK1. *Cancer Science*, *114*(3), 896–907. https://doi.org/10.1111/cas.15347

He, Y., Kan, W., Li, Y., Hao, Y., Huang, A., Gu, H., Wang, M., Wang, Q., Chen, J., Sun, Z., Liu, M., Chen, Y., & Yi, Z. (2021). A potent and selective small molecule inhibitor of myoferlin attenuates colorectal cancer progression. *Clinical and Translational Medicine*, *11*(2). https://doi.org/10.1002/ctm2.289

Heck, K. A., Lindholm, H. T., Niederdorfer, B., Tsirvouli, E., Kuiper, M., Flobak, Å., Lægreid, A., & Thommesen, L. (2023). Characterisation of Colorectal Cancer Cell Lines through Proteomic Profiling of Their Extracellular Vesicles. *Proteomes*, *11*(1), 3. https://doi.org/10.3390/proteomes11010003

Helenius, A., & Aebi, A. M. (2001). Intracellular Functions of N-Linked Glycans. *Science*, *291*(5512), 2364–2369. https://doi.org/10.1126/science.291.5512.2364

Hernández-Caselles, T., Miguel, R. C.-S., Ruiz-Alcaraz, A. J., & García-Peñarrubia, P. (2019). CD33 (Siglec-3) Inhibitory Function: Role in the NKG2D/DAP10 Activating Pathway. *Journal of Immunology Research*, *2019*, 1–15. https://doi.org/10.1155/2019/6032141

Hiers, N. M., Li, T., Traugot, C. M., & Xie, M. (2024). Target-directed MICRORNA degradation: Mechanisms, significance, and functional implications. *WIREs RNA*, *15*(2), e1832. https://doi.org/10.1002/wrna.1832

Hirano, T. (2021). IL-6 in inflammation, autoimmunity and cancer. *International Immunology*, *33*(3), 127–148. https://doi.org/10.1093/intimm/dxaa078

Hiruma, Y., Hirai, T., & Tsuda, E. (2011). Siglec-15, a member of the sialic acid-binding lectin, is a novel regulator for osteoclast differentiation. *Biochemical and Biophysical Research Communications*, *409*(3), 424–429. https://doi.org/10.1016/j.bbrc.2011.05.015

Hoffmeister, B. R., Adib-Razavi, M. S., Jakupec, M. A., Galanski, M. S., & Keppler, B. K. (2012). Diamminetetrakis(carboxylato)platinum(IV) Complexes – Synthesis, Characterization, and Cytotoxicity. *Chemistry & Biodiversity*, *9*(9), 1840–1848. https://doi.org/10.1002/cbdv.201200019

Holdbrooks, A. T., Ankenbauer, K. E., Hwang, J., & Bellis, S. L. (2020). Regulation of inflammatory signaling by the ST6Gal-I sialyltransferase. *PLOS ONE*, *15*(11), e0241850. https://doi.org/10.1371/journal.pone.0241850

Holme, Ø., Bretthauer, M., Eide, T. J., Løberg, E. M., Grzyb, K., Løberg, M., Kalager, M., Adami, H.-O., Kjellevold, Ø., & Hoff, G. (2015). Long-term risk of colorectal cancer in individuals with serrated polyps. *Gut*, *64*(6), 929–936. https://doi.org/10.1136/gutjnl-2014-307793

Holowatyj, A. N., Haffa, M., Lin, T., Scherer, D., Gigic, B., Ose, J., Warby, C. A., Himbert, C., Abbenhardt-Martin, C., Achaintre, D., Boehm, J., Boucher, K. M., Gicquiau, A., Gsur, A., Habermann, N., Herpel, E., Kauczor, H.-U., Keski-Rahkonen, P., Kloor, M., … Ulrich, C. M. (2020). Multi-omics Analysis Reveals Adipose–tumor Crosstalk in Patients with Colorectal Cancer. *Cancer Prevention Research*, *13*(10), 817–828. https://doi.org/10.1158/1940-6207.capr-19-0538

Hong, S. N. (2018). Genetic and epigenetic alterations of colorectal cancer. *Intestinal Research*, *16*(3), 327. https://doi.org/10.5217/ir.2018.16.3.327

Hosokawa, H., & Rothenberg, E. V. (2018). Cytokines, Transcription Factors, and the Initiation of T-Cell Development. *Cold Spring Harbor Perspectives in Biology*, *10*(5), a028621. https://doi.org/10.1101/cshperspect.a028621

Hou, X., Chen, C., He, X., & Lan, X. (2022). Siglec-15 Silencing Inhibits Cell Proliferation and Promotes Cell Apoptosis by Inhibiting STAT1/STAT3 Signaling in Anaplastic Thyroid Carcinoma. *Disease Markers*, *2022*, 1–16. https://doi.org/10.1155/2022/1606404

Hou, X., Chen, C., Lan, X., & He, X. (2022). Unveiling the molecular features, relevant immune and clinical characteristics of SIGLEC15 in thyroid cancer. *Frontiers in Immunology*, *13*, 975787. https://doi.org/10.3389/fimmu.2022.975787

Hsieh, C.-C., Shyr, Y.-M., Liao, W.-Y., Chen, T.-H., Wang, S.-E., Lu, P.-C., Lin, P.-Y., Chen, Y.-B., Mao, W.-Y., Han, H.-Y., Hsiao, M., Yang, W.-B., Li, W.-S., Sher, Y.-P., & Shen, C.-N. (2017). Elevation of β-galactoside α2,6-sialyltransferase 1 in a fructose-responsive manner promotes pancreatic cancer metastasis. *Oncotarget*, *8*(5), 7691–7709. https://doi.org/10.18632/oncotarget.13845

Hsieh, T.-C., & Hsu, C.-W. (2019). Breast metastasis from colorectal cancer treated by multimodal therapy: Case report and literature review. *Medicine*, *98*(51), e18016. https://doi.org/10.1097/MD.0000000000018016

Hsueh, C., Lin, J.-D., Chang, Y.-S., Hsueh, S., Chao, T.-C., Yu, J.-S., Jung, S.-M., Tseng, N.-M., Sun, J.-H., Kuo, S.-Y., & Ueng, S.-H. (2013). Prognostic significance of pituitary tumour-transforming gene-binding factor (PBF) expression in papillary thyroid carcinoma. *Clinical Endocrinology*, *78*(2), 303–309. https://doi.org/10.1111/cen.12007

Hu, J., Yu, A., Othmane, B., Qiu, D., Li, H., Li, C., Liu, P., Ren, W., Chen, M., Gong, G., Guo, X., Zhang, H., Chen, J., & Zu, X. (2021). Siglec15 shapes a non-inflamed tumor microenvironment and predicts the molecular subtype in bladder cancer. *Theranostics*, *11*(7), 3089–3108. https://doi.org/10.7150/thno.53649

Hu, P., Shimoji, S., & Hart, G. W. (2010). Site-specific interplay between O-GlcNAcylation and phosphorylation in cellular regulation. *FEBS Letters*, *584*(12), 2526–2538. https://doi.org/10.1016/j.febslet.2010.04.044

Huang, B., Lang, X., & Li, X. (2022). The role of IL-6/JAK2/STAT3 signaling pathway in cancers. *Frontiers in Oncology*, *12*, 1023177. https://doi.org/10.3389/fonc.2022.1023177

Huang, D., Sun, W., Zhou, Y., Li, P., Chen, F., Chen, H., Xia, D., Xu, E., Lai, M., Wu, Y., & Zhang, H. (2018). Mutations of key driver genes in colorectal cancer progression and metastasis. *Cancer and Metastasis Reviews*, *37*(1), 173–187. https://doi.org/10.1007/s10555-017-9726-5

Huang, R., Zheng, J., Shao, Y., Zhu, L., & Yang, T. (2023). Siglec-15 as multifunctional molecule involved in osteoclast differentiation, cancer immunity and microbial infection. *Progress in Biophysics and Molecular Biology*, *177*, 34–41. https://doi.org/10.1016/j.pbiomolbio.2022.10.006

Huang, Y., Hong, W., & Wei, X. (2022). The molecular mechanisms and therapeutic strategies of EMT in tumor progression and metastasis. *Journal of Hematology & Oncology*, *15*(1). https://doi.org/10.1186/s13045-022-01347-8

Huang, Y., Zhou, J., Zhong, H., Xie, N., Zhang, F.-R., & Zhang, Z. (2022). Identification of a novel lipid metabolism-related gene signature for predicting colorectal cancer survival. *Frontiers in Genetics*, *13*, 989327. https://doi.org/10.3389/fgene.2022.989327

Huang, Z., Guo, Y., Li, B., Shen, M., Yi, Y., Li, L., Zhao, X., & Yang, L. (2023). Siglec-15 on macrophages suppress the immune microenvironment in patients with PD-L1 negative non-metastasis lung adenocarcinoma. *Cancer Gene Therapy*. https://doi.org/10.1038/s41417-023-00713-z

Huang, Z., Yang, Q., & Huang, Z. (2018). Identification of Critical Genes and Five Prognostic Biomarkers Associated with Colorectal Cancer. *Medical Science Monitor*, *24*, 4625–4633. https://doi.org/10.12659/MSM.907224

Hugonnet, M., Singh, P., Haas, Q., & Von Gunten, S. (2021). The Distinct Roles of Sialyltransferases in Cancer Biology and Onco-Immunology. *Frontiers in Immunology*, *12*, 799861. https://doi.org/10.3389/fimmu.2021.799861

Hung, J.-S., Huang, J., Lin, Y.-C., Huang, M.-J., Lee, P.-H., Lai, H.-S., Liang, J.-T., & Huang, M.-C. (2014). C1GALT1 overexpression promotes the invasive behavior of colon cancer cells through modifying O-glycosylation of FGFR2. *Oncotarget*, *5*(8), 2096–2106. https://doi.org/10.18632/oncotarget.1815

Hunter, S. A., & Cochran, J. R. (2016). Cell-Binding Assays for Determining the Affinity of Protein–Protein Interactions. In *Methods in Enzymology* (Vol. 580, pp. 21–44). Elsevier. https://doi.org/10.1016/bs.mie.2016.05.002

Hussen, B. M., Hidayat, H. J., Salihi, A., Sabir, D. K., Taheri, M., & Ghafouri-Fard, S. (2021). MicroRNA: A signature for cancer progression. *Biomedicine & Pharmacotherapy*, *138*, 111528. https://doi.org/10.1016/j.biopha.2021.111528

Ibrahim, H., & Lim, Y. C. (2020). KRAS-associated microRNAs in colorectal cancer. *Oncology Reviews*, *14*(2). https://doi.org/10.4081/oncol.2020.454

Ikehara, Y., Kojima, N., Kurosawa, N., Kudo, T., Kono, M., Nishihara, S., Issiki, S., Morozumi, K., Itzkowitz, S., Tsuda, T., Nishimura, S.-I., Tsuji, S., & Narimatsu, H.

(1999). Cloning and expression of a human gene encoding an N-acetylgalactosamine-2,6-sialyltransferase (ST6GalNAc I): A candidate for synthesis of cancer-associated sialyl-Tn antigens. *Glycobiology*, *9*(11), 1213–1224. https://doi.org/10.1093/glycob/9.11.1213

Imruetaicharoenchoke, W., Fletcher, A., Lu, W., Watkins, R. J., Modasia, B., Poole, V. L., Nieto, H. R., Thompson, R. J., Boelaert, K., Read, M. L., Smith, V. E., & McCabe, C. J. (2017). Functional consequences of the first reported mutations of the proto-oncogene PTTG1IP/PBF. *Endocrine-Related Cancer*, *24*(9), 459–474. https://doi.org/10.1530/ERC-16-0340

Ingelson-Filpula, W. A., & Storey, K. B. (2023). Hibernation-Induced microRNA Expression Promotes Signaling Pathways and Cell Cycle Dysregulation in Ictidomys tridecemlineatus Cardiac Tissue. *Metabolites*, *13*(10), 1096. https://doi.org/10.3390/metabo13101096

Ingersoll, M. A., Platt, A. M., Potteaux, S., & Randolph, G. J. (2011). Monocyte trafficking in acute and chronic inflammation. *Trends in Immunology*, *32*(10), 470–477. https://doi.org/10.1016/j.it.2011.05.001

Ishida-Kitagawa, N., Tanaka, K., Bao, X., Kimura, T., Miura, T., Kitaoka, Y., Hayashi, K., Sato, M., Maruoka, M., Ogawa, T., Miyoshi, J., & Takeya, T. (2012). Siglec-15 Protein Regulates Formation of Functional Osteoclasts in Concert with DNAX-activating Protein of 12 kDa (DAP12). *Journal of Biological Chemistry*, *287*(21), 17493–17502. https://doi.org/10.1074/jbc.M111.324194

Iwama, T., Mishima, Y., & Utsunomiya, J. (1993). The Impact of Familial Adenomatous Polyposis on the Tumorigenesis and Mortality at the Several Organs: Its Rational Treatment. *Annals of Surgery*, *217*(2), 101–108. https://doi.org/10.1097/00000658-199302000-00002

Iwanejko, J., Wojaczyńska, E., & Olszewski, T. K. (2018). Green chemistry and catalysis in Mannich reaction. *Current Opinion in Green and Sustainable Chemistry*, *10*, 27–34. https://doi.org/10.1016/j.cogsc.2018.02.006

Iwaya, T., Sawada, G., Amano, S., Kume, K., Ito, C., Endo, F., Konosu, M., Shioi, Y., Akiyama, Y., Takahara, T., Otsuka, K., Nitta, H., Koeda, K., Mizuno, M., Nishizuka, S., Sasaki, A., & Mimori, K. (2017). Downregulation of ST6GALNAC1 is associated with esophageal squamous cell carcinoma development. *International Journal of Oncology*, *50*(2), 441–447. https://doi.org/10.3892/ijo.2016.3817

Jain, S., Maque, J., Galoosian, A., Osuna-Garcia, A., & May, F. P. (2022). Optimal Strategies for Colorectal Cancer Screening. *Current Treatment Options in Oncology*, *23*(4), 474–493. https://doi.org/10.1007/s11864-022-00962-4

Jame-Chenarboo, Z., Gray, T. E., & Macauley, M. S. (2024). Advances in understanding and exploiting Siglec–glycan interactions. *Current Opinion in Chemical Biology*, *80*, 102454. https://doi.org/10.1016/j.cbpa.2024.102454

Jančík, S., Drábek, J., Radzioch, D., & Hajdúch, M. (2010). Clinical Relevance of KRAS in Human Cancers. *Journal of Biomedicine and Biotechnology*, *2010*, 1–13. https://doi.org/10.1155/2010/150960

Jandus, C., Boligan, K. F., Chijioke, O., Liu, H., Dahlhaus, M., Démoulins, T., Schneider, C., Wehrli, M., Hunger, R. E., Baerlocher, G. M., Simon, H.-U., Romero, P., Münz, C., & Von Gunten, S. (2014). Interactions between Siglec-7/9 receptors and ligands influence NK cell–dependent tumor immunosurveillance. *Journal of Clinical Investigation*, *124*(4), 1810–1820. https://doi.org/10.1172/JCI65899

Jia, L., Luo, S., Ren, X., Li, Y., Hu, J., Liu, B., Zhao, L., Shan, Y., & Zhou, H. (2017). miR-182 and miR-135b Mediate the Tumorigenesis and Invasiveness of Colorectal Cancer Cells via Targeting ST6GALNAC2 and PI3K/AKT Pathway. *Digestive Diseases and Sciences*, *62*(12), 3447–3459. https://doi.org/10.1007/s10620-017-4755-z

Jia, Y., Liu, J., Wang, G., & Song, Z. (2022). miR-484: A Potential Biomarker in Health and Disease. *Frontiers in Oncology*, *12*, 830420. https://doi.org/10.3389/fonc.2022.830420

Jiang, K.-Y., Qi, L.-L., Kang, F.-B., & Wang, L. (2022). The intriguing roles of Siglec family members in the tumor microenvironment. *Biomarker Research*, *10*(1), 22. https://doi.org/10.1186/s40364-022-00369-1

Jin, Y., Chen, Z., Dong, J., Wang, B., Fan, S., Yang, X., & Cui, M. (2021). SREBP1/FASN/cholesterol axis facilitates radioresistance in colorectal cancer. *FEBS Open Bio*, *11*(5), 1343–1352. https://doi.org/10.1002/2211-5463.13137

Jing, W., Guo, X., Wang, G., Bi, Y., Han, L., Zhu, Q., Qiu, C., Tanaka, M., & Zhao, Y. (2020). Breast cancer cells promote CD169+ macrophage-associated immunosuppression through JAK2-mediated PD-L1 upregulation on macrophages. *International Immunopharmacology*, *78*, 106012. https://doi.org/10.1016/j.intimp.2019.106012

Jingu, K., Matsushita, H., Yamamoto, T., Umezawa, R., Ishikawa, Y., Takahashi, N., Katagiri, Y., Takeda, K., & Kadoya, N. (2018). Stereotactic Radiotherapy for Pulmonary Oligometastases From Colorectal Cancer: A Systematic Review and Meta-Analysis.

Technology in Cancer Research & Treatment, *17*, 153303381879493. https://doi.org/10.1177/1533033818794936

Johdi, N. A., & Sukor, N. F. (2020). Colorectal Cancer Immunotherapy: Options and Strategies. *Frontiers in Immunology*, *11*, 1624. https://doi.org/10.3389/fimmu.2020.01624

Johnson, C. M., Hill, C. S., Chawla, S., Treisman, R., & Bading, H. (1997). Calcium Controls Gene Expression via Three Distinct Pathways That Can Function Independently of the Ras/Mitogen-Activated Protein Kinases (ERKs) Signaling Cascade. *The Journal of Neuroscience*, *17*(16), 6189–6202. https://doi.org/10.1523/JNEUROSCI.17-16-06189.1997

Johnson, D. E., O'Keefe, R. A., & Grandis, J. R. (2018). Targeting the IL-6/JAK/STAT3 signalling axis in cancer. *Nature Reviews. Clinical Oncology*, *15*(4), 234–248. https://doi.org/10.1038/nrclinonc.2018.8

Johnston, P. A., & Grandis, J. R. (2011). STAT3 SIGNALING: Anticancer Strategies and Challenges. *Molecular Interventions*, *11*(1), 18–26. https://doi.org/10.1124/mi.11.1.4

Joo, Y.-E. (2015). Prognostic Significance of CpG Island Methylator Phenotype in Colorectal Cancer. *Gut and Liver*, *9*(2), 139–140. https://doi.org/10.5009/gnl15023

Jost, P. J., Grabow, S., Gray, D., McKenzie, M. D., Nachbur, U., Huang, D. C. S., Bouillet, P., Thomas, H. E., Borner, C., Silke, J., Strasser, A., & Kaufmann, T. (2009). XIAP discriminates between type I and type II FAS-induced apoptosis. *Nature*, *460*(7258), 1035–1039. https://doi.org/10.1038/nature08229

Ju, T., Aryal, R. P., Kudelka, M. R., Wang, Y., & Cummings, R. D. (2014). The Cosmc connection to the Tn antigen in cancer. *Cancer Biomarkers*, *14*(1), 63–81. https://doi.org/10.3233/CBM-130375

Jung, J., Enterina, J. R., Bui, D. T., Mozaneh, F., Lin, P.-H., Nitin, Kuo, C.-W., Rodrigues, E., Bhattacherjee, A., Raeisimakiani, P., Daskhan, G. C., St. Laurent, C. D., Khoo, K.-H., Mahal, L. K., Zandberg, W. F., Huang, X., Klassen, J. S., & Macauley, M. S. (2021). Carbohydrate Sulfation As a Mechanism for Fine-Tuning Siglec Ligands. *ACS Chemical Biology*, *16*(11), 2673–2689. https://doi.org/10.1021/acschembio.1c00501

Kamanu, T. K. K., Radovanovic, A., Archer, J. A. C., & Bajic, V. B. (2013). Exploration of miRNA families for hypotheses generation. *Scientific Reports*, *3*(1), 2940. https://doi.org/10.1038/srep02940

Kameda, Y., Takahata, M., Komatsu, M., Mikuni, S., Hatakeyama, S., Shimizu, T., Angata, T., Kinjo, M., Minami, A., & Iwasaki, N. (2013). Siglec-15 Regulates Osteoclast

Differentiation by Modulating RANKL-Induced Phosphatidylinositol 3-Kinase/Akt and Erk Pathways in Association With Signaling Adaptor DAP12. *Journal of Bone and Mineral Research*, *28*(12), 2463–2475. https://doi.org/10.1002/jbmr.1989

Kanehisa, M., Araki, M., Goto, S., Hattori, M., Hirakawa, M., Itoh, M., Katayama, T., Kawashima, S., Okuda, S., Tokimatsu, T., & Yamanishi, Y. (2007). KEGG for linking genomes to life and the environment. *Nucleic Acids Research*, *36*(Database), D480–D484. https://doi.org/10.1093/nar/gkm882

Kara, G., Calin, G. A., & Ozpolat, B. (2022). RNAi-based therapeutics and tumor targeted delivery in cancer. *Advanced Drug Delivery Reviews*, *182*, 114113. https://doi.org/10.1016/j.addr.2022.114113

Kaur, P., Singh, A., & Chana, I. (2021). Computational Techniques and Tools for Omics Data Analysis: State-of-the-Art, Challenges, and Future Directions. *Archives of Computational Methods in Engineering*, *28*(7), 4595–4631. https://doi.org/10.1007/s11831-021-09547-0

Kellici, T. F., Pilka, E. S., & Bodkin, M. J. (2021). Therapeutic Potential of Targeting Plasminogen Activator Inhibitor-1 in COVID-19. *Trends in Pharmacological Sciences*, *42*(6), 431–433. https://doi.org/10.1016/j.tips.2021.03.006

Kenneth, M. J., Shishir, T. A., & Haque, F. K. M. (2023). In silico analysis reveals mir-98-5p as a potential inhibitor of tumor cell proliferation and metastasis in colorectal cancer by targeting the fzd3 receptor of the Wnt signaling pathway. *Journal of Genetic Engineering and Biotechnology*, *21*(1), 79. https://doi.org/10.1186/s43141-023-00532-7

Kenzelmann Broz, D., Spano Mello, S., Bieging, K. T., Jiang, D., Dusek, R. L., Brady, C. A., Sidow, A., & Attardi, L. D. (2013). Global genomic profiling reveals an extensive p53-regulated autophagy program contributing to key p53 responses. *Genes & Development*, *27*(9), 1016–1031. https://doi.org/10.1101/gad.212282.112

Khiaowichit, J., Talabnin, C., Dechsukhum, C., Silsirivanit, A., & Talabnin, K. (2022). Down-Regulation of C1GALT1 Enhances the Progression of Cholangiocarcinoma through Activation of AKT/ERK Signaling Pathways. *Life*, *12*(2), 174. https://doi.org/10.3390/life12020174

Kidwai, M., Bhatnagar, D., Mishra, N. K., & Bansal, V. (2008). CAN catalyzed synthesis of β-amino carbonyl compounds via Mannich reaction in PEG. *Catalysis Communications*, *9*(15), 2547–2549. https://doi.org/10.1016/j.catcom.2008.07.010

Kish, T., & Uppal, P. (2016). Trifluridine/Tipiracil (Lonsurf) for the Treatment of Metastatic Colorectal Cancer. *P & T: A Peer-Reviewed Journal for Formulary Management*, *41*(5), 314–325.

Klampfer, L. (2011). Cytokines, Inflammation and Colon Cancer. *Current Cancer Drug Targets*, *11*(4), 451–464. https://doi.org/10.2174/156800911795538066

Kobayashi, H., Terkawi, M. A., Ota, M., Hasegawa, T., Yamamoto, T., Shimizu, T., Sato, D., Fujita, R., Murakami, T., Amizuka, N., Iwasaki, N., & Takahata, M. (2024). Involvement of Siglec-15 in regulating RAP1/RAC signaling in cytoskeletal remodeling in osteoclasts mediated by macrophage colony-stimulating factor. *Bone Research*, *12*(1), 35. https://doi.org/10.1038/s41413-024-00340-w

Kobiela, J., Spychalski, P., Marvaso, G., Ciardo, D., Dell'Acqua, V., Kraja, F., Błażyńska-Spychalska, A., Łachiński, A. J., Surgo, A., Glynne-Jones, R., & Jereczek-Fossa, B. A. (2018). Ablative stereotactic radiotherapy for oligometastatic colorectal cancer: Systematic review. *Critical Reviews in Oncology/Hematology*, *129*, 91–101. https://doi.org/10.1016/j.critrevonc.2018.06.005

Krol, J., Loedige, I., & Filipowicz, W. (2010). The widespread regulation of microRNA biogenesis, function and decay. *Nature Reviews Genetics*, *11*(9), 597–610. https://doi.org/10.1038/nrg2843

Kudelka, M. R., Ju, T., Heimburg-Molinaro, J., & Cummings, R. D. (2015). Simple Sugars to Complex Disease—Mucin-Type O-Glycans in Cancer. In *Advances in Cancer Research* (Vol. 126, pp. 53–135). Elsevier. https://doi.org/10.1016/bs.acr.2014.11.002

Kumaran Satyanarayanan, S., El Kebir, D., Soboh, S., Butenko, S., Sekheri, M., Saadi, J., Peled, N., Assi, S., Othman, A., Schif-Zuck, S., Feuermann, Y., Barkan, D., Sher, N., Filep, J. G., & Ariel, A. (2019). IFN-β is a macrophage-derived effector cytokine facilitating the resolution of bacterial inflammation. *Nature Communications*, *10*(1), 3471. https://doi.org/10.1038/s41467-019-10903-9

Kvorjak, M., Ahmed, Y., Miller, M. L., Sriram, R., Coronnello, C., Hashash, J. G., Hartman, D. J., Telmer, C. A., Miskov-Zivanov, N., Finn, O. J., & Cascio, S. (2020). Cross-talk between Colon Cells and Macrophages Increases ST6GALNAC1 and MUC1-sTn Expression in Ulcerative Colitis and Colitis-Associated Colon Cancer. *Cancer Immunology Research*, *8*(2), 167–178. https://doi.org/10.1158/2326-6066.CIR-19-0514

Ladabaum, U., Dominitz, J. A., Kahi, C., & Schoen, R. E. (2020). Strategies for Colorectal Cancer Screening. *Gastroenterology*, *158*(2), 418–432. https://doi.org/10.1053/j.gastro.2019.06.043

Lagos-Quintana, M., Rauhut, R., Yalcin, A., Meyer, J., Lendeckel, W., & Tuschl, T. (2002). Identification of Tissue-Specific MicroRNAs from Mouse. *Current Biology*, *12*(9), 735–739. https://doi.org/10.1016/S0960-9822(02)00809-6

Lai, C.-Y., Yeh, K.-Y., Liu, B.-F., Chang, T.-M., Chang, C.-H., Liao, Y.-F., Liu, Y.-W., & Her, G. M. (2021). MicroRNA-21 Plays Multiple Oncometabolic Roles in Colitis-Associated Carcinoma and Colorectal Cancer via the PI3K/AKT, STAT3, and PDCD4/TNF-α Signaling Pathways in Zebrafish. *Cancers*, *13*(21), 5565. https://doi.org/10.3390/cancers13215565

Lam, K. K., Thean, L. F., & Cheah, P. Y. (2021). Advances in colorectal cancer genomics and transcriptomics drive early detection and prevention. *The International Journal of Biochemistry & Cell Biology*, *137*, 106032. https://doi.org/10.1016/j.biocel.2021.106032

Läubli, H. (2024). Unraveling the impact of a glyco-immune checkpoint in bone metastasis. *Proceedings of the National Academy of Sciences*, *121*(9), e2400499121. https://doi.org/10.1073/pnas.2400499121

Läubli, H., Nalle, S. C., & Maslyar, D. (2022). Targeting the Siglec–Sialic Acid Immune Axis in Cancer: Current and Future Approaches. *Cancer Immunology Research*, *10*(12), 1423–1432. https://doi.org/10.1158/2326-6066.CIR-22-0366

Lavrsen, K., Dabelsteen, S., Vakhrushev, S. Y., Levann, A. M. R., Haue, A. D., Dylander, A., Mandel, U., Hansen, L., Frödin, M., Bennett, E. P., & Wandall, H. H. (2018). De novo expression of human polypeptide N-acetylgalactosaminyltransferase 6 (GalNAc-T6) in colon adenocarcinoma inhibits the differentiation of colonic epithelium. *Journal of Biological Chemistry*, *293*(4), 1298–1314. https://doi.org/10.1074/jbc.M117.812826

Lee, A., Chick, J. M., Kolarich, D., Haynes, P. A., Robertson, G. R., Tsoli, M., Jankova, L., Clarke, S. J., Packer, N. H., & Baker, M. S. (2011). Liver Membrane Proteome Glycosylation Changes in Mice Bearing an Extra-hepatic Tumor. *Molecular & Cellular Proteomics*, *10*(9), M900538-MCP200. https://doi.org/10.1074/mcp.M900538-MCP200

Lee, H.-T., Oh, S., Ro, D. H., Yoo, H., & Kwon, Y.-W. (2020). The Key Role of DNA Methylation and Histone Acetylation in Epigenetics of Atherosclerosis. *Journal of Lipid and Atherosclerosis*, *9*(3), 419. https://doi.org/10.12997/jla.2020.9.3.419

Lee, J.-Y., Ryu, D.-S., Kim, W.-J., & Kim, S.-J. (2016). Aberrantly expressed microRNAs in the context of bladder tumorigenesis. *Investigative and Clinical Urology*, *57*(Suppl 1), S52. https://doi.org/10.4111/icu.2016.57.S1.S52

Lee, J.-Y., Yun, S. J., Jeong, P., Piao, X.-M., Kim, Y.-H., Kim, J., Subramaniyam, S., Byun, Y. J., Kang, H. W., Seo, S. P., Kim, J., Kim, J. M., Yoo, E. S., Kim, I. Y., Moon, S.-K., Choi, Y. H., & Kim, W.-J. (2018). Identification of differentially expressed miRNAs and miRNA-targeted genes in bladder cancer. *Oncotarget*, *9*(45), 27656–27666. https://doi.org/10.18632/oncotarget.24441

Lee, W. J., Shin, C. H., Ji, H., Jeong, S. D., Park, M.-S., Won, H.-H., Pandey, P. R., Tsitsipatis, D., Gorospe, M., & Kim, H. H. (2021). hnRNPK-regulated LINC00263 promotes malignant phenotypes through miR-147a/CAPN2. *Cell Death & Disease*, *12*(4), 290. https://doi.org/10.1038/s41419-021-03575-1

Lee, W.-L., & Wang, P.-H. (2020). Aberrant sialylation in ovarian cancers. *Journal of the Chinese Medical Association*, *83*(4), 337–344. https://doi.org/10.1097/JCMA.0000000000000252

Lee, Y., Ahn, C., Han, J., Choi, H., Kim, J., Yim, J., Lee, J., Provost, P., Rådmark, O., Kim, S., & Kim, V. N. (2003). The nuclear RNase III Drosha initiates microRNA processing. *Nature*, *425*(6956), 415–419. https://doi.org/10.1038/nature01957

Leggett, B., & Whitehall, V. (2010). Role of the Serrated Pathway in Colorectal Cancer Pathogenesis. *Gastroenterology*, *138*(6), 2088–2100. https://doi.org/10.1053/j.gastro.2009.12.066

Leibovitz, A., Wright, W. C., Pathak, S., Siciliano, M. J., Daniels, W. P., Fogh, H., & Fogh, J. (1979). Detection and Analysis of a Glucose 6-Phosphate Dehydrogenase Phenotype B Cell Line Contamination2. *JNCI: Journal of the National Cancer Institute*, *63*(3), 635–645. https://doi.org/10.1093/jnci/63.3.635

Lenza, M. P., Egia-Mendikute, L., Antoñana-Vildosola, A., Soares, C. O., Coelho, H., Corzana, F., Bosch, A., Manisha, P., Quintana, J. I., Oyenarte, I., Unione, L., Moure, M. J., Azkargorta, M., Atxabal, U., Sobczak, K., Elortza, F., Sutherland, J. D., Barrio, R., Marcelo, F., … Ereño-Orbea, J. (2023). Structural insights into Siglec-15 reveal glycosylation dependency for its interaction with T cells through integrin CD11b. *Nature Communications*, *14*(1), 3496. https://doi.org/10.1038/s41467-023-39119-8

Li, B., Zhang, B., Wang, X., Zeng, Z., Huang, Z., Zhang, L., Wei, F., Ren, X., & Yang, L. (2020). Expression signature, prognosis value, and immune characteristics of Siglec-

15 identified by pan-cancer analysis. *OncoImmunology*, *9*(1), 1807291. https://doi.org/10.1080/2162402X.2020.1807291

Li, C., Dou, P., Wang, T., Lu, X., Xu, G., & Lin, X. (2023). Defining disease-related modules based on weighted miRNA synergistic network. *Computers in Biology and Medicine*, *152*, 106382. https://doi.org/10.1016/j.compbiomed.2022.106382

Li, C., Liu, T., Yin, L., Zuo, D., Lin, Y., & Wang, L. (2019). Prognostic and clinicopathological value of MUC1 expression in colorectal cancer: A meta-analysis. *Medicine*, *98*(9), e14659. https://doi.org/10.1097/MD.0000000000014659

Li, C.-W., Lim, S.-O., Xia, W., Lee, H.-H., Chan, L.-C., Kuo, C.-W., Khoo, K.-H., Chang, S.-S., Cha, J.-H., Kim, T., Hsu, J. L., Wu, Y., Hsu, J.-M., Yamaguchi, H., Ding, Q., Wang, Y., Yao, J., Lee, C.-C., Wu, H.-J., … Hung, M.-C. (2016). Glycosylation and stabilization of programmed death ligand-1 suppresses T-cell activity. *Nature Communications*, *7*(1), 12632. https://doi.org/10.1038/ncomms12632

Li, D., & Ji, B. (2019). Protein conformational transitions coupling with ligand interactions: Simulations from molecules to medicine. *Medicine in Novel Technology and Devices*, *3*, 100026. https://doi.org/10.1016/j.medntd.2019.100026

Li, D., & Wu, M. (2021). Pattern recognition receptors in health and diseases. *Signal Transduction and Targeted Therapy*, *6*(1), 291. https://doi.org/10.1038/s41392-021-00687-0

Li, J. (2014). TNM staging of colorectal cancer should be reconsidered by T stage weighting. *World Journal of Gastroenterology*, *20*(17), 5104. https://doi.org/10.3748/wjg.v20.i17.5104

Li, J., Cao, F., Yin, H., Huang, Z., Lin, Z., Mao, N., Sun, B., & Wang, G. (2020). Ferroptosis: Past, present and future. *Cell Death & Disease*, *11*(2), 88. https://doi.org/10.1038/s41419-020-2298-2

Li, J., Chen, H., Sun, G., Zhang, X., Ye, H., & Wang, P. (2023). Role of miR-21 in the diagnosis of colorectal cancer: Meta-analysis and bioinformatics. *Pathology - Research and Practice*, *248*, 154670. https://doi.org/10.1016/j.prp.2023.154670

Li, J., Ji, Y., Chen, N., Dai, L., & Deng, H. (2023). Colitis-associated carcinogenesis: Crosstalk between tumors, immune cells and gut microbiota. *Cell & Bioscience*, *13*(1), 194. https://doi.org/10.1186/s13578-023-01139-8

Li, J., Ma, X., Chakravarti, D., Shalapour, S., & DePinho, R. A. (2021). Genetic and biological hallmarks of colorectal cancer. *Genes & Development*, *35*(11–12), 787–820. https://doi.org/10.1101/gad.348226.120

Li, P., Zhou, L., Zhao, T., Liu, X., Zhang, P., Liu, Y., Zheng, X., & Li, Q. (2017). Caspase-9: Structure, mechanisms and clinical application. *Oncotarget*, *8*(14), 23996–24008. https://doi.org/10.18632/oncotarget.15098

Li, T., Fan, J., Wang, B., Traugh, N., Chen, Q., Liu, J. S., Li, B., & Liu, X. S. (2017). TIMER: A Web Server for Comprehensive Analysis of Tumor-Infiltrating Immune Cells. *Cancer Research*, *77*(21), e108–e110. https://doi.org/10.1158/0008-5472.CAN-17-0307

Li, X., Liang, Z., Pan, J., Zhang, M., Liu, J., Hu, R., & Liao, C. (2024). Identification of BACH1-IT2-miR-4786-Siglec-15 immune suppressive axis in bladder cancer. *BMC Cancer*, *24*(1), 328. https://doi.org/10.1186/s12885-024-12061-8

Li, X., Wu, Y., & Tian, T. (2022). TGF-β Signaling in Metastatic Colorectal Cancer (mCRC): From Underlying Mechanism to Potential Applications in Clinical Development. *International Journal of Molecular Sciences*, *23*(22), 14436. https://doi.org/10.3390/ijms232214436

Li, Y., Wang, W., Wu, M., Zhu, P., Zhou, Z., Gong, Y., & Gu, Y. (2022). LncRNA LINC01315 silencing modulates cancer stem cell properties and epithelial-to-mesenchymal transition in colorectal cancer via miR-484/DLK1 axis. *Cell Cycle*, *21*(8), 851–873. https://doi.org/10.1080/15384101.2022.2033415

Li, Y., Yang, J., Wang, H., Qiao, W., Guo, Y., Zhang, S., & Guo, Y. (2020). FNDC3B, Targeted by miR-125a-5p and miR-217, Promotes the Proliferation and Invasion of Colorectal Cancer Cells via PI3K/mTOR Signaling. *OncoTargets and Therapy*, *Volume 13*, 3501–3510. https://doi.org/10.2147/OTT.S226520

Li, Z., Yang, Z., Liu, W., Zhu, W., Yin, L., Han, Z., Xian, Y., Wen, J., Tang, H., Lin, X., Yang, Y., Wang, J., & Zhang, K. (2023). Disheveled3 enhanced EMT and cancer stem-like cells properties via Wnt/β-catenin/c-Myc/SOX2 pathway in colorectal cancer. *Journal of Translational Medicine*, *21*(1), 302. https://doi.org/10.1186/s12967-023-04120-8

Liang, H., Chen, Q., Hu, Z., Zhou, L., Meng, Q., Zhang, T., Wang, B., Ge, Y., Lu, S., Ding, W., Zhou, X., Li, X., Lin, H., Jiang, L., & Dong, J. (2022). Siglec15 facilitates the progression of non-small cell lung cancer and is correlated with spinal metastasis. *Annals of Translational Medicine*, *10*(6), 281–281. https://doi.org/10.21037/atm-22-764

Liang, L., Gao, C., Li, Y., Sun, M., Xu, J., Li, H., Jia, L., & Zhao, Y. (2017). miR-125a-3p/FUT5-FUT6 axis mediates colorectal cancer cell proliferation, migration, invasion

and pathological angiogenesis via PI3K-Akt pathway. *Cell Death & Disease*, *8*(8), e2968–e2968. https://doi.org/10.1038/cddis.2017.352

Liang, R., Zhu, X., Lan, T., Ding, D., Zheng, Z., Chen, T., Huang, Y., Liu, J., Yang, X., Shao, J., Wei, H., & Wei, B. (2021). TIGIT promotes CD8+T cells exhaustion and predicts poor prognosis of colorectal cancer. *Cancer Immunology, Immunotherapy*, *70*(10), 2781–2793. https://doi.org/10.1007/s00262-021-02886-8

Liao, Y., Chuang, Y., Lin, H., Lin, N., Hsu, T., Hsieh, S., Chen, S., Hung, J., Yang, H., Liang, J., Huang, M., & Huang, J. (2023). GALNT2 promotes invasiveness of colorectal cancer cells partly through AXL. *Molecular Oncology*, *17*(1), 119–133. https://doi.org/10.1002/1878-0261.13347

Lichtenstern, C. R., Ngu, R. K., Shalapour, S., & Karin, M. (2020). Immunotherapy, Inflammation and Colorectal Cancer. *Cells*, *9*(3), 618. https://doi.org/10.3390/cells9030618

Lila, E. M., & Martha, L. S. (2019). The functional role of miRNAs in colorectal cancer: Insights from a large population-based study. *Cancer Biology & Medicine*, *16*(2), 211. https://doi.org/10.20892/j.issn.2095-3941.2018.0514

Lim, J., Sari-Ak, D., & Bagga, T. (2021). Siglecs as Therapeutic Targets in Cancer. *Biology*, *10*(11), 1178. https://doi.org/10.3390/biology10111178

Lin, A., Zhang, J., & Luo, P. (2020). Crosstalk Between the MSI Status and Tumor Microenvironment in Colorectal Cancer. *Frontiers in Immunology*, *11*, 2039. https://doi.org/10.3389/fimmu.2020.02039

Lin, J., Xia, L., Oyang, L., Liang, J., Tan, S., Wu, N., Yi, P., Pan, Q., Rao, S., Han, Y., Tang, Y., Su, M., Luo, X., Yang, Y., Chen, X., Yang, L., Zhou, Y., & Liao, Q. (2022). The POU2F1-ALDOA axis promotes the proliferation and chemoresistance of colon cancer cells by enhancing glycolysis and the pentose phosphate pathway activity. *Oncogene*, *41*(7), 1024–1039. https://doi.org/10.1038/s41388-021-02148-y

Lin, Y., Jiang, M., Chen, W., Zhao, T., & Wei, Y. (2019). Cancer and ER stress: Mutual crosstalk between autophagy, oxidative stress and inflammatory response. *Biomedicine & Pharmacotherapy*, *118*, 109249. https://doi.org/10.1016/j.biopha.2019.109249

Lin, Y.-H., Zhu, J., Meijer, S., Franc, V., & Heck, A. J. R. (2019). Glycoproteogenomics: A Frequent Gene Polymorphism Affects the Glycosylation Pattern of the Human Serum Fetuin/α-2-HS-Glycoprotein. *Molecular & Cellular Proteomics*, *18*(8), 1479–1490. https://doi.org/10.1074/mcp.RA119.001411

Liszbinski, R. B., Romagnoli, G. G., Gorgulho, C. M., Basso, C. R., Pedrosa, V. A., & Kaneno, R. (2020). Anti-EGFR-Coated Gold Nanoparticles In Vitro Carry 5-Fluorouracil to Colorectal Cancer Cells. *Materials*, *13*(2), 375. https://doi.org/10.3390/ma13020375

Liu, B., Liu, Y., Zhao, L., Pan, Y., Shan, Y., Li, Y., & Jia, L. (2017). Upregulation of microRNA-135b and microRNA-182 promotes chemoresistance of colorectal cancer by targeting ST6GALNAC2 via PI3K/AKT pathway. *Molecular Carcinogenesis*, *56*(12), 2669–2680. https://doi.org/10.1002/mc.22710

Liu, C.-H., Hu, R.-H., Huang, M.-J., Lai, I.-R., Chen, C.-H., Lai, H.-S., Wu, Y.-M., & Huang, M.-C. (2014). C1GALT1 Promotes Invasive Phenotypes of Hepatocellular Carcinoma Cells by Modulating Integrin β1 Glycosylation and Activity. *PLoS ONE*, *9*(8), e94995. https://doi.org/10.1371/journal.pone.0094995

Liu, H., Liu, Y., Zhou, Y., Chen, X., Pan, S., Zhou, Q., Ji, H., & Zhu, X. (2024). TM7SF2-induced lipid reprogramming promotes cell proliferation and migration via CPT1A/Wnt/β-Catenin axis in cervical cancer cells. *Cell Death Discovery*, *10*(1), 207. https://doi.org/10.1038/s41420-024-01975-8

Liu, T., Zhang, L., Joo, D., & Sun, S.-C. (2017). NF-κB signaling in inflammation. *Signal Transduction and Targeted Therapy*, *2*(1), 17023. https://doi.org/10.1038/sigtrans.2017.23

Liu, Y., Li, X., Zhang, C., Zhang, H., & Huang, Y. (2020). LINC00973 is involved in cancer immune suppression through positive regulation of Siglec-15 in clear-cell renal cell carcinoma. *Cancer Science*, *111*(10), 3693–3704. https://doi.org/10.1111/cas.14611

Liu, Y., Xia, Y., & Qiu, C.-H. (2020). Functions of CD169 positive macrophages in human diseases (Review). *Biomedical Reports*, *14*(2), 26. https://doi.org/10.3892/br.2020.1402

Liu, Y., Zheng, C., Huang, Y., He, M., Xu, W. W., & Li, B. (2021). Molecular mechanisms of chemo- and radiotherapy resistance and the potential implications for cancer treatment. *MedComm*, *2*(3), 315–340. https://doi.org/10.1002/mco2.55

Liu, Z., Swindall, A. F., Kesterson, R. A., Schoeb, T. R., Bullard, D. C., & Bellis, S. L. (2011). ST6Gal-I Regulates Macrophage Apoptosis via α2-6 Sialylation of the TNFR1 Death Receptor. *Journal of Biological Chemistry*, *286*(45), 39654–39662. https://doi.org/10.1074/jbc.M111.276063

López-Velazco, J. I., Manzano, S., Otaño, M., Elorriaga, K., Bultó, N., Herrero, J., Lahuerta, A., Segur, V., Álvarez-López, I., Caffarel, M. M., & Urruticoechea, A. (2024). A prospective study on tumour response assessment methods after neoadjuvant endocrine

therapy in early oestrogen receptor-positive breast cancer. *Breast Cancer Research*, *26*(1), 3. https://doi.org/10.1186/s13058-023-01756-8

Loureiro, L. R., Sousa, D. P., Ferreira, D., Chai, W., Lima, L., Pereira, C., Lopes, C. B., Correia, V. G., Silva, L. M., Li, C., Santos, L. L., Ferreira, J. A., Barbas, A., Palma, A. S., Novo, C., & Videira, P. A. (2018). Novel monoclonal antibody L2A5 specifically targeting sialyl-Tn and short glycans terminated by alpha-2–6 sialic acids. *Scientific Reports*, *8*(1), 12196. https://doi.org/10.1038/s41598-018-30421-w

Lu, J., Getz, G., Miska, E. A., Alvarez-Saavedra, E., Lamb, J., Peck, D., Sweet-Cordero, A., Ebert, B. L., Mak, R. H., Ferrando, A. A., Downing, J. R., Jacks, T., Horvitz, H. R., & Golub, T. R. (2005). MicroRNA expression profiles classify human cancers. *Nature*, *435*(7043), 834–838. https://doi.org/10.1038/nature03702

Lu, J., & Gu, J. (2015). Significance of β-Galactoside α2,6 Sialyltranferase 1 in Cancers. *Molecules*, *20*(5), 7509–7527. https://doi.org/10.3390/molecules20057509

Lu, J., Isaji, T., Im, S., Fukuda, T., Hashii, N., Takakura, D., Kawasaki, N., & Gu, J. (2014). β-Galactoside α2,6-Sialyltranferase 1 Promotes Transforming Growth Factor-β-mediated Epithelial-Mesenchymal Transition. *Journal of Biological Chemistry*, *289*(50), 34627–34641. https://doi.org/10.1074/jbc.M114.593392

Lu, X., & Lu, J. (2015). The Significance of Detection of Serum miR-423-5p and miR-484 for Diagnosis of Colorectal Cancer. *Clinical Laboratory*, *61*(01+02/2015). https://doi.org/10.7754/Clin.Lab.2014.140625

Lu, Z., Cheng, P., Huang, F., Li, J., Wang, B., Zou, S., Zheng, Z., & Peng, C. (2023). Significance of Siglec-15 expression in colorectal cancer: Association with advanced disease stage and fewer tumor-infiltrating lymphocytes. *The Journal of Pathology: Clinical Research*, *9*(2), 121–128. https://doi.org/10.1002/cjp2.303

Lugli, A., Kirsch, R., Ajioka, Y., Bosman, F., Cathomas, G., Dawson, H., El Zimaity, H., Fléjou, J.-F., Hansen, T. P., Hartmann, A., Kakar, S., Langner, C., Nagtegaal, I., Puppa, G., Riddell, R., Ristimäki, A., Sheahan, K., Smyrk, T., Sugihara, K., … Quirke, P. (2017). Recommendations for reporting tumor budding in colorectal cancer based on the International Tumor Budding Consensus Conference (ITBCC) 2016. *Modern Pathology*, *30*(9), 1299–1311. https://doi.org/10.1038/modpathol.2017.46

Ma, S., Zhang, J., Yan, T., Miao, M., Cao, Y., Cao, Y., Zhang, L., & Li, L. (2023). Novel strategies to reverse chemoresistance in colorectal cancer. *Cancer Medicine*, *12*(10), 11073–11096. https://doi.org/10.1002/cam4.5594

Macauley, M. S., Crocker, P. R., & Paulson, J. C. (2014). Siglec-mediated regulation of immune cell function in disease. *Nature Reviews Immunology*, *14*(10), 653–666. https://doi.org/10.1038/nri3737

MacFarlane, L.-A., & R. Murphy, P. (2010). MicroRNA: Biogenesis, Function and Role in Cancer. *Current Genomics*, *11*(7), 537–561. https://doi.org/10.2174/138920210793175895

Mahmoud, N. N. (2022). Colorectal Cancer. *Surgical Oncology Clinics of North America*, *31*(2), 127–141. https://doi.org/10.1016/j.soc.2021.12.001

Majtnerová, P., & Roušar, T. (2018). An overview of apoptosis assays detecting DNA fragmentation. *Molecular Biology Reports*, *45*(5), 1469–1478. https://doi.org/10.1007/s11033-018-4258-9

Mao, X., Cai, T., Olyarchuk, J. G., & Wei, L. (2005). Automated genome annotation and pathway identification using the KEGG Orthology (KO) as a controlled vocabulary. *Bioinformatics*, *21*(19), 3787–3793. https://doi.org/10.1093/bioinformatics/bti430

Marchiori, M. F., Bortot, L. O., Carvalho, I., & Campo, V. L. (2020). Synthesis of MUC1-derived glycopeptide bearing a novel triazole STn analog. *Carbohydrate Research*, *498*, 108155. https://doi.org/10.1016/j.carres.2020.108155

Margraf-Schönfeld, S., Böhm, C., & Watzl, C. (2011). Glycosylation Affects Ligand Binding and Function of the Activating Natural Killer Cell Receptor 2B4 (CD244) Protein. *Journal of Biological Chemistry*, *286*(27), 24142–24149. https://doi.org/10.1074/jbc.M111.225334

Martínez-González, L., Sánchez-Conde, V., González-Cabezuelo, J., Antunez-Rodríguez, A., Andrés-León, E., Robles-Fernandez, I., Lorente, J., Vázquez-Alonso, F., & Alvarez-Cubero, M. (2021). Identification of MicroRNAs as Viable Aggressiveness Biomarkers for Prostate Cancer. *Biomedicines*, *9*(6), 646. https://doi.org/10.3390/biomedicines9060646

Massat, N. J., Moss, S. M., Halloran, S. P., & Duffy, S. W. (2013). Screening and Primary prevention of Colorectal Cancer: A Review of sex-specific and site-specific differences. *Journal of Medical Screening*, *20*(3), 125–148. https://doi.org/10.1177/0969141313501292

Matsuda, T., Yamashita, K., Hasegawa, H., Oshikiri, T., Hosono, M., Higashino, N., Yamamoto, M., Matsuda, Y., Kanaji, S., Nakamura, T., Suzuki, S., Sumi, Y., & Kakeji, Y. (2018). Recent updates in the surgical treatment of colorectal cancer. *Annals of Gastroenterological Surgery*, *2*(2), 129–136. https://doi.org/10.1002/ags3.12061

McCoy, M. S., Bargmann, C. I., & Weinberg, R. A. (1984). Human Colon Carcinoma Ki- *ras* 2 Oncogene and Its Corresponding Proto-Oncogene. *Molecular and Cellular Biology*, *4*(8), 1577–1582. https://doi.org/10.1128/mcb.4.8.1577-1582.1984

McVeigh, P., Cwiklinski, K., Garcia-Campos, A., Mulcahy, G., O'Neill, S. M., Maule, A. G., & Dalton, J. P. (2018). In silico analyses of protein glycosylating genes in the helminth Fasciola hepatica (liver fluke) predict protein-linked glycan simplicity and reveal temporally-dynamic expression profiles. *Scientific Reports*, *8*(1), 11700. https://doi.org/10.1038/s41598-018-29673-3

Mei, Q., Xue, G., Li, X., Wu, Z., Li, X., Yan, H., Guo, M., Sun, S., & Han, W. (2015). Methylation-induced loss of MIR -484 in microsatellite-unstable colorectal cancer promotes both viability and IL -8 production via CD137L. *The Journal of Pathology*, *236*(2), 165–174. https://doi.org/10.1002/path.4525

Meškytė, E. M., Keskas, S., & Ciribilli, Y. (2020). MYC as a Multifaceted Regulator of Tumor Microenvironment Leading to Metastasis. *International Journal of Molecular Sciences*, *21*(20), 7710. https://doi.org/10.3390/ijms21207710

Miao, X., & Zhao, Y. (2016). ST6GalNAcII mediates tumor invasion through PI3K/Akt/NF-κB signaling pathway in follicular thyroid carcinoma. *Oncology Reports*, *35*(4), 2131–2140. https://doi.org/10.3892/or.2016.4590

Minami, A., Shimono, Y., Mizutani, K., Nobutani, K., Momose, K., Azuma, T., & Takai, Y. (2013). Reduction of the ST6 β-Galactosamide α-2,6-Sialyltransferase 1 (ST6GAL1)-catalyzed Sialylation of Nectin-like Molecule 2/Cell Adhesion Molecule 1 and Enhancement of ErbB2/ErbB3 Signaling by MicroRNA-199a. *Journal of Biological Chemistry*, *288*(17), 11845–11853. https://doi.org/10.1074/jbc.M112.405993

Mirzaei, S., Paskeh, M. D. A., Entezari, M., Mirmazloomi, S. R., Hassanpoor, A., Aboutalebi, M., Rezaei, S., Hejazi, E. S., Kakavand, A., Heidari, H., Salimimoghadam, S., Taheriazam, A., Hashemi, M., & Samarghandian, S. (2022). SOX2 function in cancers: Association with growth, invasion, stemness and therapy response. *Biomedicine & Pharmacotherapy*, *156*, 113860. https://doi.org/10.1016/j.biopha.2022.113860

Mitra, N., Banda, K., Altheide, T. K., Schaffer, L., Johnson-Pais, T. L., Beuten, J., Leach, R. J., Angata, T., Varki, N., & Varki, A. (2011). SIGLEC12, a Human-specific Segregating (Pseudo)gene, Encodes a Signaling Molecule Expressed in Prostate Carcinomas. *Journal of Biological Chemistry*, *286*(26), 23003–23011. https://doi.org/10.1074/jbc.M111.244152

Mittal, V. (2018). Epithelial Mesenchymal Transition in Tumor Metastasis. *Annual Review of Pathology: Mechanisms of Disease*, *13*(1), 395–412. https://doi.org/10.1146/annurev-pathol-020117-043854

Moidu, N. A., A Rahman, N. S., Syafruddin, S. E., Low, T. Y., & Mohtar, M. A. (2020). Secretion of pro-oncogenic AGR2 protein in cancer. *Heliyon*, *6*(9), e05000. https://doi.org/10.1016/j.heliyon.2020.e05000

Molinari, C., Marisi, G., Passardi, A., Matteucci, L., De Maio, G., & Ulivi, P. (2018). Heterogeneity in Colorectal Cancer: A Challenge for Personalized Medicine? *International Journal of Molecular Sciences*, *19*(12), 3733. https://doi.org/10.3390/ijms19123733

Mondal, N., Buffone, A., Stolfa, G., Antonopoulos, A., Lau, J. T. Y., Haslam, S. M., Dell, A., & Neelamegham, S. (2015). ST3Gal-4 is the primary sialyltransferase regulating the synthesis of E-, P-, and L-selectin ligands on human myeloid leukocytes. *Blood*, *125*(4), 687–696. https://doi.org/10.1182/blood-2014-07-588590

Morad, G., Helmink, B. A., Sharma, P., & Wargo, J. A. (2021). Hallmarks of response, resistance, and toxicity to immune checkpoint blockade. *Cell*, *184*(21), 5309–5337. https://doi.org/10.1016/j.cell.2021.09.020

Munkley, J. (2016). The Role of Sialyl-Tn in Cancer. *International Journal of Molecular Sciences*, *17*(3), 275. https://doi.org/10.3390/ijms17030275

Munkley, J. (2022a). Aberrant Sialylation in Cancer: Therapeutic Opportunities. *Cancers*, *14*(17), 4248. https://doi.org/10.3390/cancers14174248

Munkley, J. (2022b). Aberrant Sialylation in Cancer: Therapeutic Opportunities. *Cancers*, *14*(17), 4248. https://doi.org/10.3390/cancers14174248

Murugaesu, N., Iravani, M., Van Weverwijk, A., Ivetic, A., Johnson, D. A., Antonopoulos, A., Fearns, A., Jamal-Hanjani, M., Sims, D., Fenwick, K., Mitsopoulos, C., Gao, Q., Orr, N., Zvelebil, M., Haslam, S. M., Dell, A., Yarwood, H., Lord, C. J., Ashworth, A., & Isacke, C. M. (2014). An *In Vivo* Functional Screen Identifies ST6GalNAc2 Sialyltransferase as a Breast Cancer Metastasis Suppressor. *Cancer Discovery*, *4*(3), 304–317. https://doi.org/10.1158/2159-8290.CD-13-0287

Murugesan, G., Correia, V. G., Palma, A. S., Chai, W., Li, C., Feizi, T., Martin, E., Laux, B., Franz, A., Fuchs, K., Weigle, B., & Crocker, P. R. (2020). Siglec-15 recognition of sialoglycans on tumor cell lines can occur independently of sialyl Tn antigen expression. *Glycobiology*, cwaa048. https://doi.org/10.1093/glycob/cwaa048

Murugesan, G., Weigle, B., & Crocker, P. R. (2021). Siglec and anti-Siglec therapies. *Current Opinion in Chemical Biology*, *62*, 34–42. https://doi.org/10.1016/j.cbpa.2021.01.001

Mustafov, D., Ahmad, M. S., Serrano, A., Braoudaki, M., & Siddiqui, S. S. (2024). MicroRNA:Siglec crosstalk in cancer progression. *Current Opinion in Chemical Biology*, *81*, 102502. https://doi.org/10.1016/j.cbpa.2024.102502

Mustafov, D., Siddiqui, S. S., Kukol, A., Lambrou, G. I., Shagufta, Ahmad, I., & Braoudaki, M. (2024). MicroRNA-Dependent Mechanisms Underlying the Function of a β-Amino Carbonyl Compound in Glioblastoma Cells. *ACS Omega*, *9*(29), 31789–31802. https://doi.org/10.1021/acsomega.4c02991

Muthusami, S., Ramachandran, I. K., Babu, K. N., Krishnamoorthy, S., Guruswamy, A., Queimado, L., Chaudhuri, G., & Ramachandran, I. (2021). Role of Inflammation in the Development of Colorectal Cancer. *Endocrine, Metabolic & Immune Disorders - Drug Targets*, *21*(1), 77–90. https://doi.org/10.2174/1871530320666200909092908

Mutka, M., Joensuu, K., Heiskala, M., Eray, M., & Heikkilä, P. (2023). Core needle biopsies alter the amounts of CCR5, Siglec-15, and PD-L1 positivities in breast carcinoma. *Virchows Archiv*, *483*(2), 215–224. https://doi.org/10.1007/s00428-023-03563-0

Nagtegaal, I. D., Odze, R. D., Klimstra, D., Paradis, V., Rugge, M., Schirmacher, P., Washington, K. M., Carneiro, F., Cree, I. A., & the WHO Classification of Tumours Editorial Board. (2020). The 2019 WHO classification of tumours of the digestive system. *Histopathology*, *76*(2), 182–188. https://doi.org/10.1111/his.13975

Ni, H., Zhang, L., Huang, H., Dai, S., & Li, J. (2020). Connecting METTL3 and intratumoural CD33+ MDSCs in predicting clinical outcome in cervical cancer. *Journal of Translational Medicine*, *18*(1), 393. https://doi.org/10.1186/s12967-020-02553-z

Nielsen, M. I., De Haan, N., Kightlinger, W., Ye, Z., Dabelsteen, S., Li, M., Jewett, M. C., Bagdonaite, I., Vakhrushev, S. Y., & Wandall, H. H. (2022). Global mapping of GalNAc-T isoform-specificities and O-glycosylation site-occupancy in a tissue-forming human cell line. *Nature Communications*, *13*(1), 6257. https://doi.org/10.1038/s41467-022-33806-8

Nikoletopoulou, V., Markaki, M., Palikaras, K., & Tavernarakis, N. (2013). Crosstalk between apoptosis, necrosis and autophagy. *Biochimica et Biophysica Acta (BBA) - Molecular Cell Research*, *1833*(12), 3448–3459. https://doi.org/10.1016/j.bbamcr.2013.06.001

Nishimura, T., & Tooze, S. A. (2020). Emerging roles of ATG proteins and membrane lipids in autophagosome formation. *Cell Discovery*, *6*(1), 32. https://doi.org/10.1038/s41421-020-0161-3

Nishiyama, A., & Nakanishi, M. (2021). Navigating the DNA methylation landscape of cancer. *Trends in Genetics*, *37*(11), 1012–1027. https://doi.org/10.1016/j.tig.2021.05.002

Niyazi, M., Niyazi, I., & Belka, C. (2007). Counting colonies of clonogenic assays by using densitometric software. *Radiation Oncology*, *2*(1), 4. https://doi.org/10.1186/1748-717X-2-4

Ogawa, T., Hirohashi, Y., Murai, A., Nishidate, T., Okita, K., Wang, L., Ikehara, Y., Satoyoshi, T., Usui, A., Kubo, T., Nakastugawa, M., Kanaseki, T., Tsukahara, T., Kutomi, G., Furuhata, T., Hirata, K., Sato, N., Mizuguchi, T., Takemasa, I., & Torigoe, T. (2017). ST6GALNAC1 plays important roles in enhancing cancer stem phenotypes of colorectal cancer via the Akt pathway. *Oncotarget*, *8*(68), 112550–112564. https://doi.org/10.18632/oncotarget.22545

Øines, M., Helsingen, L. M., Bretthauer, M., & Emilsson, L. (2017). Epidemiology and risk factors of colorectal polyps. *Best Practice & Research Clinical Gastroenterology*, *31*(4), 419–424. https://doi.org/10.1016/j.bpg.2017.06.004

Olingy, C. E., Dinh, H. Q., & Hedrick, C. C. (2019). Monocyte heterogeneity and functions in cancer. *Journal of Leukocyte Biology*, *106*(2), 309–322. https://doi.org/10.1002/JLB.4RI0818-311R

Orellana, E. A., Li, C., Lisevick, A., & Kasinski, A. L. (2019). Identification and validation of microRNAs that synergize with miR-34a – a basis for combinatorial microRNA therapeutics. *Cell Cycle*, *18*(15), 1798–1811. https://doi.org/10.1080/15384101.2019.1634956

Ortiz-Muñoz, G., Brown, M., Carbone, C. B., Pechuan-Jorge, X., Rouilly, V., Lindberg, H., Ritter, A. T., Raghupathi, G., Sun, Q., Nicotra, T., Mantri, S. R., Yang, A., Doerr, J., Nagarkar, D., Darmanis, S., Haley, B., Mariathasan, S., Wang, Y., Gomez-Roca, C., … Moussion, C. (2023). In situ tumour arrays reveal early environmental control of cancer immunity. *Nature*, *618*(7966), 827–833. https://doi.org/10.1038/s41586-023-06132-2

Ozcan, M., Janikovits, J., Von Knebel Doeberitz, M., & Kloor, M. (2018). Complex pattern of immune evasion in MSI colorectal cancer. *OncoImmunology*, *7*(7), e1445453. https://doi.org/10.1080/2162402X.2018.1445453

Pan, C., Liu, H., Robins, E., Song, W., Liu, D., Li, Z., & Zheng, L. (2020). Next-generation immuno-oncology agents: Current momentum shifts in cancer immunotherapy. *Journal of Hematology & Oncology*, *13*(1), 29. https://doi.org/10.1186/s13045-020-00862-w

Papavassiliou, K. A., Delle Cave, D., & Papavassiliou, A. G. (2023). Targeting the TGF-β Signaling Axis in Metastatic Colorectal Cancer: Where Do We Stand? *International Journal of Molecular Sciences*, *24*(23), 17101. https://doi.org/10.3390/ijms242317101

Park, G.-B., Jeong, J.-Y., & Kim, D. (2020). GLUT5 regulation by AKT1/3-miR-125b-5p downregulation induces migratory activity and drug resistance in TLR-modified colorectal cancer cells. *Carcinogenesis*, *41*(10), 1329–1340. https://doi.org/10.1093/carcin/bgaa074

Park, J.-J., & Lee, M. (2013). Increasing the α 2, 6 Sialylation of Glycoproteins May Contribute to Metastatic Spread and Therapeutic Resistance in Colorectal Cancer. *Gut and Liver*, *7*(6), 629–641. https://doi.org/10.5009/gnl.2013.7.6.629

Pashaei, E., Pashaei, E., Ahmady, M., Ozen, M., & Aydin, N. (2017). Meta-analysis of miRNA expression profiles for prostate cancer recurrence following radical prostatectomy. *PLOS ONE*, *12*(6), e0179543. https://doi.org/10.1371/journal.pone.0179543

Patel, S. J., Sanjana, N. E., Kishton, R. J., Eidizadeh, A., Vodnala, S. K., Cam, M., Gartner, J. J., Jia, L., Steinberg, S. M., Yamamoto, T. N., Merchant, A. S., Mehta, G. U., Chichura, A., Shalem, O., Tran, E., Eil, R., Sukumar, M., Guijarro, E. P., Day, C.-P., … Restifo, N. P. (2017). Identification of essential genes for cancer immunotherapy. *Nature*, *548*(7669), 537–542. https://doi.org/10.1038/nature23477

Patel, S. S., Nelson, R., Sanchez, J., Lee, W., Uyeno, L., Garcia-Aguilar, J., Hurria, A., & Kim, J. (2013). Elderly patients with colon cancer have unique tumor characteristics and poor survival. *Cancer*, *119*(4), 739–747. https://doi.org/10.1002/cncr.27753

Peixoto, A., Relvas-Santos, M., Azevedo, R., Santos, L. L., & Ferreira, J. A. (2019). Protein Glycosylation and Tumor Microenvironment Alterations Driving Cancer Hallmarks. *Frontiers in Oncology*, *9*, 380. https://doi.org/10.3389/fonc.2019.00380

Peng, X., Chen, X., Zhu, X., & Chen, L. (2021). GALNT6 Knockdown Inhibits the Proliferation and Migration of Colorectal Cancer Cells and Increases the Sensitivity of Cancer Cells to 5-FU. *Journal of Cancer*, *12*(24), 7413–7421. https://doi.org/10.7150/jca.62332

Peng, X., Wang, J., Zhang, C., Liu, K., Zhao, L., Chen, X., Huang, G., & Lai, Y. (2020). A three-miRNA panel in serum as a noninvasive biomarker for colorectal cancer detection. *The International Journal of Biological Markers*, *35*(3), 74–82. https://doi.org/10.1177/1724600820950740

Perdicchio, M., Cornelissen, L. A. M., Streng-Ouwehand, I., Engels, S., Verstege, M. I., Boon, L., Geerts, D., Van Kooyk, Y., & Unger, W. W. J. (2016). Tumor sialylation impedes

T cell mediated anti-tumor responses while promoting tumor associated-regulatory T cells. *Oncotarget*, *7*(8), 8771–8782. https://doi.org/10.18632/oncotarget.6822

Perez, S. J. L. P., Fu, C.-W., & Li, W.-S. (2021). Sialyltransferase Inhibitors for the Treatment of Cancer Metastasis: Current Challenges and Future Perspectives. *Molecules*, *26*(18), 5673. https://doi.org/10.3390/molecules26185673

Pesce, S., Greppi, M., Ferretti, E., Obino, V., Carlomagno, S., Rutigliani, M., Thoren, F. B., Sivori, S., Castagnola, P., Candiani, S., & Marcenaro, E. (2020). miRNAs in NK Cell-Based Immune Responses and Cancer Immunotherapy. *Frontiers in Cell and Developmental Biology*, *8*, 119. https://doi.org/10.3389/fcell.2020.00119

Pian, A. K., Foong, C. P., & Hamid, R. A. (2022). S-phase arrest and apoptosis in human breast adenocarcinoma MCF-7 cells via mitochondrial dependent pathway induced by tricyclohexylphosphine gold (I) n-mercaptobenzoate complexes. *Life Sciences*, *311*, 121161. https://doi.org/10.1016/j.lfs.2022.121161

Piawah, S., & Venook, A. P. (2019). Targeted therapy for colorectal cancer metastases: A review of current methods of molecularly targeted therapy and the use of tumor biomarkers in the treatment of metastatic colorectal cancer. *Cancer*, *125*(23), 4139–4147. https://doi.org/10.1002/cncr.32163

Pillsbury, C. E., Dougan, J., Rabe, J. L., Fonseca, J. A., Zhou, C., Evans, A. N., Abukharma, H., Ichoku, O., Gonzalez-Flamenco, G., Park, S. I., Aljudi, A., DeRyckere, D., Castellino, S. M., Rafiq, S., Langermann, S., Liu, L. N., Henry, C. J., & Porter, C. C. (2023). Siglec-15 Promotes Evasion of Adaptive Immunity in B-cell Acute Lymphoblastic Leukemia. *Cancer Research Communications*, *3*(7), 1248–1259. https://doi.org/10.1158/2767-9764.CRC-23-0056

Pimentel, J. M., Zhou, J.-Y., & Wu, G. S. (2023). The Role of TRAIL in Apoptosis and Immunosurveillance in Cancer. *Cancers*, *15*(10), 2752. https://doi.org/10.3390/cancers15102752

Pinho, S. S., & Reis, C. A. (2015). Glycosylation in cancer: Mechanisms and clinical implications. *Nature Reviews Cancer*, *15*(9), 540–555. https://doi.org/10.1038/nrc3982

Pirro, M., Mohammed, Y., De Ru, A. H., Janssen, G. M. C., Tjokrodirijo, R. T. N., Madunić, K., Wuhrer, M., Van Veelen, P. A., & Hensbergen, P. J. (2021). Oxonium Ion Guided Analysis of Quantitative Proteomics Data Reveals Site-Specific O-Glycosylation of Anterior Gradient Protein 2 (AGR2). *International Journal of Molecular Sciences*, *22*(10), 5369. https://doi.org/10.3390/ijms22105369

Pointreau, Y., Moreau, J., Vendrely, V., & Schipman, B. (2022). Quel apport de la modulation d'intensité pour la radiothérapie des cancers du rectum ? *Cancer/Radiothérapie*, *26*(6–7), 865–870. https://doi.org/10.1016/j.canrad.2022.06.001

Porta, C., Hadj-Slimane, R., Nejmeddine, M., Pampin, M., Tovey, M. G., Espert, L., Alvarez, S., & Chelbi-Alix, M. K. (2005). Interferons α and γ induce p53-dependent and p53-independent apoptosis, respectively. *Oncogene*, *24*(4), 605–615. https://doi.org/10.1038/sj.onc.1208204

Pothuraju, R., Khan, I., Jain, M., Bouvet, M., Malafa, M., Roy, H. K., Kumar, S., & Batra, S. K. (2024). Colorectal cancer murine models: Initiation to metastasis. *Cancer Letters*, *587*, 216704. https://doi.org/10.1016/j.canlet.2024.216704

Pugh, S., Thiébaut, R., Bridgewater, J., Grisoni, M.-L., Moutasim, K., Rousseau, F., Thomas, G. J., Griffiths, G., Liebaert, F., Primrose, J., & Laurent-Puig, P. (2017). Association between miR-31-3p expression and cetuximab efficacy in patients with KRAS wild-type metastatic colorectal cancer: A post-hoc analysis of the New EPOC trial. *Oncotarget*, *8*(55), 93856–93866. https://doi.org/10.18632/oncotarget.21291

Purushothaman, A., Mohajeri, M., & Lele, T. P. (2023). The role of glycans in the mechanobiology of cancer. *Journal of Biological Chemistry*, *299*(3), 102935. https://doi.org/10.1016/j.jbc.2023.102935

P□rez, A., Andrade-Da-Costa, J., De Souza, W., De Souza Ferreira, M., Boroni, M., De Oliveira, I., Freire-Neto, C., Fernandes, P., De Lanna, C., Souza-Santos, P., Morgado-D□az, J., & De-Freitas-Junior, J. C. (2020). N-glycosylation and receptor tyrosine kinase signaling affect claudin-3 levels in colorectal cancer cells. *Oncology Reports*. https://doi.org/10.3892/or.2020.7727

Qi, F., Isaji, T., Duan, C., Yang, J., Wang, Y., Fukuda, T., & Gu, J. (2020). ST3GAL3, ST3GAL4, and ST3GAL6 differ in their regulation of biological functions via the specificities for the α2,3-sialylation of target proteins. *The FASEB Journal*, *34*(1), 881–897. https://doi.org/10.1096/fj.201901793R

Qian, J., Olbrecht, S., Boeckx, B., Vos, H., Laoui, D., Etlioglu, E., Wauters, E., Pomella, V., Verbandt, S., Busschaert, P., Bassez, A., Franken, A., Bempt, M. V., Xiong, J., Weynand, B., Van Herck, Y., Antoranz, A., Bosisio, F. M., Thienpont, B., … Lambrechts, D. (2020). A pan-cancer blueprint of the heterogeneous tumor microenvironment revealed by single-cell profiling. *Cell Research*, *30*(9), 745–762. https://doi.org/10.1038/s41422-020-0355-0

Quan, J., Bode, A. M., & Luo, X. (2021). ACSL family: The regulatory mechanisms and therapeutic implications in cancer. *European Journal of Pharmacology*, *909*, 174397. https://doi.org/10.1016/j.ejphar.2021.174397

Quirke, P., West, N. P., & Nagtegaal, I. D. (2014). EURECCA consensus conference highlights about colorectal cancer clinical management: The pathologists expert review. *Virchows Archiv*, *464*(2), 129–134. https://doi.org/10.1007/s00428-013-1534-x

Ramírez, A. S., De Capitani, M., Pesciullesi, G., Kowal, J., Bloch, J. S., Irobalieva, R. N., Reymond, J.-L., Aebi, M., & Locher, K. P. (2022). Molecular basis for glycan recognition and reaction priming of eukaryotic oligosaccharyltransferase. *Nature Communications*, *13*(1), 7296. https://doi.org/10.1038/s41467-022-35067-x

Ranasinghe, R., Mathai, M. L., & Zulli, A. (2022). Cisplatin for cancer therapy and overcoming chemoresistance. *Heliyon*, *8*(9), e10608. https://doi.org/10.1016/j.heliyon.2022.e10608

Rawla, P., Sunkara, T., & Barsouk, A. (2019). Epidemiology of colorectal cancer: Incidence, mortality, survival, and risk factors. *Gastroenterology Review*, *14*(2), 89–103. https://doi.org/10.5114/pg.2018.81072

Read, M. L., Seed, R. I., Modasia, B., Kwan, P. P. K., Sharma, N., Smith, V. E., Watkins, R. J., Bansal, S., Gagliano, T., Stratford, A. L., Ismail, T., Wakelam, M. J. O., Kim, D. S., Ward, S. T., Boelaert, K., Franklyn, J. A., Turnell, A. S., & McCabe, C. J. (2016). The proto-oncogene PBF binds p53 and is associated with prognostic features in colorectal cancer: OVEREXPRESSION OF PBF IN COLORECTAL CANCER. *Molecular Carcinogenesis*, *55*(1), 15–26. https://doi.org/10.1002/mc.22254

Redza-Dutordoir, M., & Averill-Bates, D. A. (2016). Activation of apoptosis signalling pathways by reactive oxygen species. *Biochimica et Biophysica Acta (BBA) - Molecular Cell Research*, *1863*(12), 2977–2992. https://doi.org/10.1016/j.bbamcr.2016.09.012

Rehwinkel, J., Behm-Ansmant, I., Gatfield, D., & Izaurralde, E. (2005). A crucial role for GW182 and the DCP1:DCP2 decapping complex in miRNA-mediated gene silencing. *RNA*, *11*(11), 1640–1647. https://doi.org/10.1261/rna.2191905

Reid, G., Pel, M. E., Kirschner, M. B., Cheng, Y. Y., Mugridge, N., Weiss, J., Williams, M., Wright, C., Edelman, J. J. B., Vallely, M. P., McCaughan, B. C., Klebe, S., Brahmbhatt, H., MacDiarmid, J. A., & Van Zandwijk, N. (2013). Restoring expression of miR-16: A novel approach to therapy for malignant pleural mesothelioma. *Annals of Oncology*, *24*(12), 3128–3135. https://doi.org/10.1093/annonc/mdt412

Reis, C. A., Osorio, H., Silva, L., Gomes, C., & David, L. (2010). Alterations in glycosylation as biomarkers for cancer detection. *Journal of Clinical Pathology*, *63*(4), 322–329. https://doi.org/10.1136/jcp.2009.071035

Remya, C., Dileep, K. V., Variyar, E. J., Omkumar, R. V., & Sadasivan, C. (2023). Lobeline: A multifunctional alkaloid modulates cholinergic and glutamatergic activities. *IUBMB Life*, iub.2762. https://doi.org/10.1002/iub.2762

Ren, Y., Lyu, J., Guo, Y., Yao, Y., & Hu, L. (2022). Long Noncoding RNA TUG1 Inhibits Tumor Progression through Regulating Siglec-15-Related Anti-Immune Activity in Hepatocellular Carcinoma. *Journal of Immunology Research*, *2022*, 1–24. https://doi.org/10.1155/2022/9557859

Riley, N. M., Malaker, S. A., Driessen, M. D., & Bertozzi, C. R. (2020). Optimal Dissociation Methods Differ for *N*—And *O* -Glycopeptides. *Journal of Proteome Research*, *19*(8), 3286–3301. https://doi.org/10.1021/acs.jproteome.0c00218

Rodrigues, E., Jung, J., Park, H., Loo, C., Soukhtehzari, S., Kitova, E. N., Mozaneh, F., Daskhan, G., Schmidt, E. N., Aghanya, V., Sarkar, S., Streith, L., St. Laurent, C. D., Nguyen, L., Julien, J.-P., West, L. J., Williams, K. C., Klassen, J. S., & Macauley, M. S. (2020). A versatile soluble siglec scaffold for sensitive and quantitative detection of glycan ligands. *Nature Communications*, *11*(1), 5091. https://doi.org/10.1038/s41467-020-18907-6

Rodrigues, E., & Macauley, M. (2018). Hypersialylation in Cancer: Modulation of Inflammation and Therapeutic Opportunities. *Cancers*, *10*(6), 207. https://doi.org/10.3390/cancers10060207

Rodrigues, J. G., Duarte, H. O., Gomes, C., Balmaña, M., Martins, Á. M., Hensbergen, P. J., De Ru, A. H., Lima, J., Albergaria, A., Van Veelen, P. A., Wuhrer, M., Gomes, J., & Reis, C. A. (2021). Terminal α2,6-sialylation of epidermal growth factor receptor modulates antibody therapy response of colorectal cancer cells. *Cellular Oncology*, *44*(4), 835–850. https://doi.org/10.1007/s13402-021-00606-z

Rodriguez, E., Boelaars, K., Brown, K., Eveline Li, R. J., Kruijssen, L., Bruijns, S. C. M., Van Ee, T., Schetters, S. T. T., Crommentuijn, M. H. W., Van Der Horst, J. C., Van Grieken, N. C. T., Van Vliet, S. J., Kazemier, G., Giovannetti, E., Garcia-Vallejo, J. J., & Van Kooyk, Y. (2021). Sialic acids in pancreatic cancer cells drive tumour-associated macrophage differentiation via the Siglec receptors Siglec-7 and Siglec-9. *Nature Communications*, *12*(1), 1270. https://doi.org/10.1038/s41467-021-21550-4

Rogler, G. (2014). Chronic ulcerative colitis and colorectal cancer. *Cancer Letters*, *345*(2), 235–241. https://doi.org/10.1016/j.canlet.2013.07.032

Roh, M. S., Lee, H. W., Jung, S. B., Kim, K., Lee, E. H., Park, M., Lee, J. S., & Kim, M.-S. (2018). Expression of miR-200c and its clinicopathological significance in patients with colorectal cancer. *Pathology - Research and Practice*, *214*(3), 350–355. https://doi.org/10.1016/j.prp.2018.01.005

Roman, G. (2015). Mannich bases in medicinal chemistry and drug design. *European Journal of Medicinal Chemistry*, *89*, 743–816. https://doi.org/10.1016/j.ejmech.2014.10.076

Roper, J., Tammela, T., Cetinbas, N. M., Akkad, A., Roghanian, A., Rickelt, S., Almeqdadi, M., Wu, K., Oberli, M. A., Sánchez-Rivera, F. J., Park, Y. K., Liang, X., Eng, G., Taylor, M. S., Azimi, R., Kedrin, D., Neupane, R., Beyaz, S., Sicinska, E. T., … Yilmaz, Ö. H. (2017). In vivo genome editing and organoid transplantation models of colorectal cancer and metastasis. *Nature Biotechnology*, *35*(6), 569–576. https://doi.org/10.1038/nbt.3836

Rosenstock, P., & Kaufmann, T. (2021). Sialic Acids and Their Influence on Human NK Cell Function. *Cells*, *10*(2), 263. https://doi.org/10.3390/cells10020263

Ross, A. B., Langer, J. D., & Jovanovic, M. (2021). Proteome Turnover in the Spotlight: Approaches, Applications, and Perspectives. *Molecular & Cellular Proteomics*, *20*, 100016. https://doi.org/10.1074/mcp.R120.002190

Ru, B., Wong, C. N., Tong, Y., Zhong, J. Y., Zhong, S. S. W., Wu, W. C., Chu, K. C., Wong, C. Y., Lau, C. Y., Chen, I., Chan, N. W., & Zhang, J. (2019). TISIDB: An integrated repository portal for tumor–immune system interactions. *Bioinformatics*, *35*(20), 4200–4202. https://doi.org/10.1093/bioinformatics/btz210

Ruan, G., Xie, H., Yuan, K., Lin, S., Zhang, H., Liu, C., Shi, J., Ge, Y., Song, M., Hu, C., Zhang, X., Liu, X., Yang, M., Wang, K., Zheng, X., Chen, Y., Hu, W., Cong, M., Zhu, L., … Shi, H. (2023). Prognostic value of systemic inflammation and for patients with colorectal cancer cachexia. *Journal of Cachexia, Sarcopenia and Muscle*, *14*(6), 2813–2823. https://doi.org/10.1002/jcsm.13358

Rusiniak, M. E., Punch, P. R., Hait, N. C., Maiti, A., Burns, R. T., Chapla, D., Moremen, K. W., Zhao, P., Wells, L., Hoffmeister, K., & Lau, J. T. Y. (2022). Extracellular ST6GAL1 regulates monocyte–macrophage development and survival. *Glycobiology*, *32*(8), 701–711. https://doi.org/10.1093/glycob/cwac032

Saeui, C. T., Cho, K., Dharmarha, V., Nairn, A. V., Galizzi, M., Shah, S. R., Gowda, P., Park, M., Austin, M., Clarke, A., Cai, E., Buettner, M. J., Ariss, R., Moremen, K. W., Zhang,

H., & Yarema, K. J. (2020). Cell Line-, Protein-, and Sialoglycosite-Specific Control of Flux-Based Sialylation in Human Breast Cells: Implications for Cancer Progression. *Frontiers in Chemistry*, *8*, 13. https://doi.org/10.3389/fchem.2020.00013

Safari, E., Ghorghanlu, S., Ahmadi-khiavi, H., Mehranfar, S., Rezaei, R., & Motallebnezhad, M. (2019). Myeloid-derived suppressor cells and tumor: Current knowledge and future perspectives. *Journal of Cellular Physiology*, *234*(7), 9966–9981. https://doi.org/10.1002/jcp.27923

Sakuma, K., Aoki, M., & Kannagi, R. (2012). Transcription factors c-Myc and CDX2 mediate E-selectin ligand expression in colon cancer cells undergoing EGF/bFGF-induced epithelial–mesenchymal transition. *Proceedings of the National Academy of Sciences*, *109*(20), 7776–7781. https://doi.org/10.1073/pnas.1111135109

Saliminejad, K., Khorram Khorshid, H. R., Soleymani Fard, S., & Ghaffari, S. H. (2019). An overview of microRNAs: Biology, functions, therapeutics, and analysis methods. *Journal of Cellular Physiology*, *234*(5), 5451–5465. https://doi.org/10.1002/jcp.27486

Sameer, A. S. (2013). Colorectal Cancer: Molecular Mutations and Polymorphisms. *Frontiers in Oncology*, *3*. https://doi.org/10.3389/fonc.2013.00114

Sanghvi, V. R., & Steel, L. F. (2011). The Cellular TAR RNA Binding Protein, TRBP, Promotes HIV-1 Replication Primarily by Inhibiting the Activation of Double-Stranded RNA-Dependent Kinase PKR. *Journal of Virology*, *85*(23), 12614–12621. https://doi.org/10.1128/JVI.05240-11

Sanz-Martinez, I., Pereira, S., Merino, P., Corzana, F., & Hurtado-Guerrero, R. (2023). Molecular Recognition of GalNAc in Mucin-Type O-Glycosylation. *Accounts of Chemical Research*, *56*(5), 548–560. https://doi.org/10.1021/acs.accounts.2c00723

Sawicki, T., Ruszkowska, M., Danielewicz, A., Niedźwiedzka, E., Arłukowicz, T., & Przybyłowicz, K. E. (2021). A Review of Colorectal Cancer in Terms of Epidemiology, Risk Factors, Development, Symptoms and Diagnosis. *Cancers*, *13*(9), 2025. https://doi.org/10.3390/cancers13092025

Schein, C. H. (2021). Repurposing approved drugs for cancer therapy. *British Medical Bulletin*, *137*(1), 13–27. https://doi.org/10.1093/bmb/ldaa045

Scheper, A. F., Schofield, J., Bohara, R., Ritter, T., & Pandit, A. (2023). Understanding glycosylation: Regulation through the metabolic flux of precursor pathways. *Biotechnology Advances*, *67*, 108184. https://doi.org/10.1016/j.biotechadv.2023.108184

Schjoldager, K. T., Narimatsu, Y., Joshi, H. J., & Clausen, H. (2020). Global view of human protein glycosylation pathways and functions. *Nature Reviews Molecular Cell Biology*, *21*(12), 729–749. https://doi.org/10.1038/s41580-020-00294-x

Schneider, F., Kemmner, W., Haensch, W., Franke, G., Gretschel, S., Karsten, U., & Schlag, P. M. (2001). Overexpression of sialyltransferase CMP-sialic acid:Galbeta1,3GalNAc-R alpha6-Sialyltransferase is related to poor patient survival in human colorectal carcinomas. *Cancer Research*, *61*(11), 4605–4611.

Schroy, P. C., Brown-Shimer, S., Kim, K., Johnson, K. A., Murnane, M. J., Yang, S., O'brein, M. J., Carney, W. P., & Kupchik, H. Z. (1995). Detection of p21ras mutations in colorectal adenomas and carcinomas by enzyme-linked immunosorbent assay. *Cancer*, *76*(2), 201–209. https://doi.org/10.1002/1097-0142(19950715)76:2<201::AID-CNCR2820760207>3.0.CO;2-T

Sena, P., Mancini, S., Pedroni, M., Reggiani Bonetti, L., Carnevale, G., & Roncucci, L. (2022). Expression of Autophagic and Inflammatory Markers in Normal Mucosa of Individuals with Colorectal Adenomas: A Cross Sectional Study among Italian Outpatients Undergoing Colonoscopy. *International Journal of Molecular Sciences*, *23*(9), 5211. https://doi.org/10.3390/ijms23095211

Sewell, R., Bäckström, M., Dalziel, M., Gschmeissner, S., Karlsson, H., Noll, T., Gätgens, J., Clausen, H., Hansson, G. C., Burchell, J., & Taylor-Papadimitriou, J. (2006). The ST6GalNAc-I Sialyltransferase Localizes throughout the Golgi and Is Responsible for the Synthesis of the Tumor-associated Sialyl-Tn O-Glycan in Human Breast Cancer. *Journal of Biological Chemistry*, *281*(6), 3586–3594. https://doi.org/10.1074/jbc.M511826200

Shafi, S., Aung, T. N., Xirou, V., Gavrielatou, N., Vathiotis, I. A., Fernandez, A., Moutafi, M., Yaghoobi, V., Herbst, R. S., Liu, L. N., Langermann, S., & Rimm, D. L. (2022). Quantitative assessment of Siglec-15 expression in lung, breast, head, and neck squamous cell carcinoma and bladder cancer. *Laboratory Investigation*, *102*(10), 1143–1149. https://doi.org/10.1038/s41374-022-00796-6

Shang, A., Gu, C., Wang, W., Wang, X., Sun, J., Zeng, B., Chen, C., Chang, W., Ping, Y., Ji, P., Wu, J., Quan, W., Yao, Y., Zhou, Y., Sun, Z., & Li, D. (2020). Exosomal circPACRGL promotes progression of colorectal cancer via the miR-142-3p/miR-506-3p- TGF-β1 axis. *Molecular Cancer*, *19*(1), 117. https://doi.org/10.1186/s12943-020-01235-0

Shang, R., Lee, S., Senavirathne, G., & Lai, E. C. (2023). microRNAs in action: Biogenesis, function and regulation. *Nature Reviews Genetics*, *24*(12), 816–833. https://doi.org/10.1038/s41576-023-00611-y

Sharma, B. R., & Kanneganti, T.-D. (2023). Inflammasome signaling in colorectal cancer. *Translational Research*, *252*, 45–52. https://doi.org/10.1016/j.trsl.2022.09.002

Sharma, B. R., Karki, R., Sundaram, B., Wang, Y., Vogel, P., & Kanneganti, T.-D. (2022). The Transcription Factor IRF9 Promotes Colorectal Cancer via Modulating the IL-6/STAT3 Signaling Axis. *Cancers*, *14*(4), 919. https://doi.org/10.3390/cancers14040919

Sharma, P. C., & Gupta, A. (2020). MicroRNAs: Potential biomarkers for diagnosis and prognosis of different cancers. *Translational Cancer Research*, *9*(9), 5798–5818. https://doi.org/10.21037/tcr-20-1294

Sharma, P., Hu-Lieskovan, S., Wargo, J. A., & Ribas, A. (2017). Primary, Adaptive, and Acquired Resistance to Cancer Immunotherapy. *Cell*, *168*(4), 707–723. https://doi.org/10.1016/j.cell.2017.01.017

Shayimu, P., Yusufu, A., Rehemutula, A., Redati, D., Jiapaer, R., & Tuerdi, R. (2020). MicroRNA-377 Counteracts With Cancer Stem Cell Phenotypes and Epithelial Mesenchymal Transformation by Targeting ZEB2 in Colon Cancer. *Technology in Cancer Research & Treatment*, *19*, 153303382096747. https://doi.org/10.1177/1533033820967475

Shi, C., Wang, Y., Wu, M., Chen, Y., Liu, F., Shen, Z., Wang, Y., Xie, S., Shen, Y., Sang, L., Zhang, Z., Gao, Z., Yang, L., Qu, L., Yang, Z., He, X., Guo, Y., Pan, C., Che, J., … Lin, A. (2022). Promoting anti-tumor immunity by targeting TMUB1 to modulate PD-L1 polyubiquitination and glycosylation. *Nature Communications*, *13*(1), 6951. https://doi.org/10.1038/s41467-022-34346-x

Shi, J., Li, F., Luo, M., Wei, J., & Liu, X. (2017). Distinct Roles of Wnt/*β*-Catenin Signaling in the Pathogenesis of Chronic Obstructive Pulmonary Disease and Idiopathic Pulmonary Fibrosis. *Mediators of Inflammation*, *2017*, 1–16. https://doi.org/10.1155/2017/3520581

Shi, S., Qiu, W., Miao, P., Li, R., Lin, X., & Sun, Z. (2021). Three-component radical homo Mannich reaction. *Nature Communications*, *12*(1), 1006. https://doi.org/10.1038/s41467-021-21303-3

Shihan, M. H., Novo, S. G., Le Marchand, S. J., Wang, Y., & Duncan, M. K. (2021). A simple method for quantitating confocal fluorescent images. *Biochemistry and Biophysics Reports*, *25*, 100916. https://doi.org/10.1016/j.bbrep.2021.100916

Shin, A. E., Giancotti, F. G., & Rustgi, A. K. (2023). Metastatic colorectal cancer: Mechanisms and emerging therapeutics. *Trends in Pharmacological Sciences*, *44*(4), 222–236. https://doi.org/10.1016/j.tips.2023.01.003

Shukla, G. C., Singh, J., & Barik, S. (2011). MicroRNAs: Processing, Maturation, Target Recognition and Regulatory Functions. *Molecular and Cellular Pharmacology*, *3*(3), 83–92.

Shum, E., Myint, H., Shaik, J., Zhou, Q., Barbu, E., Morawski, A., Abukharma, H., Liu, L., Nelson, M., Zeidan, S., Cusumano, Z., Tolcher, A., Langermann, S., Gutierrez, M., & Hamid, O. (2021). 490 Clinical benefit through Siglec-15 targeting with NC318 antibody in subjects with Siglec-15 positive advanced solid tumors. *Journal for ImmunoTherapy of Cancer*, *9*(Suppl 2), A520–A521. https://doi.org/10.1136/jitc-2021-SITC2021.490

Siddiqui, S. S. (2023). Non-canonical roles of Siglecs: Beyond sialic acid-binding and immune cell modulation. *Molecular Aspects of Medicine*, *90*, 101145. https://doi.org/10.1016/j.mam.2022.101145

Siddiqui, S. S., Vaill, M., Do, R., Khan, N., Verhagen, A. L., Zhang, W., Lenz, H., Johnson-Pais, T. L., Leach, R. J., Fraser, G., Wang, C., Feng, G., Varki, N., & Varki, A. (2021). Human-specific polymorphic pseudogenization of *SIGLEC12* protects against advanced cancer progression. *FASEB BioAdvances*, *3*(2), 69–82. https://doi.org/10.1096/fba.2020-00092

Siegel, R. L., Miller, K. D., Fedewa, S. A., Ahnen, D. J., Meester, R. G. S., Barzi, A., & Jemal, A. (2017). Colorectal cancer statistics, 2017. *CA: A Cancer Journal for Clinicians*, *67*(3), 177–193. https://doi.org/10.3322/caac.21395

Siegel, R. L., Miller, K. D., Goding Sauer, A., Fedewa, S. A., Butterly, L. F., Anderson, J. C., Cercek, A., Smith, R. A., & Jemal, A. (2020). Colorectal cancer statistics, 2020. *CA: A Cancer Journal for Clinicians*, *70*(3), 145–164. https://doi.org/10.3322/caac.21601

Siegel, R. L., Wagle, N. S., Cercek, A., Smith, R. A., & Jemal, A. (2023). Colorectal cancer statistics, 2023. *CA: A Cancer Journal for Clinicians*, *73*(3), 233–254. https://doi.org/10.3322/caac.21772

Singh, P., & Lim, B. (2022). Targeting Apoptosis in Cancer. *Current Oncology Reports*, *24*(3), 273–284. https://doi.org/10.1007/s11912-022-01199-y

Singh, R., & Choi, B. K. (2019). Siglec1-expressing subcapsular sinus macrophages provide soil for melanoma lymph node metastasis. *eLife*, *8*, e48916. https://doi.org/10.7554/eLife.48916

Singh, R., & Manna, P. P. (2022). Reactive oxygen species in cancer progression and its role in therapeutics. *Exploration of Medicine*, 43–57. https://doi.org/10.37349/emed.2022.00073

Skriver, S. K., Jensen, M.-B., Knoop, A. S., Ejlertsen, B., & Laenkholm, A.-V. (2020). Tumour-infiltrating lymphocytes and response to neoadjuvant letrozole in patients with early oestrogen receptor-positive breast cancer: Analysis from a nationwide phase II DBCG trial. *Breast Cancer Research*, *22*(1), 46. https://doi.org/10.1186/s13058-020-01285-8

Slattery, M. L., Mullany, L. E., Sakoda, L. C., Samowitz, W. S., Wolff, R. K., Stevens, J. R., & Herrick, J. S. (2018). Expression of Wnt-signaling pathway genes and their associations with miRNAs in colorectal cancer. *Oncotarget*, *9*(5), 6075–6085. https://doi.org/10.18632/oncotarget.23636

Sleire, L., Førde, H. E., Netland, I. A., Leiss, L., Skeie, B. S., & Enger, P. Ø. (2017). Drug repurposing in cancer. *Pharmacological Research*, *124*, 74–91. https://doi.org/10.1016/j.phrs.2017.07.013

Smith, B. A. H., & Bertozzi, C. R. (2021). The clinical impact of glycobiology: Targeting selectins, Siglecs and mammalian glycans. *Nature Reviews Drug Discovery*, *20*(3), 217–243. https://doi.org/10.1038/s41573-020-00093-1

Smith, B. A. H., Deutzmann, A., Correa, K. M., Delaveris, C. S., Dhanasekaran, R., Dove, C. G., Sullivan, D. K., Wisnovsky, S., Stark, J. C., Pluvinage, J. V., Swaminathan, S., Riley, N. M., Rajan, A., Majeti, R., Felsher, D. W., & Bertozzi, C. R. (2023). MYC-driven synthesis of Siglec ligands is a glycoimmune checkpoint. *Proceedings of the National Academy of Sciences*, *120*(11), e2215376120. https://doi.org/10.1073/pnas.2215376120

Smith, K. M., & Desai, J. (2018). Nivolumab for the treatment of colorectal cancer. *Expert Review of Anticancer Therapy*, *18*(7), 611–618. https://doi.org/10.1080/14737140.2018.1480942

Smith, V. E., Sharma, N., Watkins, R. J., Read, M. L., Ryan, G. A., Kwan, P. P., Martin, A., Watkinson, J. C., Boelaert, K., Franklyn, J. A., & McCabe, C. J. (2013). Manipulation of PBF/PTTG1IP Phosphorylation Status; a Potential New Therapeutic Strategy for

Improving Radioiodine Uptake in Thyroid and Other Tumors. *The Journal of Clinical Endocrinology & Metabolism*, *98*(7), 2876–2886. https://doi.org/10.1210/jc.2012-3640

Smithson, M., Diffalha, S. A., Irwin, R. K., Williams, G., McLeod, M. C., Somasundaram, V., Bellis, S. L., & Hardiman, K. M. (2024). ST6GAL1 is associated with poor response to chemoradiation in rectal cancer. *Neoplasia*, *51*, 100984. https://doi.org/10.1016/j.neo.2024.100984

Smithson, M., Irwin, R., Williams, G., Alexander, K. L., Smythies, L. E., Nearing, M., McLeod, M. C., Al Diffalha, S., Bellis, S. L., & Hardiman, K. M. (2022). Sialyltransferase ST6GAL-1 mediates resistance to chemoradiation in rectal cancer. *Journal of Biological Chemistry*, *298*(3), 101594. https://doi.org/10.1016/j.jbc.2022.101594

Soares, C. O., Grosso, A. S., Ereño-Orbea, J., Coelho, H., & Marcelo, F. (2021). Molecular Recognition Insights of Sialic Acid Glycans by Distinct Receptors Unveiled by NMR and Molecular Modeling. *Frontiers in Molecular Biosciences*, *8*, 727847. https://doi.org/10.3389/fmolb.2021.727847

Song, K., Ma, J., Gao, Y., Qu, Y., Ren, C., Yan, P., Zheng, B., & Yue, B. (2022). Knocking down Siglec-15 in osteosarcoma cells inhibits proliferation while promoting apoptosis and pyroptosis by targeting the Siglec-15/STAT3/Bcl-2 pathway. *Advances in Medical Sciences*, *67*(2), 187–195. https://doi.org/10.1016/j.advms.2022.03.001

Song, M., Chan, A. T., & Sun, J. (2020). Influence of the Gut Microbiome, Diet, and Environment on Risk of Colorectal Cancer. *Gastroenterology*, *158*(2), 322–340. https://doi.org/10.1053/j.gastro.2019.06.048

Song, X.-J., Liu, Z.-L., Zeng, R., Ye, W., & Liu, C.-W. (2019). A meta-analysis of laparoscopic surgery versus conventional open surgery in the treatment of colorectal cancer. *Medicine*, *98*(17), e15347. https://doi.org/10.1097/MD.0000000000015347

Speiser, D. E., Chijioke, O., Schaeuble, K., & Münz, C. (2023). CD4+ T cells in cancer. *Nature Cancer*, *4*(3), 317–329. https://doi.org/10.1038/s43018-023-00521-2

Spiro, R. G. (2002). Protein glycosylation: Nature, distribution, enzymatic formation, and disease implications of glycopeptide bonds. *Glycobiology*, *12*(4), 43R-56R. https://doi.org/10.1093/glycob/12.4.43R

Stachowiak, M., Flisikowska, T., Bauersachs, S., Perleberg, C., Pausch, H., Switonski, M., Kind, A., Saur, D., Schnieke, A., & Flisikowski, K. (2017). Altered microRNA profiles during early colon adenoma progression in a porcine model of familial adenomatous

polyposis. *Oncotarget*, *8*(56), 96154–96160. https://doi.org/10.18632/oncotarget.21774

Stanczak, M. A., Rodrigues Mantuano, N., Kirchhammer, N., Sanin, D. E., Jacob, F., Coelho, R., Everest-Dass, A. V., Wang, J., Trefny, M. P., Monaco, G., Bärenwaldt, A., Gray, M. A., Petrone, A., Kashyap, A. S., Glatz, K., Kasenda, B., Normington, K., Broderick, J., Peng, L., … Läubli, H. (2022). Targeting cancer glycosylation repolarizes tumor-associated macrophages allowing effective immune checkpoint blockade. *Science Translational Medicine*, *14*(669), eabj1270. https://doi.org/10.1126/scitranslmed.abj1270

Stang, A., Weilert, H., Lipp, M. J., Oldhafer, K. J., Hoheisel, J. D., Zhang, C., & Bauer, A. S. (2021). MicroRNAs in blood act as biomarkers of colorectal cancer and indicate potential therapeutic targets. *Molecular Oncology*, *15*(9), 2480–2490. https://doi.org/10.1002/1878-0261.13065

Stevenson, T. K., Moore, S. J., Murphy, G. G., & Lawrence, D. A. (2022). Tissue Plasminogen Activator in Central Nervous System Physiology and Pathology: From Synaptic Plasticity to Alzheimer's Disease. *Seminars in Thrombosis and Hemostasis*, *48*(03), 288–300. https://doi.org/10.1055/s-0041-1740265

Stoffel, E. M., & Murphy, C. C. (2020). Epidemiology and Mechanisms of the Increasing Incidence of Colon and Rectal Cancers in Young Adults. *Gastroenterology*, *158*(2), 341–353. https://doi.org/10.1053/j.gastro.2019.07.055

Storey, J. D., & Tibshirani, R. (2003). Statistical significance for genomewide studies. *Proceedings of the National Academy of Sciences*, *100*(16), 9440–9445. https://doi.org/10.1073/pnas.1530509100

Stowell, S. R., Ju, T., & Cummings, R. D. (2015). Protein Glycosylation in Cancer. *Annual Review of Pathology: Mechanisms of Disease*, *10*(1), 473–510. https://doi.org/10.1146/annurev-pathol-012414-040438

Stuelten, C. H., Parent, C. A., & Montell, D. J. (2018). Cell motility in cancer invasion and metastasis: Insights from simple model organisms. *Nature Reviews Cancer*, *18*(5), 296–312. https://doi.org/10.1038/nrc.2018.15

Stuible, M., Moraitis, A., Fortin, A., Saragosa, S., Kalbakji, A., Filion, M., & Tremblay, G. B. (2014). Mechanism and Function of Monoclonal Antibodies Targeting Siglec-15 for Therapeutic Inhibition of Osteoclastic Bone Resorption. *Journal of Biological Chemistry*, *289*(10), 6498–6512. https://doi.org/10.1074/jbc.M113.494542

Suarez-Arnedo, A., Torres Figueroa, F., Clavijo, C., Arbeláez, P., Cruz, J. C., & Muñoz-Camargo, C. (2020). An image J plugin for the high throughput image analysis of in vitro scratch wound healing assays. *PLOS ONE*, *15*(7), e0232565. https://doi.org/10.1371/journal.pone.0232565

Subramanian, I., Verma, S., Kumar, S., Jere, A., & Anamika, K. (2020). Multi-omics Data Integration, Interpretation, and Its Application. *Bioinformatics and Biology Insights*, *14*, 117793221989905. https://doi.org/10.1177/1177932219899051

Suda, T., Takahashi, N., Udagawa, N., Jimi, E., Gillespie, M. T., & Martin, T. J. (1999). Modulation of Osteoclast Differentiation and Function by the New Members of the Tumor Necrosis Factor Receptor and Ligand Families. *Endocrine Reviews*, *20*(3), 345–357. https://doi.org/10.1210/edrv.20.3.0367

Sullivan, B. A., Noujaim, M., & Roper, J. (2022). Cause, Epidemiology, and Histology of Polyps and Pathways to Colorectal Cancer. *Gastrointestinal Endoscopy Clinics of North America*, *32*(2), 177–194. https://doi.org/10.1016/j.giec.2021.12.001

Sun, H., Li, Y., Zhang, P., Xing, H., Zhao, S., Song, Y., Wan, D., & Yu, J. (2022). Targeting toll-like receptor 7/8 for immunotherapy: Recent advances and prospectives. *Biomarker Research*, *10*(1), 89. https://doi.org/10.1186/s40364-022-00436-7

Sun, J., Lu, Q., Sanmamed, M. F., & Wang, J. (2021). Siglec-15 as an Emerging Target for Next-generation Cancer Immunotherapy. *Clinical Cancer Research*, *27*(3), 680–688. https://doi.org/10.1158/1078-0432.CCR-19-2925

Sun, J.-Y., Zhang, D., Wu, S., Xu, M., Zhou, X., Lu, X.-J., & Ji, J. (2020). Resistance to PD-1/PD-L1 blockade cancer immunotherapy: Mechanisms, predictive factors, and future perspectives. *Biomarker Research*, *8*(1), 35. https://doi.org/10.1186/s40364-020-00212-5

Sun, K., Lv, Y., Zhu, Z., Zhang, L., Wu, H., Liu, L., Jiang, Y., Xiao, B., & Wang, X. (2015). Oxidative C–S bond cleavage reaction of DMSO for C–N and C–C bond formation: New Mannich-type reaction for β-amino ketones. *RSC Advances*, *5*(4), 3094–3097. https://doi.org/10.1039/C4RA14249G

Sun, L., Su, Y., Jiao, A., Wang, X., & Zhang, B. (2023). T cells in health and disease. *Signal Transduction and Targeted Therapy*, *8*(1), 235. https://doi.org/10.1038/s41392-023-01471-y

Sun, R., Yang, Y., Lü, W., Yang, Y., Li, Y., Liu, Z., Diao, D., Wang, Y., Chang, S., Lu, M., Jiang, Q., Dai, B., Ma, X., Zhao, C., Lü, M., Zhang, J., Ding, C., Li, N., Zhang, J., … Huang, C. (2023). Single-cell transcriptomic analysis of normal and pathological

tissues from the same patient uncovers colon cancer progression. *Cell & Bioscience*, *13*(1), 62. https://doi.org/10.1186/s13578-023-01002-w

Sun, X., Ju, T., & Cummings, R. D. (2018). Differential expression of Cosmc, T-synthase and mucins in Tn-positive colorectal cancers. *BMC Cancer*, *18*(1), 827. https://doi.org/10.1186/s12885-018-4708-8

Sunada, S., Saito, H., Zhang, D., Xu, Z., & Miki, Y. (2021). CDK1 inhibitor controls G2/M phase transition and reverses DNA damage sensitivity. *Biochemical and Biophysical Research Communications*, *550*, 56–61. https://doi.org/10.1016/j.bbrc.2021.02.117

Swindall, A. F., & Bellis, S. L. (2011). Sialylation of the Fas Death Receptor by ST6Gal-I Provides Protection against Fas-mediated Apoptosis in Colon Carcinoma Cells. *Journal of Biological Chemistry*, *286*(26), 22982–22990. https://doi.org/10.1074/jbc.M110.211375

Syrkina, M., Viushkov, V., Potashnikova, D., Veiko, V., Vassetzky, Y., & Rubtsov, M. (2019). From an increase in the number of tandem repeats through the decrease of sialylation to the downregulation of MUC1 expression level. *Journal of Cellular Biochemistry*, *120*(3), 4472–4484. https://doi.org/10.1002/jcb.27735

Szabo, R., & Skropeta, D. (2017). Advancement of Sialyltransferase Inhibitors: Therapeutic Challenges and Opportunities. *Medicinal Research Reviews*, *37*(2), 219–270. https://doi.org/10.1002/med.21407

Takamiya, R., Ohtsubo, K., Takamatsu, S., Taniguchi, N., & Angata, T. (2013). The interaction between Siglec-15 and tumor-associated sialyl-Tn antigen enhances TGF- secretion from monocytes/macrophages through the DAP12-Syk pathway. *Glycobiology*, *23*(2), 178–187. https://doi.org/10.1093/glycob/cws139

Tan, L., Peng, D., & Cheng, Y. (2022). Significant position of C-myc in colorectal cancer: A promising therapeutic target. *Clinical and Translational Oncology*, *24*(12), 2295–2304. https://doi.org/10.1007/s12094-022-02910-y

Tan, X., Zhang, S., Gao, H., He, W., Xu, M., Wu, Q., Ni, X., & Jiang, H. (2019). Hypermethylation of the PTTG1IP promoter leads to low expression in early-stage non-small cell lung cancer. *Oncology Letters*. https://doi.org/10.3892/ol.2019.10400

Tan, Y., Wang, K., & Kong, Y. (2022). Circular RNA ZFR promotes cell cycle arrest and apoptosis of colorectal cancer cells via the miR-147a/CACUL1 axis. *Journal of Gastrointestinal Oncology*, *13*(4), 1793–1804. https://doi.org/10.21037/jgo-22-672

Tang, F., Cao, F., Lu, C., He, X., Weng, L., & Sun, L. (2022). Dvl2 facilitates the coordination of NF-κB and Wnt signaling to promote colitis-associated colorectal progression. *Cancer Science*, *113*(2), 565–575. https://doi.org/10.1111/cas.15206

Tang, L., Zhou, L., Wu, S., Shi, X., Jiang, G., Niu, S., & Ding, D. (2019). miR-125a-5p inhibits colorectal cancer cell epithelial–mesenchymal transition, invasion and migration by targeting TAZ. *OncoTargets and Therapy*, *Volume 12*, 3481–3489. https://doi.org/10.2147/OTT.S191247

Tang, Q., Chen, Y., Li, X., Long, S., Shi, Y., Yu, Y., Wu, W., Han, L., & Wang, S. (2022). The role of PD-1/PD-L1 and application of immune-checkpoint inhibitors in human cancers. *Frontiers in Immunology*, *13*, 964442. https://doi.org/10.3389/fimmu.2022.964442

Taniuchi, I. (2018). CD4 Helper and CD8 Cytotoxic T Cell Differentiation. *Annual Review of Immunology*, *36*(1), 579–601. https://doi.org/10.1146/annurev-immunol-042617-053411

Tantin, D. (2013). Oct transcription factors in development and stem cells: Insights and mechanisms. *Development*, *140*(14), 2857–2866. https://doi.org/10.1242/dev.095927

Tapia Rico, G., & Price, T. J. (2018). Atezolizumab for the treatment of colorectal cancer: *The latest evidence and clinical potential*. *Expert Opinion on Biological Therapy*, *18*(4), 449–457. https://doi.org/10.1080/14712598.2018.1444024

Tasdemir, E., Maiuri, M. C., Galluzzi, L., Vitale, I., Djavaheri-Mergny, M., D'Amelio, M., Criollo, A., Morselli, E., Zhu, C., Harper, F., Nannmark, U., Samara, C., Pinton, P., Vicencio, J. M., Carnuccio, R., Moll, U. M., Madeo, F., Paterlini-Brechot, P., Rizzuto, R., … Kroemer, G. (2008). Regulation of autophagy by cytoplasmic p53. *Nature Cell Biology*, *10*(6), 676–687. https://doi.org/10.1038/ncb1730

Teh, H. S., Kisielow, P., Scott, B., Kishi, H., Uematsu, Y., Blüthmann, H., & Von Boehmer, H. (1988). Thymic major histocompatibility complex antigens and the αβ T-cell receptor determine the CD4/CD8 phenotype of T cells. *Nature*, *335*(6187), 229–233. https://doi.org/10.1038/335229a0

Templeton, K., Ramos, M., Rose, J., Le, B., Zhou, Q., Cressman, A., Ferreyra, S., Lebrilla, C. B., & Fierro, F. A. (2021). Mesenchymal Stromal Cells Regulate Sialylations of N-Glycans, Affecting Cell Migration and Survival. *International Journal of Molecular Sciences*, *22*(13), 6868. https://doi.org/10.3390/ijms22136868

Tewari, D., Bawari, S., Sharma, S., DeLiberto, L. K., & Bishayee, A. (2021). Targeting the crosstalk between canonical Wnt/β-catenin and inflammatory signaling cascades: A

novel strategy for cancer prevention and therapy. *Pharmacology & Therapeutics*, *227*, 107876. https://doi.org/10.1016/j.pharmthera.2021.107876

The Cancer Genome Atlas Network. (2012). Comprehensive molecular characterization of human colon and rectal cancer. *Nature*, *487*(7407), 330–337. https://doi.org/10.1038/nature11252

Tian, H., Yu, J.-L., Chu, X., Guan, Q., Liu, J., & Liu, Y. (2024). Unraveling the role of C1GALT1 in abnormal glycosylation and colorectal cancer progression. *Frontiers in Oncology*, *14*, 1389713. https://doi.org/10.3389/fonc.2024.1389713

Tian, S., Chu, Y., Hu, J., Ding, X., Liu, Z., Fu, D., Yuan, Y., Deng, Y., Wang, G., Wang, L., & Wang, Z. (2022). Tumour-associated neutrophils secrete AGR2 to promote colorectal cancer metastasis via its receptor CD98hc–xCT. *Gut*, *71*(12), 2489–2501. https://doi.org/10.1136/gutjnl-2021-325137

To, K. K., Tong, C. W., Wu, M., & Cho, W. C. (2018). MicroRNAs in the prognosis and therapy of colorectal cancer: From bench to bedside. *World Journal of Gastroenterology*, *24*(27), 2949–2973. https://doi.org/10.3748/wjg.v24.i27.2949

Tomita, N., Jiang, W., Hibshoosh, H., Warburton, D., Kahn, S. M., & Weinstein, I. B. (1992). Isolation and characterization of a highly malignant variant of the SW480 human colon cancer cell line. *Cancer Research*, *52*(24), 6840–6847.

Tzavlaki, K., & Moustakas, A. (2020). TGF-β Signaling. *Biomolecules*, *10*(3), 487. https://doi.org/10.3390/biom10030487

Ueno, H., Kajiwara, Y., Shimazaki, H., Shinto, E., Hashiguchi, Y., Nakanishi, K., Maekawa, K., Katsurada, Y., Nakamura, T., Mochizuki, H., Yamamoto, J., & Hase, K. (2012). New Criteria for Histologic Grading of Colorectal Cancer. *American Journal of Surgical Pathology*, *36*(2), 193–201. https://doi.org/10.1097/PAS.0b013e318235edee

Umar, A., Boland, C. R., Terdiman, J. P., Syngal, S., Chapelle, A. D. L., Ruschoff, J., Fishel, R., Lindor, N. M., Burgart, L. J., Hamelin, R., Hamilton, S. R., Hiatt, R. A., Jass, J., Lindblom, A., Lynch, H. T., Peltomaki, P., Ramsey, S. D., Rodriguez-Bigas, M. A., Vasen, H. F. A., … Srivastava, S. (2004). Revised Bethesda Guidelines for Hereditary Nonpolyposis Colorectal Cancer (Lynch Syndrome) and Microsatellite Instability. *JNCI Journal of the National Cancer Institute*, *96*(4), 261–268. https://doi.org/10.1093/jnci/djh034

Urh, K., Zidar, N., Tomažič, A., & Boštjančič, E. (2022). Intra-tumor heterogeneity of cancer stem cell-related genes and their potential regulatory microRNAs in metastasizing

colorectal carcinoma. *Oncology Reports*, *48*(5), 193. https://doi.org/10.3892/or.2022.8408

Valle, L., De Voer, R. M., Goldberg, Y., Sjursen, W., Försti, A., Ruiz-Ponte, C., Caldés, T., Garré, P., Olsen, M. F., Nordling, M., Castellvi-Bel, S., & Hemminki, K. (2019). Update on genetic predisposition to colorectal cancer and polyposis. *Molecular Aspects of Medicine*, *69*, 10–26. https://doi.org/10.1016/j.mam.2019.03.001

Van Cutsem, E., Cervantes, A., Nordlinger, B., & Arnold, D. (2014). Metastatic colorectal cancer: ESMO Clinical Practice Guidelines for diagnosis, treatment and follow-up. *Annals of Oncology*, *25*, iii1–iii9. https://doi.org/10.1093/annonc/mdu260

Van De Velde, C. J. H., Boelens, P. G., Tanis, P. J., Espin, E., Mroczkowski, P., Naredi, P., Pahlman, L., Ortiz, H., Rutten, H. J., Breugom, A. J., Smith, J. J., Wibe, A., Wiggers, T., & Valentini, V. (2014). Experts reviews of the multidisciplinary consensus conference colon and rectal cancer 2012. *European Journal of Surgical Oncology (EJSO)*, *40*(4), 454–468. https://doi.org/10.1016/j.ejso.2013.10.013

Van Der Zanden, S. Y., Luimstra, J. J., Neefjes, J., Borst, J., & Ovaa, H. (2020). Opportunities for Small Molecules in Cancer Immunotherapy. *Trends in Immunology*, *41*(6), 493–511. https://doi.org/10.1016/j.it.2020.04.004

Van Houtum, E. J. H., Büll, C., Cornelissen, L. A. M., & Adema, G. J. (2021). Siglec Signaling in the Tumor Microenvironment. *Frontiers in Immunology*, *12*, 790317. https://doi.org/10.3389/fimmu.2021.790317

Van Zandwijk, N., Pavlakis, N., Kao, S. C., Linton, A., Boyer, M. J., Clarke, S., Huynh, Y., Chrzanowska, A., Fulham, M. J., Bailey, D. L., Cooper, W. A., Kritharides, L., Ridley, L., Pattison, S. T., MacDiarmid, J., Brahmbhatt, H., & Reid, G. (2017). Safety and activity of microRNA-loaded minicells in patients with recurrent malignant pleural mesothelioma: A first-in-man, phase 1, open-label, dose-escalation study. *The Lancet Oncology*, *18*(10), 1386–1396. https://doi.org/10.1016/S1470-2045(17)30621-6

Varadi, M., Anyango, S., Deshpande, M., Nair, S., Natassia, C., Yordanova, G., Yuan, D., Stroe, O., Wood, G., Laydon, A., Žídek, A., Green, T., Tunyasuvunakool, K., Petersen, S., Jumper, J., Clancy, E., Green, R., Vora, A., Lutfi, M., … Velankar, S. (2022). AlphaFold Protein Structure Database: Massively expanding the structural coverage of protein-sequence space with high-accuracy models. *Nucleic Acids Research*, *50*(D1), D439–D444. https://doi.org/10.1093/nar/gkab1061

Varki, A. (2008). Sialic acids in human health and disease. *Trends in Molecular Medicine*, *14*(8), 351–360. https://doi.org/10.1016/j.molmed.2008.06.002

Vashchenko, B. V., Geraschenko, O., & Grygorenk, O. O. (2023). HETEROCYCLIC α-OXOESTERS (HETARYL GLYOXYLATES): SYNTHESIS AND CHEMICAL TRANSFORMATIONS. Part 1. *Targets in Heterocyclic Systems*, *26*, 533. https://doi.org/10.17374/targets.2023.26.533

Venturi, G., Gomes Ferreira, I., Pucci, M., Ferracin, M., Malagolini, N., Chiricolo, M., & Dall'Olio, F. (2019). Impact of sialyltransferase ST6GAL1 overexpression on different colon cancer cell types. *Glycobiology*, *29*(10), 684–695. https://doi.org/10.1093/glycob/cwz053

Venugopal, A., & Carethers, J. M. (2022). Epidemiology and biology of early onset colorectal cancer. *EXCLI Journal; 21:Doc162; ISSN 1611-2156*. https://doi.org/10.17179/EXCLI2021-4456

Vieira, A. R., Abar, L., Chan, D. S. M., Vingeliene, S., Polemiti, E., Stevens, C., Greenwood, D., & Norat, T. (2017). Foods and beverages and colorectal cancer risk: A systematic review and meta-analysis of cohort studies, an update of the evidence of the WCRF-AICR Continuous Update Project. *Annals of Oncology*, *28*(8), 1788–1802. https://doi.org/10.1093/annonc/mdx171

Vilar, E., & Gruber, S. B. (2010). Microsatellite instability in colorectal cancer—The stable evidence. *Nature Reviews Clinical Oncology*, *7*(3), 153–162. https://doi.org/10.1038/nrclinonc.2009.237

Vodenkova, S., Buchler, T., Cervena, K., Veskrnova, V., Vodicka, P., & Vymetalkova, V. (2020). 5-fluorouracil and other fluoropyrimidines in colorectal cancer: Past, present and future. *Pharmacology & Therapeutics*, *206*, 107447. https://doi.org/10.1016/j.pharmthera.2019.107447

Vojta, A., Samaržija, I., Bočkor, L., & Zoldoš, V. (2016). Glyco-genes change expression in cancer through aberrant methylation. *Biochimica et Biophysica Acta (BBA) - General Subjects*, *1860*(8), 1776–1785. https://doi.org/10.1016/j.bbagen.2016.01.002

Von Gunten, S., & Bochner, B. S. (2008). Basic and Clinical Immunology of Siglecs. *Annals of the New York Academy of Sciences*, *1143*(1), 61–82. https://doi.org/10.1196/annals.1443.011

Wan, M., Wang, Y., Zeng, Z., Deng, B., Zhu, B., Cao, T., Li, Y., Xiao, J., Han, Q., & Wu, Q. (2020). Colorectal cancer (CRC) as a multifactorial disease and its causal correlations with multiple signaling pathways. *Bioscience Reports*, *40*(3), BSR20200265. https://doi.org/10.1042/BSR20200265

Wandall, H. H., Nielsen, M. A. I., King-Smith, S., De Haan, N., & Bagdonaite, I. (2021). Global functions of O-glycosylation: Promises and challenges in O-glycobiology. *The FEBS Journal*, *288*(24), 7183–7212. https://doi.org/10.1111/febs.16148

Wang, H. (2020). MicroRNAs and Apoptosis in Colorectal Cancer. *International Journal of Molecular Sciences*, *21*(15), 5353. https://doi.org/10.3390/ijms21155353

Wang, H., Guo, M., Wei, H., & Chen, Y. (2023). Targeting p53 pathways: Mechanisms, structures and advances in therapy. *Signal Transduction and Targeted Therapy*, *8*(1), 92. https://doi.org/10.1038/s41392-023-01347-1

Wang, J., Cao, Z., Wang, P., Zhang, X., Tang, J., He, Y., Huang, Z., Mao, X., Shi, S., & Kou, X. (2021). Apoptotic Extracellular Vesicles Ameliorate Multiple Myeloma by Restoring Fas-Mediated Apoptosis. *ACS Nano*, *15*(9), 14360–14372. https://doi.org/10.1021/acsnano.1c03517

Wang, J., Manni, M., Bärenwaldt, A., Wieboldt, R., Kirchhammer, N., Ivanek, R., Stanczak, M., Zippelius, A., König, D., Rodrigues Manutano, N., & Läubli, H. (2022). Siglec Receptors Modulate Dendritic Cell Activation and Antigen Presentation to T Cells in Cancer. *Frontiers in Cell and Developmental Biology*, *10*, 828916. https://doi.org/10.3389/fcell.2022.828916

Wang, J., Sun, J., Liu, L. N., Flies, D. B., Nie, X., Toki, M., Zhang, J., Song, C., Zarr, M., Zhou, X., Han, X., Archer, K. A., O'Neill, T., Herbst, R. S., Boto, A. N., Sanmamed, M. F., Langermann, S., Rimm, D. L., & Chen, L. (2019). Siglec-15 as an immune suppressor and potential target for normalization cancer immunotherapy. *Nature Medicine*, *25*(4), 656–666. https://doi.org/10.1038/s41591-019-0374-x

Wang, J., Xu, L., Ding, Q., Li, X., Wang, K., Xu, S., & Liu, B. (2023). Siglec15 is a prognostic indicator and a potential tumor-related macrophage regulator that is involved in the suppressive immunomicroenvironment in gliomas. *Frontiers in Immunology*, *14*, 1065062. https://doi.org/10.3389/fimmu.2023.1065062

Wang, W., He, Y., Rui, J., & Xu, M. (2018). miR-410 acts as an oncogene in colorectal cancer cells by targeting dickkopf-related protein 1 via the Wnt/β-catenin signaling pathway. *Oncology Letters*. https://doi.org/10.3892/ol.2018.9710

Wang, X., He, Y., Mackowiak, B., & Gao, B. (2021). MicroRNAs as regulators, biomarkers and therapeutic targets in liver diseases. *Gut*, *70*(4), 784–795. https://doi.org/10.1136/gutjnl-2020-322526

Wang, Y., He, M., Zhang, C., Cao, K., Zhang, G., Yang, M., Huang, Y., Jiang, W., & Liu, H. (2023). Siglec-9 $^{+}$ tumor-associated macrophages delineate an immunosuppressive

subset with therapeutic vulnerability in patients with high-grade serous ovarian cancer. *Journal for ImmunoTherapy of Cancer*, *11*(9), e007099. https://doi.org/10.1136/jitc-2023-007099

Wang, Y., Johnson, K. C. C., Gatti-Mays, M. E., & Li, Z. (2022). Emerging strategies in targeting tumor-resident myeloid cells for cancer immunotherapy. *Journal of Hematology & Oncology*, *15*(1), 118. https://doi.org/10.1186/s13045-022-01335-y

Wang, Y., Xu, Z., Wu, K.-L., Yu, L., Wang, C., Ding, H., Gao, Y., Sun, H., Wu, Y.-H., Xia, M., Chen, Y., & Xiao, H. (2024). Siglec-15/sialic acid axis as a central glyco-immune checkpoint in breast cancer bone metastasis. *Proceedings of the National Academy of Sciences*, *121*(5), e2312929121. https://doi.org/10.1073/pnas.2312929121

Wang, Y., Zeng, Z., Lu, J., Wang, Y., Liu, Z., He, M., Zhao, Q., Wang, Z., Li, T., Lu, Y., Wu, Q., Yu, K., Wang, F., Pu, H.-Y., Li, B., Jia, W., Shi, M., Xie, D., Kang, T., … Xu, R. (2018). CPT1A-mediated fatty acid oxidation promotes colorectal cancer cell metastasis by inhibiting anoikis. *Oncogene*, *37*(46), 6025–6040. https://doi.org/10.1038/s41388-018-0384-z

Wang, Y.-L., Wei, M.-B., Zhao, W.-W., Feng, L.-L., Yin, X.-K., Bai, S.-M., Wan, X.-B., Hung, M.-C., Zou, A. Z., Wang, M. H., Zheng, J., Qin, C., & Fan, X.-J. (2021). Glycosylation of Siglec15 promotes immunoescape and tumor growth. *American Journal of Cancer Research*, *11*(5), 2291–2302.

Warde-Farley, D., Donaldson, S. L., Comes, O., Zuberi, K., Badrawi, R., Chao, P., Franz, M., Grouios, C., Kazi, F., Lopes, C. T., Maitland, A., Mostafavi, S., Montojo, J., Shao, Q., Wright, G., Bader, G. D., & Morris, Q. (2010). The GeneMANIA prediction server: Biological network integration for gene prioritization and predicting gene function. *Nucleic Acids Research*, *38*(suppl_2), W214–W220. https://doi.org/10.1093/nar/gkq537

Watkins, R. J., Read, M. L., Smith, V. E., Sharma, N., Reynolds, G. M., Buckley, L., Doig, C., Campbell, M. J., Lewy, G., Eggo, M. C., Loubiere, L. S., Franklyn, J. A., Boelaert, K., & McCabe, C. J. (2010). Pituitary Tumor Transforming Gene Binding Factor: A New Gene in Breast Cancer. *Cancer Research*, *70*(9), 3739–3749. https://doi.org/10.1158/0008-5472.CAN-09-3531

Weber, R., Fleming, V., Hu, X., Nagibin, V., Groth, C., Altevogt, P., Utikal, J., & Umansky, V. (2018). Myeloid-Derived Suppressor Cells Hinder the Anti-Cancer Activity of Immune Checkpoint Inhibitors. *Frontiers in Immunology*, *9*, 1310. https://doi.org/10.3389/fimmu.2018.01310

Wei, A., Fan, B., Zhao, Y., Zhang, H., Wang, L., Yu, X., Yuan, Q., Yang, D., & Wang, S. (2016). ST6Gal-I overexpression facilitates prostate cancer progression via the PI3K/Akt/GSK-3β/β-catenin signaling pathway. *Oncotarget*, *7*(40), 65374–65388. https://doi.org/10.18632/oncotarget.11699

Wei, C., Yang, C., Wang, S., Shi, D., Zhang, C., Lin, X., Liu, Q., Dou, R., & Xiong, B. (2019). Crosstalk between cancer cells and tumor associated macrophages is required for mesenchymal circulating tumor cell-mediated colorectal cancer metastasis. *Molecular Cancer*, *18*(1), 64. https://doi.org/10.1186/s12943-019-0976-4

Wei, K., Shi, J., Xiao, Y., Wang, W., Yang, Q., & Chen, C. (2023). [MiR-30e-5p overexpression promotes proliferation and migration of colorectal cancer cells by activating the CXCL12 axis via downregulating PTEN]. *Nan Fang Yi Ke Da Xue Xue Bao = Journal of Southern Medical University*, *43*(7), 1081–1092. https://doi.org/10.12122/j.issn.1673-4254.2023.07.04

Weinhold, L., Wahl, S., Pechlivanis, S., Hoffmann, P., & Schmid, M. (2016). A statistical model for the analysis of beta values in DNA methylation studies. *BMC Bioinformatics*, *17*(1), 480. https://doi.org/10.1186/s12859-016-1347-4

Wen, Y., Zhu, Y., Zhang, C., Yang, X., Gao, Y., Li, M., Yang, H., Liu, T., & Tang, H. (2022). Chronic inflammation, cancer development and immunotherapy. *Frontiers in Pharmacology*, *13*, 1040163. https://doi.org/10.3389/fphar.2022.1040163

Weng, J., Li, S., Zhu, Z., Liu, Q., Zhang, R., Yang, Y., & Li, X. (2022). Exploring immunotherapy in colorectal cancer. *Journal of Hematology & Oncology*, *15*(1), 95. https://doi.org/10.1186/s13045-022-01294-4

West, N. P., Morris, E. J., Rotimi, O., Cairns, A., Finan, P. J., & Quirke, P. (2008). Pathology grading of colon cancer surgical resection and its association with survival: A retrospective observational study. *The Lancet Oncology*, *9*(9), 857–865. https://doi.org/10.1016/S1470-2045(08)70181-5

Westholm, J. O., & Lai, E. C. (2011). Mirtrons: microRNA biogenesis via splicing. *Biochimie*, *93*(11), 1897–1904. https://doi.org/10.1016/j.biochi.2011.06.017

White, A., Ironmonger, L., Steele, R. J. C., Ormiston-Smith, N., Crawford, C., & Seims, A. (2018). A review of sex-related differences in colorectal cancer incidence, screening uptake, routes to diagnosis, cancer stage and survival in the UK. *BMC Cancer*, *18*(1), 906. https://doi.org/10.1186/s12885-018-4786-7

Wightman, B., Ha, I., & Ruvkun, G. (1993). Posttranscriptional regulation of the heterochronic gene lin-14 by lin-4 mediates temporal pattern formation in C. elegans. *Cell*, *75*(5), 855–862. https://doi.org/10.1016/0092-8674(93)90530-4

Wu, H., Chen, J., Li, D., Liu, X., Li, L., & Wang, K. (2017). MicroRNA-30e Functions as a Tumor Suppressor in Cervical Carcinoma Cells through Targeting GALNT7. *Translational Oncology*, *10*(6), 876–885. https://doi.org/10.1016/j.tranon.2017.08.006

Wu, L., Saxena, S., & Singh, R. K. (2020). Neutrophils in the Tumor Microenvironment. In A. Birbrair (Ed.), *Tumor Microenvironment* (Vol. 1224, pp. 1–20). Springer International Publishing. https://doi.org/10.1007/978-3-030-35723-8_1

Wu, M., Jing, H., & Chang, T. (2007). Synthesis of β-amino carbonyl compounds via a Mannich reaction catalyzed by SalenZn complex. *Catalysis Communications*, *8*(12), 2217–2221. https://doi.org/10.1016/j.catcom.2007.05.011

Wu, Q., Qian, W., Sun, X., & Jiang, S. (2022). Small-molecule inhibitors, immune checkpoint inhibitors, and more: FDA-approved novel therapeutic drugs for solid tumors from 1991 to 2021. *Journal of Hematology & Oncology*, *15*(1). https://doi.org/10.1186/s13045-022-01362-9

Wu, Q., Wei, X., Chen, F., Huang, M., Zhang, S., Zhu, L., Zhou, L., Yang, C., & Song, Y. (2023). Aptamer-Assisted Blockade of the Immune Suppressor Sialic Acid-Binding Immunoglobulin-Like Lectin-15 for Cancer Immunotherapy. *Angewandte Chemie International Edition*, e202312609. https://doi.org/10.1002/anie.202312609

Wu, X., Zhang, J., He, X., Wang, C., Lian, L., Liu, H., Wang, J., & Lan, P. (2012). Postoperative Adjuvant Chemotherapy for Stage II Colorectal Cancer: A Systematic Review of 12 Randomized Controlled Trials. *Journal of Gastrointestinal Surgery*, *16*(3), 646–655. https://doi.org/10.1007/s11605-011-1682-8

Wu, Y.-F., Wang, C.-Y., Tang, W.-C., Lee, Y.-C., Ta, H. D. K., Lin, L.-C., Pan, S.-R., Ni, Y.-C., Anuraga, G., & Lee, K.-H. (2021). Expression Profile and Prognostic Value of Wnt Signaling Pathway Molecules in Colorectal Cancer. *Biomedicines*, *9*(10), 1331. https://doi.org/10.3390/biomedicines9101331

Wu, Z., Wang, Z., Wu, H., Zheng, N., Huang, D., Huang, Z., Han, H., Bao, J., Xu, H., Zhang, R., Du, Z., & Wu, D. (2023). The pan-cancer multi-omics landscape of key genes of sialylation combined with RNA-sequencing validation. *Computers in Biology and Medicine*, *166*, 107556. https://doi.org/10.1016/j.compbiomed.2023.107556

Xia, L., Lin, J., Peng, M., Jiang, X., Peng, Q., Cui, S., Zhang, W., Li, S., Wang, J., Oyang, L., Tan, S., Hu, Z., Wu, N., Tang, Y., Luo, X., Ren, Z., Shi, Y., Liao, Q., & Zhou, Y.

(2024). Diallyl disulfide induces DNA damage and growth inhibition in colorectal cancer cells by promoting POU2F1 ubiquitination. *International Journal of Biological Sciences*, *20*(4), 1125–1141. https://doi.org/10.7150/ijbs.91206

Xiang, H., Toyoshima, Y., Shen, W., Wang, X., Okada, N., Kii, S., Sugiyama, K., Nagato, T., Kobayashi, H., Ikeo, K., Hashimoto, S., Tanino, M., Taketomi, A., & Kitamura, H. (2022). IFN -α/β-mediated NK2R expression is related to the malignancy of colon cancer cells. *Cancer Science*, *113*(8), 2513–2525. https://doi.org/10.1111/cas.15397

Xiang, T., Qiao, M., Xie, J., Li, Z., & Xie, H. (2022). Emerging Roles of the Unique Molecular Chaperone Cosmc in the Regulation of Health and Disease. *Biomolecules*, *12*(12), 1732. https://doi.org/10.3390/biom12121732

Xiao, S., Yang, C., Zhang, Y., & Lai, C. (2022). Downregulation of B3GNT6 is a predictor of poor outcomes in patients with colorectal cancer. *World Journal of Surgical Oncology*, *20*(1), 110. https://doi.org/10.1186/s12957-022-02561-x

Xie, Y., Hou, W., Song, X., Yu, Y., Huang, J., Sun, X., Kang, R., & Tang, D. (2016). Ferroptosis: Process and function. *Cell Death & Differentiation*, *23*(3), 369–379. https://doi.org/10.1038/cdd.2015.158

Xie, Y.-H., Chen, Y.-X., & Fang, J.-Y. (2020). Comprehensive review of targeted therapy for colorectal cancer. *Signal Transduction and Targeted Therapy*, *5*(1), 22. https://doi.org/10.1038/s41392-020-0116-z

Xing, X., Cao, F., Gao, L., & Song, M. (2023). AHSG, a Gene Promoting Tumour Proliferation, Migration and Invasion, is an Independent Prognostic Factor for Poor Overall Survival in Lung Adenocarcinoma. *Molecular Biology Reports*, *50*(9), 7659–7666. https://doi.org/10.1007/s11033-023-08623-x

Xing, Y., Wang, Z., Lu, Z., Xia, J., Xie, Z., Jiao, M., Liu, R., & Chu, Y. (2021). MicroRNAs: Immune modulators in cancer immunotherapy. *Immunotherapy Advances*, *1*(1), ltab006. https://doi.org/10.1093/immadv/ltab006

Xiong, X., Wen, Y.-A., Fairchild, R., Zaytseva, Y. Y., Weiss, H. L., Evers, B. M., & Gao, T. (2020). Upregulation of CPT1A is essential for the tumor-promoting effect of adipocytes in colon cancer. *Cell Death & Disease*, *11*(9), 736. https://doi.org/10.1038/s41419-020-02936-6

Xiu, B., Chi, Y., Liu, L., Chi, W., Zhang, Q., Chen, J., Guo, R., Si, J., Li, L., Xue, J., Shao, Z.-M., Wu, Z.-H., Huang, S., & Wu, J. (2019). LINC02273 drives breast cancer metastasis by epigenetically increasing AGR2 transcription. *Molecular Cancer*, *18*(1), 187. https://doi.org/10.1186/s12943-019-1115-y

Xu, Z., Qu, H., Ren, Y., Gong, Z., Ri, H. J., & Chen, X. (2021). An Update on the Potential Roles of E2F Family Members in Colorectal Cancer. *Cancer Management and Research*, *Volume 13*, 5509–5521. https://doi.org/10.2147/cmar.s320193

Xu, Z., Qu, H., Ren, Y., Gong, Z., Ri, H. J., Zhang, F., Shao, S., Chen, X., & Chen, X. (2022). Systematic Analysis of E2F Expression and Its Relation in Colorectal Cancer Prognosis. *International Journal of General Medicine*, *Volume 15*, 4849–4870. https://doi.org/10.2147/IJGM.S352141

Yan, L., Wang, D., Liu, X., Gu, C., & Gao, S. (2021). Actein antagonizes colorectal cancer through blocking PI3K/Akt pathways by downregulating IMPDH2. *Anti-Cancer Drugs*, *32*(8), 864–874. https://doi.org/10.1097/CAD.0000000000001080

Yang, J., Ma, D., Fesler, A., Zhai, H., Leamniramit, A., Li, W., Wu, S., & Ju, J. (2017). Expression analysis of microRNA as prognostic biomarkers in colorectal cancer. *Oncotarget*, *8*(32), 52403–52412. https://doi.org/10.18632/oncotarget.14175

Yang, J., Roy, A., & Zhang, Y. (2012). BioLiP: A semi-manually curated database for biologically relevant ligand–protein interactions. *Nucleic Acids Research*, *41*(D1), D1096–D1103. https://doi.org/10.1093/nar/gks966

Yang, J., Roy, A., & Zhang, Y. (2013). Protein–ligand binding site recognition using complementary binding-specific substructure comparison and sequence profile alignment. *Bioinformatics*, *29*(20), 2588–2595. https://doi.org/10.1093/bioinformatics/btt447

Yao, Y., Jiao, D., Liu, Z., Chen, J., Zhou, X., Li, Z., Li, J., & Han, X. (2020). Novel miRNA Predicts Survival and Prognosis of Cholangiocarcinoma Based on RNA-seq Data and In Vitro Experiments. *BioMed Research International*, *2020*, 1–14. https://doi.org/10.1155/2020/5976127

Yashiro, M. (2014). Ulcerative colitis-associated colorectal cancer. *World Journal of Gastroenterology*, *20*(44), 16389. https://doi.org/10.3748/wjg.v20.i44.16389

Ye, Z., & Vakhrushev, S. Y. (2021). The Role of Data-Independent Acquisition for Glycoproteomics. *Molecular & Cellular Proteomics*, *20*, 100042. https://doi.org/10.1074/mcp.R120.002204

Yeung, T. M., Gandhi, S. C., Wilding, J. L., Muschel, R., & Bodmer, W. F. (2010). Cancer stem cells from colorectal cancer-derived cell lines. *Proceedings of the National Academy of Sciences*, *107*(8), 3722–3727. https://doi.org/10.1073/pnas.0915135107

Yi, R., Qin, Y., Macara, I. G., & Cullen, B. R. (2003). Exportin-5 mediates the nuclear export of pre-microRNAs and short hairpin RNAs. *Genes & Development*, *17*(24), 3011–3016. https://doi.org/10.1101/gad.1158803

Yu, F.-X., Zhao, B., & Guan, K.-L. (2015). Hippo Pathway in Organ Size Control, Tissue Homeostasis, and Cancer. *Cell*, *163*(4), 811–828. https://doi.org/10.1016/j.cell.2015.10.044

Yu, S.-Y., Hsiao, C.-T., Izawa, M., Yusa, A., Ishida, H., Nakamura, S., Yagi, H., Kannagi, R., & Khoo, K.-H. (2018). Distinct substrate specificities of human GlcNAc-6-sulfotransferases revealed by mass spectrometry–based sulfoglycomic analysis. *Journal of Biological Chemistry*, *293*(39), 15163–15177. https://doi.org/10.1074/jbc.RA118.001937

Zaki, T. A., Singal, A. G., May, F. P., & Murphy, C. C. (2022). Increasing Incidence Rates of Colorectal Cancer at Ages 50–54 Years. *Gastroenterology*, *162*(3), 964-965.e3. https://doi.org/10.1053/j.gastro.2021.10.039

Zeng, Z., Lu, J., Wang, Y., Sheng, H., Wang, Y., Chen, Z., Wu, Q., Zheng, J., Chen, Y., Yang, D., Yu, K., Mo, H., Hu, J., Hu, P., Liu, Z., Ju, H., & Xu, R. (2021). The lncRNA XIST/miR-125b-2-3p axis modulates cell proliferation and chemotherapeutic sensitivity via targeting Wee1 in colorectal cancer. *Cancer Medicine*, *10*(7), 2423–2441. https://doi.org/10.1002/cam4.3777

Zenonos, K. (2013). RAS signaling pathways, mutations and their role in colorectal cancer. *World Journal of Gastrointestinal Oncology*, *5*(5), 97. https://doi.org/10.4251/wjgo.v5.i5.97

Zhai, W., Zhou, X., Du, J., & Gao, Y. (2019). In vitro assay for the development of small molecule inhibitors targeting PD-1/PD-L1. In *Methods in Enzymology* (Vol. 629, pp. 361–381). Elsevier. https://doi.org/10.1016/bs.mie.2019.05.051

Zhang, C., Liu, J., Xu, D., Zhang, T., Hu, W., & Feng, Z. (2020). Gain-of-function mutant p53 in cancer progression and therapy. *Journal of Molecular Cell Biology*, *12*(9), 674–687. https://doi.org/10.1093/jmcb/mjaa040

Zhang, H., Li, Z., Jiang, J., Lei, Y., Xie, J., Liu, Y., & Yi, B. (2023). SNTB1 regulates colorectal cancer cell proliferation and metastasis through YAP1 and the WNT/β-catenin pathway. *Cell Cycle*, *22*(17), 1865–1883. https://doi.org/10.1080/15384101.2023.2244778

Zhang, H., Zhu, H.-T., Wang, D., Yang, C.-R., & Zhang, Y.-J. (2019). Sphingofungins G and H: New five-membered lactones from *Aspergillus penicilliodes* Speg. *Natural Product Research*, *33*(9), 1284–1291. https://doi.org/10.1080/14786419.2018.1470627

Zhang, J., Yang, W., Xiao, Y., & Shan, L. (2022). MiR-125b Inhibits Cell Proliferation and Induces Apoptosis in HumanColon Cancer SW480 Cells via Targeting STAT3. *Recent Patents on Anti-Cancer Drug Discovery*, *17*(2), 187–194. https://doi.org/10.2174/1574892816666210708165037

Zhang, L., & Shay, J. W. (2017). Multiple Roles of APC and its Therapeutic Implications in Colorectal Cancer. *Journal of the National Cancer Institute*, *109*(8), djw332. https://doi.org/10.1093/jnci/djw332

Zhang, N., Hu, X., Du, Y., & Du, J. (2021). The role of miRNAs in colorectal cancer progression and chemoradiotherapy. *Biomedicine & Pharmacotherapy*, *134*, 111099. https://doi.org/10.1016/j.biopha.2020.111099

Zhang, P., Lu, X., Tao, K., Shi, L., Li, W., Wang, G., & Wu, K. (2015). Siglec-10 is associated with survival and natural killer cell dysfunction in hepatocellular carcinoma. *Journal of Surgical Research*, *194*(1), 107–113. https://doi.org/10.1016/j.jss.2014.09.035

Zhang, S., Lu, J., Xu, Z., Zou, X., Sun, X., Xu, Y., Shan, A., Lu, J., Yan, X., Cui, Y., Yan, W., Du, Y., Gu, J., Zheng, M., Feng, B., & Zhang, Y. (2017). Differential expression of ST6GAL1 in the tumor progression of colorectal cancer. *Biochemical and Biophysical Research Communications*, *486*(4), 1090–1096. https://doi.org/10.1016/j.bbrc.2017.03.167

Zhang, X., Cui, S., Ding, Y., Li, Y., Wu, B., Gao, J., Li, M., Xu, L., & Xia, H. (2024). Downregulation of B4GALT5 attenuates cardiac fibrosis through Lumican and Akt/GSK-3β/β-catenin pathway. *European Journal of Pharmacology*, *963*, 176263. https://doi.org/10.1016/j.ejphar.2023.176263

Zhang, X., Shi, J., Jin, S., Wang, R., Li, M., Zhang, Z., Yang, X., & Ma, H. (2024). Metabolic landscape of head and neck squamous cell carcinoma informs a novel kynurenine/Siglec-15 axis in immune escape. *Cancer Communications*, *44*(6), 670–694. https://doi.org/10.1002/cac2.12545

Zhang, X., Xu, Y., Yamaguchi, K., Hu, J., Zhang, L., Wang, J., Tian, J., & Chen, W. (2020). Circular RNA circVAPA knockdown suppresses colorectal cancer cell growth process by regulating miR-125a/CREB5 axis. *Cancer Cell International*, *20*(1), 103. https://doi.org/10.1186/s12935-020-01178-y

Zhang, Y., Sun, H., Huang, F., Chen, Y., Ding, X., Zhou, C., Wu, Y., Zhang, Q., Ma, X., Wang, J., Yue, R., Shen, L., Sun, X., & Ye, Z. (2024). The chromatin remodeling factor Arid1a cooperates with Jun/Fos to promote osteoclastogenesis by epigenetically upregulating *Siglec15* expression. *Journal of Bone and Mineral Research*, *39*(6), 775–790. https://doi.org/10.1093/jbmr/zjae042

Zhang, Y., Xia, M., Jin, K., Wang, S., Wei, H., Fan, C., Wu, Y., Li, X., Li, X., Li, G., Zeng, Z., & Xiong, W. (2018). Function of the c-Met receptor tyrosine kinase in carcinogenesis and associated therapeutic opportunities. *Molecular Cancer*, *17*(1), 45. https://doi.org/10.1186/s12943-018-0796-y

Zhang, Z., Zhang, H., Liao, X., & Tsai, H. (2023). KRAS mutation: The booster of pancreatic ductal adenocarcinoma transformation and progression. *Frontiers in Cell and Developmental Biology*, *11*. https://doi.org/10.3389/fcell.2023.1147676

Zhao, H., Ming, T., Tang, S., Ren, S., Yang, H., Liu, M., Tao, Q., & Xu, H. (2022). Wnt signaling in colorectal cancer: Pathogenic role and therapeutic target. *Molecular Cancer*, *21*(1). https://doi.org/10.1186/s12943-022-01616-7

Zhao, J., Yang, H., Hu, H., Liu, C., Wei, M., Zhao, Y., Chen, Y., Cui, Y., Chen, P., Xiong, K., Lu, Y., Yang, H., & Yang, L. (2022). Prognostic value of PD-L1 and Siglec-15 expression in patients with nasopharyngeal carcinoma. *Scientific Reports*, *12*(1), 10401. https://doi.org/10.1038/s41598-022-13997-2

Zhao, Q., Cheng, Y., & Xiong, Y. (2021). LTF Regulates the Immune Microenvironment of Prostate Cancer Through JAK/STAT3 Pathway. *Frontiers in Oncology*, *11*, 692117. https://doi.org/10.3389/fonc.2021.692117

Zheng, B., Song, K., Sun, L., Gao, Y., Qu, Y., Ren, C., Yan, P., Chen, W., Guo, W., Zhou, C., & Yue, B. (2022). Siglec-15-induced autophagy promotes invasion and metastasis of human osteosarcoma cells by activating the epithelial–mesenchymal transition and Beclin-1/ATG14 pathway. *Cell & Bioscience*, *12*(1), 109. https://doi.org/10.1186/s13578-022-00846-y

Zheng, Y., Ma, X., Su, D., Zhang, Y., Yu, L., Jiang, F., Zhou, X., Feng, Y., & Ma, F. (2020). The Roles of Siglec7 and Siglec9 on Natural Killer Cells in Virus Infection and Tumour Progression. *Journal of Immunology Research*, *2020*, 1–9. https://doi.org/10.1155/2020/6243819

Zhong, L., Li, Y., Xiong, L., Wang, W., Wu, M., Yuan, T., Yang, W., Tian, C., Miao, Z., Wang, T., & Yang, S. (2021). Small molecules in targeted cancer therapy: Advances,

challenges, and future perspectives. *Signal Transduction and Targeted Therapy*, *6*(1), 201. https://doi.org/10.1038/s41392-021-00572-w

Zhong, S., Jeong, J.-H., Chen, Z., Chen, Z., & Luo, J.-L. (2020). Targeting Tumor Microenvironment by Small-Molecule Inhibitors. *Translational Oncology*, *13*(1), 57–69. https://doi.org/10.1016/j.tranon.2019.10.001

Zhou, H., Shen, Y., Zheng, G., Zhang, B., Wang, A., Zhang, J., Hu, H., Lin, J., Liu, S., Luan, X., & Zhang, W. (2024). Integrating single-cell and spatial analysis reveals MUC1-mediated cellular crosstalk in mucinous colorectal adenocarcinoma. *Clinical and Translational Medicine*, *14*(5), e1701. https://doi.org/10.1002/ctm2.1701

Zhou, L., Zhang, S., Zou, X., Lu, J., Yang, X., Xu, Z., Shan, A., Jia, W., Liu, F., Yan, X., Su, H., Liang, T., Zheng, M., Zhang, Y., & Feng, B. (2019). The β-galactoside α2,6-sialyltranferase 1 (ST6GAL1) inhibits the colorectal cancer metastasis by stabilizing intercellular adhesion molecule-1 via sialylation. *Cancer Management and Research*, *Volume 11*, 6185–6199. https://doi.org/10.2147/CMAR.S208631

Zhou, R. W., Harpaz, N., Itzkowitz, S. H., & Parsons, R. E. (2023). Molecular mechanisms in colitis-associated colorectal cancer. *Oncogenesis*, *12*(1), 48. https://doi.org/10.1038/s41389-023-00492-0

Zhou, S., Wang, X., Zhao, C., Liu, Q., Zhou, H., Zheng, Z., Zhou, Z., Wang, X., & Liang, J. (2019). Laparoscopic vs open colorectal cancer surgery in elderly patients: Short- and long-term outcomes and predictors for overall and disease-free survival. *BMC Surgery*, *19*(1), 137. https://doi.org/10.1186/s12893-019-0596-3

Zhou, S., Wang, Y., Zhang, R., Zeng, W., Liu, S., Liu, S., Liu, M., Yang, H., & Xi, M. (2023). Association of Sialic Acid–Binding Immunoglobulin-Like Lectin 15 With Phenotypes in Esophageal Squamous Cell Carcinoma in the Setting of Neoadjuvant Chemoradiotherapy. *JAMA Network Open*, *6*(1), e2250965. https://doi.org/10.1001/jamanetworkopen.2022.50965

Zhou, W., Xia, L., Wang, Z., Cao, G., Chen, L., Chen, E., Zhang, W., & Song, Z. (2022). Transanal Minimally Invasive Surgery for Rectal Anastomotic Stenosis After Colorectal Cancer Surgery. *Diseases of the Colon & Rectum*, *65*(8), 1062–1068. https://doi.org/10.1097/DCR.0000000000002361

Zhou, X., Yang, G., & Guan, F. (2020). Biological Functions and Analytical Strategies of Sialic Acids in Tumor. *Cells*, *9*(2), 273. https://doi.org/10.3390/cells9020273

Zlobec, I., Berger, M. D., & Lugli, A. (2020). Tumour budding and its clinical implications in gastrointestinal cancers. *British Journal of Cancer*, *123*(5), 700–708. https://doi.org/10.1038/s41416-020-0954-z

Appendix 1 - Sequence alignment of the conserved human Siglec proteins: Siglec-15 (NP_998767.1), Siglec-1 (NP_075556.1), Siglec-2 (NP_001762.2) and Siglec-4 (NP_002352.1).

CLUSTAL 2.1 multiple sequence alignment

```
NP_001762.2     MHLLGPWLLLLVLEYLAFSDSSKWVFEHPETLYAWEGACVWIPCTYRALDGDLESFILFH
NP_002352.1     --MIFLTALPLFWIMISASRGGHWGAWMPSSISAFEGTCVSIPCRFDFPD-ELRPAVVHG
NP_075556.1     ---MGFLPKLLLLASFFPAGQASWGVSSPQDVQGVKGSCLLIPCIFSFPADVEVPDGITA
NP_998767.1     ----------MEKSIWLLACLAWVLPTGSFVRTKIDTTENLLN----------------
                .  :     *    . :   .:  :

NP_001762.2     NPEYNKNTSKFDGTRLYESTKDGKVPSEQKRVQFLGDK-NKNCTLSIHPVHLNDSGQLGL
NP_002352.1     VWYFNSPYPKNYPPVVFKSRTQVVHESFQGRSRLLGDLGLRNCTLLLSNVSPELGGKYYF
NP_075556.1     IWYY--DYSGQRQVVSHSADPKLVEARFRGRTEFMGNPEHRVCNLLLKDLQPEDSGSYNF
NP_998767.1     ------------TEVHSSPAQRWSMQVPPEVSAEAGDAAVLPCTFTHPHRHYDGP-----
                    ..            *:    *.:     :

NP_001762.2     RMESKTEKWMERIH---LNVSERPFPPHIQLPPEIQESQEVTLTCLLNFSCYGYPIQLQW
NP_002352.1     RGDLGGYNQYTFSE---HSVLDIVNTPNIVVPPEVVAGTEVEVSCMVPDNCPELRPELSW
NP_075556.1     RFEISEVNRWSDVKGTLVTVTEEPRVPTIASPVELLEGTEVDFNCSTPYVCLQEQVRLQW
NP_998767.1     -----------------LTAIWRAGEPYAGPQVFRCAAARGSELCQTALSLHGR------
                    ..     *        . .   *

NP_001762.2     LLEGVPMRQAAVTSTSLTIKSVFTRSELKFSPQWSHHGKIVTCQLQDADGKFLSNDTVQL
NP_002352.1     LGHEGLGEPAVLGRLREDEGTWVQVSLLHFVPTREANGHRLGCQASFPNTTLQFEGYASM
NP_075556.1     QGQD-PARSVTFNSQKFEPTGVGHLETLHMAMSWQDHGRILRCQLSVANHRAQSEIHLQV
NP_998767.1     --------------FRLLGNPRRNDLSLRVERLALADDRRYFCRVEFAG-DVHDRYESRH
                          *:.     ..:   *: . ..    .

NP_001762.2     NVKHTPKLEIKVTPSDAIVREGDSVTMTCEVSSSNPEYTTVSWLKDGTSLKKQN------
NP_002352.1     DVKYPPVIVEMN--SSVEAIEGSHVSLLCGADSNPPPLLTWMRDGTVLREAVAE------
NP_075556.1     KYAPKGVKILLS-PSGRNILPGELVTLTCQVNSSYPAVSSIKWLKDGVRLQTKTGVLHLP
NP_998767.1     GVRLHVTAAPRIVNISVLPSPAHAFRALCTAEGEPPPALAWSGPALGNSLAAVRS-----
                  .    . .  * .... *  :

NP_001762.2     ------------------------------------------------------------
NP_002352.1     ------------------------------------------------------------
NP_075556.1     QAAWSDAGVYTCQAENGVGSLVSPPISLHIFMAEVQVSPAGPILENQTVTLVCNTPNEAP
NP_998767.1     ------------------------------------------------------------


NP_001762.2     ------------------TFTLNLREVTKDQSGKYCCQVSNDVGPGRSEEVFLQVQYAPE
NP_002352.1     ------------------SLLLELEEVTPAEDGVYACLAENAYGQD-NRTVGLSVMYAPW
NP_075556.1     SDLRYSWYKNHVLLEDAHSHTLRLHLATRADTGFYFCEVQNVHGSERSGPVSVVVNHPPL
NP_998767.1     -------------PREGHGHLVTAELPALTHDGRYTCTAANSLG----------------
                        : . : . * * * . *  *

NP_001762.2     PSTVQILHSP-------------------------------------------------
NP_002352.1     KPTVNGTMV--------------------------------------------------
NP_075556.1     TPVLTAFLETQAGLVGILHCSVVSEPLATLVLSHGGHILASTSGDSDHSPRFSGTSGPNS
NP_998767.1     ------------------------------------------------------------


NP_001762.2     ----------------------------------------------AVEGSQVEFLCMS
NP_002352.1     ----------------------------------------------AVEGETVSILCST
NP_075556.1     LRLEIRDLEETDSGEYKCSATNSLGNATSTLDFHANAARLLISPAAEVVEGQAVTLSCRS
NP_998767.1     ------------------------------------------------------------


NP_001762.2     LANPLPTNYTWYHN---------------------------------------------
NP_002352.1     QSNPDPILTIFKEKQ--------------------------------------------
NP_075556.1     GLSPTPDARFSWYLNGALLHEGPGSSLLLPAASSTDAGSYHCRARDGHSASGPSSPAVLT
```

```
NP_998767.1    ------------------------------------------------------------

NP_001762.2    ------------------------------------------------------------
NP_002352.1    ------------------------------------------------------------
NP_075556.1    VLYPPRQPTFTTRLDLDAAGAGAGRRGLLLCRVDSDPPARLQLLHKDRVVATSLPSGGGC
NP_998767.1    ------------------------------------------------------------

NP_001762.2    ---------GKEMQGRTEEKVHIPKILPWHAGTYSCVAENILGTG---------------
NP_002352.1    --------ILSTVIYESELQLELPAVSPEDDGEYWCVAENQYG-----------------
NP_075556.1    STCGGCSPRMKVTKAPNLLRVEIHNPLLEEEGLYLCEASNALGNASTSATFNGQATVLAI
NP_998767.1    ------------------------------------------------------------

NP_001762.2    ------------------------------------------------------------
NP_002352.1    ------------------------------------------------------------
NP_075556.1    APSHTLQEGTEANLTCNVSREAAGSPANFSWFRNGVLWAQGPLETVTLLPVARTDAALYA
NP_998767.1    ------------------------------------------------------------

NP_001762.2    ---------QRGPGAELDVQYPPKK-----------------------------------
NP_002352.1    ---------QRATAFNLSVEFAP-------------------------------------
NP_075556.1    CRILTEAGAQLSTPVLLSVLYPPDRPKLSALLDMGQGHMALFICTVDSRPLALLALFHGE
NP_998767.1    ------------------------------------------------------------

NP_001762.2    ------------------------------------------------------------
NP_002352.1    ------------------------------------------------------------
NP_075556.1    HLLATSLGPQVPSHGRFQAKAEANSLKLEVRELGLGDSGSYRCEATNVLGSSNTSLFFQV
NP_998767.1    ------------------------------------------------------------

NP_001762.2    --VTTVIQNPMPIREGDTVTLSCNYNSSNPSVTRYEWKPHGAWEEPSLGVLKIQNVGWDN
NP_002352.1    ----VLLLESHCAAARDTVQCLCVVKS-NP-------EPSVAFELPSRNVTVNE------
NP_075556.1    RGAWVQVSPSPELQEGQAVVLSCQVHTGVPEGTSYRWYRDGQPLQESTSATLRFAAITLT
NP_998767.1    ------------------------------------------------------------

NP_001762.2    TTIACAACNSWCSWASPVALNVQYAPRDVRVRKIKPLSEIHSGNSVSLQCDFSSSHPKEV
NP_002352.1    ------------------------------------------------------SER
NP_075556.1    QAGAYHCQAQAPGSATTSLAAPISLHVSYAPRHVTLTTLMDTGPGRLGLLLCRVDSDPPA
NP_998767.1    ------------------------------------------------------------

NP_001762.2    QFFWEKNGRLLGKESQ----------------------LNFDSISPEDAGSYSCWVNNSI
NP_002352.1    EFVYS---------------------------------------ERSGLVLTSILTLR
NP_075556.1    QLRLLHGDRLVASTLQGVGGPEGSSPRLHVAVAPNTLRLEIHGAMLEDEGVYICEASNTL
NP_998767.1    ------------------------------------------------------------

NP_001762.2    GQTASKAWTLEVLYAPRRLR-------------------------------------
NP_002352.1    GQAQAPPRVICTARN-------------------------------------------
NP_075556.1    GQASASADFDAQAVNVQVWPGATVREGQLVNLTCLVWTTHPAQLTYTWYQDGQQRLDAHS
NP_998767.1    ------------------------------------------------------------

NP_001762.2    ------------------------------------------------------------
NP_002352.1    ------------------------------------------------------------
NP_075556.1    IPLPNVTVRDATSYRCGVGPPGRAPRLSRPITLDVLYAPRNLRLTYLLESHGGQLALVLC
NP_998767.1    ------------------------------------------------------------

NP_001762.2    ------------------------------------------------------------
NP_002352.1    ------------------------------------------------------------
NP_075556.1    TVDSRPPAQLALSHAGRLLASSTAASVPNTLRLELRGPQPRDEGFYSCSARSPLGQANTS
NP_998767.1    ------------------------------------------------------------
```

```
NP_001762.2     ---------VSMSPGDQVMEGKSATLTCESDANPPVSHYTWFDWNNQSLPYHSQKLRLEP
NP_002352.1     ----------------------------------------------LYGAKSLELP
NP_075556.1     LELRLEGVRVILAPEAAVPEGAPITVTCADPAAHAPTLYTWYHNGRWLQEGPAASLSFLV
NP_998767.1     ------------------------------------------------------------


NP_001762.2     VKVQHSGAYWCQGTNSVGKGRSPLSTLTVYYSPETIGRRVA-------------------
NP_002352.1     FQGAHRLMWAKIGP-----------------------------------------------
NP_075556.1     ATRAHAGAYSCQAQDAQGTRSSRPAALQVLYAPQDAVLSSFRDSRARSMAVIQCTVDSEP
NP_998767.1     ------------------------------------------------------------


NP_001762.2     --------------------------VGLGSCLAILILAICGLKLQRRWKRTQSQQGLQE
NP_002352.1     --------------------------VGAVVAFAILIAIVCYITQTRRKKNVTESPSFSA
NP_075556.1     PAELALSHDGKVLATSSGVHSLASGTGHVQVARNALRLQVQDVPAGDDTYVCTAQNLLGS
NP_998767.1     ----------------------------RSEASVYLFRFHGASGASTVALLLGALGFKA
                                       .              :

NP_001762.2     NSSGQSFFVRNKKVRRAPLSEGPHSLGCYNPMMEDGIS----------------------
NP_002352.1     GDNPPVLFSSDFRISGAPEK--------YESERRLGSE----------------------
NP_075556.1     ISTIGRLQVEGARVVAEPGLDVPEGAALNLSCRLLGGPGPVGNSTFAWFWNDRRLHAEPV
NP_998767.1     LLLLGVLAARAARR-----------------------------------------------
                :    :

NP_001762.2     ---------------YTTLRFPEMNIPRTGDAESSEMQRPPPDCDDTVTYSALHKRQVGD
NP_002352.1     ---------------RRLLG----------------LRGEPPELDLSYSHSDLGKRPTKD
NP_075556.1     PTLAFTHVARAQAGMYHCLAELPTGAAASAPVMLRVLYPPKTPTMMVFVEPEGGLRGILD
NP_998767.1     ------------------------------------RPEHLDTPDTPPRSQAQESNYEN
                                           .      :

NP_001762.2     YENVIPDFPEDEGIHYSELIQFGVGERPQAQENVDYVILKH--------------------
NP_002352.1     SYTLTEELAEYAEIRVK----------------------------------------------
NP_075556.1     CRVDSEPLASLTLHLGSRLVASSQPQGAPAEPHIHVLASPNALRVDIEALRPSDQGEYIC
NP_998767.1     LSQMNPRSPPATMCSP-----------------------------------------------
                .

NP_001762.2     ------------------------------------------------------------
NP_002352.1     ------------------------------------------------------------
NP_075556.1     SASNVLGSASTSTYFGVRALHRLHQFQQLLWVLGLLVGLLLLLLGLGACYTWRRRRVCKQ
NP_998767.1     ------------------------------------------------------------


NP_001762.2     -----------------------------------
NP_002352.1     -----------------------------------
NP_075556.1     SMGENSVEMAFQKETTQLIDPDAATCETSTCAPPLG
NP_998767.1     -----------------------------------
```

Appendix 2 - Patient information of IHC staining cores for ST6GalNAc1 and ST6GalNAc2 staining.

Position	No.	Age	Sex	Organ/Anatomic Site	Pathology diagnosis	TNM	Grade	Stage	Type
A1	1	32	F	Colon	Adenocarcinoma	T3N0M0	1		Malignant
A2	2	32	F	Colon	Cancer adjacent colon tissue (chronic inflammation of mucous membrane)	-	-		AT
A3	3	32	F	Colon	Adjacent normal colon tissue (chronic inflammation of mucous membrane)	-	-		NAT
A4	4	42	M	Colon	Adenocarcinoma	T3N1M0	1		Malignant
A5	5	42	M	Colon	Cancer adjacent colon tissue (chronic inflammation of mucous membrane)	-	-		AT
A6	6	42	M	Colon	Adjacent normal colon tissue (chronic inflammation of mucous membrane)	-	-		NAT
A7	7	55	F	Colon	Mucinous adenocarcinoma	T3N1M0	1		Malignant
A8	8	55	F	Colon	Cancer adjacent colon tissue (chronic inflammation of mucous membrane)	-	-		AT
A9	9	55	F	Colon	Adjacent normal colon tissue (chronic inflammation of mucous membrane)	-	-		NAT
B1	10	50	M	Colon	Adenocarcinoma	T3N0M0	1		Malignant
B2	11	50	M	Colon	Cancer adjacent colon tissue	-	-		AT
B3	12	50	M	Colon	Adjacent normal colon tissue	-	-		NAT
B4	13	68	F	Colon	Adenocarcinoma	T4N2M0	1		Malignant
B5	14	68	F	Colon	Cancer adjacent colon tissue	-	-		AT
B6	15	68	F	Colon	Adjacent normal colon tissue	-	-		NAT
B7	16	62	M	Colon	Adenocarcinoma	T4N0M0	1--2		Malignant
B8	17	62	M	Colon	Cancer adjacent colon tissue	-	-		AT
B9	18	62	M	Colon	Adjacent normal colon tissue	-	-		NAT
C1	19	62	F	Colon	Adenocarcinoma	T4N1M0	1--2		Malignant
C2	20	62	F	Colon	Cancer adjacent colon tissue	-	-		AT
C3	21	62	F	Colon	Adjacent normal colon tissue	-	-		NAT

C4	22	59	F	Colon	Adenocarcinoma	T3N1M0	2	Malignant
C5	23	59	F	Colon	Cancer adjacent colon tissue	-	-	AT
C6	24	59	F	Colon	Adjacent normal colon tissue	-	-	NAT
C7	25	46	F	Colon	Mucinous adenocarcinoma	T3N0M0	2	Malignant
C8	26	46	F	Colon	Cancer adjacent colon tissue (chronic inflammation of mucous membrane)	-	-	AT
C9	27	46	F	Colon	Adjacent normal colon tissue (chronic inflammation of mucous membrane)	-	-	NAT
D1	28	52	F	Colon	Adenocarcinoma	T3N1M0	2	Malignant
D2	29	52	F	Colon	Cancer adjacent colon tissue	-	-	AT
D3	30	52	F	Colon	Adjacent normal colon tissue (chronic inflammation of mucous membrane)	-	-	NAT
D4	31	33	F	Colon	Adenocarcinoma	T4N1M0	2	Malignant
D5	32	33	F	Colon	Cancer adjacent colon tissue (chronic inflammation of mucous membrane)	-	-	AT
D6	33	33	F	Colon	Adjacent normal colon tissue (chronic inflammation of mucous membrane)	-	-	NAT
D7	34	61	M	Colon	Adenocarcinoma	T4N0M0	1	Malignant
D8	35	61	M	Colon	Cancer adjacent colon tissue	-	-	AT
D9	36	61	M	Colon	Adjacent normal colon tissue	-	-	NAT
E1	37	67	M	Colon	Adenocarcinoma	T3N1M0	2	Malignant
E2	38	67	M	Colon	Cancer adjacent colon tissue (chronic inflammation of mucous membrane)	-	-	AT
E3	39	67	M	Colon	Adjacent normal colon tissue (chronic inflammation of mucous membrane)	-	-	NAT
E4	40	53	F	Colon	Adenocarcinoma	T3N0M0	-	Malignant
E5	41	53	F	Colon	Cancer adjacent colon tissue (chronic inflammation of mucous membrane)	-	-	AT
E6	42	53	F	Colon	Adjacent normal colon tissue	-	-	NAT
E7	43	53	F	Colon	Adenocarcinoma	T3N0M0	3	Malignant
E8	44	53	F	Colon	Cancer adjacent colon tissue	-	-	AT

E9	45	53	F	Colon	Adjacent normal colon tissue	-	-	NAT
F1	46	34	F	Colon	Adenocarcinoma	T2N0M0	2	Malignant
F2	47	34	F	Colon	Cancer adjacent colon tissue (chronic inflammation of mucous membrane)	-	-	AT
F3	48	34	F	Colon	Adjacent normal colon tissue	-	-	NAT
F4	49	74	F	Colon	Adenocarcinoma	T3N1M0	3	Malignant
F5	50	74	F	Colon	Cancer adjacent colon tissue	-	-	AT
F6	51	74	F	Colon	Adjacent normal colon tissue	-	-	NAT
F7	52	52	F	Colon	Adenocarcinoma	T3N1M0	3	Malignant
F8	53	52	F	Colon	Cancer adjacent colon tissue (chronic inflammation of mucous membrane)	-	-	AT
F9	54	52	F	Colon	Adjacent normal colon tissue (chronic inflammation of mucous membrane)	-	-	NAT

Appendix 3 - List of attended Researcher Development Programme sessions and continuous professional development

3.1 Development programmes:

2021:

- Getting published and promoting your research
- How to stop procrastination
- Thriving resiliently
- Maximise your memory
- Developing your impact plan

2022:

- Literature review
- Overcoming the challenges of research
- How to cope with stress
- Public speaking for PGR's and academics
- Social media bootcamp
- Thesis writing
- How to write a scientific paper
- How to Write and Publish a Paper
- Writing for Publication in Scientific Journals
- Quantitative Data Analysis 1: Hypothesis Testing, Sample Size & Power
- Quantitative Data Analysis 2: Correlation & Regression Methods
- Getting to Know R
- Data Analysis in R
- Getting Started with Statistics
- Writing for and submitting to a journal
- Public speaking for PGR's and academics
- Registration and Doctoral Review Assessment
- RDP Summer school programme

2023:

- A Guide to Applying for External Research Funding for New Researchers
- Research Ethics
- The Viva and Process of Research Degree Examination
- A Guide to Applying for External Research Funding for New Researchers
- Build a Research Website in Under 3 hours
- CVs, Application Forms and Personal Statements
- Advanced Excel for Data Management and Analysis
- Attracting Funding: Writing & Applying for Fellowships
- Grant Writing Workshop for PhD and MSc by Research Students
- How to Write a Scientific Paper (and Get it Published)

3.2 Seminars/Workshops:

- Patient and Public Involvement (PPI) workshops – 23rd March 2023, 12th April 2023, 10th May 2023

3.3 Attended Conferences/Webinars:

- SIALOGLYCO 2024 Research Conference, Lille, France – 4th-7th June 2024
- UH LMS Annual Research Conference, Hatfield, UK – 11th June 2024
- Berlin Early Cancer Forum, Berlin, Germany – 21st-22nd November 2023
- UH LMS Annual Research Conference, Hatfield, UK – 13th June 2023
- PGR Student Conference – Sustainability and Research, Hatfield, UK – 9th June 2023
- Illumina Webinar: Empower your Research with RNA sequencing (online) – 23rd May 2023
- 17th RNA Microsymposium, Vienna, Austria – 3rd-5th May 2023
- 7th Annual Next-Gen Immuno-Oncology Conference, London, UK – 9th-10th March 2023
- The Festival of Genomics & Biodata, London, UK – 25th-26th January 2023
- 4th Annual Biomarker and Companion Diagnostics Conference, London, UK – 6th-7th October 2022
- The RNA Isoform Landscape of Cancer (online) – 20th July 2022
- UH LMS Research Conference, Hatfield, UK – 21st June 2022
- Cell Symposium: Translational Immunometabolism, Basel, Switzerland – 19th March 2022

Appendix 4 – List of Publications

4.1 Peer reviewed journal publications

Ahmad, M.S., Braoudaki, M., Siddiqui, S.S**. (2024).** Differential expression of ST6GALNAC1 and ST6GALNAC2 and their clinical relevance to colorectal cancer progression. *PLOS ONE*.

Mustafov, D*., **Ahmad, M***., Serrano, A., Braoudaki, B., Siddiqui, S.S. **(2024)**. MicroRNA:Siglec crosstalk in cancer progression. *Current Opinion in Chemical Biology*. https://doi.org/10.1016/j.cbpa.2024.102502 (*shared first author).

Ahmad M.S, Braoudaki M, Patel H, Ahmad I, Shagufta, Siddiqui SS. **(2023)**. Novel Siglec-15-Sia axis inhibitor leads to colorectal cancer cell death by targeting miR-6715b-3p and oncogenes. *Frontiers in Immunology*. 2023;14: 1254911. doi:10.3389/fimmu.2023.1254911

Braoudaki, M., **Ahmad, M. S**., Mustafov, D., Seriah, S., Siddiqui, M. N., & Siddiqui, S. S. **(2022)**. Chemokines and chemokine receptors in colorectal cancer; multifarious roles and clinical impact. *Seminars in cancer biology*, 86 (Pt 2), 436–449.https://doi.org/10.1016/j.semcancer.2022.06.002

4.2 Journal papers in press

Ahmad, M.S., Braoudaki, M., Candil-Barrado, A., Siddiqui, S.S. **(2024)**. Deciphering the role of aleplasinin as a viable small molecule inhibitor of Siglec-15 in colorectal cancer progression. *Life Sciences.*

4.3 Book chapters

Ahmad, M.S., Seriah, S., Siddiqui, S.S. **(2024)**. Impact of the Siglec-Sialoglycan Axis on the Cancer Immune Response. *Springer Nature.* DOI:https://doi.org/10.1007/16833_2024_272

Appendix 5 - List of abstracts, poster presentations and oral talks

5.1 List of abstracts

Ahmad M.S; Braoudaki M.; Siddiqui S.S. Characterisation of aleplasinin as a small molecule inhibitor targeting Siglec-15 in colorectal cancer – UH LMS conference, Hatfield, UK, April 2024

Ahmad M.S; Braoudaki M.; Siddiqui S.S. Repurposing of aleplasinin as a small molecule inhibitor targeting Siglec-15 in colorectal cancer – Sialoglyco 2024 Research Conference, Lille, France, June 2024

Ahmad M.S, Braoudaki M, Patel H, Ahmad I, Shagufta, Siddiqui S.S Novel Siglec-15-Sialoglycan axis inhibitor leads to colorectal cancer cell death targeting multiple oncogenic pathways - Early Cancer Forum Berlin, Germany, November 2023.

Ahmad M.S., Braoudaki M., Siddiqui S.S. New β-amino ketone compound regulates cell death in vitro and upregulates miR-6715b-3p in colon cancer cells. – 17th Microsymposium on RNA Biology, Vienna, Austria May 2023.

Ahmad M.S; Braoudaki M., Patel H., Siddiqui S.S.; Supervisor: Dr Shoib Siddiqui. Small molecule inhibitor regulates cell death through the Siglec15/Sia and miR-6715b-3p/PTTG1IP axes in colon cancer cells – UH LMS conference, Hatfield, UK, April 2023

Ahmad M.S., Lione., L., Braoudaki M., Siddiqui S.S. MiR-203a-3p and miR-512-3p mimic mediated cancer immunotherapy against Siglec-15; clinical implications in

colorectal cancer progression – UH LMS conference, Hatfield, UK, April 2022

5.2 Poster presentations

June 2024 **Ahmad M.S.,** Braoudaki M., Siddiqui S.S. Validation of aleplasinin as a small molecule inhibitor targeting Siglec15 *in vitro* – UH LMS conference, Hatfield, UK

June 2024 Candil-Barrado, A.; Diz. C., Madejón, C., **Ahmad M.S**; García-Cela, E., Siddiqui S.S. Exploring the toxicological implications of Ochratoxin α on human colorectal cancer cell line – UH LMS conference, Hatfield, UK

June 2024 **Ahmad M.S;** Braoudaki M.; Siddiqui S.S. Repurposing of aleplasinin as a small molecule inhibitor targeting Siglec-15 in colorectal cancer – Sialoglyco 2024 conference, Lille, France

June 2023 **Ahmad, M.S.,** Waseem, S., Ahmad, I., Braoudaki, M., Siddiqui, S.S. Small molecule inhibitor regulates cell death and upregulates miR-6715b-3p in colon cancer cells – 17th Microsymposium on RNA Biology, Vienna, Austria

April 2023 **Ahmad, M.S.,** Waseem, S., Ahmad, I., Braoudaki, M., Siddiqui, S.S. Small molecule inhibitor synthesised with sustainable method regulates cytotoxicity in colon cancer cells– UH LMS conference, Hatfield, UK

June 2022 Ahmad M.S., Lione., L., Braoudaki M., Siddiqui S.S. MiR-203a-3p and miR-512-3p mimic mediated cancer immunotherapy against Siglec-15; clinical implications in

colorectal cancer progression – UH LMS conference, Hatfield, UK

5.3 Oral presentations

June 2024 **Ahmad, M.S.** "Repurposing of aleplasinin as a small molecule inhibitor targeting Siglec-15 in Colorectal cancer" – Sialoglyco 2024 Poster talk Lille, France

November 2023 **Ahmad, M.S.** "Novel Siglec-15-Sialoglycan axis inhibitor leads to colorectal cancer cell death targeting multiple oncogenic pathways" **-** Early Cancer Forum Berlin, Germany

Appendix 6 – List of grant funding, awards and nominations

May 2024	**School of Life and Medical Sciences Dean's awards nomination**
June 2023	**3 min thesis competition winner at the University of Hertfordshire**
April 2023	**Funding support for conference attendance from the UH doctoral college**
April 2022	**Funding support for conference attendance from the UH doctoral college**

Available online at www.sciencedirect.com

ScienceDirect

Current Opinion in Chemical Biology

MicroRNA:Siglec crosstalk in cancer progression

D. Mustafov[1,2,a], M. S. Ahmad[1,a], A. Serrano[3], M. Braoudaki[1,b] and S. S. Siddiqui[1,b]

Abstract

Aberrant Siglec expression in the tumour microenvironment has been implicated in tumour malignancies and can impact tumour behaviour and patient survival. Further to this, engagement with sialoglycans induces masked antigen recognition and promotes immune evasion, highlighting deregulated immune function. This necessitates the elucidation of their expression profiles in tumour progression. MicroRNAs (miRNAs) mediated targeting represents a novel approach to further elucidate Siglec potential and clinical relevance. Although miRNA activity in Siglec expression remains limited, we highlight current literature detailing miRNA:Siglec interactions within the tumour landscape and provide insights for possible diagnostic and therapeutic strategies in targeting the Siglec/sialic acid axis.

Addresses

[1] School of Life and Medical Sciences, University of Hertfordshire, Hatfield, AL10 9AB, UK

[2] College of Health, Medicine and Life Sciences, Brunel University London, Uxbridge UB8 3PH, UK

[3] Francisco de Vitoria University, Ctra. M-515 Pozuelo-Majadahonda, Km. 1,800, Pozuelo de Alarcón, 28223, Madrid, Spain

Corresponding authors: Siddiqui, Shoib Sarwar (s.siddiqui3@herts.ac.uk); Braoudaki, Maria (m.braoudaki@herts.ac.uk)

(Serrano A.)

[a] Equal contribution.[b] Equal contribution and shared Correspondence.

Current Opinion in Chemical Biology 2024, **81**:102502

This review comes from a themed issue on **Glycobiology (2024)**

Edited by **Peng Wu** and **Mia Huang**

For complete overview of the section, please refer the article collection - Glycobiology (2024)

Available online 18 July 2024

https://doi.org/10.1016/j.cbpa.2024.102502

General overview

Human cells express a great variety of receptors and ligands on their membranes that enable optimal homeostasis and intact cellular processes. The aberrant expression of membrane glycolipids and glycoproteins in addition to the unique distribution of surface molecules, including sialic acid (Sia)-containing glycoconjugates, have attracted research attention due to their involvement in various pathologies including cancer [1]. The acquisition of further scientific findings and knowledge needs to be elucidated to fully understand their comprehensive functions and implications in health and pathogenesis.

Under normal homeostatic conditions, glycans exhibit multiple functions, such as enabling communication with both neighbouring cells and the immune system. In the tumour landscape, the role of sialic acid–binding immunoglobulin-type lectins (Siglecs) disrupts normal immune signalling, thus promoting tumour progression [2]. This review provides an opinion regarding recently studied miRNA-Siglec interactions and their effects on tumour progression.

Siglec structure, function, and ligand interaction

To date, a total of 15 human and 9 murine Siglec proteins have been identified and are classified into distinct groups based on sequence homology and domain conservation [3]. The groups that share high sequence and functional homology are outlined as Sialoadhesin (Siglec-1), cluster of differentiation 22 (CD22 or Siglec-2), myelin-associated glycoprotein (MAG or Siglec-4), and Siglec-15 with approximately 50%–80% similarity. In contrast, the remaining Siglec family members are characterised by lower sequence similarity (25–30%), due to structural heterogeneity related to less conserved Ig-domain-encoding due to rapid evolutionary events [4].

Siglecs are type-I transmembrane proteins consisting of several structural domains. Each Siglec possesses a variable number of C2-type domains and an N-terminal V–set binding domain located on the extracellular region, essential for sialoglycan binding [5]. Moreover, each Siglec has preferential complementarity towards respective sialoglycan ligands, such as those exhibiting α2,8-, α2,6- or α2,3 glycosidic linkages [6,7]. The intracellular constituent motifs displayed can be either immunoreceptor tyrosine-based inhibition or activation motifs (ITIM and ITAM, respectively) and define the overall functionality of the Siglec receptor in relation to immune function [8]. Upon sialoglycan engagement, activating Siglec signalling occurs via the recruitment and interaction with the adapter protein DNAX-activation protein 12 (DAP12). In comparison to their ITIM inhibitory Siglec counterparts, canonical downstream signalling is determined via the recruitment of

Src tyrosine phosphatases SHP1 and SHP2, reducing immune activation [9].

Siglec role in cancer

Aberrant expression of Siglecs and the overall Siglec/Sia axis are implicated in tumour onset and progression, displaying increased receptor–ligand interactions that pose detrimental effects on immune signalling [10]. Immune cells express Siglecs to interact with surface-exposed sialoglycans. This interaction triggers inhibitory signalling, hindering the detection and elimination of tumour cells via effective immune response generation [11]. Further to this, tumour cells highly express sialoglycans to induce Siglec engagement to evade immune surveillance, posing as a unique driver that emphasises enhanced binding and masked antigen recognition, preventing immune cell activation [11]. For instance, Siglec-15 expression is exhibited on the surface of tumours cells and TAMs. Upon binding with the STn antigen, Siglec-15 plays a role in immune modulation and the development of a heterogeneous TME [12]. Furthermore, Siglec-7/-9 activity modulates the activation of NK cell mediated cytotoxicity. Sialoglycan engagement with these inhibitory Siglecs stimulates downstream immunosuppressive signalling that down-regulates NK cell activation. Moreover, this interaction diminishes NK cells' ability to effectively release cytotoxic granules and IFN-γ, reducing the anti-tumour response [13]. Additionally, Siglec-10/CD24 activity facilitate monocytic differentiation to pro-tumorigenic polarised macrophage and enhances tumour growth and metastasis through the release of IL-10 and TGF-β [14].

Dysregulation of sialylation expression patterns and glycosylation post-translational modifications are typically associated with cancer hallmarks. These changes include erroneous branching of N-glycans, incomplete O-glycan sequences, truncation and hypersialylation resulting from the deregulation of sialyltransferase and neuraminidase activity [15]. As a result, modified sialoglycan production increases Siglec engagement on tumour cell membranes, leading to immune evasion, increased tumour growth and metastasis [16].

In addition to this, Siglecs exhibit distinct expression profiles across several myeloid cell populations, thus playing a key role in immune regulation. In particular, Siglec activity promotes tumour microenvironment (TME) development, including polarization of monocytic differentiation to pro-tumorigenic polarised macrophage phenotype or the altered cytotoxic functionality and activation of immune cells [12].

Mutually exclusive expression of Siglec-15 and PD-L1 on cancer populations underscores Siglec-15 targeting in PD-L1 negative patients. Encouraging patient response with a Siglec-15 monoclonal antibody (NC318) was shown in PD-L1 treatment resistant patients, leading to possible combination therapeutic strategies [17]. Furthermore, a humanised monoclonal antibody (Epratzumab) was shown to have a positive response in CD22 targeting and was well tolerated in non-Hodgkin's lymphoma patients in early phase I/II clinical trials [18]. Pre-clinical models also highlight potential implications of Siglec expression patterns in tumour progression. Blocking the Siglec-10/CD24 axis via a CD24-Fc vaccine emphasised reduced immune related adverse events in neuroblastoma murine models [19]. Similarly, CAR-T therapies targeting CD22 in B cell malignancies have shown promising patient response, having been investigated in pre-clinical and clinical trials, following patient relapses with CD19 CAR-T therapies [20].

Overall, the alteration of the homeostatic balance between Siglec/Sia engagement has been demonstrated to lead to an immunosuppressive TME, which corresponds to an increasingly described feature in cancer [21]. However, there is a need for further elucidation of their gene expression regulation in tumour progression. One such instance involves miRNA mediated Siglec regulation in cancer. Although the context of Siglec:miRNA interactions remains limited in the literature, there is a correlation linking deregulated Siglec expression patterns and miRNA activity on advanced tumour stage and tumour type. A previous study exhibited LINC00973 acting as a molecular sponge of miR-7109, preventing its binding to *SIGLEC15*. In addition, their interactions were associated with advanced tumour grades in clear cell renal cell carcinoma (ccRCC) and modulated *SIGLEC15* expression at the transcriptional level [22]. Similarly, overexpression of miR-494 in CD33 MDSCs constituted to greater tumour heterogeneity and significantly correlated with advanced tumour stage and histological grade [23]. Thus, this could outline the development of new miRNA-based therapeutic approaches targeting the Siglec/Sia axis in immunotherapy (Figure 1).

MicroRNA biogenesis and function

MicroRNAs (miRNAs) are small, non-coding single-stranded RNA molecules that regulate gene expression [24,25]. MiRNAs have been related to many biological processes, such as embryonal development, human cancer, neurodegenerative and cardiovascular disorders, diabetes, and metabolic diseases [26–29]. Given their multifunctional biological relevance, miRNAs have gained significant importance as potential candidates for diagnostic and prognostic biomarkers and possible therapeutic agents [26]. Thus, it is important to understand how miRNAs are synthesized and how they can modulate gene expression. There are two pathways that define the biogenesis of miRNAs, namely the canonical and non-canonical pathways (Figure 2).

Figure 1

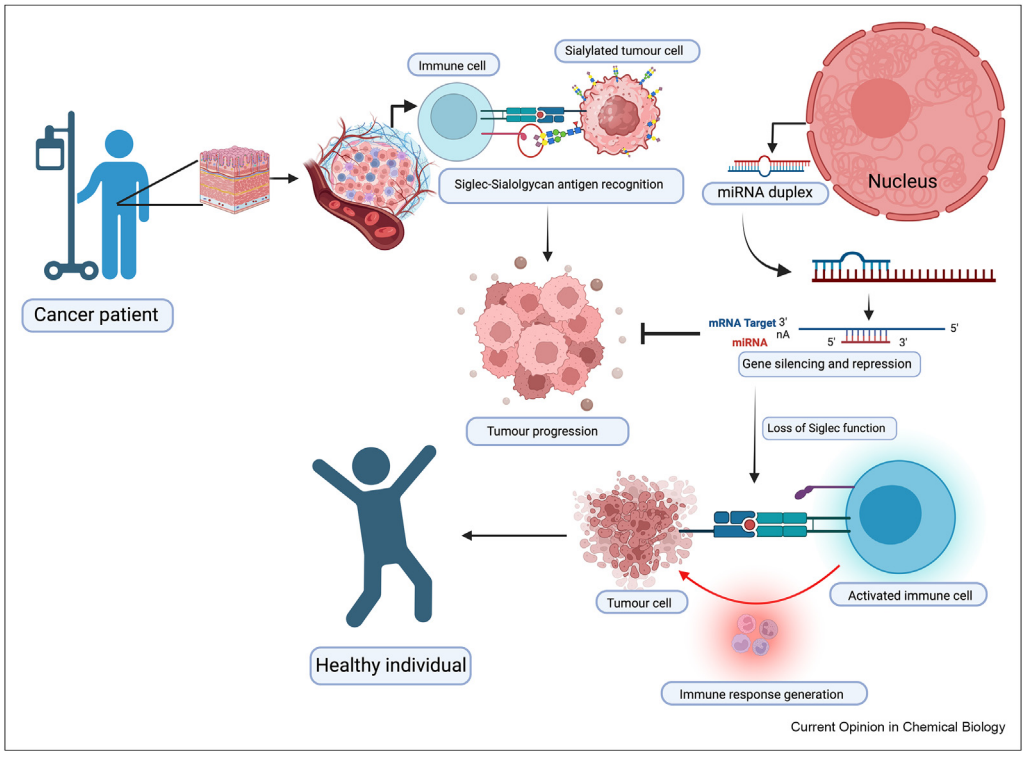

MicroRNA mediated Siglec regulation. Within the TME, Siglec-sialoglycan interactions mask antigen recognition on tumour cells, promoting tumour progression and metastasis. The involvement of microRNA on Siglec gene regulation has the potential to impact Siglec loss of function and revert the activation of the immune response against tumour cells. This figure was created with BioRender.com.

Canonical miRNA biogenesis

The canonical miRNA biogenesis is a multistep process that transforms primary miRNA transcripts (pri-miRNAs) into functional, mature single-stranded miRNAs that associate with Argonaute (Ago) proteins to form the Ago complex, which usually is referred to as the RNA-induced silencing complex (RISC) [30].

MiRNA synthesis begins within the nucleus, where RNA polymerase II transcribes a DNA sequence encoding a miRNA gene. This results in the formation of a long, 5′ capped, and 3′ polyadenylated pri-miRNA transcript characterised with a hairpin structure [31]. Within the nucleus, the pri-miRNA encounters the microprocessor complex, a trimer formed by one Drosha and two DiGeorge syndrome critical region gene 8 (DGCR8) molecules [32]. Drosha, an RNase III enzyme, recognizes and cleaves the pri-miRNA, releasing a shorter, hairpin-shaped RNA molecule called a precursor miRNA (pre-miRNA) [30]. Following Drosha-DGCR8 processing, the pre-miRNA is exported from the nucleus to the cytoplasm. This step is facilitated by the Exportin-5 (XPO5)/RanGTP complex. XPO5 interacts with pre-miRNA in a sequence-independent manner and in the presence of a GTP-binding nuclear protein Ran (RanGTP) [33].

Once in the cytoplasm, the pre-miRNA encounters the Dicer complex. Dicer, another RNase III enzyme, recognises the pre-miRNA and cleaves it at a defined position. This cleavage event generates a short, double-stranded miRNA duplex containing the mature miRNA and its passenger strand [34]. Once the miRNA duplex is formed, it is loaded into an Ago protein with the help of the Hsc70/Hsp90 chaperone machinery in an ATP dependent manner [35]. This miRNA duplex can be loaded into any of the four proteins of the Ago proteins, with preferential loading on the most abundant Ago2 paralog [36]. Upon Ago complex association, one miRNA duplex strand (mature guide miRNA) is retained, while the other (passenger strand) is discarded, forming a single-stranded RNA-induced silencing complex (RISC). Notably, both 5' (5p) and 3' (3p) derived miRNAs could exert functionality on target mRNAs [37].

The mature miRNA loaded onto the RISC complex is guided towards its complementary mRNA targets within the cytosol. Target recognition primarily relies on base-pairing interactions between the miRNA seed region (nucleotides 2–7/8 of the mature miRNA) and the complementary sequence within the mRNA 3′ untranslated region (UTR) [38]. This interaction leads to

Figure 2

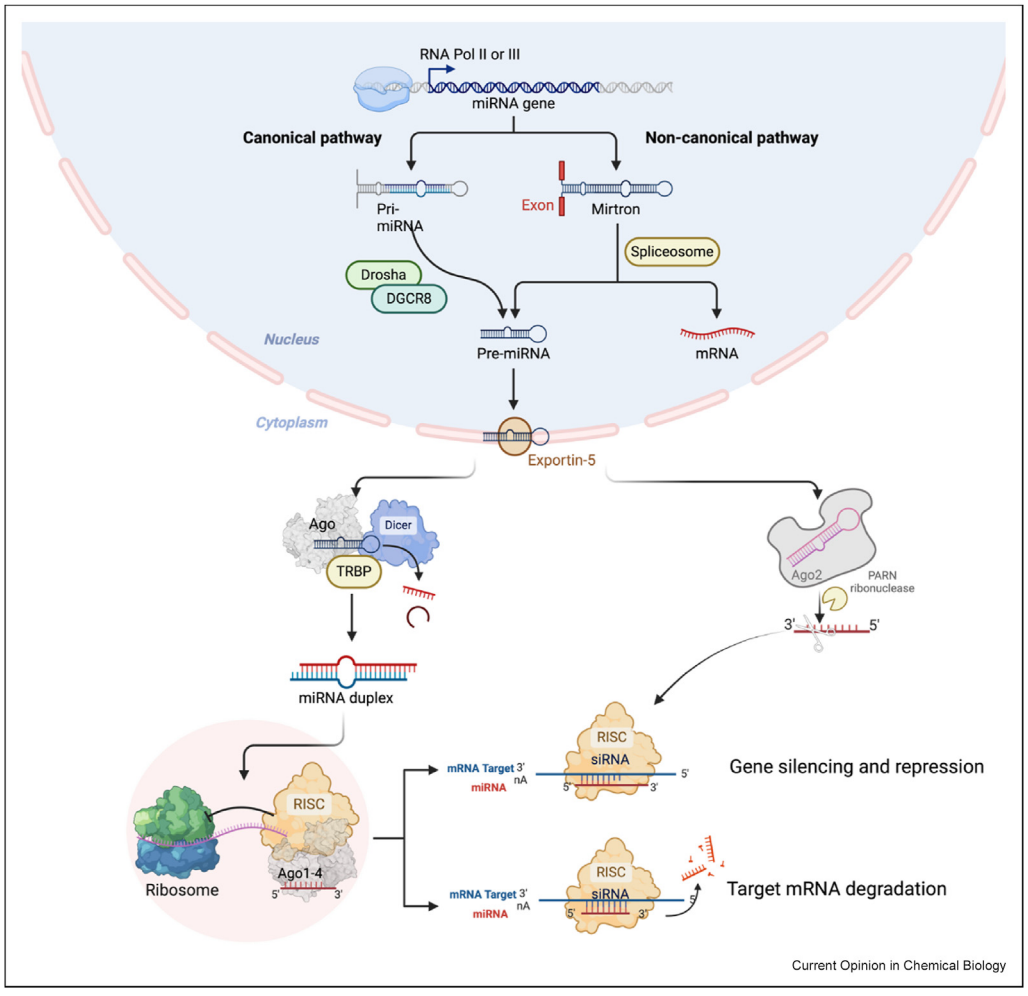

An overview of the canonical and non-canonical pathways of miRNA biogenesis. The canonical miRNA biosynthesis commences with the transcription of miRNA genes by RNA polymerase II or III, producing primary miRNA transcripts (pri-miRNA), which can be several hundred to thousands of nucleotides (nts) long and might contain more than one hairpin structure. In the nucleus, the pri-miRNA transcripts are recognised and cleaved by the Drosha enzyme (RNase III enzyme) and its co-factor, the Di-George Syndrome Critical Region 8 (DGCR8) enzyme. Once bound to each other, they form a microprocessor complex which recognises the RNA stem loop and cleaves pri-miRNA to form 65–70 nts long precursor-miRNA (pre-miRNA). The produced pre-miRNA is characterised by a two-nucleotide-long 3′ overhang, which is subsequently recognised by a transmembrane protein, exportin 5, which facilitates the export of the pre-miRNA to the cytoplasm, where its processing continues with the aid of Dicer. Dicer associates with the TAR-RNA binding protein (TRBP) cofactor forming the Dicer-TRBP, which is incorporated in the removal of the terminal loop of the pre-miRNA and thus the production of the mature double-stranded miRNA (dsRNA). The formed mature dsRNA is approximately 18–22 nts long and constitutes of a miRNA-guide strand and a miRNA-passenger strand (miRNA/miRNA* or miR-3p/miR-5p, respectively). The strand with a lower 5′-end stability, usually the guide strand, subsequently associates with an RNA-induced silencing complex (RISC), which contains Argonaute (AGO 1–4) proteins. The miRNA-RISC complex is then guided to a complementary mRNA sequence where it acts as a post-transcriptional regulator via inducing degradation or translational inhibition of the target mRNA. This translational silencing occurs at the 3′ untranslated region (UTR) region of the target mRNA. The non-canonical miRNA biosynthesis includes pathways such as mirtron (a non-coding RNA molecule derived from introns) processing, omitting the Drosha/DGCR8 microprocessor complex interaction and thus expanding the diversity of miRNA origins. This involves introns cleavage by spliceosomes or other debranching enzymes present in the nucleus, resulting in the exclusion of the pre-miRNA hairpin, thus making the pre-miRNA ready for nucleus export via exportin 5 and further processing by Dicer. Another non-canonical miRNA biogenesis mechanism aids the generation of miR-3p strands via omitting the Dicer cleavage. Instead, Ago2 and PARN ribonucleases remove the hairpin structure of the pre-miRNA and produce a miR-3p strand which can then act upon its mRNA targets. This figure was created with BioRender.com.

various modes of translational repression based on the complementarity binding between the miRNA:mRNA complex. During full complementarity binding, the RISC complex can directly cleave the target mRNA, leading to its full degradation. In contrast, partial complementarity induces a wider range of regulatory effects such as partial gene silencing and mRNA destabilisation (Figure 2) [39].

Non-canonical miRNA biogenesis

In brief, non-canonical biogenesis utilises the Drosha/DGCR8-independent and Dicer-independent pathways in pre-miRNA transcript production. Mirtrons and viral tRNA-like structures bypass the Drosha/DGCR8 microprocessor complex to generate the pre-miRNA transcript. Additionally, m7G-capped pre-miRNAs utilise a distinct export pathway and favour 3p-miRNA incorporation into the silencing complex (Figure 2) [40]. Meanwhile, the Dicer-independent pathway requires pre-miRNA cleavage supervised by Ago2, resulting in the formation of a mature miRNA strand. Further processing via 3′ trimming is mediated by the PARN ribonuclease enzyme, which can only generate functional miRNA-3p [41].

MiRNA–Siglec interaction network

MiRNA–Siglec interactions represent an exciting avenue for research in elucidating their therapeutic potential and clinical relevance across the tumour landscape (Table 1). This type of association has been recently reported in bladder cancer. The upregulation of *BACH1-IT2* and its consequential impact on Siglec-15 expression, orchestrated by miR-4786-5p, offers a compelling glimpse into the molecular intricacies underlying cancer development [42]. *BACH1-IT2* was seen to promote tumour progression by suppressing miR-4786, consequently increasing *SIGLEC15* expression on tumour cells facilitating greater immunosuppression and heterogenous TME.

Similarly, the involvement of miRNAs such as miR-582-5p and miR-7109 in the negative regulation of Siglec-15 expression in hepatocellular carcinoma (HCC) and ccRCC respectively, has been reported [22,43]. In HCC, the effect of sponging upon miR-582-5p by *TUG1* resulted in elevated *SIGLEC15* expression patterns, indicating enhanced immunosuppression within HCC cells and a greater number of inactivated T-cells [43]. Similarly, in ccRCC, the sponging of miR-7109 by LINC00973 prevented effective miRNA binding and regulation of the *SIGLEC15* gene. This prompted greater *SIGLEC15* expression and immunosuppression in the tumour cells [22]. These findings not only shed light on the molecular interactions between miRNAs and Siglecs in cancer progression but also hold promise for the identification of potential diagnostic and therapeutic biomarkers.

Ahmad et al. explored the interplay between Siglec-15 and miRNAs in colorectal cancer (CRC) progression. Utilisation of a small molecule inhibitor (SHG-8) was predicted to bind to the Siglec-15 protein via the ARG143 residue. Exposure to SHG-8 reduced tumour progression and stimulated cytokine production from differentiated macrophages. Therefore, this suggested a potential activation of immune cells for an effective immune response. Simultaneously, small RNA sequencing analysis demonstrated significant upregulation of miR-6715b-3p, potentially targeting *PTTG1IP*, a possible oncogene in CRC. This suggested a potential regulatory axis involving Siglec-15 inhibition and subsequent miRNA-driven oncogene suppression. Further investigation into this regulatory axis is necessitated to elucidate its clinical relevance to CRC progression. However, its therapeutic potential holds promise for novel CRC treatment strategies [44].

MiRNA–Siglec interactions can also act as a potential therapeutic avenue in acute myeloid leukaemia (AML). The interplay between miRNA-125b with the cell surface marker *CD33/SIGLEC3* is of growing interest. A study investigated the potential of red blood cell-derived extracellular vesicles (RBCEVs) for directed delivery of anti-FLT3-ITD and anti-miR-125b oligonucleotides in AML. CD33 conjugated antibody-coated RBCEVs allowing for $CD33^{+}$ specific targeting of AML cells were loaded with antisense oligonucleotides (ASOs) to inhibit FLT3-ITD or miR-125b. The observed results demonstrated that the engineered EVs reduced cellular viability and suppressed leukaemia progression *in vitro* and *in vivo* due to the significant increase in the uptake of RBCEVs. These results highlight the importance of miR-125b and its regulation of the *CD33* gene [45].

Another report suggested that miRNA-Siglec interactions have emerged as a valuable tool for cholangiocarcinoma (CCA) diagnosis and treatment [46]. MiR-3913-5p was identified as an independent prognostic factor for CCA, with lower expression correlating with poor survival outcomes. Further *in vitro* experiments validated the differential expression of miR-3913-5p in CCA, whereas computational target gene prediction analysis identified *RNF24* and *SIGLEC10* as potential downstream effectors of miR-3913-5p, warranting further investigation [46]. MiR-3913-5p was associated with the negative regulation of cell metabolism, thus promoting tumour growth. Conversely, *SIGLEC10* potentially influenced metastasis in CCA by altering cellular adhesion, whilst *RNF24* affected tumour cell proliferation. Furthermore, a computational approach highlighted miRNA involvement in *SIGLEC12* mediated tumorigenesis in kidney renal papillary cell carcinomas (KRCC). Deregulated expression of miR-133b/miR-654 and miR-574 was predicted to modulate *SIGLEC12* expression patterns. Moreover, data may suggest *Siglec-12*$^{+}$ KRCC tumours upon miRNA exertion exhibit greater sensitisation to immunotherapeutic checkpoint blockade [47]. Further investigations highlighting the synergistic therapeutic potentials of miR-319-5p and *SIGLEC10*, as well as the miR-133b/miR-654 and miR-574/Siglec-12 axis, are necessitated to validate their clinical relevance in CCA and KRCC onset, respectively. Emerging technologies such as small RNA-sequencing (sRNA-seq) and spatial

Table 1

miRNA involvement in Siglec regulation in cancer.

Siglec protein	Observed myeloid expression in situ	Cytoplasmic tail	Preferential Sialoglycan binding	miRNA involvement	Reference.
Siglec-1	Monocytes, Macrophages, Dendritic cells	ITIM	α2,3 linked sialoglycans	N/A	
Siglec-2	B-cells, Mast cells, Dendritic cells	ITIM	α2,6 linked sialoglycans	miR-17~92	[49]
Siglec-3	Monocytes, Macrophages, NK cells, Myeloid progenitor cells, Microglia	ITIM	α2,3 and α2,6 linked sialoglycans GD1a and GT1b gangliosides	miR-125b, miRNA-494	[23,45,50]
Siglec-4	Mast cells, Oligodendrocytes, Schwann cells	ITIM	α2,3 linked sialoglycans	N/A	
Siglec-5	Neutrophils, Mast cells, B-cells, Monocytes, Activated T-lymphocytes	ITIM	α2,3 linked sialoglycans	N/A	
Siglec-6	Mast cells, B-cells, Basophils	ITIM	α2,6 linked sialoglycans Leptin Glycodelin-A STn antigen	N/A	[51]
Siglec-7	NK cells, Monocytes, Mast cells	ITIM	α2,8 linked sialoglycans CD43 Gangliosides (GD3, GD2, GD1b, GT1b, DSGb5 Disialyl-T antigen	N/A	[52–54]
Siglec-8	Eosinophils, Mast cells, Basophils	ITIM	α2,3 linked sialoglycans	N/A	
Siglec-9	Monocytes, Neutrophils, NK cells	ITIM	α2,3, α2,6 linked sialoglycans	N/A	
Siglec-10	NK cells, B-cells, activated $CD4^+$ T-cells, Monocytes, Eosinophils	ITIM	α2,3, α2,6 linked sialoglycans	miR-561-5p	[55,56]
Siglec-11	Macrophages, Brain microglial cells	ITIM	α2,8 linked sialoglycans	N/A	
Siglec-14	Granulocytes, Monocytes	Interact with DAP-containing ITAM	α2,3 linked sialoglycans	N/A	
Siglec-15	Osteoclasts, TAMs	Interact with DAP-containing ITAM	Sialyl-Tn antigen CD11b α2,3, α2,6 linked sialoglycans	miR-6715b-3p, miR-4786, miR-582-5p, miR-7109	[6,22,42–44,57,58]
Siglec-16	Macrophages, Microglia	Interact with DAP-containing ITAM	α2,8 linked sialoglycans	N/A	

transcriptomics approaches have provided insights to our understanding of miRNA:Siglec interactions. Sequencing analysis in combination with a multiomics approach offered comprehensive insights into the complex regulatory networking involving miRNAs and Siglecs. These approaches identified regulatory pathways and characterisation of oncogenic targets that impact the Siglec/Sia axis and its interactions on tumour progression. The findings of Ahmad et al. suggested the interplay of miR-6715b-3p with *SIGLEC15* via *PTTG1IP* through the use of sRNA-seq analysis, which suggested a regulatory pathway associated with CRC progression [44]. Furthermore, Rodriguez et al. bulk tissue transcriptomics analysis revealed that the expression of Siglec-7/-9 both correlated with myeloid cell markers (TYROBP, FCER1G, C1QR and CD14) and co-expressed on $CD14^+$ myeloid cells in pancreatic ductal adenocarcinoma (PDAC), suggesting these sialylated tumour cells can play a part in controlling immune suppression and provide new targets for cancer immunotherapy [48].

Deregulated Siglec/miRNA networks may play a crucial role in reducing sensitisation to immunotherapeutic treatment. MiRNAs can modulate the expression of Siglec genes to inhibit T-cell activation and promote immunosuppression. It has been demonstrated that miRNAs could impact immune checkpoint inhibitor (ICI) efficacy. MiR-21, let-7a/b and miR-155 were shown to regulate the polarisation of tumorigenic macrophages [59–61]. In contrast, miR-28, miR-138 and miR-149 exhibited greater association for enhanced T-cell exhaustion [62–64]. This may suggest possible implications of miRNA activity in enhancing treatment resistance in cancer. Nevertheless, preclinical studies suggest a combination of miRNA-based therapies with ICIs could overcome resistance mechanisms and potentiate the treatment response to immune checkpoint blockade in cancer patients. The miRNA/Siglec network in initiating resistance to immunotherapy remains largely unexplored. However, further investigations on the Siglec/miRNA mediated interactions could provide potential avenues for the development of targeted immunotherapies that could effectively overcome resistance.

However, miRNA-mediated Siglec regulation is not solely limited to cancer. One study indicated upregulated sialoadhesin expression in chronic obstructive pulmonary disease (COPD) and presented miR-195-5p targeting sialoadhesin expression, possibly emphasising as a potential target in COPD treatment [65]. Similarly, an *in vivo* study demonstrated that miR-1260 blocking impeded sialoadhesin activity and inhibited the occurrence of inflammation in COPD murine models [66]. This highlights the interplay of miRNA-Siglec involvement having significant implications in patient health. The pathogenesis of Hirschsprung's disease (HSCR), a rare congenital disorder characterised by the absence of enteric neurons, has been linked to the interplay between miR-215 and its host gene, isoleucyl-tRNA synthetase 2 (*IARS2*), along with their target *SIGLEC8*. Expression analyses revealed that miR-215 levels were significantly lower in the colon tissues of HSCR patients, positively correlating with *IARS2* levels and negatively with *SIGLEC8* expression. These findings suggest that the *IARS2*/miR-215/*SIGLEC8* axis is a critical factor in the development of HSCR [67]. A recent study has demonstrated that in chronic hepatitis C virus (HCV), miR-124 expression was associated with STAT3 signalling promoting $CD33^+$ MDSC differentiation. They also suggested that the interaction between miR-124 and RUNX1 stimulated the release of immunosuppressive markers, such as iNOS and STAT3. Silencing these interactions prevented MDSC differentiation and enhanced $CD4^+$ T-cell activity, suggesting a possible therapeutic application in conjunction with antiviral treatment [68].

Elucidating miRNA:Siglec interactions present several challenges within the clinical setting. Firstly, the interactions involved between miRNA and Siglec activity are highly complicated, leading to the difficult identification of downstream therapeutic targets. Furthermore, tissue specific expression patterns of miRNAs and Siglecs pose challenges related to non-specific interactions and off-target effects. Moreover, delivery systems for miRNA-based therapeutics require further optimisation for efficient and efficacious delivery to the tumour site. In addition, variability in patient response and individual differences related to genetic polymorphisms and gene heterogeneity may influence the miRNA:Siglec interactive networks across patients. Addressing these possible challenges is crucial for elucidating the clinical relevance of miRNA:Siglec interactions to enable their transition to clinical settings.

Conclusion

The intricate interplay among Siglecs, miRNAs, and cancer progression unveils a compelling narrative within the domains of immunology and oncology research. Through meticulous investigations into various malignancies, scientists have illuminated the crucial role of miRNAs in modulating Siglec expression. This modulation significantly impacts tumour behaviour and patient prognosis. While these examples suggest miRNA-Siglec interactions can influence gene regulation, the field is still developing. In conclusion, continued exploration of these intricate molecular networks promises to unravel possible diagnostic and therapeutic avenues to enhance our understanding of cancer biology and immune regulation.

Funding

There is no funding associated with this work.

Declaration of competing interest

The authors declare that they have no known competing financial interests or personal relationships that could have appeared to influence the work reported in this paper.

Data availability

No data was used for the research described in the article.

Acknowledgements

We would like to thank Alejandro Candil-Barrado and Patricia Rodrigues for their contributions to this work.

References

Papers of particular interest, published within the period of review, have been highlighted as:

* of special interest
** of outstanding interest

1. Filipsky F, Läubli H: **Regulation of sialic acid metabolism in cancer**. *Carbohydr Res* 2024, **539**, 109123.
2. Jiang K-Y, Qi L-L, Kang F-B, Wang L: **The intriguing roles of Siglec family members in the tumor microenvironment**. *Biomark Res* 2022, **10**:22.
3. Stanczak MA, Läubli H: **Siglec receptors as new immune checkpoints in cancer**. *Mol Aspect Med* 2023, **90**, 101112.
4. Van De Wall S, Santegoets KCM, Van Houtum EJH, Büll C, Adema GJ: **Sialoglycans and Siglecs can shape the tumor immune microenvironment**. *Trends Immunol* 2020, **41**: 274–285.
5. Van Houtum EJH, Büll C, Cornelissen LAM, Adema GJ: **Siglec signaling in the tumor microenvironment**. *Front Immunol* 2021, **12**, 790317.
6. Lenza MP, Egia-Mendikute L, Antoñana-Vildosola A, Soares CO, Coelho H, Corzana F, Bosch A, Manisha P, Quintana JI, Oyenarte I, *et al.*: **Structural insights into Siglec-15 reveal glycosylation dependency for its interaction with T cells through integrin CD11b**. *Nat Commun* 2023, **14**:3496.
7. Zheng Y, Ma X, Su D, Zhang Y, Yu L, Jiang F, Zhou X, Feng Y, Ma F: **The roles of Siglec7 and Siglec9 on natural killer cells in virus infection and tumour progression**. *Journal of Immunology Research* 2020, **2020**:1–9.
8. Siddiqui SS: **Non-canonical roles of Siglecs: beyond sialic acid-binding and immune cell modulation**. *Mol Aspect Med* 2023, **90**, 101145.
9. Murugesan G, Weigle B, Crocker PR: **Siglec and anti-Siglec therapies**. *Curr Opin Chem Biol* 2021, **62**:34–42.
10. Läubli H, Nalle SC, Maslyar D: **Targeting the siglec–sialic acid immune Axis in cancer: current and future approaches**. *Cancer Immunol Res* 2022, **10**:1423–1432.
11. Zhou X, Chi K, Zhang C, Liu Q, Yang G: **Sialylation: a cloak for tumors to trick the immune system in the microenvironment**. *Biology* 2023, **12**:832.
12. Huang Z, Guo Y, Li B, Shen M, Yi Y, Li L, Zhao X, Yang L: **Siglec-15 on macrophages suppress the immune microenvironment in patients with PD-L1 negative non-metastasis lung adenocarcinoma**. *Cancer Gene Ther* 2023, https://doi.org/10.1038/s41417-023-00713-z.
13. Daly J, Sarkar S, Natoni A, Stark JC, Riley NM, Bertozzi CR, Carlsten M, O'Dwyer ME: **Targeting hypersialylation in multiple myeloma represents a novel approach to enhance NK cell–mediated tumor responses**. *Blood Advances* 2022, **6**: 3352–3366.
14. Barkal AA, Brewer RE, Markovic M, Kowarsky M, Barkal SA, Zaro BW, Krishnan V, Hatakeyama J, Dorigo O, Barkal LJ, *et al.*: **CD24 signalling through macrophage Siglec-10 is a target for cancer immunotherapy**. *Nature* 2019, **572**:392–396.
15. Munkley J: **Aberrant sialylation in cancer: therapeutic opportunities**. *Cancers* 2022, **14**:4248.
16. Stanczak MA, Siddiqui SS, Trefny MP, Thommen DS, Boligan KF, Von Gunten S, Tzankov A, Tietze L, Lardinois D, Heinzelmann-Schwarz V, *et al.*: **Self-associated molecular patterns mediate cancer immune evasion by engaging Siglecs on T cells**. *J Clin Invest* 2018, **128**:4912–4923.
17. Wang J, Sun J, Liu LN, Flies DB, Nie X, Toki M, Zhang J, Song C, Zarr M, Zhou X, *et al.*: **Siglec-15 as an immune suppressor and potential target for normalization cancer immunotherapy**. *Nat Med* 2019, **25**:656–666.
18. Lim J, Sari-Ak D, Bagga T: **Siglecs as therapeutic targets**. ***Cancer***. *Biology* 2021, **10**:1178.
19. Wu X, Srinivasan P, Basu M, Zimmerman T, Li S, Wang Y, Zheng P, Liu Y, Sandler AD: **CD24-Fc suppression of immune related adverse events in a therapeutic cancer vaccine model of murine neuroblastoma**. *Front Immunol* 2023, **14**, 1176370.
20. Adeel K, Fergusson NJ, Shorr R, Atkins H, Hay KA: **Efficacy and safety of CD22 chimeric antigen receptor (CAR) T cell therapy in patients with B cell malignancies: a protocol for a systematic review and meta-analysis**. *Syst Rev* 2021, **10**:35.
21. Läubli H, Kawanishi K, George Vazhappilly C, Matar R, Merheb M, Sarwar Siddiqui S: **Tools to study and target the Siglec–sialic acid axis in cancer**. *FEBS J* 2021, **288**: 6206–6225.
22. Liu Y, Li X, Zhang C, Zhang H, Huang Y: **LINC00973 is involved in cancer immune suppression through positive regulation of Siglec-15 in clear-cell renal cell carcinoma**. *Cancer Sci* 2020, **111**:3693–3704.
23. Moaaz M, Lotfy H, Elsherbini B, Motawea M, Fadali G: **TGF-β enhances the anti-inflammatory effect of tumor- infiltrating CD33+11b+HLA-DR myeloid-derived suppressor cells in gastric cancer: a possible relation to MicroRNA-494**. *Asian Pac J Cancer Prev APJCP* 2020, **21**:3393–3403.
24. Mustafov D, Siddiqui SS, Klena L, Karteris E, Braoudaki M: **SV2B/miR-34a/miR-128 axis as prognostic biomarker in glioblastoma multiforme**. *Sci Rep* 2024, **14**:6647.
25. Braoudaki M, Sarafidis M, Koutsouris DD, Koutsouri G, Lambrou GI: **Bioinformatics analysis reveals ki-67 specific microRNA functions in pediatric embryonal tumors**. In *2019 41st annual international conference of the IEEE engineering in medicine and biology society (EMBC)*. IEEE; 2019:1346–1349.
26. Ho PTB, Clark IM, Le LTT: **MicroRNA-based diagnosis and therapy**. *IJMS* 2022, **23**:7167.
27. Braoudaki M, Koutsouris D-D, Kouris I, Paidi A, Koutsouri G, Lambrou GI: **Bioinformatics and regression analyses manifest tumor-specific miRNA expression dynamics in pediatric embryonal malignancies**. In *2018 40th annual international conference of the IEEE engineering in medicine and biology society (EMBC)*. IEEE; 2018:5834–5837.
28. Lykoudi A, Kolialexi A, Lambrou GI, Braoudaki M, Siristatidis C, Papaioanou GK, Tzetis M, Mavrou A, Papantoniou N: **Dysregulated placental microRNAs in early and late onset preeclampsia**. *Placenta* 2018, **61**:24–32.
29. Ntoumou E, Tzetis M, Braoudaki M, Lambrou G, Poulou M, Malizos K, Stefanou N, Anastasopoulou L, Tsezou A: **Serum microRNA array analysis identifies miR-140-3p, miR-33b-3p and miR-671-3p as potential osteoarthritis biomarkers involved in metabolic processes**. *Clin Epigenet* 2017, **9**:127.
30. Shang R, Lee S, Senavirathne G, Lai EC: **microRNAs in action: biogenesis, function and regulation**. *Nat Rev Genet* 2023, **24**: 816–833.
31. Bofill-De Ros X, Vang Ørom UA: **Recent progress in miRNA biogenesis and decay**. *RNA Biol* 2024, **21**:1–8.

32. Nguyen HM, Nguyen TD, Nguyen TL, Nguyen TA: **Orientation of human microprocessor on primary MicroRNAs**. *Biochemistry* 2019, **58**:189–198.

33. Wu K, He J, Pu W, Peng Y: **The role of exportin-5 in MicroRNA biogenesis and cancer**. *Dev Reprod Biol* 2018, **16**:120–126.

34. Luo Q-J, Zhang J, Li P, Wang Q, Zhang Y, Roy-Chaudhuri B, Xu J, Kay MA, Zhang QC: **RNA structure probing reveals the structural basis of Dicer binding and cleavage**. *Nat Commun* 2021, **12**:3397.

35. Lee S, Jee D, Srivastava S, Yang A, Ramidi A, Shang R, Bortolamiol-Becet D, Pfeffer S, Gu S, Wen J, *et al.*: **Promiscuous splicing-derived hairpins are dominant substrates of tailing-mediated defense of miRNA biogenesis in mammals**. *Cell Rep* 2023, **42**, 112111.

36. Nakanishi K: **Anatomy of four human Argonaute proteins**. *Nucleic Acids Res* 2022, **50**:6618–6638.

37. Medley JC, Panzade G, Zinovyeva AY: **microRNA strand selection: unwinding the rules**. *WIREs RNA* 2021, **12**, e1627.

38. Gan HH, Gunsalus KC: **The role of tertiary structure in MicroRNA target recognition**. In *MicroRNA target identification*. Edited by Laganà A, New York: Springer; 2019:43–64.

39. Iwakawa H, Tomari Y: **Life of RISC: formation, action, and degradation of RNA-induced silencing complex**. *Mol Cell* 2022, **82**:30–43.

40. Mustafov D, Seriah S, Malik R, Braoudaki M: **MicroRNA biomarkers in primary brain malignancies**. In *Epigenetics - regulation and new perspectives*. Edited by Huang T, IntechOpen; 2023.

41. Lee Y-Y, Lee H, Kim H, Kim VN, Roh S-H: **Structure of the human DICER–pre-miRNA complex in a dicing state**. *Nature* 2023, **615**:331–338.

42. * Li X, Liang Z, Pan J, Zhang M, Liu J, Hu R, Liao C: **Identification of BACH1-IT2-miR-4786-Siglec-15 immune suppressive axis in bladder cancer**. *BMC Cancer* 2024, **24**:328.
This study identified a molecular pathway involving the *BACH1-IT2*/miR-4786/*SIGLEC15* axis that contributes to immune evasion and progression of bladder cancer. This pathway suggested potential targets for new therapeutic approaches and prediction for patient survival outcomes.

43. ** Ren Y, Lyu J, Guo Y, Yao Y, Hu L: **Long noncoding RNA TUG1 inhibits tumor progression through regulating siglec-15-related anti-immune activity in hepatocellular carcinoma**. *Journal of Immunology Research* 2022, **2022**:1–24.
Researchers demonstrated the involvement of miR-582-5p in directly targeting *SIGLEC15* and *TUG1*, implicated in liver cancer tumorigenesis. By acting as a "sponge" for miR-582-5p, *TUG1* allowed *SIGLEC15* to suppress the immune response in liver cancer. Silencing *TUG1* with miR-582-5p-RNA inhibitor therapy proposes alternative treatment strategies for normalising the immune response and reduction of tumour growth.

44. ** Ahmad MS, Braoudaki M, Patel H, Ahmad I, Shagufta Siddiqui SS: **Novel Siglec-15-Sia axis inhibitor leads to colorectal cancer cell death by targeting miR-6715b-3p and oncogenes**. *Front Immunol* 2023, **14**, 1254911.
This research incorporated the development and utilisation of a small molecule inhibitor (SHG-8) that targeted Siglec-15 *in vitro* in colon cancer. Small RNA sequencing analysis identified deregulated expression of miR-6715b-3p, possibly acting as a tumour suppressor following SHG-8 exposure. In addition, miR-6715b-3p targeted *PTTG1IP* emphasising possible interaction with the *SIGLEC15*/Sia axis. These findings suggested a combination strategy with PD-L1 antagonists for colon cancer patients.

45. * Chen H, Jayasinghe MK, Yeo EYM, Wu Z, Pirisinu M, Usman WM, Pham TT, Lim KW, Tran NV, Leung AYH, *et al.*: **CD33 -targeting extracellular vesicles deliver antisense oligonucleotides against FLT3-ITD and miR -125b for specific treatment of acute myeloid leukaemia**. *Cell Prolif* 2022, **55**, e13255.
Chen et al. exhibited engineered vesicles (RBCEVs) for drug delivery capable of gene and miRNA targeting in AML. Moreover, the designed carriers also targeted CD33 (Siglec-3), a highly expressed protein on AML cells. Therapeutic agent loaded RBCEVs directly targeting the *FLT3-ITD* gene or miR-125b exerted tumour suppression of AML *in vitro* and *in vivo*. This provided a promising avenue for effective AML treatment.

46. Yao Y, Jiao D, Liu Z, Chen J, Zhou X, Li Z, Li J, Han X: **Novel miRNA predicts survival and prognosis of cholangiocarcinoma based on RNA-seq data and in vitro experiments**. *BioMed Res Int* 2020, **2020**:1–14.

47. ** Ogbodo AK, Mustafov D, Arora M, Lambrou GI, Braoudaki M, Siddiqui SS: **Analysis of SIGLEC12 expression, immunomodulation and prognostic value in renal cancer using multiomic databases**. *Heliyon* 2024, **10**, e24286.
This research focused on the investigation of Siglec-12 expression profiles in kidney cancer (KRCC). While the mechanisms of Siglec-12 action within KRCC remain unclear, it was suggested that high protein levels might be associated with poor patient prognosis. Further compactional analyses predicted that miR-133b/miR-654/miR-574 were involved in the modulation of *SIGLEC12* expression. The researchers proposed that miRNA blockade of *SIGLEC12* might inhibit cancer-promoting pathways and induce sensitisation to immunotherapeutic treatment within KRCC patients.

48. Rodriguez E, Boelaars K, Brown K, Eveline Li RJ, Kruijssen L, Bruijns SCM, Van Ee T, Schetters STT, Crommentuijn MHW, Van Der Horst JC, *et al.*: **Sialic acids in pancreatic cancer cells drive tumour-associated macrophage differentiation via the Siglec receptors Siglec-7 and Siglec-9**. *Nat Commun* 2021, **12**:1270.

49. Psathas JN, Doonan PJ, Raman P, Freedman BD, Minn AJ, Thomas-Tikhonenko A: **The Myc-miR-17-92 axis amplifies B-cell receptor signaling via inhibition of ITIM proteins: a novel lymphomagenic feed-forward loop**. *Blood* 2013, **122**:4220–4229.

50. Gonzalez-Gil A, Schnaar RL: **Siglec ligands**. *Cells* 2021, **10**:1260.

51. Robida PA, Rische CH, Morgenstern NB-B, Janarthanam R, Cao Y, Krier-Burris RA, Korver W, Xu A, Luu T, Schanin J, *et al.*: **Functional and phenotypic characterization of siglec-6 on human mast cells**. *Cells* 2022, **11**:1138.

52. Büll C, Nason R, Sun L, Van Coillie J, Madriz Sørensen D, Moons SJ, Yang Z, Arbitman S, Fernandes SM, Furukawa S, *et al.*: **Probing the binding specificities of human Siglecs by cell-based glycan arrays**. *Proc Natl Acad Sci USA* 2021, **118**, e2026102118.

53. Yamakawa N, Yasuda Y, Yoshimura A, Goshima A, Crocker PR, Vergoten G, Nishiura Y, Takahashi T, Hanashima S, Matsumoto K, *et al.*: **Discovery of a new sialic acid binding region that regulates Siglec-7**. *Sci Rep* 2020, **10**:8647.

54. Chang L-Y, Liang S-Y, Lu S-C, Tseng HC, Tsai H-Y, Tang C-J, Sugata M, Chen Y-J, Chen Y-J, Wu S-J, *et al.*: **Molecular basis and role of siglec-7 ligand expression on chronic lymphocytic leukemia B cells**. *Front Immunol* 2022, **13**, 840388.

55. Liu J, Yan C, Xu S: **LncRNA IL21-AS1 facilitates tumour progression by enhancing CD24-induced phagocytosis inhibition and tumorigenesis in ovarian cancer**. *Cell Death Dis* 2024, **15**:313.

56. Bandala-Sanchez E, Bediaga NG, Naselli G, Neale AM, Harrison LC: **Siglec-10 expression is up-regulated in activated human CD4+ T cells**. *Hum Immunol* 2020, **81**:101–104.

57. Läubli H: **Unraveling the impact of a glyco-immune checkpoint in bone metastasis**. *Proc Natl Acad Sci USA* 2024, **121**, e2400499121.

58. Boelaars K, Van Kooyk Y: **Targeting myeloid cells for cancer immunotherapy: siglec-7/9/10/15 and their ligands**. *Trends in Cancer* 2024, **10**:230–241.

59. Xi J, Huang Q, Wang L, Ma X, Deng Q, Kumar M, Zhou Z, Li L, Zeng Z, Young KH, *et al.*: **miR-21 depletion in macrophages promotes tumoricidal polarization and enhances PD-1 immunotherapy**. *Oncogene* 2018, **37**:3151–3165.

60. Yu D, Liu X, Han G, Liu Y, Zhao X, Wang D, Bian X, Gu T, Wen L: **The let-7 family of microRNAs suppresses immune evasion in head and neck squamous cell carcinoma by promoting PD-L1 degradation**. *Cell Commun Signal* 2019, **17**:173.

61. Huffaker TB, Lee S-H, Tang WW, Wallace JA, Alexander M, Runtsch MC, Larsen DK, Thompson J, Ramstead AG, Voth WP,

et al.: **Antitumor immunity is defective in T cell–specific microRNA-155–deficient mice and is rescued by immune checkpoint blockade**. *J Biol Chem* 2017, **292**:18530–18541.

62. Li Q, Johnston N, Zheng X, Wang H, Zhang X, Gao D, Min W: **miR-28 modulates exhaustive differentiation of T cells through silencing programmed cell death-1 and regulating cytokine secretion**. *Oncotarget* 2016, **7**:53735–53750.

63. Wei J, Nduom EK, Kong L-Y, Hashimoto Y, Xu S, Gabrusiewicz K, Ling X, Huang N, Qiao W, Zhou S, *et al.*: **MiR-138 exerts anti-glioma efficacy by targeting immune checkpoints**. *Neuro Oncol* 2016, **18**:639–648.

64. Zhang M, Gao D, Shi Y, Wang Y, Joshi R, Yu Q, Liu D, Alotaibi F, Zhang Y, Wang H, *et al.*: **miR-149-3p reverses CD8 $^{+}$ T-cell exhaustion by reducing inhibitory receptors and promoting cytokine secretion in breast cancer cells**. *Open Biol* 2019, **9**, 190061.

65. Li S, Jiang L, Yang Y, Cao J, Zhang Q, Zhang J, Wang R, Deng X, Li Y: **MiR-195-5p inhibits the development of chronic obstructive pulmonary disease via targeting siglec1**. *Hum Exp Toxicol* 2020, **39**:1333–1344.

66. Li S, Jiang L, Yang Y, Cao J, Zhang Q, Zhang J, Wang R, Deng X, Li Y: **Siglec1 enhances inflammation through miR-1260-dependent degradation of IκBα in COPD**. *Exp Mol Pathol* 2020, **113**, 104398.

67. Lei H, Li H, Xie H, Du C, Xia Y, Tang W: **Role of MiR-215 in hirschsprung's disease pathogenesis by targeting SIGLEC-8**. *Cell Physiol Biochem* 2016, **40**:1646–1655.

68. Thakuri BKC, Zhang J, Zhao J, Nguyen LN, Nguyen LNT, Schank M, Khanal S, Dang X, Cao D, Lu Z, *et al.*: **HCV-associated exosomes upregulate RUNXOR and RUNX1 expressions to promote MDSC expansion and suppressive functions through STAT3–miR124 Axis**. *Cells* 2020, **9**:2715.

PLOS ONE

RESEARCH ARTICLE

Differential expression of ST6GALNAC1 and ST6GALNAC2 and their clinical relevance to colorectal cancer progression

Mohammed Saqif Ahmad, Maria Braoudaki, Shoib Sarwar Siddiqui*

School of Life and Medical Sciences, University of Hertfordshire, Hatfield, United Kingdom

* s.siddiqui3@herts.ac.uk

OPEN ACCESS

Citation: Ahmad MS, Braoudaki M, Siddiqui SS (2024) Differential expression of ST6GALNAC1 and ST6GALNAC2 and their clinical relevance to colorectal cancer progression. PLoS ONE 19(9): e0311212. https://doi.org/10.1371/journal.pone.0311212

Editor: James Mockridge, PLOS: Public Library of Science, UNITED KINGDOM OF GREAT BRITAIN AND NORTHERN IRELAND

Received: May 1, 2024

Accepted: September 13, 2024

Published: September 30, 2024

Data Availability Statement: All relevant data are within the manuscript and its Supporting Information files.

Funding: The author(s) received no specific funding for this work.

Competing interests: The authors have declared that no competing interests exist.

Abbreviations: AGR2, anterior gradient 2; AHSG, α-2-HS-glycoprotein; ALCC, average local

Abstract

Colorectal cancer (CRC) has become a significant global health concern and ranks among the leading causes of morbidity and mortality worldwide. Due to its malignant nature, current immunotherapeutic treatments are used to tackle this issue. However, not all patients respond positively to treatment, thereby limiting clinical effectiveness and requiring the identification of novel therapeutic targets to optimise current strategies. The putative ligand of Siglec-15, Sialyl-Tn (STn), is associated with tumour progression and is synthesised by the sialyltransferases ST6GALNAC1 and ST6GALNAC2. However, the deregulation of both sialyltransferases within the literature remain limited, and the involvement of microRNAs (miRNAs) in STn production require further elucidation. Here, we identified miRNAs involved in the regulation of *ST6GALNAC1* via a computational approach and further analysis of miRNA binding sites were determined. *In silico* tools predicted miR-21, miR-30e and miR-26b to regulate the *ST6GALNAC1* gene, all of which had shown significant upregulated expression in the tumour cohort. Moreover, each miRNA displayed a high binding affinity towards the seed region of *ST6GALNAC1*. Additionally, enrichment analysis outlined pathways associated with several cancer hallmarks, including epithelial to mesenchymal transition (EMT) and MYC targets associated with tumour progression. Furthermore, our *in silico* findings demonstrated that the *ST6GALNAC1* expression profile was significantly downregulated in CRC tumours, and its low expression correlated with poor survival outcomes when compared with patient survival data. In comparison to its counterpart, there were no significant differences in the expression of *ST6GALNAC2* between normal and malignant tissues, which was further evidenced in our immunohistochemistry analysis. Immunohistochemistry staining highlighted significantly higher expression was more prevalent in normal human tissues with regard to *ST6GALNAC1*. In conclusion, the integrated *in silico* analysis highlighted that STn production is not reliant on deregulated sialyltransferase expression in CRC, and *ST6GALNAC1* expression is regulated by several oncomirs. We proposed the involvement of other sialyltransferases in the production of the STn antigen and CRC progression via the Siglec-15/Sia axis.

clustering coefficient; AT, cancer adjacent colon tissue; C1GALT1, Core-1 synthase-glycoprotein-*N*-acetylgalactosamine 3-b-galactosyltransferase- 1; C1GALT1C1, C1GALT1 Specific Chaperone 1; ccRCC, clear-cell renal cell carcinoma; CI, confidence interval; CIMP, CpG island methylation; CIN, chromosomal instability; COAD, colon adenocarcinoma; CRC, colorectal cancer; CTLA4, Cytotoxic T-lymphocyte associated protein 4; EEF, eukaryotic elongation factor; EEF1A2, Elongation factor 1-a 2; EMT, epithelial-mesenchymal transition; ER, endoplasmic reticulum; EZH2, Enhancer of zeste homolog 2; FDR, false discovery rate; FTC, follicular thyroid carcinomas; GALNT, *N*-acetylgalactosaminyltransferase; GALNT, N-acetylgalactosaminyltransferase; GSEA, Gene Set Enrichment Analysis; HR, hazard ratio; IHC, immunohistochemistry; LAG3, Lymphocyte-activation gene 3; LUAD, lung adenocarcinoma; LUSC, lung squamous cell carcinoma; miRNAs, microRNAs; MSI, microsatellite instability; NAT, adjacent normal colon tissue; OS, overall survival; PD-L1, programmed death-ligand 1; PPI, protein-protein interactions; PPS, post-progression survival; RECIST, response evaluation criteria in solid tumours; RFS, relapse-free survival; RT, room temperature; Sfold, statistical folding of nucleic acids and studies of regulatory RNAs; Siglec, Sialic acid-binding immunoglobulin-type lectin; SNAIL, Zinc finger protein SNAI1SNTB1—syntrophin beta 1; SRCC, spearman's rank correlation coefficient; STn, Sialyl Tn; STRING, Search Tool for the Retrieval of Interacting Genes/Proteins; TAMs, tumour-associated macrophages; TIGIT, T-cell immunoreceptor with Ig and ITIM domains; TILs, tumour-infiltrating lymphocytes; TIMER, tumour IMmune Estimation Resource analysis; TME, tumour microenvironment; TPM, transcript per million; Tregs, regulatory T-cells; UTR, untranslated region.

Introduction

Colorectal cancer (CRC) is one of the most prevalent and lethal malignancies worldwide, with patient diagnoses increasing each consecutive year [1]. Due to its malignant nature, CRC treatment is heavily reliant on early screening and detection to improve patient survival [2]. Current immune checkpoint blockade therapies have shown positive patient responses against programmed cell death protein-1 (PD-1), with blocking antibodies such as pembrolizumab and nivolumab being food and drug administration (FDA) approved for treatment in metastatic CRC patients with significant microsatellite instability (MSI) mutations [3]. However, not all patients respond positively to immunotherapeutic treatments, limiting clinical effectiveness and resulting in a poor prognosis. There is an urgent need to further identify therapeutic targets to optimise current treatment strategies for CRC.

The sialic acid-binding immunoglobulin-type lectin (Siglec)/sialic acid (Sia) axis is an immunoregulatory pathway that establishes immune tolerance to self-cells. More recently, this has been implicated in several cancer types, with Siglecs being focused upon as emerging therapeutic cancer targets [4]. Siglec-15 is one such promising immune checkpoint protein that exhibits distinct expression on cancer subpopulations compared to other immune checkpoints, such as programmed death-ligand 1 (PD-L1) [5]. The interaction of sialoglycan ligands upon Siglec-15 engagement prevents effective activation of T-lymphocytes [6]. The implications of Siglec-15 binding to sialoglycan ligands are those of inducing hypersialylation and promoting immunosuppression, consequently resulting in the immune evasion of tumour cells [7]. Several treatment strategies are being employed in the disruption of the Siglec-15/Sia axis. Current therapeutic strategies involve blocking antibodies (NC318) that are in clinical trials [8]. Similarly, another study highlighted the development of a monoclonal antibody (1-15D1) that had a high binding affinity to the Siglec-15 protein and was capable of stimulating T-cell response *in vitro* [9]. Moreover, other approaches for Siglec-15 disruption have utilised protein aptamers to assist in checkpoint blockade and have high affinity against the Siglec-15 protein [10]. Further to this, our previous study also highlighted the development of a small molecule inhibitor binding to the V-set binding domain to prevent sialoglycan binding [11]. Interestingly, upregulation of these Sia glycans has also been correlated with cancer-specific glycosylation and serves as a unique driver in cancer onset and progression [12]. More specifically, Siglec-15/Sia binding is dependent on Sialyl-Tn (STn), likely synthesised by glycosyltransferases such as *ST6GALNAC1*, which have shown aberrant expression in cancer [13]. *ST6GALNAC1*'s involvement in STn antigen presentation is frequently upregulated in multiple cancer types and has shown poor prognosis in CRC and prostate cancer (PCa) [14,15]. Similarly, *ST6GALNAC2* participates in STn antigen generation to a lesser extent and demonstrates high expression in CRC, and exhibits advanced cancer progression in follicular thyroid carcinomas (FTC) [16,17]. Targeting sialyltransferases such as *ST6GALNAC1* and *ST6GALNAC2* may provide anti-tumour immunity and a greater response in current immune checkpoint blockade therapies. However, evidence regarding miRNAs involved in their regulation and STn production in the literature remain limited.

MiRNAs are small single-stranded RNA molecules capable of modulating gene expression via 3' untranslated region (UTR) binding post-transcriptionally [18]. Furthermore, the interplay of miRNAs enhances cancer hallmarks and its regulation, and correlates with targeting key genes involved in promoting angiogenesis, cancer proliferation, and metastasis [19,20]. Similarly, the Siglec/Sia axis can also be modulated via miRNA expression. The upregulation of miR-135b and miR-182 directly targets *ST6GALNAC2* via the phosphoinositide 3-kinase/protein kinase B (PI3K)/AKT signalling pathway, enhancing chemoresistance in CRC [21].

The crosstalk between miRNA expression patterns and the Siglec-15/Sia axis could underline certain dysregulated mechanisms.

In the current study, a multiomics approach was adopted to investigate the roles of *ST6GALNAC1* and *ST6GALNAC2* in mediating the Siglec/Sia axis and its clinical relevance to CRC tumorigenesis at the gene and protein levels. We further highlighted enriched pathways associated with cancer hallmarks and identified possible signalling pathways related to tumour onset. Moreover, we addressed the impact of each corresponding gene on the infiltration of myeloid cells and their association with prominent immune checkpoints and immune function. This may provide insights into highlighting their roles in cancer progression.

Methodology

Search Tool for the Retrieval of Interacting Genes/Proteins (STRING)

The STRING database identifies known and predicted protein-protein interactions (PPI) and displays direct associations via computational data mining. The STRING 11.0 (https://version-11-0b.string-db.org/cgi/input?sessionId=brxKfZgAG9Au&input_page_show_search=on; accessed 2 August 2023) software highlighted PPI relationships in *ST6GALNAC1* and *ST6GALNAC2*. The development of the full PPI network included both functional and physical protein associations with $\leq$ 10 protein interactors. Additionally, each individual protein queried and $\leq$ 20 protein interactors were included in the second expansion of the framework with a high confidence interval, with $\geq$ 0.700 considered significant.

GeneMANIA

The GeneMANIA database (https://genemania.org/; accessed 26 July 2023) predicts functional information based on corresponding genes and gene datasets. The gene framework highlights functional communication between genes via criterion comprising of physical interactions, co-expression, predicted datamining, co-localisation, genetic interactions, and common pathway interactions with respect to *ST6GALNAC1* and *ST6GALNAC2*. Correlating genes with a high degree of association were also represented [22].

UALCAN

The UALCAN database (http://ualcan.path.uab.edu; accessed 26 July 2023) is used as a tool for cancer transcriptomics. Utilising TCGA genomic data for analysis, the mRNA expression of *ST6GALNAC1* (ENSG00000070526) and *ST6GALNAC2* (ENSG00000070731) were compared for normal and colon adenocarcinoma (COAD) cohorts. Similarly, gene expression of identified protein targets obtained from the STRING analysis were determined and compared between normal and COAD subgroups. Additionally, predicted miRNA candidates involved in gene regulation were also compared for normal and COAD cohorts. Statistical significance of gene expression data (transcript per million; TPM) generated by the UALCAN database for box plot construction was assessed via a Welch's t-test PERL script encoded to identify significant differences between cohorts based on clinicopathological features [23]. $P < 0.05$ was considered statistically significant.

In silico miRNA datamining

In silico analysis tools were utilised to determine common miRNA targets predicted to modulate *ST6GALNAC1* expression and possible clinical relevance to CRC across several databases. Venn diagrams (Venny 2.1.0) (https://bioinfogp.cnb.csic.es/tools/venny/; accessed 28 July 2023) were constructed using three separate miRNA prediction databases including

TargetScan (https://www.targetscan.org/vert_80/; accessed 28 July 2023), MiRSystem (http://mirsystem.cgm.ntu.edu.tw/index.php; accessed 28 July 2023), and MiRWalk (http://mirwalk.umm.uni-heidelberg.de/; accessed 28 July 2023), and were further cross-referenced. Furthermore, common miRNA candidates were also determined for the identified *in silico* targets that were shown to interact with *ST6GALNAC1* and *ST6GALNAC2*. The most frequent miRNA hits associated with *ST6GALNAC1* were further explored for predicted binding sites via statistical folding of nucleic acids and studies of regulatory RNAs (Sfold) software (https://sfold.wadsworth.org/cgi-bin/starmir.pl; accessed 13 September 2023).

Gene Set Enrichment Analysis (GSEA)

GSEA of *ST6GALNAC1* and *ST6GALNAC2* were obtained via the TCGA dataset (TCGA, PanCancer Atlas) from cBioPortal for Cancer Genomics (http://cbioportal.org/ accessed on 19 September 2023). CBioPortal is offered as an open access repository for interactive omics patient data. The dataset for COAD tumours was selected, comprising of a total of 524 patient samples. Each of the corresponding genes were submitted as the queried gene and modified to include the differential mRNA expression relative to the normal cohort with a z-score threshold of ± 2.0. Following this, the mRNA comparative data between the altered (differentially expressed group) and unaltered group (unchanged expression group) was separated. Following this, the altered group containing only the significant differentially expressed genes between the normal and COAD subgroups were selected, which also included the query genes *ST6GALNAC1* and *ST6GALNAC2*, respectively. The number of differentially expressed genes for each dataset were recorded as 6667 genes for the *ST6GALNAC1* dataset and 4331 genes for the *ST6GALNAC2* dataset and exported as TSV files. The datasetswere uploaded into the GSEA v4.3.2 software as rnk files (https://www.gsea-msigdb.org/ accessed on 19 January 2023) and enriched pathways and cancer hallmarks were identified (FDR < 0.25 and $p < 0.05$).

TISIDB

The TISIDB database (http://cis.hku.hk/TISIDB/index.php; accessed on 26 July 2023) provides an integrated repository for identifying interactions between tumours and the immune system. The TISIDB database collates information via several datasets including TCGA transcriptomics and clinical data pertaining to multiple cancer types. The Spearman's rank correlation between the abundance of macrophages, activated $CD4^+$ T-cells, activated $CD8^+$ T-cells, regulatory T-cells (Tregs), and monocytes were assessed in conjunction with the expression of both sialyltransferases, *ST6GALNAC1* and *ST6GALNAC2*, in COAD tumours [24].

Tumour IMmune Estimation Resource (TIMER) analysis

The TIMER database (https://cistrome.shinyapps.io/timer/, accessed on 1 August 2023) serves as an extensive platform to systematically analyse immune infiltrates over several cancer types. For this study, specific parameters relating to the correlation of immune checkpoint protein genes, including *SIGLEC15*, *PDCD1*, *CD274*, cytotoxic T-lymphocyte associated protein 4 (*CTLA4*), T-cell immunoreceptor with Ig and ITIM domains *(TIGIT)*, and Lymphocyte-activation gene 3 (*LAG3*), were all compared with the abundance of *ST6GALNAC1* and *ST6GALNAC2*. Spearman's rank correlation coefficient and $p < 0.05$ for log2 TPM was used to determine the statistical significance of COAD tumours [25].

Kaplan-Meier Plotter (KM PLOTTER)

The Kaplan-Meier plotter (https://kmplot.com/analysis/, accessed on 26 July 2023) database tool was used to identify the prognostic association between the genomic expression data for *ST6GALNAC1* and *ST6GALNAC2*, along with corresponding patient survival outcomes in COAD tumours. The prognostic expression of each highlighted sialyltransferase in CRC patients was analysed over a period of time based on overall survival criterion (OS), relapse-free survival (RFS), post-progression survival (PPS), hazard ratio (HR), 95% confidence interval (CI), and Log-rank P-value [26].

Immunohistochemistry (IHC)

Colorectal cancer tissue array (BC05023a) obtained from Biomax (TissueArray.Com LLC, Maryland, USA), containing 54 cores (18 COAD, 18 cancer adjacent colon tissue (AT), and 18 adjacent normal colon tissue (NAT), was subjected to histological staining. Deparaffinisation was achieved by treating the sections with histoclean/ethanol followed by antigen retrieval via sodium citrate treatment, and subsequently washed in 0.025% triton-x/PBS and incubated in 3% hydrogen peroxide:PBS for a period of 15 min. The slides were washed an additional three times with Triton-X100/PBS for 5 min. Blocking of non-specific binding sites was performed using 5% BSA/PBS, and the sections were then incubated in a humidity chamber for 1h at room temperature (RT) whilst wrapped in parafilm. The slides were incubated overnight at 4˚C with the primary *ST6GALNAC1* antibody (1:50) (Proteintech Group, Inc., Manchester, UK) and *ST6GALNAC2* antibody (1:100) (Life Technologies Limited, Renfrewshire, UK) respectively. The slides were washed with 0.025% Triton X-100/PBS, followed by incubation with a biotin-labelled anti-rabbit secondary antibody. Subsequently, the sections were washed using a 0.025% Triton X-100/PBS wash step and 1h incubation with a streptavidin-HRP conjugate. Visualisation of both *ST6GALNAC1* and *ST6GALNAC2* antibody staining was achieved via addition of DAB solution (Zytomed Systems GmBH, Berlin, Germany) and haematoxylin as the nuclei stain for a period of 10 min at RT. Quantification of the staining was conducted via an AxioCam Hrc (Zeiss Microscopy, Oberkochen, Germany) microscope at x4 and x10 magnifications. Both normal and malignant tissues were compared via the unpaired student's t-test.

Results

ST6GALNAC1 and *ST6GALNAC2* gene and protein-protein molecular networks

The STRING and GeneMANIA databases highlight predicted genes and PPI between interacting queried proteins/genes. The *ST6GALNAC1* gene framework, produced by GeneMANIA, shows co-expression (purple) with anterior gradient 2 (*AGR2*) (Fig 1A) (Fig 1A). The *ST6GALNAC1* PPI network (Fig 1B) has shown multiple hits that correspond with N-acetylgalactosaminyltransferase (GALNT) enzymes and other sialyltransferases. Likewise, the average local clustering coefficient (ALCC) (0.83) shows a strong correlation with multiple protein targets, and the PPI enrichment score upon normalization shows significant node interactions at the highest confidence interval (< 1.0 x 10–16) (S1 Table). Predicted gene communication involving *ST6GALNAC2* has shown significant physical interactions with the MUC gene family (Fig 1C). The *ST6GALNAC2* PPI framework (Fig 1D) has also demonstrated a comprehensive predicted interaction clustering of several protein targets with 26 nodes. The ALCC score (0.708) and PPI enrichment (1.09×10^{-5}) (S1 Table) show strong correlation between several protein targets and with primary interactions associated with α-2-HS-glycoprotein (AHSG).

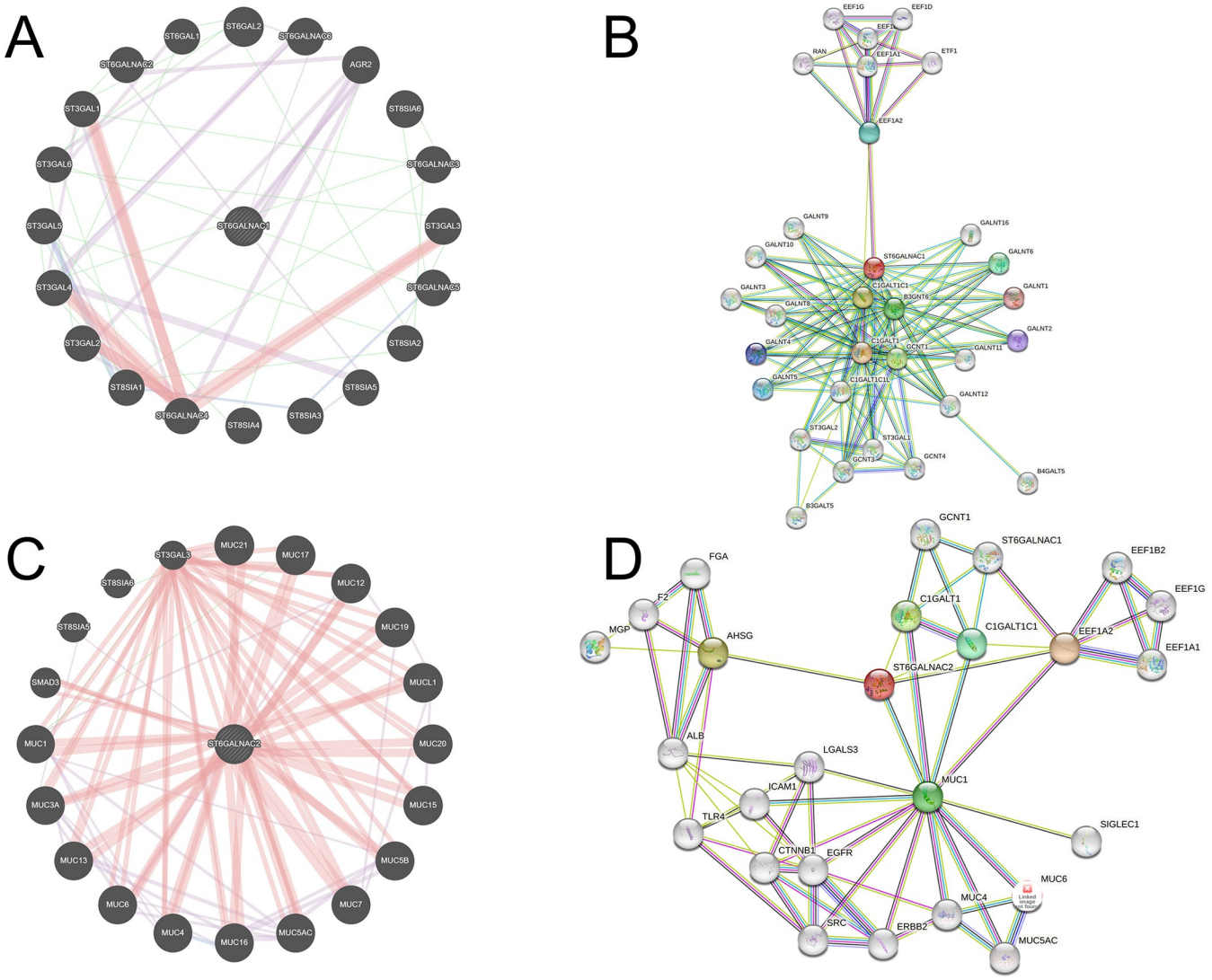

Fig 1. *ST6GALNAC1* and *ST6GALNAC2* share significant gene and protein-protein interactions and may highlight key novel targets. (**A**) *ST6GALNAC1* gene framework predicts functional information based on corresponding genes and gene datasets. (**B**) *ST6GALNAC1* STRING framework highlighting possible PPI from interacting proteins and direct associations via computational datamining. The framework is developed with a confidence interval of ≥ 0.700. (**C**) S*T6GALNAC2* gene framework predicts functional information based on corresponding genes and gene datasets. (**D**) *ST6GALNAC2* STRING framework highlighting possible PPI from interacting proteins and direct associations via computational datamining. The framework is developed with a confidence interval of ≥ 0.700.

https://doi.org/10.1371/journal.pone.0311212.g001

Furthermore, both sialyltransferases show interactions with a cluster of EEF1 enzymes, particularly with EEF1A2, and communication with Core-1 synthase-glycoprotein-*N*-acetylgalactosamine 3-b-galactosyltransferase-1 (C1GALT1) and C1GALT1 Specific Chaperone 1 (C1GALT1C1) (Fig 1B and 1D).

Candidate miRNAs predicted in gene regulation and possible binding sites

UALCAN TCGA datamining highlighted the sialyltransferase expression profile of *ST6GALNAC1* and *ST6ALNAC2* in CRC (Fig 2A). *ST6GALNAC1* shows significant gene downregulation in the tumour cohort of 46.056 TPM in comparison to the normal subgroup with a mean expression of 173.703 TPM ($p < 0.0001$). Additionally, UALCAN expression analysis shows

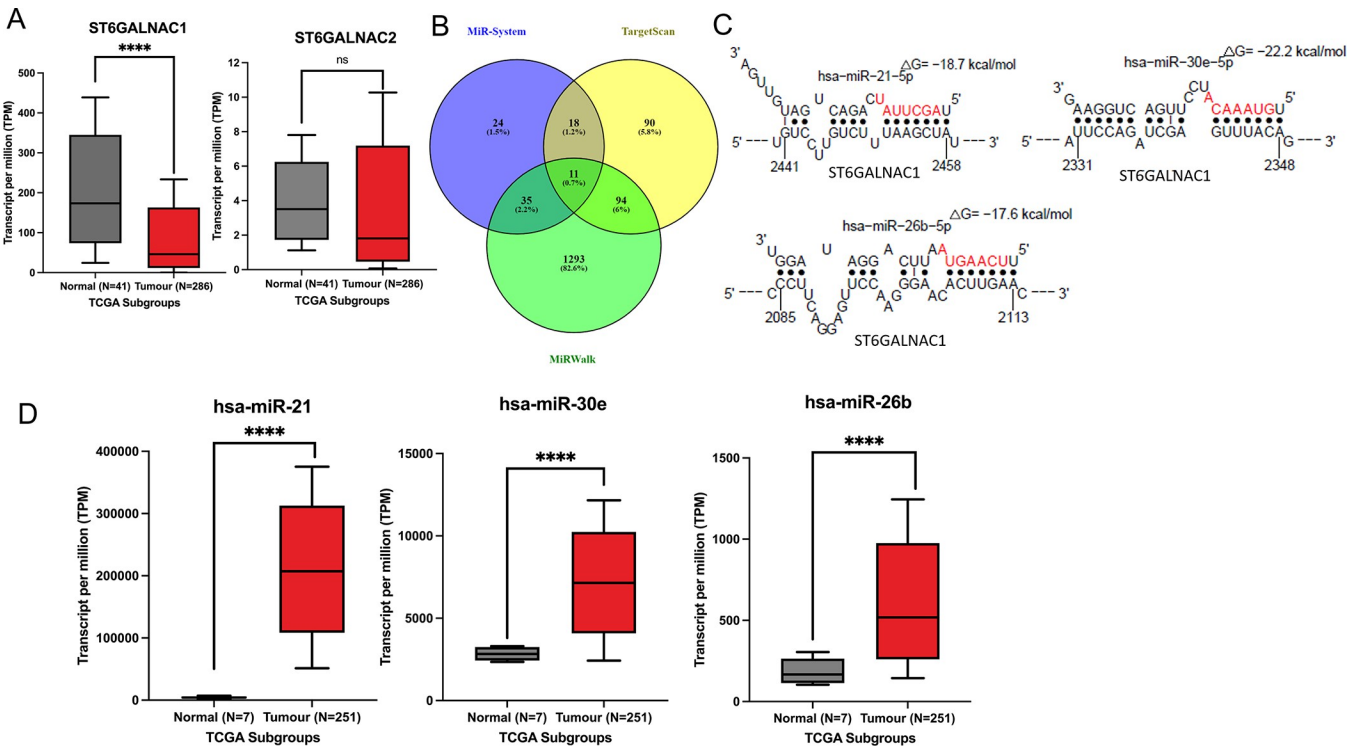

Fig 2. *In silico* analysis demonstrates that sialyltransferase expression is downregulated in COAD tumours. (**A**) TCGA genomic data demonstrating the mRNA expression of *ST6GALNAC1* for both normal and colon adenocarcinoma (COAD) cohorts. Welch's t-test PERL script. **** $P < 0.0001$ (**B**) *In silico* analysis tools were utilised to construct Venn diagrams identifying common miRNA targets predicted to modulate *ST6GALNAC1* expression. (**C**) The most frequent miRNA hits associated with *ST6GALNAC1* were further explored for predicted binding sites via the Sfold software. (**D**) TCGA genomic data demonstrating the mRNA expression of candidate miRNAs with the highest binding affinities for normal and colon adenocarcinoma (COAD) cohorts. Welch's t-test PERL script; **** $P < 0.0001$.

https://doi.org/10.1371/journal.pone.0311212.g002

no significant change in the expression of *ST6GALNAC2* between normal (3.509 TPM) and tumour (1.813 TPM) cohorts. Similarly, the gene expression of the predicted targets *AGR2* and *AHSG* were also determined between normal and CRC tumour groups. UALCAN expression identified significant expression of *AHSG* in the tumour subgroup (0.032 TPM) in comparison to the normal tissue subgroup (0.00 TPM) (S1B Fig). In contrast, *AGR2* had shown no significant difference in the expression of both subgroups. Furthermore, only *ST6GALNAC2* displays enhanced promoter methylation in the tumour cohort (S2B Fig). Moreover, the Pearson correlation between both *ST6GALNAC1* and *ST6GALNAC2* expression in CRC shows a low association between the two genes, but the relationship has been shown to be significant (S3 Fig).

To identify the miRNAs involved in regulating the gene expression of *ST6GALNAC1*, several databases were compared to identify the most frequent hits (Fig 2B). Of the multiple miRNAs cross-referenced, a total of 11 were predicted to be involved in the regulation of *ST6GALNAC1* based on targetscan, miRsystem and miRwalk databases (Fig 2B) (S2 Table). We have found that none of the 11 commonly deregulated miRNAs (Fig 2B) were regulating *ST6GALNAC1* as their expression levels seem to be downregulated as well. Hence, we focused on the miRNAs found common between Targetscan and miRsystem, and we found that miR-21-5p, miR-30e-5p and miR-26b-5p as potential regulators of *ST6GALNAC1* promoting CRC progression when overexpressed (Fig 2C and 2D). All three miRNAs were also shown to regulate ST6GALNAC1 by miRPathDB database as well (data not shown). Moreover, common miRNAs from the TargetScan database were identified between regulating *AHSG* and *AGR2*

in association with *ST6GALNAC1* and *ST6GALNAC2* (S4A Fig). Although no singular miRNA was shown to regulate all four genes, common miRNAs across other predicted protein targets were also determined. The common miRNA element that correlated between the targets *GALNT3*, *GALNT8*, *B3GNT6* and *ST6GALNAC1* identified hsa-miR-30a-5p to be involved in gene regulation (S4B Fig). Similarly, predicted targets *C1GALT1*, *C1GALT1C1*, *AHSG* and *ST6GALNAC2* were compared for any common miRNA elements, although none were identified (S4C Fig). Further to this, predicted miRNAs involved in *ST6GALNAC1* expression were further investigated, and the binding affinities to key binding sites were identified (Fig 2C). MiRNA activity for gene regulation typically occurs at the 3' end of the UTR. MiR-21-5p exhibited a high binding affinity (-18.700 kcal/mol) towards the seed region of the target *ST6GALNAC1* mRNA strand at position 2441–2458. Similarly, the predicted binding of miR-30e-5p and miR-26b-5p also displayed high binding affinities to the target mRNA strand at -22.200 kcal/mol and -17.600 kcal/mol, respectively. MiR-30e-5p had a predicted binding site at position 2331–2348. In contrast, miR-26b-5p had demonstrated a predicted binding site at position 2085–2113, all of which indicated a strong association between nucleotide bases.

To understand the role of these identified candidate miRNAs and their relevance in relation to CRC (Fig 2D), UALCAN data demonstrated significantly upregulated expression of all three miRNAs in the COAD tumour subgroup. MiR-21 displayed a mean expression of 207,192.191 TPM in comparison to normal colon tissues. This was also similarly observed by the mean expression of miR-30e with 7142.537 TPM and a mean expression of 518.048 TPM for miR-26b in comparison to the normal colon tissue cohort.

GSEA analysis of sialyltransferases and cancer hallmarks

To identify various enriched pathways relating to *ST6GALNAC1* and *ST6GALNAC2* and cancer hallmarks, the GSEA of the TCGA, PanCancer Atlas dataset with a specific focus on significantly differentially expressed (DE) genes relating to CRC were highlighted with respect to *ST6GALNAC1* (Fig 3) and *ST6ALNAC2* (Fig 4). Out of a total of 47 gene sets displayed for *ST6GALNAC1* and the CRC phenotype, three gene sets were identified as significantly upregulated, whilst seven gene sets were identified as being significantly downregulated with respect to CRC (FDR < 0.25 and $p < 0.05$) (Fig 3A and 3B, S3 Table). Significant enrichment of EMT, MYC targets, and hallmarks related to myogenesis were identified as being significantly enriched. Additionally, enriched gene sets that had shown downregulation including the inflammatory response, IL-6 mediated JAK/STAT3 signalling, and deregulated KRAS signalling, among others. Similarly, *ST6GALNAC2* highlighted 10 significantly enriched gene sets as being upregulated (FDR < 0.25 and $p < 0.05$) (Fig 4A), and seven gene sets that were significantly enriched as being downregulated out of a total of 42 gene sets (S4 Table). Upregulated gene sets included the enrichment of E2F targets, MYC targets, the G2M checkpoint, mTOR signalling, and other pathways (Fig 4A). Downregulated gene sets that were also enriched included KRAS signalling, allograft rejection, EMT, inflammatory response, and IFNγ response, among other pathways (Fig 4B).

Sialyltransferase expression correlates to the abundance of myeloid cells

To determine the role of both sialyltransferases and immune infiltration *in situ*, the abundance of immune infiltrating cell populations correlating with *ST6GALNAC1* and *ST6GALNAC2* expression in colon adenocarcinomas (COAD) was determined (Figs 5A and 6A). Spearman's rank correlation coefficient (SRCC) significantly associated the abundance of activated $CD4^+$ T-lymphocytes and monocyte populations with *ST6GALNAC1* expression (Fig 5A). In

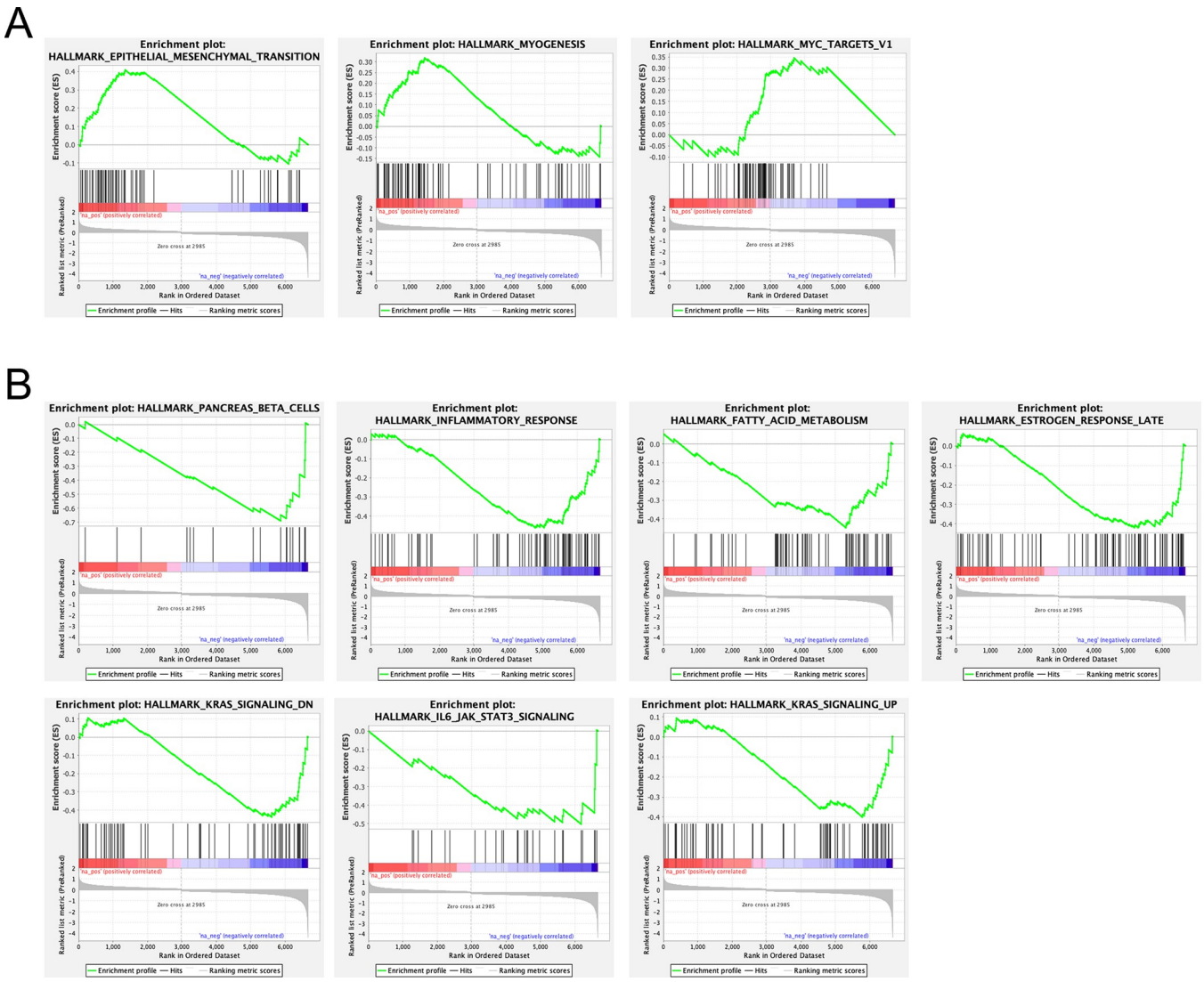

Fig 3. GSEA of *ST6GALNAC1* identified significant enrichment between DEG's and the CRC phenotype. GSEA of *ST6GALNAC1* was obtained via the TCGA dataset (TCGA, PanCancer Atlas) from cBioPortal outlining DEG's and a total of 47 gene sets associated with cancer hallmarks. (**A**) The enrichment of three gene sets was identified as being upregulated. FDR < 0.25 and p < 0.05. (**B**) Enrichment of seven gene sets was identified as being downregulated. FDR < 0.25 and p < 0.05.

https://doi.org/10.1371/journal.pone.0311212.g003

comparison, *ST6GALNAC2* expression correlated with the abundance of several infiltrating immune cell populations including activated $CD4^+$ T-lymphocytes, activated $CD8^+$ T-lymphocytes, Tregs, monocytes, and macrophages, with the most significant SRCC correlation with the latter (0.206) (Fig 6A). Additionally, the association between the abundance of both *ST6GALNAC1* and *ST6GALNAC2* and pro-tumorigenic immune checkpoints were also determined via TIMER analyses (Figs 5B and 6B). *ST6GALNAC1* expression showed no significant correlation with other pro-tumorigenic immune checkpoints (Fig 5B). However, *ST6GALNAC2* expression displayed an association with most pro-tumorigenic immune checkpoints, excluding Siglec-15 (Fig 6B).

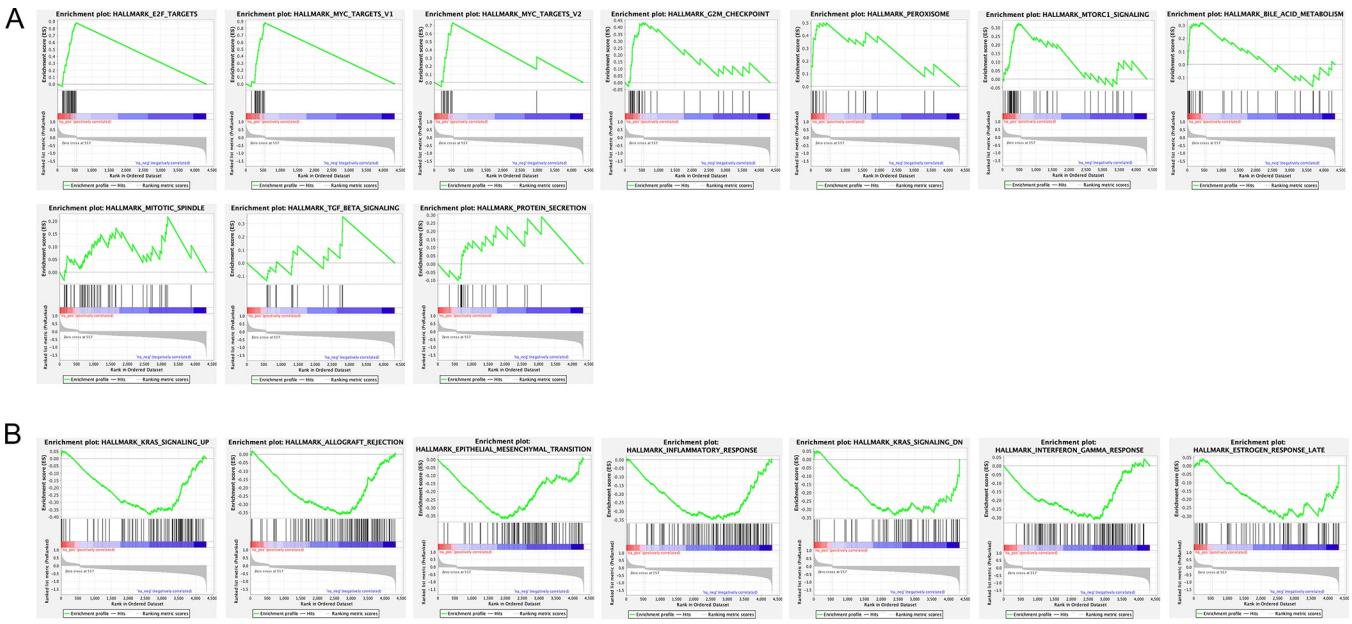

Fig 4. GSEA of *ST6GALNAC2* identified significant enrichment between DEG's and the CRC phenotype. GSEA of *ST6GALNAC2* was obtained via the TCGA dataset (TCGA, PanCancer Atlas) from cBioPortal outlining DEG's and a total of 42 gene sets associated with cancer hallmarks. (**A**) *ST6GALNAC2* highlighted 10 significantly enriched gene sets. FDR < 0.25 and p < 0.05. (**B**) Significant enrichment of seven gene sets was identified as being significantly downregulated. FDR < 0.25 and p < 0.05.

https://doi.org/10.1371/journal.pone.0311212.g004

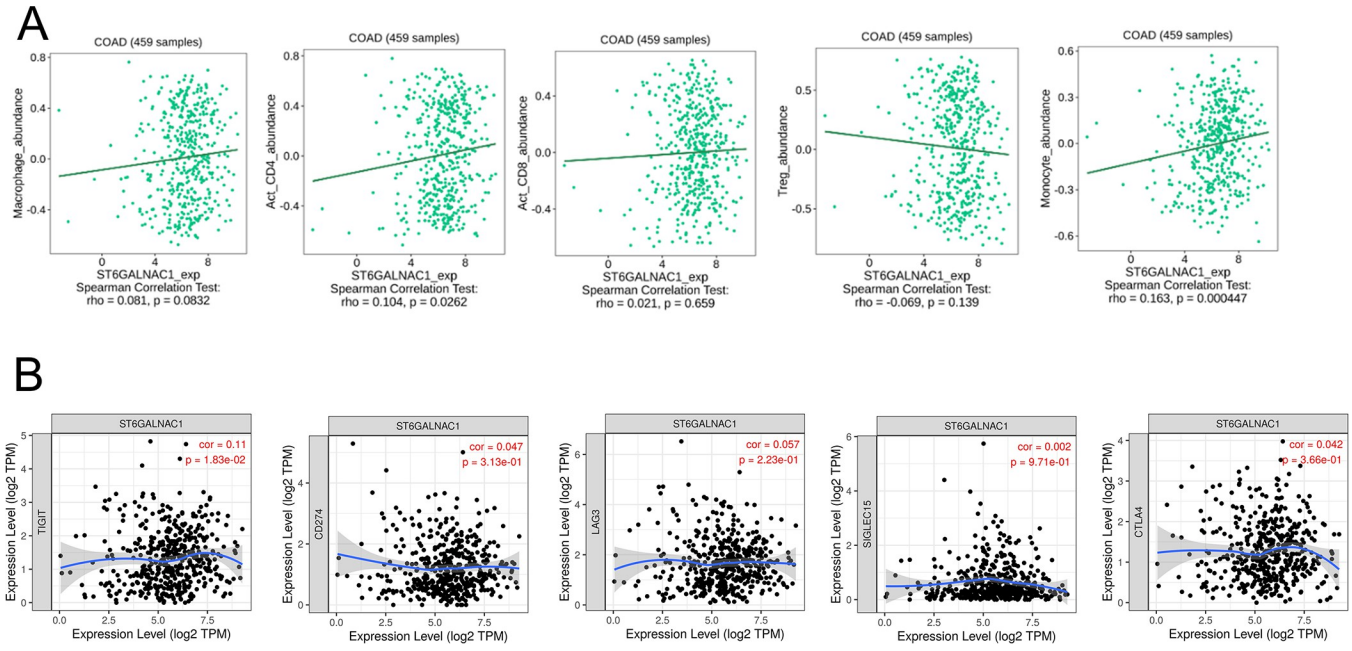

Fig 5. *ST6GALNAC1* correlates with CD4$^+$ T-lymphocytes and monocyte populations but shows no significant correlation with other pro-tumorigenic immune checkpoints. (**A**) SRCC between the abundance of macrophages, activated CD4$^+$ T-cells, activated CD8$^+$ T-cells, regulatory T-cells (Tregs), and monocytes were assessed in conjunction with the expression of *ST6GALNAC1* in COAD tumours. P < 0.05 was considered statistically significant. (**B**) The association between the abundance of *ST6GALNAC1* and pro-tumorigenic immune checkpoints was determined via TIMER analysis.

https://doi.org/10.1371/journal.pone.0311212.g005

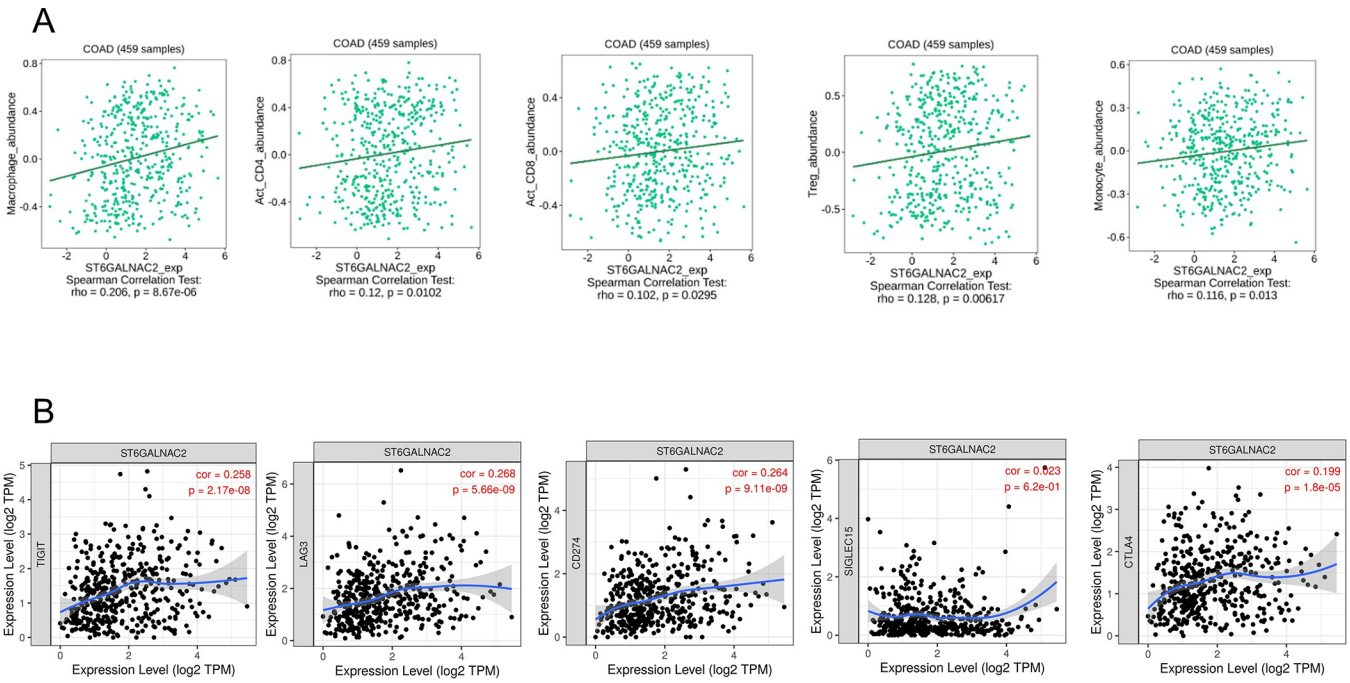

Fig 6. *ST6GALNAC2* correlated with the abundance of several infiltrating immune cell populations and displayed an association with most pro-tumorigenic immune checkpoints, excluding Siglec-15. (**A**) SRCC between the abundance of macrophages, activated $CD4^+$ T-cells, activated $CD8^+$ T-cells, regulatory T-cells (Tregs), and monocytes were assessed in conjunction with the expression of *ST6GALNAC2* in COAD tumours. $P < 0.05$ was considered statistically significant. (**B**) The association between the abundance of *ST6GALNAC2* and pro-tumorigenic immune checkpoints was determined via TIMER analysis.

https://doi.org/10.1371/journal.pone.0311212.g006

Dysregulated sialyltransferase expression correlated with poor clinical outcomes

To correlate the expression of *ST6GALNAC1* and *ST6GALNAC2* to patient survival data, survival curves outlining overall survival (OS), post-progression survival (PPS), and relapse-free survival (RFS) were determined (Fig 7). *ST6GALNAC1* shows low expression that is significantly correlated to poor prognosis based on OS criteria ($p < 0.05$), the RFS criterion ($p < 0.05$), and PPS ($p < 0.05$) survival in CRC patients (Fig 7A). Moreover, high *ST6GALNAC2* expression was significantly associated with poor prognosis in CRC patients under all survival criteria ($p < 0.05$) (Fig 7B).

ST6GALNAC1 protein expression is more prevalent in normal colon tissues

IHC analysis was performed to investigate the presence of *ST6GALNAC1* and *ST6GALNAC2* proteins in CRC tissues (Fig 8). Minimal staining for *ST6GALNAC1* and *ST6GALNAC2* was observed in the malignant tumour tissue cores, with representative images of *ST6GALNAC1* and *ST6GALNAC2* staining in the tissue sections shown (Fig 8A and 8B). Quantitative analysis of the staining revealed a significant decrease in the expression of *ST6GALNAC1* between normal and malignant tumour cores, with non-significant staining found in both subgroups for *ST6GALNAC2* staining.

Discussion

The current study has highlighted the multifaceted roles of both *ST6GALNAC1* and *ST6GALNAC2* and their collective association with the Siglec-15/Sia axis and its clinical relevance to

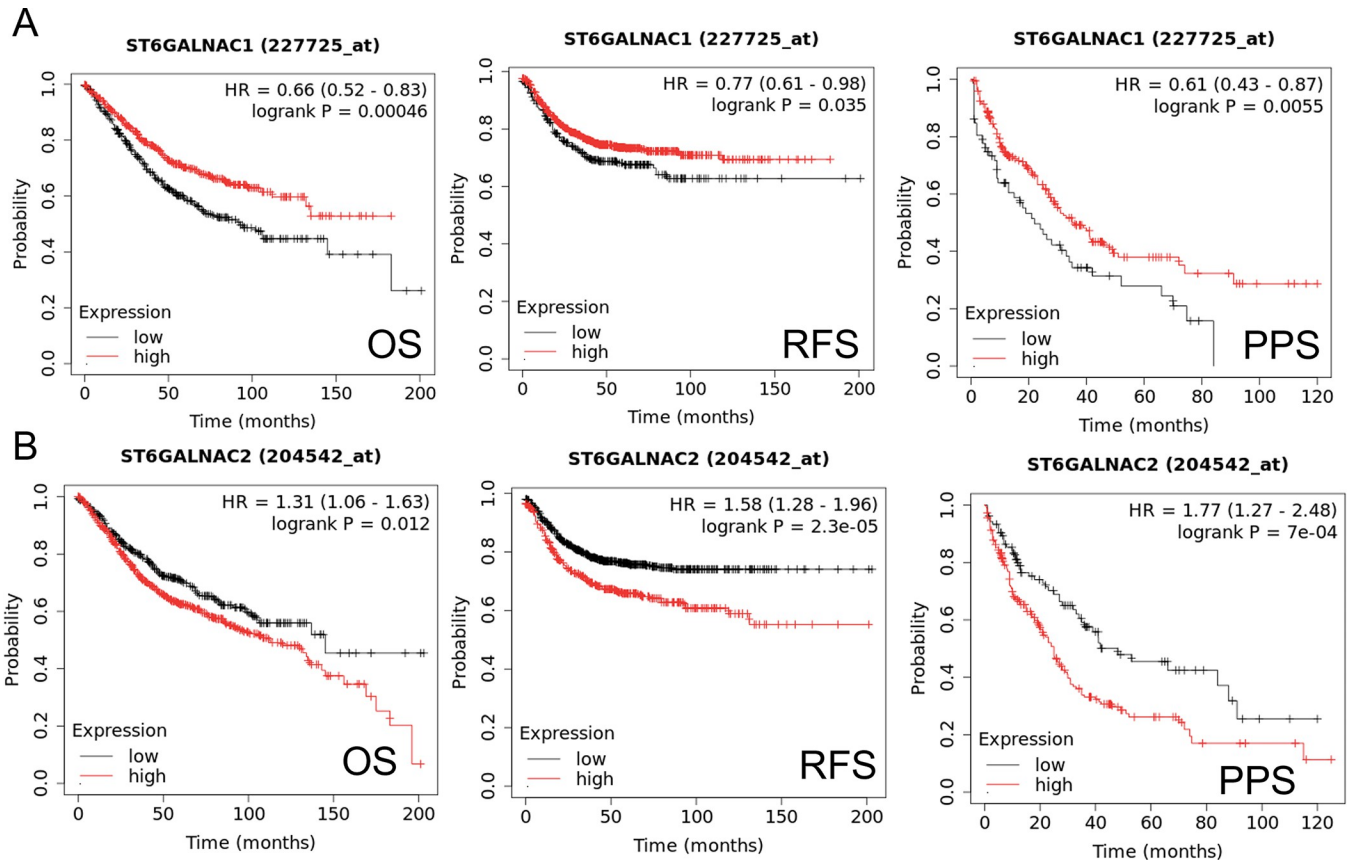

Fig 7. *ST6GALNAC1* shows low expression to be significantly correlated to poor prognosis based on survival criteria. High *ST6GALNAC2* expression was significantly associated with poor prognosis under all survival criteria. Only miR-940 OS criteria highlighted that low expression was associated with poor prognosis. (**A**) Survival curves outlining *ST6GALNAC1* expression with regard to patient survival data outlining overall survival (OS), post-progression survival (PPS), and relapse-free survival (RFS) criteria. $P < 0.05$ was considered statistically significant. (**B**) Survival curves outlining *ST6GALNAC2* expression with regard to patient survival data outlining overall survival (OS), post-progression survival (PPS), and relapse-free survival (RFS) criteria. $P < 0.05$ was considered statistically significant.

https://doi.org/10.1371/journal.pone.0311212.g007

CRC tumorigenesis. However, the regulatory mechanisms underlying their expression profiles remain unclear. Hence, we have identified possible regulatory mechanisms and miRNA candidates that seem to be involved in their regulation and, thereby, have some possible involvement in STn production.

The GeneMANIA database predicted *ST6GALNAC1* co-expression with *AGR2*. *AGR2* is localised to the endoplasmic reticulum (ER) and plays a crucial role in maintaining ER homeostasis via the formation, breakage, and isomerisation of the disulphide bonds involved in nascent protein maturation [27]. *AGR2* has also been found to be a prominent pro-tumorigenic gene that has consistently been associated with tumour onset and progression in a number of cancer types, including CRC [28,29]. Although AGR2 is predominantly localised in the ER, there is also evidence suggesting the extracellular secretion of AGR2 [30], where ER-resident AGR2 displays disparate O-glycosylation patterns compared to secreted AGR2 [31]. Similarly, *ST6GALNAC2* was shown to be co-expressed with and function alongside *AHSG*, an oncogene that is commonly associated with metabolic processes that have shown abnormal expression in multiple cancer types [32]. Furthermore, PPI interactions have highlighted that both sialyltransferases interact with a cluster of EEF1 proteins, particularly with EEF1A2. EEF1A2 serves an important role in modulating protein translation elongation and can play

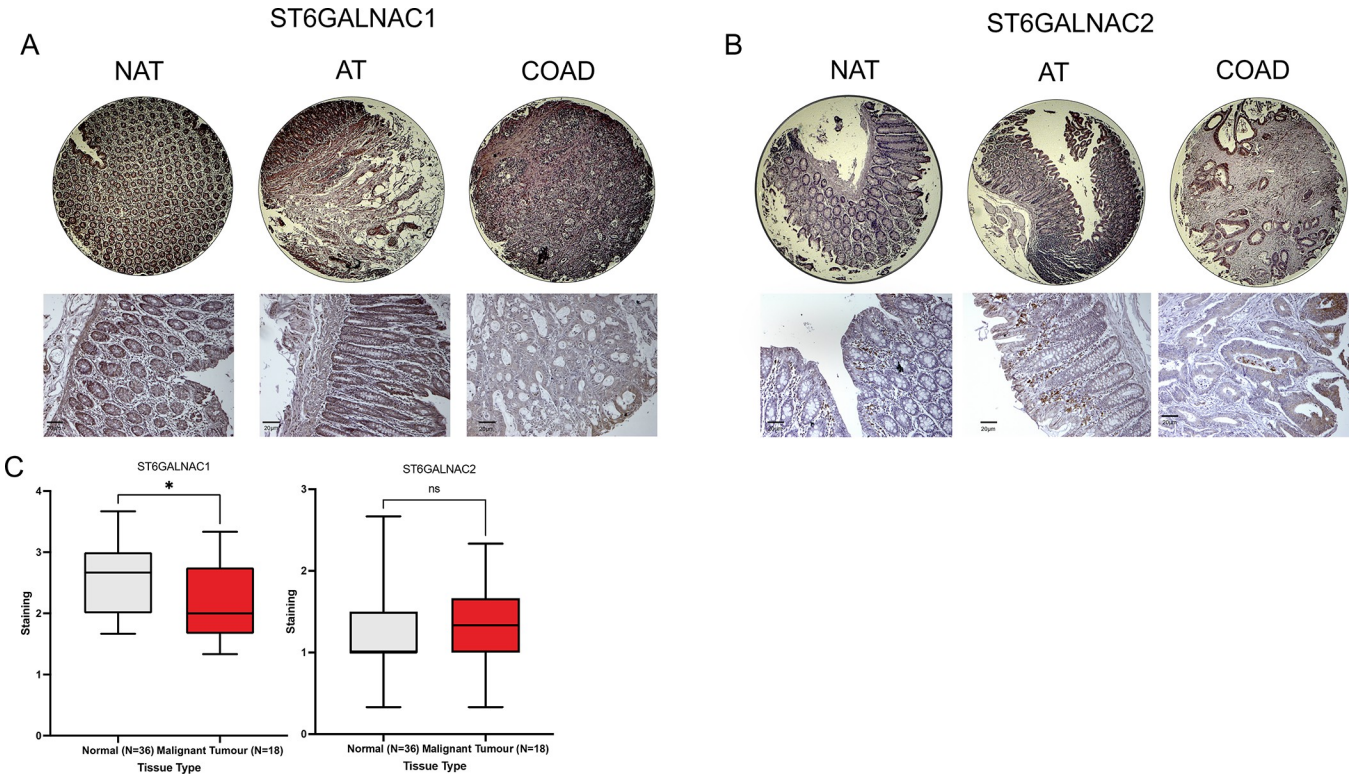

Fig 8. Low staining of *ST6GALNAC1* and *ST6GALNAC2* was observed in malignant tumour tissues. (**A**) IHC analysis was performed to investigate the presence of *ST6GALNAC1* in CRC tissues (BC05023a). Representative images of a total of 54 core tissue samples representing normal and malignant tissue cores were stained and visualised. (**B**) IHC analysis was performed to investigate the presence of *ST6GALNAC2* in CRC tissues (BC05023a). Representative images of a total of 54 core tissue samples, representing both normal and malignant tissue cores, were stained and visualised. (**C**) Quantitative analysis of the IHC staining for both *ST6GALNAC1* and *ST6GALNAC2* was performed for normal (clear) and malignant (red) tumour tissues. Unpaired student's t-test. $^{*}P < 0.05$.

https://doi.org/10.1371/journal.pone.0311212.g008

key roles in several biological processes [33]. To note, little is mentioned in the literature regarding the interactions between sialyltransferases and EEF1A2. However, *in vitro* studies have demonstrated that EEF1A2 is capable of regulating several signalling pathways, including PI3K/AKT and mTOR, via p53 inactivation [34]. Interaction with EEF1A2 could modulate the activity of ST6GALNAC1/ST6GALNAC2 and sialoglycan synthesis differently in normal and malignant tumour tissues.

Several previous studies have highlighted the aberrant expression of both sialyltransferase enzymes in multiple cancer types and the overexpression of the STn antigen [35,36]. However, TCGA genomic analysis highlighted significantly downregulated expression in the COAD subgroups for *ST6GALNAC1*. A previous study highlighted that increased *ST6GALNAC1* expression was only observed in the presence of M2 tumorigenic macrophages and CRC cells *in vitro*, which also stimulated the production of the STn antigen [37]. Moreover, another study outlined deficient mismatch repair (dMMR) CRC molecular subtype tumours displayed significantly downregulated expression of *GALNT6*, a prominent glycosyltransferase in glycan synthesis [38]. Consequently, this enhanced the pro-tumorigenic characteristics of SW480 cells *in vitro* and increased the expression of the Tn antigen, the precursor of the STn antigen. Additionally, GALNT6 was observed to interact with ST6GALNAC1 via our STRING analysis. This could suggest increased expression of the Tn antigen precursor molecule, and overexpression of STn may be independent of deregulated *ST6GALNAC1* expression in CRC and may require intercellular signalling to facilitate STn production in the TME. Further to this point,

interactions with TAMs may be necessary for enhanced expression patterns that drive tumour heterogeneity within the TME and CRC progression. Further evidence also highlighted the downregulated expression of *ST6GALNAC2* in CRC cells [39]. This was also similarly observed in CRC tumour samples [40]. Possible epigenetic mechanisms and regulatory expression through miRNA activity may indicate dysregulated sialyltransferase activity. In addition, both Tn and STn antigens are more prevalent in CRC tumours, correlating with poor prognosis and reduced clinical survival outcomes in patients [40,41].

UALCAN datamining also indicated enhanced methylation of the promoter region of *ST6GALNAC2* in primary COAD tumours, suggesting a possible explanation for silencing gene expression. Additionally, enhanced CpG island methylation in the promoter regions of tumour-specific genes has also been associated with CRC tumorigenesis and further presents as one of the molecular subtypes of CRC [42]. Enhanced methylation and subsequent silencing of *ST6GALNAC2* expression could prevent its expression. Similarly, epigenetic modifications of histone proteins, including deacetylation may also repress *ST6GALNAC2* transcription [43].

Simultaneously, predicted miRNA candidates involved in sialyltransferase regulation have exhibited high binding affinities for the seed regions on the 3' UTR of the mRNA target strand, suggesting a high likelihood of gene silencing [44]. Further to this point, full complementarity binding of the miRNA candidate to the target mRNA strand will lead to directed target degradation. In contrast, partial complementary binding can exhibit translational repression [45]. The role of pro-tumorigenic miR-21 has been characterised in the development and progression of multiple tumour malignancies, including CRC, which has also been highlighted as a potential tumour biomarker [46]. Furthermore, miR-21 was shown to induce advanced stage MSI type CRC tumours in conjunction with miR-335 activity, leading to poor prognosis in CRC patients [47]. In addition to this, miR-21 may play a role in tumour associated signalling pathways, including PI3K/AKT and TGF-β signalling [48,49]. This could suggest likely signalling pathways that stimulate CRC progression. Similarly, miR-30e has also been suggested as a potential biomarker for CRC development [50]. Moreover, miR-30e exhibited overexpression in CRC *in vitro* via stimulating the CXCL12 axis [51]. MiR-30e has also been demonstrated to be consistently deregulated in chemoresistant CRC patients [52]. The overexpression of miR-26b has also been observed in CRC and was identified to correlate with the expression of MMP-9 [53]. However, the role of miR-26b as an oncomir in CRC remains limited and requires further elucidation. Additionally, several miRNAs may facilitate the progression of the TME. Extracellular vesicles containing miR-21 stimulated tumour immune evasion in CRC via upregulated expression of the immune checkpoint PD-L1 in TAMs, thus enhancing tumour migration and invasion [54,55]. It has been understood that changes in miRNA expression patterns drive the onset of malignancies [56]. Moreover, the significance between these miRNA interactions on the seed region of the 3' UTR and *ST6GALNAC1* expression may address its downregulated expression in CRC tumour malignancies. Additionally, it may suggest miRNAs are involved in modulating tumour heterogeneity in CRC and their activity enhanced pro-tumorigenic characteristics including treatment resistance, which inevitably results in poor survival outcomes. However, other epigenetic modifications as were observed with *ST6GALNAC2* may downplay the roles of these sialyltransferases in STn production. Therefore, this may provide insights into how *ST6GALNAC1* can become deregulated and may suggest the involvement of other sialyltransferase proteins to play a role in STn production.

We have correlated the role of *ST6GALNAC1* and *ST6GALNAC2* expression and the enrichment of specific gene sets associated with cancer hallmarks.

With respect to *ST6GALNAC1*, upregulation of EMT and MYC targets provide ample evidence, as reported in the literature, of its role as a possible oncogene, and may also outline

possible signalling pathways through which to carry out tumorigenesis [57,58]. Of note, several downregulated mechanisms relating to *ST6GALNAC1* also involve IL-6-mediated JAK/STAT3 signalling. Pro-inflammatory stimulation of IL-6 underlines signalling via JAK/STAT3, which promote EMT in multiple cancer types [59]. JAK/STAT3 signalling pathways mediate the activation of EMT through a series of tyrosine and serine/threonine kinases [59]. A previous study associated EMT with CRC metastasis, emphasising crosstalk between CRC tumour cells and TAMs [60] *ST6GALNAC1* may facilitate TME heterogeneity following interactions with myeloid cells and EMT pathways. However, the observation of both this pathway and the inflammatory response showing downregulated enrichment supported our findings that EMT is mediated through another mechanism. This may suggest the activity of MYC targets in CRC progression. Disheveled-3 was shown to induce EMT in CRC progression mediated through MYC signalling and Wnt/β-catenin activity [61]. Moreover, syntrophin beta 1 (SNTB1) was shown to mediate EMT progression in CRC through a similar mechanism in knockdown studies [62]. Furthermore, enriched MYC targets may highlight the involvement of Zinc finger protein SNAI1 (SNAIL), a key regulator of the EMT process. Indeed, MYC was shown to induce SNAIL transcription and promote EMT via TGF-β action [63]. Characterisation of *ST6GALNAC1* and other gene targets in the MYC/Wnt/β-catenin crosstalk may propose a possible axis in CRC tumorigenesis.

ST6GALNAC2 enrichment exhibited E2F and MYC targets. E2F target involvement in transcriptional regulation can be correlated with the development of multiple tumour malignancies [64]. Moreover, upregulation of E2F activity was exhibited upon the characterisation of deregulated CRC KRAS mutant tumours and CIN type tumours [65]. E2F expression is also directly associated with clinicopathological features of CRC and correlated with poor clinical outcomes [66]. In addition, synergistic signalling between E2F1/MYC can mediate epigenetic modulation in CRC with targeted inhibition of the axis inducing p-53 independent arrest [67]. Furthermore, a recent study identified the expression of E2F7 activating the transcription of enhancer of zeste homolog 2 (EZH2), thus inducing mTOR signalling in glioblastoma progression [68]. Upon identifying that mTOR signalling is also enriched with regard to *ST6GALNAC2*, this could possibly indicate that a similar interaction could induce the PI3K/AKT/mTOR signalling pathway, possibly through EEF1A2 and MYC. Similarly, another pro-tumorigenic signalling pathway associated with CRC progression had identified TGF-β signalling as significantly enriched. TGF-β signalling is associated with several characteristics of CRC tumours including EMT, angiogenesis and immunosuppression [69]. Interestingly, the downregulated enrichment of the inflammatory response and IFNγ response were revealed. The downregulation of both pathways may indicate CRC tumours associated with *ST6GALNAC2* expression is not dependent on inflammatory stimuli. Stimulated IFNγ response is an immunomodulatory mechanism directed against infection, inflammation and anti-tumour activity [70]. Further to this, several inflammatory mediated diseases, including inflammatory bowel disease and ulcerative colitis, could manifest to colitis-associated CRC as a consequence of chronic inflammation [71]. Therefore, the downregulated enrichment of both pathways in GSEA analysis could suggest *ST6GALNAC2* expression is not mediated by inflammatory stimuli and its expression profile may be context-dependent.

The role of sialyltransferases and their involvement with immune infiltration highlighted possible interactions within the TME. Although the exhibited SRCC scores outline a non-correlative relationship > 0.2, there is significance in the expression of *ST6GALNAC1* and activated $CD4^+$ T-lymphocytes. A pan-cancer transcriptomics analysis identified monocytes and macrophages accounted for the largest proportion of tumour infiltrating myeloid cells [72]. The heterogeneity of the TME could possibly coincide with the pro-tumorigenic nature of several myeloid cell populations, including $CD4^+$ T-lymphocytes [73]. A pan-cancer analysis of

stromal heterogeneity was also able to predict the naïve $CD4^+$ T-lymphocyte response to immunotherapeutic treatment [74]. Furthermore, monocyte depletion is also correlated to an immunosuppressive phenotype [75]. Moreover, a previous study highlighted the differential expression of *ST6GALNAC1* and its regulatory miRNAs, corresponding with intra-tumour heterogeneity in CRC metastasis [76]. Immunotherapeutic treatment has shown positive treatment responses in patients. However, further targeting additional myeloid cell populations may drive clinical effectiveness. Monocytes exhibit heterogeneity and plasticity within the TME through differentiation to the polarised M2 immunosuppressive phenotype. Blocking M2 polarisation or stimulating M1 monocyte differentiation may reduce the presence of TAMs, thus improving immunotherapeutic approaches in CRC [77]. Furthermore, stimulating $CD4^+$ T-cells to Th1 cells could enhance $CD8^+$ T-cell activation, promoting anti-tumour activity [78]. Although *ST6GALNAC1* shares a weak association with *TIGIT*, the sialyltransferase also shares significant expression with *TIGIT*, another immune checkpoint associated with cancer progression [76]. TIGIT has been shown to promote myeloid cell exhaustion, including $CD8^+$ T-lymphocytes and enhanced expression profiles correlated with poor clinical outcomes in CRC [79]. This highlights the possibility of other immune checkpoint-related pathways contributing to tumour onset and tumour heterogeneity.

ST6GALNAC2 had shown significant association with several subsets of myeloid cells and immune infiltration. By directly interacting with cellular components associated with the TME, their interaction could modulate the induction of metastasis and immune tolerance [80]. Additionally, solid tumours could display immunogenicity due to the heterogeneous nature of the TME, largely characterised by an immune-induced inflammatory phenotype [81]. The correlation between *ST6GALNAC2* expression and immune cell infiltration may offer insights for improving the efficacy of immunotherapeutic approaches. Further to this, reducing the sialylation of glycans will allow greater antigen recognition and promote anti-tumour immunity [82]. The binding of the STn antigen and Siglec-15 drives TGF-β secretion via monocytes and macrophages, possibly establishing tumoral recruitment and enhancing tumour heterogeneity via *ST6GALNAC2* overexpression [83]. Likewise, associations with immune checkpoints excluding Siglec-15 highlight potential combination treatment therapies for immune checkpoint blockade, although the literature associating *ST6GALNAC2* and immune checkpoints remains limited.

Several studies have indicated enhanced expression of *ST6GALNAC1* in several cancer tissues, including lung adenocarcinoma (LUAD), lung squamous cell carcinoma (LUSC), and clear-cell renal cell carcinoma (ccRCC) samples [84,85]. However, the outlined survival curves obtained via datamining demonstrated low *ST6GALNAC1* expression correlated with poor clinical outcomes across all survival criteria ($p < 0.05$). Similarly, this also corroborated the *in silico* data and IHC staining, outlining higher expression of *ST6GALNAC1* in normal tissues. This possibly highlights the involvement of other sialyltransferases in the production of the STn antigen, and inducing effective binding with Siglec-15.

Interestingly, high levels of *ST6GALNAC2* expression were statistically significant in all survival criteria ($p < 0.05$) and were associated with poor clinical outcomes. However, this was not seen at the gene and protein levels obtained via *in silico* datamining and IHC staining. One possible explanation could stem from silenced gene expression and modulated expression via miRNA binding. Previous studies have highlighted miR-182 and miR-135b were shown to modulate the expression of *ST6GALNAC2* via the PI3K/AKT pathway, promoting chemoresistance and tumour invasiveness [21,86]. This could prove similar as mTOR signalling was significantly enriched with regard to *ST6GALNAC2* expression.

To illustrate the role of the STn antigen in the CRC landscape, multiple studies have shown the abnormal expression of the STn antigen and its precursor Tn antigen molecule in CRC

tumours [87]. Moreover, the expression of the STn antigen is not directly limited to solid CRC epithelial tumours. Circulating tumour cells of metastatic CRC patients expressed enhanced STn production, indicating its role in CRC metastasis to secondary organ sites [88]. Although the present study has identified possible miRNA candidates involved in the regulation of *ST6GALNAC1* and *ST6GALNAC2*, further sialyltransferase family members could play roles in CRC development. The STn antigen displays high binding affinity towards Siglec-15 [89]; however, other sialylated glycans have also displayed elevated binding affinity for Siglec-15 via *ST3GAL4* and *ST6GAL1* modulation [90]. Furthermore, GALNT enzymes highlighted by the STRING analysis are also heavily involved in GalNAc type-O glycosylation, this could suggest that members of the GALNT family including GALNT2 and GALNT6 facilitate glycan sialylation, including STn production. In addition, many GALNT genes have displayed dysregulated expression in CRC [91,92]. Therefore, this may suggest that downregulated *ST6GALNAC1* expression is independent to STn production. Elevated levels of STn and Tn antigens were also identified in CRC samples. However, their expression was induced by the loss of function of other glycosyltransferases, including C1GALT1 and COSMC, through promoter methylation or mutation [40]. Additionally, sulphation modifications of sialoglycans can also contribute to immune evasion and possible tumorigenesis. The overexpression of carbohydrate sulphotransferases, including *CHST1* and *CHST2*, can greatly induce the occurrence of hypersialylation and Siglec binding [93]. Furthermore, *CHST1* exhibited an accentuated effect on sialoglycan ligand binding and greatly impacted Siglec preference for O-glycans [94]. Further elucidation of the Siglec/Sia axis may highlight the role of other sialyltransferases in STn production.

Our findings highlighted a different view in the deregulated expression profiles of *ST6GALNAC1* and *ST6GALNAC2* in comparison to the literature. We believe that epigenetic modifications in conjunction with miRNA activity greatly impact gene expression and may outline sialyltransferase expression in relation to CRC as tumour specific. Furthermore, we provided insights into possible regulatory pathways and signalling pathways associated with their clinical relevance to CRC. Moreover, we believe that *ST6GALNAC1* and *ST6GALNAC2* is a minor player in the STn production in the case of CRC. The other sialyltransferase enzymes, such as *ST6GAL1*, *ST3GAL1*, and sulphotransferases *CHST1* might play a vital role in the production of the STn antigen in CRC.

Whilst a mutliomics approach identified the crosstalk of potential gene targets and regulatory pathways of sialyltransferase expression from the integration of several key datasets. There are significant limitations to consider when utilising multiple databases. Firstly, the well-defined regulatory pathways identified through *in silico* analysis may not fully highlight the interplay of sialylation and sialyltransferase activity without experimental validation to directly support their potential impact on cellular behaviour [95,96]. Further to this point, variation in methodologies may introduce false discoveries which highlight difficulties for data comparability [97]. Moreover, limited sample size and availability may impact *in silico* software thus creating challenges that require further sophisticated data mining tools. Additionally, there are also difficulties in histological staining for truncated O-glycan structures. Antibodies are required to have high specificity for antigen staining to prevent non-specific cross-reactive staining of similarly structured glycans [98]. However, addressing these limiting factors in association with experimental validation with further studies will provide more robust data interpretation and elucidation of sialyltransferase regulation.

In conclusion, the present study has predicted possible oncomirs involved in the regulation of *ST6GALNAC1* with high binding affinities, all of which displayed significantly upregulated expression in CRC tumours. However, downregulated expression of *ST6GALNAC1* in CRC might highlight the involvement of other sialyltransferases in the production of the STn

antigen and have suggested the interplay of several key sialyltransferases that could play a role. Moreover, we have identified several regulatory signalling pathways that have highlighted the clinical relevance of both *ST6GALNAC1* and *ST6GALNAC2* to CRC progression. Further elucidation of this pathway will give significant insights into the regulation of the Siglec-15/Sia axis.

Supporting information

S1 Table. Sialyltransferase predicted PPI relationships and targets. STRING network analysis for predicted protein-protein interactions and direct associations obtained via computational data mining for ST6GALNAC1 and ST6GALNAC2 sialyltransferase enzymes. The obtained framework was developed with a high confidence interval $\geq$0.700.
(DOCX)

S2 Table. Predicted miRNA binding targets for sialyltransferase gene regulation. *In silico* analysis to determine common miRNA targets predicted to modulate *ST6GALNAC1* via Venn diagrams.
(DOCX)

S3 Table. Enriched signalling pathways corresponding with cancer hallmarks relating to *ST6GALNAC1* expression. GSEA enrichment scores for the association of ST6GALNAC1 with cancer hallmarks *(*FDR $<$ 0.25 and p $<$ 0.05*)*.
(DOCX)

S4 Table. Enriched signalling pathways corresponding with cancer hallmarks relating to *ST6GALNAC2* expression. GSEA enrichment scores for the association of ST6GALNAC2 with cancer hallmarks *(*FDR $<$ 0.25 and p $<$ 0.05*)*.
(DOCX)

S1 Fig. *AHSG* exhibits upregulated expression in CRC tumours. UALCAN genomic data was used to determine the gene expression of STRING protein targets *AGR2* (ENSG00000106541) and *AHSG* (ENSG00000145192) and were compared between normal and tumour cohorts.
(TIF)

S2 Fig. The promoter region for ST6GALNAC2 is highly methylated in COAD tumours. UALCAN TCGA genomic data was used to identify promoter methylation of *ST6GALNAC1* (ENSG00000070526) and *ST6GALNAC2* (ENSG00000070731) and were compared between normal and colon adenocarcinoma (COAD) cohorts.
(TIF)

S3 Fig. The association between ST6GALNAC1 and ST6GALNAC2 gene expression was considered significant. The Pearson correlation coefficient comparing *ST6GALNAC1* and *ST6GALNAC2* gene expression was determined.
(TIF)

S4 Fig. Common miRNA targets between predicted PPI targets associated with ST6GALNAC1 and ST6GALNAC2. (**A**) No common miRNAs were predicted between *AGR2*, *AHSG*, *ST6GALNAC1* and *ST6GALNAC2*. MiR-432 was common between AGR2, ST6GALNAC1 and ST6GALNAC2. (**B**) Common miRNAs were determined between *GALNT3*, *GALNT8*, *B3GNT6* and *ST6GALNAC1*. MiR-30a-5p was predicted as the common miRNA between all four genes. (**C**) Common miRNAs were determined between *AHSG*, *C1GALT1C1*, *C1GALT1* and *ST6GALNAC2*. No common miRNAs were determined between each gene.
(TIF)

Acknowledgments

We are grateful to the School of Life and Medical Sciences, University of Hertfordshire, United Kingdom, for their support during this work.

Author Contributions

Conceptualization: Shoib Sarwar Siddiqui.

Data curation: Mohammed Saqif Ahmad.

Investigation: Mohammed Saqif Ahmad, Maria Braoudaki, Shoib Sarwar Siddiqui.

Methodology: Mohammed Saqif Ahmad, Maria Braoudaki, Shoib Sarwar Siddiqui.

Supervision: Maria Braoudaki, Shoib Sarwar Siddiqui.

Writing – original draft: Mohammed Saqif Ahmad.

Writing – review & editing: Mohammed Saqif Ahmad, Maria Braoudaki, Shoib Sarwar Siddiqui.

References

1. Xie Y-H, Chen Y-X, Fang J-Y. Comprehensive review of targeted therapy for colorectal cancer. Sig Transduct Target Ther. 2020; 5: 22. https://doi.org/10.1038/s41392-020-0116-z PMID: 32296018
2. Lam KK, Thean LF, Cheah PY. Advances in colorectal cancer genomics and transcriptomics drive early detection and prevention. The International Journal of Biochemistry & Cell Biology. 2021; 137: 106032. https://doi.org/10.1016/j.biocel.2021.106032 PMID: 34182137
3. Fan A, Wang B, Wang X, Nie Y, Fan D, Zhao X, et al. Immunotherapy in colorectal cancer: current achievements and future perspective. Int J Biol Sci. 2021; 17: 3837–3849. https://doi.org/10.7150/ijbs.64077 PMID: 34671202
4. Läubli H, Nalle SC, Maslyar D. Targeting the Siglec–Sialic Acid Immune Axis in Cancer: Current and Future Approaches. Cancer Immunology Research. 2022; 10: 1423–1432. https://doi.org/10.1158/2326-6066.CIR-22-0366 PMID: 36264237
5. Sun J, Lu Q, Sanmamed MF, Wang J. Siglec-15 as an Emerging Target for Next-generation Cancer Immunotherapy. Clinical Cancer Research. 2021; 27: 680–688. https://doi.org/10.1158/1078-0432.CCR-19-2925 PMID: 32958700
6. Wang Y, Xu Z, Wu K-L, Yu L, Wang C, Ding H, et al. Siglec-15/sialic acid axis as a central glyco-immune checkpoint in breast cancer bone metastasis. Proc Natl Acad Sci USA. 2024; 121: e2312929121. https://doi.org/10.1073/pnas.2312929121 PMID: 38252825
7. Gianchecchi E, Arena A, Fierabracci A. Sialic Acid-Siglec Axis in Human Immune Regulation, Involvement in Autoimmunity and Cancer and Potential Therapeutic Treatments. IJMS. 2021; 22: 5774. https://doi.org/10.3390/ijms22115774 PMID: 34071314
8. Siglec-15: An Attractive Immunotherapy Target. Cancer Discovery. 2020; 10: 7–8. https://doi.org/10.1158/2159-8290.CD-NB2019-136 PMID: 31806628
9. Ding H, Yao B, Ci L, Feng J, Ouyang P, Chen G, et al. Enhancing the Anti-tumor Potency of a Novel Siglec-15 Antibody by Engineering its Fc-mediated Effector Functions. Journal of Immunotherapy. 2023; 46: 161–169. https://doi.org/10.1097/CJI.0000000000000465 PMID: 37103472
10. Wu Q, Wei X, Chen F, Huang M, Zhang S, Zhu L, et al. Aptamer-Assisted Blockade of the Immune Suppressor Sialic Acid-Binding Immunoglobulin-Like Lectin-15 for Cancer Immunotherapy. Angew Chem Int Ed. 2023; e202312609. https://doi.org/10.1002/anie.202312609 PMID: 37955317
11. Ahmad MS, Braoudaki M, Patel H, Ahmad I, Shagufta, Siddiqui SS. Novel Siglec-15-Sia axis inhibitor leads to colorectal cancer cell death by targeting miR-6715b-3p and oncogenes. Front Immunol. 2023; 14: 1254911. https://doi.org/10.3389/fimmu.2023.1254911
12. Stanczak MA, Rodrigues Mantuano N, Kirchhammer N, Sanin DE, Jacob F, Coelho R, et al. Targeting cancer glycosylation repolarizes tumor-associated macrophages allowing effective immune checkpoint blockade. Sci Transl Med. 2022; 14: eabj1270. https://doi.org/10.1126/scitranslmed.abj1270 PMID: 36322632

13. Angata T, Tabuchi Y, Nakamura K, Nakamura M. Siglec-15: an immune system Siglec conserved throughout vertebrate evolution. Glycobiology. 2007; 17: 838–846. https://doi.org/10.1093/glycob/cwm049 PMID: 17483134

14. Munkley J, Oltean S, Vodák D, Wilson BT, Livermore KE, Zhou Y, et al. The androgen receptor controls expression of the cancer-associated sTn antigen and cell adhesion through induction of ST6GalNAc1 in prostate cancer. Oncotarget. 2015; 6: 34358–34374. https://doi.org/10.18632/oncotarget.6024 PMID: 26452038

15. Ogawa T, Hirohashi Y, Murai A, Nishidate T, Okita K, Wang L, et al. ST6GALNAC1 plays important roles in enhancing cancer stem phenotypes of colorectal cancer via the Akt pathway. Oncotarget. 2017; 8: 112550–112564. https://doi.org/10.18632/oncotarget.22545 PMID: 29348846

16. Schneider F, Kemmner W, Haensch W, Franke G, Gretschel S, Karsten U, et al. Overexpression of sialyltransferase CMP-sialic acid:Galbeta1,3GalNAc-R alpha6-Sialyltransferase is related to poor patient survival in human colorectal carcinomas. Cancer Res. 2001; 61: 4605–4611. PMID: 11389097

17. Miao X, Zhao Y. ST6GalNAcII mediates tumor invasion through PI3K/Akt/NF-κB signaling pathway in follicular thyroid carcinoma. Oncology Reports. 2016; 35: 2131–2140. https://doi.org/10.3892/or.2016.4590

18. Ali Syeda Z, Langden SSS, Munkhzul C, Lee M, Song SJ. Regulatory Mechanism of MicroRNA Expression in Cancer. IJMS. 2020; 21: 1723. https://doi.org/10.3390/ijms21051723 PMID: 32138313

19. Ghafouri-Fard S, Hussen BM, Badrlou E, Abak A, Taheri M. MicroRNAs as important contributors in the pathogenesis of colorectal cancer. Biomedicine & Pharmacotherapy. 2021; 140: 111759. https://doi.org/10.1016/j.biopha.2021.111759 PMID: 34091180

20. Shi Y, Liu Z, Lin Q, Luo Q, Cen Y, Li J, et al. MiRNAs and Cancer: Key Link in Diagnosis and Therapy. Genes. 2021; 12: 1289. https://doi.org/10.3390/genes12081289 PMID: 34440464

21. Jia L, Luo S, Ren X, Li Y, Hu J, Liu B, et al. miR-182 and miR-135b Mediate the Tumorigenesis and Invasiveness of Colorectal Cancer Cells via Targeting ST6GALNAC2 and PI3K/AKT Pathway. Dig Dis Sci. 2017; 62: 3447–3459. https://doi.org/10.1007/s10620-017-4755-z PMID: 29030743

22. Warde-Farley D, Donaldson SL, Comes O, Zuberi K, Badrawi R, Chao P, et al. The GeneMANIA prediction server: biological network integration for gene prioritization and predicting gene function. Nucleic Acids Research. 2010; 38: W214–W220. https://doi.org/10.1093/nar/gkq537 PMID: 20576703

23. Chandrashekar DS, Karthikeyan SK, Korla PK, Patel H, Shovon AR, Athar M, et al. UALCAN: An update to the integrated cancer data analysis platform. Neoplasia. 2022; 25: 18–27. https://doi.org/10.1016/j.neo.2022.01.001 PMID: 35078134

24. Ru B, Wong CN, Tong Y, Zhong JY, Zhong SSW, Wu WC, et al. TISIDB: an integrated repository portal for tumor–immune system interactions. Wren J, editor. Bioinformatics. 2019; 35: 4200–4202. https://doi.org/10.1093/bioinformatics/btz210

25. Li T, Fan J, Wang B, Traugh N, Chen Q, Liu JS, et al. TIMER: A Web Server for Comprehensive Analysis of Tumor-Infiltrating Immune Cells. Cancer Research. 2017; 77: e108–e110. https://doi.org/10.1158/0008-5472.CAN-17-0307 PMID: 29092952

26. Győrffy B. Survival analysis across the entire transcriptome identifies biomarkers with the highest prognostic power in breast cancer. Computational and Structural Biotechnology Journal. 2021; 19: 4101–4109. https://doi.org/10.1016/j.csbj.2021.07.014 PMID: 34527184

27. Moidu NA A Rahman NS, Syafruddin SE, Low TY, Mohtar MA. Secretion of pro-oncogenic AGR2 protein in cancer. Heliyon. 2020; 6: e05000. https://doi.org/10.1016/j.heliyon.2020.e05000

28. Xiu B, Chi Y, Liu L, Chi W, Zhang Q, Chen J, et al. LINC02273 drives breast cancer metastasis by epigenetically increasing AGR2 transcription. Mol Cancer. 2019; 18: 187. https://doi.org/10.1186/s12943-019-1115-y PMID: 31856843

29. Tian S, Chu Y, Hu J, Ding X, Liu Z, Fu D, et al. Tumour-associated neutrophils secrete AGR2 to promote colorectal cancer metastasis via its receptor CD98hc–xCT. Gut. 2022; 71: 2489–2501. https://doi.org/10.1136/gutjnl-2021-325137 PMID: 35086885

30. Fessart D, Domblides C, Avril T, Eriksson LA, Begueret H, Pineau R, et al. Secretion of protein disulphide isomerase AGR2 confers tumorigenic properties. eLife. 2016; 5: e13887. https://doi.org/10.7554/eLife.13887 PMID: 27240165

31. Pirro M, Mohammed Y, De Ru AH, Janssen GMC, Tjokrodirijo RTN, Madunić K, et al. Oxonium Ion Guided Analysis of Quantitative Proteomics Data Reveals Site-Specific O-Glycosylation of Anterior Gradient Protein 2 (AGR2). IJMS. 2021; 22: 5369. https://doi.org/10.3390/ijms22105369 PMID: 34065225

32. Xing X, Cao F, Gao L, Song M. AHSG, a Gene Promoting Tumour Proliferation, Migration and Invasion, is an Independent Prognostic Factor for Poor Overall Survival in Lung Adenocarcinoma. Mol Biol Rep. 2023; 50: 7659–7666. https://doi.org/10.1007/s11033-023-08623-x PMID: 37535244

33. Shen Z, Li Y, Fang Y, Lin M, Feng X, Li Z, et al. SNX16 activates c-Myc signaling by inhibiting ubiquitin-mediated proteasomal degradation of eEF1A2 in colorectal cancer development. Molecular Oncology. 2020; 14: 387–406. https://doi.org/10.1002/1878-0261.12626 PMID: 31876369

34. Pellegrino R, Calvisi DF, Neumann O, Kolluru V, Wesely J, Chen X, et al. EEF1A2 inactivates p53 by way of PI3K/AKT/mTOR-dependent stabilization of MDM4 in hepatocellular carcinoma: Pellegrino et al. Hepatology. 2014; 59: 1886–1899. https://doi.org/10.1002/hep.26954

35. Munkley J. The Role of Sialyl-Tn in Cancer. IJMS. 2016; 17: 275. https://doi.org/10.3390/ijms17030275 PMID: 26927062

36. Sanz-Martinez I, Pereira S, Merino P, Corzana F, Hurtado-Guerrero R. Molecular Recognition of GalNAc in Mucin-Type O-Glycosylation. Acc Chem Res. 2023; 56: 548–560. https://doi.org/10.1021/acs.accounts.2c00723 PMID: 36815693

37. Kvorjak M, Ahmed Y, Miller ML, Sriram R, Coronnello C, Hashash JG, et al. Cross-talk between Colon Cells and Macrophages Increases ST6GALNAC1 and MUC1-sTn Expression in Ulcerative Colitis and Colitis-Associated Colon Cancer. Cancer Immunology Research. 2020; 8: 167–178. https://doi.org/10.1158/2326-6066.CIR-19-0514 PMID: 31831633

38. Noda M, Okayama H, Tachibana K, Sakamoto W, Saito K, Thar Min AK, et al. Glycosyltransferase Gene Expression Identifies a Poor Prognostic Colorectal Cancer Subtype Associated with Mismatch Repair Deficiency and Incomplete Glycan Synthesis. Clinical Cancer Research. 2018; 24: 4468–4481. https://doi.org/10.1158/1078-0432.CCR-17-3533 PMID: 29844132

39. Fernández-Ponce C, Geribaldi-Doldán N, Sánchez-Gomar I, Navarro Quiroz R, Atencio Ibarra L, Gomez Escorcia L, et al. The Role of Glycosyltransferases in Colorectal Cancer. IJMS. 2021; 22: 5822. https://doi.org/10.3390/ijms22115822 PMID: 34070747

40. Sun X, Ju T, Cummings RD. Differential expression of Cosmc, T-synthase and mucins in Tn-positive colorectal cancers. BMC Cancer. 2018; 18: 827. https://doi.org/10.1186/s12885-018-4708-8 PMID: 30115016

41. Tian H, Yu J-L, Chu X, Guan Q, Liu J, Liu Y. Unraveling the role of C1GALT1 in abnormal glycosylation and colorectal cancer progression. Front Oncol. 2024; 14: 1389713. https://doi.org/10.3389/fonc.2024.1389713 PMID: 38699634

42. Nishiyama A, Nakanishi M. Navigating the DNA methylation landscape of cancer. Trends in Genetics. 2021; 37: 1012–1027. https://doi.org/10.1016/j.tig.2021.05.002 PMID: 34120771

43. Erfani M, Zamani M, Mokarram P. Evidence of histone modification affecting ARID1A expression in colorectal cancer cell lines. Gastroenterol Hepatol Bed Bench. 2022; 15: 32–38. PMID: 35611248

44. Wang X, He Y, Mackowiak B, Gao B. MicroRNAs as regulators, biomarkers and therapeutic targets in liver diseases. Gut. 2021; 70: 784–795. https://doi.org/10.1136/gutjnl-2020-322526 PMID: 33127832

45. Shang R, Lee S, Senavirathne G, Lai EC. microRNAs in action: biogenesis, function and regulation. Nat Rev Genet. 2023; 24: 816–833. https://doi.org/10.1038/s41576-023-00611-y PMID: 37380761

46. Li J, Chen H, Sun G, Zhang X, Ye H, Wang P. Role of miR-21 in the diagnosis of colorectal cancer: Meta-analysis and bioinformatics. Pathology—Research and Practice. 2023; 248: 154670. https://doi.org/10.1016/j.prp.2023.154670 PMID: 37418993

47. Calvo-López T, Paz-Cabezas M, Llovet P, Ibañez MD, Sastre J, Alonso-Orduña V, et al. Association of miR-21 and miR-335 to microsatellite instability and prognosis in stage III colorectal cancer. CBM. 2022; 34: 201–210. https://doi.org/10.3233/CBM-210353 PMID: 34958006

48. Lai C-Y, Yeh K-Y, Liu B-F, Chang T-M, Chang C-H, Liao Y-F, et al. MicroRNA-21 Plays Multiple Oncometabolic Roles in Colitis-Associated Carcinoma and Colorectal Cancer via the PI3K/AKT, STAT3, and PDCD4/TNF-α Signaling Pathways in Zebrafish. Cancers. 2021; 13: 5565. https://doi.org/10.3390/cancers13215565

49. Despotovic J, Dragicevic S, Nikolic A. Effects of Chemotherapy for Metastatic Colorectal Cancer on the TGF-β Signaling and Related miRNAs hsa-miR-17-5p, hsa-miR-21-5p and hsa-miR-93-5p. Cell Biochem Biophys. 2021; 79: 757–767. https://doi.org/10.1007/s12013-021-00980-3

50. Peng X, Wang J, Zhang C, Liu K, Zhao L, Chen X, et al. A three-miRNA panel in serum as a noninvasive biomarker for colorectal cancer detection. Int J Biol Markers. 2020; 35: 74–82. https://doi.org/10.1177/1724600820950740 PMID: 32914665

51. Wei K, Shi J, Xiao Y, Wang W, Yang Q, Chen C. [MiR-30e-5p overexpression promotes proliferation and migration of colorectal cancer cells by activating the CXCL12 axis via downregulating PTEN]. Nan Fang Yi Ke Da Xue Xue Bao. 2023; 43: 1081–1092. https://doi.org/10.12122/j.issn.1673-4254.2023.07.04 PMID: 37488790

52. Han J, Sun W, Liu R, Zhou Z, Zhang H, Chen X, et al. Plasma Exosomal miRNA Expression Profile as Oxaliplatin-Based Chemoresistant Biomarkers in Colorectal Adenocarcinoma. Front Oncol. 2020; 10: 1495. https://doi.org/10.3389/fonc.2020.01495 PMID: 33072545

53. Farouk S, El-Shenawy R, Khairy AM, Bader El-Din NG. Overexpression of Mirna 26A and 26B with Mmp-9 are Valuable Diagnostic Biomarkers for Colorectal Cancer Patients. Biomark Med. 2023; 17: 159–169. https://doi.org/10.2217/bmm-2022-0861 PMID: 37097025

54. Yin Y, Liu B, Cao Y, Yao S, Liu Y, Jin G, et al. Colorectal Cancer-Derived Small Extracellular Vesicles Promote Tumor Immune Evasion by Upregulating PD-L1 Expression in Tumor-Associated Macrophages. Advanced Science. 2022; 9: 2102620. https://doi.org/10.1002/advs.202102620 PMID: 35356153

55. Lan J, Sun L, Xu F, Liu L, Hu F, Song D, et al. M2 Macrophage-Derived Exosomes Promote Cell Migration and Invasion in Colon Cancer. Cancer Research. 2019; 79: 146–158. https://doi.org/10.1158/0008-5472.CAN-18-0014 PMID: 30401711

56. Hussen BM, Hidayat HJ, Salihi A, Sabir DK, Taheri M, Ghafouri-Fard S. MicroRNA: A signature for cancer progression. Biomedicine & Pharmacotherapy. 2021; 138: 111528. https://doi.org/10.1016/j.biopha.2021.111528

57. Gao F, Li X, Xu K, Wang R, Guan X. c-MYC mediates the crosstalk between breast cancer cells and tumor microenvironment. Cell Commun Signal. 2023; 21: 28. https://doi.org/10.1186/s12964-023-01043-1 PMID: 36721232

58. Shin AE, Giancotti FG, Rustgi AK. Metastatic colorectal cancer: mechanisms and emerging therapeutics. Trends in Pharmacological Sciences. 2023; 44: 222–236. https://doi.org/10.1016/j.tips.2023.01.003 PMID: 36828759

59. Huang B, Lang X, Li X. The role of IL-6/JAK2/STAT3 signaling pathway in cancers. Front Oncol. 2022; 12: 1023177. https://doi.org/10.3389/fonc.2022.1023177 PMID: 36591515

60. Wei C, Yang C, Wang S, Shi D, Zhang C, Lin X, et al. Crosstalk between cancer cells and tumor associated macrophages is required for mesenchymal circulating tumor cell-mediated colorectal cancer metastasis. Mol Cancer. 2019; 18: 64. https://doi.org/10.1186/s12943-019-0976-4 PMID: 30927925

61. Li Z, Yang Z, Liu W, Zhu W, Yin L, Han Z, et al. Disheveled3 enhanced EMT and cancer stem-like cells properties via Wnt/β-catenin/c-Myc/SOX2 pathway in colorectal cancer. J Transl Med. 2023; 21: 302. https://doi.org/10.1186/s12967-023-04120-8

62. Zhang H, Li Z, Jiang J, Lei Y, Xie J, Liu Y, et al. SNTB1 regulates colorectal cancer cell proliferation and metastasis through YAP1 and the WNT/β-catenin pathway. Cell Cycle. 2023; 22: 1865–1883. https://doi.org/10.1080/15384101.2023.2244778

63. Meškytė EM, Keskas S, Ciribilli Y. MYC as a Multifaceted Regulator of Tumor Microenvironment Leading to Metastasis. IJMS. 2020; 21: 7710. https://doi.org/10.3390/ijms21207710 PMID: 33081056

64. He J, Gao R, Yang J, Li F, Fu Y, Cui J, et al. NCAPD2 promotes breast cancer progression through E2F1 transcriptional regulation of CDK1. Cancer Science. 2023; 114: 896–907. https://doi.org/10.1111/cas.15347 PMID: 35348268

65. Chong W, Zhu X, Ren H, Ye C, Xu K, Wang Z, et al. Integrated multi-omics characterization of KRAS mutant colorectal cancer. Theranostics. 2022; 12: 5138–5154. https://doi.org/10.7150/thno.73089 PMID: 35836817

66. Xu Z, Qu H, Ren Y, Gong Z, Ri HJ, Zhang F, et al. Systematic Analysis of E2F Expression and Its Relation in Colorectal Cancer Prognosis. IJGM. 2022;Volume 15: 4849–4870. https://doi.org/10.2147/IJGM.S352141

67. Jeon D, Kim N, Um S-J. BET Inhibitors Induce p53-Independent Growth Arrest in HCT116 Cells *via* Epigenetic Control of the E2F1/c-MYC Axis. Biological & Pharmaceutical Bulletin. 2023; 46: 12–18. https://doi.org/10.1248/bpb.b22-00343

68. Yang R, Wang M, Zhang G, Bao Y, Wu Y, Li X, et al. E2F7−EZH2 axis regulates PTEN/AKT/mTOR signalling and glioblastoma progression. Br J Cancer. 2020; 123: 1445–1455. https://doi.org/10.1038/s41416-020-01032-y PMID: 32814835

69. Li X, Wu Y, Tian T. TGF-β Signaling in Metastatic Colorectal Cancer (mCRC): From Underlying Mechanism to Potential Applications in Clinical Development. IJMS. 2022; 23: 14436. https://doi.org/10.3390/ijms232214436

70. Coelho MA, Cooper S, Strauss ME, Karakoc E, Bhosle S, Gonçalves E, et al. Base editing screens map mutations affecting interferon-γ signaling in cancer. Cancer Cell. 2023; 41: 288–303.e6. https://doi.org/10.1016/j.ccell.2022.12.009

71. Zhou RW, Harpaz N, Itzkowitz SH, Parsons RE. Molecular mechanisms in colitis-associated colorectal cancer. Oncogenesis. 2023; 12: 48. https://doi.org/10.1038/s41389-023-00492-0 PMID: 37884500

72. Cheng S, Li Z, Gao R, Xing B, Gao Y, Yang Y, et al. A pan-cancer single-cell transcriptional atlas of tumor infiltrating myeloid cells. Cell. 2021; 184: 792–809.e23. https://doi.org/10.1016/j.cell.2021.01.010 PMID: 33545035

73. Zhao Q, Cheng Y, Xiong Y. LTF Regulates the Immune Microenvironment of Prostate Cancer Through JAK/STAT3 Pathway. Front Oncol. 2021; 11: 692117. https://doi.org/10.3389/fonc.2021.692117 PMID: 34868909

74. Qian J, Olbrecht S, Boeckx B, Vos H, Laoui D, Etlioglu E, et al. A pan-cancer blueprint of the heterogeneous tumor microenvironment revealed by single-cell profiling. Cell Res. 2020; 30: 745–762. https://doi.org/10.1038/s41422-020-0355-0 PMID: 32561858

75. Ortiz-Muñoz G, Brown M, Carbone CB, Pechuan-Jorge X, Rouilly V, Lindberg H, et al. In situ tumour arrays reveal early environmental control of cancer immunity. Nature. 2023; 618: 827–833. https://doi.org/10.1038/s41586-023-06132-2 PMID: 37258670

76. Urh K, Zidar N, Tomažič A, Boštjančič E. Intra-tumor heterogeneity of cancer stem cell-related genes and their potential regulatory microRNAs in metastasizing colorectal carcinoma. Oncol Rep. 2022; 48: 193. https://doi.org/10.3892/or.2022.8408

77. Olingy CE, Dinh HQ, Hedrick CC. Monocyte heterogeneity and functions in cancer. Journal of Leukocyte Biology. 2019; 106: 309–322. https://doi.org/10.1002/JLB.4RI0818-311R PMID: 30776148

78. Speiser DE, Chijioke O, Schaeuble K, Münz C. CD4+ T cells in cancer. Nat Cancer. 2023; 4: 317–329. https://doi.org/10.1038/s43018-023-00521-2 PMID: 36894637

79. Liang R, Zhu X, Lan T, Ding D, Zheng Z, Chen T, et al. TIGIT promotes CD8+T cells exhaustion and predicts poor prognosis of colorectal cancer. Cancer Immunol Immunother. 2021; 70: 2781–2793. https://doi.org/10.1007/s00262-021-02886-8 PMID: 33634371

80. Bai Z, Yan C, Chang D. Prediction and therapeutic targeting of the tumor microenvironment-associated gene CTSK in gastric cancer. Discov Onc. 2023; 14: 200. https://doi.org/10.1007/s12672-023-00821-0 PMID: 37930479

81. Chen DS, Mellman I. Elements of cancer immunity and the cancer–immune set point. Nature. 2017; 541: 321–330. https://doi.org/10.1038/nature21349 PMID: 28102259

82. Munkley J. Aberrant Sialylation in Cancer: Therapeutic Opportunities. Cancers. 2022; 14: 4248. https://doi.org/10.3390/cancers14174248

83. Hugonnet M, Singh P, Haas Q, Von Gunten S. The Distinct Roles of Sialyltransferases in Cancer Biology and Onco-Immunology. Front Immunol. 2021; 12: 799861. https://doi.org/10.3389/fimmu.2021.799861 PMID: 34975914

84. Bai Q, Liu L, Xi W, Wang J, Xia Y, Qu Y, et al. Prognostic significance of ST6GalNAc-1 expression in patients with non-metastatic clear cell renal cell carcinoma. Oncotarget. 2018; 9: 3112–3120. https://doi.org/10.18632/oncotarget.11258 PMID: 29423033

85. Alabiad M, Harb O, Abozaid M, Embaby A, Mandour D, Hemeda R, et al. The Diagnostic and Prognostic Roles of Combined Expression of Novel Biomarkers in Lung Adenocarcinoma (LUAD) and Lung Squamous Cell Carcinoma (LUSC); An Immunohistochemical Study. Iran J Pathol. 2021; 16: 162–173. https://doi.org/10.30699/ijp.2020.130944.2452

86. Liu B, Liu Y, Zhao L, Pan Y, Shan Y, Li Y, et al. Upregulation of microRNA-135b and microRNA-182 promotes chemoresistance of colorectal cancer by targeting ST6GALNAC2 via PI3K/AKT pathway. Molecular Carcinogenesis. 2017; 56: 2669–2680. https://doi.org/10.1002/mc.22710 PMID: 28767179

87. Dombek GE, Ore AS, Cheng J, Matsumoto Y, Glickman JN, Fleishman A, et al. Immunohistochemical analysis of Tn antigen expression in colorectal adenocarcinoma and precursor lesions. BMC Cancer. 2022; 22: 1281. https://doi.org/10.1186/s12885-022-10376-y PMID: 36476111

88. Neves M, Azevedo R, Lima L, Oliveira MI, Peixoto A, Ferreira D, et al. Exploring sialyl-Tn expression in microfluidic-isolated circulating tumour cells: A novel biomarker and an analytical tool for precision oncology applications. New Biotechnology. 2019; 49: 77–87. https://doi.org/10.1016/j.nbt.2018.09.004 PMID: 30273682

89. Murugesan G, Weigle B, Crocker PR. Siglec and anti-Siglec therapies. Current Opinion in Chemical Biology. 2021; 62: 34–42. https://doi.org/10.1016/j.cbpa.2021.01.001 PMID: 33607404

90. Briard JG, Jiang H, Moremen KW, Macauley MS, Wu P. Cell-based glycan arrays for probing glycan–glycan binding protein interactions. Nat Commun. 2018; 9: 880. https://doi.org/10.1038/s41467-018-03245-5 PMID: 29491407

91. Liao Y, Chuang Y, Lin H, Lin N, Hsu T, Hsieh S, et al. GALNT2 promotes invasiveness of colorectal cancer cells partly through AXL. Molecular Oncology. 2023; 17: 119–133. https://doi.org/10.1002/1878-0261.13347

92. Lavrsen K, Dabelsteen S, Vakhrushev SY, Levann AMR, Haue AD, Dylander A, et al. De novo expression of human polypeptide N-acetylgalactosaminyltransferase 6 (GalNAc-T6) in colon adenocarcinoma inhibits the differentiation of colonic epithelium. Journal of Biological Chemistry. 2018; 293: 1298–1314. https://doi.org/10.1074/jbc.M117.812826 PMID: 29187600

93. Jung J, Enterina JR, Bui DT, Mozaneh F, Lin P-H, Nitin, et al. Carbohydrate Sulfation As a Mechanism for Fine-Tuning Siglec Ligands. ACS Chem Biol. 2021; 16: 2673–2689. https://doi.org/10.1021/acschembio.1c00501

94. Büll C, Nason R, Sun L, Van Coillie J, Madriz Sørensen D, Moons SJ, et al. Probing the binding specificities of human Siglecs by cell-based glycan arrays. Proc Natl Acad Sci USA. 2021; 118: e2026102118. https://doi.org/10.1073/pnas.2026102118 PMID: 33893239

95. Kaur P, Singh A, Chana I. Computational Techniques and Tools for Omics Data Analysis: State-of-the-Art, Challenges, and Future Directions. Arch Computat Methods Eng. 2021; 28: 4595–4631. https://doi.org/10.1007/s11831-021-09547-0

96. Subramanian I, Verma S, Kumar S, Jere A, Anamika K. Multi-omics Data Integration, Interpretation, and Its Application. Bioinform Biol Insights. 2020; 14: 117793221989905. https://doi.org/10.1177/1177932219899051 PMID: 32076369

97. Ye Z, Vakhrushev SY. The Role of Data-Independent Acquisition for Glycoproteomics. Molecular & Cellular Proteomics. 2021; 20: 100042. https://doi.org/10.1074/mcp.R120.002204

98. Loureiro LR, Sousa DP, Ferreira D, Chai W, Lima L, Pereira C, et al. Novel monoclonal antibody L2A5 specifically targeting sialyl-Tn and short glycans terminated by alpha-2–6 sialic acids. Sci Rep. 2018; 8: 12196. https://doi.org/10.1038/s41598-018-30421-w PMID: 30111774

frontiers | Frontiers in Immunology

TYPE Original Research
PUBLISHED 06 October 2023
DOI 10.3389/fimmu.2023.1254911

OPEN ACCESS

EDITED BY
Leonardo Freire-de-Lima,
Federal University of Rio de Janeiro, Brazil

REVIEWED BY
Raphael Carmo Valente,
Universidade Federal do Rio de Janeiro, Brazil
Leonardo Marques da Fonseca,
Federal University of Rio de Janeiro, Brazil
Natalia Rodrigues Mantuano,
University Hospital of Basel, Switzerland

*CORRESPONDENCE
Shoib Sarwar Siddiqui
s.siddiqui3@herts.ac.uk
Shagufta
shagufta.waseem@aurak.ac.ae

RECEIVED 07 July 2023
ACCEPTED 22 September 2023
PUBLISHED 06 October 2023

CITATION
Ahmad MS, Braoudaki M, Patel H, Ahmad I, Shagufta and Siddiqui SS (2023) Novel Siglec-15-Sia axis inhibitor leads to colorectal cancer cell death by targeting miR-6715b-3p and oncogenes. *Front. Immunol.* 14:1254911. doi: 10.3389/fimmu.2023.1254911

Novel Siglec-15-Sia axis inhibitor leads to colorectal cancer cell death by targeting miR-6715b-3p and oncogenes

Mohammed Saqif Ahmad[1], Maria Braoudaki[1], Hershna Patel[1], Irshad Ahmad[2], Shagufta[2]* and Shoib Sarwar Siddiqui[1]*

[1]School of Life and Medical Sciences, University of Hertfordshire, Hatfield, United Kingdom, [2]Department of Biotechnology, School of Arts and Sciences, American University of Ras Al Khaimah, Ras Al Khaimah, United Arab Emirates

Siglecs are well known immunotherapeutic targets in cancer. Current checkpoint inhibitors have exhibited limited efficacy, prompting a need for novel therapeutics for targets such as Siglec-15. Presently, small molecule inhibitors targeting Siglec-15 are not explored alongside characterised regulatory mechanisms involving microRNAs in CRC progression. Therefore, a small molecule inhibitor to target Siglec-15 was elucidated *in vitro* and microRNA mediated inhibitor effects were investigated. Our research findings demonstrated that the SHG-8 molecule exerted significant cytotoxicity on cell viability, migration, and colony formation, with an IC_{50} value of approximately 20μM. SHG-8 exposure induced late apoptosis *in vitro* in SW480 CRC cells. Notably, miR-6715b-3p was the most upregulated miRNA in high-throughput sequencing, which was also validated via RT-qPCR. MiR-6715b-3p may regulate *PTTG1IP*, a potential oncogene which was validated via RT-qPCR and *in silico* analysis. Additionally, molecular docking studies revealed SHG-8 interactions with the Siglec-15 binding pocket with the binding affinity of -5.4 kcal/mol, highlighting its role as a small molecule inhibitor. Importantly, Siglec-15 and PD-L1 are expressed on mutually exclusive cancer cell populations, suggesting the potential for combination therapies with PD-L1 antagonists.

KEYWORDS

colorectal cancer, Siglec-15, sialic acid, inhibitor, miRNA, gene expression

1 Background

Colorectal cancer (CRC) has been referred to as the fourth most diagnosed cancer worldwide and the third leading cause of patient mortality in humans (1). Approximately, 1,931,590 new cases of CRC were reported with 935,137 patient deaths worldwide in 2020 (1). CRC has become increasingly prevalent worldwide as well, with statistical trends indicated cancer-related deaths could reach as high as 71.5% by 2035 (2). Currently,

conventional treatments for CRC patients have fallen short as successful therapeutic strategies, due to lacking in patient response, severe side effects and modest specificity consequently resulting in patient mortality and/or tumour recurrence (3). The recent trend of immunotherapy in solid cancers such as melanoma have shown success with blocking antibodies including Nivolumab and Pembrolizumab (4).

The blocking antibodies have also been approved for the treatment of CRC that have a high number of mutations with high microsatellite instability type (MSI-H) tumours (5). However, immunotherapy treatment has some limitations such as effectiveness in limited patient numbers, with acquired resistance to treatment a likely possibility (3). Therefore, a necessity to develop a novel approach to proficiently treat CRC has emerged.

Sialic acid-binding immunoglobulin-type of lectin 15 (Siglec-15) is a recently emerging immune checkpoint protein involved in suppressing the immune system and inducing cancer progression (6). An overexpression of Siglec-15 is commonly observed in various cell types. Most notably, it is upregulated on the surface of tumour cells. Pan-cancer analysis identified that this included various cancers such as CRC, non-small cell lung cancer (NSCLC), lung squamous cell carcinoma (SCC), ovarian cancer (OV), and others (7). Additionally, high Siglec-15 expression has been shown to correlate with increased MSI-H type tumours of CRC patients (8). Interestingly, the expression of both PDL-1 and Siglec-15 are mutually exclusive on cancer cell populations. Therefore, further treatments targeting Siglec-15 are required for Siglec-15 positive tumours.

MicroRNAs (miRNAs) are small non-coding RNA molecules approximately 20-25 nucleotides long capable of binding to the 3' untranslated region (UTR) of mRNA target molecules and regulating gene expression post-transcriptionally (9). Several miRNAs have shown differential expression profiles in CRC malignancies indicating oncogenic/tumour suppressive roles within CRC development and progression (10). The identification of specific miRNAs that is explicitly involved in CRC progression remains largely unclear. Interestingly, this study has given insights into the possible interactions between miRNAs and oncogenes for considerable strategies for the treatment of *SIGLEC15* positive CRC tumours.

The class of compounds, β-amino ketones, bearing an amino group at the beta carbon to ketone functional group is an important pharmacophoric feature employed in the synthesis of numerous natural products, drugs, and bioactive molecules (11). These compounds are biologically active scaffolds that exhibit a wide range of activities including anticancer, anti-inflammatory, antibacterial, antiviral, and antidiabetic etc. (12). In addition, several β-amino derived drugs are currently available for the treatment of various diseases and disorders (13).

Small drug-like molecules that modulate the immune system by targeting defined pathways or cells can improve the effectiveness of cancer immunotherapy (14). As far as our understanding with the literature, small molecules have not been explored for the treatment of Siglec-15 positive tumours by targeting Siglec-15. Considering the β-amino ketone's biological significance, we synthesised 3-(4-bromophenyl)-1-phenyl-3-(phenylamino)propan-1-one (SHG-8) through a one-step catalytic route using an environmentally benign solid acid nano-catalyst. We believed that the molecule SHG-8 being a small molecule in nature could possibly interact with the therapeutic target Siglec-15 and this could be our leading point towards the development of strategies for CRC treatment. Furthermore, the β-amino ketones affecting miRNA expression and subsequent interactions with genes and pathways in CRC development remains largely unknown. Therefore, it may be possible to identify miRNAs as targets for therapeutic treatment by elucidating their role in CRC development and their association to *SIGLEC15* regulation.

2 Materials and methods

2.1 Reagents and instruments

All the starting materials, reagents, and solvents were obtained from Merck and Spectrochem. The synthesis and characterization data of the sulfonic acid-functionalized silica nanospheres (SAFSNS), an environmentally benign solid acid nano-catalyst is available in our recent publication (15). The progress of the synthesis reaction of the SHG-8 molecule was monitored by using thin-layer chromatography (TLC) on silica gel plates and the spots were visualized under ultraviolet light (UV, λ254 nm). Infrared spectra were recorded on a PerkinElmer FTIR spectrophotometer. Mass spectra were measured with an electrospray (ESI-MS) on Shimadzu LCMS-spectrophotometer. ^{1}H and ^{13}C NMR spectra of the SHG-8 molecule were recorded using the Bruker AV-400 NMR spectrometer with tetramethylsilane as an internal standard. High Resolution Mass Spectrum (HRMS) was recorded on an Agilent 6540 HD Accurate Mass QTOF/LC/MS with electrospray ionization (ESI) technique.

2.1.1 Synthesis of 3-(4-bromophenyl)-1-phenyl-3-(phenylamino)propan-1-one

The SHG-8 molecule was prepared in a one-step catalytic reaction by a stirring mixture of acetophenone (1.1 mmol), 4-Bromo benzaldehyde (1 mmol), and aniline (1 mmol) in 1mL of ethanol at room temperature (RT), the sulfonic acid functionalized silica nano spheres (SAFSNS) nano-catalyst (0.03 g) was added. The reaction mixture was stirred at RT for 4h. After completion of the reaction as indicated by Thin Layer Chromatography (TLC), the reaction mixture was placed at ambient temperature to evaporate ethanol and water to obtain a yellow solid. The solid was dissolved in dichloromethane (5mL) at 35°C and filtered to remove the catalyst. The crude product was purified by the recrystallization technique, using an ethanol solvent to afford compound SHG-8 as a light-yellow solid: yield 85%.

2.2 Cell culture and treatments

Human CRC SW480 and GBM cell line U87MG were obtained from ATCC (ATCC, Virginia, USA). Human monocytic cell lines THP-1 and U937 were obtained from ATCC (ATCC, Virginia, USA). Additionally, the human normal colon tissue HcoEPiC cell line was obtained from iXcells Biotechnologies (iXcells Biotechnologies, San

Diego, USA). The adherent cell lines SW480 and U87MG were grown using DMEM (Gibco, Bleiswijk, Netherlands) and MEM (Gibco, Bleiswijk, Netherlands) media respectively, and supplemented with 10% FBS (Gibco, Bleiswijk, Netherlands) and 1% penicillin/streptomycin (Gibco, Bleiswijk, Netherlands). Both THP-1 and U937 suspension cell lines were grown using DMEM (Gibco, Bleiswijk, Netherlands) media respectively, and supplemented with 10% FBS (Gibco, Bleiswijk, Netherlands) and 1% penicillin/streptomycin (Gibco, Bleiswijk, Netherlands). Both cell lines were also differentiated into macrophages 48h post- phorbol 12-myristate 13-acetate (PMA) treatment (50ng/mL) for determining cytokine expression. The HcoEPiC cell line was grown using epithelial cell growth media (iXcells Biotechnologies, San Diego, USA) supplemented with 1% antibiotic-antimycotics (iXcells Biotechnologies, San Diego, USA). All cell lines were incubated at 37°C, 5% CO_2 and further experimental work was conducted upon reaching a minimum confluency of 80%. SHG-8 was solubilised in DMSO at a stock concentration of 10mM and further diluted for various assay experiments.

2.3 MTT assay

SW480 CRC cells ($1.5x10^4$ cells/well) and HcoEPiC cells were seeded at a cellular density of $2.5x10^4$ cells/well onto a 96 well-plate and left to incubate at 37°C, 5% CO_2 overnight. Following cell adherence, all wells were treated with varying SHG-8 concentrations: 20μM, 40μM, 60μM, 80μM, 100μM and were incubated for 24h at 37°C, 5% CO_2. Following overnight incubation, all wells were treated with 20μL MTT (0.5mg/mL) and were left to incubate for a further 2h at 37°C. The MTT was then removed, and the remaining crystals were treated and solubilised with isopropanol for 30 min on a shaker. Absorbance was then recorded at 540nm using a CLARIOstar plus multi-mode microplate reader (BMG LABTECH, Aylesbury, UK). Average percentage cell viability was calculated.

2.4 Migration assay

In total, $4x10^5$ cells/well were seeded onto a 12-well plate and left to incubate overnight at 37°C, 5% CO_2. Following cell adherence, vertical and horizontal scratches were made for each well using a 2μL pipette tip. The wells were then washed with PBS twice. All wells were treated with SHG-8 at 10μM and 40μM concentrations alongside control treatments. Images of the wound area were taken at 0h, 24h, 48h using an Olympus CKX41 inverted microscope (Olympus Life Science Solutions, Stansted, UK) at 4x magnification. All images taken relating to the wound area were then analysed using ImageJ analysis. Plugins for wound healing analysis were obtained from a previous study (16).

2.5 Colony formation assay

In total, $1x10^3$ cells/well were seeded onto a 12-well plate and left to incubate overnight at 37°C, 5% CO_2. Following cell adherence, the cells were then treated in triplicate with SHG-8 concentrations at 10μM and 40μM and were placed into the incubator for 24h. Following the 24h treatment period, the treatment was replaced with fresh media and left to incubate at 37°C, 5% CO_2 for a period of 7 days. The incubation period was determined by the total number of colonies formed in the DMSO control (colonies were determined as a cluster of cells totalling larger >30 cells). Following the 7-day incubation period, all wells were fixed with 4% PFA for total of 20 min. After fixation, all wells were washed with PBS three times for 5 min each before being stained with 0.1% crystal violet (Pro-Lab Diagnostics, Wirral, UK) for 45 min on a rocker. Following staining, all wells were washed with PBS for 3 min and images of all colonies were taken at 4x and 10x magnifications using an Olympus CKX41 inverted microscope (Olympus Life Science Solutions, Stansted, UK).

2.6 Nuclear fragmentation assay

SW480 cells ($4x10^5$ cells/well) were seeded onto coverslips within a 12 well-plate and left to adhere overnight at 37°C, 5% CO_2. The cells were treated with: DMSO, 10μM and 40μM SHG-8 as well as 100μM cisplatin for 24h. After the incubation period, all wells were washed with PBS. The cells were then fixed with 4% PFA for a period of 15-20 minutes and kept at RT. The fixation was removed and washed again with PBS. The coverslips were removed and placed onto slides with DAPI Antifade Mounting Medium (2Bscientific, Hatfield, UK). Fluorescent images were taken with an EVOS XL Core Imaging system (Fisher Scientific, Hemel Hempstead, UK) at 40x magnification with the DAPI filter.

2.7 Annexin-V/propidium iodide staining

To determine the stage of apoptosis induction post SHG-8 treatment, a total of $3x10^6$ cells/well were seeded onto a 6 well plate and left to adhere overnight. Following cellular adherence, all wells were treated with control conditions and SHG-8 at 10μM and 40μM conditions for a period of 24h. Following treatment, all wells were washed with ice-cold PBS and $1x10^6$ cells were harvested to 100μL suspensions. The SW480 cells were treated with 1μL of RNase A (10mg/mL) before being labelled with Annexin-V FITC (5μL) and propidium iodide (100μg/mL). Using the dead cell apoptosis kit with Annexin-V FITC and propidium iodide for flow cytometry (Invitrogen, Inchinnan, UK) to each 100μL cell suspension following the manufacturer's instructions. The cell suspensions were left to incubate at RT for a period of 15 min. Following incubation, 400μL of 1x binding buffer was added to each sample and left on ice before analysing via the Guavasoft 3.1.1 software and guava easyCyte HT system (Merck Millipore, Watford, UK).

2.8 Cell cycle arrest via flow cytometry method

Cell cycle analysis of SW480 cells at sub-G0/G1/S/G2/M phases post SHG-8 treatment was performed via PI staining using the dead

cell apoptosis kit with Annexin-V FITC and propidium iodide (Invitrogen, Inchinnan, UK) as per the manufacturer's instructions. The cells were harvested and treated with 100µg/mL PI and left to incubate for 15 min at RT. The cell suspensions were analysed using the Guavasoft 3.1.1 software and guava easyCyte HT system (Merck Millipore, Watford, UK).

2.9 ROS assay

To determine ROS production, SW480 ($1.5x10^4$ cells/well) cells were seeded onto a 96 well-plate and left to incubate overnight at 37°C, 5% CO_2. ROS production was determined using the Reactive Oxygen Species (ROS) Detection Assay Kit (Abcam, Cambridge, UK). Following cell adherence, 20µL ROS red dye was added to each of the wells and left to incubate at 37° C, 5% CO_2 for 1 hour. After the incubation period, 20µL of each sample treatment was added to each of the wells following manufacturer's instructions. Fluorescence readings were obtained at 15-, 30-, 45-, 60- and 75-minute intervals at Ex/Em = 520/605 nm using a CLARIOstar plus multi-mode microplate reader (BMG LABTECH, Aylesbury, UK).

2.10 Molecular docking study methods

A model of the Siglec-15 structure was downloaded from the AlphaFold Protein Structure Database with the corresponding UniProt entry Q6ZMC9, as there was no experimental structure available in the Protein Data Bank (17). The COACH server was used to predict protein-ligand binding sites on the AlphaFold model (18). The chemical structure of SHG-8 was obtained in SDF format. Molecular docking was carried out using the web app Webina 1.0.3 which runs Autodock Vina entirely in the web browser (19). The Siglec-15 AlphaFold model was uploaded as the receptor and the SHG-8 SDF file was uploaded as the ligand, both files were automatically converted to the PDBQT format for docking. The grid box was centred around the ARG143 binding site, and the parameters were set as follows: centre_x = -23, center_y = 6, center_z = 13.272 and size_x = 28, size_y =21, size_z = 22. The default settings of 2 CPUs and exhaustiveness of the global search set as 8 were used for docking.

2.11 IF staining

SW480 and U87MG cells ($3x10^5$ cells/well) were seeded onto coverslips onto a 12-well plate and left to incubate overnight. Following cell adherence, all wells were washed with PBS three times for 5 min each and then fixed with 4% PFA for a total of 15 min. With the fixation removed and washed with PBS, all wells were treated with a 1% BSA/PBS blocking buffer for 1h before incubating the primary Siglec-15 antibody (Life Technologies Limited, Renfrewshire, UK) at a dilution of 1:500 at 4°C overnight. Following this, the antibody is removed and washed with PBS before treating with an anti-rabbit Alexa-488 secondary antibody (Life Technologies Limited, Renfrewshire, UK) at a dilution of 1:500 for 1h at RT. The coverslips were then placed onto microscope slides and visualised with an EVOS XL Core Imaging system (Fisher Scientific, Hemel Hempstead, UK) at 40x magnification with the DAPI and GFP filter.

2.12 Siglec-15 expression via flow cytometry method

SW480 cells were seeded at a density of $3x10^6$ cells/well onto a 6 well plate and left to adhere overnight. Following cell adherence, the cells were treated with varying SHG-8 concentrations and controls for 24h. Post-treatment, the cells were washed with ice-cold PBS and harvested with 10mM EDTA at a cellular density of $1x10^6$ cells and resuspended in 2% BSA : PBS (fluorescence activated cell sorting buffer- FACS buffer). The cells were washed with ice-cold PBS and centrifuged at 200xg for 5 min twice. The cell samples were then resuspended in FACS buffer alongside the addition of a monoclonal Siglec-15 primary antibody (R&D Systems, Minneapolis, USA) (0.25µg) raised in mouse and left to incubate on ice for a period of 45 min. Following incubation, the cells were washed with ice-cold PBS and centrifuged at 200xg for 5 min twice before being resuspended in FACS buffer. Each cell suspension was treated with an anti-mouse Alexa- 488 secondary antibody (Life Technologies Limited, Renfrewshire, UK) and left to incubate on ice for a period of 30 min in the dark. After the secondary antibody incubation, the cells were washed once more with ice-cold PBS and centrifuged before being resuspended in FACS buffer for analysis via the guava easyCyte HT system (Merck Millipore, Watford, UK) and Guavasoft 3.1.1 software.

2.13 Cytokine expression via enzyme-linked immunosorbent assay method

The secretion of pro-inflammatory cytokines TNF-α and IL-1β were evaluated in THP-1 and U937 differentiated macrophages following SHG-8 treatment. Both cell lines were differentiated into macrophages with PMA (50ng/mL) for 48h prior to 40µM SHG-8 treatment and LPS (50ng/mL) stimulation for 24h. The supernatant was harvested and were placed as duplicates onto microwell strips alongside standards using the respective cytokine human ELISA kit (Life Technologies Limited, Renfrewshire, UK) after several wash steps as per the manufacturer's instructions. 50µL of biotin-conjugate were added to all the strips and were left to incubate at RT for 2h on a microplate shaker. Following the incubation period, the strips were washed and 100µL of streptavidin-HRP were added to all the strips for 1h. The strips were then washed again following the incubation period. After consecutive wash steps, 100µL of TMB substrate solution were added to all wells and left to incubate at RT for 10 min or until a noticeable colour change was observed. Following colour development, 100µL of stop solution were added to each of the strips and was then measured at 620nm using a CLARIOstar microplate reader (BMG LABTECH, Aylesbury, UK).

2.14 RNA extraction and RT-qPCR methods

Total RNA was extracted from SW480 cultured cells 24hrs post-treatment under the following conditions: DMSO, SHG-8 10μM and 40μM as well as 100μM cisplatin using the TRIzol method (Life Technologies Limited, Renfrewshire, UK). RNA quality and quantity of all treated samples for gene and miRNA expression analyses were evaluated using a Nanodrop ND-1000 spectrophotometer UV-Vis Nanogen Inc. (Marshall Scientific, Hampton, USA). Following quantification, expression measurement analysis of treated samples had undergone Dnase treatment with the Rnase-free Dnase set respectively (Qiagen, Hilden, Germany). In brief, the mRNA samples for gene analysis were directly subjected to cDNA synthesis and subsequent RT-qPCR was performed using the High-Capacity cDNA reverse transcription kit (Applied Biosystems, Massachusetts, USA) followed by the Taqman Fast Advanced Mastermix, no UNG (Applied Biosystems, Massachusetts, USA) and PowerUp SYBR Green Mastermix (Applied Biosystems, Massachusetts, USA for probe-based and SYBR green qPCR analyses. SYBR green primer sequences involved in analysis are as follows: *GAPDH* forward (GGAGCGAGATCCCTCCAAAAT) and reverse (GGCTG TTGTCATACTTCTCATGG) and *PTTG1IP* forward (GTCT GGACTACCCAGTTACAAGC) and reverse (CGCCTCAA AGTTCACCCAA). All treated samples collected for miRNA expression analysis were further purified and subjected to miRNA enrichment with the miRvana miRNA Isolation Kit (Life Technologies Limited, Renfrewshire, UK). Following this, miRNA samples were further quantified for their RNA quality and quantity prior to reverse transcription with the TaqMan MicroRNA Reverse Transcription kit (Applied Biosystems, Massachusetts, USA). RT-qPCR of individual Taqman miRNA assays (Applied Biosystems, Massachusetts, USA) were performed using the TaqMan Universal Mastermix II, no UNG (Applied Biosystems, Massachusetts, USA) following manufacturer's instructions. All samples were performed in triplicate using the QuantStudio 7 Flex Real-Time PCR System (Applied Biosystems, Massachusetts, USA). GAPDH and U47 used as housekeeping controls respectively. Relative expression of *SIGLEC15* and candidate miRNAs and genes were performed using the $\mathbf{2^{-\Delta\Delta Ct}}$ **method.**

2.15 Small-RNA sequencing

To determine the differential expression of miRNAs treated with SHG-8, sRNA-seq was outsourced to Biomarker Technologies (Biomarker Technologies, Inc., CA, USA). SW480 cells were subjected to 24hrs SHG-8 treatment prior to total RNA extraction via TRIzol reagent method. The purity and quantity of each RNA sample was processed using a Nanodrop ND-1000 spectrophotometer UV-Vis Nanogen Inc. (Marshall Scientific, Hampton, USA) and 4150 TapeStation System (Agilent Technologies, California, USA). All samples were recorded with RIN numbers >7.0. The resulting data was subjected to Kyoto Encyclopedia of Genes and Genomes (KEGG), Gene Set Enrichment Analysis (GSEA) and Gene Ontology (GO) to identify enriched pathways, biological processes, molecular function, and cellular components in relation to CRC.

2.16 UALCAN datamining

The UALCAN database (http://ualcan.path.uab.edu, accessed on 9 May 2023) was utilised for TCGA cancer genomic analysis and is presented as a tool for cancer transcriptomics. Utilising TCGA genomic data, the expression of selected miRNAs was compared among both tumour and normal subgroups. *PTTG1IP* expression in normal and tumour subgroups were also compared at the protein level.

2.17 Statistical analysis

MTT assays for both SW480 and HcoEPiC cell lines and colony formation assays evaluating the effect of SHG-8 on cancer cells and cytokine secretion of SHG-8 treated THP-1 and U937 differentiated macrophages were compared using the one-way ANOVA statistical test followed by Dunnett's multiple comparison *post-hoc* test to identify any statistical significance. The migration assay compared all treatment conditions with Welch's one-way ANOVA followed by Dunnett's multiple comparison *post-hoc* test. Additionally, determining the effect of ROS production in the induction of apoptosis used the two-way ANOVA statistical test followed by Dunnett's multiple comparison *post-hoc* test. RT-qPCR expression analyses of *SIGLEC15*, gene targets and candidate miRNAs were compared with the one-way ANOVA statistical test and Dunnett's multiple comparison test. Genomic and proteomic data of candidate miRNAs and gene targets between normal and tumour subgroups were compared with an unpaired student's t-test. Statistical analysis was performed using GraphPad prism 8. **P<0.05, **P<0.01, ***P<0.001, **** P<0.0001* were considered as statistically significant.

3 Results

3.1 Synthesis and characterisation of β-amino ketones

The 3-(4-bromophenyl)-1-phenyl-3-(phenylamino)propan-1-one SHG-8 molecule was synthesised efficiently using our in-house developed environmentally benign solid acid nano-catalyst (SAFSNS) at ambient temperature and in good yield. The compound SHG-8 was characterized by spectroscopic techniques including IR, Mass, ^{1}HNMR and ^{13}C NMR and melting point that accurately matches with the literature data (20). The observed melting point of compound SHG-8 was 122-126°C that corresponds to the literature melting point (123–127°C). The sharp peak at 3391 (medium) and 1667 (strong) cm^{-1} in IR spectrum indicated the presence of -NH and C=O group respectively (Figure 1A). In the ^{1}H NMR spectrum of compound SHG-8 (Figure 1B), the two $COCH_2$ protons appeared as multiplet

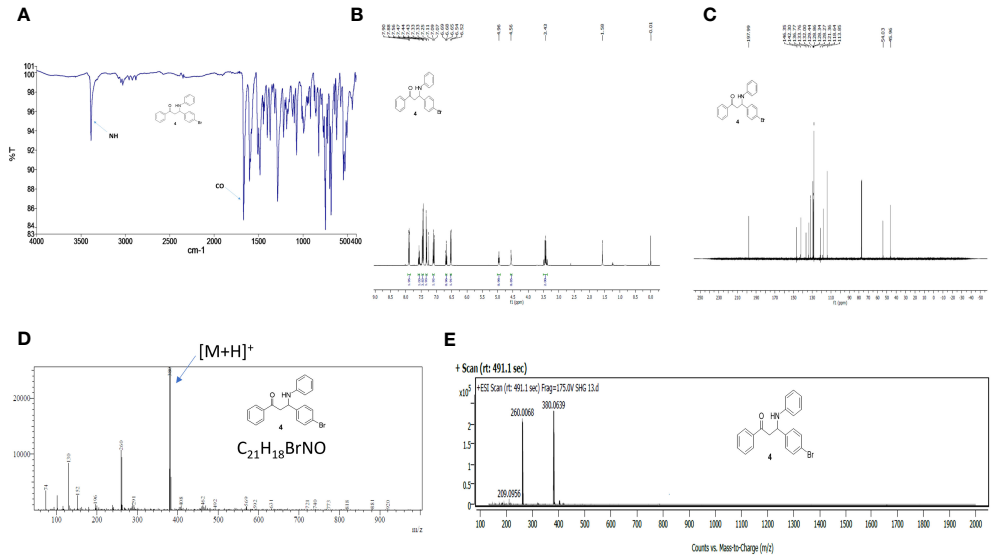

FIGURE 1
Spectra of compound 4 (SHG-8). **(A)** FTIR spectrum. **(B)** ^{1}H NMR spectrum in $CDCl_3$. **(C)** ^{13}C NMR spectrum $CDCl_3$. **(D)** ESI-MS spectrum. **(E)** High-resolution mass spectrum (HRMS).

at δ 3.41-3.45 and the one NH proton appeared as singlet at δ 4.56. The one CH proton next to NH group appeared as a triplet at δ 4.96. The fourteen aromatic protons were observed in the downfield region, including a doublet at δ 6.53 (J = 8 Hz) for two protons, triplet at δ 6.68 for one proton, multiplet at δ 7.07-7.11 for two protons, doublet at δ 7.31 (J = 8Hz) for two protons, multiplet at δ 7.42-7.57 for four protons, multiplet at δ 7.55-7.57 for one proton and a doublet at δ 7.79 (J = 8 Hz) for two protons. The ^{13}C NMR spectrum of compound SHG-8 (Figure 1C) was also in full agreement with the assigned structures showing fifteen peaks at δ 45.9, 54.1, 113.8, 118.6, 121.3, 128.2, 128.3, 128.8, 129.4, 132.0, 133.7, 136.7, 142.3, 146.3, 197.9. The MS (ESI) spectra showed M+ +H peak at m/z 380 (Figure 1D) and in the HRMS (ESI) spectra (Figure 1E) the m/z peak is found at 380.0639 matching with the calculated m/z for $C_{21}H_{19}BrNO$ $[M+H]^+$ which is 380.0645, showing the delta value 0.0006.

3.2 Cytotoxic ability of SHG-8 on CRC cells

The cytotoxic effect of SHG-8 was evaluated *in vitro* on the SW480 CRC cell line via MTT, wound healing and colony formation assays (Figure 2). Using cisplatin as a positive control, SHG-8 has demonstrated a significant dose-dependent cytotoxic effect on the SW480 cell line with an IC_{50} value of ~20μM, and significant cell death of ~90% upon reaching 80-100μM concentrations ($p<0.0001$) (Figure 2B). Wound healing has also shown an anti-tumour effect on cellular migration with the SHG-8 40μM concentration showing significant reduction of 15.37% at 24 hours ($p<0.05$) (Figure 2C). Additionally, both SHG-8 10μM and 40μM concentrations have shown similar reductions for 48 hours at 13.22% and 13.28% respectively in comparison to the DMSO control, possibly only effective in the early time points. SHG-8 has also shown a significant negative effect on colonisation of cancer cells (Figures 2E-G). Both 10μM and 40μM SHG-8 concentrations produced no colonies on the plate as also observed with the cisplatin control ($p<0.0001$) (Figure 2G).

3.3 SHG-8 induced apoptosis in SW480

SHG-8 was evaluated on whether it could induce apoptotic cell death to produce its cytotoxic effect (Figure 3). DAPI staining was performed to see cell fragmentation as a marker of apoptosis. Initially, SHG-8 induced apoptosis in a dose-dependent manner with nuclear fragmentation occurring at both 10μM and 40μM concentrations (Figure 3A). Morphological changes of the cancer cells were also apparent; with irregular structural changes indicating a consequential effect of nuclear fragmentation; shown with white arrows. Furthermore, dual staining with Annexin-V and PI has shown significant apoptosis induction in cisplatin 100μM, SHG-8 10μM and 40μM conditions in comparison to the DMSO control (Figure 3B). The cisplatin condition had a larger percentage of cells within early apoptosis at 13.88% (lower right quadrant) whilst both SHG-8 10μM and 40μM conditions had a larger percentage of cells exhibiting late apoptosis induction (upper right quadrant) at 15.74% and 17.75% respectively when compared to DMSO. All conditions have shown a minimal number of cells exhibiting necrotic like features (upper left quadrant). Moreover, cell cycle arrest analysis of SHG-8 treated SW480 cells have shown an increased presence in the G2/M phase with SHG-8 at 10μM (13.314%) and 40μM (16.168%) which demonstrated the greatest increase in comparison to the DMSO control condition (10.968%) (Figure 3C). Cisplatin shows the greatest number of cells present in the S phase (12.802%) of the cell cycle in comparison to SHG-8 treatments of 10μM and 40μM at 5.954% and 5.975% respectively. Further to this, there are minimal

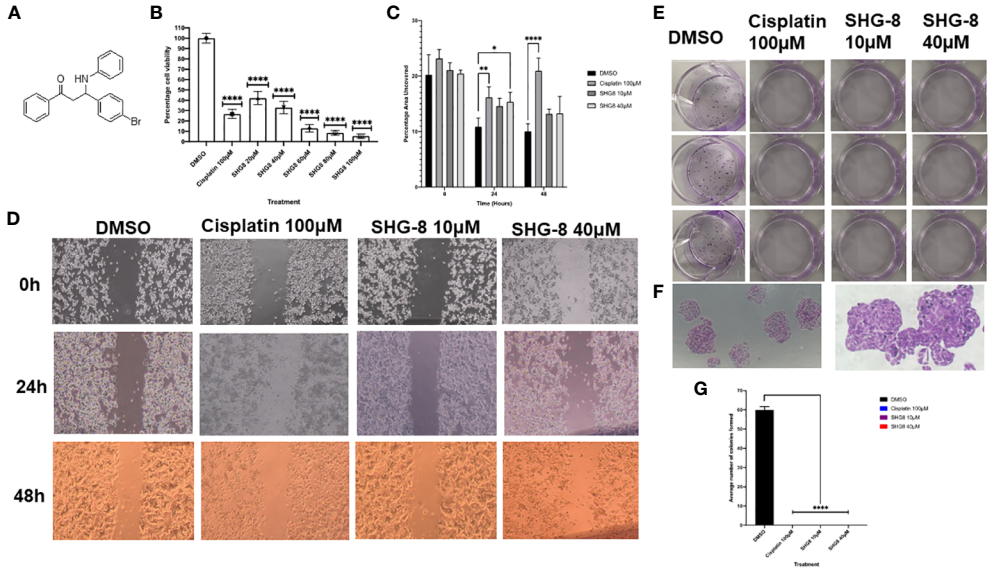

FIGURE 2
The anti-tumorigenic effect of the β-amino ketone SHG-8 against SW480 CRC cancer cells *in vitro*. **(A)** The molecular structure of compound SHG-8. **(B)** MTT assay was conducted to determine the IC_{50} of SHG-8 24 h post-treatment and to evaluate its cytotoxic effects *in vitro* (N=5). Data is presented as mean ± SEM. One-Way ANOVA statistical test followed by Dunnett's multiple comparison *post-hoc* test **** P<0.0001. **(C)** Migration assay was conducted to evaluate the effect of SHG-8 on cellular migration following 48h post-treatment (N=3). Data is presented as mean ± SEM. Welch's One-Way ANOVA followed by Dunnett's multiple comparison *post-hoc* test. *P<0.05, **P<0.01, ***P<0.001, **** P<0.0001. **(D)** 4x microscopic images taken of the wound area across all treatment conditions over the 48h treatment period. Images were analysed via ImageJ with inserted plugins outlined by Suarez-Arnedo et al., 2020. **(E)** Visual image outlining the 12-well plate utilised for the colony formation assay 7-days post-treatment. **(F)** 4x and 10x microscopic images taken of SW480 cellular colonies of the DMSO condition 7-days post-treatment. Colonies were counted as clusters of cells >30. **(G)** Colony formation assay outlining the effect of SHG-8 on SW480 colony formation and cell proliferation 7 days post-treatment (N=3). Data is presented as mean ± SD. One-way ANOVA statistical test followed by Dunnett's multiple comparison *post-hoc* test. **** P<0.0001 were considered as statistically significant.

cell populations present in the sub-G0 phase in all treatment conditions. Additionally, a ROS assay was performed to investigate the role of ROS production on the likelihood of apoptosis induction (Figure 3D). From this, it can be inferred that ROS production seemingly exhibited no effect on cell death.

3.4 Molecular docking of Siglec-15 and expression analysis

The top ranked binding site predicted by the COACH server included the amino acid residues of Siglec-15 at positions: 44, 70, 143,152,153,154,155 and 157 (Supplementary Figure 1) and the region selected as the target site for docking was predicted with very high confidence by AlphaFold. The highest predicted binding affinity between SHG-8 and Siglec-15 was -5.4 kcal/mol and the docking pose revealed that SHG-8 binds around a narrow cleft on the surface of the protein. The amino acid residues that form the cleft and are within 5.0 Å of SHG-8 include: Arg153, Glu145, Ala147, Phe146, Pro76, Ala97, Ala96, Ala98, Arg94 and Ala107 (Figure 4A). The binding affinity for mode two was -5.2 kcal/mol. The amino acid residues with atoms within 5.0 Å of SHG-8 mode 2 include: Trp44, Tyr87, Tyr154, Arg143, Asp152, Arg153. Later investigations looked at Siglec-15 expression *in vitro* which tested positive for expression with a highly expressed Siglec-15 positive cell line (U87MG) for comparison via fluorescence staining methods (Figure 4B). RT-qPCR methods were used to determine the expression of *SIGLEC15* when treated with SHG-8. RT-qPCR methods have shown that SHG-8 regulates *SIGLEC15* expression. We have identified a downregulation of *SIGLEC15* respectively at both SHG-8 10μM and 40μM treated conditions ($p<0.5$, $p<0.01$, $p<0.0001$) (Figure 4C). However, Siglec-15 protein expression via flow cytometry methods highlighted no significant difference in expression level when treated with SHG-8 at 10μM and 40μM conditions in comparison to the DMSO control (Figure 4D).

3.5 SHG-8 toxicity is reduced in colon epithelial cells and inhibits pro-inflammatory cytokine secretion in stimulated macrophages

To determine if SHG-8 poses a cytotoxic effect on normal colon epithelial cells, an MTT assay was conducted using HCoEPiC cells at varying SHG-8 concentrations (Figure 5A). SHG-8 has shown no significant difference in cell viability at 20μM which was the determined IC_{50} value in SW480 cells. However, increasing SHG-8 concentrations affect cell viability ranging from 77.18% at 40μM to 45.26% at 100μM concentration in comparison to 32.97% at 40μM to 5.41% at 100μM at the same concentration range in SW480 cells. Moreover, the IC_{50} value for HCoEPiC treated cells was found around 90μM, which is significantly higher than SW480 cells

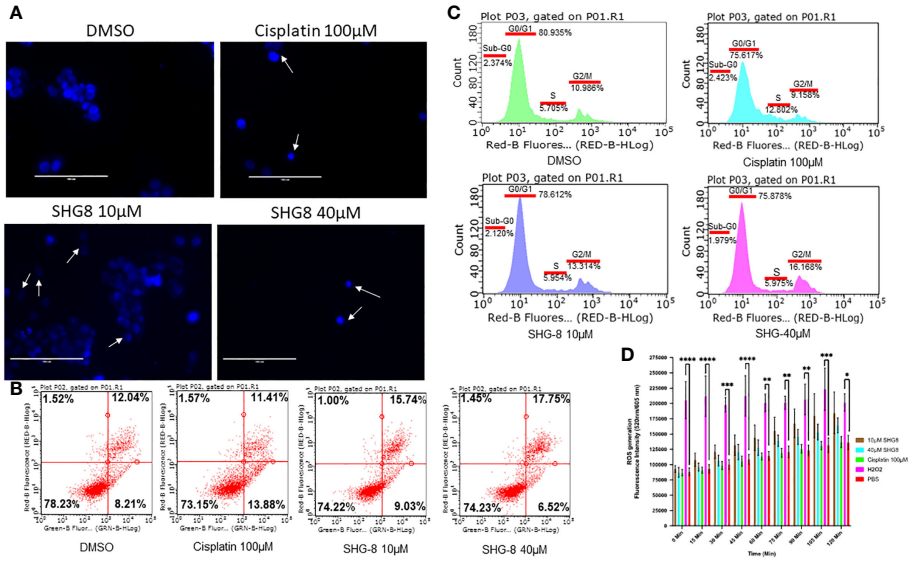

FIGURE 3
SHG-8 induced concentration-dependant apoptosis however the mechanism of action is not ROS-mediated. **(A)** Nuclear fragmentation assay determined if SHG-8 could induce apoptosis at various treatment concentrations, white arrows indicate nuclear fragments and irregular cellular morphology 24 h post-treatment at all treated conditions (N=3). **(B)** Annexin-V/propidium iodide (PI) staining of SW480 cells treated with SHG-8 at 10μM and 40μM conditions via flow cytometry to determine apoptosis induction post-treatment, dot plots are divided into four quadrants. FITC negative and PI positive (upper left quadrant) represents cells undergoing necrosis. FITC positive and PI positive (upper right quadrant) represents cells undergoing late apoptosis. FITC negative and PI negative (lower left quadrant) represents live viable cells. FITC positive and PI negative (lower right quadrant) represents cells undergoing early apoptosis. **(C)** Cell cycle arrest analysis of SW480 cells at sub-G0/G1/S/G2/M phases of the cell cycle when treated with DMSO control (green), cisplatin 100μM (light blue), SHG-8 10μM (dark blue) and SHG-8 40μM (pink) conditions. **(D)** ROS assay was utilised to determine if SHG8 could induce ROS production to infer a mechanism of action to promote apoptosis. Fluorescence intensity was measured at 520/605nm over a 2-hour period at 15 min intervals (N=4). Data is presented as mean ± SD. Two-way ANOVA followed by Dunnett's multiple comparison *post-hoc* test was conducted. *P<0.05, **P<0.01, ***P<0.001, **** P<0.0001 were considered as statistically significant.

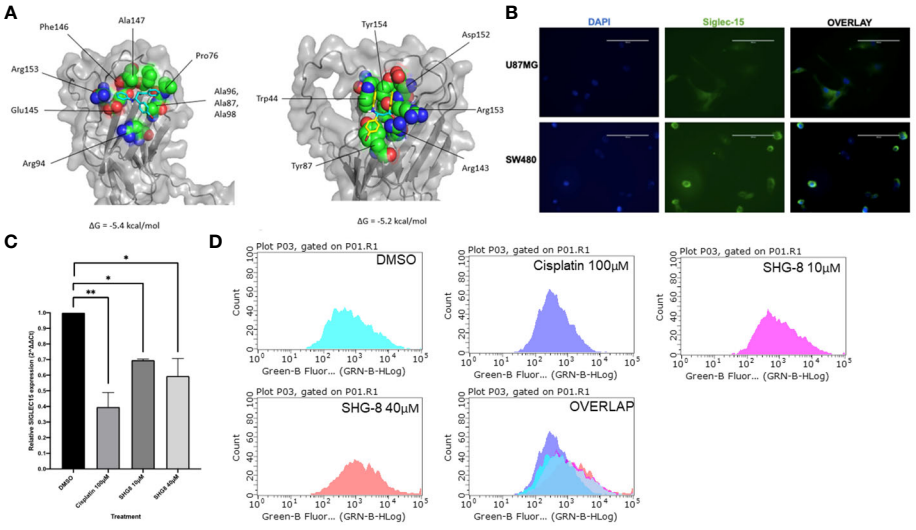

FIGURE 4
The effect of SHG8 treatment on *SIGLEC15* expression. **(A)** Docking study for SHG-8 binding on the Siglec-15 protein structure. **(B)** Positive Siglec-15 protein expression validated *in vitro* on SW480 CRC cancer cells in comparison to the U87MG Siglec-15 positive cell line (N=3). **(C)** *SIGLEC15* expression across various treated SHG-8 conditions 24h post- treatment via RT-qPCR methods (N=3). SHG-8 was shown to reduce *SIGLEC15* expression *in vitro*. One-way ANOVA statistical test followed by Dunnett's multiple comparison *post-hoc* test, *P<0.05, **P<0.01. **(D)** Flow cytometry analysis of Siglec-15 protein expression of SW480 cells when treated with DMSO control (light blue), cisplatin 100μM (dark blue), SHG-8 10μM (pink) and SHG-8 40μM (red). There was no significant difference in the level of protein expression upon SHG-8 treatment exposure.

10.3389/fimmu.2023.1254911

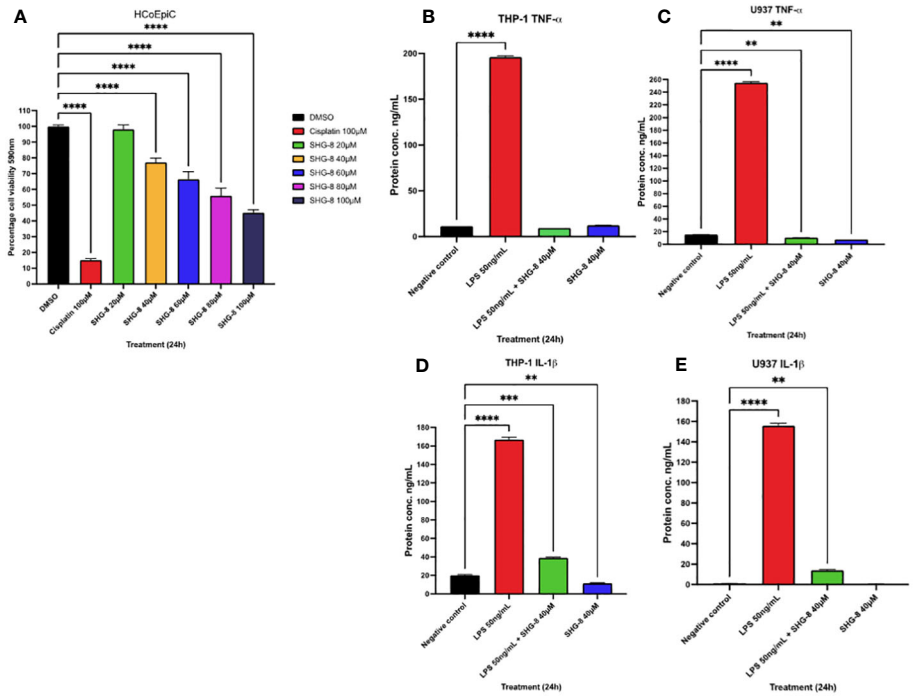

FIGURE 5
SHG-8 toxicity is reduced in colon epithelial cells and inhibits pro-inflammatory cytokine secretion in stimulated macrophages **(A)** MTT assay was conducted on normal colon epithelial HCoEPiC cells to determine the IC_{50} of SHG-8 24h post-treatment and to evaluate its cytotoxic effects *in vitro*. Data is presented as mean ± SEM. One-way ANOVA statistical test followed by Dunnett's multiple comparison *post-hoc* test **** P<0.0001. **(B)** TNF-α cytokine secretion in LPS stimulated THP-1 differentiated macrophages post SHG-8 exposure. SHG-8 normalises TNF-α secretion following LPS stimulation. Data is presented as mean ± SD. One-way ANOVA statistical test followed by Dunnett's multiple comparison *post-hoc* test **** P<0.0001. **(C)** TNF-α cytokine secretion in LPS stimulated U937 differentiated macrophages post SHG-8 exposure. SHG-8 normalises TNF-α secretion in stimulated macrophages and inhibited the presence of the pro-inflammatory cytokine at the 40µM only condition. Data is presented as mean ± SD. One-way ANOVA statistical test followed by Dunnett's multiple comparison *post-hoc* test **** P<0.0001, ** 0.01. **(D)** IL-1β cytokine secretion in LPS stimulated THP-1 differentiated macrophages post SHG-8 exposure. SHG-8 reduced IL-1β secretion and inhibited the presence of the pro-inflammatory cytokine at 40µM only condition in comparison to the control group. Data is presented as mean ± SD. One-way ANOVA statistical test followed by Dunnett's multiple comparison *post-hoc* test **** P<0.0001, *** 0.001, **0.01. **(E)** IL-1β cytokine secretion in LPS stimulated U937 differentiated macrophages post SHG-8 exposure. SHG-8 reduced IL-1β secretion following LPS stimulation. Data is presented as mean ± SD. One-way ANOVA statistical test followed by Dunnett's multiple comparison *post-hoc* test **** P<0.0001, **0.01.

highlighting lower toxicity. In addition to this, to determine the effect of pro-inflammatory cytokine secretion in immune cells in the presence of SHG-8, the cytokine levels of TNF-α and IL-1β were determined 24h post SHG-8 treatment and LPS (50ng/mL) stimulation (Figures 5B-E). LPS stimulation significantly enhanced pro-inflammatory cytokine secretion of TNF-α and IL-1β in both differentiated macrophage cell lines in comparison to the control group (p<0.0001). In addition to this, SHG-8 treatment at 40µM reduced the LPS-triggered pro-inflammatory cytokine release from differentiated macrophages in all variable conditions. Furthermore, upon exposure to SHG-8 only at 24h, there is a significant reduction in inflammatory cytokine secretion with lower TNF-α secreted in U937 (7.731ng/mL) and IL-1β in THP-1 cells (11.52ng/mL).

3.6 sRNA-seq revealed dysregulation of miRNAs by the treatment of SHG-8 on CRC cells

SRNA-seq analysis of mRNA SHG-8 treated samples identified clear differential miRNA expression between SHG-8 treatment and control conditions via constructed heat map (Figure 6A). Analysis also identified 185 differentially expressed miRNAs via volcano plot (Figure 6B). Of those, 106 genes were identified as significantly downregulated, and 79 genes were significantly upregulated having shown a two-fold change in expression. The top 5 most significantly downregulated miRNAs were identified as novel miR-1031/1130/503/993 whilst the top 5 most significantly upregulated miRNAs were listed as novel miR-1401/1065/233/1431 and hsa-miR-6715b-3p. Differential expression also classified COG functions which were correlated largely with signal transduction mechanisms and functions related to translation, ribosomal structure, and biogenesis (Figure 6C). KEGG pathway analysis depicted that signalling pathways related to autophagy and senescence were all enriched (Figure 6D). GO classification identified several biological processes were elevated including regulation of cellular components, cellular response, and regulation of immune cell apoptotic processes (Figure 6E). Additionally, cellular components relating to lysosomes and vesicles were enriched (Figure 6F). Furthermore, nucleic acid binding displayed the most enriched molecular function followed by GTP binding and specific protein domain binding (Figure 6G).

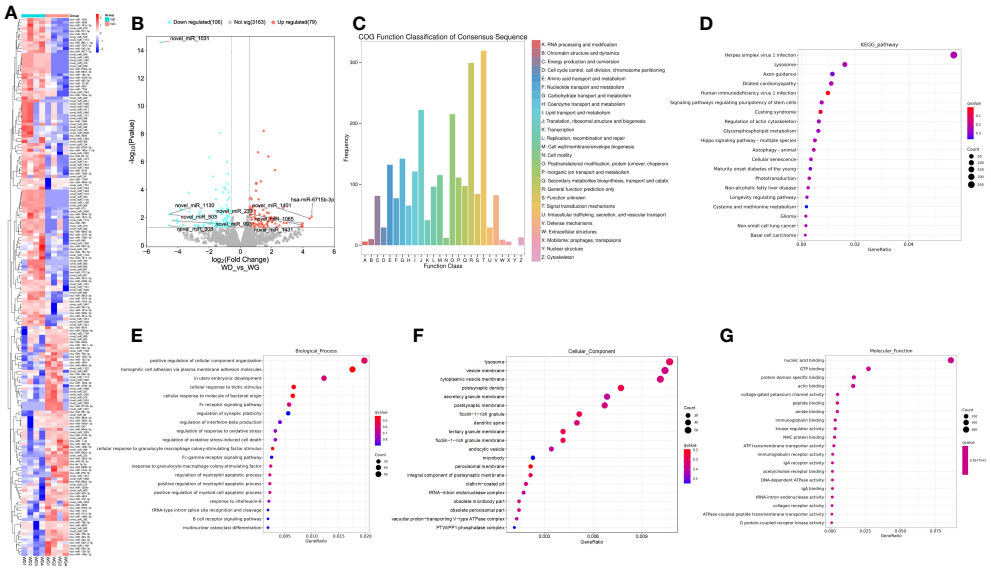

FIGURE 6
SHG-8 induces differential expression of miRNAs in CRC cells. **(A)** A constructed heat map illustrating differential miRNA expression in the SHG-8 treated and untreated group. **(B)** A volcano plot was constructed to illustrate the top 5 upregulated and downregulated miRNAs between the SHG-8 treated and untreated groups. **(C)** COG functional analysis was conducted to determine the differential expression of miRNAs and associated enriched pathways. **(D)** KEGG pathway analysis identifying enriched signalling pathways between SHG-8 treated and untreated groups. **(E)** GO classification determining enriched biological processes relating to differentially expressed miRNAs. **(F)** GO classification for enriched cellular components relating to differentially expressed miRNAs. **(G)** GO classification for molecular function relating to differentially expressed miRNAs.

3.6 RT-qPCR and *in silico* analysis of miR-6715b-3p and *PTTG1IP* in SW480 cells

To investigate the expression profile of miR-6715b-3p in CRC, UALCAN TCGA genomic data was used to confirm sRNA-seq findings (Figure 7) and analysed its expression in the CRC tumour group compared to a normal subgroup (Figure 7A). The mean expression level of miR-6715b-3p in the tumour group was 0.655 while in the normal tissue subgroup, the mean expression level was 6.949, indicating a significant substantial dysregulation ($p<0.05$) of miR-6715b-3p in CRC. To confirm the validity of miR-6715b-3p expression in CRC outlined via *in silico* analysis, RT-qPCR analysis determined the relative expression of miR-6715b-3p *in vitro* between SHG-8 treated and untreated conditions (Figure 7B). The resulting data demonstrated a significant increase in the expression of miR-6715b-3p ($p<0.01$) following SHG-8 treatment at both 10μM and 40μM concentrations in comparison to the untreated control. Therefore, confirming the observed increase in miR-6715b-3p expression identified by high-throughput sequencing. Furthermore, sRNA-seq analysis identified that miR-6715b-3p is involved in regulating *PTTG1IP*, a possible oncogene in CRC. To investigate the differential expression of the PTTG1IP protein between normal and tumour subgroups, *in silico* analysis was performed using proteomics data (Figure 7C). *In silico* analysis revealed significant upregulation of PTTG1IP protein expression in the CRC tumour subgroup with a mean expression of 0.00 compared to their corresponding normal tissue subgroup with a mean expression of -0.554 ($p<0.05$). To assess the expression profile of *PTTG1IP* at the gene level in CRC cells, RT-qPCR analysis on SHG-8 treated and control subgroups was conducted to evaluate its relevance in CRC (Figure 7D). The RT-qPCR results revealed that *PTTG1IP* expression was significantly downregulated in both 10μM and 40μM SHG-8 treated conditions with a relative expression of 0.525 and 0.449 respectively compared to the control group ($p<0.01$, $p<0.001$). The mean relative expression of *PTTG1IP* in treated SW480 cells were 1.12-fold lower than in untreated cells, indicating an SHG8-treatment induced effect on *PTTG1IP* regulation in SW480 cells.

4 Discussion

To treat CRC cases, conventional front-line treatments would involve the usage of chemotherapy, surgery and radiotherapy or a combination of each to improve patient response (21). Despite several advances in CRC diagnosis, prognosis, and disease management and even development of new treatment strategies, ultimately it has fallen short (22). In last few decades, the targeted anticancer drugs including small molecules and macromolecules, have gained much attention due to their ability to specifically target cancer cells and spare normal cells and thus they possess high potency and low toxicity. In comparison to macromolecular targeted drugs, the small molecule targeted drugs have several advantages such as low cost, better pharmacokinetic properties, patient compliance, and easy storage and transportation and therefore considered favourable for anti-cancer drug development (23).

In recent years, small molecule targeted therapies have emerged as a promising approach for the treatment of various cancers including CRC preventing metastasis and cancer progression (24).

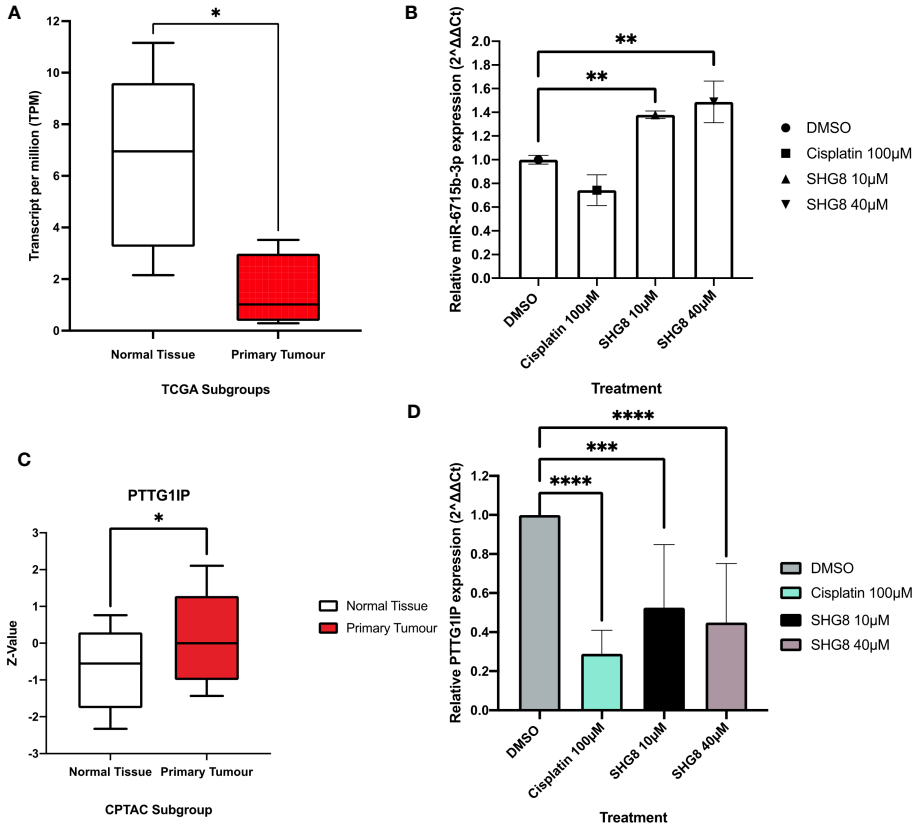

FIGURE 7
In silico analysis and RT-qPCR validation of sRNA-seq analysis. **(A)** TCGA genomic data for miR-6715b-3p expression in normal (clear) and CRC tumour groups (red) box plots. Unpaired student's t-test *P<0.05. **(B)** Relative expression of miR-6715b-3p in SHG-8 treated and untreated conditions *in vitro*. One way ANOVA followed by Dunnett's multiple comparison *post-hoc* test **P<0.01. (N=3). **(C)** TCGA proteomics data for PTTG1IP expression in normal (clear) and CRC tumour groups (red) box plots. Unpaired student's t-test *P<0.05. **(D)** Relative expression of *PTTG1IP* in SHG-8 treated and untreated conditions *in vitro*. One way ANOVA followed by Dunnett's multiple comparison *post-hoc* test ***P<0.001, ****P<0.0001. (N=3).

Bearing in mind the significance of small molecules for CRC, we decided to explore the efficacy of the β-amino ketone (SHG-8) for CRC by targeting the Siglec-15/Sia axis.

The SHG-8 compound is a small molecule that contains three aromatic rings connected by a β-amino ketone. A halogen group is introduced to an aromatic ring to enhance lipophilicity and hydrophobicity. The efficient synthesis of β-amino ketones can be achieved through a one-step three-component Mannich reaction involving an amine, aldehyde, ketone, and a catalyst (25). Various catalytic systems have been explored, however, they suffer from drawbacks such as long reaction times, high temperatures, cost, low recyclability, and challenges in product separation and purification (26). Moreover, some catalysts pose environmental risks due to their corrosiveness and toxicity. In line with the United Nations Sustainable Goals (SDGs), a suitable and recyclable heterogenous catalyst for the Mannich reaction was developed. The heterogenous nano-catalyst SAFSNS, was synthesised and characterized by our reported procedure (15).

This study presents the development of an efficient, environmentally friendly catalytic process using a solid acid nano-catalyst (SAFSNS) for the one-pot condensation of aromatic ketones, aldehydes, and amines to yield the β-amino carbonyl compound (SHG-8). Further investigations are underway to explore the synthesis of a range of β-amino carbonyl compounds using the SAFSNS nano-catalyst.

It's evident from the experimental results that the β-amino ketone compound SHG-8 has significant cytotoxicity *in vitro*. At an IC_{50} of approximately 20μM, SHG-8 has shown a higher treatment efficacy in comparison to current available treatments such as cisplatin. It has been reported that cisplatin displayed an IC_{50} of 23.61μM in CRC cells (27). Similar to what was observed in this study. This suggests the use of SHG-8 as a small molecule inhibitor as more effective at displaying anti-tumorigenic properties in comparison to cisplatin. Similarly, combination therapies were required to increase the efficacy of cisplatin drug treatment due to cancer cells developing resistance (28). In addition, wound healing assays demonstrated that cisplatin and the 40μM SHG-8 treated condition significantly reduced cellular migration across 24 hours. However, at the 48-hour time point, only cisplatin was able to achieve this effect. Moreover, all treated conditions displayed significant inhibition on cell proliferation as no colonies were formed. This also correlated similarly with other treatments including combination therapies and small molecule inhibitors inhibiting the proliferation of CRC cells *in vitro* (29).

The nuclear fragmentation assay inferred the occurrence of apoptotic cell death at increasing SHG-8 concentrations. This observation correlated with several other compounds including conventional and non-conventional treatment methods such as cisplatin which are also capable of modulating apoptosis in multiple cancer types (30). These images corresponded with cellular features commonly associated with apoptosis including nucleus fragmentation, irregular morphology, and cell shrinkage via caspase functional activity cleaving peptide bonds of nuclear proteins (31). In contrast, induced cell cycle arrest at the G2/M phase post-treatment observed via PI staining suggests prolonged generation of double stranded breaks within the DNA helical structure, hence the possibility of apoptosis induction (32). However, the rate of apoptosis induced by SHG-8 treatment was rather low, thus suggesting that other types of cell death pathways may be triggered by SHG-8.

The transition from G2 to M phase is highly regulated via several proteins including p53. Cellular exposure to SHG-8 might enhance the activity of p53 prompting p53-dependant G2 cell cycle arrest thereby inhibiting cancer proliferation (33). It could further propose specific mechanistic action of SHG-8 to inhibit tumour proliferation. Furthermore, SHG-8 exhibits similar apoptotic induction to other small molecule inhibitors including DMOCPTL, MLN4924 and RGX-202 used in several cancer types including triple negative breast cancer (TNBC), lung cancer and CRC (34–36). Additionally, there are previous reports stating that cisplatin significantly enhanced the presence of cells within the S phase of the cell cycle, this is in agreement with our findings (37). Another possible mechanistic explanation may involve ROS production and could be the underlying cause for which apoptosis occurs. Overstimulated ROS production within a tumour microenvironment could cause severe damage to various proteins and metabolites inducing the activation of apoptosis and related signalling pathways (38). However, this is not the case of SHG-8 as ROS production remained consistent throughout with only the positive control showing significant ROS generation. This suggested that apoptosis induction is modulated via a similar yet distinct signalling pathway, although the exact mechanism of activation remains unclear up to this point (39).

There is also growing evidence associating *SIGLEC15* upregulation with the development of cancer and its role in the progression of various types of tumours comprising of head and neck squamous cell carcinomas (HNSCC), liver hepatocellular carcinomas (LIHC), lung adenocarcinoma (LUAD), prostate adenocarcinoma (PRAD), rectum adenocarcinoma (READ), thyroid carcinoma (THCA) and many others including colorectal adenocarcinomas (COAD) tumours (7, 8, 40). Simultaneously, immune checkpoint proteins including Siglec-15 and PD-L1 have specified key roles in the proliferation of cancer cells and are able to modulate cancer progression (41, 42). In particular, Siglec-15 is also expressed on mutually exclusive populations of cancer cells with respect to PD-L1 (43). Therefore, this could pave the way for combination therapies with PD-L1 and Siglec-15 antagonists. Thus, in this study, elucidating candidate miRNAs as therapeutic targets for CRC progression could provide insights to treating Siglec-15 positive tumours and PD-L1 negative tumour patients.

Notably, it is understood that Siglec-15 functional activity requires canonical glycan binding. It has been reported that interactions with essential arginine amino acid residues were necessary for the formation of salt bridges with sialic acid carboxylates (44). Our docking studies aimed to elucidate potential binding sites of the Siglec-15 protein structure. The docking study located amino acid residues within 5.0 Å of SHG-8 including ARG143, an amino acid residue that has been previously reported for glycan ligand binding (45). Thereby suggesting SHG-8's role as a small molecule inhibitor.

To determine the role of SHG-8 on CRC, Siglec-15 was shown to have positive expression *in vitro*. With SHG-8 treatment, RT-qPCR methods indicated *SIGLEC15* expression was significantly reduced. Several mechanisms maybe involved in the regulation of *SIGLEC15* expression. A previous report identified *hsa-miR-582-5p/TUG1* axis to be involved in pancreatic adenocarcinomas (PAAD) (46). Similarly, the *LINC02432/hsa-miR-98–5p/HK2* axis also correlated with *SIGLEC15* regulation in hepatocellular carcinomas (HCC) (47). Therefore, it may be possible that *SIGLEC15* is regulated through a similar mechanism. However, we have found no significant difference in Siglec-15 protein expression upon SHG-8 treatment. It may be possible that Siglec-15 binding and regulation at the gene level could in fact regulate apoptosis induction and subsequent pathways resulting in cancer cell death. It was previously reported that Siglec-15 knockdown could reduce STAT3 signalling thus inhibiting cellular proliferation and inducing apoptosis in osteosarcomas (48).

The effect of SHG-8 on HCoEPiC cells has demonstrated that the IC_{50} value at 90μM shares significantly lower potency in epithelial cells in comparison to the IC_{50} value at 20μM in SW480 cells. Similarly, a previous study highlighted Actein, a triterpene glycoside, significantly inhibited SW480 and HT-29 cells *in vitro* whilst exhibiting reduced anti-proliferation effects in HCoEPiC cells (49). Furthermore, MOG13 a selective inhibitor for CRC treatment, witnessed a concentration-dependant reduction in cellular viability when exposed to drug treatment (50). This could suggest that significantly higher concentrations from 40μM onwards could sensitise HCoEPiC cells towards SHG-8 treatment. Although, there was cell death at higher SHG-8 concentrations, the toxicity that was observed emphasises the effectiveness of SHG-8 as a treatment alternative and suggests reduced adverse effects in comparison to cisplatin treatment.

Chronic inflammation can play a crucial role in cancer development and progression (51). Secretion of pro-inflammatory cytokines including TNF-α and IL-1β can intrinsically contribute to the formation of the TME and systemic immunosuppression could be stimulated by cell populations including TAMs (52). Consequently, resulting in chronic inflammation and cancer progression. SHG-8 exposure has indicated a suppressive effect on the secretion of both TNF-α and IL-1β in the presence of LPS stimulated macrophages highlighting a possibility in preventing the occurrence of inflammation and the TME. In addition to this, reduced inflammatory cytokine secretion could also correlate with negligible ROS production as was seen in the ROS assay for SW480 cells.

The constructed heat map identified several clusters of miRNAs that were differentially expressed between the SHG-8 treated and untreated groups. Mir-1303 is one such differentially expressed

miRNA which showed downregulated expression in the treatment group. This miRNA has typically shown upregulated expression and was capable of inducing tumour cell proliferation and invasion in various cancer types including CRC (53). Likewise, miR-940 has shown differential expression displaying downregulated expression in the treatment group. MiR-940 upregulation has consistently been shown to contribute to tumour progression in cancer types such as PAAD and cervical carcinomas (CC) (54). Moreover, miR-543 was shown to be downregulated in several tumour types including CRC by exhibiting a tumour suppressive role and inhibiting tumorigenesis (55). In the treatment group, miR-543 has shown increased expression supporting the conclusion in its role as a tumour suppressor. In addition to this, there have also been several reports of anti-tumorigenic drug compounds capable of affecting miRNA expression (56–58). Therefore, it is highly likely that SHG-8 could is involved in modulating miRNA expression profiles in order to inhibit cancer progression.

The differential expression for many miRNAs has shown that SHG-8 is compatible as a small molecule inhibitor and is capable of inducing changes to miRNA expression to inhibit cancer proliferation. To answer the question of whether the downregulation of *SIGLEC15* is mediated by miRNAs, sRNA-seq analysis was performed between SHG-8 treated and untreated conditions. Several miRNAs were shown to be differentially expressed with the SHG-8 treatment; however, we did not find miRNAs that significantly affect *SIGLEC15* expression with the treatment. The downregulation of Siglec-15 could be an effect of DNA methylation and/or by an effect of transcriptional regulation. Nevertheless, we found miR-6715b-3p to be the most upregulated miRNA. With minimal evidence in the literature for the novel miRNAs, miR-6715b-3p has been previously identified as integral in the modulation of autophagy through SESN1 targeting in Huntington's disease and was also found to be downregulated in prostate adenocarcinomas (59, 60). In this study, *in silico* analysis and RT-qPCR methods confirmed miR-6715b-3p expression *in vitro* in SHG-8 treated conditions. It is possible that miR-6715b-3p acts as a tumour suppressor miRNA and could regulate oncogenes in regard to CRC progression. It has been reported that miR-6715b-3p could work in conjunction with other miRNAs to display superior anti-proliferative activity such as miR-34a (61). Supporting the likelihood that miR-6715b-3p could possess an important role in regulating key gene targets associated with CRC progression and improve on current therapeutics.

sRNA analysis has shown gene targets to be involved in multiple pathways and biological/molecular functions. KEGG pathway analysis detailed enriched signalling pathways related to autophagy and senescence when subjected to SHG-8 treatment. It is possible that miRNAs can regulate these pathways to inhibit tumorigenesis. Several miRNAs including miR-145 have been reported to promote autophagy via various signalling pathways (62–64). Likewise, several miRNAs including miR-15/17/19/21/24/29/34/101 have shown signs of modulating senescence in cancer development (65). MiRNA's have also shown involvement in tumorigenic signalling regulation as well.

Several biological processes that were enriched included the regulation of immune cell apoptosis and cellular response. It is possible that miRNAs can regulate apoptotic processes in cancer. Mir-448 and miR-148a-3p were both reported to regulate immune cell apoptosis which inhibited cancer progression (66, 67).

Based on differentially expressed miRNAs induced via SHG-8 treatment; miR-6715b-3p was predicted to interact and significantly regulate *PTTG1IP*, a possible oncogene in CRC. Proteomics data outlined higher levels of PTTG1IP expression in *COAD* tumours with significant downregulation in the SHG-8 treated conditions confirming sequencing analysis. The expression of *PTTG1IP* has been reported in other malignant cancers including, CRC breast and thyroid cancers supporting its role as an oncogene (68–70). However, *PTTG1IP* has also shown low expression in malignancies which correlated with poor survival (71). It was also highlighted that the overexpression of *PTTG1IP* in malignant tumours are the main driving force for tumour progression whilst genetic mutations are likely to establish minimal effects on *PTTG1IP* function (72). Although, there are conflicting reports for the expression of *PTTG1IP* in malignant tumours, further assessment of the mechanistic action of the miR-6715b-3p/*PTTG1IP* axis in correlation with the Siglec-15/Sia axis could shed some light on CRC progression and maybe a promising approach for treatment.

Subsequent studies to decipher further mechanistic action of SHG-8 on cancer survival could elaborate on key intrinsic pathways particularly regarding the induction of apoptosis. Caspases and their cleaved counterparts including cleaved caspase-3 and cleaved caspase-9 maybe involved in the induction of apoptosis as a possible method for cancer death to exert SHG-8's therapeutic potential (73). Furthermore, the expression of *SIGLEC15* at the gene level demonstrated reduced expression from SHG-8 treatment, knockdown studies may provide further mechanistic insights in SHG-8's therapeutic potential. Similarly, we hypothesise that the role of SHG-8 as a Siglec-15 antagonist will have no effect on the expression of PD-L1. However, due to the mutual exclusivity in the expression of both inhibitory checkpoints, SHG-8 targeting of Siglec-15 in combination with PD-L1 antagonists may share synergistic effects. Further experimental analysis could underline and discern their role in cancer progression. Moreover, it may offer a more complete and robust approach in CRC treatment.

5 Conclusion

To conclude the small molecule SHG-8 has shown significant anti-tumour properties against SW480 cancer cells. Although indications do identify that SHG-8 does induce late apoptosis at higher concentrations with elevated cell cycle arrest at the G2/M phase of the cell cycle, further mechanistic studies are needed to gain insights as to how this phenomenon is generated. The molecule SHG-8 binding to ARG143 confirms its role as a novel small molecule inhibitor in Siglec-15 positive tumours. Moreover, it outlines the tumorigenic role of the Siglec-15/Sia and miR-6715b-3p/*PTTG1IP* axes in the progression of CRC. It is worth noting that Siglec-15 expression is exclusively expressed on distinct

subpopulations of cancer cells with respect to PDL-1. Therefore, our study indicates the possibility of combination therapies utilising both PDL-1 and Siglec-15 antagonists to induce a successful patient response and prevent tumour recurrence. These findings offer a promising avenue for future investigations for CRC treatment. Notably, SHG-8 is the first known inhibitor to target Siglec-15, with current clinical trials so far has only focused on the development of blocking antibodies to inhibit the Siglec-15/Sia axis. SHG-8 could be a gamechanger in the way CRC and other Siglec-15 positive cancers will be treated in the future.

Data availability statement

The data presented in the study are deposited in the Mendeley repository, accession number doi: 10.17632/r2xdf868k9.1; release date 3 Aug 2023.

Ethics statement

Ethical approval was not required for the studies on humans in accordance with the local legislation and institutional requirements because only commercially available established cell lines were used.

Author contributions

MA: data curation, methodology, writing – original draft, writing – review & editing. MB: conceptualization, supervision, writing – review & editing. HP: data curation, methodology, writing – original draft, writing – review & editing. IA: data curation, funding acquisition, methodology, writing – original draft, writing – review & editing. S: conceptualization, data curation, methodology, writing – original draft, writing – review & editing. SS: conceptualization, project administration, supervision, writing – review & editing.

Funding

The authors IA and S appreciate the financial support provided by the School of Graduate Studies and Research, American University of Ras Al Khaimah, Ras Al Khaimah, UAE through seed grant funded project no. AAS/002/19.

Acknowledgments

We are grateful to the School of Life and Medical Sciences, University of Hertfordshire, United Kingdom for the support in this work.

Conflict of interest

The authors declare that the research was conducted in the absence of any commercial or financial relationships that could be construed as a potential conflict of interest.

Publisher's note

Supplementary material

The Supplementary Material for this article can be found online at: https://www.frontiersin.org/articles/10.3389/fimmu.2023.1254911/full#supplementary-material

References

1. *Cancer today*. Available at: http://gco.iarc.fr/today/home (Accessed May 26, 2023).

2. Sawicki T, Ruszkowska M, Danielewicz A, Niedźwiedzka E, Arłukowicz T, Przybyłowicz KE. A review of colorectal cancer in terms of epidemiology, risk factors, development, symptoms and diagnosis. *Cancers* (2021) 13:2025. doi: 10.3390/cancers13092025

3. Weng J, Li S, Zhu Z, Liu Q, Zhang R, Yang Y, et al. Exploring immunotherapy in colorectal cancer. *J Hematol Oncol* (2022) 15:95. doi: 10.1186/s13045-022-01294-4

4. Kishore C, Bhadra P. Current advancements and future perspectives of immunotherapy in colorectal cancer research. *Eur J Pharmacol* (2021) 893:173819. doi: 10.1016/j.ejphar.2020.173819

5. Fan A, Wang B, Wang X, Nie Y, Fan D, Zhao X, et al. Immunotherapy in colorectal cancer: current achievements and future perspective. *Int J Biol Sci* (2021) 17:3837–49. doi: 10.7150/ijbs.64077

6. Wang J, Sun J, Liu LN, Flies DB, Nie X, Toki M, et al. Siglec-15 as an immune suppressor and potential target for normalization cancer immunotherapy. *Nat Med* (2019) 25:656–66. doi: 10.1038/s41591-019-0374-x

7. Li B, Zhang B, Wang X, Zeng Z, Huang Z, Zhang L, et al. Expression signature, prognosis value, and immune characteristics of Siglec-15 identified by pan-cancer analysis. *OncoImmunology* (2020) 9:1807291. doi: 10.1080/2162402X.2020.1807291

8. Du H, Tang J, Li X, Wang X, Wu L, Zhang R, et al. Siglec-15 is an immune suppressor and potential target for immunotherapy in the pre-metastatic lymph node of colorectal cancer. *Front Cell Dev Biol* (2021) 9:691937. doi: 10.3389/fcell.2021.691937

9. Zhang N, Hu X, Du Y, Du J. The role of miRNAs in colorectal cancer progression and chemoradiotherapy. *Biomed Pharmacother* (2021) 134:111099. doi: 10.1016/j.biopha.2020.111099

10. To KK, Tong CW, Wu M, Cho WC. MicroRNAs in the prognosis and therapy of colorectal cancer: From bench to bedside. *WJG* (2018) 24:2949–73. doi: 10.3748/wjg.v24.i27.2949

11. Hammouda MM, Elattar KM. Recent progress in the chemistry of β-aminoketones. *RSC Adv* (2022) 12:24681–712. doi: 10.1039/D2RA03864A

12. Roman G. Mannich bases in medicinal chemistry and drug design. *Eur J Medicinal Chem* (2015) 89:743–816. doi: 10.1016/j.ejmech.2014.10.076

13. Farzaneh S, Shahhosseini S, Arefi H, Daraei B, Esfahanizadeh M, Zarghi A. Design, synthesis and biological evaluation of new 1,3-diphenyl-3- (phenylamino)

propan-1-ones as selective cyclooxygenase (COX-2) inhibitors. *MC* (2018) 14:652–9. doi: 10.2174/1573406414666180525133221

14. Van Der Zanden SY, Luimstra JJ, Neefjes J, Borst J, Ovaa H. Opportunities for small molecules in cancer immunotherapy. *Trends Immunol* (2020) 41:493–511. doi: 10.1016/j.it.2020.04.004

15. Ahmad I, Shagufta, Dhar R, Hisaindee S, Hasan K. An environmentally benign solid acid nanocatalyst for the green synthesis of carboxylic acid ester. *ChemistrySelect* (2021) 6:9645–52. doi: 10.1002/slct.202102230

16. Suarez-Arnedo A, Torres Figueroa F, Clavijo C, Arbeláez P, Cruz JC, Muñoz-Camargo C. An image J plugin for the high throughput image analysis of in *vitro* scratch wound healing assays. *PloS One* (2020) 15:e0232565. doi: 10.1371/journal.pone.0232565

17. Varadi M, Anyango S, Deshpande M, Nair S, Natassia C, Yordanova G, et al. AlphaFold Protein Structure Database: massively expanding the structural coverage of protein-sequence space with high-accuracy models. *Nucleic Acids Res* (2022) 50:D439–44. doi: 10.1093/nar/gkab1061

18. Yang J, Roy A, Zhang Y. Protein–ligand binding site recognition using complementary binding-specific substructure comparison and sequence profile alignment. *Bioinformatics* (2013) 29:2588–95. doi: 10.1093/bioinformatics/btt447

19. Kochnev Y, Hellemann E, Cassidy KC, Durrant JD. Webina: an open-source library and web app that runs AutoDock Vina entirely in the web browser. *Bioinformatics* (2020) 36:4513–5. doi: 10.1093/bioinformatics/btaa579

20. Kidwai M, Bhatnagar D, Mishra NK, Bansal V. CAN catalyzed synthesis of β-amino carbonyl compounds via Mannich reaction in PEG. *Catalysis Commun* (2008) 9:2547–9. doi: 10.1016/j.catcom.2008.07.010

21. Johdi NA, Sukor NF. Colorectal cancer immunotherapy: options and strategies. *Front Immunol* (2020) 11:1624. doi: 10.3389/fimmu.2020.01624

22. Piawah S, Venook AP. Targeted therapy for colorectal cancer metastases: A review of current methods of molecularly targeted therapy and the use of tumor biomarkers in the treatment of metastatic colorectal cancer. *Cancer* (2019) 125:4139–47. doi: 10.1002/cncr.32163

23. Zhong L, Li Y, Xiong L, Wang W, Wu M, Yuan T, et al. Small molecules in targeted cancer therapy: advances, challenges, and future perspectives. *Sig Transduct Target Ther* (2021) 6:201. doi: 10.1038/s41392-021-00572-w

24. He Y, Kan W, Li Y, Hao Y, Huang A, Gu H, et al. A potent and selective small molecule inhibitor of myoferlin attenuates colorectal cancer progression. *Clin Trans Med* (2021) 11. doi: 10.1002/ctm2.289

25. Iwanejko J, Wojaczyńska E, Olszewski TK. Green chemistry and catalysis in Mannich reaction. *Curr Opin Green Sustain Chem* (2018) 10:27–34. doi: 10.1016/j.cogsc.2018.02.006

26. Cai X, Xie B. Recent advances on organocatalysed asymmetric Mannich reactions. *Arkivoc* (2013) 2013:264–93. doi: 10.3998/ark.5550190.p007.839

27. Zhang H, Zhu H-T, Wang D, Yang C-R, Zhang Y-J. Sphingofungins G and H: new five-membered lactones from *Aspergillus penicilliodes* Speg. *Natural Product Res* (2019) 33:1284–91. doi: 10.1080/14786419.2018.1470627

28. Hoffmeister BR, Adib-Razavi MS, Jakupec MA, Galanski MS, Keppler BK. Diammine tetrakis(carboxylato)platinum(IV) complexes – synthesis, characterization, and cytotoxicity. *Chem Biodiver* (2012) 9:1840–8. doi: 10.1002/cbdv.201200019

29. Chen P, Li X, Zhang R, Liu S, Xiang Y, Zhang M, et al. Combinative treatment of β-elemene and cetuximab is sensitive to KRAS mutant colorectal cancer cells by inducing ferroptosis and inhibiting epithelial-mesenchymal transformation. *Theranostics* (2020) 10:5107–19. doi: 10.7150/thno.44705

30. Singh P, Lim B. Targeting apoptosis in cancer. *Curr Oncol Rep* (2022) 24:273–84. doi: 10.1007/s11912-022-01199-y

31. Majtnerová P, Roušar T. An overview of apoptosis assays detecting DNA fragmentation. *Mol Biol Rep* (2018) 45:1469–78. doi: 10.1007/s11033-018-4258-9

32. Sunada S, Saito H, Zhang D, Xu Z, Miki Y. CDK1 inhibitor controls G2/M phase transition and reverses DNA damage sensitivity. *Biochem Biophys Res Commun* (2021) 550:56–61. doi: 10.1016/j.bbrc.2021.02.117

33. Lu W-J, Peng W, Sun Q-Q, Li Y-H, Chen B, Yu L-T, et al. #2714, a novel active inhibitor with potent G2/M phase arrest and antitumor efficacy in preclinical models. *Cell Death Discovery* (2018) 4:24. doi: 10.1038/s41420-018-0032-y

34. Kurth I, Yamaguchi N, Andreu-Agullo C, Tian HS, Sridhar S, Takeda S, et al. Therapeutic targeting of SLC6A8 creatine transporter suppresses colon cancer progression and modulates human creatine levels. *Sci Adv* (2021) 7:eabi7511. doi: 10.1126/sciadv.abi7511

35. Ding Y, Chen X, Liu C, Ge W, Wang Q, Hao X, et al. Identification of a small molecule as inducer of ferroptosis and apoptosis through ubiquitination of GPX4 in triple negative breast cancer cells. *J Hematol Oncol* (2021) 14:19. doi: 10.1186/s13045-020-01016-8

36. Xu T, Ma Q, Li Y, Yu Q, Pan P, Zheng Y, et al. A small molecule inhibitor of the UBE2F-CRL5 axis induces apoptosis and radiosensitization in lung cancer. *Sig Transduct Target Ther* (2022) 7:354. doi: 10.1038/s41392-022-01182-w

37. Pian AK, Foong CP, Hamid RA. S-phase arrest and apoptosis in human breast adenocarcinoma MCF-7 cells via mitochondrial dependent pathway induced by tricyclohexylphosphine gold (I) n-mercaptobenzoate complexes. *Life Sci* (2022) 311:121161. doi: 10.1016/j.lfs.2022.121161

38. Redza-Dutordoir M, Averill-Bates DA. Activation of apoptosis signalling pathways by reactive oxygen species. *Biochim Biophys Acta (BBA) - Mol Cell Res* (2016) 1863:2977–92. doi: 10.1016/j.bbamcr.2016.09.012

39. Tang R, Xu J, Zhang B, Liu J, Liang C, Hua J, et al. Ferroptosis, necroptosis, and pyroptosis in anticancer immunity. *J Hematol Oncol* (2020) 13:110. doi: 10.1186/s13045-020-00946-7

40. Hu J, Yu A, Othmane B, Qiu D, Li H, Li C, et al. Siglec15 shapes a non-inflamed tumor microenvironment and predicts the molecular subtype in bladder cancer. *Theranostics* (2021) 11:3089–108. doi: 10.7150/thno.53649

41. Mehdizadeh S, Bayatipoor H, Pashangzadeh S, Jafarpour R, Shojaei Z, Motallebnezhad M. Immune checkpoints and cancer development: Therapeutic implications and future directions. *Pathol - Res Pract* (2021) 223:153485. doi: 10.1016/j.prp.2021.153485

42. BaSudan AM. The role of immune checkpoint inhibitors in cancer therapy. *Clinics Pract* (2022) 13:22–40. doi: 10.3390/clinpract13010003

43. Shafi S, Aung TN, Robbins C, Zugazagoitia J, Vathiotis I, Gavrielatou N, et al. Development of an immunohistochemical assay for Siglec-15. *Lab Invest* (2022) 102:771–8. doi: 10.1038/s41374-022-00785-9

44. Crocker PR, Paulson JC, Varki A. Siglecs and their roles in the immune system. *Nat Rev Immunol* (2007) 7:255–66. doi: 10.1038/nri2056

45. Murugesan G, Weigle B, Crocker PR. Siglec and anti-Siglec therapies. *Curr Opin Chem Biol* (2021) 62:34–42. doi: 10.1016/j.cbpa.2021.01.001

46. Ren Y, Lyu J, Guo Y, Yao Y, Hu L. Long noncoding RNA TUG1 inhibits tumor progression through regulating siglec-15-related anti-immune activity in hepatocellular carcinoma. *J Immunol Res* (2022) 2022:1–24. doi: 10.1155/2022/9557859

47. Tan P, Li M, Liu Z, Li T, Zhao L, Fu W. Glycolysis-related LINC02432/hsa-miR-98–5p/HK2 axis inhibits ferroptosis and predicts immune infiltration, tumor mutation burden, and drug sensitivity in pancreatic adenocarcinoma. *Front Pharmacol* (2022) 13:937413. doi: 10.3389/fphar.2022.937413

48. Song K, Ma J, Gao Y, Qu Y, Ren C, Yan P, et al. Knocking down Siglec-15 in osteosarcoma cells inhibits proliferation while promoting apoptosis and pyroptosis by targeting the Siglec-15/STAT3/Bcl-2 pathway. *Adv Med Sci* (2022) 67:187–95. doi: 10.1016/j.advms.2022.03.001

49. Yan L, Wang D, Liu X, Gu C, Gao S. Actein antagonizes colorectal cancer through blocking PI3K/Akt pathways by downregulating IMPDH2. *Anti-Cancer Drugs* (2021) 32:864–74. doi: 10.1097/CAD.0000000000001080

50. Maderer A, Plutizki S, Kramb J-P, Göpfert K, Linnig M, Khillimberger K, et al. Moguntinones—New selective inhibitors for the treatment of human colorectal cancer. *Mol Cancer Ther* (2014) 13:1399–409. doi: 10.1158/1535-7163.MCT-13-0224

51. Muthusami S, Ramachandran IK, Babu KN, Krishnamoorthy S, Guruswamy A, Queimado L, et al. Role of inflammation in the development of colorectal cancer. *EMIDDT* (2021) 21:77–90. doi: 10.2174/1871530320666200909092908

52. Wen Y, Zhu Y, Zhang C, Yang X, Gao Y, Li M, et al. Chronic inflammation, cancer development and immunotherapy. *Front Pharmacol* (2022) 13:1040163. doi: 10.3389/fphar.2022.1040163

53. Urh K, Žlajpah M, Zidar N, Boštjančič E. Identification and validation of new cancer stem cell-related genes and their regulatory microRNAs in colorectal cancerogenesis. *Biomedicines* (2021) 9:179. doi: 10.3390/biomedicines9020179

54. Li H, Li Y, Tian D, Zhang J, Duan S. miR-940 is a new biomarker with tumor diagnostic and prognostic value. *Mol Ther - Nucleic Acids* (2021) 25:53–66. doi: 10.1016/j.omtn.2021.05.003

55. Fan C, Lin Y, Mao Y, Huang Z, Liu AY, Ma H, et al. MicroRNA-543 suppresses colorectal cancer growth and metastasis by targeting KRAS, MTA1 and HMGA2. *Oncotarget* (2016) 7:21825–39. doi: 10.18632/oncotarget.7989

56. Jung HM, Benarroch Y, Chan EKL. Anti-Cancer Drugs Reactivate Tumor Suppressor miR-375 Expression in Tongue Cancer Cells: miR-375 REACTIVATION BY ANTI-CANCER DRUGS. *J Cell Biochem* (2015) 116:836–43. doi: 10.1002/jcb.25039

57. Tormo E, Pineda B, Serna E, Guijarro A, Ribas G, Fores J, et al. MicroRNA profile in response to doxorubicin treatment in breast cancer: MICRORNA PROFILE IN RESPONSETO DOXORUBICIN. *J Cell Biochem* (2015) 116:2061–73. doi: 10.1002/jcb.25162

58. Al-Kawlani B, Murrieta-Coxca JM, Chaiwangyen W, Fröhlich K, Fritzsche A, Winkler S, et al. Doxorubicin induces cytotoxicity and miR-132 expression in granulosa cells. *Reprod Toxicol* (2020) 96:95–101. doi: 10.1016/j.reprotox.2020.06.001

59. Anderson KE, Stevenson M, Varghese R, Hebron ML, Koppel E, McCartin M, et al. Alteration of autophagy and glial activity in nilotinib-treated huntington's disease patients. *Metabolites* (2022) 12:1225. doi: 10.3390/metabo12121225

60. Martínez-González L, Sánchez-Conde V, González-Cabezuelo J, Antunez-Rodríguez A, Andrés-León E, Robles-Fernandez I, et al. Identification of microRNAs as viable aggressiveness biomarkers for prostate cancer. *Biomedicines* (2021) 9:646. doi: 10.3390/biomedicines9060646

61. Orellana EA, Li C, Lisevick A, Kasinski AL. Identification and validation of microRNAs that synergize with miR-34a – a basis for combinatorial microRNA therapeutics. *Cell Cycle* (2019) 18:1798–811. doi: 10.1080/15384101.2019.1634956

62. Wu H, Liu C, Yang Q, Xin C, Du J, Sun F, et al. *MIR145-3p* promotes autophagy and enhances bortezomib sensitivity in multiple myeloma by targeting. *HDAC4. Autophagy* (2020) 16:683–97. doi: 10.1080/15548627.2019.1635380

63. Zhou C, Liang Y, Zhou L, Yan Y, Liu N, Zhang R, et al. TSPAN1 promotes autophagy flux and mediates cooperation between WNT-CTNNB1 signaling and autophagy via the *MIR454* -FAM83A-TSPAN1 axis in pancreatic cancer. *Autophagy* (2021) 17:3175–95. doi: 10.1080/15548627.2020.1826689

64. Zhang Z, Zhu H, Hu J. CircRAB11FIP1 promoted autophagy flux of ovarian cancer through DSC1 and miR-129. *Cell Death Dis* (2021) 12:219. doi: 10.1038/s41419-021-03486-1

65. Tacutu R, Budovsky A, Yanai H, Fraifeld VE. Molecular links between cellular senescence, longevity and age-related diseases – a systems biology perspective. *Aging* (2011) 3:1178–91. doi: 10.18632/aging.100413

66. Lou Q, Liu R, Yang X, Li W, Huang L, Wei L, et al. miR-448 targets IDO1 and regulates CD8+ T cell response in human colon cancer. *J Immunother Cancer* (2019) 7:210. doi: 10.1186/s40425-019-0691-0

67. Ashizawa M, Okayama H, Ishigame T, Thar Min AK, Saito K, Ujiie D, et al. miRNA-148a-3p regulates immunosuppression in DNA mismatch repair–deficient colorectal cancer by targeting PD-L1. *Mol Cancer Res* (2019) 17:1403–13. doi: 10.1158/1541-7786.MCR-18-0831

68. Read ML, Seed RI, Modasia B, Kwan PPK, Sharma N, Smith VE, et al. The proto-oncogene PBF binds p53 and is associated with prognostic features in colorectal cancer: OVEREXPRESSION OF PBF IN COLORECTAL CANCER. *Mol Carcinog* (2016) 55:15–26. doi: 10.1002/mc.22254

69. Watkins RJ, Read ML, Smith VE, Sharma N, Reynolds GM, Buckley L, et al. Pituitary tumor transforming gene binding factor: A new gene in breast cancer. *Cancer Res* (2010) 70:3739–49. doi: 10.1158/0008-5472.CAN-09-3531

70. Hsueh C, Lin J-D, Chang Y-S, Hsueh S, Chao T-C, Yu J-S, et al. Prognostic significance of pituitary tumour-transforming gene-binding factor (PBF) expression in papillary thyroid carcinoma. *Clin Endocrinol* (2013) 78:303–9. doi: 10.1111/cen.12007

71. Tan X, Zhang S, Gao H, He W, Xu M, Wu Q, et al. Hypermethylation of the PTTG1IP promoter leads to low expression in early–stage non–small cell lung cancer. *Oncol Lett* (2019) 18:1278–86. doi: 10.3892/ol.2019.10400

72. Imruetaicharoenchoke W, Fletcher A, Lu W, Watkins RJ, Modasia B, Poole VL, et al. Functional consequences of the first reported mutations of the proto-oncogene PTTG1IP/PBF. *Endocrine-Related Cancer* (2017) 24:459–74. doi: 10.1530/ERC-16-0340

73. Lin F, Zhang G, Yang X, Wang M, Wang R, Wan M, et al. A network pharmacology approach and experimental validation to investigate the anticancer mechanism and potential active targets of ethanol extract of Wei-Tong-Xin against colorectal cancer through induction of apoptosis via PI3K/AKT signaling pathway. *J Ethnopharmacol* (2023) 303:115933. doi: 10.1016/j.jep.2022.115933

10.3389/fimmu.2023.1254911

Glossary

SHG8	3-(4-bromophenyl)-1-phenyl-3-(phenylamino)propan-1-one
CC	cervical carcinomas
COAD	Colorectal adenocarcinomas
CRC	Colorectal cancer
ESI	Electrospray ionization
ESI-MS	Electrospray ionization Mass spectra
FACS	fluorescence-activated cell sorting
GO	Gene Ontology
GSEA	Gene Set Enrichment Analysis
HCC	Hepatocellular carcinomas
HNSCC	Head and Neck Squamous Cell Carcinomas
HRMS	High Resolution Mass Spectra
IF	Immunofluorescence
KEGG	Kyoto Encyclopaedia of Genes and Genomes
LIHC	Liver Hepatocellular Carcinomas
LUAD	Lung Adenocarcinoma
MiRNAs	MicroRNAs
MSI-H	High Microsatellite Instability
NSCLC	Non-Small Cell Lung Cancer
OV	Ovarian Cancer
PAAD	Pancreatic Adenocarcinomas
PRAD	Prostate Adenocarcinoma
PI	Propidium Iodide
READ	Rectum Adenocarcinoma
ROS	Reactive Oxygen Species
RT	Room Temperature
RT-qPCR	Real Time- Quantitative Polymerase Chain Reaction
SAFSNS	Sulfonic Acid-Functionalized Silica Nanospheres
SCC	Lung Squamous Cell Carcinoma
SDG's	United Nations Sustainable Goals
Siglec-15	Sialic acid-binding immunoglobulin-type of lectin 15
THCA	Thyroid Carcinoma
TLC	Thin-layer Chromatography
UTR	Untranslated Region.